

Universidade Federal de Minas Gerais  
Instituto de Ciências Exatas  
Departamento de Química

Amalyn Nain Perez

**SYNTHESIS AND BIOLOGICAL ACTIVITIES OF AMINOQUINONES,  
QUINOLINES AND THEIR RUTHENIUM(II) COMPLEXES**

Belo Horizonte  
2018

UFMG/ICEx/DQ.1300<sup>a</sup>

T.588<sup>a</sup>

Amalyn Nain Perez

**SYNTHESIS AND BIOLOGICAL ACTIVITIES OF AMINOQUINONES,  
QUINOLINES AND THEIR RUTHENIUM(II) COMPLEXES**

Tese apresentada ao Departamento de Química do Instituto de Ciências Exatas da Universidade Federal de Minas Gerais como requisito parcial para obtenção do grau de Doutor em Ciências Químicas.

Belo Horizonte

2018

Ficha Catalográfica

P438s Perez, Amalyn Nain  
2018 Synthesis and biological activities of  
T aminoquinones, quinolines and their ruthenium(II)  
complexes [manuscrito] / Amalyn Nain Perez. 2018.  
[xi], 289 f. : il.

Orientador: Luiz Cláudio de Almeida Barbosa.  
Coorientadora: Maria Helena de Araújo.

Tese (doutorado) - Universidade Federal de Minas  
Gerais - Departamento de Química.  
Inclui bibliografia.

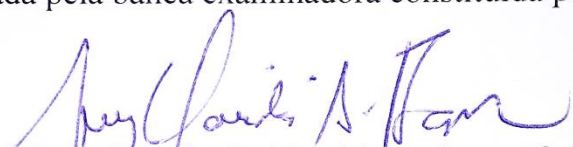
1. Química orgânica - Teses 2. Quinona - Teses 3.  
Compostos de rutênio - Teses 4. Agentes  
antineoplásicos - Teses 5. Herbicidas - Teses 6.  
Aminoquinolinas - Teses 7. Produtos de ação  
antimicrobiana - Teses I. Barbosa, Luiz Cláudio de  
Almeida, Orientador II. Araújo, Maria Helena de,  
Coorientadora III. Título.

CDU 043

## "Synthesis and Biological Activities of Aminoquinones, Quinolines and Their Ruthenium(II) Complexes"

**Amalyn Nain Perez**

Tese aprovada pela banca examinadora constituída pelos Professores:




Prof. Luiz Cláudio de Almeida Barbosa - Orientador  
UFMG



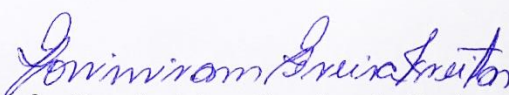
Profa. Maria Helena de Araujo - Coorientadora  
UFMG



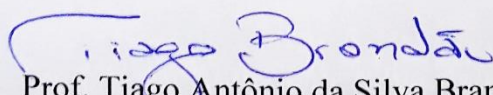
Prof. Hélio Alexandre Stefani  
USP



Prof. Silvio do Desterro Cunha  
UFBA



Profa. Rossimiriam Pereira de Freitas  
UFMG



Prof. Tiago Antônio da Silva Brandão  
UFMG

Belo Horizonte, 28 de agosto de 2018.



*“Each of us must work for his own improvement, and at the same time share a general responsibility for all humanity”*

*Marie Curie*

## ACKNOWLEDGEMENTS

I would like to thank Coordination for the Improvement of Higher Education Personnel, (CAPES), Government of Brazil, for the fellowship during this PhD.

I would like to thank Professor Luiz Cláudio de Almeida Barbosa for his expert advice and encouragement throughout this difficult project and for trust in me.

I would like to thank Professor Maria Helena de Araújo for her extraordinary support in this PhD process.

This project would have been impossible without the collaboration of the Professor Giuseppe Forlani (University of Ferrara) for herbicide and cyanobactericide experiments. As well as Professor René Csuk (Martin Luther University) for the cytotoxic studies and elemental analysis. Also, the Professor Taibi Ben Hadda (Mohammed First University), for the idea in form ruthenium complexes with aminoquinones. To all of you, thanks.

I would like to thank Professor Jacqueline Takahashi (UFMG) for her collaboration in the antibacterial studies. As well as Professor Renata Diniz (UFMG) for her collaboration in the study of x-ray.

I would like to thank my family for support me, motivate me and always believe in me. I would like to thank my colleagues: Isabel, Thaís, Samara, Jaime, Milandip, Muhammad, Izabel, Wagner, for their wonderful collaboration. You supported me greatly and were always willing to help me. Specially, to Diego my colleague, my confidant and my partner for giving me support at all times, especially in the most difficult.

I would like to thanks to post graduation secretary: Alessandra, Lilian, Fabiana, Ana Carolina, Alex, for their great service and always be there with a good smile.

I would like to thank Universidade Federal de Minas Gerais, especially to Chemistry Department. My thanks to all professors, technicians, and workers that contributed in some way in this process.

## CONTENT

ABBREVIATIONS	iv
LIST OF FIGURES	v
LIST OF TABLES	vii
ABSTRACT	viii
RESUMO	xi
<b>GENERAL INTRODUCTION</b>	<b>1</b>
1. AMINOQUINONES	2
1.1. Biological functions	3
1.1.1. Chemistry of aminoquinones: mechanism of action	5
1.2. Aminoquinones as ligand in organometallics	8
1.3. Ruthenium	9
1.4. Ruthenium based on <i>N,O</i> -type ligands	10
2. OBJECTIVES	11
3. REFERENCES	13
<b>CHAPTER 1</b>	
<b>FIRST SYNTHESIS OF ABENQUINES A-D</b>	<b>16</b>
1. INTRODUCTION	17
2. RESULTS AND DISCUSSION	20
2.1. Synthesis	20
2.2. Characterization	26
3. CONCLUSIONS	31
4. EXPERIMENTAL PART	32
4.1. General Information	32
4.2. Synthesis of <i>N</i> -(2,5-Dimethoxyphenyl)acetamide	32
4.3. Synthesis of 2-Acetamido-1,4-benzoquinone	33
4.4. Synthesis of <i>N</i> -(4-Bromo-2,5-dimethoxyphenyl)acetamide	34
4.5. Synthesis of 2-Acetamido-5-bromo-1,4-benzoquinone	34
4.6. Synthesis of Abenquines A-D	35
4.7. Synthesis of 2-Acetamido-5-benzylamino-1,4-benzoquinone	39
5. REFERENCES	40
<b>CHAPTER 2</b>	
<b>NATURAL ABENQUINES AND ANALOGUES: SYNTHESIS AND EVALUATIONS OF THEIR ALGICIDAL AND CYTOTOXIC ACTIVITY</b>	<b>42</b>
1. INTRODUCTION	43
2. RESULTS AND DISCUSSION	45
2.1. Synthesis	45
2.1.1. Synthesis of analogues of acetyl group	45
2.1.2. Characterization	46
2.1.3. Synthesis of analogues of benzoyl group	50
2.1.4. Characterization	51
2.2. Biological assay	54

2.2.1.	Cyanobacteria inhibition	54
2.2.2.	Inhibition of cyanobacterial growth	55
2.2.3.	Cytotoxicity assay	60
2.2.4.	Biological activity	60
3.	CONCLUSIONS	63
4.	EXPERIMENTAL PART	64
4.1.	Synthesis of analogue	64
4.2.	Synthesis of <i>N</i> -(2,5-dimethoxyphenyl)benzamide	66
4.3.	Synthesis of 2-benzamido-1,4-benzoquinone	67
4.4.	Synthesis of analogues (amino acids)	67
4.5.	Synthesis of analogues (amines)	70
4.6.	Biological assay	73
4.6.1.	Cyanobacterial cultures	73
4.6.2.	Cytotoxicity	73
5.	REFERENCES	75

**CHAPTER 3**  
**SYNTHETIC ANALOGUES OF ABENQUINES AS INHIBITORS OF THE PHOTOSYNTHETIC ELECTRON TRANSPORT CHAIN** 76

1.	INTRODUCTION	77
2.	RESULTS AND DISCUSSION	79
2.1.	Synthesis	79
2.1.1.	Synthesis of analogues (benzylamines)	79
2.1.2.	Characterization	80
2.1.3.	Synthesis of analogues (amides)	83
2.1.4.	Characterization	84
2.2.	Biological assay	87
2.2.1.	Inhibition of photosynthetic electron transport chain	87
2.2.2.	Molecular docking studies	90
3.	CONCLUSION	92
4.	EXPERIMENTAL PART	93
4.1.	Synthesis of benzylamines	93
4.2.	Synthesis of analogues	93
4.3.	Biological assay	100
4.3.1.	Measurement of the photosynthetic electron transport	100
4.3.2.	Molecular docking	102
5.	REFERENCES	103

**CHAPTER 4**  
**SYNTHESIS AND CHARACTERIZATION OF NEW RUTHENIUM COMPLEXES WITH 2,5-D(ALKYLAMINO)-1,4-BENZOQUINONE** 105

1.	INTRODUCTION	106
2.	RESULTS AND DISCUSSION	110
2.1.	Synthesis of ligands 2,5-diamino-1,4-benzoquinone	110
2.1.1.	Characterization	112
2.2.	Synthesis of $\mu$ -dichloro( <i>p</i> -cymene)ruthenium(II) dimer	113
2.2.1.	Characterization	113
2.3.	Synthesis of ruthenium complexes	114

2.3.1.	Characterization	116
2.4.	Biological evaluation	122
3.	CONCLUSION	124
4.	EXPERIMENTAL PART	125
4.1.	General Information	125
4.2.	Synthesis of ligands 2,5-diamino-1,4-benzoquinone	125
4.3.	Synthesis of $\mu$ -dichloro( <i>p</i> -cymene)ruthenium(II) dimer	129
4.4.	Synthesis of complexes	129
4.5.	Cytotoxic assay	132
5.	REFERENCES	133

## CHAPTER 5

### SYNTHESIS OF NEW RUTHENIUM COMPLEXES WITH QUINOLINE DERIVATIVES AND THEIR EVALUATION AS ANTIMICROBIAL AGENTS

		135
1.	INTRODUCTION	136
2.	RESULTS AND DISCUSSION	138
2.1.	Synthesis of 8-hydroxy-2-methylquinolines derivatives	138
2.1.1.	Characterization	140
2.1.2.	Synthesis of complexes	144
2.1.3.	Characterization	145
2.2.	Biological assay	150
2.2.1.	Antimicrobial activity	150
2.2.2.	Cytotoxic activity	154
3.	CONCLUSION	156
4.	EXPERIMENTAL PART	157
4.1.	General information	157
4.2.	Synthesis of 5-bromo-8-hydroxy-2-methylquinoline	157
4.3.	Synthesis of 5-(aryl)-8-hydroxy-2-methylquinoline derivatives	158
4.4.	Synthesis of 5,7-dibromo-8-hydroxy-2-methylquinoline	162
4.5.	Synthesis of complexes	163
4.6.	X-ray Crystallography	170
4.7.	Antimicrobial activity	170
4.8.	Cytotoxic activity	171
5.	REFERENCES	172

### FINAL CONSIDERATIONS

		174
		177
APPENDIX	Infrared, $^1\text{H}$ and $^{13}\text{C}$ NMR Spectra of compounds	

ANNEXES	Doctoral articles and patent	273
---------	------------------------------	-----

CHART OF PRODUCTS		280
-------------------	--	-----

## ABBREVIATIONS

$\delta$	Chemical shift relative to tetramethylsilane
$J$	Coupling Constant
$\nu_{\max}$	Frequency of maximum absorption
$\eta^6$	Hapticity, number of coordination = 6
$\mu\text{M}$	Micro molar
$[\text{M}+\text{H}]^+$	Molecular ion (positive ion mode)
$\text{EC}_{50}$	Half maximal effective concentration
Hex	Hexane
HRMS (ESI)	High Resolution Mass Spectrometry – Electrospray Ionization
$\text{IC}_{50}$	Half maximal inhibitory concentration
IR	Infrared Spectroscopy
NMR	Nuclear Magnetic Resonance
$^1\text{H}$ NMR	Hydrogen Nuclear Magnetic Resonance
$^{13}\text{C}$ NMR	Carbon Nuclear Magnetic Resonance
br.	Broad (NMR)
s	Singlet (NMR)
d	Doublet (NMR)
t	Triplet (NMR)
m	Multiplet (NMR)
sept	Septuplet (NMR)
MHz	Megahertz
Mp	Melting point
$m/z$	Mass of ion

## LIST OF FIGURES

<b>Figure 1.</b>	Chemical structures of amino-benzoquinones	2
<b>Figure 2.</b>	Natural products and analogues synthetic of aminoquinones	4
<b>Figure 3.</b>	Mechanism of reduction of aziridiny-1,4-benzoquinone	5
<b>Figure 4.</b>	Reduction in one and two electrons of benzoquinone	6
<b>Figure 5.</b>	Aminoquinones as anti-cancer compounds	7
<b>Figure 6.</b>	The complex formed by streptonigrin fragment and Ru(II)	8
<b>Figure 7.</b>	Aminoquinone as a ligand and complex aminoquinone-ruthenium	9
<b>Figure 8.</b>	Structure activity relationship of Ru(II)-arene quinolinol complexes	10
<b>Figure 1.1.</b>	Natural aminoquinones	17
<b>Figure 1.2.</b>	Structure of Abenquines A-D	19
<b>Figure 1.3.</b>	Retrosynthetic analysis	20
<b>Figure 1.4.</b>	First step: acetylation of 2,5-dimethoxyaniline ( <b>1.13</b> )	20
<b>Figure 1.5.</b>	Route 1 to obtain abenquine B2 ( <b>1.8</b> )	21
<b>Figure 1.6.</b>	Proposed mechanism for oxidation of hydroquinone to benzoquinone	21
<b>Figure 1.7.</b>	Route 2 to obtain abenquine B2 ( <b>1.8</b> )	22
<b>Figure 1.8.</b>	The mechanism proposed for oxidation with PIDA	23
<b>Figure 1.9.</b>	Aza-Michael addition of amino acid to the 2-acetamido-1,4-benzoquinone	24
<b>Figure 1.10.</b>	Route 3 to obtain abenquine B2 ( <b>1.8</b> )	24
<b>Figure 1.11.</b>	Synthesis of abenquines A, C and D	25
<b>Figure 1.12.</b>	Analogues of abenquines	25
<b>Figure 1.13.</b>	<sup>1</sup> H NMR spectra (400 MHz, CD <sub>3</sub> OD) of compounds <b>1.6</b> , <b>1.8-1.10</b> and <b>1.11</b>	27
<b>Figure 2.1.</b>	Abenquine analogues type 2,5-diaminoquinones	43
<b>Figure 2.2.</b>	Suggested amines as pharmacophores	44
<b>Figure 2.3.</b>	Proposed of change the acyl group by the benzoyl group to give new abenquine analogues	44
<b>Figure 2.4.</b>	Variation in the core of abenquine	45
<b>Figure 2.5.</b>	Preparation of analogue of acetyl group with different amines	46
<b>Figure 2.6.</b>	Infrared spectrum in KBr of compound <b>2.3</b>	46
<b>Figure 2.7.</b>	<sup>1</sup> H NMR (DMSO- <sub>d6</sub> , 300 MHz) of compound <b>2.3</b>	47
<b>Figure 2.8.</b>	<sup>13</sup> C NMR (DMSO- <sub>d6</sub> , 75 MHz) of compound <b>2.3</b>	48
<b>Figure 2.9.</b>	Preparation of analogue of benzoyl group with different amino acids	50
<b>Figure 2.10.</b>	Preparation of analogue of benzoyl group with different amines	50
<b>Figure 2.11.</b>	Infrared spectrum in KBr of compound <b>2.11</b>	51
<b>Figure 2.12.</b>	<sup>1</sup> H NMR (CDCl <sub>3</sub> , 400 MHz) of compound <b>2.11</b>	52
<b>Figure 2.13.</b>	<sup>13</sup> C NMR (CDCl <sub>3</sub> , 100 MHz) of compound <b>2.11</b>	53
<b>Figure 2.14.</b>	Effect of increasing concentrations of natural and synthetic abenquines	57
<b>Figure 2.15.</b>	Effect of abenquines and analogues on the photosynthetic electron transport chain in isolated spinach chloroplast in concentration of 50 and 100 μM	59

<b>Figure 3.1.</b>	Variations in the abenquine scaffold for analogues <b>3.1-3.9</b> and <b>3.12-3.16</b>	79
<b>Figure 3.2.</b>	Preparation of compounds <b>3.1-3.9</b>	80
<b>Figure 3.3.</b>	Infrared spectrum in KBr of compound <b>3.7</b>	81
<b>Figure 3.4.</b>	$^1\text{H}$ NMR (DMSO- $d_6$ , 400 MHz) of compound <b>3.7</b>	82
<b>Figure 3.5.</b>	$^{13}\text{C}$ NMR (DMSO- $d_6$ , 100 MHz) of compound <b>3.7</b>	83
<b>Figure 3.6.</b>	Preparation of compounds <b>3.12-3.16</b>	84
<b>Figure 3.7.</b>	Infrared spectrum in KBr of compound <b>3.13</b>	85
<b>Figure 3.8.</b>	$^1\text{H}$ NMR ( $\text{CDCl}_3$ , 400 MHz) of compound <b>3.13</b>	85
<b>Figure 3.9.</b>	$^{13}\text{C}$ NMR ( $\text{CDCl}_3$ , 100 MHz) of compound <b>3.13</b>	86
<b>Figure 3.10.</b>	Effects of increasing concentrations of compound <b>3.6</b> on ferricyanide reduction under basal, uncoupling, or phosphorylating conditions Infrared	90
<b>Figure 3.11.</b>	Binding models of abenquine analogue <b>3.6</b> with the pocket site of PSII from <i>Spinacia oleracea</i> (PDB ID: 3JCU)	91
<b>Figure 4.1.</b>	Octahedrally coordinated Ru(III)	107
<b>Figure 4.2.</b>	Structural formula for compounds <b>4.1</b> and <b>4.2</b>	108
<b>Figure 4.3.</b>	Ruthenium complexes, enzyme inhibitor and antitumor agents	108
<b>Figure 4.4.</b>	Synthesis of 2,5-bis-(alkyl/arylamino)-1,4-benzoquinones <b>4.8-4.20</b>	112
<b>Figure 4.5.</b>	Synthesis of $[\text{Ru}(\text{p-Cym})\text{Cl}_2]_2$	113
<b>Figure 4.6.</b>	Expansion of $^1\text{H}$ NMR spectrum ( $\text{CDCl}_3$ , 200 MHz) of compound <b>4.21</b>	113
<b>Figure 4.7.</b>	Expansion of $^{13}\text{C}$ NMR spectrum ( $\text{CDCl}_3$ , 75 MHz) of compound <b>4.21</b>	114
<b>Figure 4.8.</b>	Dinuclear ruthenium complexes ( <b>4.23-4.26</b> )	116
<b>Figure 4.9.</b>	Expansion of $^1\text{H}$ NMR spectrum ( $\text{CD}_2\text{Cl}_2$ , 400 MHz) of compound <b>4.23</b>	118
<b>Figure 4.10.</b>	Expansion of $^1\text{H}$ NMR spectrum of compound <b>4.21</b> , isomer ratio 4:1 <i>syn:anti</i>	120
<b>Figure 4.11.</b>	Expansion of $^{13}\text{C}$ NMR spectrum ( $\text{CD}_2\text{Cl}_2$ , 100 MHz) of compound <b>4.23</b>	121
<b>Figure 5.1.</b>	Structural representation of ruthenium complex of pyrazolone as <i>N,O</i> -ligands.	136
<b>Figure 5.2.</b>	Structure of 5,7-dibromo-8-hydroxyquinoline and their ruthenium complex	137
<b>Figure 5.3.</b>	Retrosynthetic analysis	138
<b>Figure 5.4.</b>	Synthesis of the quinoline derivatives ( <b>5.2-5.9</b> )	139
<b>Figure 5.5.</b>	Synthesis of the quinoline derivatives ( <b>5.10-5.11</b> )	139
<b>Figure 5.6.</b>	Infrared spectrum in KBr of compound <b>5.4</b>	140
<b>Figure 5.7.</b>	Synthesis of complexes <b>5.12-5.22</b>	144
<b>Figure 5.8.</b>	Infrared spectrum in KBr of complex <b>5.14</b>	145
<b>Figure 5.9.</b>	$^1\text{H}$ NMR spectrum ( $\text{CDCl}_3$ , 400 MHz) of compound <b>5.14</b>	146
<b>Figure 5.10.</b>	Expansion of $^1\text{H}$ NMR spectrum of compound <b>5.14</b>	147
<b>Figure 5.11.</b>	Expansion of $^1\text{H}$ NMR spectrum of compound <b>5.14</b>	147
<b>Figure 5.12.</b>	$^{13}\text{C}$ NMR spectrum ( $\text{CDCl}_3$ , 100 MHz) of compound <b>5.14</b>	148
<b>Figure 5.13.</b>	ORTEP representation of the complex <b>5.14</b>	149
<b>Figure 5.14.</b>	Inhibition of the yeast <i>C. albicans</i> by compound <b>5.3</b>	151



## LIST OF TABLES

<b>Table 1.1.</b>	Comparative <sup>1</sup> H NMR data of natural and synthetic Abenquines in CD <sub>3</sub> OD, 400 MHz	28
<b>Table 1.2.</b>	Comparative <sup>13</sup> C NMR data of natural and synthetic Abenquines in CD <sub>3</sub> OD, 100 MHz	30
<b>Table 2.1.</b>	<sup>1</sup> H NMR data for compounds <b>2.1-2.3</b> in DMSO- <i>d</i> <sub>6</sub> (400 MHz)	49
<b>Table 2.2.</b>	<sup>13</sup> C NMR data for compounds <b>2.1-2.3</b> in DMSO- <i>d</i> <sub>6</sub> (100 MHz)	49
<b>Table 2.3.</b>	Inhibitory effect of abenquines and analogues with acetyl group on cyanobacterial growth	55
<b>Table 2.4.</b>	Inhibitory effect of abenquines analogues with benzoyl group on cyanobacterial growth	56
<b>Table 2.5.</b>	Concentrations of natural and synthetic abenquines able to inhibit by 50% (IC <sub>50</sub> ) the growth of the model cyanobacterial strain <i>Synechococcus elongatus</i> PCC 6301	58
<b>Table 2.6.</b>	Concentrations of <b>2.11</b> and <b>2.12</b> able to inhibit by 50% the growth of various organisms	59
<b>Table 2.7.</b>	Cytotoxicity for abenquines <b>1.6-1.10</b> and analogues <b>1.17-1.20</b> , <b>2.1-2.3</b> and <b>2.6-2.13</b> ; employing human tumor cell lines and non-malignant mouse fibroblasts (NIH 3T3)	61
<b>Table 3.1.</b>	Effect of abenquines ( <b>1.6-1.10</b> ) and analogues ( <b>1.17-1.19</b> ) on the photosynthetic electron transport chain	87
<b>Table 3.2.</b>	Effect of synthetic analogues of abenquines with an acetyl group ( <b>1.20</b> , <b>2.1-2.3</b> ) on the photosynthetic electron transport chain	88
<b>Table 3.3.</b>	Effect of synthetic analogues of abenquines with benzoyl group ( <b>2.6-2.13</b> ) on the photosynthetic electron transport chain	88
<b>Table 3.4.</b>	Concentrations inhibiting by 50% the light-dependent ferricyanide reduction in spinach chloroplasts for compounds ( <b>3.1-3.9</b> and <b>3.12-3.16</b> )	89
<b>Table 4.1.</b>	Optimization of the reaction conditions	110
<b>Table 4.2.</b>	Bases to generate deprotonated ligand	115
<b>Table 4.3.</b>	Comparative <sup>1</sup> H NMR data for starting material and product	119
<b>Table 4.4.</b>	Isomer ratio of complexes <b>3.22-2.26</b>	119
<b>Table 4.5.</b>	Comparative <sup>13</sup> C NMR data for starting material and product	122
<b>Table 4.6.</b>	Cytotoxicity for quinoline derivatives and complexes employing human tumor cell lines and non-malignant mouse fibroblasts (NIH3T3)	123
<b>Table 5.1.</b>	Comparative <sup>1</sup> H NMR data of 8-hydroxy-2-methylquinoline derivatives <b>5.2-5.11</b> in CDCl <sub>3</sub> (400 MHz)	142
<b>Table 5.2.</b>	Comparative <sup>13</sup> C NMR data of 8-hydroxy-2-methylquinoline derivatives <b>5.2-5.11</b> in CDCl <sub>3</sub> (100 MHz)	143
<b>Table 5.3.</b>	Concentration of compounds <b>5.2-5.22</b> able to inhibit by 50% the growth of six organisms.	152
<b>Table 5.4.</b>	Cytotoxicity for compounds <b>5.2-5.11</b> and <b>5.12-5.22</b>	155

## ABSTRACT

Aminoquinones are an important class of naturally-occurring and synthetic compounds with a wide variety of biological functions. Although several studies address pharmacological activity, only a few studies about these compounds exhibiting agrochemical activity have been reported to date. In this context, this project will address the synthesis of a class of aminoquinones called abenquines. Moreover, an investigation about both agrochemical and cytotoxic activities of this class of compounds is reported. Additionally, this work presents an exploration of the synthesis and biological activities of ruthenium complexes. Metals have been used for medicinal purposes for decades; among them, ruthenium compounds. There is increasing interest in the use of the latter because of their biological activities. Consequently, organic compounds such as aminoquinones or quinolines, with known biological activities, are used as *N,O*-type ligands to form stable complexes with ruthenium. In this regard, the synthesis of ruthenium complexes containing this class of ligands, as well as the evaluation of cytotoxic or antimicrobial property is described.

Thereby, this thesis is divided into five chapters. In Chapter one, the first total synthesis of Abenquines **A**, **B2**, **C**, and **D**, is described. Abenquines have been achieved in three steps, with overall yields of 41-61%. The key steps of synthesis include (i) acylation of the aniline, (ii) oxidative demethoxylation, and (iii) oxidative addition of the amino acid moiety. Using the same methodology described above, in chapter two the synthesis of new analogues of abenquines is then discussed. Replacing the acetyl by a benzoyl group in the quinone core and changing the amino acid moiety with different amine groups results in 11 analogues with yields between 45-85%. The two most effective analogues carrying ethylpyrrolidinyl and ethylpyrimidinyl with either an acetyl group (**2.1**, **2.2**) or a benzoyl group (**2.11**, **2.12**), inhibited the proliferation of all five cyanobacterial strains tested, with  $IC_{50}$  values ranging from 0.3 to 3  $\mu$ M. Furthermore, analogues **2.1**, **2.2**, **2.11**, and **2.12**, were the most potent against all human cancer cell lines and displayed  $EC_{50}$  between a range of 0.6–3.4  $\mu$ M. Other series of analogues of abenquines were prepared by changing the amino acid group on abenquine with benzylamines and the acetyl with different acyl groups. This resulted in 14

new analogues in 68-95% yield as described in Chapter 3. Some analogues **3.2**, **3.3**, **3.6**, and **3.7** presented high effectiveness ( $IC_{50} = 0.1-0.4 \mu M$ ), comparable with the commercial herbicide diuron ( $IC_{50} = 0.3 \mu M$ ).

In chapter four the synthesis of 2,5-dialkylamino- and 2,5-diarylaminoquinones is described through an established protocol using a 1:3 ratio of amine/quinone, affording 13 aminoquinones in favourable yields (46-93%). Reactions of these aminoquinones in their doubly-deprotonated form with dichloro *p*-cymene ruthenium (II) dimer, afforded 5 new dinuclear complexes in yields within 65-95%. All aminoquinones and their ruthenium complexes were evaluated against six different cancer cell lines. Results displayed values of effective concentration ( $EC_{50}$ ) higher than 60  $\mu M$  for all the different cancer cell.

Chapter five describes the synthesis of new derivatives to 8-hydroxy-2-methylquinoline in high yield (65-90%). These quinoline derivatives and commercial 8-hydroxy-2-methylquinoline were reacted with dichloro *p*-cymene ruthenium (II) dimer, resulting 11 new ruthenium-quinolines complexes in 51-94% yields. For all quinolines derivatives and their complexes their antimicrobial activity against five microorganisms was evaluated. Results revealed active quinolines (**5.6** and **5.4**) with  $IC_{50} = 2.30$  and  $4.66 \mu g mL^{-1}$ . Whereas for complexes (**5.13** and **5.15**) an increase in the antimicrobial activity was demonstrated, which presented  $IC_{50}$  as low as 9.37 and  $4.64 \mu g mL^{-1}$ .

**Keywords:** Aminoquinones, quinolines, ruthenium complexes, herbicide, anticancer.

## RESUMO

As aminoquinonas são uma classe importante de compostos naturais e sintéticos com uma ampla variedade de funções biológicas. Apesar de vários estudos abordem a atividade farmacológica, apenas alguns estudos sobre estes compostos exibindo atividade agroquímica foram relatados até o momento. Neste contexto, este projeto abordará a síntese de uma classe de aminoquinonas chamadas abenquinas. Além disso, uma investigação sobre as atividades agroquímicas e citotóxicas desta classe de compostos é relatada. Adicionalmente, este trabalho apresenta uma exploração da síntese e atividades biológicas de complexos de rutênio. Os metais têm sido utilizados para fins medicinais por décadas; entre eles, compostos de rutênio. Há um crescente interesse no uso deste último por causa de suas atividades biológicas. Conseqüentemente, compostos orgânicos tais como aminoquinonas ou quinolinas, com actividades biológicas conhecidas, são utilizados como ligandos do tipo *N*, *O* para formar complexos estáveis com rutênio. A este respeito, descreve-se a síntese de complexos de rutênio contendo esta classe de ligantes, bem como a avaliação da propriedade citotóxica ou antimicrobiana.

Assim, esta tese é dividida em cinco capítulos. No primeiro capítulo, é descrita a primeira síntese total de abenquinas **A**, **B2**, **C** e **D**. As abenquinas foram alcançadas em três etapas, com rendimentos globais de 41-61%. Os passos chave da síntese incluem (i) acilação da anilina, (ii) desmetoxilação oxidativa e (iii) adição oxidativa do aminoácido. Usando a mesma metodologia descrita acima, no capítulo dois a síntese de novos análogos das abenquinas é então discutida, substituindo o acetila por um grupo benzoíla no núcleo quinona e alterando a porção aminoácido com diferentes grupos amina resulta em 11 análogos com rendimentos entre 45-85%. Os dois análogos mais eficazes transportando etilpirrolidinila e etilpirimidinila com um grupo acetilo (**2.1**, **2.2**) ou um grupo benzoíla (**2.11**, **2.12**). Eles inibiram a proliferação de todas as cinco espécies de cianobactérias testadas, com valores de  $IC_{50}$  variando entre 0,3 e 3,0  $\mu$ M. Além disso, os análogos **2.1**, **2.2**, **2.11** e **2.12**, foram os mais potentes contra todas as linhas celulares de câncer humano e exibiram  $EC_{50}$  entre um intervalo de 0,6 a 3,4  $\mu$ M. Outras séries de análogos das abenquinas foram

preparadas alterando o grupo aminoácido na abenquina com benzilaminas e o grupo acetila com diferentes grupos acila. Isso resultou em 14 novos análogos em 68-95% de rendimento como descrito no capítulo 3. Alguns análogos **3.2**, **3.3**, **3.6** e **3.7** apresentaram alta efetividade inibitória ( $IC_{50} = 0,1-0,4 \mu M$ ), comparável com o herbicida comercial diuron ( $IC_{50} = 0,3 \mu M$ ).

No capítulo quatro a síntese de 2,5-dialquil/arilamino-1,4-benzoquinonas é descrita através de um protocolo estabelecido usando uma proporção de 1:3 de amina/quinona, produzindo 13 aminoquinonas em rendimentos favoráveis (46-93%). As reações destas aminoquinonas na sua forma duplamente desprotonada com o dímero de dicloro *p*-cimeno rutênio (II), proporcionou 5 novos complexos dinucleares com rendimentos entre 65-95%. Todos os compostos preparados foram avaliados contra seis diferentes linhagens celulares de câncer. Os resultados apresentaram valores de concentração efetiva ( $EC_{50}$ ) maiores que 60  $\mu M$  para todas as diferentes células cancerígenas.

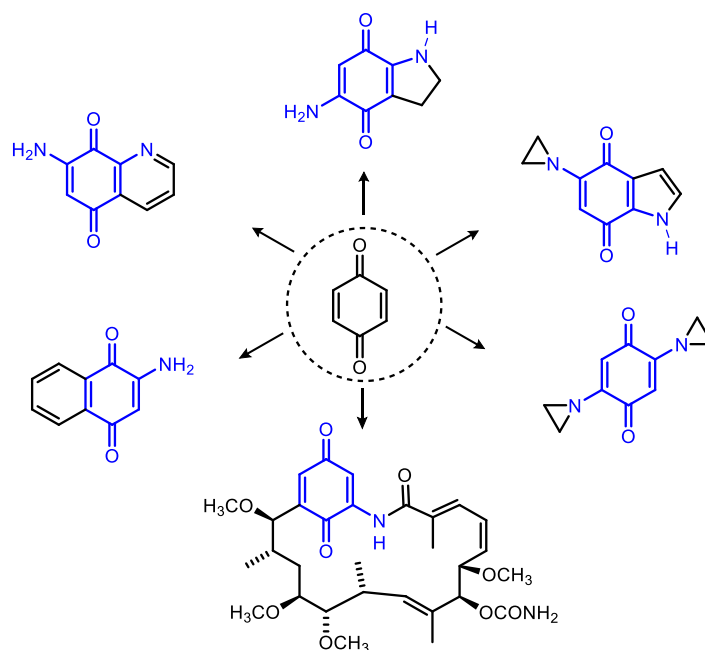
O capítulo cinco descreve a síntese de novos derivados para 8-hidroxi-2-metilquinolina em alto rendimento (65-90%). Estes derivados reagiram com o dímero de dicloro *p*-cimeno rutênio (II), resultando em 11 novos complexos de rutênio com 51-94% de rendimento. Para todos os derivados das 8-hidroxi-2-metilquinolina e seus complexos, foi avaliada sua atividade antimicrobiana contra cinco microorganismos. Os resultados revelaram quinolinas ativas (**5.6** e **5.4**) com  $IC_{50} = 2,30$  e  $4,66 \mu g/mL$ . Já para os complexos (**5.13** e **5.15**), foi demonstrado o  $IC_{50}$  tão baixo quanto  $9,37$  e  $4,64 \mu g/mL$ .

**Palavras-chave:** Aminoquinonas, quinolinas, complexos de rutênio, herbicida, anticâncer.

## **GENERAL INTRODUCTION**

## 1. AMINOQUINONES

Aminoquinones belong to a class of quinones compounds, that consist in a core of *para*-benzoquinone or naphthoquinone bearing amine as substituents (Figure 1). These class of compounds are widely distributed in nature and present several important biological effects as antibiotic, anticancer, antioxidant among others [1–4].



**Figure 1.** Chemical structures of amino-benzoquinones.

Aminoquinones are found in a variety of microorganism, for instance, in bacteria such as *Streptomyces caespitosus* [5], *Rhodospirillum rubrum* [6], *Streptomyces hygrosopicus* [7,8], *Photorhabdus luminescens* TT01 [9], *Salinispora arenicora* [10] and *Streptomyces* sp. [11]. They are also produced by marine sponge *Dactylospongia elegans* [12], *Dysidea* sp [13], *Spongia* sp [14], *Spongiidae* [15] as well as by marine bryozoan *Caulibugula intermist* Hamer [16]. In addition, they can be found in plants, such as *Murraya euchrestifolia* Hayata [17], *Coriander sativum* L [18], as well as in different species of toadstools such as *Lepiota Americana* [19], *Lactarius lilacinus* Fr. [20] and *Lactarius blennius* Fr. [21].

## 1.1. Biological functions

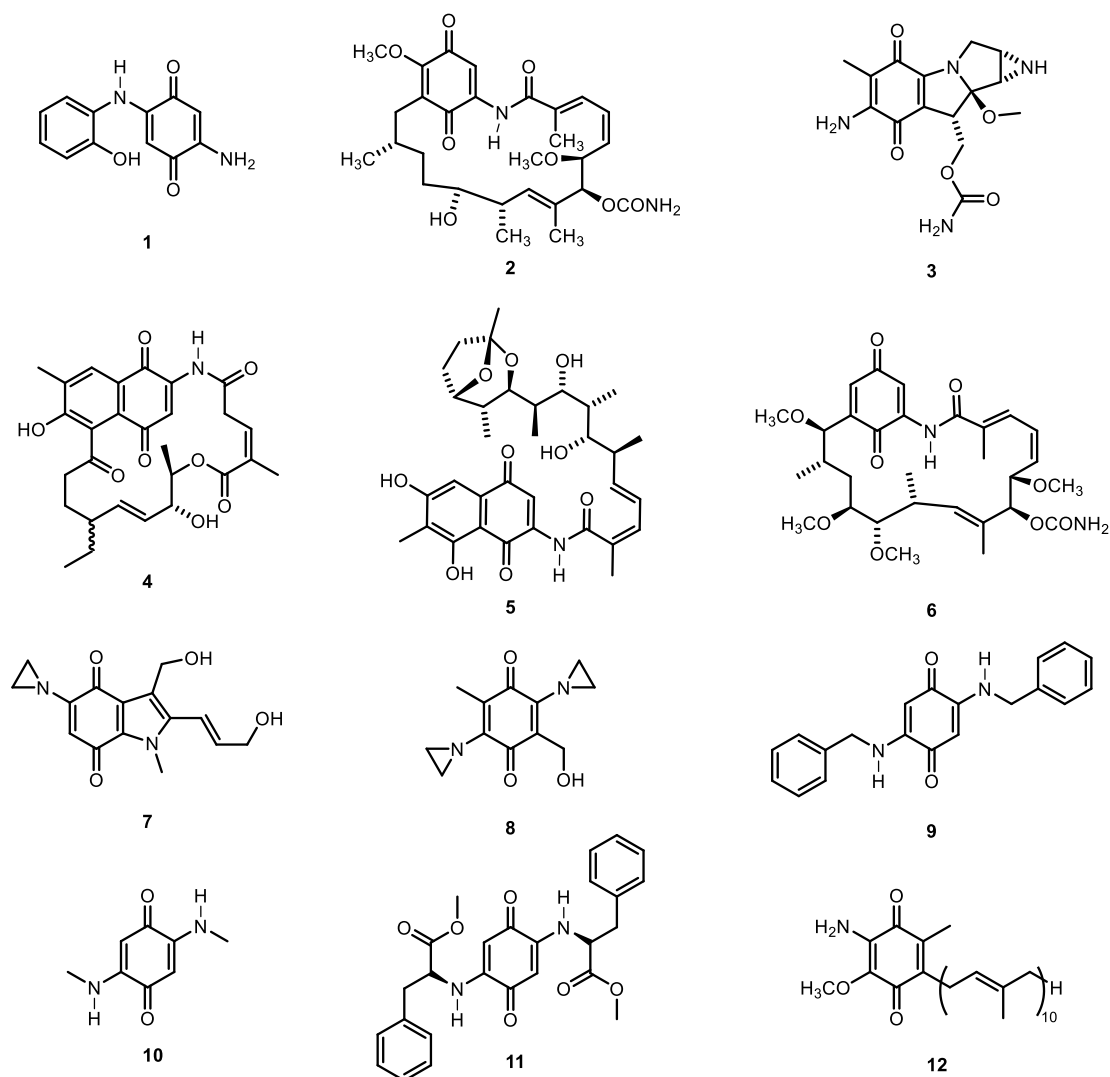
Some secondary metabolites shown in Figure 2 play an important role in biological functions. Due to their wide occurrence in nature, aminoquinones correspond to a well-studied class of compounds. For example, lepiotaquinone (**1**) is responsible for the red color in toadstools of the genera *Lepiota* and *Macrolepiota* [19]. On the other hand, geldanamycin (**2**) had been originally isolated as a natural product with anti-fungal activity. Additionally, it has been found as anti-proliferative activity in tumor cells and is known as the major inhibitor of molecular chaperone Hsp90 (Heat shock proteins) [22,23]. Another natural product of this class is mitomycin C (**3**), isolated from *Streptomyces caespitosus*, used as a chemotherapeutic agent due to antitumor and antibiotic properties [5,24]. Other examples are the natural products hygrocin A (**4**) and salinisporamycin (**5**), both of them exhibiting anticancer and antibiotic activity [8,25]. Besides, the aminonaphthoquinone herbimycin A (**6**) showed potent herbicidal and anti-tobacco mosaic virus (TMV) activity [7].

The great importance of these compounds with biological functions, owing to its structural features already mentioned, have been the basis on which new derivatives and synthetic analogues have been prepared. In Figure 2, some examples of interesting compounds are observed. In 1987, the synthetic derivative of mitomycin C known as EO9 (**7**) was developed as targeted therapeutic agent, hence clinical evaluations shown significant anti-tumor activity [26]. An additional class of potential compound is the one called RH1 (**8**), which underwent both preclinical and phase-I clinical trials [1].

Bis(benzylamino)benzoquinone (**9**) is another type of aminoquinone with a powerful electron acceptor group at the reducing side of photosystem II (PSII) and has been used as a type of herbicide [27]. This compound has been also identified as an effective inhibitor of dynamin I (belongs to the super-family GTPases) [28]. In addition, *di*-methylamino-benzoquinone (**10**) is a potential phytotoxic inhibitor against the growth of the monocotyledonous species *Sorghum bicolor*. Furthermore, these diaminoquinone compounds exerted a high inhibitory effect on a cyanobacterial model strain [29,30]. As a matter of fact,



benzoquinone with amino acid methyl ester (**11**) was the most powerful inhibitor against ScGT1 cells [31].



**Figure 2.** Natural products and analogues synthetic of aminoquinones.

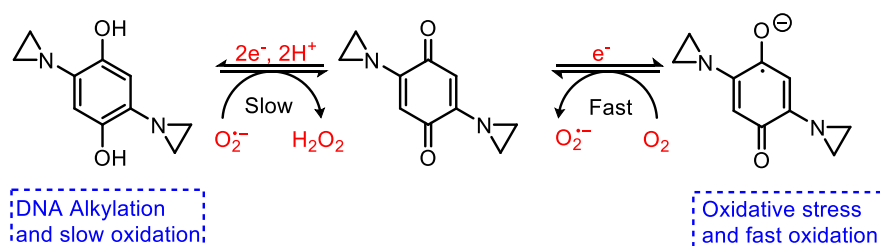
Likewise, rholoquinone (**12**) is an important cofactor involved in the anaerobic energy metabolism of *Rhodospirillum rubrum*. Compound **12** is structurally similar to ubiquinone (coenzyme Q) which is involved in the aerobic respiratory chain. Also, this compound is found in several eukaryotic species that employ a fumarate reductase pathway for anaerobic respiration, being the parasitic helminths an important example. This cofactor is found neither in humans nor in mammals, and inhibition of its biosynthesis may provide a parasite-specific drug target [6].

Aminoquinones also show a different activities, acting as antimicrobial [10] anti fungicide [9], antibacterial [32–34], anti-inflammatory and antiallergic [35,36], antibiotic [24,25], antiparasitic [37], urease inhibitor [38], anti-malarial [39], anti-leukemia [12], neuroprotective [13], and anti-cancer [1,2,5,11,15,16,40].

### 1.1.1. Chemistry of aminoquinones: mechanism of action

Many natural products and their derivatives such as the aminobenzoquinones are associated with enzyme inhibition, DNA cross-linking, antibacterial, antifungal, and anticancer activity. Concerning their medicinal effective results the striking feature of aminoquinone chemistry in a biological system is their large capacity of reduction and consequently, these compounds have the ability to act as oxidizing [41,42].

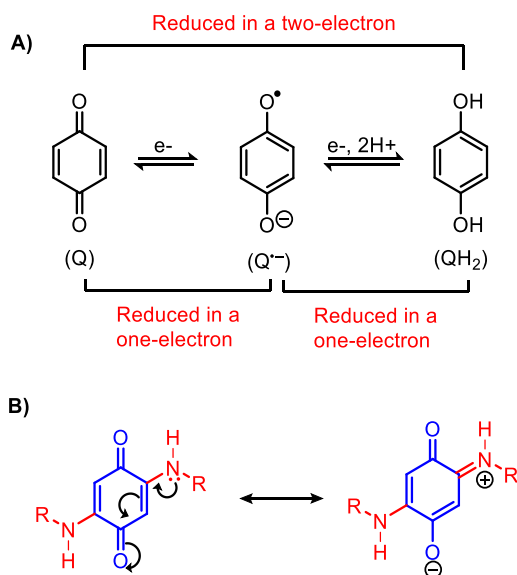
Aminoquinones play an important role in a redox system. For example, aziridiny-1,4-benzoquinones, which are potentially important antitumor agents known since the 1980s has been extensively studied their mechanism of action. It is accepted that their antitumor activity stems from the following mechanism: a) their two-electron enzymatic reduction into aziridiny-hydroquinones which alkylate DNA more readily than the parent quinones; b) their oxidative stress-type cytotoxicity caused by the redox cycling of semiquinone formed during the single-electron enzymatic reduction of quinones; and c) their direct alkylation of DNA by certain aziridiny-benzoquinones with the strong electron-donating substituents [43] (Figure 3).



**Figure 3.** Mechanism of reduction of aziridiny-1,4-benzoquinone.

Similarly, there are some electrochemical properties that can be explained by the mechanism of action through the redox cycling in Figure 4. In Figure 4A, quinone (Q) are reduced in a two-electron way into hydroquinone (QH<sub>2</sub>) with a

formation of the radical semiquinone ( $Q^{\cdot-}$ ). Figure 4B shows the interaction of amino group as electron donating. On the other hand, the electron accepting substituents such as  $-Cl$ ,  $-SO_3$ , etc., increase the redox potentials of quinones, whereas the electron donating ones such as  $-CH_3$ ,  $-OCH_3$ ,  $-NH_2$ ,  $-NHR$ , and  $-OH$  decrease it when compared with 1,4-benzoquinone [43].

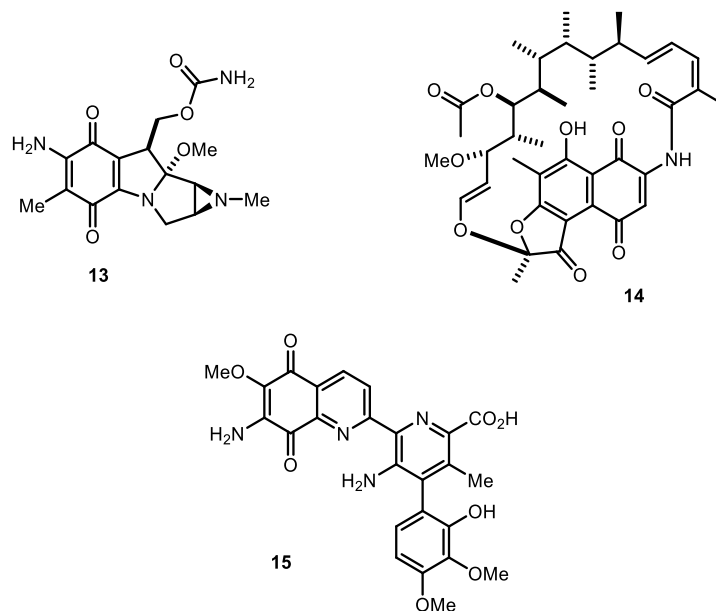


**Figure 4.** A) Reduction in one and two electrons of benzoquinone. B) Resonant effect involving the amino group.

This can be explained by considering two separate electronic effects of the amino substituents. Firstly, the inductive electron-withdrawing effect of the nitrogen atom, which operates always, regardless of the steric hindrance. Secondly, the resonance effect is commonly predominant and carries to delocalization of the lone pair of electrons of the nitrogen over the enone system on the quinone nucleus. Therefore, the amino group can adopt a conformation when the  $\pi$ -orbitals carry the lone pair of electron parallel to the  $\pi$  system of the ring [27,44,45]. For this reason, they can accept one electron, forming the semiquinone radical, followed by a further electron to give the hydroquinone system.

In general, aminoquinone has two properties: First, the quinone moiety can be reduced, thus, the cytotoxic activity may consider have a relation with the redox cycling [46]. And second, their electrophilic character enables them to undergo nucleophilic attack which may lead to enhanced toxicity [4].

As previously noted, aminoquinones represent a broad source of anti-cancer compounds such as mitomycin C (**3**), porfiromycin (**13**), rifamycin (**14**), streptonigrin (**15**) besides ansamycins as hygrocin (**4**), geldanamycin (**2**) and derivatives (Figure 5) [47].



**Figure 5.** Aminoquinones as anti-cancer compounds.

These compounds require a specific enzyme able to catalyze the bioreduction of the quinone moiety, before conversion to intermediates that can generate toxic free radical species or bind to DNA and form covalent adducts. However, one and two electron reductase are capable of activating bioreductive drugs, including NADH:Cytochrome b<sub>5</sub> reductase, cytochrome P450 reductase, and NAD(P)H:Quinone oxidoreductase (NQO1) [46].

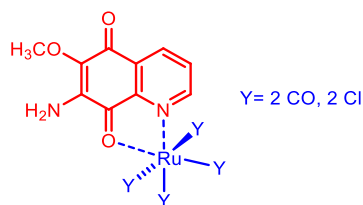
For example, mitomycin (**3**) is bioreduced by the enzyme P450R that leads to the formation of free radicals causing lipid peroxidation as well as damage to protein and DNA, then resulting in cell death [4]. Regarding the mechanism of action, it is well known that streptonigrin (**15**) interact with DNA, causing some DNA degradations when is chemically reduced. Particularly, this compound requires oxygen and electron source to exert its lethal effect [48].

## 1.2. Aminoquinones as ligand in organometallics

Organometallic compounds are an important area of chemistry, so they play crucial roles in biological and biomedical processes because they offer the potential for the design of novel therapeutic and diagnostic agents [49].

It has been shown that a range of divalent transition metal ions improves the biological activity of different fragment of streptonigrin. For example metal complexes of streptonigrin fragment with zinc(II), copper(II), cadmium(II), cobalt(II), iron(II), manganese(II), palladium(II) and ruthenium(II), are more cytotoxic than the corresponding uncomplexed organic moiety [50].

The formation of complex with the fragment of the core of streptonigrin and ruthenium (II) (Figure 6) forms stable, redox-active. Metal coordination alters the charge distribution across the molecule, affecting the redox potential of the quinone and therefore influences directly the rate of generation of DNA-damaging radical species. The coordination also influences the conformational flexibility of the drug, which may have significant consequences *in vivo* [50].



**Figure 6.** The complex formed by streptonigrin fragment and Ru(II).

In fact, organometallics offer many opportunities in the design of innovative classes of medicinal compounds, potentially with new metal specific modes of action [51–53].

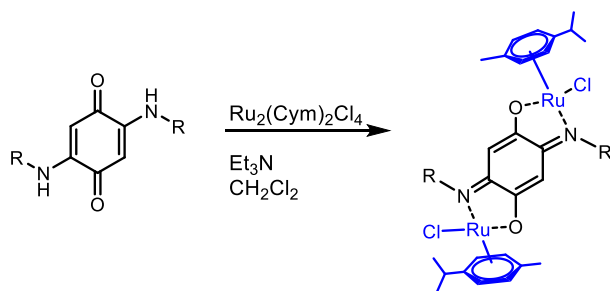
Recently, the use of aminoquinones as ligands in the preparation of several organometallic compounds have been reported. This is due to its role in the electrons transference process with transition metals, as well as its importance in biological systems [54,55]. The development of ruthenium complexes as an alternative to platinum-based tumor inhibitors is of special interest due their antitumor and antimetastatic activity [56].

### 1.3. Ruthenium

Ruthenium has a combination of properties which makes this metal an ideal candidate to form an organometallic compound as bioactive species [57]. Some of these features include:

- ✓ Ruthenium is able to form substitutional inert coordinate bonds.
- ✓ Ruthenium has a low general toxicity.
- ✓ Synthetic routes to ruthenium-containing compounds can be planned and predicted similarly to purely organic molecules.
- ✓ Due to the kinetic inertness of coordinate bonds of ruthenium, compounds can generally be purified in the same manner as purely organic compounds, using standard silica gel chromatography.

The interaction between ruthenium centers and non-innocent ligands, such as aminoquinones (Figure 7), has fascinated chemists by virtue of the valence ambiguity arising in such complexes as a cause of the close proximity of the metal  $d\pi$  and ligand based  $\pi$  orbitals. The non-innocent character of ligands has led to the concept of electron reservoirs, leading to the activation of small molecules [58].



**Figure 7.** Aminoquinone as a ligand and complex of aminoquinone-ruthenium.

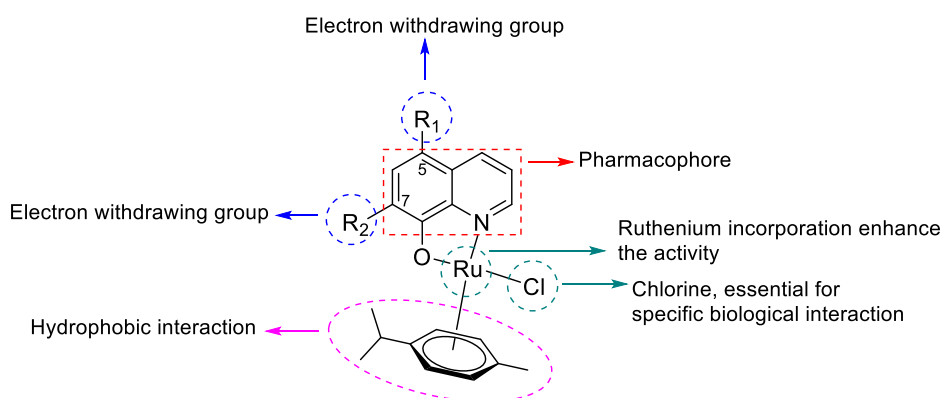
The biological potential and the usefulness involved in the production of metal complexes with organic compounds rise to an interest in the synthesis of aminoquinone complex. Hence, the present work proposes the synthesis of the aminoquinone-ruthenium complex. For the synthesis, new compounds with different amino groups as a substitute on the benzoquinone core will be employed. Also, this investigation has as a final objective, the preparation of new organometallic compounds to evaluate their biological potential such as cytotoxic activities.

#### 1.4. Ruthenium based on *N,O*-type ligands

Dimer of  $\text{Ru}(\text{Cym})\text{Cl}_2$  can be used as a scaffold to build compounds with promising biological activity using chelating ligands [59,60]. A chelating agent contains two or more electron donor atoms that can form coordinate bonds to a single metal atom, where each donor atom bound creates a ring containing the metal atom and this cyclic structure is called a chelation complex [61,62]. The principal donor atoms in practical use are N, O and S; they formed chelate rings usually of five or six members and have been the most stable and most useful in chemistry [62].

An approach in metallodrug design is the use of nature inspired, bioactive ligands such as flavones or quinones [63], however, another approach is the use of privileged structures. Nowadays, privileged structures refer to substructures or scaffold which appear in drugs, natural compounds or bioactive molecules. Among them, the nitrogen-containing heterocycle 8-hydroxyquinoline and its derivatives has been explored as chelating agent due to a broad variety of pharmacological properties, which make them an ideal bioactive building block in the development of metal drugs [64].

Several ruthenium complexes of 8-hydroxyquinoline derivatives have been reported [65,66]. Although, there is a gap in terms of a systematic study on the effect of the variation of substituents at the 5 and 7 positions, recently was establish a structure activity relationship based on the best cytotoxicity in different cancer cell lines (see Figure 8).



**Figure 8.** Structure activity relationship of Ru(II)-arene quinolinol complexes.

In terms of cytotoxic activity Moldal *et al.*, [67] reported that (i) spatial arrangement of arene is essential for hydrophobic and specific biological interaction with the target (ii) electron withdrawing halogen substitution at 5 and 7 positions of hydroxyquinoline is crucial for cytotoxicity (iii) labile chlorine group is essential for several biological interactions with DNA and protein.

In this context, 8-hydroxy-2-methylquinoline will be employed as model to synthesize new derivatives, in order to form ruthenium complexes and explore their potential as antimicrobial and cytotoxic agents.

## 2. OBJECTIVES

Considering the positive results already described in the literature for the synthesis of similar compounds to aminoquinones, the present work aims to synthesize new natural aminoquinones as well as the synthesis of different analogues. Also, it is propose the synthesis of ligands bearing *N,O*-atoms for the formation of ruthenium complexes, in order to obtain products with potential biological activity.

Specifically, aims are:

- ✓ Synthesize 2,5-di(alkyl/arylamino)-1,4-benzoquinones
- ✓ Synthesize natural abenquines and analogues
- ✓ Synthesize ruthenium complexes with the ligands 2,5-di(alkyl/arylamino)-1,4-benzoquinones
- ✓ Synthesize ruthenium complexes with ligands derivates of 8-hydroxy-2-methylquinoline
- ✓ Evaluate the phytotoxic, cytotoxic and antimicrobial potential of the synthesized compounds.

Thus, to achieve the above objectives, this Doctoral Thesis is divided into the following chapters.



**Chapter 1:** It describes the approach of the new methodology for the first total synthesis of natural aminoquinone abenquines (A-D). Moreover, it is presented the synthesis of four analogues of abenquines as well as the characterization of the compounds.

**Chapter 2:** In this section the synthesis of analogues to natural abenquines changing the substitutions of the core of abenquines is described. This chapter also shows all the characterization data of the compounds and a detailed discussion on both the algicidal and cytotoxic activity.

**Chapter 3:** In this chapter the synthesis of abenquine analogues containing the benzylamine with or without substitution is discussed. A complete characterization of the compounds and the study of herbicide activity targeting photosynthesis is also described.

**Chapter 4:** This chapter describes the synthesis of new complexes between 2,5-di(alkyl/arylamino)-1,4-benzoquinones and ruthenium. In addition, a complete characterization of the compounds is discussed as well as a brief screening of their cytotoxic potential.

**Chapter 5:** It describes the synthesis of 8-hydroxy-2-methylquinolines derivatives that used *N,O*-ligands to form new ruthenium complexes. Also, the antibacterial activity against *S. aureus*, *B. cereus*, *S. typhimurium*, *E. coli* and *C. albicans* is discussed.

### 3. REFERENCES

- [1] A. Nemeikaitė-Čėnienė, R. Jarašienė, H. Nivinskas, J. Šarlauskas, N. Čėnas, *Chemija*. 26 (2015) 46–50.
- [2] M. Itoigawa, Y. Kashiwada, C. Ito, H. Furukawa, Y. Tachibana, K. Bastow, K.-H. Lee, *J. Nat. Prod.* 63 (2000) 893–897.
- [3] T.J. Donohoe, C.R. Jones, A.F. Kornahrens, L.C.A. Barbosa, L.J. Walport, M.R. Tatton, M. O'Hagan, A.H. Rathi, D.B. Baker, *J. Org. Chem.* 78 (2013) 12338–12350.
- [4] N. El-Najjar, H. Gali-Muhtasib, R.A. Ketola, P. Vuorela, A. Urtti, H. Vuorela, *Phytochem. Rev.* 10 (2011) 353–370.
- [5] M. Tomasz, *Chem. Biol.* 2 (1995) 575–579.
- [6] B.C. Brajcich, A.L. Iarocci, L.A.G. Johnstone, R.K. Morgan, Z.T. Lonjers, M.J. Hotchko, J.D. Muhs, A. Kieffer, B.J. Reynolds, S.M. Mandel, B.N. Marbois, C.F. Clarke, J.N. Shepherd, *J. Bacteriol.* 192 (2010) 436–445.
- [7] Y. Iwai, A. Nakagawa, N. Sadakane, S. Omura, *J. Antibiot. (Tokyo)*. 33 (1980) 1114–1119.
- [8] P. Cai, F. Kong, M.E. Ruppen, G. Glasier, G.T. Carter, *J. Nat. Prod.* 68 (2005) 1736–1742.
- [9] H.B. Park, J.M. Crawford, *J. Nat. Prod.* 78 (2015) 1437–1441.
- [10] S. Matsuda, K. Adachi, Y. Matsuo, M. Nukina, Y. Shizuri, *J. Antibiot. (Tokyo)*. 62 (2009) 519–26.
- [11] U.W. Hawas, M. Shaaban, K.A. Shaaban, M. Speitling, A. Maier, G. Kelter, H.H. Fiebig, M. Meiners, E. Helmke, H. Laatsch, *J. Nat. Prod.* 72 (2009) 2120–4.
- [12] D. Kong, *Mar. Drugs*. 6 (2008) 480–488.
- [13] H. Suna, M. Arai, Y. Tsubotani, A. Hayashi, A. Setiawan, M. Kobayashi, *Bioorg. Med. Chem.* 17 (2009) 3968–72.
- [14] N.K. Utkina, V. a. Denisenko, O. V. Scholokova, M. V. Virovaya, N.G. Prokof'eva, *Tetrahedron Lett.* 44 (2003) 101–102.
- [15] J. Kobayashi, T. Madono, H. Shigemori, *Tetrahedron*. 51 (1995) 10867–10874.
- [16] D.J. Milanowski, K.R. Gustafson, J. a. Kelley, J.B. McMahon, *J. Nat. Prod.* 67 (2004) 70–73.
- [17] K. Ramesh, R.S. Kapil, *J. Nat. Prod.* 50 (1987) 932–934.
- [18] R. Dharmalingam, P. Nazni, *Int. J. Food Nutr. Sci.* 2 (2013) 34–39.
- [19] K. Aulinger, N. Arnold, W. Steglich, *Z. Naturforsch.* 55c (2000) 481–484.
- [20] P. Spiteller, N. Arnold, M. Spiteller, W. Steglich, *J. Nat. Prod.* 66 (2003) 1402–3.
- [21] P. Spiteller, W. Steglich, *J. Nat. Prod.* 65 (2002) 725–727.
- [22] Y. Miyata, *Curr. Pharm. Des.* 11 (2005) 1131–1138.
- [23] M. Zhang, S. Gaisser, M. Nur-E-Alam, L.S. Sheehan, W.A. Vousden, N. Gaitatzis, G. Peck, N.J. Coates, S.J. Moss, M. Radzom, T.A. Foster, R.M. Sheridan, M.A. Gregory, S.M. Roe, C. Prodromou, L. Pearl, S.M. Boyd, B. Wilkinson, C.J. Martin, *J. Med. Chem.* 51 (2008) 5494–5497.
- [24] N. Danshiitsoodol, C.A. de Pinho, Y. Matoba, T. Kumagai, M. Sugiyama, *J. Mol. Biol.* 360 (2006) 398–408.
- [25] C.C. Nawrat, L.I. Palmer, A.J. Blake, C.J. Moody, *J. Org. Chem.* 78 (2013) 5587–5603.
- [26] R.M. Phillips, H.R. Hendriks, G.J. Peters, *Br. J. Pharmacol.* 168 (2013) 11–

- 18.
- [27] B. Lotina-Hennsen, L. Achnine, N.M. Ruvalcaba, A. Ortiz, J. Hernández, N. Farfán, M. Aguilar-Martínez, *J. Agric. Food Chem.* 46 (1998) 724–730.
- [28] K.A. MacGregor, M.K. Abdel-Hamid, L.R. Odell, N. Chau, A. Whiting, P.J. Robinson, A. McCluskey, *Eur. J. Med. Chem.* 85 (2014) 191–206.
- [29] L.C.A. Barbosa, U.A. Pereira, C.R.A. Maltha, R.R. Teixeira, V.M. Moreira Valente, J.R. Oliveira Ferreira, L.V. Costa-Lotufo, M.O. Moraes, C. Pessoa, *Molecules.* 15 (2010) 5629–5643.
- [30] A. Nain-Perez, L.C.A. Barbosa, M.C. Picanço, S. Giberti, G. Forlani, *Chem. Biodivers.* 13 (2016) 1008–1017.
- [31] H. Ngoc, A. Tran, S. Bongarzone, P. Carloni, G. Legname, M. Laura, 20 (2010) 1866–1868.
- [32] B. Chakraborty, S. Chakraborty, C. Saha, *Int. J. Microbiol.* 2014 (2014) 1–8.
- [33] C. Sudhakar, K.R. Raju, M.K. Reddy, 6 (2014) 664–668.
- [34] M.K. Reddy, K.R. Raju, 4 (2014) 47–53.
- [35] R. Filosa, A. Peduto, A.M. Schaible, V. Krauth, C. Weinigel, D. Barz, C. Petronzi, F. Bruno, F. Roviezzo, G. Spaziano, B. D’Agostino, M. De Rosa, O. Werz, *Eur. J. Med. Chem.* 94 (2015) 132–139.
- [36] W.-H. Jiao, T.-T. Xu, F. Zhao, H. Gao, G.-H. Shi, J. Wang, L.-L. Hong, H.-B. Yu, Y.-S. Li, F. Yang, H.-W. Lin, *European J. Org. Chem.* 2015 (2015) 960–966.
- [37] N. Mathew, T. Karunan, L. Srinivasan, K. Muthuswamy, *Drug Dev. Res.* 71 (2010) 188–196.
- [38] Z.-L. You, D.-M. Xian, M. Zhang, X.-S. Cheng, X.-F. Li, *Bioorg. Med. Chem.* 20 (2012) 4889–4894.
- [39] W.A. Guiguemde, A.A. Shelat, D. Bouck, S. Duffy, G.J. Crowther, P.H. Davis, D.C. Smithson, M. Connelly, J. Clark, F. Zhu, M.B. Jiménez-Díaz, M.S. Martinez, E.B. Wilson, A.K. Tripathi, J. Gut, E.R. Sharlow, I. Bathurst, F. El Mazouni, J.W. Fowble, I. Forquer, P.L. McGinley, S. Castro, I. Angulo-Barturen, S. Ferrer, P.J. Rosenthal, J.L. DeRisi, D.J. Sullivan, J.S. Lazo, D.S. Roos, M.K. Riscoe, M.A. Phillips, P.K. Rathod, W.C. Van Voorhis, V.M. Avery, R.K. Guy, *Nature.* 465 (2010) 311–315.
- [40] A.K. Vadukoot, S.F. AbdulSalam, M. Wunderlich, E.D. Pullen, J. Landero-Figueroa, J.C. Mulloy, E.J. Merino, *Bioorg. Med. Chem.* 22 (2014) 6885–6892.
- [41] C. Asche, *Mini Rev. Med. Chem.* 5 (2005) 449–467.
- [42] H. Lee, E.A. Theodorakis, *Sci. Synth.* 28 (2006) 71–86.
- [43] J. Šarlauskas, *Chemij.* 26 (2015) 208–217.
- [44] J. Elving, S.I. Pace, *Biological Aspects of Electrochemistry*, Springer Basel AG, 1971.
- [45] S. Bayen, N. Barooah, R.J. Sarma, T.K. Sen, A. Karmakar, J.B. Baruah, *Dye. Pigment.* 75 (2007) 770–775.
- [46] G.F. Weber, *Molecular Therapies of Cancer*, Springer, 2015.
- [47] F.E. Hahn, *Mechanism of Action of Antieukaryotic and Antiviral Compounds*, Springer-Verlag, Berlin Heidelberg New York, 1979.
- [48] H. Kersten, W. Kersten, *Inhibitors of Nucleic Acid Synthesis: Biophysical and Biochemical Aspects*, Springer-Verlag, Berlin-Heidelberg-New York, 1974.
- [49] Z. Guo, P.J. Sadler, *Angew. Chem. Int. Ed. Engl.* 38 (1999) 1512–1531.

- [50] P.I. Anderberg, M.M. Harding, I.J. Luck, P. Turner, *Inorg. Chem.* 41 (2002) 1365–1371.
- [51] S. Medici, M. Peana, V.M. Nuchi, J.I. Lachowicz, *Coord. Chem. Rev.* 284 (2015) 329–350.
- [52] A. Bergamo, G. Sava, *Dalt. Trans.* 40 (2011) 7817–7823.
- [53] F. Li, J.G. Collins, F.R. Keene, *Chem Soc Rev.* 44 (2015) 2529–2542.
- [54] S. Scheuermann, T. Kretz, H. Vitze, J.W. Bats, M. Bolte, H.-W. Lerner, M. Wagner, *Chemistry.* 14 (2008) 2590–601.
- [55] W.G. Jia, Y.F. Han, Y.J. Lin, L.H. Weng, G.X. Jin, *Organometallics.* 28 (2009) 3459–3464.
- [56] W. Peti, T. Pieper, M. Sommer, K.B. Keppler, G. Giester, *Eur. J. Inorg. Chem.* (1999) 1551–1555.
- [57] E. Meggers, *Curr. Opin. Chem. Biol.* 11 (2007) 287–292.
- [58] H.S. Das, D. Schweinfurth, J. Fiedler, M.M. Khusniyarov, S.M. Mobin, B. Sarkar, *Chem. - A Eur. J.* 20 (2014) 4334–4346.
- [59] R. Pettinari, F. Marchetti, C. Pettinari, A. Petrini, R. Scopelliti, C.M. Clavel, P.J. Dyson, *Inorg. Chem.* 53 (2014) 13105–13111.
- [60] F. Aman, M. Hanif, W.A. Siddiqui, A. Ashraf, L.K. Filak, T. So, S.M.F. Jamieson, C.G. Hartinger, (2014).
- [61] J.L. Domingo, *Reprod. Toxicol. Rev.* 12 (1998) 499–510.
- [62] H.W. L., W. David, Chelating Agents, in: Kirk-Othmer Encycl. Chem. Technol., American Cancer Society, 2003.
- [63] M. Kubanik, H. Holtkamp, T. Söhnel, S.M.F. Jamieson, C.G. Hartinger, *Organometallics.* 34 (2015) 5658–5668.
- [64] Y.Q. Hu, C. Gao, S. Zhang, L. Xu, Z. Xu, L.S. Feng, X. Wu, F. Zhao, *Eur. J. Med. Chem.* 139 (2017) 22–47.
- [65] M. Malipeddi, C. Lakhani, M. Chhabra, P. Paira, R. Vidya, *Bioorg. Med. Chem. Lett.* 25 (2015) 2892–2896.
- [66] M.H. Kaulage, B. Maji, S. Pasadi, S. Bhattacharya, K. Muniyappa, 139 (2017) 1016–1029.
- [67] A. Mondal, S. De, S. Maiti, B. Sarkar, A.K. Sk, R. Jacob, A. Moorthy, P. Paira, *J. Photochem. Photobiol. B Biol.* 178 (2018) 380–394.

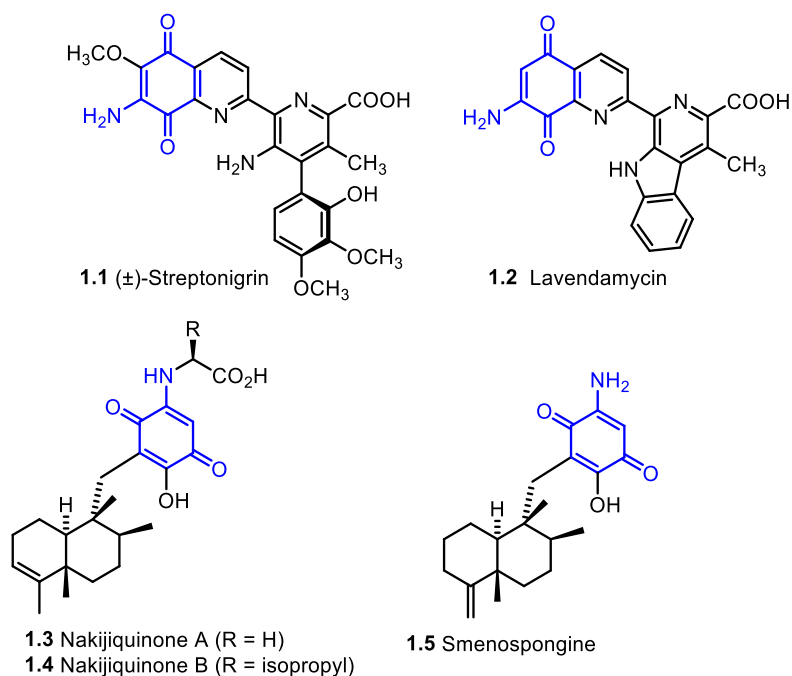
## **CHAPTER 1**

### **FIRST SYNTHESIS OF ABENQUINES A-D**

## 1. INTRODUCTION

Natural products generally mean secondary metabolite, a small molecule that is not essential to the growth and development of the producing organism [1]. The existence of well over 300,000 secondary metabolites has been estimated and it is thought that their primary function consists of increasing the likelihood of an organism survival, by repelling or attracting other organisms [2,3]. Nowadays, one-third of clinically used drugs come from nature, they are either directly isolated from natural products or synthesized by structural modification of their natural compounds [1].

Among the plethora of natural products, such as polyketides, terpenoids, steroids and alkaloids, the quinones represent an important class of substances endowed with a vast array of biological activities [4,5]. These compounds are found in plants, microorganisms and marine organisms [4,5]. Despite the large structural variation among the natural quinones, those bearing an amino group *ortho* to the carbonyl group are less common.



**Figure 1.1.** Natural aminoquinones.

One of the earliest natural aminoquinones identified was the streptonigrin (1.1) (Figure 1.1), a highly functionalized antibiotic isolated from *Streptomyces*

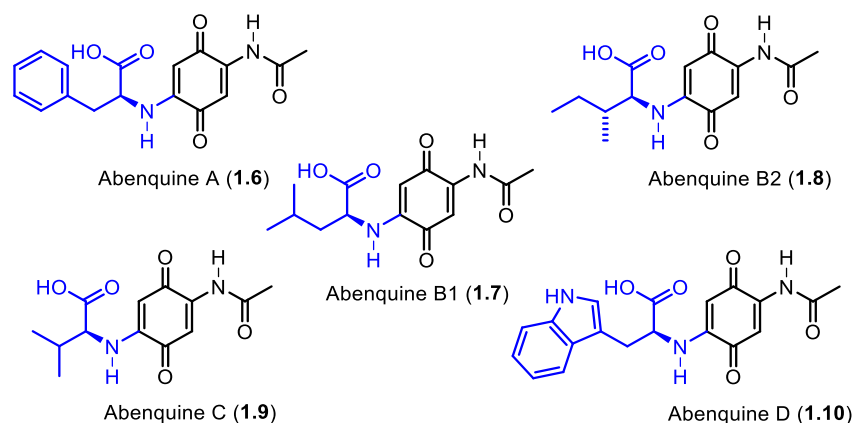
*flocculus* in 1959 [6]. In the 1970s, this compound entered phase II clinical trials as an anticancer agent and has attracted considerable attention of many research groups [7–11].

In the early 1980s, lavendamycin (**1.2**), structurally related to streptonigrin, was isolated from *Streptomyces lavendulae* and it was shown to exert cytotoxic and antimicrobial activities [12,13]. Lavendamycin was also the object of synthetic investigations, including the preparation of analogues for biological studies [8,14].

In 1994, two new terpenoid aminoquinones, nakijiquinones A (**1.3**) and B (**1.4**), were isolated from a marine sponge (family Spongidae). Besides representing the first sesquiterpenoid quinones with amino acid residues of natural origin, they also exhibited cytotoxic activity against some cancer cell lines [15]. This discovery was followed by the isolation [16–18] and synthesis [19,20] of several new nakijiquinones and analogues bearing amino acid residues. Furthermore, one aminoquinone structurally related to nakijiquinones was then isolated from the marine sponge *Dactylospongia elegans* and named smenospongine [21]. This compound, and other natural analogues isolated from marine sources, presented antimicrobial and cytotoxic activities [22–25]. Moreover, other natural aminoquinones endowed with biological activities include metachromins [26,27], geldanamycin [28], mytomicin [29,30], and dysifragilones [31].

Many aminoquinones are also found in *Streptomyces*, these bacteria grow in a different environment, and have a filamentous form similar to fungi. *Streptomyces* are the most important source to produce bioactive secondary metabolites such as antifungals, antivirals, antitumoral, anti-hypertensives, and mainly antibiotics as well as immunosuppressive [32,33]. In other words, it is known that *Streptomyces* produces more than 5000 known bioactive compounds [34].

Recently, a new group of benzoquinones bearing natural amino acid residues [35] called abenquines A-D (**1.6-1.10**) (Figure 1.2) were isolated from a strain of *Streptomyces* sp. collected from the Atacama desert in Chile.



**Figure 1.2.** The structure of Abenquines A-D.

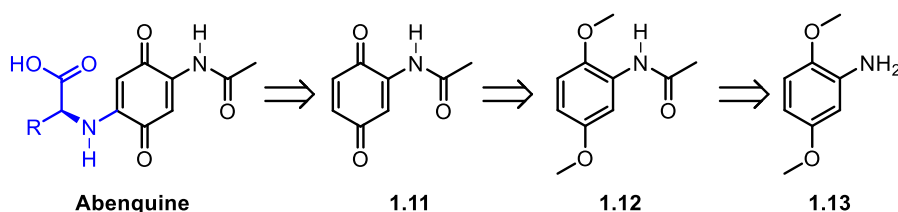
These abenquines showed cytotoxic activity against bacteria and dermatophytic fungi and were an inhibitor of phosphodiesterase type 4b [35]. Meanwhile, the abenquines are a linkage of *N*-acetyl-aminobenzoquinones with amino acids groups, this new group of secondary metabolites exhibit a rare connection with benzoquinones. In view of our interest in bioactive natural products and considering that abenquines are available in short supply, this chapter will report our achievements that culminated in the first total synthesis of such compounds.



## 2. RESULTS AND DISCUSSION

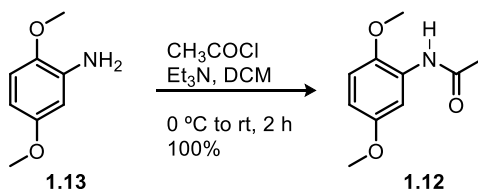
### 2.1. Synthesis

Initially, we envisaged that all abenquines could be obtained from quinone **1.11** (2-acetamido-1,4-benzoquinone), which in turn could easily be prepared from the commercially available *N*-2,5-dimethoxyaniline **1.13** (Figure 1.3).



**Figure 1.3.** Retrosynthetic analysis.

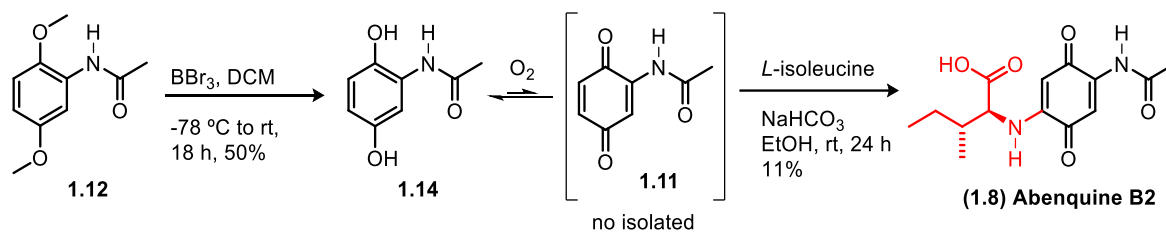
Initially, the precursor *N*-(2,5-dimethoxyphenyl) acetamide (**1.12**) was prepared from the commercially available 2,5-dimethoxyaniline (**1.13**). Thus, compound **1.13** reacts with acetyl chloride in the presence of triethylamine to produce the desired acetamide (**1.12**) in 100% yield (Figure 1.4). Then, from this intermediate, different kinds of routes for the synthesis of abenquines were proposed.



**Figure 1.4.** First step: acetylation of 2,5-dimethoxyaniline (**1.13**).

One of the proposals, route 1 (Figure 1.5), required demethylation of compound **1.12** through treatment with  $\text{BBr}_3$ , to obtain the desired hydroquinone **1.14** in 50% yield. No attempt was made to optimize this reaction step since the focus is the direct conversion of **1.14** into abenquine B2 using the methodology proposed by Zhong-Lu *et al.*, [36]. Hence, the reaction of **1.14** with isoleucine in ethanol for 24 h, rendered the required product **1.8** in only 11% yield. This low yield was not surprising since we have recently shown that a direct amination

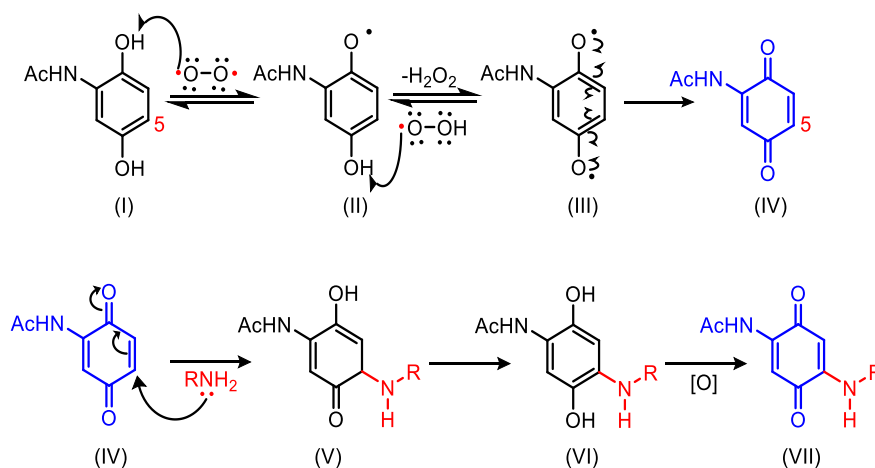
followed by spontaneous oxidation of hydroquinone is a low efficiency process [37].



**Figure 1.5.** Route 1 to obtain abenquine B2 (1.8).

This result may suggest that unfavorable yield is partially attributed to the low formation of benzoquinone 1.11. Despite our efforts, low yields were obtained from the reaction between the starting hydroquinone which produced the aminoquinone compounds [37].

Figure 1.6 shows the proposed mechanism that explains the oxidation of hydroquinone into the benzoquinone core in the presence of molecular oxygen and the subsequent aza-Michael addition.

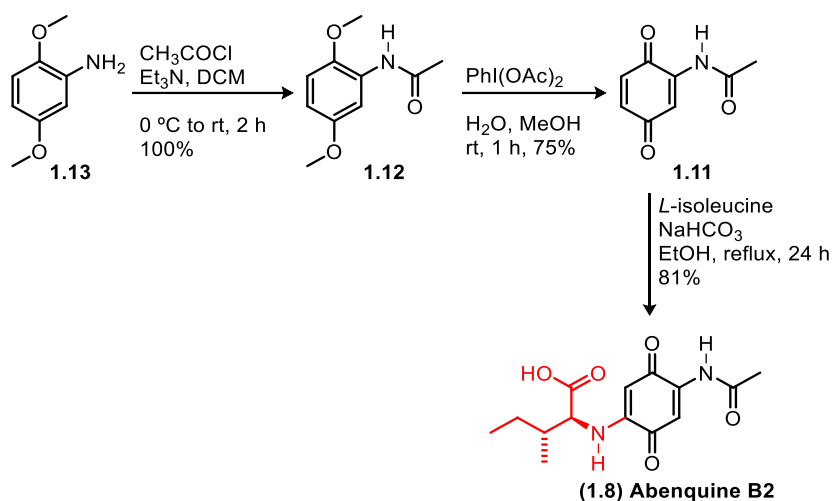


**Figure 1.6.** Proposed mechanism for oxidation of hydroquinone to benzoquinone.

The molecular oxygen takes a hydrogen from the hydroxyl in intermediate (I), to form the radical intermediate (II). Simultaneously, the formation of hydrogen peroxide is favored by the capture of the hydrogen in the intermediate (II) and, consequently, the formation of the di-radical (III). Intermediate (III) is converted into the benzoquinone core (IV). Finally, benzoquinone (IV) in the presence of the

amino group undergoes an addition reaction to produce the intermediate (V) in a keto-enol equilibrium with (VI). Consequently, (VI) undergoes oxidation leading to the final di-substituted benzoquinone (VII).

Since the obtained results from route 1 were not favored considerably, another method for obtaining abenquines (route 2) was designed. Such method was performed through the oxidation of the compound **1.12** as shown in Figure 1.7. From the benzoquinone **1.11**, which was proposed in the retrosynthetic analysis, the aza-Michael addition could be favorable, thus leading to the expected adduct, abenquine.

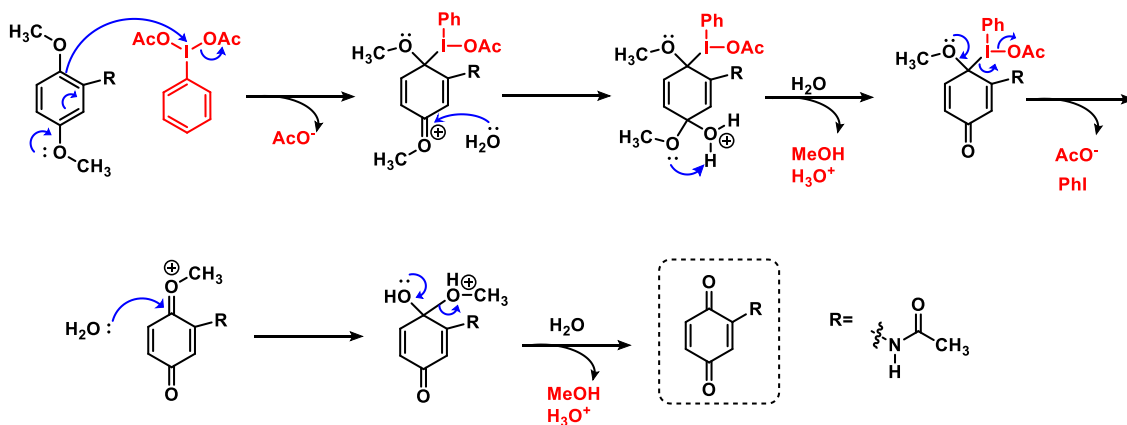


**Figure 1.7.** Route 2 to obtain abenquine B2 (**1.8**).

As reported by Whiteley [38], the oxidation of **1.12** with a large excess of cerium ammonium nitrate (CAN) in acetonitrile and water can afford the target product **1.11**. However, when attempted the reaction using only two CAN equivalents was attempted, the reaction produced a complex mixture of polar compounds. This result is in agreement with previous data, showing that 1,4-dimethoxybenzene with one substituent, gives rise to a dimerization reaction [39–42]. An alternative treatment of **1.12** with Dess-Martin periodinane (DMP), resulted in the required quinone **1.11** in a better yield (50%). To improve the yield further, a hypervalent iodine reagent, namely phenyliodine diacetate (PIDA) [43], was used affording the quinone **1.11** in a 75% yield. Despite repeating this reaction several times, the yield could not be increased, and other byproducts were always formed.

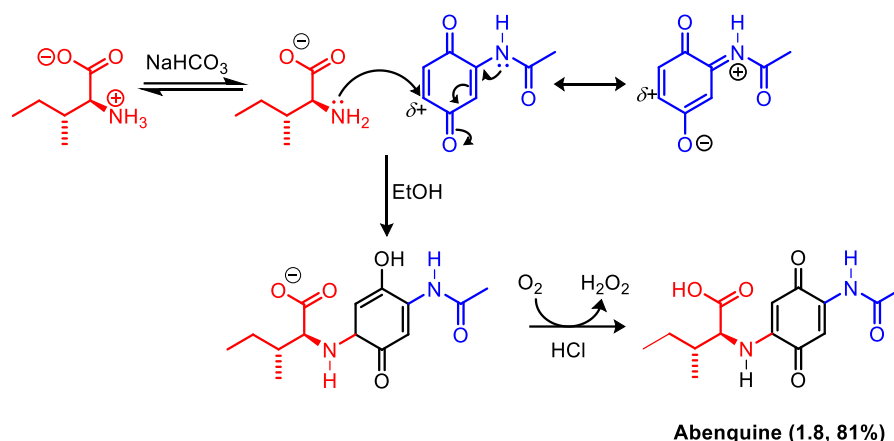
Compound **1.11** was subsequently reacted with isoleucine in the presence of sodium bicarbonate in ethanol. After 2 hours at reflux, the required abenquine B2 (**1.8**) was isolated in 81% yield. Conversely, starting from the commercially available aniline **1.13**, abenquine B2 was obtained in just three steps and 61% global yield (Figure 1.7).

In Figure 1.8, it is shown the proposal of the oxidation mechanism using  $\text{PhI}(\text{OAc})_2$ . The electrophilic aromatic substitution in the first step is favored by resonance afforded by the methoxyl group in the *para* position, as well as the acetamide group in the *ortho* position. Hence, this arrangement favors the dissociation of an acetoxy group of the PIDA reagent and in turn, generates the good leaving group,  $\text{PhI}$ . After stabilization through resonance and the presence of water, the desired quinone is generated.



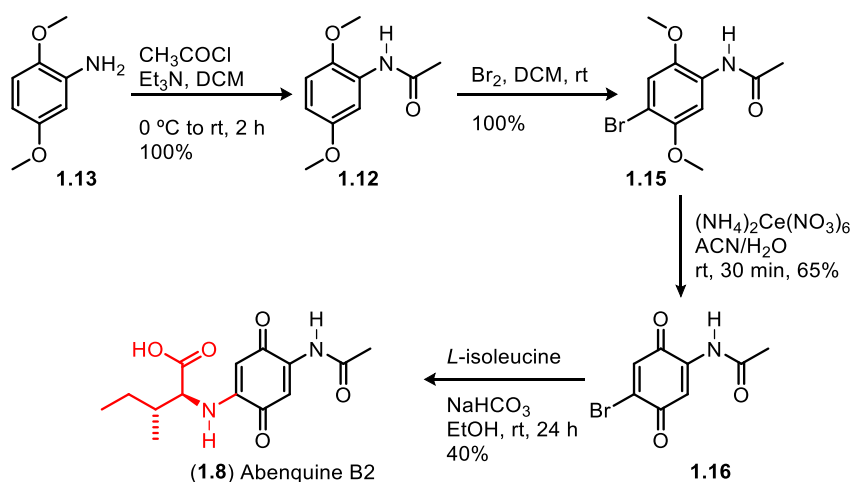
**Figure 1.8.** The mechanism proposed for oxidation with PIDA.

Finally, once the expected compound **1.11** was obtained, the last step occurred through the addition of an amino acid (*L*-isoleucine) to the strong acceptor in an aza-Michael reaction, as shown in Figure 1.9. Treatment of the amino acid with sodium bicarbonate leads to its non-ionic form, allowing the nitrogen to behave as the nucleophile. The nucleophilic attack therefore occurs at the electrophilic position (C-5) of the 2-acetamido-1,4-benzoquinone (**1.11**). Additionally, the resonance contribution of the nitrogen of the acetamido group contributes to increasing the electrophilic effect in C-5. Lastly, by spontaneous oxidation, the adduct is transformed into the desired abenquine **1.8**.



**Figure 1.9.** Aza-Michael addition of amino acid to the 2-acetamido-1,4-benzoquinone.

A further attempt (route 3) to improve the overall yield of this synthesis involved the initial bromination of amide **1.12** to afford **1.15** in quantitative yield (Figure 1.10). The rationale for this transformation is based on work by Hayashi *et al* [42], where the oxidation of disubstituted 1,4-dimethoxybenzene derivative proceeds in better yield and produces less dimers than compound **1.12**. Proceeding, oxidation of compound **1.15** was realized employing the same reagents used for the production of **1.11**. As a result, it was observed that the use of CAN and PIDA afforded the bromoquinone **1.16** in 70% yield, while treatment with DMP did not produce the required compound.

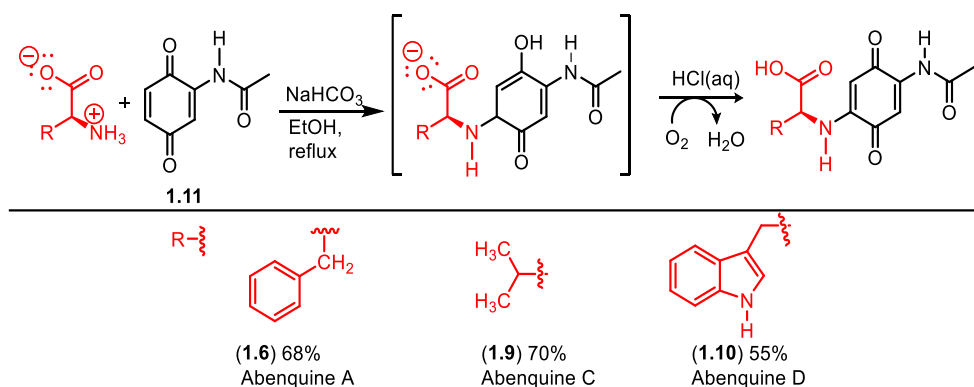


**Figure 1.10.** Route 3 to obtain abenquine B2 (**1.8**).

Based on the efficient substitution of a bromine for an amino group in case of 2,3-dibromofuran-2(5*H*)-one [44,45], it was expected that the same reaction

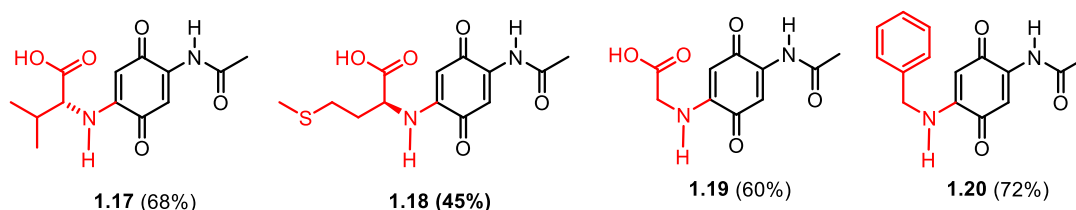
would take place with compound **1.16**. Consequently, a reaction was attempted between compound **1.16** and isoleucine under the conditions reported above. However, abenquine **B2** was formed in a disappointing 40% yield.

Finally, from the three different routes, the route 2 was chosen as a reference for obtaining abenquines. This procedure, involving an aza-Michael addition with the benzoquinone (**1.11**) and different amino acid groups as the last reaction step (Figure 1.11), afforded abenquines A (**1.6**), C (**1.9**), and D (**1.10**) in 68%, 70%, and 55% yield, respectively. The total yields for the synthesis of natural compounds were 51% (A, **1.6**), 61 % (B2, **1.8**), 53% (C, **1.9**), and 41% (D, **1.10**).



**Figure 1.11.** Synthesis of abenquines A, C and D.

We have produced for the first time four natural abenquines, the newly developed methodology was applied for the synthesis of analogues, studied later regard their biological activities. The enantiomer of abenquine C (**1.17**) was prepared in 68% yield from intermediate **1.11**. Other abenquine analogues (**1.18** and **1.19**) were obtained in 45% and 60% yield. A simple derivative of benzylamine (**1.20**) was also obtained in 72% yield (Figure 1.12).



**Figure 1.12.** Analogues of abenquines.

## 2.2. Characterization

The structure of abenquines and analogues was determined by extensive spectroscopic analysis and the molecular formula was established by HRMS (ESI). All compounds have shown similar characteristics throughout the different spectroscopic analysis.

According to infrared spectra, typical absorption of amino acid groups in their zwitterionic form is evidenced by a broad band at the region of 3554-2794  $\text{cm}^{-1}$  ( $\text{NH}_3^+$ ). The stretch band related to N-H of the amide group is between 3279-3302  $\text{cm}^{-1}$ . Another important absorption is related to the  $-\text{COO}^-$  group in 1701-1722  $\text{cm}^{-1}$ . The absorption of the carbonyl group of the quinone at the region 1648-1656  $\text{cm}^{-1}$  was observed [46,47].

In the  $^1\text{H}$  NMR analysis it was possible to make a comparison between the starting material benzoquinone **1.11** and abenquines A-D (Figure 1.13). For instance, the signal corresponding to hydrogen H-2'' of the methyl group in abenquines was observed in the region of  $\delta = 2.06\text{-}2.22$ , being slightly more shielded than the benzoquinone **1.11** at  $\delta = 2.23$ , and the signal related to hydrogen H-2' was observed at  $\delta = 5.24\text{-}5.46$ , even more shielded than the benzoquinone **1.11** at  $\delta = 6.82$ . As well as the signal corresponded to hydrogen H-5' at  $\delta = 7.16\text{-}7.32$ , the analysis reveals it to be slightly more shielded than the benzoquinone **1.11** at  $\delta = 7.50$ .

Additionally, all these data were compared with the natural product initially isolated by Schulz and collaborators [35], and it is present in Table 1.1 (all the spectra of compounds are present in Appendix 1).

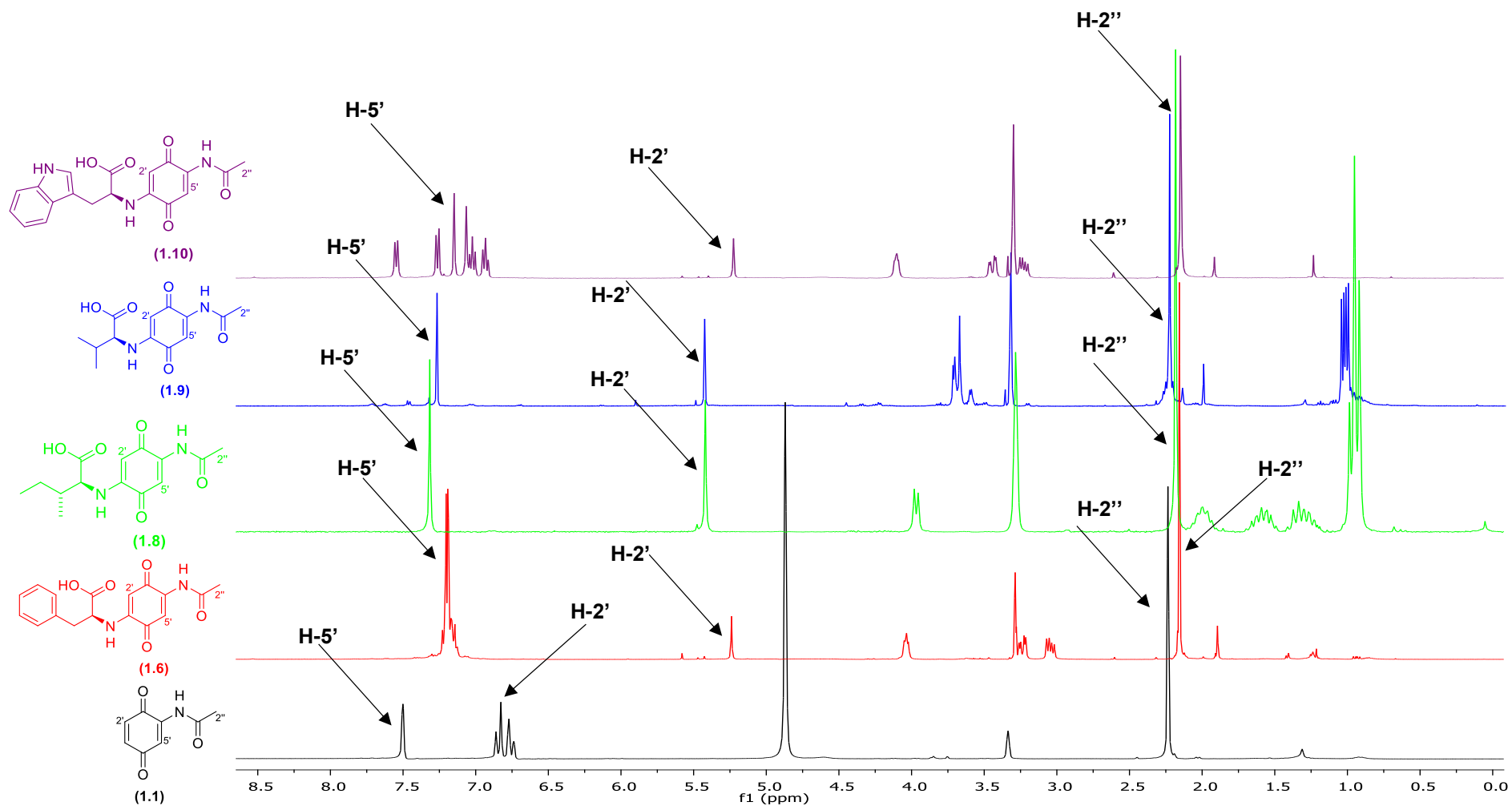
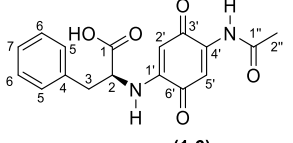
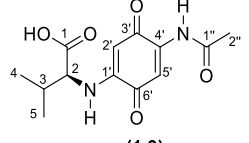
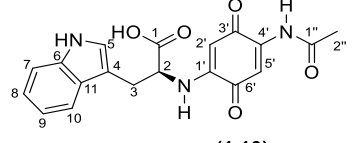


Figure 1.13. <sup>1</sup>H NMR spectra (400 MHz, CD<sub>3</sub>OD) of compounds 1.6, 1.8-1.10 and 1.11.



**Table 1.1.** Comparative  $^1\text{H}$  NMR data of natural and synthetic abenquines in  $\text{CD}_3\text{OD}$ , 400 MHz

N <sup>o</sup> H	 (1.6)		 (1.9)		 (1.10)	
	<b>Abenquine A</b> <i>*Schulz et al.</i>	<b>Abenquine A</b> <i>This work</i>	<b>Abenquine C</b> <i>*Schulz et al.</i>	<b>Abenquine C</b> <i>This work</i>	<b>Abenquine D</b> <i>*Schulz et al.</i>	<b>Abenquine D</b> <i>This work</i>
	$\delta_{\text{H}}$ (J in Hz)	$\delta_{\text{H}}$ (J in Hz)	$\delta_{\text{H}}$ (J in Hz)	$\delta_{\text{H}}$ (J in Hz)	$\delta_{\text{H}}$ (J in Hz)	$\delta_{\text{H}}$ (J in Hz)
<b>2'</b>	5.45, s	5.25, s	5.49, s	5.43, s	5.48	5.24, s
<b>5'</b>	7.27, s	7.17, s	7.31	7.28, s	7.27, s	7.16, s
<b>2''</b>	2.24, s	2.18, s	2.27, s	2.23, br s	2.25, s	2.17, s
<b>2</b>	4.52, dd (7.0, 5.2)	4.05, dd, (6.8, 4.8)	4.05, d (5.4)	3.71, d (4.7)	4.55, dd (6.4, 5.3)	4.12, dd (6.9, 4.3)
<b>3</b>	(a) 3.36, dd (14.0, 5.2) (b) 3.25, dd (14.0, 7.0)	(a) 3.26, dd (13.7, 4.8) (b) 3.07, dd (13.7, 6.8)	(a) 2.35, d (5.4, 7.0)	2.23, br s	(a) 3.53, ddd (14.8, 5.3, 0.8) (b) 3.45, ddd (14.8, 6.4, 0.5)	(a) 3.24, dd (14.6, 6.9) (b) 3.46, dd (14.6, 4.3)
<b>4</b>			1.08, d (7.0)	1.00, d (6.8)		
<b>5</b>	7.21-7.26, m	7.14-7.20, m	1.02, d (7.0)	1.03, d (6.8)	7.24, br s	7.08, s
<b>6</b>	7.21-7.26, m	7.14-7.20, m				
<b>7</b>	7.21-7.26, m	7.14-7.20, m			7.35, dt (8.0, 0.9)	7.28, d (7.9)
<b>8</b>					7.07, ddd (8.0, 7.0, 1.3)	7.04, dd (7.9, 7.3)
<b>9</b>					6.98, ddd (8.0, 7.0, 0.9)	6.95, dd (7.9, 7.3)
<b>10</b>					7.57, ddd (8.0, 1.3, 0.9)	7.56, d (7.9)

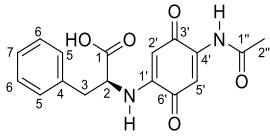
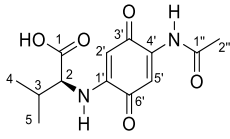
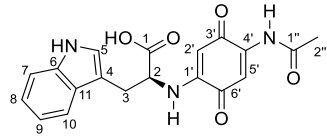
\*The NMR data of *Schulz et al.*, [35] were performed at 500 MHz, in acetone- $d_6$ .

In the  $^{13}\text{C}$  NMR spectra, it was confirmed all the signal corresponded to the abenquines. In this regard, the common signal corresponded to the carbon C-2'' at  $\delta = 59.7-64.4$  confirms the formation of the product.

Amongst the most relevant signals are the vinyl carbon C-3 and C-6 at  $\delta = 110.0-110.9$  and  $\delta = 110.0-110.9$ , in addition to the signal related to the carbonyl of the amide at  $\delta = 94.7-102.7$ . Finally, it is worth mentioning the signal pertaining to the carbonyl of the acid group at  $\delta = 173.1-174.4$ . The  $^{13}\text{C}$  NMR data was compared and confirmed as shown in Table 1.2.

In accordance with the spectroscopy data, all synthesized compounds match with what is expected. In total, four abenquines and four new analogues of abenquines were obtained and fully characterized (all the spectra data of compounds are present in Appendix 1).

**Table 1.2.** Comparative  $^{13}\text{C}$  NMR data of natural and synthetic abenquines in  $\text{CD}_3\text{OD}$ , 100 MHz.

N° C	 (1.6)		 (1.9)		 (1.10)	
	<i>Abenquine A</i> *Schulz et al.	<i>AbenquineA</i> This work	<i>Abenquine C</i> *Schulz et al.	<i>Abenquine C</i> This work	<i>Abenquine D</i> *Schulz et al.	<i>AbenquineD</i> This work
$\delta_{\text{C}}$						
1'	147.5	148.5	148.0	149.1	147.6	148.9
2'	95.9	95.0	95.9	95.0	95.8	94.7
3'	179.6	180.1	179.8	180.2	179.7	179.9
4'	142.4	143.2	142.5	143.4	142.4	143.3
5'	109.7	110.7	109.7	110.7	109.7	110.6
6'	183.9	184.7	184.0	184.7	183.9	184.7
1''	170.9	172.8	171.0	172.7	171.0	172.6
2''	24.7	24.6	24.8	24.62	24.7	24.5
1	171.6	174.4	171.7	172.7	171.9	177.1
2	56.3	59.8	60.6	64.1	55.9	59.7
3	37.2	38.7	31.5	32.5	27.4	29.0
4	137.2	138.5	18.9	19.8	109.8	111.3
5	130.2	130.4	18.6	19.0	124.7	124.5
6	129.3	129.3			137.4	137.9
7	127.8	127.6			112.2	112.1
8					122.3	122.3
9					119.8	119.7
10					119.1	119.3
11					128.5	129.0

\*The NMR data of Schulz et al.,[35] were performed at 125 MHz.

### 3. CONCLUSIONS

This chapter reported the first total synthesis of four abenquines **A (1.6)**, **B2 (1.8)**, **C (1.9)**, and **D (1.10)** in three steps. The synthesis was performed throughout the study of three synthetic routes. Route 1 demonstrated that the simple Michael addition of the amino acid to hydroquinone **1.14** led to product **1.8** in low yield (11%). Meanwhile, the yield of compound **1.8** was greatly improved in the route 2 to about 81% starting from compound **1.11**. Oxidation, the key step of this route, required the use of different oxidative reagents for the obtention of benzoquinone **1.11**, with phenyl iodobenzene diacetate being the best oxidant. The last route (3) was then explored using the intermediate **1.16** (2-acetamido-5-bromo-1,4-benzoquinone), but afforded a moderate yield of compound **1.8** (40%).

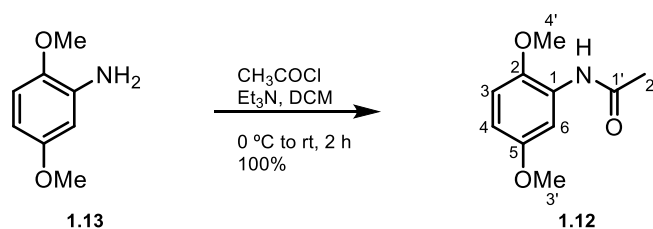
Once route 2 was selected for the synthesis of the natural aminoquinones, abenquines **A (1.6)**, **B2 (1.8)**, **C (1.9)**, and **D (1.10)** were obtained in excellent total yields, 51% (**1.6**), 61 % (**1.8**), 53% (**1.9**), and 41% (**1.10**). In fact, the improved synthetic route allowed the synthesis of four analogues **1.17-1.20** in good yields (45-72%). We expected that this synthetic contribution will be of interest for future studies about the biological potential of these types of compounds.

## 4. EXPERIMENTAL PART

### 4.1. General Information

All solvents were purchased from Sigma Aldrich. All reactions were monitored by TLC using Merck silica gel plates. Purifications were performed with column chromatography using silica gel (Merck 60, 230–400 mesh). Infrared spectra were recorded on a Perkin-Elmer Paragon 1000 FTIR spectrophotometer using potassium bromide disks (1% w/w).  $^1\text{H}$  NMR spectra were recorded at 400 MHz and  $^{13}\text{C}$  NMR spectra at 100 MHz with a Bruker Avance spectrometer. Chemical shifts ( $\delta$ ) are reported from tetramethylsilane with the solvent resonance as the internal standard. Data are reported as follows: chemical shift ( $\delta$ ), multiplicity (s= singlet, d= doublet, t= triplet, q= quartet, br= broad, m= multiplet), integration, coupling constants ( $J$  = Hz) and assignment. High-resolution mass spectra were recorded on a Bruker Micro ToF (resolution= 10,000 FWHM) under electrospray ionization (ESI) and are given to four decimal figures. Melting points were determined on an MQAPF-301 apparatus.

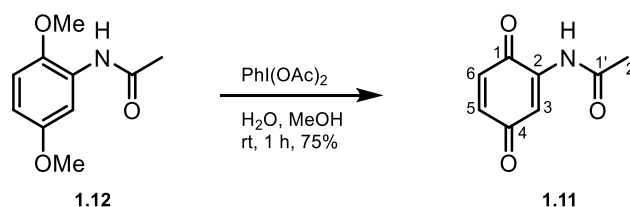
### 4.2. Synthesis of *N*-(2,5-Dimethoxyphenyl)acetamide 1.12



To a round-bottomed flask (100 mL) were added 2,5-dimethoxyaniline **1.13** (2.0 g, 13.1 mmol) and triethylamine (2.1 mL, 15.2 mmol) dissolved in dichloromethane (50 mL). Then, to the stirred solution was added acetyl chloride (1.1 mL, 15.2 mmol) and was left stirring at  $0\text{ }^\circ\text{C}$  for two hours under  $\text{N}_2$  atmosphere. The resulting solution was warmed to room temperature over 30 min. When TLC analysis revealed the consumption of the starting material, the mixture was washed with water (3 x 50 mL), saturated aqueous sodium hydrogen carbonate solution (100 mL) and brine (100 mL), and then dried over  $\text{MgSO}_4$ . The solution was filtered and concentrated under reduced pressure to give a brown solid. The residue was purified by column chromatography on silica gel, eluting

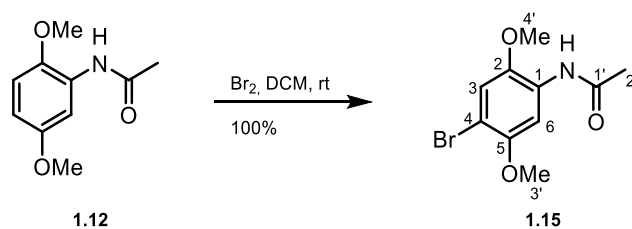
with ethyl acetate:hexane 1:3 v/v, to give the title compound as a white solid in 100% yield (2.54 g, 13.0 mmol). Mp: 90-92 °C, (lit. [48], 91-92 °C). IR: ( $\nu_{\max}/\text{cm}^{-1}$ ) 3250, 2992, 1662, 1592.  $^1\text{H}$  NMR ( $\text{CDCl}_3$ , 400 MHz)  $\delta$ : 2.14 (s, 3H, H-2'), 3.72 and 3.77 (s, 3H, H-3' and H-4'), 6.52 (dd,  $J = 8.9$ ; 3.0 Hz, 1H, H-4), 6.74 (d,  $J = 8.9$  Hz, 1H, H-3), 7.82 (s, 1H, N-H), 8.05 (d,  $J = 3.0$  Hz, 1H, H-6).  $^{13}\text{C}$  NMR ( $\text{CDCl}_3$ , 100 MHz)  $\delta$ : 24.8 (C-2'), 55.6 and 56.0 (C-3' and C-4'), 106.1 (C-6), 108.0 (C-4), 110.5 (C-3), 128.3 (C-1), 141.9 (C-2), 153.7 (C-5), 168.2 (C-1'). The spectroscopy data matched with those reported by Nawrat *et al.*, 2011 [43].

#### 4.3. Synthesis of 2-Acetamido-1,4-benzoquinone 1.11



To a round-bottomed flask (50 mL) was added 2,5- dimethoxyacetanilide **1.12** (1.0 g, 5.1 mmol) in water (25 mL) and MeOH (0.64 mL). The mixture was stirred until the suspension was homogenized before a slow addition of phenyliodine diacetate (2.5 g, 7.7 mmol). The resulting suspension was stirred for 1.5 h, and the mixture solution was diluted with water (50 mL) and extracted with dichloromethane (3 x 50 mL). The combined extracts were washed with water (50 mL), saturated aqueous sodium hydrogen carbonate solution (50 mL), dried ( $\text{Na}_2\text{SO}_4$ ), filtered and the solvent was concentrated under reduced pressure. The residue was purified by column chromatography on silica gel, eluting with ethyl acetate:hexane 1:2 v/v, to give the title compound as a golden-yellow solid in 75% yield (0.64 g, 3.87 mmol). Mp: 146-148 °C, (lit. [48], 148-149 °C). IR: ( $\nu_{\max}/\text{cm}^{-1}$ ) 3224, 3088, 1694, 1510.  $^1\text{H}$  NMR ( $\text{CD}_3\text{OD}$ , 300 MHz)  $\delta$ : 2.23 (s, 3H, H-2'), 6.75 (d,  $J = 10.2$  Hz, 1H, H-5), 6.84 (d,  $J = 10.2$  Hz, 1H, H-6), 7.50 (br s, 1H, H-3).  $^{13}\text{C}$  NMR ( $\text{CD}_3\text{OD}$ , 75 MHz)  $\delta$ : 24.4 (C-2'), 115.6 (C-3), 135.1 (C-6), 138.4 (C-5), 140.8 (C-2), 172.9 (C-1'), 183.6 (C-1), 190.1 (C-4). The spectroscopy data matched with those reported by Nawrat *et al.*, 2011 [43].

#### 4.4. Synthesis of *N*-(4-Bromo-2,5-dimethoxyphenyl)acetamide **1.15**



To a round-bottomed flask (50 mL) was added 2,5-dimethoxyacetanilide **1.12** (1.0 g, 5.1 mmol) in dichloromethane (10 mL), followed by dropwise addition of bromine (0.35 mL, 6.8 mmol) at room temperature. The solution was stirred overnight under N<sub>2</sub> atmosphere and then washed with saturated aqueous sodium thiosulfate solution (20 mL), saturated aqueous sodium bicarbonate solution (20 mL), water (20 mL) and brine (20 mL). The organic phase was dried over Na<sub>2</sub>SO<sub>4</sub>, filtered and concentrated under reduced pressure to afford the compound as a grey solid in 100% yield (1.40 g, 5.1 mmol), which did not require further purification. Mp: 118-120 °C, (lit.[49], 123 °C). IR: ( $\nu_{\text{max}}/\text{cm}^{-1}$ ) 3425, 3008, 1689, 1518. <sup>1</sup>H NMR (CDCl<sub>3</sub>, 400 MHz)  $\delta$ : 2.16 (s, 3H, H-2'), 3.82 and 3.86 (s, 3H, H-3' and H-4'), 7.56 (s, 1H, H-6), 8.25 (s, 1H, H-3), 9.57 (s, 1H, N-H). <sup>13</sup>C NMR (CDCl<sub>3</sub>, 100 MHz)  $\delta$ : 24.7 (C-2'); 56.9 and 57.0 (C-3' and C-4'), 105.7 (C-3), 108.2 (C-6), 132.5 (C-5), 134.7 (C-2), 141.8 (C-1), 148.5 (C-4), 170.3 (C-1'). The spectroscopy data matched with those reported by Nawrat *et. al.*, 2011 [43].

#### 4.5. Synthesis of 2-Acetamido-5-bromo-1,4-benzoquinone **1.16**

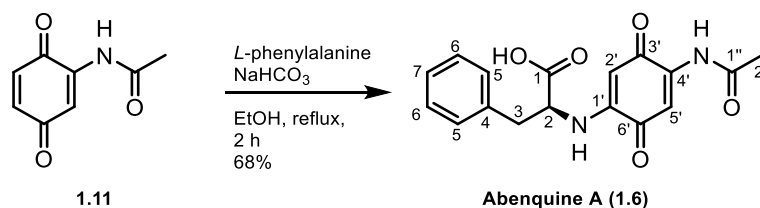


To a one neck round-bottomed flask (50 mL) was added *N*-(4-Bromo-2,5-dimethoxyphenyl)acetamide **1.13** (0.5 g, 1.8 mmol) in acetonitrile (5 mL). The mixture was stirred until the suspension was homogenized, then *ceric ammonium nitrate* (2.4 g, 4.5 mmol) in water (5 mL) was added slowly. The resulting suspension was stirred for 0.5 h before it was quenched by addition of water (20 mL). The product was extracted with dichloromethane (3 x 20 mL). The combined

extracts were washed with water (50 mL), dried (Na<sub>2</sub>SO<sub>4</sub>), filtered and the solvent removed under reduced pressure to afford the compound as a golden-yellow solid in 70% yield (0.31 g, 1.27 mmol), which did not require further purification. Mp: 185-186 °C, (lit. [43], 184-185 °C). IR: ( $\nu_{\text{max}}/\text{cm}^{-1}$ ) 3374, 3012, 1668, 1503. <sup>1</sup>H NMR (CDCl<sub>3</sub>, 400 MHz)  $\delta$ : 2.24 (s, 3H, H-2'), 7.28 (s, 1H, H-3), 7.75 (s, 1H, H-6), 8.08 (s, 1H, N-H). The spectroscopy data matched with those reported by Nawrat *et. al.*, 2011 [43].

#### 4.6. Synthesis of Abenquines A

(2S)-2-((4-acetamido-3,6-dioxocyclohexa-1,4-dien-1-yl)amino)-3-phenylpropanoic acid (**1.6**):



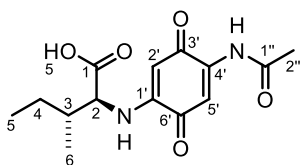
To a one neck round-bottomed flask (25 mL) was added the L-phenylalanine (0.07 g, 0.42 mmol) and sodium bicarbonate (0.071 g, 0.84 mmol), dissolved in EtOH (5 mL). To this mixture 2-acetamido-1,4-benzoquinone (**1.11**) (0.07 g, 0.42 mmol) was added and the reaction mixture was stirred at reflux under an oxygen atmosphere. Initially, there was a change of solution colour from yellow to dark red. The reaction was monitored by TLC and stopped after 2 h. The reaction mixture was filtered to remove the sodium bicarbonate salt and washed with ethanol. Consequently, the resulting residual mixture was acidified to pH 4-5 with hydrochloric acid 1 M, and dissolved with 5.0 mL of distilled water. The mixture was extracted with EtOAc (3 x 25 mL). The organic extracts were combined, and the resulting organic phase was dried over Na<sub>2</sub>SO<sub>4</sub>, filtered and the solvent removed under reduced pressure to afford the crude product. The residue was purified by silica gel column chromatography eluting with Hex/EtOAc 1:1 v/v, and then with acetone/methanol 1:1 v/v to afford compound **1.6** as red crystals in 68% yield (0.095 g, 0.29 mmol). Mp: > 185 °C (Decomposition). IR: ( $\nu_{\text{max}}/\text{cm}^{-1}$ ) 3456, 2794, 3366, 3302, 2924, 1712, 1656, 1596. <sup>1</sup>H NMR (CD<sub>3</sub>OD, 400 MHz)  $\delta$ : 2.18 (s, 3H, H2''), 3.07 (dd, *J* = 13.7; 6.8 Hz, 1H, H3b), 3.26 (dd, *J*



= 13.7; 4.8 Hz, 1H, H3a,), 4.05 (dd,  $J = 6.8$ ; 4.8 Hz, 1H, H-2), 5.25 (s, 1H, H-2'), 7.14-7.20 (m, 6H, H-5-7 and H-5').  $^{13}\text{C}$  NMR ( $\text{CD}_3\text{OD}$ , 100 MHz)  $\delta$ : 24.6 (C-2''), 38.7 (C-3), 59.8 (C-2), 95.0 (C-2'), 110.7 (C-5'), 127.6 (C-7), 129.3 (C-6), 130.4 (C-5), 138.5 (C-4), 143.2 (C-4'), 148.5 (C-1'), 172.8 (C-1''), 174.4 (C-1), 180.1 (C-3'), 184.7 (C-6'). HRMS (ESI)  $m/z$  calculated for  $\text{C}_{17}\text{H}_{16}\text{N}_2\text{O}_5$   $[\text{M}+\text{H}]^+$ : 329.1132, found 329.1136. The spectroscopy data matched with those reported by Schulz *et al.*, 2011 [35].

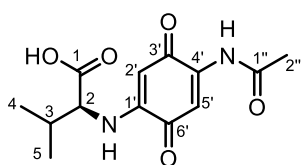
Compounds **1.8-1.10** and **1.17-1.19** were synthesized using a similar method to that of **1.6**.

*(2S-3S)-2-((4-acetamido-3,6-dioxocyclohexa-1,4-dien-1-yl)amino)-3-methylpentanoic acid (1.8):*



Quantities used for the synthesis: *L*-isoleucine (0.06 g, 0.48 mmol); compound **1.11** (0.079 g, 0.48 mmol). Red solid. Mp: > 195 °C (Decomposition). Yield: 81% (0.12 g, 0.39 mmol). IR: ( $\nu_{\text{max}}/\text{cm}^{-1}$ ) 3466, 2749, 3340, 3280, 2964, 1722, 1656, 1556.  $^1\text{H}$  NMR ( $\text{CD}_3\text{OD}$ , 400 MHz)  $\delta$ : 0.96-1.03 (m, 6H, H5 and H-6), 1.26-1.41 (m, 1H, H-4a), 1.53-1.70 (m, 1H, H-4b), 1.97-2.11 (m, 1H, H-3), 2.22 (s, 3H, H-2''), 3.99 (d,  $J = 10.5$  Hz, 1H, H-2), 5.43 (s, 1H, H-2'), 7.32 (s, 1H, H-5').  $^{13}\text{C}$  NMR ( $\text{CD}_3\text{OD}$ , 100 MHz)  $\delta$ : 11.7 (C-5), 15.6 (C-6), 24.5 (C-2''), 26.6 (C-4), 38.2 (C-3), 64.4 (C-2), 95.9 (C-2'), 111.0 (C-5'), 143.1 (C-4'), 148.7 (C-1'), 172.7 (C-1''), 173.1 (C-1) 180.8 (C-3'), 184.6 (C-6'). HRMS (ESI)  $m/z$  calculated for  $\text{C}_{14}\text{H}_{18}\text{N}_2\text{O}_5$   $[\text{M}+\text{H}]^+$ : 295.1288, found 295.1290.

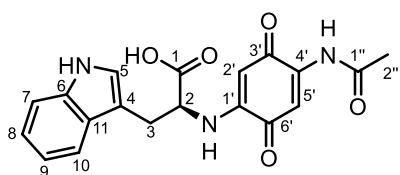
*(2S)-2-((4-acetamido-3,6-dioxocyclohexa-1,4-dien-1-yl)amino)-3-methylbutanoic acid (1.9):*



Quantities used for the synthesis: *L*-valine (0.04 g, 0.3 mmol); compound **1.11** (0.05 g, 0.3 mmol). Red solid. Mp: > 209 °C (Decomposition). Yield: 70% (0.06 g, 0.21 mmol). IR: ( $\nu_{\text{max}}/\text{cm}^{-1}$ ) 3554, 2875, 3442, 3338, 2963, 1718, 1654, 1594.  $^1\text{H}$  NMR ( $\text{CD}_3\text{OD}$ , 400 MHz)  $\delta$ : 1.00 (d,  $J = 6.8$  Hz, 3H, H-5), 1.03 (d,  $J = 6.8$  Hz, 3H, H-4), 2.23 (br s, 4H, H-3 and H-2''), 3.71 (d,  $J = 4.7$  Hz, 1H, H-2), 5.43 (s, 1H, H-2'), 7.28 (s, 1H, H-5').  $^{13}\text{C}$  NMR ( $\text{CD}_3\text{OD}$ , 100 MHz)  $\delta$ :

19.0 (C-5), 19.8 (C-4), 24.62 (C-2''), 32.5 (C-3), 64.1 (C-2), 95.0 (C-2'), 110.7 (C-5'), 143.4 (C-4'), 149.1 (C-1'), 172.7 (C-1''), 180.2 (C-3'), 184.7 (C-6'). HRMS (ESI)  $m/z$  calculated for  $C_{13}H_{16}N_2O_5$   $[M+H]^+$ : 281.1132, found 281.1128. The spectroscopy data matched with those reported by Schulz *et al.*, 2011 [35].

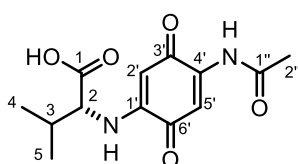
*(2S)-2-((4-acetamido-3,6-dioxocyclohexa-1,4-dien-1-yl)amino)-3-(1H-indol-3-yl)propanoic acid (1.10):*



Quantities used for the synthesis: *L*-tryptophane (0.07 g, 0.35 mmol); compound **1.11** (0.06 g, 0.35 mmol). Red solid. Mp: > 175 °C (Decomposition). Yield: 55% (0.073 g, 0.19 mmol). IR: ( $\nu_{max}/cm^{-1}$ )

3527, 2854, 3421, 3336, 2926, 1702, 1654, 1590.  $^1H$  NMR ( $CD_3OD$ , 400 MHz)  $\delta$ : 2.17 (s, 3H, H-2''), 3.23 (dd,  $J = 14.6$ ; 6.9 Hz, 1H, H-3a), 3.46 (dd,  $J = 14.6$ ; 4.3 Hz, 1H, H-3b), 4.12 (dd,  $J = 6.9$ ; 4.3 Hz, 1H, H-2), 5.24 (s, 1H, H-2'), 6.95 (dd,  $J = 7.9$ ; 7.3 Hz, 1H, H-9) 7.04 (dd,  $J = 7.9$ ; 7.3 Hz, 1H, H-8), 7.08 (s, 1H, H-5), 7.16 (s, 1H, H-5'), 7.28 (d,  $J = 7.9$  Hz, 1H, H-7), 7.56 (d,  $J = 7.9$  Hz, 1H, H-10).  $^{13}C$  NMR ( $CD_3OD$ , 100 MHz)  $\delta$ : 24.5 (C-2''), 29.0 (C-3), 59.7 (C-2), 94.7 (C-2'), 110.6 (C-5'), 111.3 (C-4), 112.1 (C-7), 119.3 (C-10), 119.7 (C-9), 122.3 (C-8), 124.5 (C-5), 129.0 (C-11), 137.9 (C-6), 143.3 (C-4'), 148.9 (C-1') 172.6 (C-1''), 177.1 (C-1), 179.9 (C-3'), 184.7 (C-6'). HRMS (ESI)  $m/z$  calculated for  $C_{19}H_{17}N_3O_5$   $[M+H]^+$ : 368.1241, found 368.1247. The spectroscopy data matched with those reported by Schulz *et al.*, 2011 [35].

*(2R)-2-((4-acetamido-3,6-dioxocyclohexa-1,4-dien-1-yl)amino)3-methylbutanoic acid (1.17):*

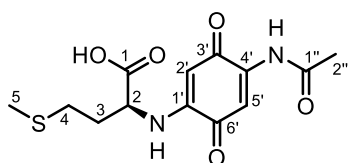


Quantities used for the synthesis: *D*-valine (0.05 g, 0.41 mmol); compound **1.11** (0.07 g, 0.41 mmol). Red solid. Mp: 220-222°C. Yield: 68% (0.078 g, 0.28 mmol). IR: ( $\nu_{max}/cm^{-1}$ )

$^1$  3441, 2853, 3325, 3285, 2926, 1702, 1648, 1508.  $^1H$  NMR ( $CD_3OD$ , 400 MHz)  $\delta$ : 1.66 (d,  $J = 6.9$  Hz, 3H, H-5), 1.75 (d,  $J = 6.9$  Hz, 3H, H-4), 2.91-2.96 (m, 1H, H-3), 3.00 (s, 3H, H-2''), 4.38 (dd,  $J = 7.4$ ; 3.9 Hz, 1H, H-2), 6.17 (s, 1H, H-2'), 8.00 (s, 1H, H-5'), 8.14 (d,  $J = 7.4$  Hz, 1H, N-H), 10.40 (s, 1H, N-H).  $^{13}C$  NMR ( $CD_3OD$ , 100 MHz)  $\delta$ : 28.2 (C-5), 28.5 (C-4), 34.0 (C-2''), 40.1 (C-3), 71.0 (C-2), 102.7 (C-2'), 118.1 (C-5'), 151.9 (C-4'), 156.3 (C-1'), 180.6

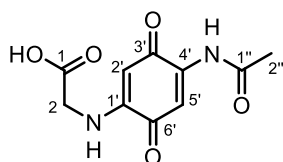
(C-1''), 187.2 (C-3'), 192.8 (C-6'). HRMS (ESI)  $m/z$  calculated for  $C_{13}H_{16}N_2O_5$  [M+H]<sup>+</sup>: 281.1132, found 281.1137.

(2S)-2-((4-acetamido-3,6-dioxocyclohexa-1,4-dien-1-yl)amino)-4-(methylthio)butanoic acid (**1.18**):



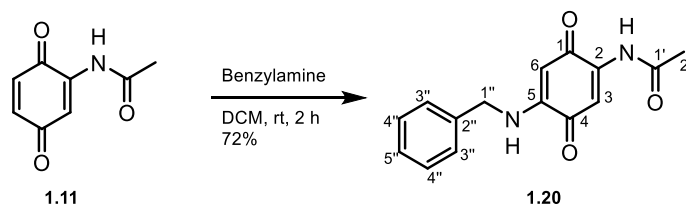
Quantities used for the synthesis: L-methionine (0.07 g, 0.49 mmol); compound **1.11** (0.08 g, 0.49 mmol). Red solid. Mp: 145-147 °C. Yield: 45% (0.07 g, 0.22 mmol). R: ( $\nu_{\max}/\text{cm}^{-1}$ )3510, 2742, 3336, 3289, 2921, 1718, 1654, 1594. <sup>1</sup>H NMR (CD<sub>3</sub>OD, 400 MHz)  $\delta$ : 2.06 (s, 3H, H-2''), 2.11-2.18 (m, 2H, H-3), 2.21 (s, 3H, H-5), 2.50-2.62 (m, 2H, H-4), 4.14 (s, 1H, H-2), 5.46 (s, 1H, H-2') 7.23 (s, 1H, H-5'). <sup>13</sup>C NMR (CD<sub>3</sub>OD, 100 MHz)  $\delta$ : 15.3 (C-5), 24.6 (C-2''), 31.0 (C-4), 32.0 (C-3), 95.6 (C-2'), 110.9 (C-5'), 143.0 (C-4'), 148.7 (C-1'), 172.7 (C-1''), 180.4 (C-3'), 184.6 (C-6'). HRMS (ESI)  $m/z$  calculated for  $C_{13}H_{16}N_2O_5S$  [M+H]<sup>+</sup>: 313.0853, found 313.0850.

(2S)-2-((4-acetamido-3,6-dioxocyclohexa-1,4-dien-1-yl)amino) ethanoic acid (**1.19**):



Quantities used for the synthesis: glycine (0.03 g, 0.40 mmol); compound **1.11** (0.07 g, 0.40 mmol). Red solid. Mp: > 238 °C (Decomposition). Yield: 60% (0.058 g, 0.24 mmol). IR: ( $\nu_{\max}/\text{cm}^{-1}$ )3568, 2855, 3400, 3267, 2927, 1718, 1654, 1598. <sup>1</sup>H NMR (CD<sub>3</sub>OD, 400 MHz)  $\delta$ : 2.20 (s, 3H, H-2''), 3.76 (br s, 2H, H-2), 5.31 (s, 1H, H-2'), 7.25 (s, 1H, H-5'). <sup>13</sup>C NMR (CD<sub>3</sub>OD, 100 MHz)  $\delta$ : 24.5 (C-2''), 45.9 (C-2), 103.3 (C-2'), 105.3 (C-5'), 154.5 (C-4'), 157.3 (C-1'), 170.3 (C-1'' and C-3'), 180.2 (C-6'). HRMS (ESI)  $m/z$  calculated for  $C_{10}H_{10}N_2O_5$  [M+H]<sup>+</sup>: 239.0662, found 239.0668.

#### 4.7. Synthesis of 2-Acetamido-5-benzylamino-1,4-benzoquinone **1.20**



To a one neck round-bottomed flask (25 mL) was added 2-acetamido-1,4-benzoquinone (**1.11**) (0.19 g, 1.1 mmol) in dichloromethane (5 mL), followed by benzylamine (0.12 mL, 1.1 mmol). The reaction mixture was stirred at room temperature under molecular oxygen atmosphere. Initially, there was a change of solution colour from yellow to dark red. The reaction was monitored by TLC and stopped after 2 h. The solvent was removed under reduced pressure to afford the crude product as a dark red solid. The compound was purified by silica gel column chromatography with Hex/EtOAc 1:1 v/v to afford the required product **1.20** as red crystals in 72% yield (0.22 g, 0.81 mmol). Mp: 240-241 °C. IR: ( $\nu_{\max}/\text{cm}^{-1}$ ) 3301, 3279, 2958, 2923, 2853, 1654, 1570.  $^1\text{H}$  NMR (DMSO- $d_6$ , 400 MHz)  $\delta$ : 2.16 (s, 3H, H-2'), 4.37 (d,  $J = 8.6$  Hz, 2H, H-1''), 5.31 (s, 1H, H-6), 7.19 (s, 1H, H-3), 7.23-7.34 (m, 5H, H-3''-5''), 8.30 (t,  $J = 8.6$  Hz, 1H, N-H), 9.56 (s, 1H, N-H).  $^{13}\text{C}$  NMR (DMSO- $d_6$ , 100 MHz)  $\delta$ : 24.6 (C-2'), 45.0 (C-1''), 94.4 (C-6), 109.1 (C-3), 127.2 (C-3'' and C5''), 128.5 (C-4''), 137.1 (C-2''), 142.0 (C-2), 148.1 (C-5), 171.2 (C-1'), 178.2 (C-1), 183.7 (C-4). HRMS (ESI)  $m/z$  calculated for  $\text{C}_{15}\text{H}_{14}\text{N}_2\text{O}_3$   $[\text{M}+\text{H}]^+$ : 271.1077, found 271.1070.

## 5. REFERENCES

- [1] R.-S. Xu, Introduction, in: *Introd. to Nat. Prod. Chem.*, CRC Press, **2011**: pp. 1–3.
- [2] T. Kutchan, R. a. Dixon, *Curr. Opin. Plant Biol.* **8** (2005) 227–229.
- [3] J. McMurry, *Organic Chemistry*, 5th ed., Brooks/Cole, **2000**.
- [4] N. El-Najjar, H. Gali-Muhtasib, R.A. Ketola, P. Vuorela, A. Urtti, H. Vuorela, *Phytochem. Rev.* **10** (2011) 353–370.
- [5] I. Abraham, R. Joshi, P. Pardasani, R.T. Pardasani, *J. Braz. Chem. Soc.* **22** (2011) 385–421.
- [6] K. V. Rao, W.P. Cullen, *Antibiot Annu.* **7** (1960) 950–953.
- [7] F.Z. Basha, S. Hibino, D. Kim, W.E. Pye, T.-T. Wu, S.M. Weinreb, *J. Am. Chem. Soc.* **102** (1980) 3962–3964.
- [8] S. Kende, F.H. Ebetino, *Tetrahedron Lett.* **25** (1984) 923–926.
- [9] D.L. Boger, J.S. Panek, *J. Am. Chem. Soc.* **107** (1985) 5745–5754.
- [10] T.J. Donohoe, C.R. Jones, L.C.A. Barbosa, *J. Am. Chem. Soc.* **133** (2011) 16418–16421.
- [11] T.J. Donohoe, C.R. Jones, A.F. Kornahrens, L.C.A. Barbosa, L.J. Walport, M.R. Tatton, M. O'Hagan, A.H. Rathi, D.B. Baker, *J. Org. Chem.* **78** (2013) 12338–12350.
- [12] W. Doyle, D.M. Bahtz, R.E. Gruhch, D.E. Nettleton, *Tetrahedron Lett.* **22** (1981) 4595–4598.
- [13] D.M. Balitz, J.A. Bush, W.T. Bradner, T.W. Doyle, *J. Antibiot. (Tokyo).* **35** (1982) 259–265.
- [14] A. Nourry, S. Legoupy, F. Huet, *Tetrahedron Lett.* **48** (2007) 6014–6018.
- [15] H. Shigemori, T. Madono, T. Sasaki, Y. Mikami, J. Kobayashi, *Tetrahedron.* **50** (1994) 8347–8354.
- [16] J. Kobayashi, T. Madono, H. Shigemori, *Tetrahedron.* **51** (1995) 10867–10874.
- [17] Y. Takahashi, M. Ushio, T. Kubota, S. Yamamoto, J. Fromont, J. Kobayashi, *J. Nat. Prod.* **73** (2010) 467–471.
- [18] G. Daletos, N.J. de Voogd, W.E.G. Müller, V. Wray, W. Lin, D. Feger, M. Kubbutat, A.H. Aly, P. Proksch, *J. Nat. Prod.* **77** (2014) 218–226.
- [19] P. Stahl, L. Kissau, R. Mazitschek, A. Huwe, P. Furet, A. Giannis, H. Waldmann, *J. Am. Chem. Soc.* **123** (2001) 11586–11593.
- [20] L. Kissau, P. Stahl, R. Mazitschek, A. Giannis, H. Waldmann, *J. Med. Chem.* **46** (2003) 2917–2931.
- [21] M.-L. Kondracki, M. Guyot, *Tetrahedron Lett.* **28** (1987) 5815–5818.
- [22] S. Aoki, D. Kong, K. Matsui, R. Rachmat, M. Kobayashi, *Chem. Pharm. Bull. (Tokyo).* **52** (2004) 935–937.
- [23] N.K. Utkina, V. a. Denisenko, O. V. Scholokova, M. V. Virovaya, N.G. Prokof'eva, *Tetrahedron Lett.* **44** (2003) 101–102.
- [24] C. Giannini, C. Debitus, R. Lucas, a Ubeda, M. Payá, J.N. Hooper, M. V D'Auria, *J. Nat. Prod.* **64** (2001) 612–5.
- [25] J. Rodríguez, E. Quiñoá, R. Riguera, B.M. Peters, L.M. Abrell, P. Crews, *Tetrahedron.* **48** (1992) 6667–6680.
- [26] Y. Takahashi, T. Kubota, J. Fromont, J. Kobayashi, *Tetrahedron.* **63** (2007) 8770–8773.
- [27] Y. Takahashi, T. Kubota, S. Yamamoto, J. Kobayashi, *Bioorg. Med. Chem. Lett.* **23** (2013) 117–8.

- [28] Y. Miyata, *Curr. Pharm. Des.* 11 (2005) 1131–1138.
- [29] N. Danshiitsoodol, C.A. Pinho, Y. Matoba, T. Kumagai, M. Sugiyama, *J. Mol. Biol.* 360 (2006) 398–408.
- [30] M. Tomasz, *Chem. Biol.* 2 (1995) 575–579.
- [31] W.-H. Jiao, T.-T. Xu, F. Zhao, H. Gao, G.-H. Shi, J. Wang, L.-L. Hong, H.-B. Yu, Y.-S. Li, F. Yang, H.-W. Lin, *European J. Org. Chem.* 2015 (2015) 960–966.
- [32] K.F. Chater, *Philos. Trans. R. Soc. B Biol. Sci.* 361 (2006) 761–768.
- [33] R.E. de Lima Procópio, I.R. da Silva, M.K. Martins, J.L. de Azevedo, J.M. de Araújo, *Brazilian J. Infect. Dis.* 16 (2012) 466–471.
- [34] P. Kämpfer, The Family Streptomycetaceae, Part I: Taxonomy, in: M. Dworkin, S. Falkow, E. Rosenberg, K.-H. Schleifer, E. Stackebrandt (Eds.), *Prokaryotes SE* - 22, Springer New York, 2006: pp. 538–604.
- [35] D. Schulz, P. Beese, B. Ohlendorf, A. Erhard, H. Zinecker, C. Dorador, J.F. Imhoff, *J. Antibiot. (Tokyo)*. 64 (2011) 763–768.
- [36] Z.-L. You, D.-M. Xian, M. Zhang, X.-S. Cheng, X.-F. Li, *Bioorg. Med. Chem.* 20 (2012) 4889–4894.
- [37] A. Nain-Perez, L.C.A. Barbosa, M.C. Picanço, S. Giberti, G. Forlani, *Chem. Biodivers.* 13 (2016) 1008–1017.
- [38] C.G. Whiteley, *Bioorganic Med. Chem.* 10 (2002) 1221–1227.
- [39] H. Tohma, H. Morioka, Y. Harayama, M. Hashizume, Y. Kita, *Tetrahedron Lett.* 42 (2001) 6899–6902.
- [40] B.E. Love, J. Bonner-Stewart, L.A. Forrest, *Synlett.* 1 (2009) 813–817.
- [41] L.C.A. Barbosa, E.S. Alvarenga, A.J. Demuner, L.S. Virtuoso, A.A. Silva, *Chem. Biodivers.* 3 (2006) 553–567.
- [42] N. Hayashi, K. Matsui, A. Kanda, T. Yoshikawa, H. Nakagawa, J. Yoshino, H. Higuchi, *Chem. Lett.* 40 (2011) 947–949.
- [43] C.C. Nawrat, W. Lewis, C.J. Moody, *J. Org. Chem.* 76 (2011) 7872–7881.
- [44] S. Cunha, C.C. Oliveira, J.R. Sabino, *J. Braz. Chem. Soc.* 22 (2011) 598–603.
- [45] T. Yuehe, H. Zhifeng, L. Jianxiao, *Chinese J. Org. Chem.* 31 (2011) 1222–1229.
- [46] A. Leifer, E.R. Lippincott, *J. Am. Chem. Soc.* 79 (1957) 5098–5101.
- [47] L.C.A. Barbosa, *Espectroscopia no Infravermelho na caracterização de compostos orgânicos*, Editora UFV, 2011.
- [48] S.J. Gould, B. Shen, Y.G. Whittle, 111 (1989) 7932–7938.
- [49] J.M. Gulland, R. Robinson, J. Scott, S. Thornley, *J. Chem. Soc.* (1929) 2924–2941.

## **CHAPTER 2**

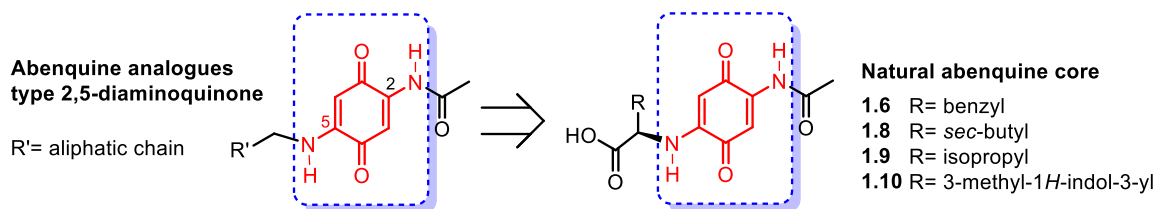
### **NATURAL ABENQUINES AND ANALOGUES: SYNTHESIS AND EVALUATION OF THEIR ALGICIDAL AND CYTOTOXIC ACTIVITY**

## 1. INTRODUCTION

Over the last decades, natural products have been used as tools for drug discovery. The structural complexity of natural products can be reduced by the chemical synthesis of smaller fragments while retaining or sometimes improving desired biological parameters such as potency or selectivity [1]. The continuous search for bioactive compounds has led to great contributions in both agrochemical and pharmaceutical areas. Drugs and agrochemicals tend to be moderately sized organic molecules with a smattering of functional groups to provides specific binding and the right physical properties [2].

It is well known that plants, animals, bacteria and fungi lives depend on enzymes and protein receptors, and the interference with these proteins is the main way that bioactive compounds exert their effect. Furthermore, the target binding sites for drugs and agrochemicals are very similar (enzyme active sites and receptor binding sites) and the path these compounds must traverse to reach them are comparable [2]. The existent similarities between the molecules produced by the pharmaceutical and agrochemical research show that there are potential opportunities to exploit the structural properties of natural products or analogues.

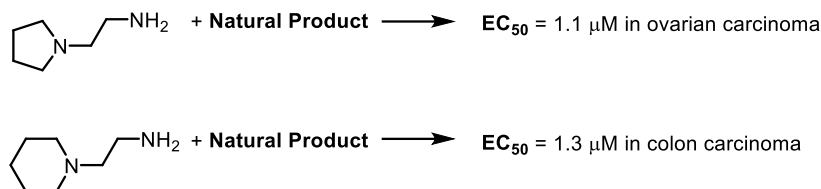
Since in Chapter 1, an accessible route was described for the synthesis of natural abenquines and some analogues of 2,5-diamino-benzoquinones, herein, abenquines will be used as a model to prepare analogues type 2,5-diamino-benzoquinone that could present both biological potential, as drugs or agrochemicals (Figure 2.1).



**Figure 2.1.** Abenquine analogues type 2,5-diaminoquinones.

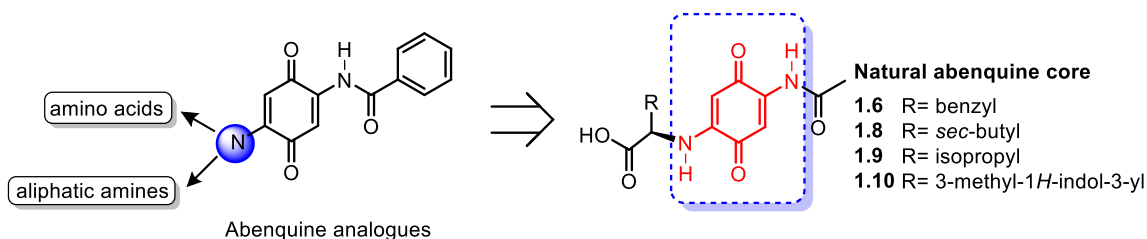


Looking for new substances that could show those biological activity, analogues to abenquines will be prepared using a known pharmacophore. Since our laboratory was reported that some amines could increase the cytotoxic activity when introduced to some natural products different ethan-1,2-diamine will be employed in the synthesis of abenquines analogues (Figure 2.2).



**Figure 2.2.** Suggested amines as pharmacophores.

Given that amino acids fragments of aminoquinones will be changed by different amino groups, herein, the acetyl group will also be replaced by the benzoyl group to explore deeply the structure-activity relationship of the abenquine core.



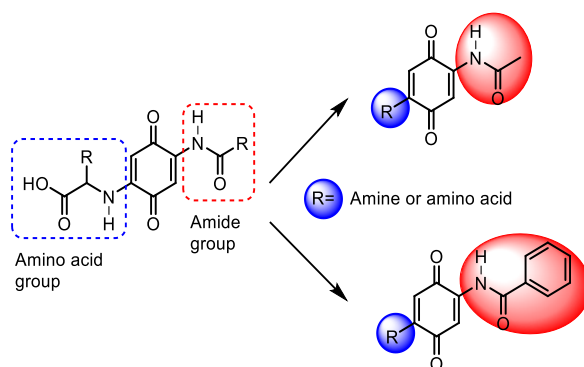
**Figure 2.3.** Proposed of change the acyl group by the benzoyl group to give new abenquine analogues.

In this context, further we will describe the synthesis of new analogues to abenquines and both, the ability of abenquines analogues to inhibit the growth of a cyanobacteria strain, and inhibit the viability of different cancer cells.

## 2. RESULTS AND DISCUSSION

### 2.1. Synthesis

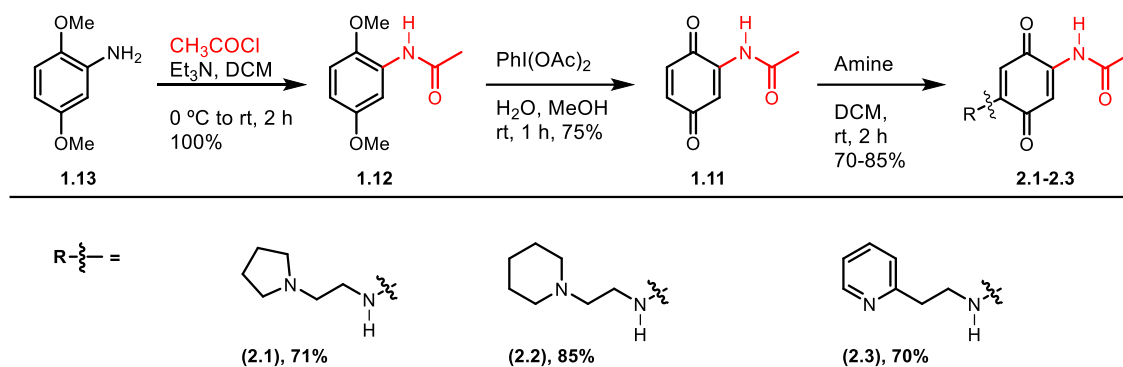
The synthesis of analogues was performed through variations in the benzoquinone core of abenquine (Figure 2.4). The structure of abenquine is divided into two fragments: first an amido group and second a fragment with amino acid groups. In the first chapter, the preparation and characterization of some analogues (**1.17-1.20**) were presented. The substitution of the amino acid group by different amino groups was planned, maintaining fixed the acetamide moiety to retain the abenquine core. On this chapter the synthesis of analogues of the acetyl and benzoyl groups are discussed.



**Figure 2.4.** Variation in the core of abenquine.

#### 2.1.1. Synthesis of analogues of acetyl group

Regarding route 2 described in the first chapter, Figure 2.5 presents the preparation of analogues **2.1-2.3**. Initially, the commercially available starting material (**1.13**) was acetylated, rendering the intermediate **1.12** in 100% conversion. This intermediate was then oxidized with phenyliodine diacetate, producing compound **1.11** in 75% yield. Subsequently, treatment of the benzoquinone **1.11** with different amines, in dichloromethane (since in ethanol compound **1.11** showed low solubility) for two hours at room temperature, afforded the required compounds (**2.1-2.3**) with yields of 70-85%.

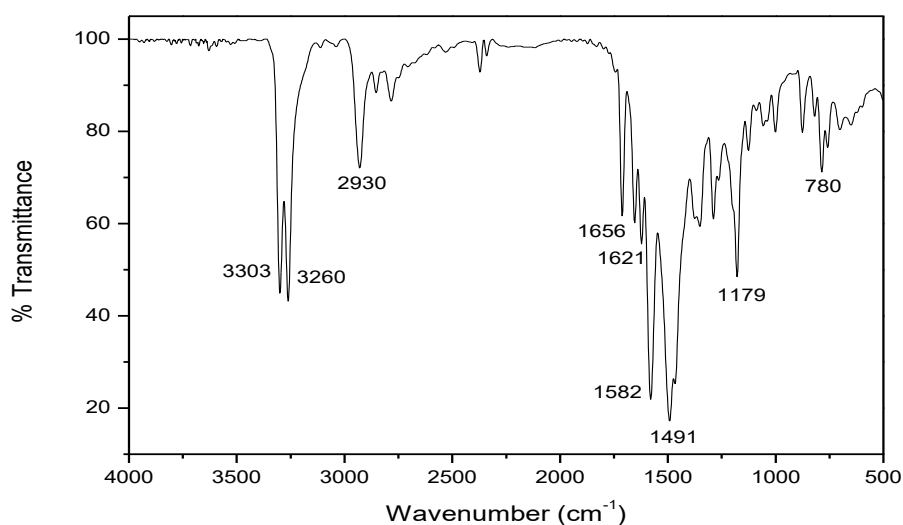


**Figure 2.5.** Preparation of analogue of acetyl group of abenquine with different amines.

### 2.1.2. Characterization

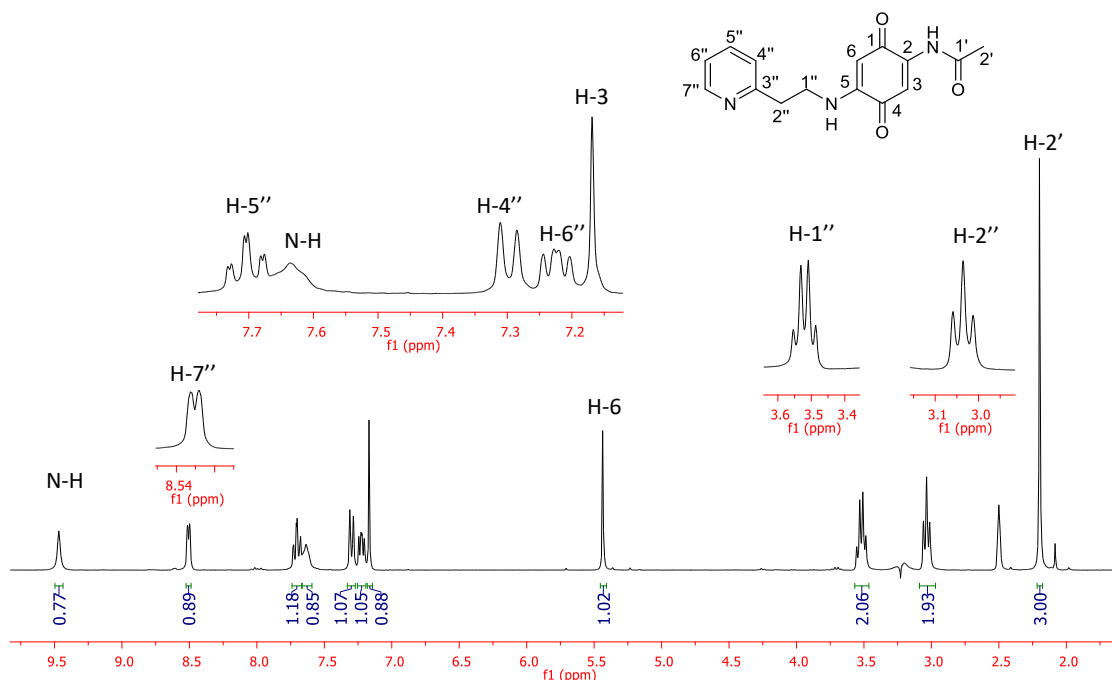
Characterization and purity of compounds were determined by microanalysis, IR,  $^1\text{H}$  and  $^{13}\text{C}$  NMR. Due to that fact that these compounds share spectroscopic characteristics. Only the characterization of compound **2.3** is explained in detail and this description can be extended for **2.1** and **2.2**.

In the infrared spectrum (Figure 2.6), a similarity between the absorption bands for the amino and the acetamide group was observed in the range of 3303-3260  $\text{cm}^{-1}$ , respectively. In addition to this, absorption bands corresponded to stretching of the carbonyl of the quinone system at 1656  $\text{cm}^{-1}$  and 1621  $\text{cm}^{-1}$  in the acetamide group was observed.



**Figure 2.6.** Infrared spectrum in KBr of compound **2.3**.

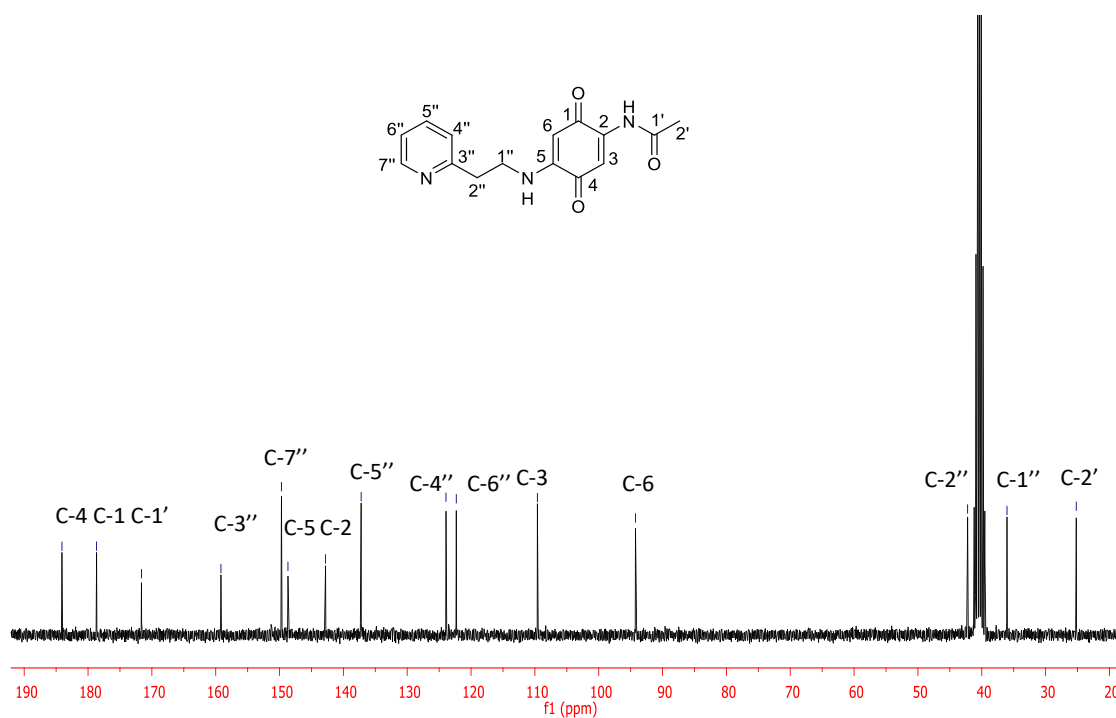
In the  $^1\text{H}$  NMR spectrum (Figure 2.7), the acetyl group was characterized by the singlet at  $\delta = 2.19$  ( $\text{CH}_3\text{CO}$ -). A triplet signal at  $\delta = 3.03$  ( $J = 6.8$  Hz) and a doublet of doublets at  $\delta = 3.51$  ( $J = 13.4$ ; 6.8 Hz) are associated to the ethylene chain of the amino group ( $\text{CH}_2\text{CH}_2$  unit). The two  $-\text{CH}$  of the quinone core are characterized by the singlet at  $\delta = 7.16$  and 5.43.



**Figure 2.7.**  $^1\text{H}$  NMR spectrum ( $\text{DMSO-}d_6$ , 300 MHz) of compound **2.3**.

The hydrogens related to the pyridinyl group are observed between 7.2-8.5 ppm. Signal related to H-6'' is seen as a doublet of doublets at  $\delta = 7.22$  ( $J = 7.5$ ; 4.8 Hz). The doublet at  $\delta = 7.29$  ( $J = 7.5$  Hz) is associated to H-4'' and the signal related to the N-H of the amino group is observed as a broad singlet ( $\delta = 7.63$ ). Then, the H-7'' signal, which is a doublet at  $\delta = 8.50$  ( $J = 4.8$  Hz). The NH amide is characterized by a singlet at  $\delta = 9.46$ . All this data is summarized in a comparative table of compounds **2.1-2.3** (Table 2.1).

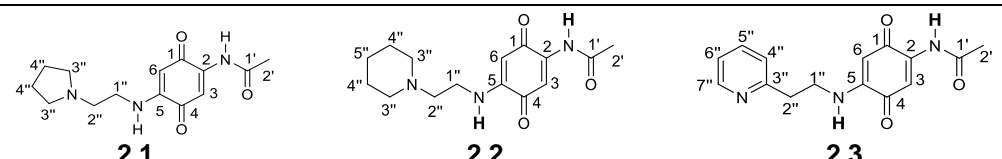
In the  $^{13}\text{C}$  NMR spectrum (Figure 2.8), 15 signals are observed for the compound **2.3**. Firstly, the signal belonging to methyl-2' is seen at  $\delta = 25.1$  as well as the carbons associated to the ethylene groups at  $\delta = 36.0$  and 42.2 for C-1'' and C-2'', respectively.



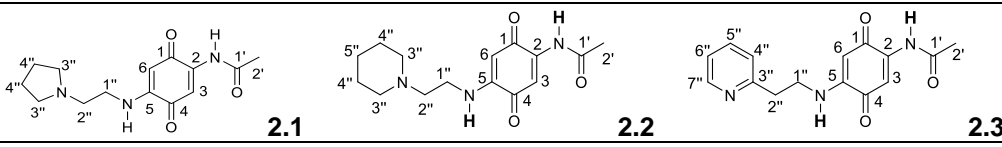
**Figure 2.8.**  $^{13}\text{C}$  NMR spectrum ( $\text{DMSO-}d_6$ , 75 MHz) of compound **2.3**.

Additionally, the signals of the vinylic carbons are observed at the region of  $\delta = 94.2$  for C-6 and  $\delta = 109.6$  for C-3. Another group of carbon signal corresponded to carbonyl C-1', C-1, and C-4 at  $\delta = 171.6$ , 178.6, and 184.0, respectively. This data is summarized in Table 2.2 with the corresponding data for compounds **2.1-2.3**.

**Table 2.1.**  $^1\text{H}$  NMR data for compounds **2.1-2.3** in  $\text{DMSO-d}_6$  (400 MHz)

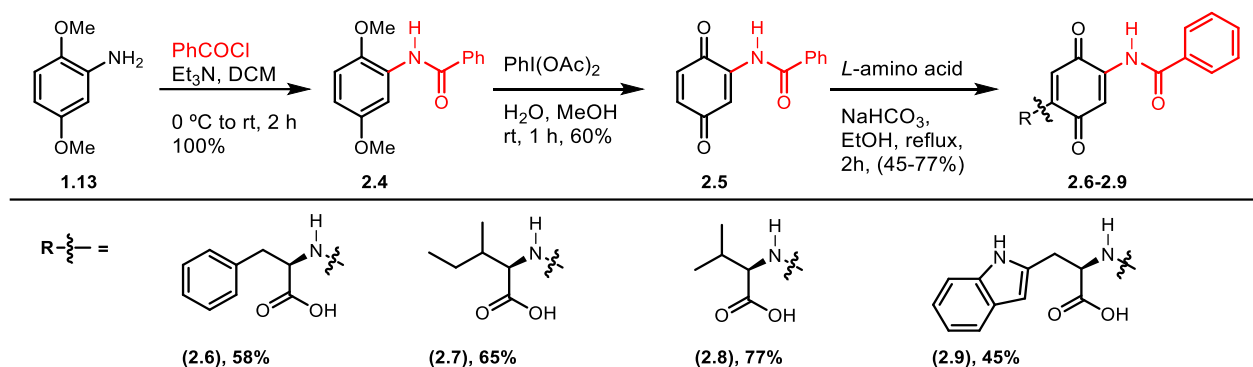
N° H			
	$\delta$ (J in Hz)		
<b>3</b>	7.21, s	7.17, s	7.16, s
<b>6</b>	5.45, s	5.40, s	5.43, s
<b>2'</b>	2.22, s	2.18, s	2.19, s
<b>1''</b>	3.26, t ( $J = 6.4$ )	3.19, dd ( $J = 10.7; 6.5$ )	3.51, dd ( $J = 13.4; 6.8$ )
<b>2''</b>	2.65, t ( $J = 6.4$ )	2.45, t ( $J = 6.5$ )	3.03, t ( $J = 6.8$ )
<b>3''</b>	(a) 1.79, br s; (b) 2.54, m	2.32-2.39, m	
<b>4''</b>	1.66-1.75, m	1.44-1.49, m	7.29, d ( $J = 7.5$ )
<b>5''</b>		1.33-1.36, m	7.70, td ( $J = 7.5; 1.7$ )
<b>6''</b>			7.22, dd ( $J = 7.5; 4.8$ )
<b>7''</b>			8.50, d ( $J = 4.8$ )

**Table 2.2.**  $^{13}\text{C}$  NMR data for compounds **2.1-2.3** in  $\text{DMSO-d}_6$  (100 MHz)

N° C			
	$\delta$		
<b>1</b>	178.1	178.0	178.6
<b>2</b>	142.4	142.3	142.7
<b>3</b>	109.0	108.9	109.6
<b>4</b>	183.6	183.5	184.0
<b>5</b>	148.0	147.9	148.6
<b>6</b>	93.6	93.6	94.2
<b>1'</b>	171.4	171.3	171.6
<b>2'</b>	24.7	24.6	25.1
<b>1''</b>	40.8	39.0	36.0
<b>2''</b>	52.8	55.5	42.2
<b>3''</b>	53.5	53.8	159.1
<b>4''</b>	23.2	25.6	123.9
<b>5''</b>		24.0	137.2
<b>6''</b>			122.3
<b>7''</b>			149.7

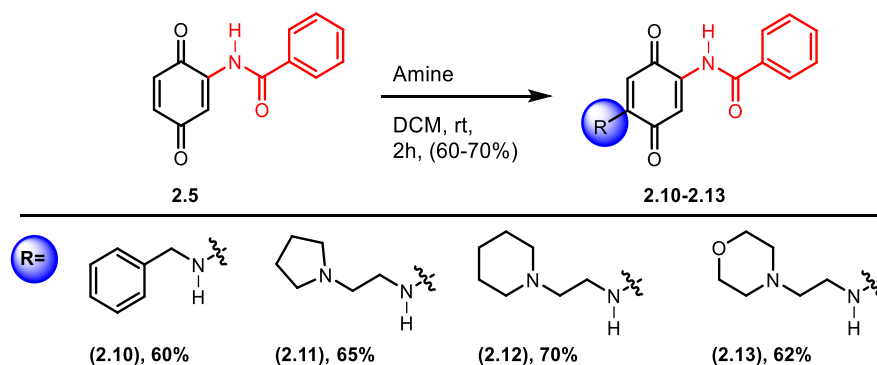
### 2.1.3. Synthesis of analogues of benzoyl group of abenquines

Substitution of the acetyl by the benzoyl group afforded a new series of analogues bearing a bulky group. Additionally, substitution of amines or amino acid groups provide the analogues to benzoyl group of abenquines. Figure 2.9 demonstrates the preparation of the compounds **2.6-2.9**. Firstly, *N*-(2,5-dimethoxyphenyl) benzamide (**2.4**) was prepared through a reaction of 2,5-dimethoxyaniline (**1.13**) with benzoyl chloride for two hours to provide **2.4** in 100% yield. The oxidation step was then attained to produce the compound **2.5** in 60% yield. Afterwards, the quinone **2.5** was reacted with the selected amino acid in ethanol using sodium bicarbonate as a base in a 2-hour reflux resulting in four analogues (**2.6-2.9**) in 45-77% yield.



**Figure 2.9.** Preparation of analogue of benzoyl group with different amino acids.

Moreover, according to the route selected for this synthesis, four new analogues were also prepared (Figure 2.10) by the addition of different amines to the intermediate **2.5** in dichloromethane for two hours at room temperature, producing the required compounds (**2.10-2.13**) with yields between 60-70%.



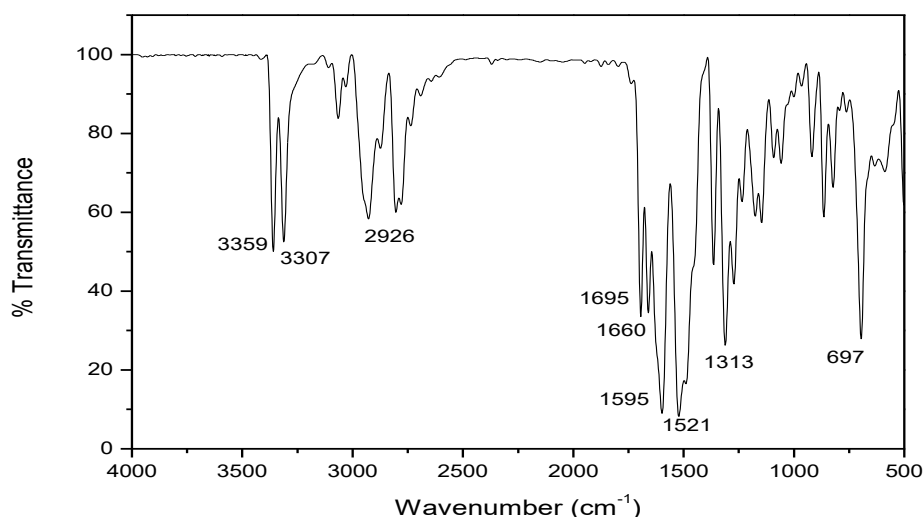
**Figure 2.10.** Preparation of analogue of benzoyl group with different amines.

#### 2.1.4. Characterization

Compound **2.11** was selected to describe its structural characterization through the analysis in IR,  $^1\text{H}$ , and  $^{13}\text{C}$  NMR. The spectra of synthesized compounds were shown to be greatly similar, with the only noticeable variations observed referring to the substituents of each amine initially used in the reactions. Therefore, the following discussion is based on data of compound **2.11**, although this analysis can be extended to other synthesized products.

Compound 2-benzamido-5-((2-(pyrrolidin-1-yl)ethyl)amino)-1,4-benzoquinone (**2.11**):

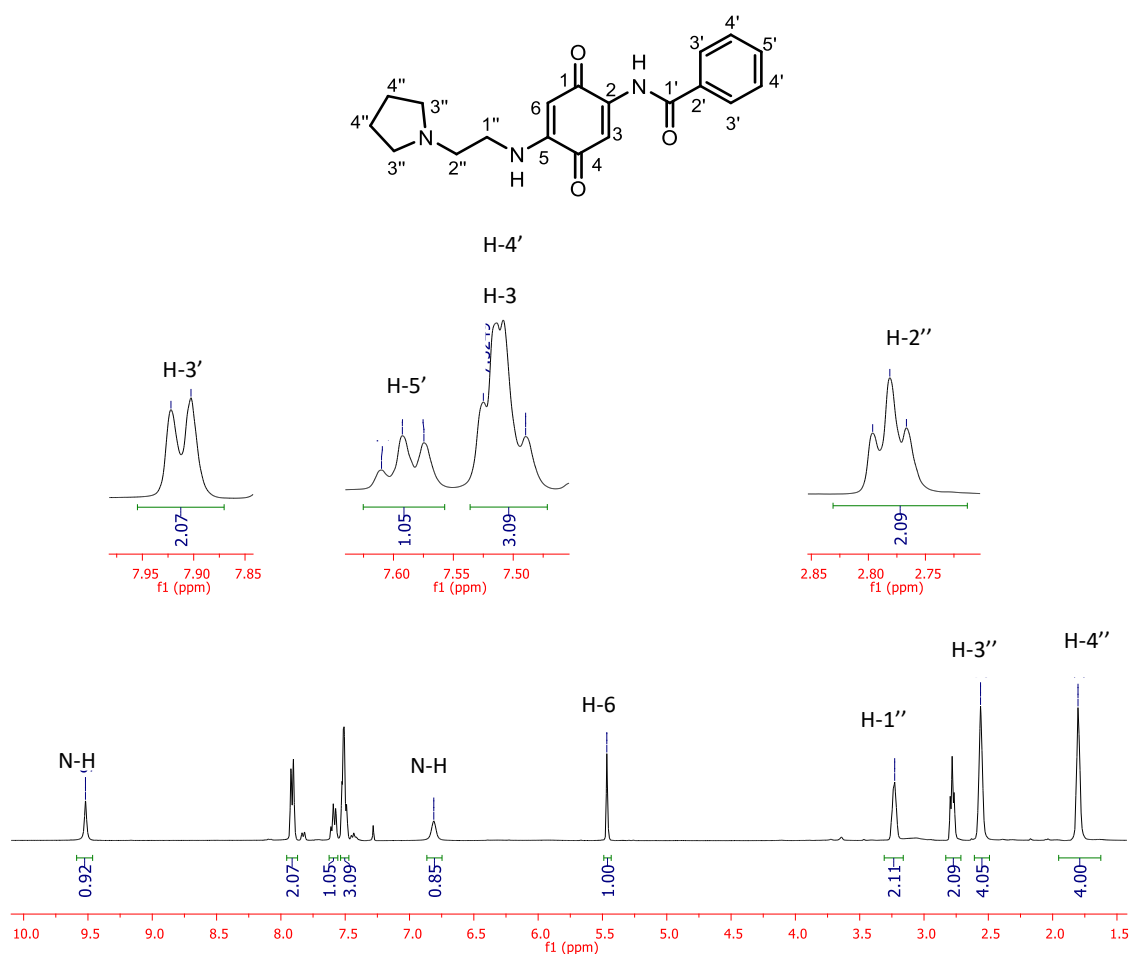
ESI-MS analysis for compound **2.11** confirmed that the signal  $m/z$  340.0 corresponded to the ion  $[\text{M}+\text{H}]^+$ , while analysis of IR and NMR established the formation of the product (**2.11**). In the Infrared spectrum (Figure 2.11), the characteristic band of the stretching of the N-H bond in  $3359$  and  $3307\text{ cm}^{-1}$  for the amide group was observed. The C-H stretching was captured at  $3002$  and  $2926\text{ cm}^{-1}$  while the carbonyl band (C=O) of an  $\alpha,\beta$ -unsaturated system was detected at  $1695\text{ cm}^{-1}$ . The double bond stretching band of the conjugated C=C was recorded at  $1595\text{ cm}^{-1}$  and the C-N bond stretch at  $1521\text{ cm}^{-1}$  [3].



**Figure 2.11.** Infrared spectrum in KBr of compound **2.11**.

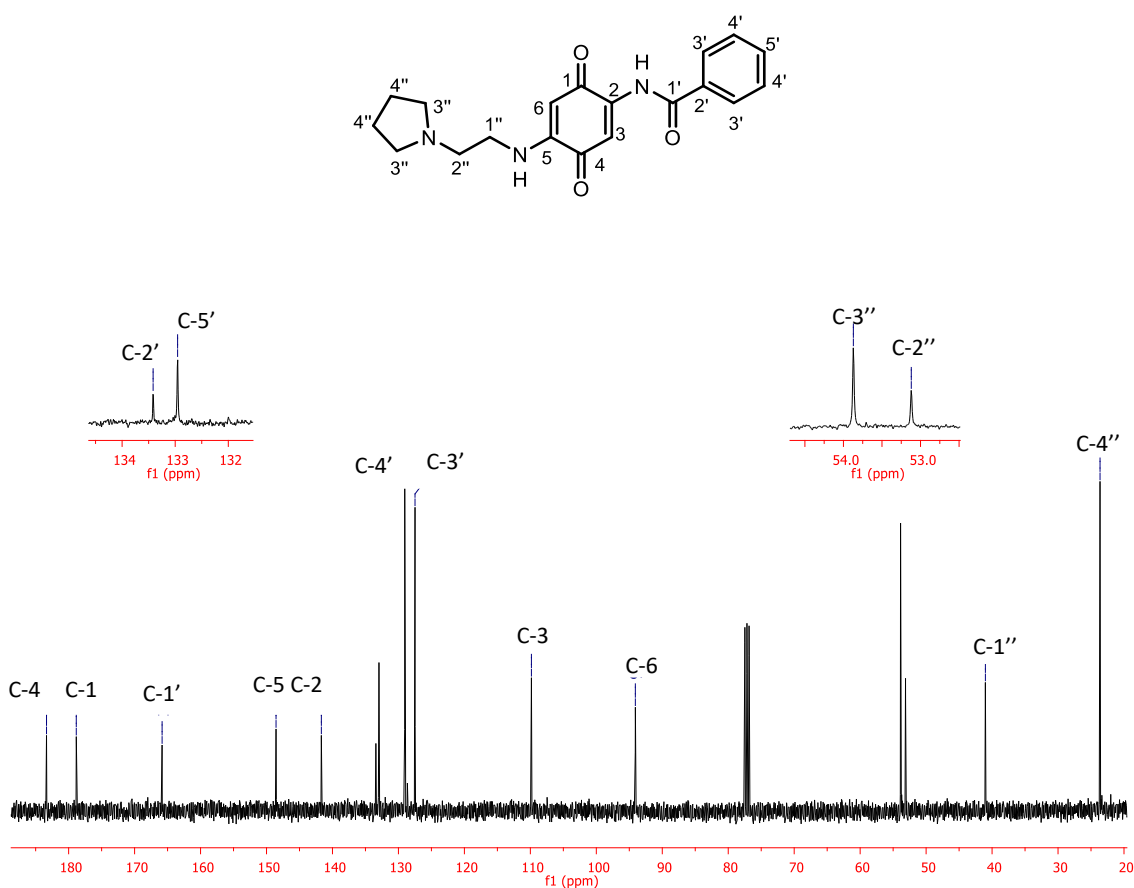


The  $^1\text{H}$  NMR spectrum (Figure 2.12) exhibited ten signals corresponding to 21 hydrogens. Among these are a broad signal at  $\delta = 1.80$  and  $2.56$ , corresponding to the methylene hydrogens-4'', as well as the methylene hydrogens-3'', both belonging to the pyrrolidiny system. A triplet signal at  $\delta = 2.78$  ( $J = 5.9$  Hz) corresponds to the ethylenic hydrogens-2'' and a broad singlet corresponds to hydrogens-1'' at  $\delta = 3.22$ . A singlet signal pertaining to the vinylic hydrogen-3 at  $\delta = 5.46$  it was also observed. Furthermore, a small broad singlet corresponds to an amino hydrogen at  $\delta = 6.8$ . Subsequently, a multiplet at  $\delta = 7.48$ - $7.52$ , associated to three hydrogens; two for the aromatic ring (H-4') and the other for the vinylic H-6, is also observed. Hydrogen-5' is assigned to the triplet at  $\delta = 7.59$  with  $J = 7.3$  Hz. A doublet ( $\delta = 7.91$ ,  $J = 7.3$  Hz) corresponds to the *ortho* coupling of the two aromatic hydrogen-3' [4]. Finally, a broad singlet at  $\delta = 9.51$  for the N-H of amide group was observed.



**Figure 2.12.**  $^1\text{H}$  NMR ( $\text{CDCl}_3$ , 400 MHz) of compound 2.11.

In the  $^{13}\text{C}$  NMR spectrum (Figure 2.13), at the region of  $\delta = 23.6\text{-}55.8$ , four signals were observed, and are associated to the ethyl pyrrolidinyl system (C1''-C4''). Between  $\delta = 23.6\text{-}55.8$  90-110, two signals are found to be related to the vinylic carbon (C-3 and C-6). The signals in the range of  $\delta = 127.4\text{-}133.4$  were attributed to the carbon of the aromatic system (C2'-C5'), while the signal related to carbon-2 and carbon-5 were assigned at  $\delta = 141.6$  and  $148.1$ , respectively. Finally, three signals at  $\delta = 165.8$ ,  $179.3$ , and  $183.4$  match to the carbonyl group of the amide (C-1'') and the carbonyl of the quinone system (C-1 and C-4).



**Figure 2.13.**  $^{13}\text{C}$  NMR ( $\text{CDCl}_3$ , 100 MHz) of compound **2.11**.

In accordance with spectroscopy data, all synthesized compounds match to what is expected. In total, three acetyl analogues of abenquines (**2.1-2.3**) and eight benzoyl analogues of abenquines (**2.6-2.13**) were obtained and fully characterized (all the spectra data of compounds are present in Appendix 2). All these compounds are novel to the existing literature.

## 2.2. Biological assay

### 2.2.1. *Cyanobacteria inhibition*

Cyanobacteria, also referred to as blue-green algae, have existed over 2.5 billion years ago. These are ancient inhabitants of aquatic and terrestrial environments that can survive in a wide variety of extreme environmental conditions when are exposed to various types of natural stresses [5,6]. A majority of cyanobacteria are Gram-negative, aerobic photoautotrophs, and their essential metabolic processes only require water, carbon dioxide, inorganic substances, and light [7,8].

In fresh and coastal salt water, under favorable conditions, *e.g.* warm temperature, sunny weather, and most importantly, increased availability of N and P as well as nutrient source, some cyanobacteria are capable of *blooming*, rapidly multiplying and forming a dense surface scum [9]. This often leads to the establishment of anoxic conditions, possibly altering the ecological order and contributing to a decline in the ecosystem's productivity [10].

Cyanobacterial blooms have become a severe problem all over the world in recent years by contributing to increasing eutrophication and climate change. They cause many problems, including severe damage to aquatic ecosystems and human health [11]. For example, the deaths of Lesser Flamingos in Lake Big Momela and Lake Manyara in Tanzania, were mostly due to cyanobacterial intoxication [12]. Thus, these organisms are known for producing toxins such as microcystins, nodularins, anatoxins, and paralytic shellfish poisons [13]. *Microcystis* is the most common bloom-forming cyanobacterium in the world's eutrophic and hypereutrophic waters. Many cyanobacteria strains are known for affecting drinking water supplies and human health by producing a wide range of toxins, especially *Microcystis* [11]. Consequently, the control of this blooming microorganism is an important matter of study.

In this context, studies of the mechanisms of action that result in the inhibition of photosynthesis are significant in the search for new algicidal agents. Therefore, a series of new analogues of abenquines is used to evaluate their phytotoxicity against different cyanobacteria strains.

### 2.2.2. Inhibition of cyanobacterial growth

Four natural abenquines (**1.6**, **1.8-1.10**) and 15 synthetic analogues (**1.17-1.20**, **2.1-2.3**, **2.6-2.13**) were firstly evaluated against the cyanobacterium *Synechococcus elongatus* for the study of the inhibitory potential for photoautotrophic growth. The assays were achieved using a concentration of each compound from 1 to 100  $\mu\text{M}$ . Aliquots of 2  $\mu\text{M}$  of this concentration were applied to 96-well plates containing 0.2 mL chlorophyll from the cyanobacteria strain. The growth of the cyanobacterial strain was determined by absorbance and the data were expressed as percentages of growth in Table 2.3.

**Table 2.3.** Inhibitory effect of abenquines (**1.6**, **1.8-1.10**) and analogues with acetyl group (**1.17-1.20**, **2.1-2.3**) on cyanobacterial growth. Results are expressed as a percentage of constant growth and are mean  $\pm$  SE over 4 replicates.

Compounds	$\mu\text{M}$						
	1	2	5	10	20	50	100
<b>1.6</b>	81.3 $\pm$ 1.6	81.2 $\pm$ 2.4	64.4 $\pm$ 5.8	59.3 $\pm$ 2.9	38.2 $\pm$ 2.2	0.0 $\pm$ 0.0	0.0 $\pm$ 0.0
<b>1.8</b>	93.7 $\pm$ 5.0	88.5 $\pm$ 1.4	83.0 $\pm$ 2.8	57.2 $\pm$ 4.8	48.7 $\pm$ 4.3	0.8 $\pm$ 0.8	0.0 $\pm$ 0.0
<b>1.9</b>	79.5 $\pm$ 3.7	77.0 $\pm$ 2.8	74.9 $\pm$ 1.5	77.3 $\pm$ 2.1	74.5 $\pm$ 2.1	63.5 $\pm$ 3.2	48.7 $\pm$ 3.5
<b>1.10</b>	82.6 $\pm$ 2.6	79.7 $\pm$ 2.8	64.1 $\pm$ 3.1	65.7 $\pm$ 2.1	50.6 $\pm$ 2.5	2.2 $\pm$ 1.3	0.0 $\pm$ 0.0
<b>1.17</b>	78.7 $\pm$ 7.1	76.8 $\pm$ 6.1	69.8 $\pm$ 7.1	75.3 $\pm$ 2.6	76.3 $\pm$ 2.8	71.9 $\pm$ 2.4	61.8 $\pm$ 5.2
<b>1.18</b>	80.7 $\pm$ 3.5	72.1 $\pm$ 1.3	64.3 $\pm$ 0.8	37.3 $\pm$ 3.2	0.0 $\pm$ 0.0	0.0 $\pm$ 0.0	0.0 $\pm$ 0.0
<b>1.19</b>	88.8 $\pm$ 4.7	82.8 $\pm$ 4.3	62.5 $\pm$ 3.5	53.1 $\pm$ 4.5	13.6 $\pm$ 3.5	0.2 $\pm$ 0.2	1.7 $\pm$ 1.3
<b>1.20</b>	68.9 $\pm$ 3.7	55.1 $\pm$ 4.5	24.5 $\pm$ 5.8	1.5 $\pm$ 1.5	0.0 $\pm$ 0.0	0.0 $\pm$ 0.0	0.0 $\pm$ 0.0
<b>2.1</b>	38.8 $\pm$ 6.0	10.1 $\pm$ 3.6	0.8 $\pm$ 0.5	0.0 $\pm$ 0.0	0.0 $\pm$ 0.0	0.0 $\pm$ 0.0	0.0 $\pm$ 0.0
<b>2.2</b>	31.2 $\pm$ 4.4	18.7 $\pm$ 5.7	2.5 $\pm$ 2.5	0.0 $\pm$ 0.0	0.0 $\pm$ 0.0	0.0 $\pm$ 0.0	0.0 $\pm$ 0.0
<b>2.3</b>	73.5 $\pm$ 2.8	69.0 $\pm$ 1.8	52.4 $\pm$ 3.4	22.8 $\pm$ 2.5	0.0 $\pm$ 0.0	0.0 $\pm$ 0.0	0.0 $\pm$ 0.0

In Table 2.3, the inhibition percentage caused by abenquines (**1.6**, **1.8-1.10**) and analogues with acetyl group (**1.17-1.20**, **2.1-2.3**) on cyanobacterial growth are presented. For the natural abenquines (**1.6**, **1.8-1.10**), the cyanobacterial growth at a concentration as low as 50  $\mu\text{M}$  was almost completely abolished, except for abenquine C (**1.9**), which was found to be significantly less effective, causing less than 36%-inhibition at 50  $\mu\text{M}$ . Concerning analogues with different amino acid groups (**1.18-1.19**), an incremental inhibition of cyanobacterial growth at a concentration as low as 20  $\mu\text{M}$  is observed.

Results for compounds **1.20** and **2.1-2.3** are also summarized in Table 2.3. It is quite obvious that in the concentration range of 20-100  $\mu\text{M}$  these compounds inhibited 100% of the growth of the cyanobacterial. Compounds **2.1** and **2.2** were

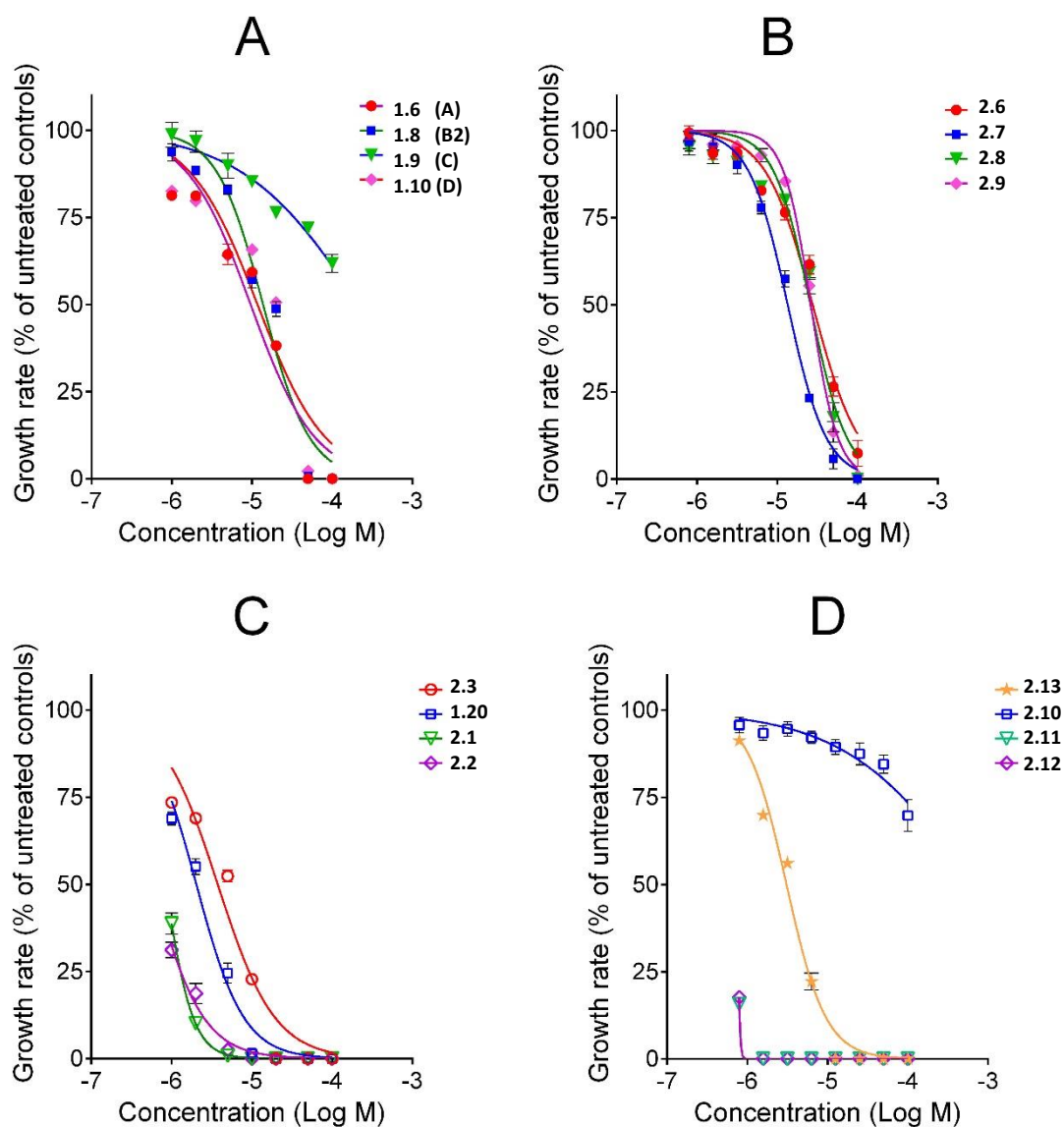
found the most potent inhibitors of the growth, with more than 80% and 60% of inhibition at concentrations as low as 1 and 2  $\mu\text{M}$  respectively.

On the other hand, the effect caused by a series of compounds with the benzoyl group (**2.6-2.13**) are summarized in Table 2.4. Compounds **2.6-2.9**, analogues with amino acids, display inhibition of 50% or more on cyanobacteria growth at a concentration of 50-100  $\mu\text{M}$ . Analogues of benzoyl moiety with amines (**2.10-2.13**), are known to be very potent even in concentration as low as 0.8  $\mu\text{M}$ . Also, results are similar or better when compared to compounds **2.1-2.3** in Table 2.3.

**Table 2.4.** Inhibitory effect of abenquines analogues with benzoyl group (**2.6-2.13**) on cyanobacterial growth. Results are expressed as a percentage of growth constant and are mean  $\pm$  SE over 4 replicates.

Compounds	$\mu\text{M}$							
	0.8	1.6	3	6	12	25	50	100
<b>2.6</b>	114.4 $\pm$ 7.7	93.5 $\pm$ 4.3	91.0 $\pm$ 3.5	77.8 $\pm$ 3.2	70.3 $\pm$ 4.3	51.6 $\pm$ 4.5	15.1 $\pm$ 3.6	2.3 $\pm$ 2.3
<b>2.7</b>	102.8 $\pm$ 5.6	95.7 $\pm$ 8.3	88.6 $\pm$ 6.2	74.6 $\pm$ 4.1	54.0 $\pm$ 5.0	0.0 $\pm$ 0.0	2.7 $\pm$ 2.7	0.0 $\pm$ 0.0
<b>2.8</b>	102.8 $\pm$ 4.4	95.2 $\pm$ 5.9	90.2 $\pm$ 3.1	81.8 $\pm$ 3.3	74.5 $\pm$ 2.4	51.2 $\pm$ 2.8	8.7 $\pm$ 4.7	0.0 $\pm$ 0.0
<b>2.9</b>	106.9 $\pm$ 5.8	101.2 $\pm$ 5.0	92.6 $\pm$ 4.1	86.0 $\pm$ 4.2	78.4 $\pm$ 4.3	42.6 $\pm$ 3.9	3.8 $\pm$ 3.4	0.0 $\pm$ 0.0
<b>2.10</b>	106.0 $\pm$ 7.1	99.2 $\pm$ 6.3	95.1 $\pm$ 5.6	93.3 $\pm$ 5.4	90.3 $\pm$ 5.7	87.8 $\pm$ 6.2	84.6 $\pm$ 6.5	73.4 $\pm$ 9.0
<b>2.11</b>	7.8 $\pm$ 5.3	0.0 $\pm$ 0.0	0.0 $\pm$ 0.0	0.0 $\pm$ 0.0	0.0 $\pm$ 0.0	0.0 $\pm$ 0.0	0.5 $\pm$ 0.5	0.7 $\pm$ 0.7
<b>2.12</b>	10.3 $\pm$ 4.8	0.0 $\pm$ 0.0	0.0 $\pm$ 0.0	0.0 $\pm$ 0.0	0.0 $\pm$ 0.0	0.0 $\pm$ 0.0	0.0 $\pm$ 0.0	0.0 $\pm$ 0.0
<b>2.13</b>	110.8 $\pm$ 5.4	77.2 $\pm$ 6.8	63.1 $\pm$ 7.5	23.0 $\pm$ 7.8	0.0 $\pm$ 0.0	0.0 $\pm$ 0.0	0.0 $\pm$ 0.0	1.6 $\pm$ 1.6

The concentrations causing 50% inhibition ( $\text{IC}_{50}$ ) were estimated by nonlinear regression analysis using Prism 6 for Windows, version 6.03 (GraphPad Software) and the data is summarized in Table 2.5. Accordingly, the results of this series of abenquines are very promising as algicidal agents. Abenquines A (**1.6**), B2 (**1.8**), and D (**1.10**) had shown inhibitory properties against the growth of the cyanobacterium *Synechococcus elongatus* PCC 6301, with concentrations causing 50% inhibition of growth rate ( $\text{IC}_{50}$ ) of about 10  $\mu\text{M}$ . Abenquine C (**1.9**) was found to be significantly less effective, promoting less than 40%-inhibition at 100  $\mu\text{M}$  (Figure 2.14A).



**Figure 2.14.** Effect of increasing concentrations of natural and synthetic abenquines on the growth rate of the model cyanobacterial strain *Synechococcus elongatus*. Panel A: natural abenquines A-D; panel B: benzoyl analogues of natural abenquines **2.6-2.9**; panel C: analogues **2.1-2.3** and **1.20** with amino instead of amino acid groups; panel D: benzoyl analogues of abenquines **2.11-2.13**.

For analogues (**2.6-2.9**), in which the acetyl moiety had been replaced by a benzoyl group, the inhibitory activity was similar (Figure 2.14B). However, in this case, compound **2.8**, an analogue of the inactive abenquine C (**1.9**), also showed some inhibitory activity. Even if the number of active substances is too small to draw general conclusions, the comparison of  $IC_{50}$  values (Table 2.5) showed that analogues with the benzoyl group are slightly less active than the acetyl counterparts when bearing aromatic amino acids (**2.6**, **2.9**). However, the activity is not influenced nor is enhanced when an aliphatic amino acid is present

(**2.7**, **2.8**). This finding is strengthened by the fact that the same effect was also evident for the other group of analogues. For instance, compound **2.10**, with an aromatic group in both sides, presented an  $IC_{50} > 100 \mu\text{M}$ , whereas an  $IC_{50}$  value of  $2.0 \mu\text{M}$  was found for its counterpart **1.20**.

**Table 2.5.** Concentrations of natural and synthetic abenquines able to inhibit by 50% ( $IC_{50}$ ) the growth of the model cyanobacterial strain *Synechococcus elongatus* PCC 6301.

Compound	$IC_{50}$ ( $\mu\text{M}$ )	Compound	$IC_{50}$ ( $\mu\text{M}$ )
<b>1.6</b>	$9.6 \pm 2.2$	<b>2.6</b>	$27.7 \pm 3.0$
<b>1.8</b>	$13.8 \pm 1.9$	<b>2.7</b>	$13.5 \pm 1.0$
<b>1.9</b>	$> 100$	<b>2.8</b>	$25.9 \pm 1.8$
<b>1.10</b>	$11.7 \pm 2.6$	<b>2.9</b>	$26.2 \pm 1.6$
<b>1.20</b>	$2.0 \pm 0.2$	<b>2.10</b>	$> 100$
<b>2.1</b>	$0.84 \pm 0.05$	<b>2.11</b>	$< 0.50$
<b>2.2</b>	$0.59 \pm 0.10$	<b>2.12</b>	$< 0.50$
<b>2.3</b>	$3.8 \pm 0.6$	<b>2.13</b>	$3.1 \pm 0.2$

On the other hand, when the amino acid moieties were replaced with some amino groups, the biological activity of abenquines was significantly enhanced. In particular, the presence of groups such as ethylpyrimidinyl and ethylpyrrolidinyl (as in compounds **2.1-2.3**) caused a ten-fold increase of the inhibitory potential (Figure 2.14C), with  $IC_{50}$  values lower than  $1 \mu\text{M}$  (Table 2.5). Being aliphatic agents, these substituents benzamide analogues **2.11-2.12** exhibited, as expected, an even higher effectiveness, promoting an almost complete suppression of cyanobacterial growth at  $1 \mu\text{M}$  (Figure 2.14D).

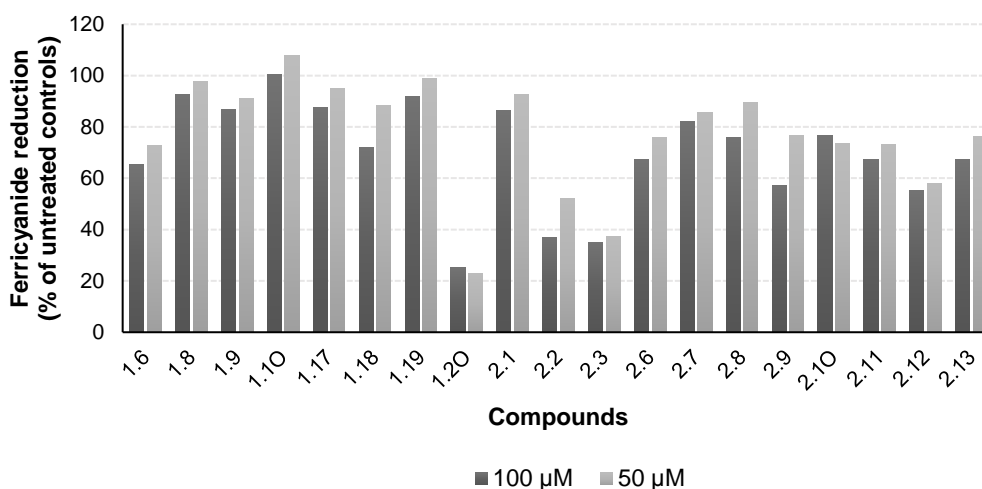
The biological activity of the two most potent analogues, **2.11** and **2.12**, was characterized in more detail. At first, the effect of increasing concentrations in the submicromolar range was assessed on a wider range of five cyanobacterial strains most commonly associated with blooms in freshwaters, namely *Nostoc* sp., *Anabaena* sp., *Microcystis aeruginosa*., *Synechocystis* sp., and *Synechococcus elongatus* [14]. Data, summarized in Table 2.6, clearly showed that all strains were highly susceptible to these aminoquinones, with  $IC_{50}$  values ranging from  $0.3$  to  $3.0 \mu\text{M}$ . The three unicellular, non-nitrogen-fixing strains belonging to the order *Chroococcales* were significantly more sensitive than the

two filamentous, nitrogen-fixing strains of the order *Nostocales*. Considering *Microcystis aeruginosa*, which is believed to be the most dangerous toxin-producing species [15], the effectiveness of compounds **2.11** and **2.12** was about one order of magnitude higher than that of some natural inhibitors recently described, comprising to two algicidal diketopiperazines produced by a *Chryseobacterium* sp. [16].

**Table 2.6.** Concentrations of **2.11** and **2.12** able to inhibit by 50% the growth of various organisms.

Species	Compound 2.11 IC <sub>50</sub> (μM)	Compound 2.12 IC <sub>50</sub> (μM)
<i>Nostoc</i> sp. PCC 7524-1	2.38 ± 0.14	2.6 ± 0.2
<i>Anabaena</i> sp. PCC 7120	3.10 ± 0.30	1.7 ± 0.2
<i>Microcystis aeruginosa</i> PCC 7941	0.76 ± 0.09	0.35 ± 0.04
<i>Synechocystis</i> sp. PCC 6803	0.38 ± 0.02	0.42 ± 0.04
<i>Synechococcus elongatus</i> PCC 6301	0.39 ± 0.03	0.31 ± 0.02

Further experiments were carried out to evaluate the ability of abenquines and analogues to inhibit chloroplastic electron transport, the light-driven reduction of ferricyanide by isolated thylakoid membranes, was measured in the absence and in the presence of a given compounds, as previously described [17]. The ability of compounds (**1.6-1.10**, **1.17-1.20**, **2.1-2.3**, **2.6-2.13**) to interfere with the light-driven ferricyanide reduction from isolated spinach chloroplasts is presented in Figure 2.15.



**Figure 2.15.** Effect of abenquines and analogues (**1.6-1.10**, **1.17-1.20**, **2.1-2.3**, **2.6-2.13**) on the photosynthetic electron transport chain in isolated spinach chloroplast in concentration of 50 and 100 μM.



In general, all the compounds have no apparent inhibition against the light-driven reduction of ferricyanide, except compound **1.20**, which exhibit inhibition of approximately 20% at concentration of 50  $\mu$ M. Contrary to what was expected, (except for compound **1.20**) no inhibition was observed and no relationship was found between this property and their biological activity as algicidal agents.

### 2.2.3. *Cytotoxicity assay*

Cancer has become a major cause of global mortality, with being approximately 12.7 million diagnosed cases per year. According to the World Health Organization, in 2012 approximately 14 million new cases of morbidity and mortality was reported worldwide along with 8.2 million cancer related deaths were recorded. Nevertheless, the number of new cases could rise about 70% along the next two decades [18]. In the developing world, cancer results from infections with viruses, bacteria, and parasites. For example, liver cancer associated with hepatitis B or human papillomavirus (HPV) cause cervical cancer [19]. On the other hand, the deadliest cancers are lung (1.59 million deaths), liver (745000 deaths), stomach (723000 deaths), colorectal (694000 deaths), breast (521000 deaths), and esophageal cancer (400000 deaths) [18].

Due to the high demand of varied treatments for each particular case, there is a tendency towards the search for new drugs to control these diseases. Historically, natural products have been present in pharmacopoeia, and have been used for the treatment and control of various diseases. Nowadays, 34% of medications are based on small molecules such as natural products or derivatives of them, furthermore, they have a diverse range of chemical structures [20].

In this context, a new series of abenquine analogues was employed to evaluate their cytotoxic profiles against several cancer cell lines.

### 2.2.4. *Biological activity*

The cytotoxic activity of abenquines and their analogues (**1.6-1.10**, **1.17-1.20**, **2.1-2.3** and **2.6-2.13**) was evaluated employing six human tumor cell lines (melanoma cells - 518A2; ovarian carcinoma - A2780; colon adenocarcinoma -

HT29; breast adenocarcinoma - MCF7; lung cancer - A549; hypopharyngeal carcinoma - FaDu) and non-malignant mouse fibroblasts (NIH 3T3) using the well-established photometric sulforhodamine B assay [21]. The results of these assays are summarized in Table 2.7.

Natural abenquines (**1.6-1.10**) and their analogues with benzamide block, bearing amino acid groups (**2.6-2.9**) revealed a low cytotoxicity ( $EC_{50} > 30 \mu\text{M}$  = cut-off of the assay) against the different cells lines tested (Table 2.7). However, the analogues with the acetamide block carrying the amino acid groups such as *D*-valine (**1.17**), an isomer of abenquine C (**1.9**) and *L*-methionine (**1.18**), revealed the activity of interest, especially the compound **1.17**. When their activity is compared to the isomer **1.9**, an improvement in the cytotoxic activity may be noticed. Hence, we could assume that analogues of abenquine possessing amino acid residue with a *D* configuration could modulate the cytotoxic activity of these compounds.

**Table 2.7.** Cytotoxicity for abenquines **1.6-1.10** and analogues **1.17-1.20**, **2.1-2.3** and **2.6-2.13** (cut-off in all experiments was  $30 \mu\text{M}$ ); employing human tumor cell lines and non-malignant mouse fibroblasts (NIH 3T3).

Comp.	$EC_{50}^a$						
	Melanoma (518A2)	Ovarian (A2780)	Colon (HT29)	Breast (MCF7)	Lung (A549)	Hyp. (FaDu)	NIH 3T3
<b>1.6</b>	> 30	> 30	> 30	> 30	> 30	> 30	> 30
<b>1.8</b>	> 30	> 30	> 30	> 30	> 30	> 30	> 30
<b>1.9</b>	> 30	> 30	> 30	> 30	> 30	> 30	> 30
<b>1.10</b>	> 30	> 30	> 30	> 30	> 30	> 30	> 30
<b>1.17</b>	7.1 ± 0.5	5.7 ± 1.8	12.7 ± 1.7	7.3 ± 0.4	6.5 ± 1.2	11.7 ± 0.5	6.6 ± 0.2
<b>1.18</b>	15.4 ± 0.5	5.9 ± 0.0	26.8 ± 1.3	15.2 ± 1.8	13.7 ± 0.3	16.7 ± 1.8	7.8 ± 0.2
<b>1.20</b>	9.7 ± 1.7	3.5 ± 0.7	18.6 ± 2.6	8.6 ± 0.5	7.4 ± 0.7	15.2 ± 1.3	6.6 ± 0.0
<b>2.1</b>	3.4 ± 0.1	1.0 ± 0.3	1.4 ± 0.1	0.9 ± 0.1	2.8 ± 0.3	2.2 ± 0.0	1.5 ± 0.0
<b>2.2</b>	2.5 ± 0.1	0.6 ± 0.0	0.9 ± 0.0	0.8 ± 0.0	2.0 ± 0.0	1.8 ± 0.0	1.2 ± 0.0
<b>2.3</b>	9.6 ± 0.3	1.4 ± 0.0	4.4 ± 0.7	2.2 ± 0.0	2.6 ± 0.0	5.8 ± 0.3	6.3 ± 0.2
<b>2.6</b>	> 30	> 30	> 30	> 30	> 30	> 30	> 30
<b>2.7</b>	> 30	> 30	> 30	> 30	> 30	> 30	> 30
<b>2.8</b>	> 30	> 30	> 30	> 30	> 30	> 30	> 30
<b>2.9</b>	> 30	> 30	> 30	> 30	> 30	> 30	> 30
<b>2.10</b>	n.s. <sup>b</sup>	n.s.	n.s.	n.s.	n.s.	n.s.	n.s.
<b>2.11</b>	1.7 ± 0.3	1.4 ± 0.0	0.9 ± 0.0	1.5 ± 0.1	1.5 ± 0.0	1.7 ± 0.1	2.0 ± 0.1
<b>2.12</b>	1.7 ± 0.1	1.3 ± 0.0	0.9 ± 0.0	1.5 ± 0.0	1.4 ± 0.0	1.7 ± 0.0	2.1 ± 0.0
<b>2.13</b>	6.5 ± 1.9	5.5 ± 0.7	3.5 ± 0.1	6.2 ± 0.2	5.4 ± 1.5	7.8 ± 0.5	7.5 ± 0.5
<b>B.A</b>	13.6±0.8	12.7±0.9	18.4±1.4	11.4±1.4	7.6±1.1	13.7±1.1	13.1±2.1

<sup>a</sup>  $EC_{50}$  values in  $\mu\text{M}$  from SRB assay after 96 h of treatment. <sup>b</sup> n.s. not soluble.

<sup>c</sup> B.A = Betulinic acid, positive control.

On the other hand, the analogues carrying the amino group, such as ethylpyrimidinyl and ethylpyrrolidinyl were the most active compounds. When comparing the abenquine analogues with the different blocks, namely acetamide (**2.1** and **2.2**) and benzamide (**2.11** and **2.12**), it can be noticed that there are no differences in their cytotoxic activity, and these compounds exhibited EC<sub>50</sub> values ranging between 0.6 and 3.4 μM (Table 2.7).

These results revealed that these compounds (**2.1**, **2.2**, **2.11** and **2.12**) are at least about 20 times more active than the natural abenquines (**1.6-1.10**). Nevertheless, they were not selective between malignant and non-malignant cells. While compound **2.10** was not soluble in the experiment of SRB, other analogues, such as **1.20**, **2.3**, and **2.13**, afforded satisfactory cytotoxicity. For example, an EC<sub>50</sub> = 3.5 and 1.4 μM, were revealed for compounds **1.20** and **2.3** when the ovarian cancer cell line A2780 was used (Table 2.7).

### 3. CONCLUSIONS

This chapter reported the synthesis of 11 new analogues of abenquines that were obtained in promising yields (45-85%) as well as the study of their potential of biological activity.

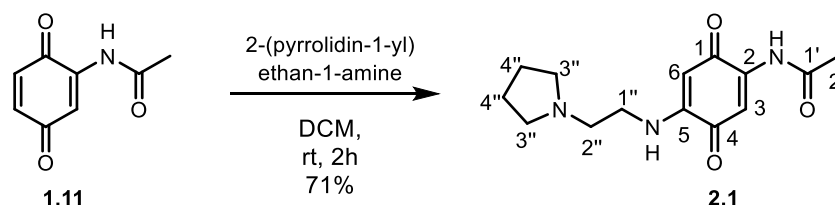
The results obtained through the efforts presented in this work indicated the potential of naturally-occurring abenquine quinones as new leads in the development of specific inhibitors of cyanobacterial proliferation. The appropriate replacement of the quinone core of the acetyl with a benzoyl moiety and of the amino acid with an ethylpyrimidinyl or an ethylpyrrolidinyl group increased their inhibitory potential up to 30-fold when compared to natural abenquines. The most active analogues exerted their effects in the range of 0.1 to 1  $\mu\text{M}$  against the following species: *Microcystis aeruginosa* PCC 7941, *Synechocystis* sp. PCC 6803, and *Synechococcus elongatus* PCC 6301. Therefore, these substances appear to be promising tools in the control of cyanobacterial blooms.

The ability of natural abenquines and their analogues as anticancer agents was also reported. From these data, the natural abenquines and their analogues, presenting a benzoyl group along with an amino acid group did not exhibit the cytotoxic activity of interest. However, the analogues carrying an ethylpyrimidinyl or an ethylpyrrolidinyl group, with either the acetyl group or benzoyl group, proved to be the most active compounds, affording  $\text{EC}_{50}$  values ranging between 0.6 and 3.4  $\mu\text{M}$ . Notably, the abenquine core was demonstrably able to act in both types of inhibitions of cyanobacteria as well as in the inhibition of cancer cells.

## 4. EXPERIMENTAL PART

### 4.1. Synthesis of analogue 2.1-2.3

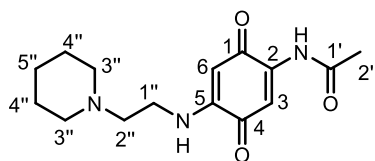
2-Acetamido-5-((2-(pyrrolidin-1-yl)ethyl)amino)-1,4-benzoquinone (**2.1**):



To a round bottom flask (25 mL) was added 2-acetamido-1,4-benzoquinone (**1.11**) (192 mg, 1.1 mmol) in dichloromethane (5 mL). Then was added 2-(pyrrolidin-1-yl)ethan-1-amine (0.14 mL, 1.1 mmol). The mixture was stirred at room temperature under oxygen atmosphere. Initially, there was a change of color solution from yellow to dark red. The reaction was monitored by TLC and stopped after 2 h. The reaction mixture was concentrated under reduced pressure. The obtained residue was purified by silica gel column chromatography with Hex/EtOAc 1:1 v/v and EtOAc/MeOH 1:0.5 v/v to give red crystals in 71% (216 mg, 0.78 mmol). Mp: 190-192 °C. IR: ( $\nu_{\max}/\text{cm}^{-1}$ ) 3303, 3260, 2961, 2778, 1712, 1651, 1578, 1474, 1170, 798.  $^1\text{H}$  NMR (DMSO- $d_6$ , 300 MHz)  $\delta$ : 1.66-1.75 (m, 4H, H-4''), 1.79 (br s, 2H, H-3''a), 2.22 (s, 3H, H-2'), 2.52-2.54 (m, 2H, H-3''b), 2.65 (t,  $J = 6.4$  Hz, 2H, H-2''), 3.26 (t,  $J = 6.4$  Hz, 2H, H-1''), 5.45 (s, 1H, H-6), 7.21 (s, 1H, H-3), 9.63 (br s, 1H, N-H).  $^{13}\text{C}$  NMR (DMSO- $d_6$ , 75 MHz)  $\delta$ : 23.2 (C-4''), 24.7 (C-2'), 40.8 (C-1''), 52.8 (C-2''), 53.5 (C-3''), 93.6 (C-6), 109.0 (C-3), 142.4 (C-2), 148.0 (C-5), 171.4 (C-1'), 178.1 (C-1), 183.6 (C-4). EIMS  $m/z$  calculated for  $\text{C}_{14}\text{H}_{19}\text{N}_3\text{O}_3$   $[\text{M}+\text{H}]^+$ : 278.1499, found: 278.4  $[\text{M}+\text{H}]^+$ , 277.5  $[\text{M}]^-$ . Elemental analysis: calculated C 60.63%; H 6.91%; N 15.15%; found C 59.80%; H 7.21%; N 15.07%.

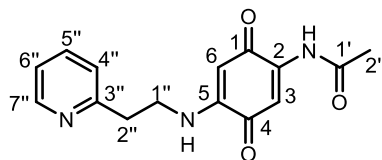
Compounds **2.2-2.3** were synthesized using a method similar to that of **2.1**.

**2-Acetamido-5-((2-(piperidin-1-yl)ethyl)amino)-1,4-benzoquinone (2.2):**



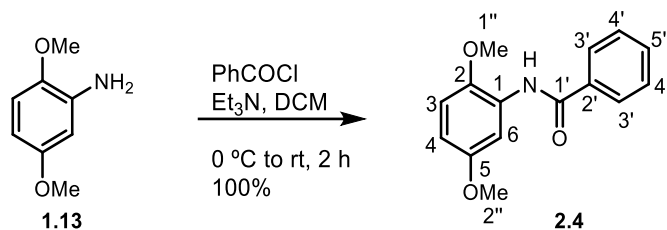
Quantities used in the reaction: amine (0.08 g, 0.59 mmol); compound **1.11** (0.09 g, 0.59 mmol). Red solid. Mp: 211-213 °C. Yield: 85% (145 mg, 0.50 mmol). IR: ( $\nu_{\max}/\text{cm}^{-1}$ ) 3303, 3260, 2930, 1712, 1656, 1621, 1582, 1491, 1179, 780.  $^1\text{H}$  NMR (DMSO- $d_6$ , 300 MHz)  $\delta$ : 1.33-1.36 (m, 2H, H-5''), 1.44-1.49 (m, 4H, H-4'') 2.18 (s, 3H, H-2'), 2.32-2.39 (m, 4H, H-3''), 2.45 (t,  $J = 6.5$  Hz, 2H, H-2''), 3.19 (dd,  $J = 10.7; 5.8$  Hz, 2H, H-1''), 5.40 (s, 1H, H-6), 7.17 (s, 1H, H-3), 9.59 (br s, 1H, N-H).  $^{13}\text{C}$  NMR (DMSO- $d_6$ , 75 MHz)  $\delta$ : 24.0 (C-5''), 24.6 (C-2'), 25.6 (C-4''), 39.0 (C-1''), 53.8 (C-3''), 55.5 (C-2''), 93.6 (C-6), 108.9 (C-3), 142.3 (C-2), 147.9 (C-5), 171.3 (C-1'), 178.0 (C-1), 183.5 (C-4). EIMS  $m/z$  calculated for  $\text{C}_{15}\text{H}_{21}\text{N}_3\text{O}_3$   $[\text{M}+\text{H}]^+$ : 292.1656, found: 292.4  $[\text{M}]^+$ . Elemental analysis: calculated C 61.84, H 7.27, N 14.42%; found C 61.62; H 7.11; N 15.01%.

**2-Acetamido-5-((2-(pyridin-2-yl)ethyl)amino)-1,4-benzoquinone (2.3):**



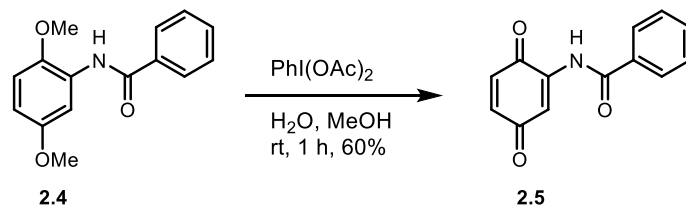
Quantities used in the reaction: amine (0.07 g, 0.60 mmol); compound **1.11** (0.09 g, 0.60 mmol). Red solid. Mp: 246-248 °C. Yield: 70% (120 mg, 0.42 mmol). IR: ( $\nu_{\max}/\text{cm}^{-1}$ ) 3273, 2939, 1703, 1651, 1569, 1482, 1179, 780.  $^1\text{H}$  NMR (DMSO- $d_6$ , 300 MHz)  $\delta$ : 2.19 (s, 3H, H-2'), 3.03 (t,  $J = 6.8$  Hz, 2H, H-2''), 3.51 (dd,  $J = 13.4; 6.8$  Hz, 2H, H-1''), 5.43 (s, 1H, H-6), 7.16 (s, 1H, H-3), 7.22 (dd,  $J = 7.5; 4.8$  Hz, 1H, H-6''), 7.29 (d,  $J = 7.5$  Hz, 1H, H-4''), 7.59-7.66 (m, 1H, N-H), 7.70 (td,  $J = 7.5; 1.7$  Hz, 1H, H-5''), 8.50 (d,  $J = 4.8$  Hz, 1H, H-7''), 9.45 (br s, 1H, N-H).  $^{13}\text{C}$  NMR (DMSO- $d_6$ , 75 MHz)  $\delta$ : 25.1 (C-2'), 36.0 (C-1''), 42.2 (C-2''), 94.2 (C-6), 109.6 (C-3), 122.3 (C-6''), 123.9 (C-4''), 137.2 (C-5''), 142.7 (C-2), 148.6 (C-5), 149.7 (C-7''), 159.1 (C-3''), 171.6 (C-1'), 178.6 (C-1), 184.0 (C-4). EIMS  $m/z$  calculated for  $\text{C}_{15}\text{H}_{15}\text{N}_3\text{O}_3$   $[\text{M}+\text{H}]^+$ : 286.1, found 286.0  $[\text{M}+\text{H}]^+$ , 285.4  $[\text{M}]^-$ . Elemental analysis: calculated C 63.15%; H 5.30%; N 14.73%; found C 63.01%; H 5.58%; N 14.43%.

#### 4.2. Synthesis of *N*-(2,5-dimethoxyphenyl)benzamide 2.4



To a round-bottomed flask (100 mL) were added 2,5-dimethoxyaniline **1.13** (2.0 g, 13.1 mmol) and triethylamine (2.1 mL, 15.2 mmol) dissolved in dichloromethane (50 mL). Then, to the stirred solution was added benzoyl chloride (1.8 mL, 15.2 mmol) and was left stirring at 0 °C for two hours. The resulting solution was warmed to room temperature over 30 min. When TLC analysis revealed the consumption of the starting material, the mixture was washed with water (3 x 50 mL), saturated aqueous sodium hydrogen carbonate solution (100 mL) and brine (100 mL), and then dried (MgSO<sub>4</sub>). Then the solution was filtered and concentrated under reduced pressure to give the compound as a brown solid. The residue was purified by column chromatography on silica gel, eluting with ethyl acetate:hexane 1:3 v/v, to give the title compound as a white solid in 100% (3.3 g, 12.84 mmol). Mp: 83-84 °C (lit. [22], 82-84°C). IR: ( $\nu_{\max}/\text{cm}^{-1}$ ) 3333, 2930, 1660, 1530, 697. <sup>1</sup>H NMR (CDCl<sub>3</sub>, 300 MHz)  $\delta$ : 3.82 and 3.88 (s, 6H, H-1'' and H-2''), 6.61 (d,  $J = 8.9$ , Hz, 1H, H-4), 6.83 (d,  $J = 8.9$  Hz, 1H, H-3), 7.47-7.57 (m, 3H, H-4' and H-5'), 7.89 (d,  $J = 6.8$  Hz, 2H, H-3'), 8.28 (s, 1H, H-6), 8.59 (br s, 1H, N-H). <sup>13</sup>C NMR (CDCl<sub>3</sub>, 75 MHz)  $\delta$ : 55.9 and 56.4 (C-1'' and C-2''), 106.0 (C-6), 109.0 (C-4), 110.8 (C-3), 127.1 (C-1), 128.5 (C-3'), 128.9 (C-4'), 131.8 (C-5'), 135.3 (C-2'), 142.4 (C-2), 154.0 (C-5), 165.3 (C-1').

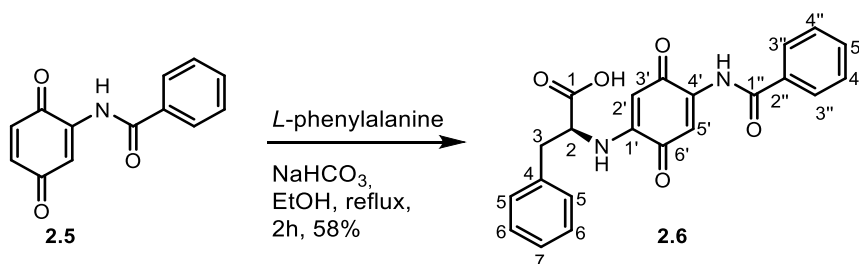
#### 4.3. Synthesis of 2-benzamido-1,4-benzoquinone **2.5**



To a round-bottomed flask (50 mL) was added 2,5-dimethoxyphenyl benzamide **2.4** (1.0 g, 3.9 mmol) in water (25 mL) and MeOH (625  $\mu\text{L}$ ). The mixture was stirred until the suspension was homogenized and then was added slowly phenyliodine diacetate (1.9 g, 5.9 mmol). The resulting suspension was stirred for 1.5 h when TLC analysis revealed the consumption of the starting material, the mixture solution was diluted with water (50 mL) and extracted with dichloromethane (3 x 50 mL). The combined extracts were washed with water (50 mL), saturated aqueous sodium hydrogen carbonate solution (50 mL), dried ( $\text{Na}_2\text{SO}_4$ ), filtered and the solvent was concentrated under reduced pressure. The compound was used for future reactions without previously purification.

#### 4.4. Synthesis of analogues **2.6-2.9**

(4-benzamido-3,6-dioxocyclohexa-1,4-dien-1-yl)-L-phenylalanine (**2.6**):



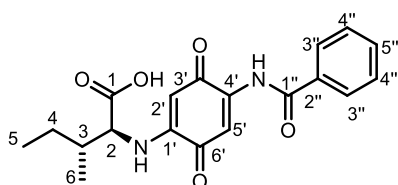
To a round bottom flask (25 mL) was added the L-phenylalanine (60 mg, 0.31 mmol) and sodium bicarbonate (52 mg, 0.62 mmol), dissolved in 5 mL of EtOH. Then was added 2-benzamido-1,4-benzoquinone (**2.5**) (70 mg, 0.31 mmol). The mixture was stirred at room temperature under an oxygen atmosphere. Initially, there was a change of solution color from yellow to dark red. The reaction was monitored by TLC and stopped after 2 h. The reaction mixture was filtered to remove the sodium bicarbonate salt and washed with ethanol.



Consequently, the resulting residual mixture was acidified to pH 4-5 with hydrochloric acid 1 M, and dissolved in 5.0 mL of distilled water. The mixture was extracted with EtOAc (3 x 25 mL). The organic extracts were combined, and the resulting organic phase was dried over Na<sub>2</sub>SO<sub>4</sub>, filtered and the solvent concentrated under reduced pressure. The obtained residue was purified by silica gel column chromatography eluting at first with Hex/EtOAc 1:1 v/v and then with acetone/methanol 1:1 v/v to give a solid as red crystals in 58% yield (70 mg, 0.18 mmol). Mp: > 180 °C (Decomposition). IR: ( $\nu_{\max}/\text{cm}^{-1}$ ) 3476, 3329, 2930, 1695, 1660, 1591, 1482, 1291, 693. <sup>1</sup>H NMR (CD<sub>3</sub>OD, 400 MHz)  $\delta$ : 3.08 (dd,  $J = 13.5$ ; 6.8 Hz, 1H, H-3a), 3.26 (d,  $J = 3.6$  Hz, 1H, H-3b), 4.09 (br s, 1H, H-2), 5.32 (s, 1H, H-2'), 7.15-7.24 (m, 5H, H5-7), 7.30 (s, 1H, H-5'), 7.49 (br t,  $J = 7.5$  Hz, 2H, H-4''), 7.59 (br t,  $J = 7.5$  Hz, 1H, H-5''), 7.85 (d,  $J = 7.5$  Hz, 2H, H-3''). <sup>13</sup>C NMR (CD<sub>3</sub>OD, 100 MHz)  $\delta$ : 38.8 (C-3), 94.8 (C-2'), 110.5 (C-5'), 127.7 (C-7), 128.4 (C-3''), 129.3 (C-4''), 130.0 (C-6), 130.4 (C-5), 134.0 (C-5''), 134.4 (C-2''), 138.5 (C-4), 143.0 (C-4'), 148.9 (C-1'), 167.5 (C-1''), 179.8 (C-3'), 184.4 (C-6'). EIMS  $m/z$  calculated for C<sub>22</sub>H<sub>18</sub>N<sub>2</sub>O<sub>5</sub> [M+H]<sup>+</sup>: 391.1, found 389.5 [M-H]<sup>-</sup>. Elemental analysis: calculated C 67.69%; H 4.65%; N 7.18%; found C 67.40%; H 4.84%; N 7.01%.

Compounds **2.7-2.9** were synthesized using a method similar to that of **2.6**.

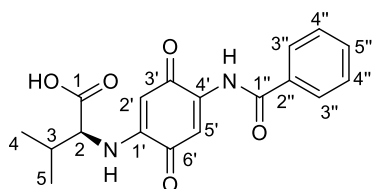
*2-((4-benzamido-3,6-dioxocyclohexa-1,4-dien-1-yl)amino)-3-methylpentanoic acid (2.7):*



Quantities used in the reaction: amino acid (0.02 g, 0.14 mmol); compound **2.5** (0.03 g, 0.14 mmol). Red solid. Mp: > 178 °C (Decomposition). Yield: 75% (40 mg, 0.11 mmol). IR: ( $\nu_{\max}/\text{cm}^{-1}$ ) 3472, 3329, 2961, 1656, 1591, 1478, 702. <sup>1</sup>H NMR (CD<sub>3</sub>OD, 400 MHz)  $\delta$ : 0.95-0.97 (m, 6H, H-5/H-6), 1.26-1.36 (m, 1H, H-3), 1.64-1.70 (m, 1H, H-4a), 1.94-1.96 (m, 1H, H-4b), 3.78 (d,  $J = 2.6$  Hz, 1H, H-2), 5.44 (s, 1H, H-2'), 7.34 (s, 1H, H-5'), 7.49 (br t,  $J = 7.5$  Hz, 2H, H-4''), 7.59 (br t,  $J = 7.5$  Hz, 1H, H-5''), 7.85 (d,  $J = 7.5$  Hz, 2H, H-3''). <sup>13</sup>C NMR (CD<sub>3</sub>OD, 100 MHz)  $\delta$ : 12.1 (C-5), 16.2 (C-6), 26.8 (C-4), 38.9 (C-3), 94.7 (C-2'), 110.5 (C-5'), 128.4 (C-3''), 130.0 (C-4''), 134.0 (C-5''), 134.4 (C-

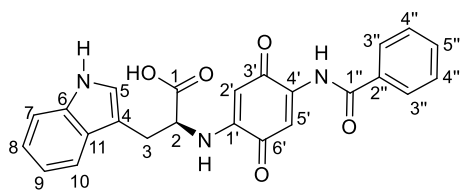
2''), 143.2 (C-4'), 149.1 (C-1'), 167.4 (C-1''), 179.7 (C-3'), 184.4 (C-6'). EIMS  $m/z$  calculated for  $C_{19}H_{20}N_2O_5$   $[M+H]^+$ : 357.1, found 355.3  $[M-H]^-$ . Elemental analysis: calculated C 64.04%; H 5.66%; N 7.86%; found C 63.86%; H 5.91%; N 7.53%.

*(4-benzamido-3,6-dioxocyclohexa-1,4-dien-1-yl)valine (2.8)*:



Quantities used in the reaction: amino acid (0.03 g, 0.25 mmol); compound **2.5** (0.06 g, 0.25 mmol). Red solid. Mp: > 180 °C (Decomposition). Yield: 70% (60 mg, 0.18 mmol). IR: ( $\nu_{max}/cm^{-1}$ ) 3442, 3333, 2961, 1695, 1660, 1591, 1481, 1179, 693.  $^1H$  NMR ( $CD_3OD$ , 400 MHz)  $\delta$ : 1.00 (d,  $J$  = 6.7 Hz, 3H, H-5), 1.04 (d,  $J$  = 6.7 Hz, 3H, H-4), 2.21-2.30 (m, 1H, H-3), 3.74 (d,  $J$  = 4.6 Hz, 1H, H-2), 5.49 (s, 1H, H-2'), 7.38 (s, 1H, H-5'), 7.52 (br t,  $J$  = 7.5 Hz, 2H, H-4''), 7.61 (br t,  $J$  = 7.5 Hz, 1H, H-5''), 7.88 (d,  $J$  = 7.5 Hz, 2H, H-3'').  $^{13}C$  NMR ( $CD_3OD$ , 100 MHz)  $\delta$ : 19.0 (C-5), 19.7 (C-4), 32.6 (C-3), 94.9 (C-2'), 110.6 (C-5'), 128.4 (C-3''), 130.1 (C-4''), 134.0 (C-5''), 134.5 (C-2''), 143.2 (C-4'), 149.5 (C-1'), 167.5 (C-1''), 180.0 (C-3'), 184.4 (C-6'). EIMS  $m/z$  calculated for  $C_{18}H_{18}N_2O_5$   $[M+H]^+$ : 343.1, found 341.1  $[M-H]^-$ . Elemental analysis: calculated C 63.15%; H 5.30%; N 8.18%; found C 62.96%; H 5.53%; N 8.01%.

*(4-benzamido-3,6-dioxocyclohexa-1,4-dien-1-yl)tryptophan (2.9)*:

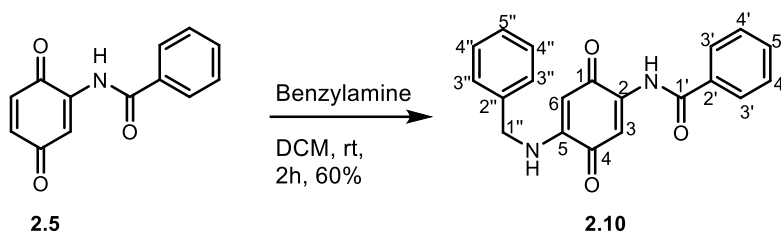


Quantities used in the reaction: amino acid (0.05 g, 0.20 mmol); compound **2.5** (0.05 g, 0.20 mmol). Red solid. Mp: > 160 °C (Decomposition). Yield: 65% (55 mg, 0.13 mmol). IR: ( $\nu_{max}/cm^{-1}$ ) 3420, 3333, 2926, 1696, 1582, 1487, 1335, 706.  $^1H$  NMR ( $CD_3OD$ , 200 MHz)  $\delta$ : 3.42-3.52 (m, 2H, H3), 4.15 (dd,  $J$  = 6.7; 4.5 Hz, 1H, H-2), 5.29 (s, 1H, H-2'), 6.91-7.06 (m, 2H, H-8 and H-9), 7.09 (s, 1H, H-5), 7.24 (s, 1H, H-5'), 7.28 (br s, 1H, H-7), 7.42-7.59 (m, 4H, H4''-5'' and H-10), 7.82 (d,  $J$  = 7.0 Hz, 2H, H-3'').  $^{13}C$  NMR ( $CD_3OD$ , 50 MHz)  $\delta$ : 29.0 (C-3), 59.7 (C-2), 94.6 (C-2'), 110.4 (C-5'), 111.2 (C-4), 112.2 (C-7), 119.3 (C-10), 119.8 (C-9), 122.3 (C-8), 124.6 (C-5), 128.3 (C-3''), 129.0 (C-11), 130.0 (C-4''), 134.0 (C-5'') 134.4 (C-2''), 137.9 (C-6), 143.0 (C-4'), 149.2 (C-1'), 167.4 (C-1''), 177.0 (C-1), 179.6 (C-3'), 184.4 (C-6'). EIMS  $m/z$  calculated for  $C_{24}H_{19}N_3O_5$   $[M+H]^+$ : 430.1397, found 428.1

[M-H]<sup>-</sup>. Elemental analysis: calculated C 67.13%; H 4.46%; N 9.79%; found C 66.86%; H 4.61%; N 9.68%.

#### 4.5. Synthesis of Analogues 2.10-2.13

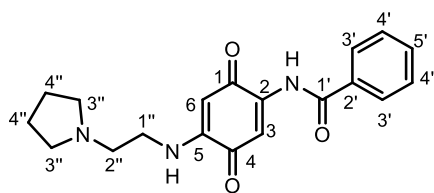
*2-benzamido-5-benzylamino-1,4-benzoquinone (2.10)*:



To a round bottom flask (25 mL) was added *2-benzamido-1,4-benzoquinone (2.5)* (150 mg, 0.6 mmol) in dichloromethane (5 mL). Then was added benzylamine (0.07 mL, 0.6 mmol). The mixture was stirred at room temperature under oxygen atmosphere. Initially, there was a change of solution color from yellow to dark red. The reaction was monitored by TLC and stopped after 2 h. The reaction mixture was concentrated under reduced pressure. The obtained residue was purified by silica gel column chromatography with Hex/EtOAc 3:1 v/v to give red crystals in 70% yield (120 mg, 0.4 mmol). Mp: 193-195 °C. IR: ( $\nu_{\text{max}}/\text{cm}^{-1}$ ) 3320, 3238, 2939, 1699, 1660, 1582, 1478, 702. <sup>1</sup>H NMR (CDCl<sub>3</sub>, 400 MHz)  $\delta$ : 4.35 (d,  $J = 5.1$  Hz, 2H, H-1''), 5.53 (s, 1H, H-6), 6.52 (br s, 1H, N-H), 7.27-7.37 (m, 5H, H-3''-5''), 7.48-7.59 (m, 4H, H-4', H-5' and H-3), 7.90 (d,  $J = 7.2$  Hz, 2H, H-3'), 9.46 (s, 1H, N-H). <sup>13</sup>C NMR (CDCl<sub>3</sub>, 100 MHz)  $\delta$ : 46.9 (C-1''), 95.0 (C-6), 109.9 (C-3), 127.5 (C-3''), 127.7 (C-4''), 128.4 (C-5''), 129.1 (C-3'), 129.2 (C-4'), 133.0 (C-5'), 133.3 (C-2'), 135.4 (C-2''), 141.5 (C-2), 148.1 (C-5), 165.8 (C-1'), 179.3 (C-1), 183.4 (C-4). EIMS  $m/z$  calculated for C<sub>20</sub>H<sub>16</sub>N<sub>2</sub>O<sub>3</sub> [M+H]<sup>+</sup>: 333.1, found 333.1 [M+H]<sup>+</sup>. Elemental analysis: calculated C 72.27%; H 4.85%; N 8.43%; found C 71.79%; H 4.99%; N 8.59%.

Compounds **2.11-2.13** were synthesized using a method similar to that of **2.10**.

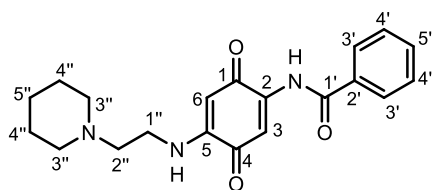
*2-Benzamido-5-((2-(pyrrolidin-1-yl)ethyl)amino)-1,4-benzoquinone (2.11)*:



Quantities used in the reaction: amine (0.04 g, 0.37 mmol); compound **2.5** (0.08 g, 0.37 mmol). Red solid. Mp: 155-157 °C. Yield: 65% (80 mg, 0.24 mmol). IR: ( $\nu_{\max}/\text{cm}^{-1}$ ) 3359, 3307, 2926,

1695, 1660, 1595, 1521, 1313, 697.  $^1\text{H}$  NMR ( $\text{CDCl}_3$ , 400 MHz)  $\delta$ : 1.80 (br s, 4H, H-4''), 2.56 (br s, 4H, H-3''), 2.78 (t,  $J = 5.9$  Hz, 2H, H-2''), 3.22 (br s, 2H, H-1''), 5.46 (s, 1H, H-6), 6.81 (br s, 1H, N-H), 7.48-7.59 (m, 4H, H-4', H-5' and H-3), 7.91 (d,  $J = 7.8$  Hz, 2H, H-3'), 9.51 (br s, 1H, N-H).  $^{13}\text{C}$  NMR ( $\text{CDCl}_3$ , 100 MHz)  $\delta$ : 23.6 (C-4''), 41.0 (C-1''), 53.1 (C-3''), 53.8 (C-2''), 94.0 (C-6), 109.8 (C-3), 127.4 (C-3'), 129.0 (C-4'), 132.9 (C-5'), 133.4 (C-2'), 141.6 (C-2), 148.5 (C-5), 165.8 (C-1'), 178.8 (C-1), 183.3 (C-4). EIMS  $m/z$  calculated for  $\text{C}_{19}\text{H}_{21}\text{N}_3\text{O}_3$   $[\text{M}+\text{H}]^+$ : 340.1, found 340.0  $[\text{M}+\text{H}]^+$ . Elemental analysis: C 67.24%; H 6.24%; N 12.38%; found C 66.97%; H 6.51%; N 12.00%.

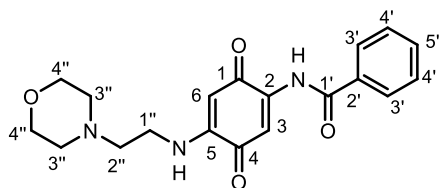
**2-Benzamido-5-((2-(piperidin-1-yl)ethyl)amino)-1,4-benzoquinone (2.12):**



Quantities used in the reaction: amine (0.04 g, 0.29 mmol); compound **2.5** (0.07 g, 0.29 mmol). Red solid. Mp: 170-171 °C. Yield: 70% (70 mg, 0.20 mmol). IR: ( $\nu_{\max}/\text{cm}^{-1}$ ) 3372, 3312, 2930,

2813, 1695, 1660, 1595, 1521, 1309, 697.  $^1\text{H}$  NMR ( $\text{CDCl}_3$ , 400 MHz)  $\delta$ : 1.45 (br s, 2H, H-5''), 1.60 (br s, 4H, H-4''), 2.41 (br s, 4H, H-3''), 2.61 (t,  $J = 5.0$  Hz, 2H, H-2''), 3.19 (d,  $J = 5.0$  Hz, 2H, H-1''), 5.45 (s, 1H, H-6), 6.88 (br s, 1H, N-H), 7.50-7.59 (m, 4H, H-4', H-5' and H-3), 7.91 (d,  $J = 7.3$  Hz, 2H, H-3'), 9.52 (s, 1H, N-H).  $^{13}\text{C}$  NMR ( $\text{CDCl}_3$ , 100 MHz)  $\delta$ : 24.3 (C-5''), 25.9 (C-4''), 38.9 (C-1''), 54.2 (C-3''), 55.6 (C-2''), 94.0 (C-6), 109.8 (C-3), 127.4 (C-3'), 129.0 (C-4'), 132.9 (C-5'), 133.4 (C-2'), 141.6 (C-2), 148.4 (C-5), 165.7 (C-1'), 178.7 (C-1), 183.3 (C-4). EIMS  $m/z$  calculated for  $\text{C}_{20}\text{H}_{23}\text{N}_3\text{O}_3$   $[\text{M}+\text{H}]^+$ : 354.1, found 354.6  $[\text{M}+\text{H}]^+$ . Elemental analysis: calculated C 67.97%; H 6.56%; N 11.89%; found C 67.70%; H 6.64%; N 11.61%.

*2-Benzamido-5-((2-morpholinoethyl)amino)-1,4-benzoquinone (2.13):*



Quantities used in the reaction: amino acid (0.04 g, 0.32 mmol); compound **2.5** (0.09 g, 0.32 mmol). Red solid. Mp: 170-172 °C. Yield: 62% (70 mg, 0.20 mmol). IR: ( $\nu_{\max}/\text{cm}^{-1}$ ) 3368, 3307,

2926, 2843, 1699, 1660, 1604, 1508, 1296, 1109, 702.  $^1\text{H}$  NMR ( $\text{CDCl}_3$ , 400 MHz)  $\delta$ : 2.49 (br s, 4H, H-4''), 2.67 (t,  $J = 5.3$  Hz, 2H, H1''), 3.21 (d,  $J = 4.9$  Hz, 2H, H-2''), 3.73 (br s, 4H, H-3''), 5.45 (br s, 1H, H-6), 6.78 (br s, 1H, N-H), 7.49-7.59 (m, 4H, H-4', H5' and H-3), 7.91 (d,  $J = 7.3$  Hz, 2H, H-3'), 9.50 (s, 1 H, N-H).  $^{13}\text{C}$  NMR ( $\text{CDCl}_3$ , 100 MHz)  $\delta$ : 38.5 (C-1''), 53.2 (C-3''), 55.4 (C-2''), 66.8 (C-4''), 94.2 (C-6), 109.7 (C-3), 127.4 (C-3'), 129.0 (C-4'), 132.9 (C-5'), 133.3 (C-2'), 141.6 (C-2), 148.3 (C-5), 165.7 (C-1'), 178.8 (C-1), 183.2 (C-4). EIMS  $m/z$  calculated for  $\text{C}_{19}\text{H}_{21}\text{N}_3\text{O}_4$   $[\text{M}+\text{H}]^+$ : 356.1, found 356.7  $[\text{M}+\text{H}]^+$ . Elemental analysis: C 64.21%; H 5.96%; N 11.82%; calculated C 63.92%; H 6.17%; N 11.58%.

## **4.6. Biological assay**

### *4.6.1. Cyanobacterial Cultures*

This study was performed by professor Giuseppe Forlani from University of Ferrara - Italy.

Cyanobacterial strains, as listed in Table 2.6, were grown in Bg11 mineral medium as described in reference [23]. Growth was followed by measuring chlorophyll concentration. Culture aliquots (0.5–1.0 mL) were withdrawn, and cells were sedimented by centrifugation for 3 min at 14000 x g. Pellets were resuspended with 1.0 mL of methanol, and solubilization was allowed to proceed for 30 min in the dark, with occasional mixing. Samples were then centrifuged again, and chlorophyll content in the supernatant was estimated spectrophotometrically at 663 nm. Late log-grown cells were sedimented by centrifugation 5 min at 4,000 x g, and used to inoculate 96-well plates, 0.2 mL per well, to an initial density of about 1.0 mg L<sup>-1</sup> chlorophyll. Aliquots (2 µL) of suitable dilutions of a given compound in DMSO were added so as to obtain final concentrations ranging from 0.1 to 100 µM. A complete randomized design with four replications was adopted. Cell growth in each well was followed for one week by daily determination of absorbance using a Ledetect 96 plate reader (Labexim, Lengau, Austria) equipped with a LED plugin at 660 nm. Following logarithmic transformation of data, growth constants were calculated and expressed as percent of the mean value for controls (no less than 8 replications) treated with the same volume of DMSO. Mean values ± SE over replicates are reported. The concentrations causing 50% inhibition (IC<sub>50</sub>) were estimated by nonlinear regression analysis using Prism 6 for Windows, version 6.03 (GraphPad Software).

### *4.6.2. Cytotoxicity assay.*

This study was performed by professor René Csuk from University Martin Luther - Germany.

The cytotoxicity of the compounds was evaluated using the sulforhodamine-B (SRB, procured from ABCR, Germany) micro-culture

colorimetric assay. This assay is grounded on the proportional binding of a rhodamine dye to surface membrane proteins, and there is a linear relationship between cell density and optical density [21]. Exponentially growing cells were seeded into a 96-well plate on day 0 at the appropriate cell densities to prevent confluence of the cells during the period of experiment. After 24 hours, the cells were treated with serial dilutions of the compounds (0-30  $\mu\text{M}$ ) for 96 hours. The final concentration of DMSO never exceeded 0.5%, which was non-toxic to the cells. The percentages of surviving cells relative to untreated controls were determined 96 h after the beginning of drug exposure. After 96 hours of treatment, the supernatant medium was discarded from the 96-well plates, and the cells were fixed with 10% TCA. For a thorough fixation, the plates were allowed to rest at 4 °C. After fixation, the cells were washed in a strip washer. The washing was done four times with water using alternate dispensing and aspiration procedures. The plates were dyed with 100  $\mu\text{L}$  of 0.4% SRB for about 20 min. After dying, the plates were washed with 1% acetic acid to remove the excess of the dye and allowed to air-dry overnight. Tris base solution (100  $\mu\text{L}$ , 10 mM) was added to each well and absorbance was measured at  $\lambda = 570 \text{ nm}$  (using a 96 well plate reader, Tecan Spectra, Crailsheim, Germany).  $\text{EC}_{50}$  values were calculated from semi logarithmic dose response curves by non-linear regression applying four parametrical Hill-slope equation. Values are given with a confidence interval CI = 95%; usually 7-13 dosage points were used.

## 5. REFERENCES

- [1] E.A. Crane, K. Gademann, *Angew. Chemie - Int. Ed.* 55 (2016) 3882–3902.
- [2] J. Delaney, E. Clarke, D. Hughes, M. Rice, *Drug Discov. Today.* 11 (2006) 839–845.
- [3] L.C.A. Barbosa, *Espectroscopia no Infravermelho na caracterização de compostos orgânicos*, Editora UFV, 2011.
- [4] R.M. Silverstein, F.X. Webster, D.J. Kiemle, *Identificação espectrométrica de compostos orgânicos*, LTC, 2007.
- [5] G.A. Codd, L.F. Morrison, J.S. Metcalf, *Toxicol. Appl. Pharmacol.* 203 (2005) 264–272.
- [6] D. Singh, J. Khattar, G. Kaur, Y. Singh, *Annu. Res. Rev. Biol.* 9 (2016) 1–39.
- [7] A.A. Issa, M.H. Abd-Alla, T. Ohyama, *Adv. Biol. Ecol. Nitrogen Fixat.* (2014) 282.
- [8] K. Krithika, R.A. Mella-Herrera, J.G. Golden, *Cold Spring Harb. Perspect. Biol.* 2 (2009) 1–19.
- [9] H.W. Paerl, T.G. Otten, *Microb. Ecol.* 65 (2013) 995–1010.
- [10] K.E. Havens, *Adv. Exp. Med. Biol.* 619 (2008) 733–747.
- [11] Z. Li, M. Geng, H. Yang, *Appl. Microbiol. Biotechnol.* 99 (2014) 981–990.
- [12] C. Lugomela, H.B. Pratap, Y.D. Mgaya, *Harmful Algae.* 5 (2006) 534–541.
- [13] S.J. Hoeger, B.C. Hitzfeld, D.R. Dietrich, *Toxicol. Appl. Pharmacol.* 203 (2005) 231–242.
- [14] J.M. O’Neil, T.W. Davis, M.A. Burford, C.J. Gobler, *Harmful Algae.* 14 (2012) 313–334.
- [15] P.J. Oberholster, A.-M. Botha, J.U. Grobbelaar, *African J. Biotechnol.* 3 (2004) 159–168.
- [16] X. Guo, X. Liu, J. Pan, H. Yang, *Sci. Rep.* 5 (2015) 14720.
- [17] J.O.S. Varejão, L.C.A. Barbosa, C.R.A. Maltha, M.R. Lage, M. Lanznaster, J.W.M. Carneiro, G. Forlani, *Electrochim. Acta.* 120 (2014) 334–343.
- [18] World Health Organization, (2014).
- [19] H. Varmus, E.L. Trimble, *Science (80).* 3 (2011) 1–4.
- [20] A.L. Harvey, R. Edrada-Ebel, R.J. Quinn, *Nat. Rev. Drug Discov.* 14 (2015) 111–129.
- [21] P. Skehan, R. Storeng, D. Scudiero, A. Monks, D. Vistica, J.T. Warren, H. Bokesch, M.R. Boyd, *J. National Cancer Inst.* 82 (1990) 1107–1112.
- [22] C.C. Nawrat, W. Lewis, C.J. Moody, *J. Org. Chem.* 76 (2011) 7872–7881.
- [23] G. Forlani, M. Bertazzini, D. Barillaro, R. Rippka, *New Phytol.* 205 (2015) 160–171.



## **CHAPTER 3**

# **SYNTHETIC ANALOGUES OF ABENQUINES AS INHIBITORS OF THE PHOTOSYNTHETIC ELECTRON TRANSPORT CHAIN**

## 1. INTRODUCTION

Herbicides are chemical compounds that disrupt physiological processes in a plant [1,2]. Since the introduction of synthetic herbicide 2,4-dichlorophenoxyacetic acid (2,4-D) in 1946, herbicides have become the primary tool for weed management [3,4].

Hence, over the last years herbicides have contributed considerably to increase crop yields providing a highly effective, economical and relatively simple means of weed control and they have been highly successful [3,5]. They can be operated through different mechanisms such as the disruption of the production of amino acids and fatty acids or the arresting of microtubule formation or the electron transport chain of photosynthesis [2]. However, the continuous use of the same herbicide with a known mechanism of action will inevitably lead to the selection of weed populations resistant to that herbicide or mechanism of herbicide action [3].

Despite important advances have been achieved in the chemical control of weeds, the identification of novel herbicides is highly desirable to overcome weed resistance [5–7]. Over the last decade analogues to natural products have been introduced to the field of herbicide discover, but there are only approximately 8% of contribution as weed management [8]. Nevertheless, the issue resistance of herbicides is not trivial for crop control since agricultures have numerous problems with the rapidly developing resistance of weeds to current herbicides.

In consequence, the need for research of new herbicides it is important. Even with their success, herbicides have not resulted in the extinction of weeds. Herbicides resistance is an evolutionary and ecological process, influenced by different factors such as the chemistry and rate of herbicides applied or the particular ecological and biological traits of the weed species [7,9].

Within the border of research plans aimed at the employment of natural products as main compounds to develop new herbicides [10–13], natural abenquines are used as a model to prepare new analogues. In Chapter 2 was

observed that compound 2-acetamido-5-benzylamino-1,4-benzoquinone (**1.20**), was the unique able to inhibit by 20% the electron transport chain in isolated spinach chloroplasts at concentration of 50  $\mu\text{M}$  (Figure 2.15).

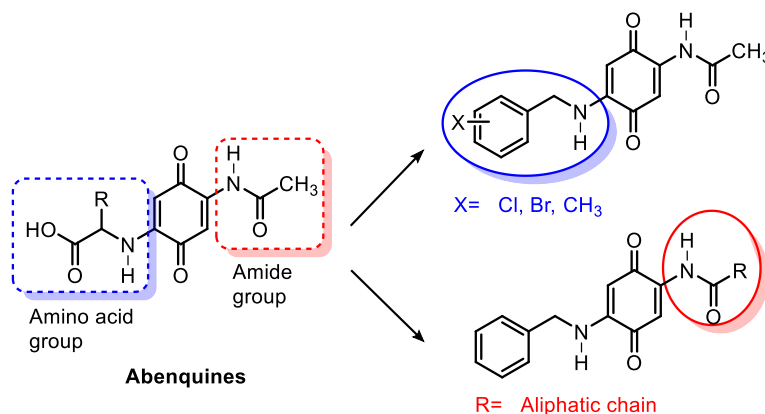
Thus, herein, compound **1.20** will be used as a model to design new analogues targeting potent substances as an herbicide. Since the structural characteristic of this compounds is that bear the benzylamine group, different substituents in the benzylamine ring such as electron withdrawing or donating groups will be envisaged. In addition, in order to evaluate the effect of the chain size on the acyl fragment, then different aliphatic chain will be introduced, and the benzylamine group will be maintaining in the quinone core.

Therefore, in this chapter, the preparation of new series of analogues to acetyl core of abenquine and a new series of amide analogues to abenquine will be described. In addition, their ability to interfere with the machinery of photosynthetic electron transport chain in isolated spinach chloroplasts will be evaluated.

## 2. RESULTS AND DISCUSSION

### 2.1. Synthesis

A new series of abenquines was planned by changing the abenquine scaffold by replacing the amino acid residue with substituted benzylamine groups or by changing the acetyl group for other acyl groups as shown in Figure 3.1. These alterations afforded the analogues **3.1-3.9** and **3.12-3.16**, respectively.

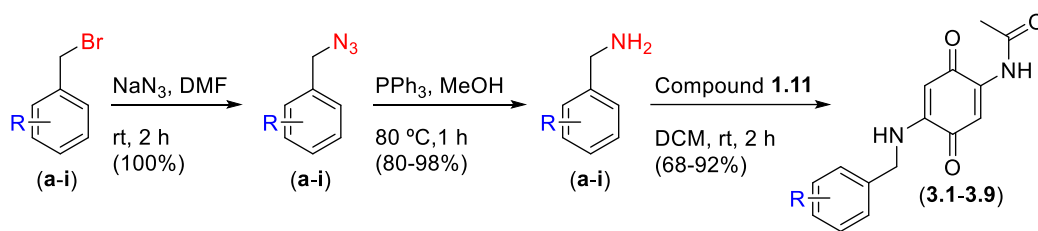


**Figure 3.1.** Variations in the abenquine scaffold for analogues **3.1-3.9** and **3.12-3.16**.

The series of analogues of abenquines could be prepared in two way, first analogues **3.1-3.9**, which correspond to the substituted benzylamines. The second series are the analogues **3.12- 3.16**, these contain the unsubstituted fixed benzylamine fixed and the acyl portion was modified.

#### 2.1.1. Synthesis of analogues **3.1-3.9**

Starting from 2-acetamido-1,4-benzoquinone (**1.11**), which was previously described in Chapter 1, whose treatment with different benzylamines at room temperature prompt an aza-Michael addition to provide the analogues 2-acetamido-5-(substituted-benzylamines)-1,4-benzoquinones (**3.1-3.9**) in favorable yields (Figure 3.2), the substituted benzylamines employed in the synthesis were prepared via a reaction of commercially available benzyl bromides with sodium azide in dimethylformamide at room temperature for two hours to promote a total conversion into benzyl azide [14].



R			Amine (%)	Abenquine analogue (%)	
<i>orto</i>	<i>meta</i>	<i>para</i>			
F	H	H	<b>a</b> (90)	<b>3.1</b>	90
H	H	Cl	<b>b</b> (85)	<b>3.2</b>	72
H	Cl	H	<b>c</b> (96)	<b>3.3</b>	68
H	H	NO <sub>2</sub>	<b>d</b> (87)	<b>3.4</b>	76
Br	H	H	<b>e</b> (80)	<b>3.5</b>	85
H	Br	H	<b>f</b> (94)	<b>3.6</b>	92
H	H	Br	<b>g</b> (90)	<b>3.7</b>	78
CH <sub>3</sub>	H	H	<b>h</b> (92)	<b>3.8</b>	70
H	CH <sub>3</sub>	H	<b>i</b> (98)	<b>3.9</b>	68

**Figure 3.2.** Preparation of 2-acetamido-5-(substituted-benzylamines)-1,4-benzoquinones (**3.1-3.9**) from 2-acetamido-1,4-benzoquinone (**1.11**) and the corresponding amines.

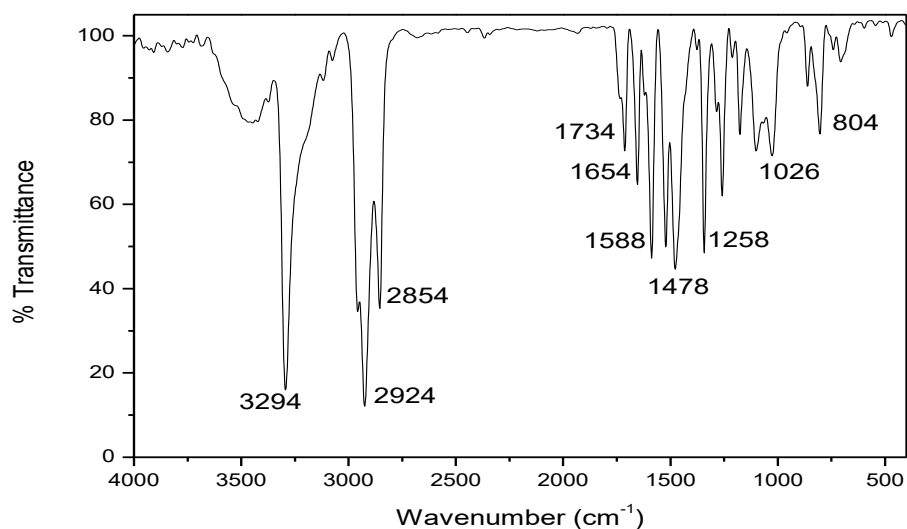
The resulted benzyl azides were reduced to the corresponding amine in favorable yield by using triphenylphosphine in methanol under reflux for one hour [15]. Therefore, with the desired amines acquired, the reaction was then proceeded by mixing the amines with the 2-acetamido-1,4-benzoquinone (**1.11**) in dichloromethane at room temperature for two hours. Such a reaction afforded the abenquines analogues (**3.1-3.9**) in promising yields ranging from 68 to 92% (Figure 3.2).

### 2.1.2. Characterization of analogues **3.1-3.9**

Concerning to these analogues, compound **3.7** was chosen to describe its structural characterization through the analysis on MS, IR, <sup>1</sup>H, and <sup>13</sup>C NMR. The spectra of compounds synthesized revealed great similarity. The only variations that were observed, referred to substituents of each benzylamine initially used in the reactions. Therefore, the following discussion is based on data of compound **3.7**, although these can be extended to other synthesized products. Compound 2-Acetamido-5-(4-bromobenzylamino)-1,4-benzoquinone (**3.7**):

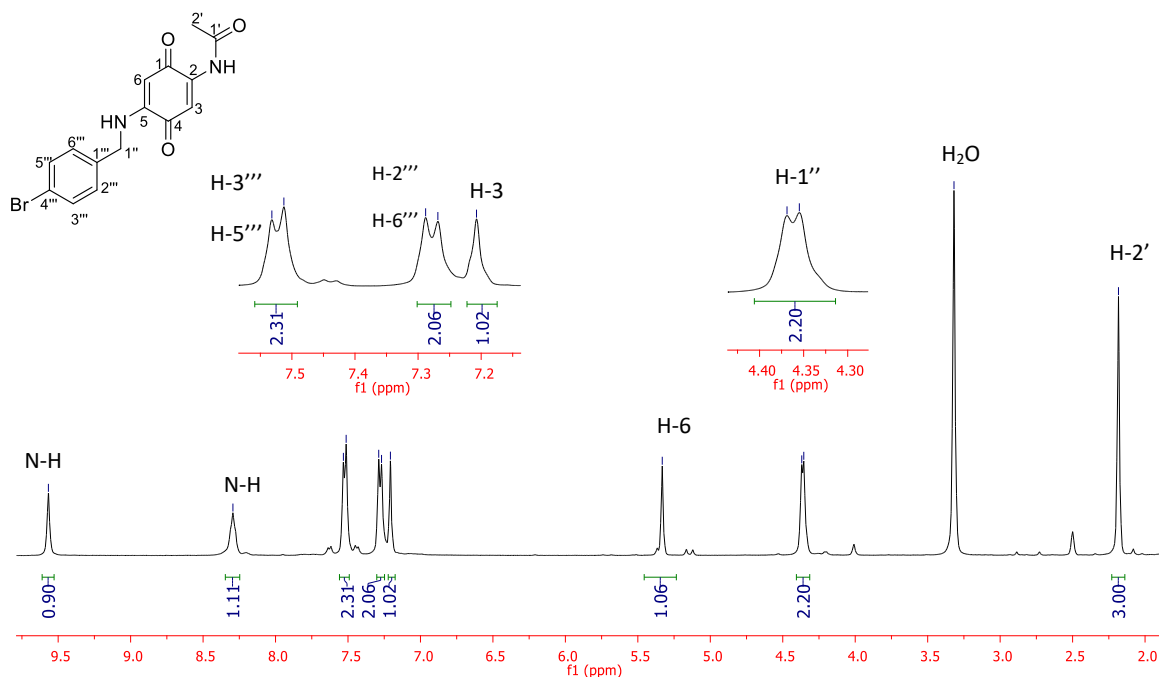
In short, mass spectra obtained under electrospray conditions (EI-MS) revealed the characteristic molecular ions as expected. EI-MS *m/z* 347.0 [M-H]<sup>-</sup>; 371.3 [M+Na]<sup>+</sup>. Through IR analysis it is possible to observe in Figure 3.3 a band

at  $3294\text{ cm}^{-1}$  corresponding to an overlap of the stretching N-H bond for the amide and the amine group. In addition to that, the stretching bond corresponding to the  $\text{CH}_3$  of the acyl fragment is seen at  $2924$  and  $2854\text{ cm}^{-1}$ . The bands related to the carbonyl group of this structure are observed at  $1734$  and  $1654\text{ cm}^{-1}$ , the first corresponds to the C=O of the quinone core and the other matching to the amide.



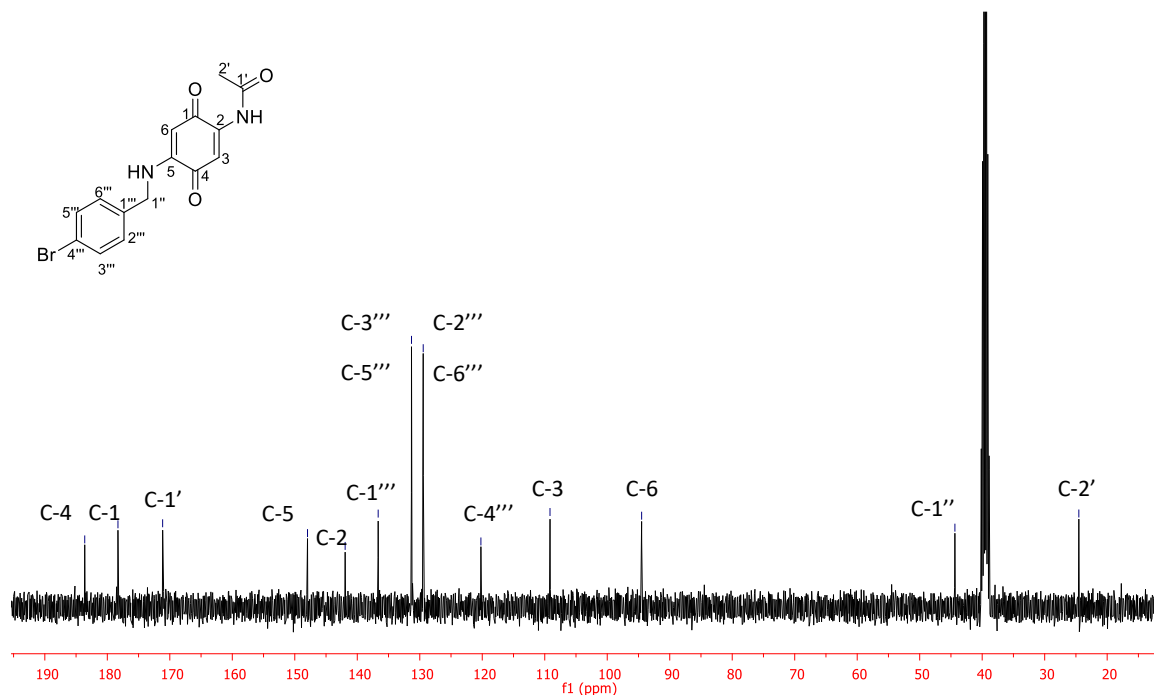
**Figure 3.3.** Infrared spectrum in KBr of compound **3.7**.

Through the analysis of  $^1\text{H-NMR}$  in Figure 3.4 it is possible to assign the 13 hydrogens of compound **3.7**. The acetyl group ( $\text{CH}_3\text{CO}$ ) was characterized by the singlet at  $\delta = 2.18$ . The methylene hydrogen-1'' of the benzylamine moiety is presented as a doublet ( $\delta = 4.36$ ,  $J = 5.6\text{ Hz}$ ) and the vinylic hydrogen-6 as a singlet at  $\delta = 5.33$ . The other vinylic hydrogen-3 of the quinone core is attributed to the singlet at  $\delta = 7.20$ . Regarding to the aromatic hydrogens, these revealed a pattern of the *para* substitution as two doublets at  $\delta = 7.28$  and  $7.52$  with a coupling constant of  $J = 7.7\text{ Hz}$ . Finally, the hydrogen in N-H bond of the amine is seen as a broad singlet at  $\delta = 8.28$  and the N-H bond of the amide appears as a strong singlet at  $\delta = 9.57$ .



**Figure 3.4.**  $^1\text{H}$  NMR (DMSO- $d_6$ , 400 MHz) of compound **3.7**.

The  $^{13}\text{C}$ -NMR spectrum is shown in the figure 3.5 and reveals 13 signals. The spectrum may be divided into four parts. In the first part the signal related to the carbon of methyl-2' and the carbon of the methylene-1'' are seen at  $\delta = 24.5$  and 44.3, respectively. In the second part, the signals relate to the vinylic carbons C-6 and C-3 at  $\delta = 94.4$  and 109.1, respectively. In the third part it is possible to attribute the carbons related to the aromatic ring showing the *para* substitution pattern. At  $\delta = 120.2$  the signal is related to C-4''', then two signals corresponding to the carbons C-2'''/C-6''' and C3'''/C-5''' are viewed at  $\delta = 129.4$  and 131.3. The signal for carbon-1''' it is assigned at  $\delta = 136.6$ , while carbon C-2 and C-5 of the quinone core are seen at  $\delta = 141.9$  and 147.9, respectively. Lastly, three signals related to the carbonyl groups of the compounds are found at  $\delta = 171.1$ , corresponding to the amide group, and the signals at  $\delta = 178.2$  and 183.6, correspond to the carbonyl of the quinone system C-1 and C-4, respectively.



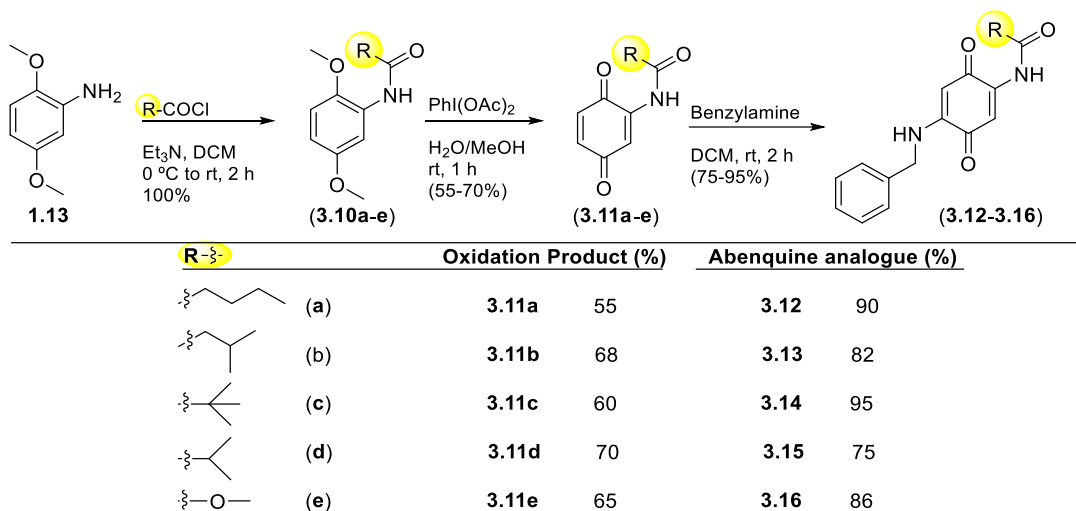
**Figure 3.5.**  $^{13}\text{C}$  NMR ( $\text{DMSO-}d_6$ , 100 MHz) of compound **3.7**.

All the synthesized compounds (**3.1-3.9**) match to what is expected, and all the spectra data of those compounds are presented in Appendix 3.

### 2.1.3. Synthesis of analogues **3.12-3.16**

Other analogues (**3.12-3.16**) were prepared as shown in Figure 3.6. The synthesis began with the reaction of **1.13** with the appropriate acyl chloride leading to 100% conversion to the desired compound (**3.10a-e**). Oxidation with phenyliodine diacetate produce the corresponding quinone (**3.11a-e**) in yields between 55 to 70%. Finally, the addition of primary benzylamine to each quinone in dichloromethane at room temperature for two hours afforded the corresponding compounds (**3.12-3.16**) in favorable yields in a range of 75-95%.





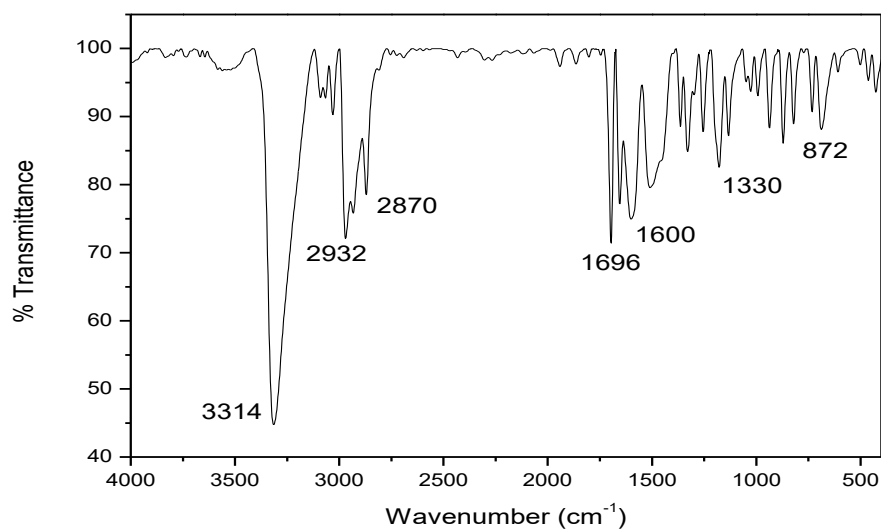
**Figure 3.6.** Preparation of 2-acetamides-5-benzylamine-1,4-benzoquinones (**3.12-3.16**).

#### 2.1.4. Characterization of analogues **3.12-3.16**

The structural characterization of the new compounds (**3.12-3.16**) was established based on their spectroscopic analysis and all compounds exhibited typical signals. Firstly, the mass spectra obtained under electrospray conditions (EI-MS) revealed the characteristic molecular ions as expected for each compound.

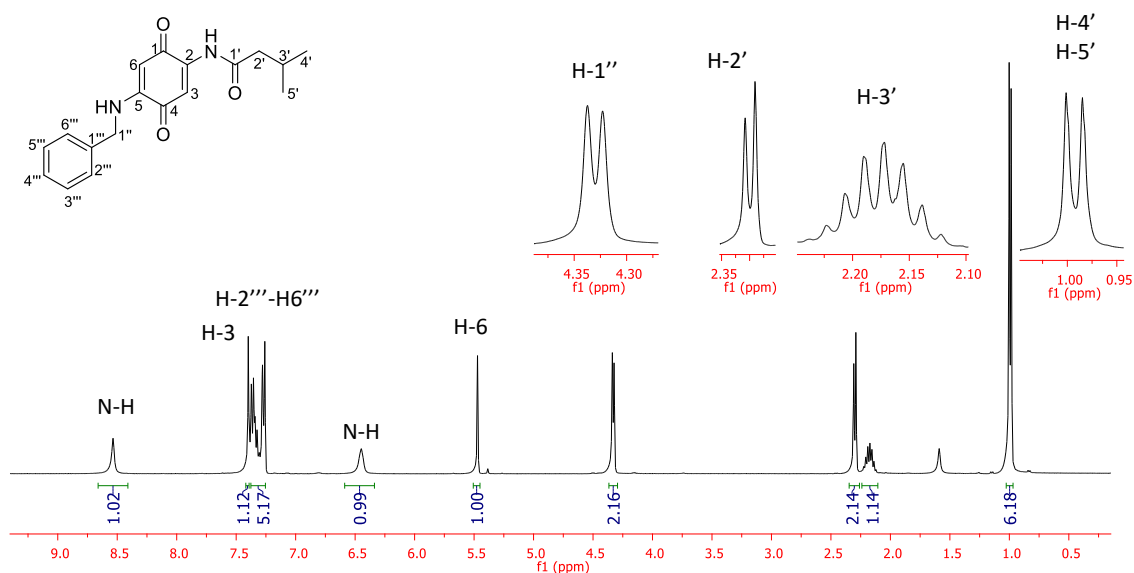
Since compounds **3.12-3.16** revealed similar spectroscopic characteristics we chose to explain the structural elucidation of compound **3.13** as an example.

In the infrared spectrum (Figure 3.7) a broad band is observed at 3314  $\text{cm}^{-1}$  which corresponds to the overlap of bands related to the N-H stretching of the amine and amide group. Also, a typical absorption in the range of 2932-2870  $\text{cm}^{-1}$ , related to the stretching vibration of the C-H bonds, were observed. Moreover, the absorption bands at a range of 1696-1650  $\text{cm}^{-1}$  that correspond to the C=O of the amide and the quinone system.



**Figure 3.7.** Infrared spectrum in KBr of compound **3.13**.

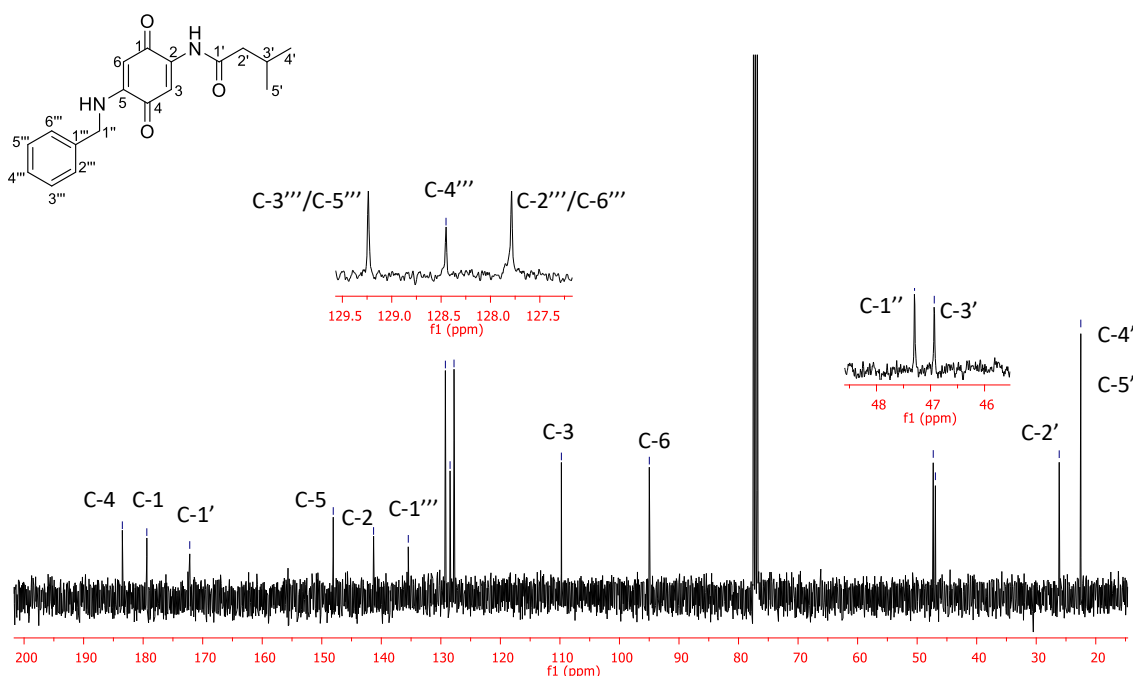
In the  $^1\text{H}$  NMR spectrum (Figure 3.8) the signal observed as a doublet at  $\delta = 0.99$  ( $J = 7.0$  Hz) correspond to the methyl group ( $-\text{CH}(\underline{\text{C}}\text{H}_3)_2$ ), followed by a multiplet at  $\delta = 2.12$ - $2.22$ , matching with the methine group ( $-\underline{\text{C}}\text{H}(\text{CH}_3)_2$ ). The signal related to hydrogen-2' appears as a doublet at  $\delta = 2.30$  ( $J = 7.0$  Hz).



**Figure 3.8.**  $^1\text{H}$  NMR spectrum ( $\text{CDCl}_3$ , 400 MHz) of compound **3.13**.

Concerning the methylene of the benzylamine fragment, ( $-\underline{\text{C}}\text{H}_2\text{NH}$ ) it appears as a doublet at  $\delta = 4.33\text{--}4.41$  ( $J = 5.8$  Hz). The signal related to hydrogen-6 is presented as a singlet at  $\delta = 5.47$ , while a broad singlet at  $\delta = 6.44$  is related to the N-H of the benzylamine. The signals related to the aromatic portion of the molecule are showed as a multiplet in the range  $\delta = 7.25\text{--}7.37$ . A singlet related to the vinylic hydrogen-3 at  $\delta = 7.39$  and a signal corresponding to the N-H of amide at  $\delta = 8.68\text{--}9.44$  were observed.

In the  $^{13}\text{C}$  NMR spectrum (Figure 3.9) 15 signals could be observed. At the region between  $\delta = 20\text{--}50$ , five signals are observed, and are related to carbons of the amide chains, as well as methylene of the benzylamine fragment ( $-\text{CH}_2\text{NH}$ ) were detected. The vinylic carbons (C-6 and C-3) at region of  $\delta = 95$  and 110, respectively, may also observed in addition to carbons related to aromatic ring at the of region  $\delta = 125\text{--}150$ . Additionally, the analysis revealed the presence of carbon-2 and carbon-5 of the quinone system and, lastly, a carbonyl group of the amide and a quinone core were observed at  $\delta = 172$ , 179, and 183, respectively.



**Figure 3.9.**  $^{13}\text{C}$  NMR spectrum ( $\text{CDCl}_3$ , 100 MHz) of compound **3.13**.

## 2.2. Biological assay

### 2.2.1. Inhibition of photosynthetic electron transport chain

Since some naturally occurring quinones are redox active molecules, the potential to interfere with electron transfer chains by the Hill reaction has been reported in available literature [16,17]. In photosynthetic organisms, plastoquinone plays a central role carrying electrons from photosystem II to the cytochrome *b<sub>6</sub>f* complex [18]. Therefore, the ability of natural abenquines and their analogues against light-driven reduction of potassium ferricyanide was evaluated by using isolated thylakoid membranes from spinach chloroplast. The results are summarized in Table 3.1 and they are expressed as a percentage of inhibition in a range of 1-100  $\mu$ M.

**Table 3.1.** Effect of abenquines (1.6-1.10) and analogues (1.17-1.19) on the photosynthetic electron transport chain. The light-driven reduction of ferricyanide by isolated spinach chloroplasts was measured in the presence of increasing concentrations of each compound, as indicated. Results were expressed as percent of untreated controls and are mean  $\pm$  SE over 4 replicates.

Compound	$\mu$ M						
	1	2	5	10	20	50	100
1.6	91.1 $\pm$ 1.1	85.9 $\pm$ 1.0	86.7 $\pm$ 1.2	89.3 $\pm$ 1.2	80.9 $\pm$ 1.1	72.8 $\pm$ 0.9	65.2 $\pm$ 1.7
1.8	101.1 $\pm$ 1.6	101.3 $\pm$ 1.9	103.1 $\pm$ 0.8	106.9 $\pm$ 1.7	105.3 $\pm$ 2.0	97.8 $\pm$ 0.5	92.8 $\pm$ 0.9
1.9	96.6 $\pm$ 0.6	98.5 $\pm$ 1.2	98.4 $\pm$ 1.4	96.4 $\pm$ 1.3	95.8 $\pm$ 1.3	91.0 $\pm$ 0.9	86.8 $\pm$ 1.3
1.10	99.0 $\pm$ 1.0	100.2 $\pm$ 0.6	104.2 $\pm$ 0.8	106.4 $\pm$ 0.6	111.0 $\pm$ 1.0	107.7 $\pm$ 2.1	100.3 $\pm$ 3.1
1.17	103.0 $\pm$ 1.7	99.5 $\pm$ 2.3	101.3 $\pm$ 1.1	99.5 $\pm$ 1.9	98.0 $\pm$ 1.8	94.8 $\pm$ 1.6	87.6 $\pm$ 1.5
1.18	100.4 $\pm$ 0.8	101.5 $\pm$ 1.2	104.2 $\pm$ 1.4	103.1 $\pm$ 3.0	102.5 $\pm$ 2.0	88.3 $\pm$ 0.9	72.1 $\pm$ 0.7
1.19	102.2 $\pm$ 0.4	103.2 $\pm$ 1.3	105.0 $\pm$ 1.4	103.7 $\pm$ 0.7	103.4 $\pm$ 0.8	98.9 $\pm$ 2.1	92.0 $\pm$ 2.2

In general, natural abenquines **1.6-1.10** exhibited low activity in the inhibition of electron transport chain. No significant difference was observed for isomer (**1.17**) of abenquine (**1.9**). Moreover, for analogues with different amino acids, such as methionine (**1.18**) or glycine (**1.19**), no change compared with natural abenquines was observed. However, for analogues with an amine group instead an amino acid, the values were enhanced. In Table 3.2, it may be noticed that compounds **1.20** and **2.1-2.3** exert a good inhibition when compared to the natural abenquines, except for compound **2.1**. In addition, in concentrations of 5  $\mu$ M compound **1.20** afforded an inhibition of the electron transport chain in more than 50%.

**Table 3.2.** Effect of synthetic analogues of abenquines with an acetyl group (**1.20**, **2.1-2.3**) on the photosynthetic electron transport chain. The light-driven reduction of ferricyanide by isolated spinach chloroplasts was measured in the presence of increasing concentrations of each compound, as indicated. Results were expressed as percent of untreated controls and are mean  $\pm$  SE over 4 replicates.

Compound	$\mu\text{M}$						
	1	2	5	10	20	50	100
<b>1.20</b>	47.6 $\pm$ 0.7	37.9 $\pm$ 0.4	24.3 $\pm$ 0.9	21.2 $\pm$ 0.8	21.9 $\pm$ 1.1	22.9 $\pm$ 1.0	25.2 $\pm$ 0.8
<b>2.1</b>	99.0 $\pm$ 0.6	98.8 $\pm$ 1.2	99.1 $\pm$ 0.4	97.8 $\pm$ 1.7	98.6 $\pm$ 1.0	92.8 $\pm$ 0.5	86.5 $\pm$ 1.2
<b>2.2</b>	97.7 $\pm$ 0.7	97.7 $\pm$ 1.4	93.6 $\pm$ 0.8	87.5 $\pm$ 1.3	73.9 $\pm$ 0.7	52.0 $\pm$ 0.9	37.0 $\pm$ 1.3
<b>2.3</b>	95.0 $\pm$ 1.4	94.5 $\pm$ 0.8	82.4 $\pm$ 0.7	70.6 $\pm$ 0.8	53.3 $\pm$ 1.1	37.4 $\pm$ 1.0	35.1 $\pm$ 2.2

The data for analogues with a benzoyl group are summarized in Table 3.3. These compounds exhibited a poor inhibition which may suggest that the aromatic group contributed to an impediment in the interaction with the photosynthetic electron transport chain. For example, in the case of compound **2.10**, which is an analogue to the more active compound with the acetyl group (**1.20**), a vast difference in the inhibition is observed.

**Table 3.3.** Effect of synthetic analogues of abenquines with benzoyl group (**2.6-2.13**) on the photosynthetic electron transport chain. The light-driven reduction of ferricyanide by isolated spinach chloroplasts was measured in the presence of increasing concentrations of each compound, as indicated. Results were expressed as percent of untreated controls and are mean  $\pm$  SE over 4 replicates.

Compound	$\mu\text{M}$							
	0.8	1.6	3	6	12	25	50	100
<b>2.6</b>	97.8 $\pm$ 0.9	94.1 $\pm$ 0.9	93.3 $\pm$ 2.0	90.6 $\pm$ 1.0	86.7 $\pm$ 0.7	81.3 $\pm$ 1.5	76.0 $\pm$ 1.0	67.3 $\pm$ 0.5
<b>2.7</b>	98.2 $\pm$ 1.3	98.1 $\pm$ 0.8	95.6 $\pm$ 2.3	94.4 $\pm$ 0.7	93.9 $\pm$ 1.9	90.8 $\pm$ 1.0	85.6 $\pm$ 0.5	82.0 $\pm$ 2.2
<b>2.8</b>	99.6 $\pm$ 1.4	97.2 $\pm$ 1.0	97.4 $\pm$ 1.0	94.9 $\pm$ 0.6	95.1 $\pm$ 1.8	94.2 $\pm$ 0.6	89.5 $\pm$ 0.5	75.8 $\pm$ 1.5
<b>2.9</b>	99.0 $\pm$ 1.1	97.8 $\pm$ 1.2	96.9 $\pm$ 1.4	95.9 $\pm$ 1.6	95.2 $\pm$ 0.4	89.4 $\pm$ 0.8	76.7 $\pm$ 0.9	57.0 $\pm$ 0.5
<b>2.10</b>	92.1 $\pm$ 1.2	90.4 $\pm$ 2.1	84.4 $\pm$ 2.6	80.5 $\pm$ 2.2	78.9 $\pm$ 1.5	75.9 $\pm$ 1.8	73.7 $\pm$ 2.5	76.8 $\pm$ 4.7
<b>2.11</b>	96.8 $\pm$ 0.9	89.5 $\pm$ 2.2	84.1 $\pm$ 2.1	77.4 $\pm$ 2.5	75.3 $\pm$ 0.9	73.5 $\pm$ 0.9	73.1 $\pm$ 1.8	67.3 $\pm$ 1.7
<b>2.12</b>	94.2 $\pm$ 2.3	91.8 $\pm$ 1.3	86.6 $\pm$ 1.4	78.0 $\pm$ 0.9	70.5 $\pm$ 1.2	63.0 $\pm$ 1.3	58.1 $\pm$ 0.6	55.3 $\pm$ 1.6
<b>2.13</b>	101.3 $\pm$ 2.8	100.3 $\pm$ 1.5	97.8 $\pm$ 1.0	96.8 $\pm$ 1.3	92.9 $\pm$ 0.6	84.9 $\pm$ 1.2	76.3 $\pm$ 0.9	67.5 $\pm$ 1.1

In view of the obtained results for the series of compounds containing the acetyl or benzoyl groups, which revealed strong inhibition of the photosynthetic electron transport chain, the most active compounds were selected to further improve their activity through structural modification. To accomplish that, a series of analogues **3.1-3.9** were prepared through a strategy previously explained,

where diverse groups with different electronic properties were introduced into a reaction system.

When analogues **3.1-3.9** were tested for their ability to interfere with the light-driven reduction of ferricyanide from spinach chloroplast, the results revealed that with the exception of **3.14**, they were all active (Table 3.4). Compounds **3.1** (*o*-fluoro-substitution) and **3.4** (*p*-nitro-substitution) exhibited IC<sub>50</sub> values in the 10 to 100 μM range, but compounds with a -Cl or -Br atom in both *meta* and *para*-position (**3.2** and **3.3**; **3.6** and **3.7**) exhibited IC<sub>50</sub> values comparable to that of the herbicide diuron (0.3 μM) [19]. Compound **3.5**, with a Br atom in *ortho*-position, was significantly less effective (IC<sub>50</sub> = 4.7 μM). A similar tendency was observed with a methyl substituent which in *ortho*-position (**3.8**) afforded an IC<sub>50</sub> = 3.6 μM, whereas in *meta*-position (**3.9**), it exhibited an IC<sub>50</sub> value of 0.38 μM.

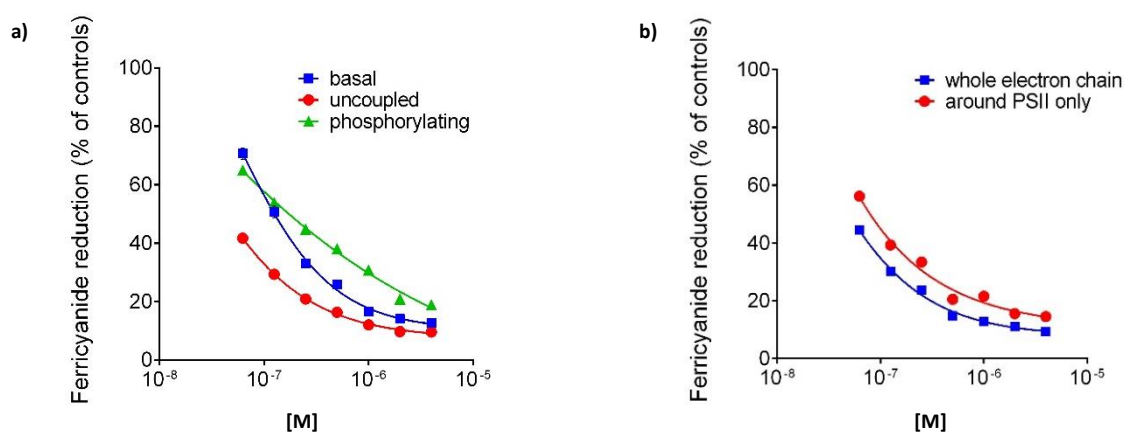
**Table 3.4.** Concentrations inhibiting by 50% the light-dependent ferricyanide reduction in spinach chloroplasts for compounds (**3.1-3.9** and **3.12-3.16**)

Compounds	IC <sub>50</sub> (μM)	Compounds	IC <sub>50</sub> (μM)
<b>3.1</b>	13	<b>3.8</b>	3.6
<b>3.2</b>	0.33	<b>3.9</b>	0.38
<b>3.2</b>	0.37	<b>3.12</b>	2.6
<b>3.4</b>	45	<b>3.13</b>	43
<b>3.5</b>	4.7	<b>3.14</b>	>100
<b>3.6</b>	0.18	<b>3.15</b>	0.27
<b>3.7</b>	0.19	<b>3.16</b>	0.95

Concerning compounds **3.12-3.16**, the compound with the *tert*-butyl moiety was inactive (**3.14**), and compound (**3.13**) was scarcely effective. However, compounds (**3.12**, **3.15-3.16**) showed IC<sub>50</sub> values in the range 0.2-2.6 μM. Nevertheless, if the effect was compared to that of the corresponding while maintaining amide keeping the benzylamino-benzoquinone moiety, the IC<sub>50</sub> value decreased to 0.27 μM for compound **3.15** bearing an isopropyl group.

With the aim of identifying where the specific interference is in the photosynthetic machinery is located the most potent compound was selected to be further characterized. Thus, the analogue **3.6** (IC<sub>50</sub> = 0.18 μM) was compared to the inhibitory pattern under basal, uncoupling, or phosphorylating conditions, which allowed us to rule out the possibility that these compounds may act as

energy coupling inhibitors or as uncouplers, thereby impeding ATP synthesis [20] (figure 3.10a).



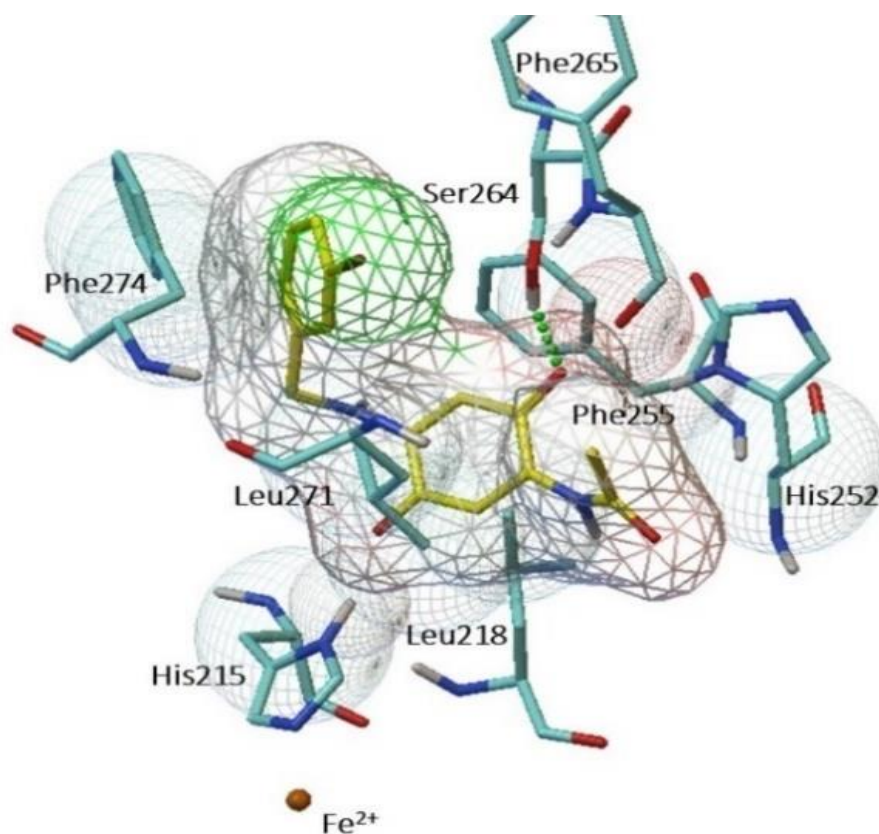
**Figure 3.10. a)** Effects of increasing concentrations of compound **3.6** on ferricyanide reduction under basal, uncoupling, or phosphorylating conditions. **b)** Comparison of the effects of compound **3.6** on the whole chloroplastic electron transport chain and on a partial electron flow involving photosystem II only.

Other experiments were performed to identify their molecular target inside the so called Z scheme, that is, if they interact with the photosynthetic machinery at photosystem II, cytochrome *b<sub>6</sub>f* complex, or photosystem I level [18,21]. When the electron flow was suppressed by addition of the cytochrome *b<sub>6</sub>f* inhibitor, 2,5-dibromo-3-methyl-6-isopropyl-*p*-benzoquinone (2 μM), and then an electron flow excluding photosystem, it was established through the addition of 0.1 mM phenylenediamine that compound **3.6** was still inhibitory (Figure 3.10b). Consequently, the compound studied is most likely interacting with the PSII.

### 2.2.2. Molecular docking studies

The great majority of herbicides inhibiting PSII are known to displace the plastoquinone Q<sub>B</sub> from its binding site and thus inhibiting the electron transfer from Q<sub>A</sub> to Q<sub>B</sub> [22,23]. *In silico* analyses of the interaction between some of these herbicides, such as diuron (3-(3,4-dichlorophenyl)-1,1-dimethylurea), atrazine, terbutryn and bromacil, and the plastoquinone binding site have been carried out using the structure of PSII from either bacteria, like *Rhodospseudomonas viridis* [24], *Tricondyloides elongatus* [25,26], *T. vulcanus* [27], and *Blastochloris viridis* [28], or plants, like *Phalaris minor* [29] and *Spinacia oleracea* [27]. For the natural

quinone, sorgoleone a docking study using the Q<sub>B</sub>-binding site of the PSII complex of bacterium *Rhodospseudomonas viridis* was performed. In this present study, a docking analysis for the most active abenquine analogue was performed (**3.6**) using the program AutoDockTools 4.2 [30,31]. Molecular docking was executed by using the crystallographic structure of the reaction center of PSII (D1) isolated from spinach (PDB ID: 3JCU). The results suggested that compound **3.6** is binding *via* oxygen and hydrogen. The carbonyl group of the quinone interacts with an OH of Ser<sub>264</sub> in 2.063 Å (Figure 3.11), with a docking score of -7.83. Moreover, hydrophobic interactions were found with Phe<sub>265</sub>, Phe<sub>274</sub>, Phe<sub>255</sub>, His<sub>252</sub>, Leu<sub>271</sub>, Leu<sub>218</sub>, and His<sub>215</sub>.



**Figure 3.11.** Binding models of abenquine analogue **3.6** with the pocket site of PSII from *Spinacia oleracea* (PDB ID: 3JCU).

Consequently, the compound **3.6** is surrounded by the above residues. Thus, the interaction of the ligands with these residues might lead to an inhibition of PSII (D1). In addition to this, most of the herbicides described above tend to occupy the position near the loop consisting of Ser<sub>264</sub>, and Phe<sub>265</sub> in the PSII.



### 3. CONCLUSION

It is clear that natural products and their analogues or derivatives have been used for decades to control pests. In the case of herbicides, it is well-established how these compounds may interfere in the vital system in the plant's metabolism. In that regard, natural abenquines were employed as a model for the synthesis of new analogues with a considerable herbicidal potential. Consequentially, modifications to the core of the quinone afforded 9 analogues, thus replacing the amino acid fragment by different substituted benzylamine groups in favourable yields (68-92%). Moreover, in 5 analogues the benzylamine fragment was maintained and the chain of the acyl moiety was modified, which also exhibited favourable yields (75-95%). Through analogues of abenquines, it was possible to determine their ability to inhibit the photosynthetic electron transport chain. In fact, one of analogues (**3.6**) presented  $IC_{50}$  values as low as  $0.18 \mu\text{M}$ , similar to that of the commercial herbicide, diuron ( $IC_{50} = 0.3 \mu\text{M}$ ). The remarkable biological activity of analogue **3.6** which bears a *m*-Br-benzylamino group, indicates that such a group is important for the inhibition of the photosynthetic machinery targeting photosystem II. Moreover, molecular docking showed interaction in the plastoquinone binding site, similar to herbicides such as atrazine or diuron which present the same mechanism of action. Finally, was found that compound **3.6** is binding with Ser<sub>f264</sub> through carbonyl of quinone fragment in the reaction centre of photosystem II.

## 4. EXPERIMENTAL PART

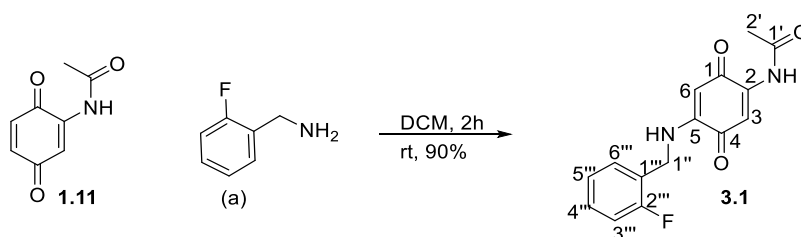
### 4.1. Synthesis of benzylamines (a-i)

#### *General procedure for synthesis of benzylamines (a-i)*

Firstly, the benzyl azides were prepared by reaction of a solution of the appropriate benzyl bromide (1.0 mmol) in DMF (10 mL) with sodium azide (100 mg; 1.5 mmol). The reaction mixture was stirred for 2 h at room temperature. The mixture was dispensed into water (50 mL), extracted with diethyl ether (2 x 30 mL), washed with brine (3 x 20 mL), dried over Na<sub>2</sub>SO<sub>4</sub>, filtered, and the filtrate was concentrated in a rotary evaporator under reduced pressure to afford the benzyl azides. Since TLC analysis of the crude products revealed only one spot, they were used without further purification. Then, the benzylamines were prepared by reaction of triphenylphosphine (1.5 mmol, 0.147 g) and the appropriate benzyl azide (1 mmol) in dry methanol (10 mL). The reaction mixture was then refluxed at 80 °C for 1 hr. After all the starting material had disappeared (monitored by TLC using 7:1 mixture of Hex/EtOAc solvent system), the reaction mixture was cooled to room temperature and the solvent was removed under reduced pressure to yield the crude amines and they were used without further purification.

### 4.2. Synthesis of analogues 3.1-3.9 and 3.12-3.16

#### *2-Acetamido-5-(2-fluorobenzylamino)-1,4-benzoquinone (3.1):*

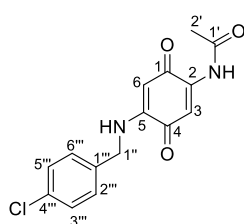


To a round-bottomed flask (25 mL) was added 2-acetamido-1,4-benzoquinone (**1.11**) previously obtained (0.12 g, 0.73 mmol) in dichloromethane (5 mL), followed by the addition of 2-fluorobenzylamine (0.10 g, 0.80 mmol). The reaction mixture was stirred at room temperature. Initially, the reaction mixture turned from yellow to red dark. The reaction was quenched after 2 h, before

removal of the solvent under reduced pressure to afford the crude product as a dark red residue. This residue was purified by silica gel column chromatography eluting with hexane/EtOAc (7:1 v/v) to afford the required product as red crystals in 90% (189 mg, 0.65 mmol). M.p 231-233 °C. IR: ( $\nu_{\max}/\text{cm}^{-1}$ ) 3290, 2934, 2856, 1725, 1664, 1590, 1500, 1470, 1355, 1056, 872  $\text{cm}^{-1}$ .  $^1\text{H}$  NMR (DMSO- $d_6$ , 400 MHz)  $\delta$ : 2.18 (s, 3H, H-2'), 4.43 (d,  $J = 6.4$  Hz, 2H, H-1''), 5.35 (s, 1H, H-6), 7.15-7.21 (m, 3H, H-3, H-5''', H-6'''), 7.30-7.36 (m, 2H, H-3''', H-4'''), 8.15 (t,  $J = 6.4$  Hz, 1H, N-H), 9.57 (s, 1H, N-H);  $^{13}\text{C}$  NMR (DMSO- $d_6$ , 100 MHz)  $\delta$ : 24.5 (C-2'), 94.2 (C-6), 109.1 (C-3), 115.1 (C-2''', C-6'''), 115.5 (C-3''', C-5'''), 124.5 (C-4'''), 129.3 (C-1'''), 141.9 (C-2), 147.9 (C-5), 171.1 (C-1'), 178.3 (C-1), 183.4 (C-4); EIMS  $m/z$  286.9 [M-H] $^-$ ; 311.1 [M+Na] $^+$ ; anal. C 62.31, H 4.72, N 9.56%, calcd for  $\text{C}_{15}\text{H}_{13}\text{FN}_2\text{O}_3$ , C 62.50, H 4.55, N 9.72%; found: C 62.31, H 4.72, N 9.56%.

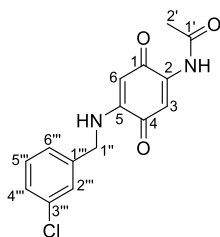
Compounds **3.2-3.9**, **3.12-3.16** were synthesized using a method similar to that of **3.1**.

**2-Acetamido-5-(4-chlorobenzylamino)-1,4-benzoquinone (3.2):**



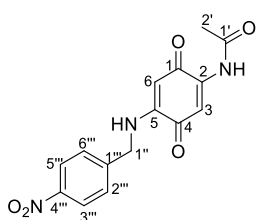
Quantities used in the reaction: amine (0.12 g, 0.82 mmol); compound **1.11** (122 mg, 0.74 mmol). Red solid; yield: 72% (160 mg, 0.53 mmol). Mp 227-229 °C. IR: ( $\nu_{\max}/\text{cm}^{-1}$ ) 3294, 2924, 2854, 1712, 1654, 1588, 1522, 1478, 1342, 1026, 862.  $^1\text{H}$  NMR (DMSO- $d_6$ , 400 MHz)  $\delta$ : 2.19 (s, 3H, H-2'), 4.39 (brs, 2H, H-1''), 5.35 (s, 1H, H-6), 7.22 (s, 1H, H-3), 7.34 (d,  $J = 6.5$  Hz, 2H, H-2''', H-6'''), 7.39 (d,  $J = 6.5$  Hz, 2H, H-3''', H-5'''), 8.30 (s, 1H, N-H), 9.57 (s, 1H, N-H).  $^{13}\text{C}$  NMR (DMSO- $d_6$ , 100 MHz)  $\delta$ : 24.5 (C-2'), 44.3 (C-1''), 94.5 (C-6), 109.2 (C-3), 128.4 (C-2''', C-6'''), 129.1 (C-3''', C-5'''), 131.7 (C-4'''), 136.2 (C-1'''), 141.9 (C-2), 147.9 (C-5), 171.1 (C-1'), 178.3 (C-1), 183.6 (C-4). EIMS  $m/z$  302.9 [M-H] $^-$ ; 327.1 [M+Na] $^+$ ; anal. C 58.92, H 4.41, N 9.02%, calcd for  $\text{C}_{15}\text{H}_{13}\text{ClN}_2\text{O}_3$ , C 59.12, H 4.30, N 9.19%; found: C 58.92, H 4.41, N 9.02%.

**2-Acetamido-5-(3-chlorobenzylamino)-1,4-benzoquinone (3.3):**



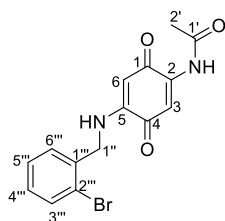
Quantities used in the reaction: amine (0.12 g, 0.82 mmol); compound **1.11** (119 mg, 0.72 mmol). Red solid; yield: 68% (151 mg, 0.49 mmol). Mp 231-232 °C. IR: ( $\nu_{\max}/\text{cm}^{-1}$ ) 3316, 2336, 2930, 1718, 1660, 1582, 1488, 1176, 722.  $^1\text{H}$  NMR (DMSO- $d_6$ , 400 MHz)  $\delta$ : 2.20 (s, 3H, H-2'), 4.41 (d,  $J = 5.0$  Hz, 2H, H-1''), 5.39 (s, 1H, H-6), 7.23 (s, 1H, H-3), 7.31-7.38 (m, 3H, H-4'''-H-6'''), 7.42 (s, 1H, H-2'''), 8.30 (s, 1H, N-H), 9.57 (s, 1H, N-H).  $^{13}\text{C}$  NMR (DMSO- $d_6$ , 100 MHz)  $\delta$ : 24.6 (C-2'), 44.4 (C-1'''), 94.5 (C-6), 109.2 (C-3), 125.9 (C-6'''), 127.1 (C-4'''), 127.2 (C-2'''), 130.3 (C-5'''), 133.2 (C-3'''), 139.9 (C-1'''), 141.9 (C-2), 148.0 (C-5), 171.2 (C-1'), 178.4 (C-1), 183.6 (C-4). EIMS  $m/z$  302.9 [M-H] $^-$ ; 326.9 [M+Na] $^+$ ; anal. C 58.85, H 4.55, N 8.97%, calcd for C<sub>15</sub>H<sub>13</sub>ClN<sub>2</sub>O<sub>3</sub>, C 59.12, H 4.30, N 9.19%; found: C 58.85, H 4.55, N 8.97%.

**2-Acetamido-5-(4-nitrobenzylamino)-1,4-benzoquinone (3.4):**



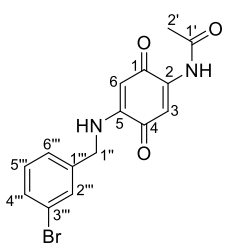
Quantities used in the reaction: amine (0.1 g, 0.66 mmol); compound **1.11** (120 mg, 0.72 mmol). Red solid; yield: 76% (175 mg, 0.55 mmol). Mp 250-252 °C. IR: ( $\nu_{\max}/\text{cm}^{-1}$ ) 3292, 2956, 2924, 2856, 1714, 1654, 1474, 1260, 1026, 804.  $^1\text{H}$  NMR (DMSO- $d_6$ , 400 MHz)  $\delta$ : 2.21 (s, 3H, H-2'), 4.57 (brs, 2H, H-1''), 5.37 (s, 1H, H-6), 7.26 (s, 1H, H-3), 7.61 (d,  $J = 6.0$  Hz, 2H, H-2''', H-6'''), 7.23 (d,  $J = 6.0$  Hz, 2H, H-3''', H-5'''), 8.65 (s, 1H, N-H), 9.61, (s, 1H, N-H).  $^{13}\text{C}$  NMR (DMSO- $d_6$ , 100 MHz)  $\delta$ : 24.5 (C-2'), 44.5 (C-1'''), 94.7 (C-6), 109.3 (C-3), 123.6 (C-2''', C-6'''), 128.3 (C-3''', C-5'''), 141.9 (C-1'''), 145.3 (C-4'''), 146.7 (C-2), 148.0 (C-5), 171.2 (C-1'), 178.5 (C-1), 183.5 (C-4). EIMS  $m/z$  314.4 [M-H] $^-$ ; 338.4 [M+Na] $^+$ ; anal. C 59.94, H 4.30, N 13.12%, calcd for C<sub>15</sub>H<sub>13</sub>N<sub>3</sub>O<sub>5</sub>, C 57.14, H 4.16, N 13.33%; found: C 59.94, H 4.30, N 13.12%.

**2-Acetamido-5-(2-bromobenzylamino)-1,4-benzoquinone (3.5):**



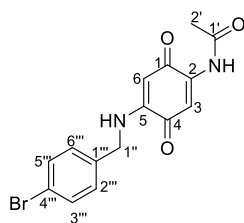
Quantities used in the reaction: amine (0.15 g, 0.79 mmol); compound **1.11** (121 mg, 0.73 mmol). Red solid; yield: 85% (217 mg, 0.62 mmol). Mp 225-227 °C. IR: ( $\nu_{\max}/\text{cm}^{-1}$ ) 3280, 2924, 2854, 1708, 1654, 1606, 1566, 1490, 1312, 1174, 1024, 750.  $^1\text{H}$  NMR ( $\text{DMSO-}d_6$ , 400 MHz)  $\delta$ : 2.18 (s, 3H, H-2'), 4.82 (brs, 2H, H-1''), 5.58 (s, 1H, H-6), 7.13 (s, 1H, H-3), 7.21-7.26 (m, 1H, H-3'''), 7.33-7.39 (m, 2H, H-5'''-H-6'''), 7.61-7.66 (m, 1H, H-4'''), 9.55 (s, 1H, N-H).  $^{13}\text{C}$  NMR ( $\text{DMSO-}d_6$ , 100 MHz)  $\delta$ : 24.5 (C-2'), 57.7 (C-1''), 100.5 (C-6), 111.6 (C-3), 121.9 (C-5'''), 127.8 (C-2'''), 128.0 (C-4'''), 129.1 (C-6'''), 132.3 (C-3'''), 132.7 (C-1'''), 140.1 (C-2), 151.1 (C-5), 171.1 (C-1'), 178.6 (C-1), 185.1 (C-4). EIMS  $m/z$  346.8  $[\text{M}-\text{H}]^-$ ; 371.0  $[\text{M}+\text{Na}]^+$ ; anal. C 51.42, H 3.84, N 7.75%, calcd for  $\text{C}_{15}\text{H}_{13}\text{BrN}_2\text{O}_3$ , C 51.59, H 3.75, N 8.02%; found: C 51.42, H 3.84, N 7.75%.

**2-Acetamido-5-(3-bromobenzylamino)-1,4-benzoquinone (3.6):**



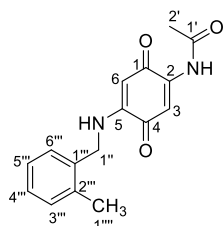
Quantities used in the reaction: amine (0.15 g, 0.79 mmol); compound **1.11** (121 mg, 0.73 mmol). Red solid; yield: 92% (235 mg, 0.67 mmol). Mp 213-215 °C. IR: ( $\nu_{\max}/\text{cm}^{-1}$ ) 3316, 3242, 2942, 1716, 1658, 1580, 1488, 1374, 1332, 1176, 718.  $^1\text{H}$  NMR ( $\text{DMSO-}d_6$ , 400 MHz)  $\delta$ : 2.21 (s, 3H, H-2'), 4.41 (d,  $J=6.0$  Hz, 2H, H-1''), 5.39 (s, 1H, H-6), 7.24 (s, 1H, H-3), 7.28-7.36 (m, 2H, H-4''', H-6'''), 7.44-7.48 (m, 1H, H-5'''), 7.56 (s, 1H, H-2'''), 8.30 (s, 1H, N-H), 9.57 (s, 1H, N-H).  $^{13}\text{C}$  NMR ( $\text{DMSO-}d_6$ , 100 MHz)  $\delta$ : 24.5 (C-2'), 44.4 (C-1''), 94.5 (C-6), 109.2 (C-3), 121.8 (C-3'''), 126.3 (C-6'''), 129.9 (C-5'''), 130.1 (C-2'''), 130.6 (C-4'''), 140.1 (C-1'''), 141.9 (C-2), 147.9 (C-5), 171.1 (C-1'), 178.4 (C-1), 183.6 (C-4). EIMS  $m/z$  347.1  $[\text{M}-\text{H}]^-$ ; 371.0  $[\text{M}+\text{Na}]^+$ ; anal. C 62.37, H 4.61, N 9.51%, calcd for  $\text{C}_{15}\text{H}_{13}\text{BrN}_2\text{O}_3$ , C 62.50, H 4.55, N 9.72%; found: C 62.37, H 4.61, N 9.51%.

**2-Acetamido-5-(4-bromobenzylamino)-1,4-benzoquinone (3.7):**



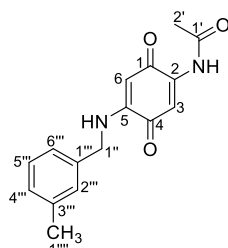
Quantities used in the reaction: amine (0.15 g, 0.79 mmol); compound **1.11** (121 mg, 0.73 mmol). Red solid; yield: 78% (199 mg, 0.57 mmol). Mp 222-225 °C. IR: ( $\nu_{\max}/\text{cm}^{-1}$ ) 3294, 2958, 2924, 2854, 1712, 1654, 1588, 1522, 1342, 1176, 1100, 862.  $^1\text{H}$  NMR (DMSO- $d_6$ , 400 MHz)  $\delta$ : 2.18 (s, 3H, H-2'), 4.36 (d,  $J = 5.6$  Hz, 2H, H-1''), 5.33 (s, 1H, H-6), 7.21 (s, 1H, H-3), 7.28 (d,  $J = 7.7$  Hz, 2H, H-2'', H-6''), 7.52 (d,  $J = 7.7$  Hz, 2H, H-3'', H-5''), 8.29 (s, 1H, N-H), 9.57 (s, 1H, N-H).  $^{13}\text{C}$  NMR (DMSO- $d_6$ , 100 MHz)  $\delta$ : 24.5 (C-2'), 44.4 (C-1''), 94.5 (C-6), 109.2 (C-3), 120.2 (C-4''), 129.4 (C-2'', C-6''), 131.1 (C-3'', C-5''), 136.7 (C-1''), 141.9 (C-2), 147.9 (C-5), 171.1 (C-1'), 178.3 (C-1), 183.6 (C-4). EIMS  $m/z$  347.0 [M-H]<sup>-</sup>; 371.3 [M+Na]<sup>+</sup>; anal. C 51.41, H 3.93, N 7.94%, calcd for C<sub>15</sub>H<sub>13</sub>BrN<sub>2</sub>O<sub>3</sub>, C 51.59, H 3.75, N 8.02%; found: C 51.41, H 3.93, N 7.94%.

**2-Acetamido-5-(2-methylbenzylamino)-1,4-benzoquinone (3.8):**



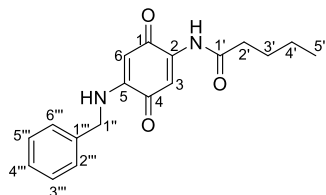
Quantities used in the reaction: amine (0.1 g, 0.81 mmol); compound **1.11** (121 mg, 0.73 mmol). Red solid; yield: 70% (145 mg, 0.51 mmol). Mp 232-235 °C. IR: ( $\nu_{\max}/\text{cm}^{-1}$ ) 3288, 2922, 2854, 1710, 1654, 1574, 1482, 1348, 1176, 758.  $^1\text{H}$  NMR (DMSO- $d_6$ , 400 MHz)  $\delta$ : 2.19 (s, 3H- H-2'), 2.28 (s, 3H, H-1'''), 4.36 (d,  $J = 5.7$  Hz, 2H, H-1''), 5.27 (s, 1H- H-6), 7.09-7.18 (m, 4H, H-3'''-H-6'''), 7.23 (s, 1H, H-3), 8.10 (s, 1H, N-H), 9.57 (s, 1H, N-H).  $^{13}\text{C}$  NMR (DMSO- $d_6$ , 100 MHz)  $\delta$ : 18.7 (C-1'''), 24.6 (C-2'), 43.5 (C-1''), 94.4 (C-6), 109.2 (C-3), 125.8 (C-6'''), 126.4 (C-5'''), 127.1 (C-4'''), 130.2 (C-3'''), 134.4 (C-2'''), 135.6 (C-1''), 142.1 (C-2), 148.3 (C-5), 171.2 (C-1'), 178.2 (C-1), 183.6 (C-4). EIMS  $m/z$  307.1 [M+Na]<sup>+</sup>; anal. C 67.30, H 5.84, N 9.61%, calcd for C<sub>16</sub>H<sub>16</sub>N<sub>2</sub>O<sub>3</sub>, C 67.59, H 5.67, N 9.85%; found: C 67.30, H 5.84, N 9.61%.

**2-Acetamido-5-(3-methylbenzylamino)-1,4-benzoquinone (3.9):**



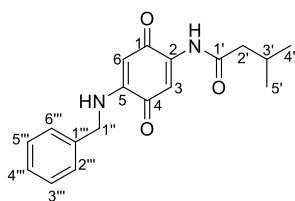
Quantities used in the reaction: amine (0.11 g, 0.87 mmol); compound **1.11** (119 mg, 0.72 mmol). Red solid; yield: 68% (141 mg, 0.49 mmol). Mp 215-217 °C. IR: ( $\nu_{\max}/\text{cm}^{-1}$ ) 3300, 3286, 3022, 2926, 2858, 1712, 1654, 1572, 1482, 1344, 1176, 768.  $^1\text{H}$  NMR (DMSO- $d_6$ , 400 MHz)  $\delta$ : 2.18 (s, 3H, H-2'), 2.28 (s, 3H, H-1'''), 4.34 (d,  $J = 5.6$  Hz, 2H, H-1''), 5.32 (s, 1H, H-6), 7.05-7.11 (m, 3H, H-4'''-H-6'''), 7.19-7.22 (m, 2H, H-3, H-2'''), 8.24 (s, 1H, N-H), 9.55 (s, 1H, N-H).  $^{13}\text{C}$  NMR (DMSO- $d_6$ , 100 MHz)  $\delta$ : 20.9 (C-1'''), 24.5 (C-2'), 45.1 (C-1'), 94.4 (C-6), 109.1 (C-3), 127.1 (C-4'''), 127.8 (C-2'''), 128.4 (C-5'''), 137.1 (C-3'''), 137.6 (C-1'''), 142.0 (C-2), 148.1 (C-5), 171.1 (C-1'), 178.2 (C-1), 183.7 (C-4). EIMS  $m/z$  282.9 [M-H] $^-$ ; 307.0 [M+Na] $^+$ ; anal. C 67.42, H 5.81, N 9.57%, calcd for C<sub>16</sub>H<sub>16</sub>N<sub>2</sub>O<sub>3</sub>, C 62.67.59, H 5.67, N 9.85%; found: C 67.42, H 5.81, N 9.57%.

**2-Pentanamido-5-(benzylamino)-1,4-benzoquinone (3.12):**



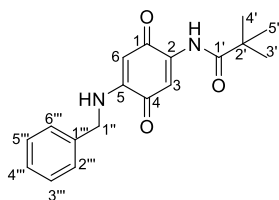
Quantities used in the reaction: amine (0.1 g, 0.92 mmol); quinone (149 mg, 0.72 mmol). Red solid. Yield: 90% (204 mg, 0.65mmol). Mp 209-211 °C. IR: ( $\nu_{\max}/\text{cm}^{-1}$ ) 3314, 2970, 2870, 1696, 1654, 1600, 1508, 1328, 1178, 870.  $^1\text{H}$  NMR (DMSO- $d_6$ , 400 MHz)  $\delta$ : 0.85 (t,  $J = 7.0$  Hz, 3H, H-5'), 1.19-1.31 (m, 2H, H-4'), 1.44-1.53 (m, 2H, H-3'), 2.41-2.59 (m, 2H, H-2'), 4.39 (s, 2H, H-1''), 5.33 (s, 1H, H-6), 7.22-7.31 (m, 6H, H-3, H-2'''-H-6'''), 8.28 (s, 1H, N-H), 9.44 (s, 1H, N-H).  $^{13}\text{C}$  NMR (DMSO- $d_6$ , 100 MHz)  $\delta$ : 13.6 (C-5'), 21.6 (C-4'), 26.7 (C-3'), 36.2 (C-2'), 45.1 (C-1'''), 94.4 (C-6), 109.0 (C-3), 127.2 (C-4''', C-2''', C-6'''), 128.5 (C-3''', C-5'''), 137.1 (C-1'''), 141.9 (C-2), 148.1 (C-5), 173.9 (C-1'), 178.2 (C-1), 183.6 (C-4). EIMS  $m/z$  311.5 [M-H] $^-$ ; 335.3 [M+Na] $^+$ ; analysis for C<sub>18</sub>H<sub>20</sub>N<sub>2</sub>O<sub>3</sub>, C 69.00, H 6.60, N 9.85%; found: C 69.21, H 6.45, N 9.97%.

**3-methylbutamido-5-(benzylamino)-1,4-benzoquinone (3.13):**



Quantities used in the reaction: amine (0.1 g, 0.92 mmol); quinone (137 mg, 0.66 mmol). Red solid; yield: 82% (186 mg, 0.59 mmol). Mp 198-200 °C. IR: ( $\nu_{\text{max}}/\text{cm}^{-1}$ ) 3318, 2975, 2872, 1698, 1652, 1605, 1502, 1324, 1179, 880.  $^1\text{H}$  NMR ( $\text{CDCl}_3$ , 400 MHz)  $\delta$ : 0.99 (d,  $J = 6.6$  Hz, 6H, H-4' and H-5'), 2.12-2.22 (m, 1H, H-3'), 2.29 (d,  $J = 7.0$  Hz, 2H, H-2'), 4.33 (d,  $J = 5.8$  Hz, 2H, H-1''), 5.47 (s, 1H, H-6), 6.44 (s br, 1H, N-H), 7.25-7.37 (m, 5H, H-2'''-H-6'''), 7.39 (s, 1H, H-3), 8.53 (s br, 1H, N-H).  $^{13}\text{C}$  NMR ( $\text{CDCl}_3$ , 100 MHz)  $\delta$ : 22.5 (C-4' and C-5'), 26.1 (C-2'), 46.9 (C-3'), 47.2 (C-1''), 94.9 (C-6), 109.7 (C-3), 127.7 (C-2'', C-6''), 128.4 (C-4''') 129.2 (C-3''', C-5'''), 135.4 (C-1'''), 141.2 (C-2), 148.0 (C-5), 172.1 (C-1'), 179.3 (C-1), 183.4 (C-4). EIMS  $m/z$  311.3  $[\text{M}-\text{H}]^-$ ; 335.7  $[\text{M}+\text{Na}]^+$ ; analysis for  $\text{C}_{18}\text{H}_{20}\text{N}_2\text{O}_3$ , C 69.08, H 6.70, N 9.80%; found: C 69.00, H 6.45, N 9.36%.

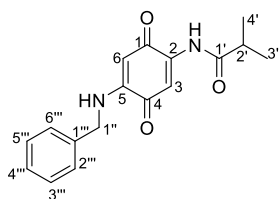
**2-Pivalamido-5-(benzylamino)-1,4-benzoquinone (3.14):**



Quantities used in the reaction: amine (0.1 g, 0.92 mmol); quinone (150 mg, 0.73 mmol). Red solid; yield: 95% (216 mg, 0.69 mmol). Mp 206-208 °C. IR: ( $\nu_{\text{max}}/\text{cm}^{-1}$ ) 3324, 3090, 3066, 3030, 2970, 2932, 2870, 1696, 1654, 1600, 1456, 1256, 992.  $^1\text{H}$  NMR ( $\text{DMSO}-d_6$ , 400 MHz)  $\delta$ : 1.20 (s, 12H, H-3', H-4', H-5'), 4.42 (s, 2H, H-1''), 5.39 (s, 1H, H-6), 7.13 (s, 1H, H-3), 7.25-7.31 (m, 5H, H-2'''-H-6'''), 8.44 (sbr, 1H, N-H), 8.93 (sbr, 1H, N-H).  $^{13}\text{C}$  NMR ( $\text{DMSO}-d_6$ , 100 MHz)  $\delta$ : 26.6 (C-3', C-4', C-5'), 40.2 (C-2'), 45.1 (C-1''), 93.9 (C-6), 108.4 (C-3), 127.1 (C-4''', C-2''', C-6'''), 128.4 (C-3''', C-5'''), 136.9 (C-1'''), 141.1 (C-2), 148.6 (C-5), 177.4 (C-1'), 177.6 (C-1), 183.2 (C-4). EIMS  $m/z$  311.4  $[\text{M}-\text{H}]^-$ ; 335.1  $[\text{M}+\text{Na}]^+$ ; analysis for  $\text{C}_{18}\text{H}_{20}\text{N}_2\text{O}_3$ , C 69.13, H 6.62, N 9.73%; found: C 69.21, H 6.45, N 9.97%.

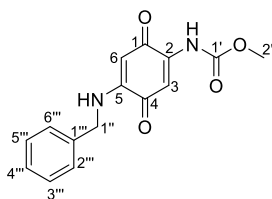


### 2-Isobutyramido-5-(benzylamino)-1,4-benzoquinone (**3.15**):



Quantities used in the reaction: amine (0.1 g, 0.92 mmol); quinone (139 mg, 0.72 mmol). Red solid; yield: 75% (163 mg, 0.54 mmol). Mp 225-228 °C. IR: ( $\nu_{\max}/\text{cm}^{-1}$ ) 3298, 3256, 2972, 2932, 1706, 1654, 1592, 1494, 1330, 1178, 734.  $^1\text{H}$  NMR (DMSO- $d_6$ , 400 MHz)  $\delta$ : 1.06 (sbr, 6H, H-3',H-4'), 2.97 (sbr, 1H, H-2'), 4.40 (s, 2H, H-1''), 5.36 (s, 1H, H-6), 7.23-7.33 (m, 6H, H-3, H-2'''-H-6'''), 8.32 (sbr, 1H, N-H), 9.42 (sbr, 1H, N-H).  $^{13}\text{C}$  NMR (DMSO- $d_6$ , 100 MHz)  $\delta$ : 19.1 (C-3', C-4'), 34.9 (C-2'), 45.1 (C-1''), 94.4 (C-6), 109.2 (C-3), 127.2 (C-4''', C-2''', C-6'''), 128.5 (C-3''', C-5'''), 137.1 (C-1'''), 142.1 (C-2), 148.2 (C-5), 155.3 (C-1'), 177.8 (C-1), 178.1 (C-4). EIMS  $m/z$  297.0 [M-H] $^-$ ; 299.4 [M+Na] $^+$ ; analysis for  $\text{C}_{17}\text{H}_{18}\text{N}_2\text{O}_3$ , C 68.21, H 6.23, N 9.27%; found: C 68.44, H 6.08, N 9.39%.

### 2-((methoxycarbonyl)amino)-5-(benzylamino)-1,4-benzoquinone (**3.16**):



Quantities used in the reaction: amine (0.1 g, 0.92 mmol); quinone (130 mg, 0.72 mmol). Red solid; yield: 86% (179 mg, 0.62 mmol). Mp 210-212 °C. IR: ( $\nu_{\max}/\text{cm}^{-1}$ ) 3318, 3230, 2946, 1742, 1654, 1578, 1370, 1342, 1186, 1050, 866 746  $\text{cm}^{-1}$ ;  $^1\text{H}$  NMR (DMSO- $d_6$ , 400 MHz)  $\delta$ : 3.70 (s, 3H, H-2'), 4.39 (s, 2H, H-1''), 5.34 (s, 1H, H-6), 6.83 (s, 1H, H-3), 7.25-7.31 (m, 5H, H-2'''-H-6'''), 8.35 (s, 1H, N-H), 8.69 (s, 1H, N-H).  $^{13}\text{C}$  NMR (DMSO- $d_6$ , 100 MHz)  $\delta$ : 45.2 (C-1''), 52.9 (C-2'), 94.2 (C-6), 107.4 (C-3), 127.2 (C-4''', C-2''', C-6'''), 128.5 (C-3''', C-5'''), 137.1 (C-1'''), 142.7 (C-2), 148.4 (C-5), 152.8 (C-1'), 177.2 (C-1), 182.7 (C-4). EIMS  $m/z$  284.9 [M-H] $^-$ ; 287.1 [M-H] $^+$ ; 309.3 [M+Na] $^+$ ; analysis for  $\text{C}_{15}\text{H}_{13}\text{BrN}_2\text{O}_3$ , C 62.77, H 5.11, N 9.57%; found: C 62.93, H 4.93, N 9.79%.

## 4.3. Biological assay

### 4.3.1. Measurement of the Photosynthetic Electron Transport

This study was performed by professor Giuseppe Forlani from University of Ferrara - Italy.

Photosynthetically active thylakoid membranes were isolated from market spinach (*Spinacia oleracea* L.) leaves. Briefly, 20 g of deveined plant material

were resuspended in 100 mL of ice-cold 20 mM Tricine/NaOH buffer (pH 8.0) containing 10 mM NaCl, 5 mM MgCl<sub>2</sub> and 0.4 M sucrose, and homogenized for 30 s in a blender at maximal speed. The homogenate was filtered through surgical gauze, and the filtrate was centrifuged at 4 °C for 1 min at 500 g; the supernatant was further centrifuged for 10 min at 1500 g. Pelleted chloroplasts were osmotically disrupted by resuspension in sucrose-lacking buffer, immediately diluted 1:1 with sucrose-containing buffer and kept on ice in the dark until used. Following dilution with 80% (v/v) acetone, the chlorophyll content was calculated using the Arnon's formula. The basal rate of photosynthetic electron transport was measured following the light-driven reduction of ferricyanide. Aliquots of membrane preparations corresponding to 15 µg of chlorophyll were incubated at 24 °C in 1 mL cuvettes containing 20 mM tricine/NaOH buffer (pH 8.0), 10 mM NaCl, 5 mM MgCl<sub>2</sub>, 0.2 M sucrose and 1 mM K<sub>3</sub>[Fe(CN)<sub>6</sub>]. The assay was initiated by exposure to saturating light (800 µmol/m<sup>2</sup>/s), and the rate of ferricyanide reduction was measured at 1 min intervals for 20 min in a Novaspec Plus spectrophotometer (GE Healthcare, Milan, Italy) at 420 nm against an exact blank. Activity was calculated over the linear portion of the curve from a molar extinction coefficient of 1000/M/cm. Compounds were dissolved in DMSO and then diluted with water, as required. Their effect on the photosynthetic electron transport chain was measured by adding concentrations in the range from 0.1 to 100 µM to the above reaction mixture and comparing the results with untreated parallel controls. Each assay was repeated in triplicate, and results were expressed as percentage of untreated controls. Phosphorylating photosynthetic electron rate was determined under the same conditions, but in the presence of 0.5 mM ADP and 2 mM K<sub>2</sub>HPO<sub>4</sub>. Uncoupled photosynthetic electron rate was measured following the addition of 1 mM NH<sub>4</sub>Cl to the basal reaction mixture. In these last two cases, ferricyanide reduction was determined at intervals of 30 s for 10 min. Reported values are mean ± SE over replicates. The concentrations causing 50% inhibition (IC<sub>50</sub>) and their confidence limits were estimated by nonlinear regression analysis using Prism 6 for Windows, version 6.03 (GraphPad Software, La Jolla, CA).

#### 4.3.2. *Molecular docking*

Molecular docking studies for compound **3.6** with the active site of spinach photosystem II (PDB: 3JCU) were performed by using AutoDockTools 4.2 program suite [30,31]. Each compound was generated using ChemDraw 14.0 followed by MM2 energy minimization. The target enzyme was prepared for molecular docking simulation using the chain A by removing water, and all hydrogens were added, Gasteiger charges were calculated and non-polar hydrogens were merged to carbon atoms. A grid box size of 40 x 40 x 40 point (x, y, z) with a spacing of 0.486 Å was centered on the X, Y, and Z at -41.788, 3.115, and -18.728, respectively. Then, to evaluate the binding free energy of the inhibitor–macromolecule, automated docking studies were carried out. The genetic algorithm with local search (GALS) was used to find the best conformers. The Lamarckian genetic algorithm with default settings was used as well. Docking experiment was performed 50 times, yielding 50 docked conformations.

## 5. REFERENCES

- [1] S.O. Duke, C.L. Cantrell, K.M. Meepagala, D.E. Wedge, N. Tabanca, K.K. Schrader, *Toxins* (Basel). 2 (2010) 1943–1962.
- [2] R.S. Baucom, *Am. J. Bot.* 103 (2016) 1–3.
- [3] D.L. Shaner, *Weed Sci.* 62 (2014) 427–431.
- [4] R.R. Teixeira, J.L. Pereira, W.L. Pereira, *Appl. Photosynth.* (2012) 3–22.
- [5] I. Heap, *Pest Manag. Sci.* 70 (2014) 1306–1315.
- [6] N.R. Burgos, P.J. Tranel, J.C. Streibig, V.M. Davis, D. Shaner, J.K. Norsworthy, C. Ritz, *Weed Sci.* 61 (2012) 4–20.
- [7] S.B. Powles, Q. Yu, *Evolution in Action: Plants Resistant to Herbicides*, 2010.
- [8] C.L. Cantrell, F.E. Dayan, S.O. Duke, *J. Nat. Prod.* 75 (2012) 1231–1242.
- [9] M. Renton, R. Busi, P. Neve, D. Thornby, M. Vila-Aiub, *Pest Manag. Sci.* 70 (2014) 1394–1404.
- [10] A.J. Demuner, L.C.A. Barbosa, A.C.M. Miranda, G.C. Geraldo, C.M. Da Silva, S. Giberti, M. Bertazzini, G. Forlani, *J. Nat. Prod.* 76 (2013) 2234–2245.
- [11] R.R. Teixeira, L.C.A. Barbosa, G. Forlani, D. Piló-Veloso, J.W.D.M. Carneiro, *J. Agric. Food Chem.* 56 (2008) 2321–2329.
- [12] L.C.A. Barbosa, M.E. Rocha, R.R. Teixeira, C.R.A. Maltha, G. Forlani, *J. Agric. Food Chem.* 55 (2007) 8562–8569.
- [13] L.C.A. Barbosa, U.A. Pereira, R.R. Teixeira, C.R.A. Maltha, S.A. Fernandes, G. Forlani, *J. Agric. Food Chem.* 56 (2008) 9434–9440.
- [14] D. Rodríguez-Hernández, A.J. Demuner, L.C.A. Barbosa, L. Heller, R. Csuk, *Eur. J. Med. Chem.* 115 (2016) 257–267.
- [15] B. Pal, P. Jaisankar, V.S. Giri, *Synth. Commun.* 34 (2004) 1317–1323.
- [16] B. Lotina-Hennsen, L. Achnine, N.M. Ruvalcaba, A. Ortiz, J. Hernández, N. Farfán, M. Aguilar-Martínez, *J. Agric. Food Chem.* 46 (1998) 724–730.
- [17] A. Nain-Perez, L.C.A. Barbosa, M.C. Picanço, S. Giberti, G. Forlani, *Chem. Biodivers.* 13 (2016) 1008–1017.
- [18] H.T. Witt, *Berichte Der Bunsengesellschaft Für Phys. Chemie* 100 (1996) 1923–1942.
- [19] A. Pereira, L.C.A. Barbosa, A.J. Demuner, A.A. Silva, M. Bertazzini, G. Forlani, *Chem. Biodivers.* 12 (2015) 987–1006.
- [20] L.C.A. Barbosa, A.J. Demuner, E.S. De Alvarenga, A. Oliveira, B. King-Diaz, B. Lotina-Hennsen, *Pest Manag. Sci.* 62 (2006) 214–222.
- [21] R.R. Teixeira, J.L. Pereira, W.L. Pereira, in: M.M. Najafpour (Ed.), *Appl. Photosynth.*, InTech, 2012, pp. 3–22.
- [22] R. Barr, F.L. Crane, *Biochem. Biophys. Res. Commun.* 67 (1981) 1190–1194.
- [23] M.D. Lambrevia, D. Russo, F. Polticelli, V. Scognamiglio, A. Antonacci, V.

- Zobnina, G. Campi, G. Rea, *Curr. Protein Pept. Sci.* 15 (2014) 285–95.
- [24] J. Xiong, S. Subramaniam, Govindjee, *Protein Sci.* 5 (1996) 2054–2073.
- [25] G. Rea, F. Polticelli, A. Antonacci, M. Lambreva, S. Pastorelli, V. Scognamiglio, V. Zobnina, M.T. Giardi, in: M. Larramendy (Ed.), *Herbic. Theory Appl.*, InTech, 2011.
- [26] M.D. Lambreva, D. Russo, F. Polticelli, V. Scognamiglio, A. Antonacci, V. Zobnina, G. Campi, G. Rea, *Curr. Protein Pept. Sci.* 15 (2014) 285–95.
- [27] S. Funar-Timofei, A. Borota, L. Crisan, *Mol. Divers.* 21 (2017) 437–454.
- [28] M. Broser, C. Glöckner, A. Gabdulkhakov, A. Guskov, J. Buchta, J. Kern, F. Müh, H. Dau, W. Saenger, A. Zouni, *J. Biol. Chem.* 286 (2011) 15964–15972.
- [29] D.V. Singh, S. Agarwal, R.K. Kesharwani, K. Misra, *J. Mol. Model.* 18 (2012) 3903–3913.
- [30] M. Sanner F., *J. Mol. Graph.* 17 (1999) 57–61.
- [31] S. Forli, R. Huey, M.E. Pique, M.F. Sanner, D.S. Goodsell, A.J. Olson, *Nat. Protoc.* 11 (2016) 905–919.

## **CHAPTER 4**

### **SYNTHESIS OF NEW RUTHENIUM COMPLEXES WITH 2,5-DI(ALKYLAMINO)-1,4-BENZOQUINONE**

## 1. INTRODUCTION

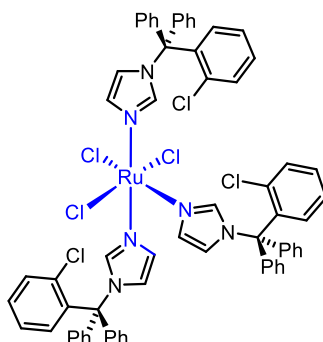
Organometallic compounds are defined as compounds in which organic groups are linked directly to the metal through at least one covalent metal-carbon bond [1,2]. These kinds of compounds have great structural variety, meaning that it goes from linear to octahedral [2]. Some other relevant characteristics include a wide range of coordination numbers, accessible redox states, and a wide structural diversity [3]. Coordination number is an attractive property of organometallic compounds, which gives different geometric possibilities, resulting from the six-coordinated metal centers to four-coordinated carbon. This property makes organometallic compounds an interesting approach for the development of the new species, that require different active sites [4]. The redox activity is interesting because enables to correlate the properties of metal compounds with electron transfer, oxidative stress, the formation of reactive oxygen species, and generally the redox status of cells [2].

Furthermore, metals play an important role in biological systems, offering potential advantages over the more common organic drugs. For instance, the discovery and development of the antitumor drug cisplatin (*cis*-[Pt(NH<sub>3</sub>)<sub>2</sub>Cl<sub>2</sub>]) had an incredible impact in the field of medicinal inorganic chemistry [5]. Due to their high effect, this compound is widely used in treatment of testicular and ovarian cancers [6].

The increasing interest in the research of metal compounds with potential applications in medicine in the last decades has come along to a deeper understanding of the reactivity of metal ions and their interaction with a wide range of biomolecules such as DNA and proteins [7]. Biological systems themselves, provide innumerable examples of 'designer ligands' that bind metal ions to perform important biological functions [5].

Ligands have importance in the biological effects on the metal used as drugs since they can modify the systemic bioavailability of metal ions and can assist in specific tissues or enzymes. Ligands can also ensure the protection of tissues from toxic metal ions or enhance uptake of pharmacologically beneficial metal ions [8].

There are some synergistic effects between the ligand, with known biological activity with a metal-containing fragment, such combinations can generate an enhanced activity of the parent drug [9]. For example, when ketoconazole and clotrimazole are ligands for Cu, Rh, Pt, Ru and Au, these complexes results in a more effective anti-malarial and anti-trypanosome in comparison with non-metal containing analogues (Figure 4.1) [8,10,11].



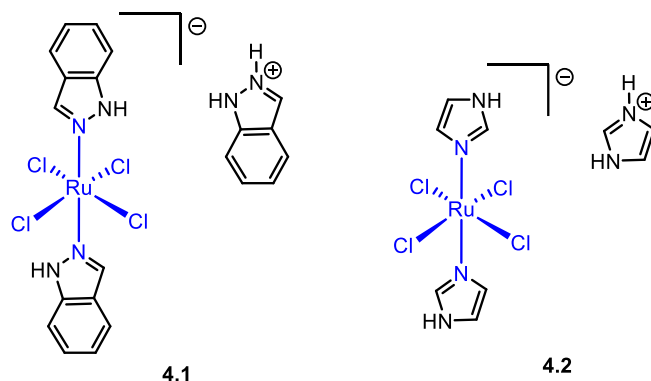
**Figure 4.1.** Octahedrally coordinated Ru(III) with three N-donor atoms of clotrimazole and three chlorides in a mer stereochemistry.

In the last decades, ruthenium has been studied from the medical scope, due to its large positive effects on various therapeutic treatments [10–17].

Ruthenium compounds containing Ru(II) or Ru(III) are considered to be appropriate candidates for anticancer drug design because they exhibit a similar spectrum of kinetics that traditional platinum-based therapeutics [3]. The spectrum of the antitumor effects of ruthenium complex differs significantly from that of cisplatin, as they show lower toxicity than platinum(II) compounds [6].

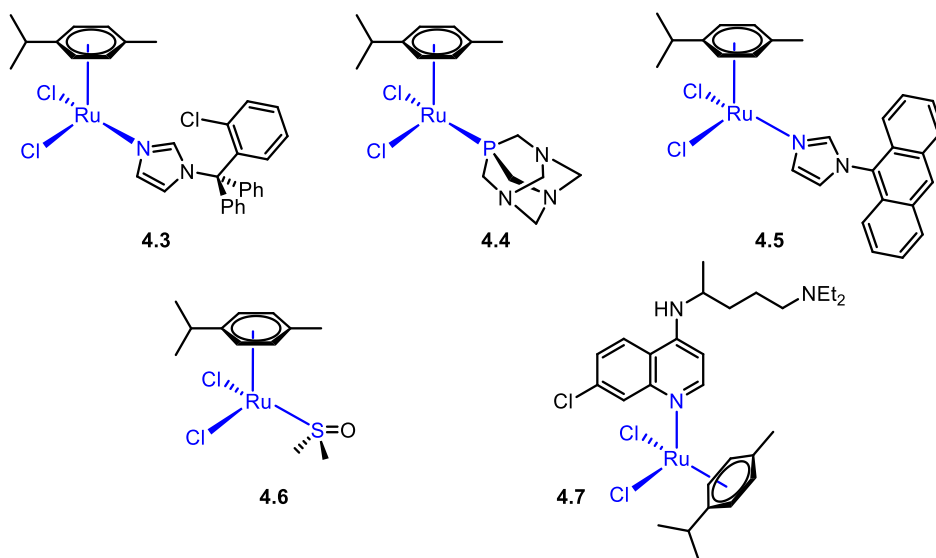
It is known that all ruthenium compounds bind to DNA and this is the main reason for their anticancer effect, similar to the platinum derivatives, causing modifications in the structure of DNA that lead to the induction of apoptosis [2]. For instance, two ruthenium(III) complexes have entered clinical trials, namely (H<sub>2</sub>im)[*trans*-RuCl<sub>4</sub>(DMSO)(Him)] (**4.1**) and (H<sub>2</sub>ind)[*trans*-RuCl<sub>4</sub>(Hind)<sub>2</sub>] (**4.2**) (Figure 4.2), where compound **4.1** is more active against metastases than against primary tumors, and compound **4.2**, which has a similar structure, is active against primary tumors [3,18,19].





**Figure 4.2.** Structural formula for compounds **4.1** and **4.2**.

There is a series of ruthenium(II) complexes (**4.3-4.7**) that have the *p*-cymene groups as a ligand, where the presence of the arene provides stability to the complexes. In addition, it has the particularity of having two chlorine atoms, which generates a similarity structure with cisplatin, and present cytotoxic activity [2,9] (Figure 4.3). Therefore, these compounds were found to be susceptible to hydrolysis and it was first anticipated that DNA was a primary target [2].



**Figure 4.3.** Ruthenium complexes, enzyme inhibitor and antitumor agents.

The mode of action of these kinds of compounds has not been fully clarified yet. One of the hypothesis is the activation-by-reduction theory, in which the reduction of Ru(III) to Ru(II) would be facilitated due to the difference in the electrochemical potential of a solid tumor and the surrounding normal tissue. The electrochemical potential of a tumor is generally lower due to the hypoxic environment of the tumor [19].

As mentioned in the general introduction, natural occurring aminoquinones core are our aim in this work, due to the wide variety of this class of compound in nature and their important biological activities [20–22]. Specifically, aminoquinones play an important role in the treatment of cancer [23–25], due to their properties in the redox cycle, allowing it to act through different mechanisms of action [26]. To the best of our knowledge, there are few studies of this class of compounds all of them are related to preparation and structural characterization [27].

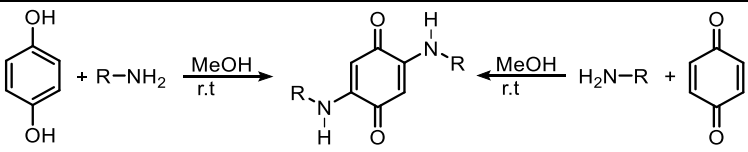
In this chapter, will be described the synthesis of a new series of compounds that combine different 2,5-di(alkyl/arylamino)-1,4-benzoquinones with ruthenium. Also, the structural characterization of the ruthenium compounds as well the biological evaluation will be discussed.

## 2. RESULTS AND DISCUSSION

### 2.1. Synthesis of ligands 2,5-di(alkyl/arylamino)-1,4-benzoquinone

One of the reports on the synthesis of alkylamino-substituted-*p*-quinones involves the reaction of the commercially available hydroquinone and amines in methanol at room temperature for one hour [28]. Following this protocol, pentylamine was reacted with hydroquinone (1:1) affording aminoquinone **4.11** in only 24% yield (Table 4.1, entry 1). Owing to the low yield obtained, the conditions of the reaction were optimized (Table 4.1).

**Table 4.1.** Optimization of the reaction conditions for synthesis of 2,5-diamino-1,4-benzoquinones



Entry	Quinone or Hydroquinone (eq)	Amine (eq)	Time (h)	Compound, Yield (%)
1	Hq (1)	A (1)	1	<b>4.11</b> , 24
2	Hq (1)	A (1)	18	<b>4.11</b> , 45
3	Hq (1)	A (1)	24	<b>4.11</b> , 48
4	Hq (1)	A (2)	36	<b>4.11</b> , 24
5	Bq (3)	A (1)	1	<b>4.11</b> , 93
6	Hq (1)	B (1)	18	<b>4.17</b> , 10
7	Hq (1)	B (1)	36	<b>4.17</b> , 45
8	Hq (1)	B (2)	36	<b>4.17</b> , 10
9	Bq (1)	B (2)	24	<b>4.17</b> , 25
10	Bq (3)	B (1)	36	<b>4.17</b> , 77

A – pentylamine; B- 3-aminobenzylalcohol; Hq= Hydroquinone; Bq= *p*-Benzoquinone.

Initially, the reaction time was increased to 18 and 24 hours, yielding the desired compound **4.11** in 45% and 48%, respectively (Table 4.1, entries 2, 3). Then, even though 2.0 equivalents of amine and 36 hours of reactions, only 24% of product **4.11** was isolated (Table 4.1, entry 4).

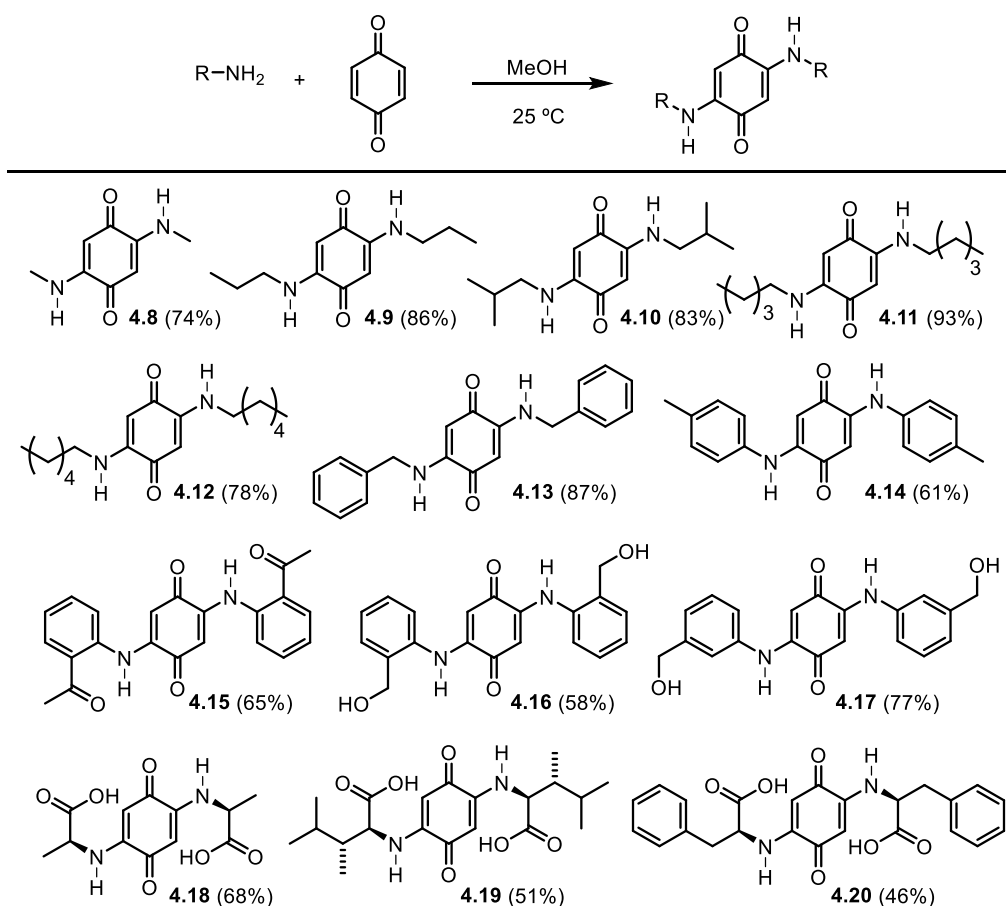
Since amination reaction employing hydroquinone as precursor gave low yields, we turned our attention to use *p*-benzoquinone as more reliable starting material [29–31]. Then, we found that using a 1:3 ratio of amine:benzoquinone

the required product **4.11** was obtained in excellent 93% yield (Table 4.1, entry 5).

Aiming to study the scope of the reaction, an aromatic amine (3-aminobenzylalcohol) was employed. Then, the reaction mixture of amine:hydroquinone (1:1 ratio) was stirred for 18 and 36 hours, yielding the desired compound **4.17** in low 10% and 45% yields, respectively (Table 4.1, entries 6, 7). When the reaction was carried out in a 2:1 ratio of amine:hydroquinone (Table 4.1, entry 8) even after 36 hours only 10% of product **4.17** was isolated. Following by using benzoquinone starting material with excess of aromatic amine (ratio to 1:2) for 24 hours the yield was not improved (Table 4.1, entry 9). Finally, the best yield for the product, 77 %, was accomplished by using and excess of benzoquinone (1:3 proportion; Table 4.1, entry 10).

Having established a protocol to produce 2,5-dialkylamino- and 2,5-diarylamino-benzoquinones in high yields, a series of analogues **4.8-4.20** were prepared (Figure 4.4). In general, the procedure involved a reaction between 1 equivalent of amine and 3 equivalents of benzoquinone, dissolved in methanol, at room temperature and for approximately 1-16 hours, under normal atmosphere. For the synthesis of compounds **4.18-4.20** it was necessary to add  $\text{NaHCO}_3$  to the ethanolic solution of the amino acids to ensure the full deprotonation of the zwitterion [32].

In general, the aliphatic amines were obtained in higher yields (74-93%), while for the less nucleophilic aromatic amines the yields were in the range of 58-87%. For the amino acids, the yields of the products varied from 46-68%. Although these yields were low, the results are good since the only report of reaction between benzoquinone and amino acids in good yields involves the use of the enzyme laccase as a catalyst [33].



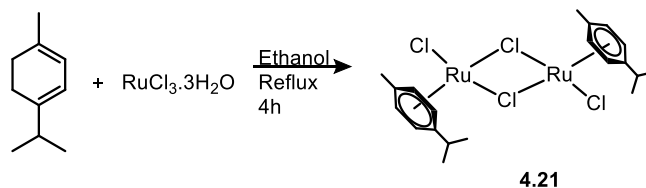
**Figure 4.4.** Synthesis of 2,5-bis-(alkyl/arylamino)-1,4-benzoquinones **4.8-4.20**.

### 2.1.1. Characterization

The structure of each compound was confirmed by extensive spectroscopic analysis. All compounds showed in their respective IR spectra typical absorptions expected for the major functional groups present. For example, a broad N-H absorption band centered around 3200 cm<sup>-1</sup> was observed. In addition, the stretch vibration of the carbonyl group of the quinone C=O was observed between 1640-1630 cm<sup>-1</sup> [34]. Through the <sup>1</sup>H-NMR spectrum, the vinylic hydrogen was confirmed at  $\delta = 5.1-6.4$  as a singlet, whereas <sup>13</sup>C-NMR analysis confirmed the carbonyl group at  $\delta = 177-181$  and the double bond of quinone (=C-H) at  $\delta = 90-110$ . A detailed assignment of the NMR spectra (<sup>1</sup>H and <sup>13</sup>C), ESI-MS and physical data for all new compounds are presented in the experimental section.

## 2.2. Synthesis of $\mu$ -dichloro(*p*-cymene)ruthenium(II) dimer (4.21)

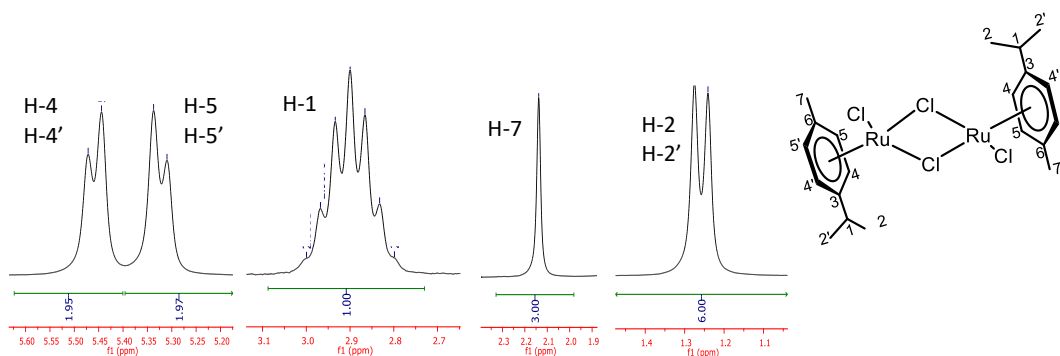
Ruthenium dimer was prepared following the methodology described by Bennett *et al* [35]. The dimer was obtained by a reaction between  $\alpha$ -phellandrene and  $\text{RuCl}_3 \cdot 3\text{H}_2\text{O}$  in ethanol at reflux for four hours (Figure 4.5). The complex was obtained as orange solid in 85% yield. Spectroscopy data matches to what is expected.



**Figure 4.5.** Synthesis of  $[\text{Ru}(p\text{-Cym})\text{Cl}_2]_2$ .

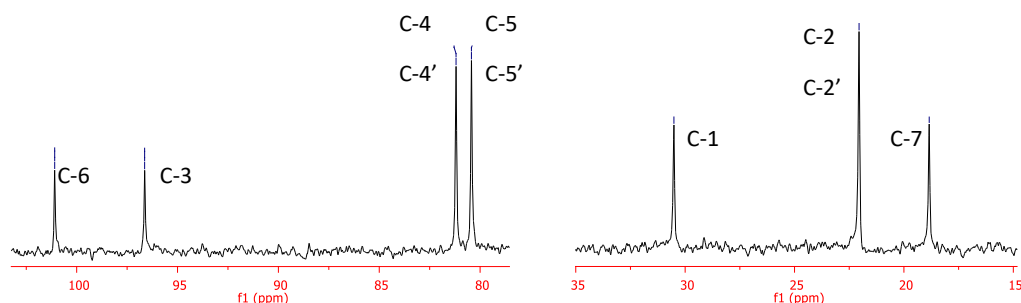
### 2.2.1. Characterization

In Figure 4.6 it is shown the  $^1\text{H}$  NMR spectra for compound **4.21**, in low frequency it was observed a signal as a doublet at  $\delta = 1.25$  ( $J = 6.8$  Hz) corresponding to the hydrogens of two methyl groups (H-2 and H-2'), and a singlet corresponding to methyl-7 at  $\delta = 2.13$ . Another signal is observed as a septet at  $\delta = 2.89$  ( $J = 6.8$  Hz) corresponding to methine-1 as expected. In addition, the signal corresponded to the hydrogens of the aromatic ring as H-5 and H-5' is observed as a doublet at  $\delta = 5.32$  ( $J = 5.5$  Hz). Finally, a doublet at  $\delta = 5.45$  ( $J = 5.5$  Hz) is related to the aromatic ring H-4 and H-4'. The spectroscopic data match with reported by Hodson *et al* [36].



**Figure 4.6.** Expansion of  $^1\text{H}$  NMR spectrum ( $\text{CDCl}_3$ , 200 MHz) of compound **4.21**.

By  $^{13}\text{C}$  NMR (Figure 4.7) it was also possible to confirm the signal relative to methyl-7 at  $\delta = 18.8$  as well as the methyl of the isopropyl group at  $\delta = 22.0$  (C-2 and C-2'). Also, the signal related to methine-1 is observed at  $\delta = 30.1$ . In the case of aromatic carbon, they are at  $\delta = 80.4$  and  $81.9$  which corresponds to C-4 and C-4' and C-5 and C-5', respectively. A signal correlated to C-3 and C-6 was observed at  $\delta = 96.6$  and  $101.0$ . The spectroscopic data match with the reported by Hodson *et al* [36].



**Figure 4.7.** Expansion of  $^{13}\text{C}$  NMR spectrum ( $\text{CDCl}_3$ , 75 MHz) of compound **4.21**.

In organometallic compounds, chemical shift values are much more variable than organic compounds, and this depends on the metal center which is bonded.  $^1\text{H}$  and  $^{13}\text{C}$  NMR of ruthenium complexes show a tendency to low frequency, due to the increased shielding from the nearby metal, since ruthenium is an electron-rich metal center [37,38].

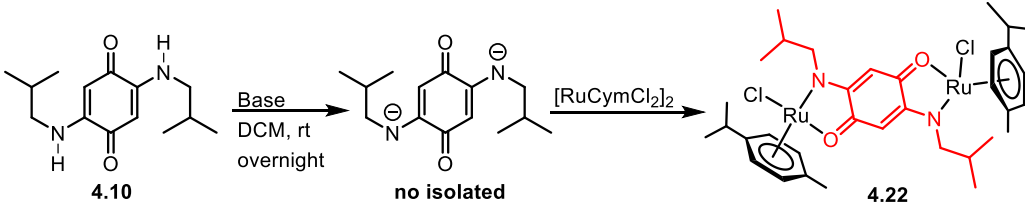
### 2.3. Synthesis of dinuclear ruthenium complexes of 2,5-dialkylamino-1,4-benzoquinone ligands

Complex 2,5-dialkylamino-1,4-benzoquinone was prepared as described by Schweinfurth *et al* [27]. In a Schlenk the ligand **4.10** and the ruthenium **4.21** were dissolved in dichloromethane in presence of triethylamine as a base to generate the deprotonated form of the ligand. The solution was left stirring overnight at room temperature, but the quinone was not totally consumed. The presence of the ligand after 24 h of reaction indicates that the base was not strong

enough, for that it was studied the same reaction using two different bases as presented in Table 4.2.

The experiment was carried out using 2.5 equivalent of the base for 1 equivalent of the ligand, knowing that one ligand has two protons to remove. A mixture of the ligand and the base, in dichloromethane, was left stirring overnight at room temperature and argon atmosphere. After the deprotonation of the ligand, the reaction was carried out by the addition of  $[\text{Ru}(p\text{-Cym})\text{Cl}_2]_2$  (**4.21**) to the solution in a ratio 1:1. This reaction mixture was left stirring at room temperature for 3 hours. In Table 4.2 it is shown that sodium hydride produces the expected compound **4.22** in 90% yield, whereas using triethylamine and potassium *tert*-butoxide afforded the product in 40% and 45% yields respectively.

**Table 4.2.** Bases to generate deprotonated ligand 2,5-diamino-1,4-benzoquinone for the synthesis of complex **4.22**

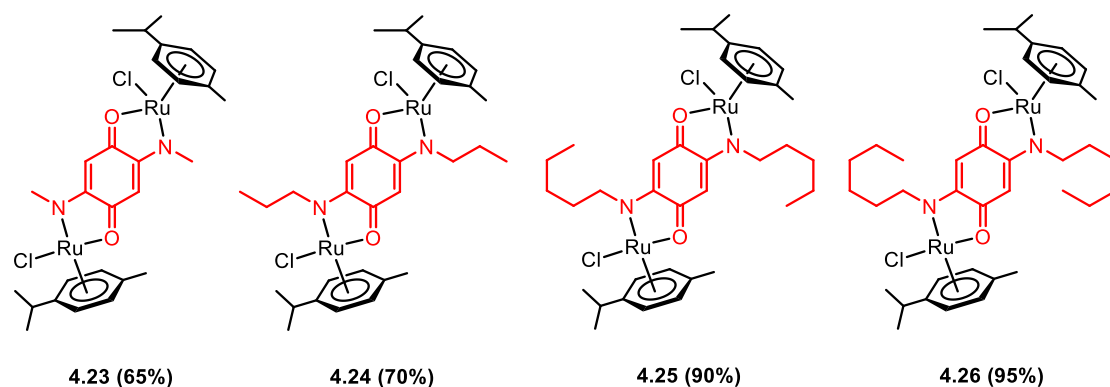


Entry	Ligand (1 equiv)	Base (2.5 equiv)	Yield of compound <b>4.22</b> (%)
1	<b>4.10</b>	$\text{Et}_3\text{N}$	40
2		<i>t</i> -BuOK	45
3		NaH	90

Once knowing the best base to generate the deprotonated ligand, the reactions to prepare de complexes with  $[\text{Ru}(p\text{-Cym})\text{Cl}_2]_2$  were carried out. A mixture of the deprotonated form of **4.10** and  $[\text{Ru}(p\text{-Cym})\text{Cl}_2]_2$  in a 1:1 ratio, dry dichloromethane, and argon atmosphere, was left stirring for three hours. Then, the solvent was reduced to half of its volume and dry hexane was added dropwise to precipitate the product. The solid was filtered under an argon atmosphere and washed with hexane and a dark red compound was obtained in 90% yield.

With this methodology four complexes were prepared **4.23** (65%), **4.24** (70%), **4.25** (90%) and **4.26** (95%), as shown in Figure 4.8.





**Figure 4.8.** Dinuclear ruthenium complexes (**4.23-4.26**).

The synthesized compounds (**4.22-4.26**) showed low solubility in different solvents (DMSO, CH<sub>3</sub>CN, MeOH, CHCl<sub>3</sub>, C<sub>6</sub>H<sub>6</sub>), in the choice of a good solvent for solubilization, it was observed that compounds had low stability in solution. Variations of color from a red solution to black as well the formation of black precipitate were observed. It is possible to suggest that might occur electron transference by ruthenium through quinone as electron acceptors (due to the reductive properties which have quinone moiety [29,30]) to lead different sub-products.

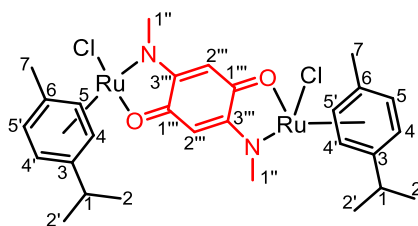
The procedure established for the synthesis of dinuclear ruthenium complexes (**4.23-4.26**) was employed for the synthesis of ruthenium with aminoquinones (**4.13-4.17**) containing the aromatic group but this results in decomposition since the desired complexes were not possible to obtain.

On the other hand, aminoquinones (**4.18-4.20**) containing amino acids groups were not possible to use as ligand since they were not soluble in the solvent selected for the preparation of complexes.

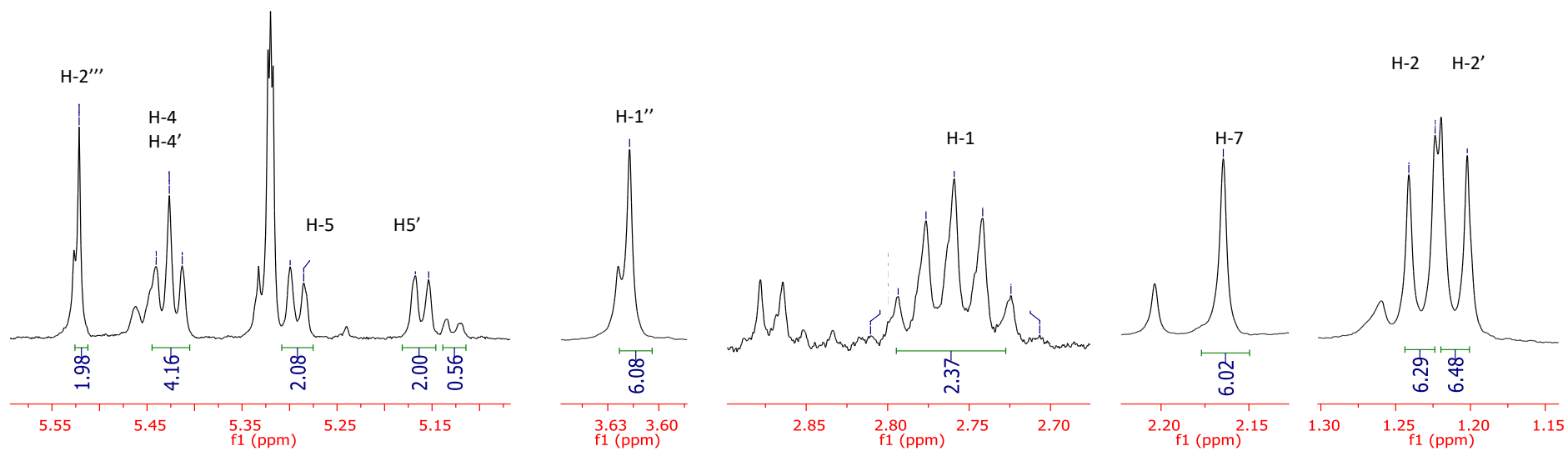
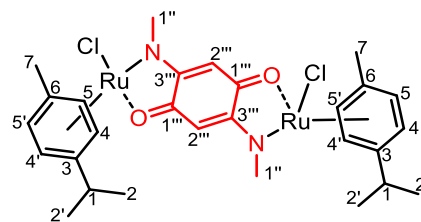
### 2.3.1. Characterization

The obtained complexes were characterized by <sup>1</sup>H and <sup>13</sup>C NMR spectroscopy. Considering that the spectra of the synthesized compounds showed great similarity, only with minor variations concerning the different substituents of each amine used in the reaction, only the characterization of

compound (**4.23**) will be presented (full spectroscopy data are in the experimental section and in Appendix 4).

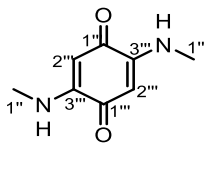
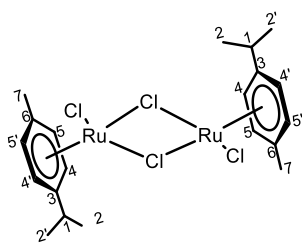
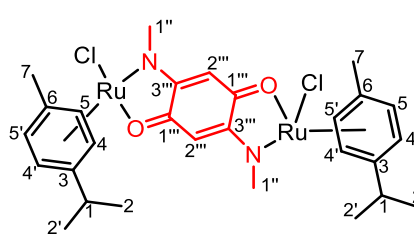


In the  $^1\text{H}$  NMR spectrum (Figure 4.9) it is observed two series of signals, the majority referent to compound **4.23** and the minority signal related to a mixture of isomer to the complex. Then, in low frequency at region  $\delta = 1.20\text{-}2.79$  are observed the signals related to the hydrogens of *p*-cymene (H-2/H-2', H-1 and H-7). First, a doublet at  $\delta = 1.21$  and  $1.23$  ( $J = 7.0$  Hz) related to methyl-2 and methyl-2'. Comparing the results presented in Table 4.3 it is possible to observe that these hydrogen (H-2/H-2') are slightly more shielded than the precursor **4.21** ( $\delta = 1.25$ ). Then, it is observed a singlet at  $\delta = 2.16$  related to methyl-7, this chemical shift is similar to observed for **4.21**, (Table 4.3). Moreover, as expected methine-1 are denoted as septet at  $\delta = 2.76$  ( $J = 7.0$  Hz). On the other hand, for the singlet concerning the methyl group of the aminoquinone moiety (H-1''), at  $\delta = 3.61$ , it is observed a deshielding effect, in comparison with the hydrogen-1'' at  $\delta = 2.75$  for the quinone precursor **4.8** (Table 4.3). In contrast, aromatic hydrogen were observed between  $\delta = 5.15\text{-}5.52$ , these hydrogens were slightly shielded than precursor **4.21** (Table 4.3). In fact, the signals resultant of the hydrogens of precursor **4.21** constitute an AA'BB' spin system, unlike in all of the complexes (**4.22-4.26**) these signals appear as an  $A_2B_2$  spin system, showing a  $J_{AB}$  approximately of 6 Hz. As suggest Hodson *et al.* [36], this is due to the rapid rotation of the *p*-cymene ring relative to the ruthenium fragment. Consequently, hydrogens H-5 and H-5' of the arene are expressive as a doublet at  $\delta = 5.16$  and  $5.29$  ( $J = 5.5$  Hz). Regarding the H-4 and H4' it would be expected a doublet for the 1,4-substitution pattern of *p*-cymene, however, it is observed a multiplet at  $\delta = 5.43$ . Finally, a singlet related to the vinylic hydrogen-2''' was observed at  $\delta = 5.52$ , slightly more deshielded than the precursor **4.8** (H-2'',  $\delta = 5.15$ ).



**Figure 4.9.** Expansion of  $^1\text{H}$  NMR spectrum ( $\text{CD}_2\text{Cl}_2$ , 400 MHz) of compound **4.23**.

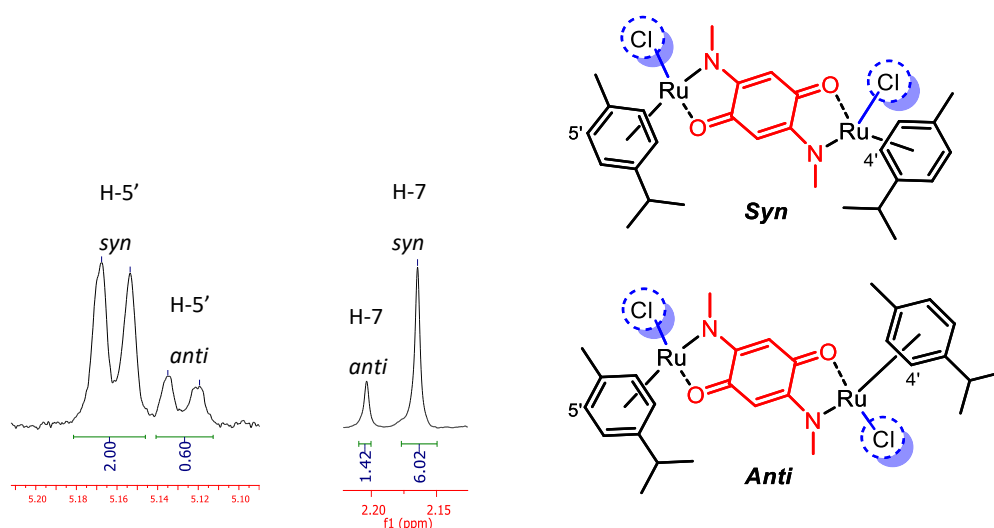
**Table 4.3.** Comparative  $^1\text{H}$  NMR data for starting material and product

					
4.8		4.21		4.23	
N° H	$\delta_{\text{H}}$ (J in Hz)	$\delta_{\text{H}}$ (J in Hz)	$\delta_{\text{H}}$ (J in Hz)	$\delta_{\text{H}}$ (J in Hz)	$\delta_{\text{H}}$ (J in Hz)
1''	2.75, (d, 5.4)			3.61, s	
2'''	5.15, (s)			5.52, s	
N-H	7.60, (s)				
1		2.83-2.96, (m)		2.72-2.79, (m)	
2/2'		1.25, d (6.8)		1.21, (d, 7.0)	
4/4'		5.45, d (5.5)		1.23, (d, 7.0)	
5/5'		5.32, d (5.5)		5.43, (m)	
7		2.13, (s)		5.16, (d, 5.5)	
				5.29, (d, 5.5)	
				2.16, (s)	

In this class of complex (**4.22-4.26**), is possible the formation of isomers *syn* and *anti*, due to the orientation of the chloro ligands with respect to the quinone moiety [27]. The  $^1\text{H}$  NMR spectrum showed two sets of signals that indicate the formation of both isomers, but the signals show the preferential formation of the *syn* isomer [27]. In an expansion of the signal related to hydrogen-5' and hydrogen-7 (Figure 4.10), it is possible to observe that the ratio is 4:1 *syn:anti*. However, when the aliphatic groups bonded to the amine are larger than the methyl group the proportion of the *syn* isomer is higher, for example, the compound **4.25** has a ratio 20:1. All the other *syn:anti* ratio is shown in Table 4.4.

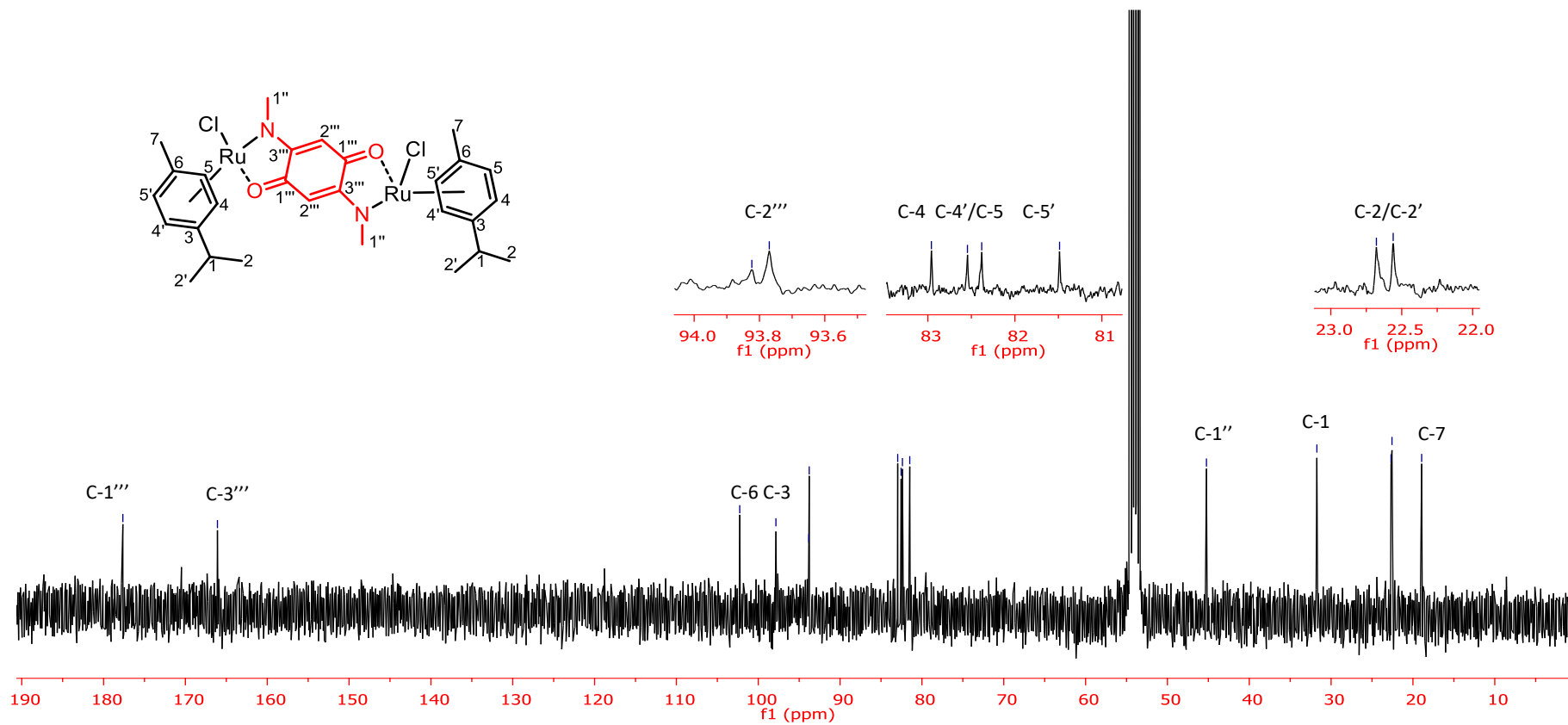
**Table 4.4.** Isomer ratio of complexes **4.22-4.26**

Compounds	Ratio <i>syn:anti</i>
<b>4.22</b>	13:1
<b>4.23</b>	4:1
<b>4.24</b>	18:1
<b>4.25</b>	20:1
<b>4.26</b>	9:1



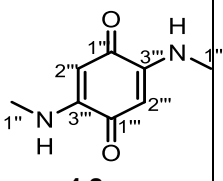
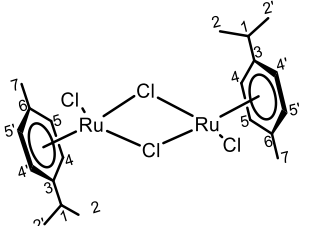
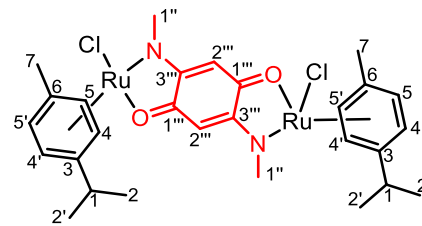
**Figure 4.10.** Expansion of  $^1\text{H}$  NMR spectrum of compound **4.21**, isomer ratio 4:1 *syn*:*anti*.

In the  $^{13}\text{C}$  NMR spectrum (Figure 4.11) it is observed the signal related to methyls C-7, C-2, C-2' and C-1 at  $\delta$  18.9, 22.5, 22.6 and 31.7, respectively. Comparing these data with precursor **4.21** in Table 3, it is possible to observe that these carbons maintain the same chemical shift. However, the deshielded effect is observed for the signal correspondent to C-1'', C-2''' and C-3''' of quinone moiety. The same tendency was observed comparing the carbons of the *p*-cymene ring (C-5, C-5', C-4, C-4', C-3 and C-6) with compound **4.23** (Table 4.5).



**Figure 4.11.** Expansion of  $^{13}\text{C}$  NMR spectrum ( $\text{CD}_2\text{Cl}_2$ , 100 MHz) of compound 4.23.

**Table 4.5.** Comparative  $^{13}\text{C}$  NMR data for starting material and product

				
		<b>4.8</b>	<b>4.21</b>	<b>4.23</b>
<b>N° C</b>	<b><math>\delta_c</math></b>		<b><math>\delta_c</math></b>	<b><math>\delta_c</math></b>
1''	28.6			45.2
1'''	177.1			177.6
2'''	91.8			93.7
3'''	152.3			93.8
1			30.1	166.1
2/2'			22.0	31.7
3			22.0	22.5
4/4'			96.6	22.6
5/5'			81.9	97.8
6			80.4	82.5
7			101.0	82.9
			18.8	81.4
				82.3
				102.3
				18.9

In accordance with spectroscopy data, all synthesized compounds match to what is expected. In total five new ruthenium complexes (**4.22-4.26**) were obtained and fully characterized (all the spectra data of compounds are present in the annex).

#### 2.4. Biological evaluation of ligands (4.8-4.20) and complexes (4.22-4.26)

All the synthesized aminoquinones (**4.8-4.20**) and the five synthesized complexes (**4.22-4.26**) were evaluated as cytotoxic activity against six human tumor cell lines (melanoma cells - 518A2; ovarian carcinoma - A2780; colon adenocarcinoma - HT29; breast adenocarcinoma - MCF7; lung cancer - A549; hypopharyngeal carcinoma - FaDu) and non-malignant mouse fibroblasts (NIH 3T3) using the established photometric sulforhodamine B [39]. The results of these assays are summarized in Table 4.6.

**Table 4.6.** Cytotoxicity for ligands (**4.8-4.20**) and complexes (**4.21-4.26**) employing human tumor cell lines and non-malignant mouse fibroblasts (NIH3T3)

Compounds	EC <sub>50</sub> <sup>a</sup>						NiH 3T3
	Melanoma (518A2)	Ovarian (A2780)	Colon (HT29)	Breast (MCF7)	Lung (A549)	Hypopharyngeal (FaDu)	
<b>4.8</b>	> 60	> 60	> 60	> 60	> 60	> 60	> 60
<b>4.9</b>	> 60	> 60	> 60	> 60	> 60	> 60	> 60
<b>4.10</b>	> 60	> 60	> 60	> 60	> 60	> 60	> 60
<b>4.11</b>	> 60	> 60	> 60	> 60	> 60	> 60	> 60
<b>4.12</b>	> 60	> 60	> 60	> 60	> 60	> 60	> 60
<b>4.13</b>	> 30	> 30	> 30	> 30	> 30	> 30	> 30
<b>4.14</b>	n.s.	n.s.	n.s.	n.s.	n.s.	n.s.	n.s.
<b>4.15</b>	n.s.	n.s.	n.s.	n.s.	n.s.	n.s.	n.s.
<b>4.16</b>	> 30	> 30	> 30	> 30	> 30	> 30	> 30
<b>4.17</b>	n.s.	n.s.	n.s.	n.s.	n.s.	n.s.	n.s.
<b>4.18</b>	> 30	> 30	> 30	> 30	> 30	> 30	> 30
<b>4.19</b>	> 60	> 60	> 60	> 60	> 60	> 60	> 60
<b>4.20</b>	> 60	> 60	> 60	> 60	> 60	> 60	> 60
<b>4.21</b>	n.s.	n.s.	n.s.	n.s.	n.s.	n.s.	n.s.
<b>4.22</b>	> 60	> 60	> 60	> 60	> 60	> 60	> 60
<b>4.23</b>	n.s.	n.s.	n.s.	n.s.	n.s.	n.s.	n.s.
<b>4.24</b>	n.s.	n.s.	n.s.	n.s.	n.s.	n.s.	n.s.
<b>4.25</b>	n.s.	n.s.	n.s.	n.s.	n.s.	n.s.	n.s.
<b>4.26</b>	n.s.	n.s.	n.s.	n.s.	n.s.	n.s.	n.s.
<b>BA</b>	13.6±0.8	12.7±0.9	18.4±1.4	11.4±1.4	7.6±1.1	13.7±1.1	13.1±2.1

<sup>a</sup> EC<sub>50</sub> values in μM from SRB assay after 96 h of treatment; the values are averaged from at least three independent experiments performed each in triplicate. Cut-off in all experiments was 60 μM)

<sup>b</sup> n.s. not soluble. BA = Betulinic acid

Aminoquinones (**4.8-4.12** and **4.19-4.20**) showed low activity for the six human cell lines (EC<sub>50</sub> > 60 μM), whereas aminoquinones (**4.16** and **4.18**) showed EC<sub>50</sub> > 30 μM. Compounds **4.14-4.15** and **4.17** were not soluble for achieving the cytotoxic evaluation.

On the other hand, complexes (**4.21**, **4.23-4.26**) presented low solubility for achieving the cytotoxic evaluation except compound **4.22** that was soluble but showed low activity (EC<sub>50</sub> > 60 μM).



### 3. CONCLUSION

Here was reported the optimization of conditions for the synthesis of thirteen 2,5-bis-(alkyl/arylamino)-1,4-benzoquinones resulting in a simple methodology with a satisfactory yield. Aminoquinones were used as a ligand for the synthesis of ruthenium complexes, where aliphatic aminoquinones (**4.8-4.12**) lead to new ruthenium complexes (**4.22-4.26**). The complexes were carried out with the doubly deprotonated forms of the related aminoquinone and were obtained in excellent yields (65-95%). When aromatic aminoquinones (**4.13-4.17**) were used as ligand were not possible to obtain the desired product. In addition aminoquinones (**4.18-4.20**) containing amino acids groups were not possible to use as ligand since they were not soluble in the condition of complexes preparation. All the compounds were characterized by spectroscopic techniques. The poor solubility of the ruthenium complexes required long acquisition times to obtain  $^{13}\text{C}$  NMR. Structural characterization of some of these complexes has shown the  $\eta^6$ -coordination mode of the *p*-cymene ligand. Due to this low solubility of complexes, the results of cytotoxic activity were obtained only for compound **4.22** with  $\text{EC}_{50} > 60 \mu\text{M}$ .

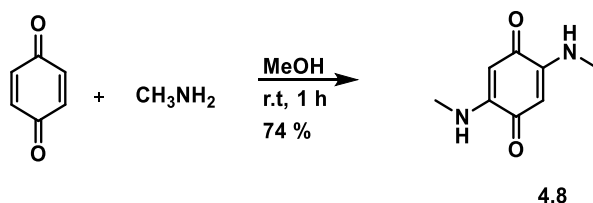
## 4. EXPERIMENTAL PART

### 4.1. General Information

RuCl<sub>3</sub>, hydroquinone and amines were purchased from Sigma-Aldrich. For the metal complexes, all manipulations were carried out under an argon atmosphere using Schlenks and a dual manifold vacuum line. The solvents were dried and distilled under argon and degassed by common techniques prior to use. Infrared spectra were recorded on a Perkin-Elmer Paragon 1000 FTIR spectrophotometer, using potassium bromide disks (1% w/w). <sup>1</sup>H NMR spectra were recorded at 400 or 200 MHz and <sup>13</sup>C NMR spectra at 100 or 75 MHz with a Bruker Avance. Chemical shifts ( $\delta$ ) are reported from tetramethylsilane with the solvent resonance as the internal standard. Data are reported as follows: chemical shift ( $\delta$ ), multiplicity (s= singlet, d= doublet, t= triplet, q= quartet, br= broad, m= multiplet), integration, coupling constants ( $J$  = Hz) and assignment.

### 4.2. Synthesis of of ligands 2,5-diamino-1,4-benzoquinone

*Procedure for 2,5-bis-(methylamino)-1,4-benzoquinone (4.8):*



To a round-bottomed flask (25 mL) were added *p*-benzoquinone (0.162 g, 1.5 mmol), methylamine (0.015 g, 0.5 mmol) and methanol (5 mL). The mixture was stirred at room temperature for 1 h under normal atmosphere. The solution changed from colorless to red. The methanol was evaporated and the residue was purified by silica gel column chromatography eluting with 2:1 v/v hexane/EtOAc to give compound **4.8** as red crystal in 74% yield (0.37 mmol, 0.061 g). Mp: 246-248 °C. IR: ( $\nu_{\max}/\text{cm}^{-1}$ ) 3284, 3002, 2929, 1642, 1568, 1500, 1410, 1360, 1290, 1234, 1062 and 706 cm<sup>-1</sup>. <sup>1</sup>H-NMR (DMSO-*d*<sub>6</sub>)  $\delta$ : 2.75 (d,  $J$  = 5.37, H-1'), 5.15 (s, H-3/H-6), 7.60 (s, H-N). <sup>13</sup>C-NMR (DMSO-*d*<sub>6</sub>)  $\delta$ : 28.61 (C-1'), 91.76 (C-3/C-6), 152.25 (C-2/C-5), 177.12 (C-1/C-4). IES-EM found (C<sub>8</sub>H<sub>11</sub>N<sub>2</sub>O<sub>2</sub>)  $m/z$  = 167.0816 [M+H]<sup>+</sup>. Calculated (C<sub>8</sub>H<sub>11</sub>N<sub>2</sub>O<sub>2</sub>)  $m/z$  = 167.0776 [M+H]<sup>+</sup>.

The other compounds **4.9-4.17** were prepared employing a procedure similar to that described for **4.8**. All the compounds were fully characterized by Mp, IR, <sup>1</sup>H-NMR and <sup>13</sup>C-NMR and mass spectrometry.

*Data for 2,5-bis-(propylamino)-1,4-benzoquinone (4.9).* Red crystals. Purified by column chromatography, eluent hexane/EtOAc 3:1 (v/v). Yield: 86%. The spectroscopy data matched with those reported by the reference [22].

*Data for 2,5-bis-(isobuthylamino)-1,4-benzoquinone (4.10).* Red crystals. Purified by column chromatography, eluent hexane/EtOAc 3:1 (v/v). Yield: 83%. The spectroscopy data matched with those reported by the reference [31].

*Data for 2,5-bis-(pentylamino)-1,4-benzoquinone (4.11).* Red crystals. Purified by column chromatography, eluent hexane/EtOAc 3:1 (v/v). Yield: 93%. The spectroscopy data matched with those reported by the reference [31].

*Data for 2,5-bis-(hexylamino)-1,4-benzoquinone (4.12).* Red crystals. Purified by column chromatography, eluent hexane/EtOAc 3:1 (v/v). Yield: 78%. The spectroscopy data matched with those reported by the reference [31].

*Data for 2,5-bis-(benzylamino)-1,4-benzoquinone (4.13).* Red crystals. Purified by column chromatography, eluent CHCl<sub>3</sub>/EtOAc 1:1 (v/v). Yield: 87%. The spectroscopy data matched with those reported by the reference [22].

*Data for 2,5-bis-(p-methylaniline)-1,4-benzoquinone (4.14).* Brown crystals. Purified by column chromatography, eluent CHCl<sub>3</sub>/hexane 1:2 (v/v). Yield: 61%. Mp: 299-300 °C. IR: ( $\nu_{\max}/\text{cm}^{-1}$ ) 3236, 2916, 1634, 1556, 1480, 1288 and 828  $\text{cm}^{-1}$ . <sup>1</sup>H-NMR (CDCl<sub>3</sub>)  $\delta$ : 2.36 (s, H-1''); 6.01 (s, H-3/H-6), 7.13 (d,  $J = 8.5$ , H-3'/H-5'), 7.20 (d,  $J = 8.5$ , H-2'/H-6'), 8.08 (s, H-N). IES-EM found (C<sub>20</sub>H<sub>18</sub>N<sub>2</sub>O<sub>2</sub>Na)  $m/z = 341.1263$  [M+Na]<sup>+</sup>. Calculated (C<sub>20</sub>H<sub>18</sub>N<sub>2</sub>O<sub>2</sub>Na)  $m/z = 341.1266$  [M+Na]<sup>+</sup>.

*Data for 2,5-bis-[2-(acetyl)phenylamino]-1,4-benzoquinone (4.15).* Brown crystals in 65% yield. Mp: 267-268 °C. IR: ( $\nu_{\max}/\text{cm}^{-1}$ ) 3206, 2922, 2980, 1652, 1642, 1604, 1566, 1454, 129 and 770  $\text{cm}^{-1}$ . <sup>1</sup>H-NMR (CDCl<sub>3</sub>)  $\delta$ : 2.67 (s, H-2''), 6.42 (s, H-3/H-6), 7.16-7.95 (m, H-3'/H-6'), 11.21 (s, H-N). <sup>13</sup>C-NMR (CDCl<sub>3</sub>)  $\delta$ :

28.65 (C-2''); 100.11 (C-3/C-6), 121.33, 123.48, 126.32, 134.20, 139.89 (C-1'/C-6'), 144.77 (C-2/C-5), 181.89 (C-1/C-4), 201.22 (C-1''). IES-EM found (C<sub>22</sub>H<sub>19</sub>N<sub>2</sub>O<sub>4</sub>)  $m/z = 375.1238$  [M+H]<sup>+</sup>. Calculated (C<sub>22</sub>H<sub>19</sub>N<sub>2</sub>O<sub>4</sub>)  $m/z = 375.1402$  [M+H]<sup>+</sup>.

*Data for 2,5-bis-[2-(hydroxymethyl)phenylamino]-1,4-benzoquinone (4.16).* Brown crystals. Purified by column chromatography, eluent EtOAc/Et<sub>2</sub>O 1:1 (v/v). Yield: 58%. Mp: 211-212 °C. IR: ( $\nu_{\max}/\text{cm}^{-1}$ ) 3383, 3180, 2872, 1632, 1576, 1484, 1286, 904, 822 and 738 cm<sup>-1</sup>. <sup>1</sup>H-NMR (DMSO-*d*<sub>6</sub>)  $\delta$ : 4.47 (*d*, *J* = 5.0, H-1'), 5.49 (*t*, *J* = 5.2, H-O), 5.53 (*s*, H-3/H-6), 7.24-7.48 (*m*, H-2'/H-6'), 9.36 (*s*, H-N). <sup>13</sup>C-NMR (DMSO-*d*<sub>6</sub>)  $\delta$ : 60.58 (C-1'), 95.02 (C-3/C-6), 124.18, 126.17, 128.07, 128.70, 135.82, 136.25 (C-1'/C-6'), 147.92 (C-2/C-5), 179.38 (C-1/C-4). IES-EM found (C<sub>20</sub>H<sub>18</sub>N<sub>2</sub>O<sub>4</sub>Na)  $m/z = 373.1149$  [M+Na]<sup>+</sup>. Calculated (C<sub>20</sub>H<sub>18</sub>N<sub>2</sub>O<sub>4</sub>Na)  $m/z = 373.1164$  [M+Na]<sup>+</sup>.

*Data for 2,5-bis-[3-(hydroxymethyl)phenylamino]-1,4-benzoquinone (4.17).* Brown crystals. Purified by column chromatography, eluent EtOAc/Et<sub>2</sub>O 3:2 (v/v). Yield: 77%. Mp: 244-245 °C. IR: ( $\nu_{\max}/\text{cm}^{-1}$ ) 3426, 3240, 2908, 1638, 1568, 1428, 1288, 934, 876 and 690 cm<sup>-1</sup>. <sup>1</sup>H-NMR (DMSO-*d*<sub>6</sub>)  $\delta$ : 4.51 (*d*, *J* = 5.2, H-1'), 5.32 (*t*, *J* = 5.2, H-O), 5.81 (*s*, H-3/C-6), 7.16-7.41 (*m*, H-2',4',5',6'), 9.34 (*s*, H-N). <sup>13</sup>C-NMR (DMSO-*d*<sub>6</sub>)  $\delta$ : 63.19 (C-1'), 95.95 (C-3/C-6), 121.98, 122.85, 124.28, 129.68, 138.29, 144.60 (C-1'/C-6'), 148.03 (C-2/C-5), 180.39 (C-1/C-4). IES-EM found (C<sub>20</sub>H<sub>18</sub>N<sub>2</sub>O<sub>4</sub>Na)  $m/z = 373.1158$  [M+Na]<sup>+</sup>. Calculated (C<sub>20</sub>H<sub>18</sub>N<sub>2</sub>O<sub>4</sub>Na)  $m/z = 373.1164$  [M+Na]<sup>+</sup>.

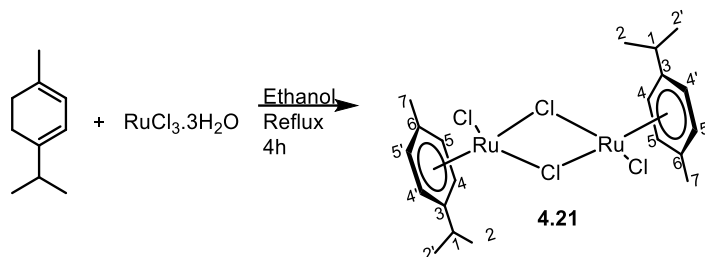
*General procedure for the synthesis of (4.18-4.20), exemplified by the synthesis of 2,5-bis-[1-(carboxy)ethylamino]-1,4-benzoquinone (4.18).* To a round bottom flask (25 mL) was added *p*-benzoquinone (0.162 g, 1.5 mmol) in ethanol (10 mL). After complete dissolution *L*-alanine (0.045 g, 0.5 mmol) and sodium bicarbonate (0.084 g, 1.0 mmol) were added. The mixture was stirred at room temperature under aerobic conditions. The reaction was monitored by TLC and stopped after 24 h. The reaction mixture was filtered to remove the sodium bicarbonate salt and unreacted amino acid, and washed with ethanol. The resulting solution was concentrated under reduced pressure. The residue obtained was acidified with 2.0 mL of concentrated hydrochloric acid and

dissolved with 5.0 mL of distilled water. The mixture was extracted with EtOAc (3 x 25 mL). The organic extracts were combined, and the resulting organic phase was dried with MgSO<sub>4</sub>, filtered and concentrated under reduced pressure. The obtained residue was purified by silica gel column chromatography eluting with acetone/MeOH 2.5:1.5 v/v to give compound **4.18** as red crystals in 68% yield (0.048 g, 0.17 mmol). Mp: 268-269 °C. IR: ( $\nu_{\max}/\text{cm}^{-1}$ ) 3444, 3318, 2992, 2934, 1636, 1594, 1308 and 780 cm<sup>-1</sup>. <sup>1</sup>H-NMR (DMSO-*d*<sub>6</sub>/D<sub>2</sub>O)  $\delta$ : 1.19 (*d*, *J* = 6.6, H-C-3'), 3.56-3.61 (*m*, H-1'), 5.13 (*s*, H-3/H-6), 7.75 (*d*, *J* = 6.6, H-N). <sup>13</sup>C-NMR (DMSO-*d*<sub>6</sub>/D<sub>2</sub>O)  $\delta$ : 17.91 (C-3'), 52.08 (C-1'), 92.13 (C-3/C-6), 150.03 (C-2/C-5), 174.08 (C-1/C-4), 177.18 (C-2'). IES-EM found (C<sub>20</sub>H<sub>18</sub>N<sub>2</sub>O<sub>4</sub>Na) *m/z* = 303.0597 [M-2H+Na]<sup>-</sup>. Calculated (C<sub>20</sub>H<sub>18</sub>N<sub>2</sub>O<sub>4</sub>Na) *m/z* = 303.0593 [M-2H+Na]<sup>-</sup>.

*Data for 2,5-bis-[(1-carboxy-2-methyl)butylamino]-1,4-benzoquinone (4.19).* Red crystals. Purified by column chromatography, eluent acetone/MeOH 2.5:1.5 (v/v). Yield: 51%. Mp: > 300 °C. IR: ( $\nu_{\max}/\text{cm}^{-1}$ ) 3418, 3320, 2966, 2934, 2876, 1574, 1494, 1404, 1352, 816 and 708 cm<sup>-1</sup>. <sup>1</sup>H-NMR (DMSO-*d*<sub>6</sub>/D<sub>2</sub>O)  $\delta$ : 0.78 (*s*, H-5'/H-6'), 1.05-1.76 (*m*, H-3'/H-4'), 3.63 (*s*, H-1'), 5.21 (*s*, H-3/H-6). <sup>13</sup>C-NMR (DMSO-*d*<sub>6</sub>/D<sub>2</sub>O)  $\delta$ : 12.68 (C-5'/C-6'), 16.68 (C-4'), 26.23 (C-3'), 62.52 (C-1'), 92.88 (C-3/C-6), 152.12 (C-2/C-5), 174.27 (C-1/C-4), 177.85 (C-2').

*Data for 2,5-bis-[1-(carboxy)phenylethanoamino]-1,4-benzoquinone (4.20).* Red crystals. Purified by column chromatography, eluent acetone/MeOH 2.5:1.5 (v/v). Yield: 46%. The spectroscopy data matched with those reported by the reference [33].

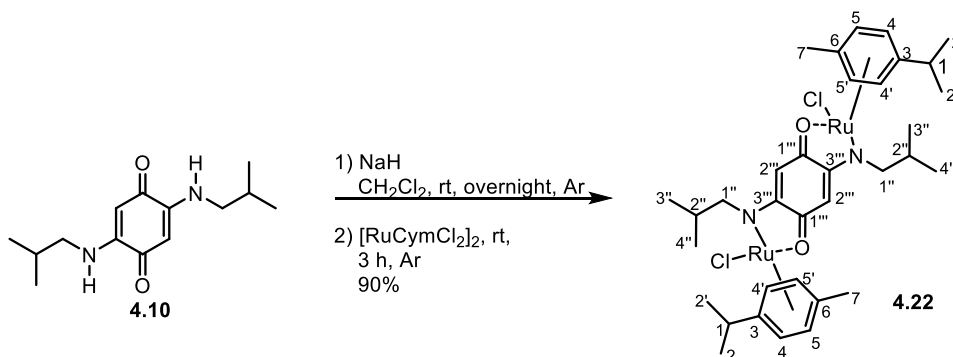
### 4.3. Synthesis of dichloro(*p*-cymene)ruthenium(II) dimer (4.21)



In a Schlenk was dissolved 1.0 g (3.82 mmol) of  $\text{RuCl}_3 \cdot 3\text{H}_2\text{O}$  in 50 mL of ethanol. Then, was added 5 mL (4.2 g, 31.0 mmol) of  $\alpha$ -phellandrene. The solution mixture was stirred at reflux for four hours under argon atmosphere. Then, the solutions were allowed to cool to room temperature, the solvent was reduced to half of volume and the red-brown solid obtained was filtrated and washed with ethanol. After drying in vacuum the yield was 1.8 g (3.15 mmol, 85%). IR: ( $\nu_{\text{max}}/\text{cm}^{-1}$ ) 2980; 1501; 998.  $^1\text{H}$  NMR ( $\text{CDCl}_3$ , 200 MHz)  $\delta$ : 1.25 (d,  $J = 6.8$  Hz, 6H, H-2 and H-2'), 2.13 (s, 3H, H-7), 2.83-2.96 (m, 1H, H-1), 5.32 (d,  $J = 5.5$  Hz, 2H, H-4 and H-4'), 5.45 (d,  $J = 5.5$  Hz, 2H, H-5 and H-5').  $^{13}\text{C}$  NMR ( $\text{CDCl}_3$ , 50 MHz)  $\delta$ : 18.8 (C-7), 22.0 (C-2 and C-2'), 30.5 (C-1), 80.4 (C-4 and C-4'), 81.1 (C-5 and C-5'), 96.6 (C-3), 101.0 (C-6). ESI  $m/z$  calculated for  $\text{C}_{22}\text{H}_{34}\text{Cl}_2\text{Ru}_2$   $[\text{M}+\text{H}]^+$ : 573.01, found 572.95.

### 4.4. Synthesis of complexes 4.22-4.26

Procedure for complex  $[\{\text{Cl}(\eta^6\text{-Cym})\text{Ru}\}_2(\mu\text{-L-}2\text{H}^4)]$ ,  $\text{L} = 2,5\text{-bis-(isobuthylamino)-1,4-benzoquinone}$  (4.22):

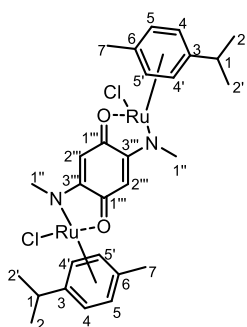


In a Schlenk was dissolved (34 mg, 0.14 mmol) of 2,5-bis-(isobuthylamino)-1,4-benzoquinone and (8.8 mg, 0.35 mmol) of sodium hydride

in dichloromethane at room temperature. The mixture was stirred overnight, then was added (92.0 mg, 0.14 mmol) of dichloro(*p*-cymene)ruthenium(II) dimer and the mixture was stirred at room temperature for 3 hours. Then, the volume of the reaction was reduce in half and hexane was added, a dark red solid was obtained, filtrated and washed with hexane. After drying in vacuum the yield was 0.110 mg (0.13 mmol, 90%). Isomerization ratio (13:1 *syn:anti*). IR: ( $\nu_{\max}/\text{cm}^{-1}$ ) 2887; 1650; 1438; 878.  $^1\text{H}$  NMR ( $\text{CD}_2\text{Cl}_2$ , 400 MHz)  $\delta$ : 0.95 (d,  $J = 6.6$  Hz, 6H, H-3''), 1.08 (d,  $J = 6.6$  Hz, 6H, H-4''), 1.20 (d,  $J = 6.9$  Hz, 6H, H-2), 1.26 (d,  $J = 6.9$  Hz, 6H, H-2'), 2.23 (s, 6H, H-7), 2.35-2.41 (m, 2H, H-2''), 2.76-2.83 (m, 2H, H-1), 3.73-3.82 (m, 4H, H-1''), 5.11 (d,  $J = 5.8$  Hz, 2H, H-5) 5.32-5.35 (m, 4H, H-5' and H-4'), 5.47 (d,  $J = 5.8$  Hz, 2H, H-4), 5.71 (s, 2H, H-1').  $^{13}\text{C}$  NMR ( $\text{CD}_2\text{Cl}_2$ , 100 MHz)  $\delta$ : 18.9 (C-7), 21.6 (C-3''), 21.7 (C-4''), 22.5 (C-2), 22.5 (C-2'), 30.2 (C-2''), 31.6 (C-1), 65.6 (C-1''), 66.2 (C-1'''), 81.2 (C-5), 82.1 (C-5'), 82.9 (C-4), 84.1 (C-4'), 94.9 (C-2'''), 96.7 (C-3), 102.7 (C-6), 166.6 (C-3'''), 178.0 (C-1'''). ESI  $m/z$  calculated for  $\text{C}_{36}\text{H}_{54}\text{Cl}_2\text{N}_2\text{O}_2\text{Ru}_2$   $[\text{M}+\text{H}]^+$ : 821.17.

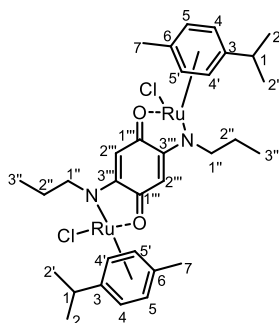
Compounds (**4.23-4.26**) were synthesized using a similar method to that of **4.22**.

$[\{\text{Cl}(\eta^6\text{-Cym})\text{Ru}\}_2(\mu\text{-L-}2\text{H}^4)]$ ,  $\text{L} = 2,5\text{-bis-(methylamino)-1,4-benzoquinone}$  (**4.23**):



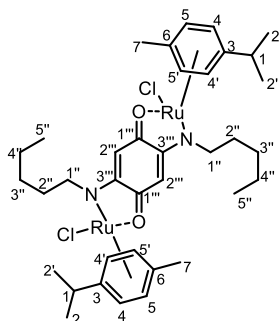
Quantities used for the synthesis: aminoquinone (23 mg, 0.14 mmol),  $[\text{Ru}(\text{cym})\text{Cl}_2]_2$  (92 mg, 0.14 mmol). Dark red solid. Yield: (63 mg, 0.09 mmol, 65%). Isomerization ratio (3:1 *syn:anti*). IR: ( $\nu_{\max}/\text{cm}^{-1}$ ) 2887; 1649; 1538; 1434; 1251; 879.  $^1\text{H}$  NMR ( $\text{CD}_2\text{Cl}_2$ , 400 MHz)  $\delta$ : 1.21 and 1.23 (d,  $J = 7.0$  Hz, 6H, H-2 and H-2'), 2.16 (s, 3H, H-7), 2.72-2.79 (m, 2H, H-1), 3.61 (s, 6H, H-1''), 5.16 (d,  $J = 5.5$  Hz, 2H, H-4), 5.29 (d,  $J = 5.5$  Hz, 2H, H-4'), 5.43 (m, 4H, H-5 and H-5'), 5.52 (s, 2H, H-2''').  $^{13}\text{C}$  NMR ( $\text{CD}_2\text{Cl}_2$ , 100 MHz)  $\delta$ : 18.9 (C-7), 22.5 (C-2), 22.6 (C-2'), 31.7 (C-1), 45.2 (C-1''), 81.4 (C-5), 82.3 (C5), 82.5 (C-4), 82.9 (C-4'), 93.7 (C-2'''), 93.8 (C-2'''), 97.8 (C-3), 102.3 (C-6), 166.0 (C-3'''), 177.6 (C-1'''). ESI  $m/z$  calculated for  $\text{C}_{30}\text{H}_{42}\text{Cl}_2\text{N}_2\text{O}_2\text{Ru}_2$   $[\text{M}+\text{H}]^+$ : 701.10.

$[\{\text{Cl}(\eta^6\text{-Cym})\text{Ru}\}_2(\mu\text{-L-}2\text{H}^4)], \text{L} = 2,5\text{-bis-}(\text{propylamino})\text{-}1,4\text{-benzoquinone (4.24):}$



Quantities used for the synthesis: aminoquinone (31 mg, 0.14 mmol),  $[\text{Ru}(\text{cym})\text{Cl}_2]_2$  (92 mg, 0.14 mmol). Dark red solid. Yield: (78 mg, 0.10 mmol, 70%). Isomerization ratio (18:1 *syn:anti*). IR: ( $\nu_{\text{max}}/\text{cm}^{-1}$ ) 2887; 2809; 1669; 1434; 889; 668.  $^1\text{H NMR}$  ( $\text{CD}_2\text{Cl}_2$ , 400 MHz)  $\delta$ : 0.98 (br s, 6H, H-3''), 1.21 and 1.24 (d,  $J = 6.0$  Hz, 6H, H-2 and H-2'), 1.63-1.81 (m, 2H, H-2''a), 1.84-1.93 (m, 2H, H-2''b), 2.19 (s, 6H, H-7), 2.72-2.89 (m, 2H, H-1), 3.75-3.99 (m, 4H, H-1''), 5.10 and 5.17 (br s, 2H, H-5 and H-5'), 5.29-5.40 (m, 4H, H-4 and H-4'), 5.60 (s, 2H, H-2''').  $^{13}\text{C NMR}$  ( $\text{CD}_2\text{Cl}_2$ , 100 MHz)  $\delta$ : 12.0 (C-3''), 18.9 (C-7), 22.5 (C-2), 22.7 (C-2'), 23.0 (C-2''), 31.6 (C-1), 60.6 (C-1''), 82.1 (C-5), 82.2 (C-5'), 82.6 (C-4), 83.3 (C-4'), 94.1 (C-2'''), 96.9 (C-3), 102.5 (C-6), 165.9 (C-3'''), 177.9 (C-1'''). ESI  $m/z$  calculated for  $\text{C}_{34}\text{H}_{50}\text{Cl}_2\text{N}_2\text{O}_2\text{Ru}_2$   $[\text{M}+\text{H}]^+$ : 793.14.

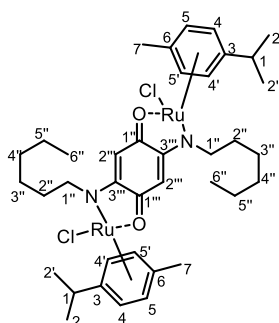
$[\{\text{Cl}(\eta^6\text{-Cym})\text{Ru}\}_2(\mu\text{-L-}2\text{H}^4)], \text{L} = 2,5\text{-bis-}(\text{pentylamino})\text{-}1,4\text{-benzoquinone (4.25):}$



Quantities used for the synthesis: aminoquinone (35 mg, 0.14 mmol),  $[\text{Ru}(\text{cym})\text{Cl}_2]_2$  (92 mg, 0.14 mmol). Red dark solid. Yield: (107 mg, 0.13 mmol, 90%). Isomerization ratio (20:1 *syn:anti*). IR: ( $\nu_{\text{max}}/\text{cm}^{-1}$ ) 2980; 1654; 1498; 868.  $^1\text{H NMR}$  ( $\text{CD}_2\text{Cl}_2$ , 400 MHz)  $\delta$ : 0.96 (t,  $J = 6.5$  Hz, 6H, H-5''), 1.22-1.24 (m, 6H, H-2), 1.27 (t,  $J = 7.3$  Hz, 6H, H-2'), 1.36-1.43 (m, 8H, H-3'' and H-4''), 1.67-1.76 (m, 2H, H-2''a), 1.90-1.99 (m, 2H, H-2''b), 2.21 (s, 6H, H-7), 2.79-2.87 (m, 2H, H-1), 3.83-3.97 (m, 4H, H1''), 5.19 and 5.31 (d,  $J = 5.6$  Hz, 2H, H-5 and H-5'), 5.42 (m, 4H, H-4 and H-4'), 5.61 (s, 2H, H-2''').  $^{13}\text{C NMR}$  ( $\text{CD}_2\text{Cl}_2$ , 100 MHz)  $\delta$ : 14.5 (C-5''), 18.8 (C-7), 22.5 (C-2), 22.7 (C-2'), 23.1 (C-4''), 29.3 (C-3''), 30.4 (C-2''), 31.6 (C-1), 58.9 (C-1''), 82.1 (C-5), 82.2 (C-5'), 82.5 (C-5), 83.3 (C-4'), 93.9 (C-2'''), 96.7 (C-3), 102.5 (C-6), 165.7 (C-3'''), 177.9 (C-1'''). ESI  $m/z$  calculated for  $\text{C}_{38}\text{H}_{58}\text{Cl}_2\text{N}_2\text{O}_2\text{Ru}_2$   $[\text{M}+\text{H}]^+$ : 847.93.



$[\{Cl(\eta^6\text{-Cym})Ru\}_2(\mu\text{-}L\text{-}2H^4)], L = 2,5\text{-bis-(hexylamino)-1,4-benzoquinone (4.26)}$ :



Quantities used for the synthesis: aminoquinone (39 mg, 0.14 mmol),  $[Ru(cym)Cl_2]_2$  (92 mg, 0.14 mmol). Red dark solid. Yield: (116 mg, 0.13 mmol, 95%). Isomerization ratio (9:1 *syn:anti*). IR: ( $\nu_{max}/cm^{-1}$ ) 2882; 1663; 1497; 1442; 861.  $^1H$  NMR ( $CD_2Cl_2$ , 400 MHz)  $\delta$ : 0.93 (t,  $J = 6.2$  Hz, 6H, H-6''), 1.19-1.22 (m, 6H, H-2), 1.25 (d,  $J = 6.9$  Hz, 6H, H-2'), 1.30-1.41 (m, 12H, H-5'', H-4'' and H-3''), 1.60-1.68 (m, 2H, H2''a), 1.83-1.92 (m, 2H, H-2''b), 2.15 (s, 6H, H-7), 2.72-2.79 (m, 2H, H-1), 3.83-3.94 (m, 4H, H-1''), 5.15 and 5.28 (d,  $J = 5.9$  Hz, 2H, H-5 and H-5'), 5.39 (m, 4H, H-4 and H-4'), 5.51 (s, 2H, H-2''').  $^{13}C$  NMR ( $CD_2Cl_2$ , 100 MHz)  $\delta$ : 13.0 (C-6''), 17.5 (C-7), 21.1 (C-5''), 21.3 (C-2), 22.0 (C-2'), 26.6 (C-4''), 28.1 (C-3''), 30.2 (C-2''), 30.9 (C-1), 57.7 (C-1'''), 80.81 (C-5), 80.87 (C-5'), 81.1 (C-4), 81.9 (C-4'), 92.6 (C-2'''), 95.4 (C-3), 101.1 (C-6), 164.3 (C-3'''), 176.5 (C-1'''). ESI  $m/z$  calculated for  $C_{40}H_{62}Cl_2N_2O_2Ru_2$   $[M+H]^+$ : 876.22.

#### 4.5. Cytotoxic assay:

*Was employed the same procedure discussed in Chapter 2.*

## 5. REFERENCES

- [1] R.C. Mehrotra, A. Singh, *Organometallic Chemistry A unified Approach*, Second Edi, New Age International (P) Ltd, **2004**.
- [2] G. Gasser, I. Ott, N. Metzler-Nolte, *J. Med. Chem.* 54 (**2011**) 3–25.
- [3] S.H. van Rijt, P.J. Sadler, *Drug Discov. Today.* 14 (**2009**) 1089–1097.
- [4] T.W. Hambley, *Science (80-. ).* 318 (**2007**) 1392–1393.
- [5] T. Storr, K.H. Thompson, C. Orvig, *Chem. Soc. Rev.* 35 (**2006**) 534–544.
- [6] J. Malina, O. Novakova, B.K. Keppler, E. Alessio, V. Brabec, *J. Biol. Inorg. Chem.* 6 (**2001**) 435–445.
- [7] A.B. Caballero, J.M. Salas, M. Sánchez-Moreno, *Met. Ther. Leishmaniasis.* (**2014**) 1–28.
- [8] K.H. Thompson, C. Orvig, *Dalton Trans.* (**2006**) 761–764.
- [9] A. Martínez, T. Carreon, E. Iniguez, A. Anzellotti, A. Sánchez, M. Tyan, A. Sattler, L. Herrera, R.A. Maldonado, R.A. Sánchez-Delgado, *J. Med. Chem.* 55 (**2012**) 3867–3877.
- [10] M. Navarro, T. Lehmann, R. a Sa, P. Silva, J. a Urbina, *Polyhedron.* 19 (**2000**) 2319–2325.
- [11] E. Iniguez, A. Sánchez, M.A. Vasquez, A. Martínez, J. Olivas, A. Sattler, R.A. Sánchez-Delgado, R.A. Maldonado, *J. Biol. Inorg. Chem.* 18 (**2013**) 779–790.
- [12] U. Schatzschneider, N. Metzler-Nolte, *Angew. Chemie - Int. Ed.* 45 (**2006**) 1504–1507.
- [13] F. Aman, M. Hanif, W.A. Siddiqui, A. Ashraf, L.K. Filak, J. Reynisson, T. Söhnel, S.M.F. Jamieson, C.G. Hartinger, *Organometallics.* 33 (**2014**) 5546–5553.
- [14] C.S. Allardyce, P.J. Dyson, *Platin. Met. Rev.* 45 (**2001**) 62–69.
- [15] M. Malipeddi, C. Lakhani, M. Chhabra, P. Paira, R. Vidya, *Bioorg. Med. Chem. Lett.* 25 (**2015**) 2892–2896.
- [16] P.I. Anderberg, M.M. Harding, I.J. Luck, P. Turner, *Inorg. Chem.* 41 (**2002**) 1365–1371.
- [17] T. Ben Hadda, M. Akkurt, M.F. Baba, M. Daoudi, B. Bennani, A. Kerbal, Z.H. Chohan, *J. Enzyme Inhib. Med. Chem.* 24 (**2009**) 457–463.
- [18] Z. Guo, P.J. Sadler, *Angew. Chem. Int. Ed. Engl.* 38 (**1999**) 1512–1531.
- [19] P. Schluga, C.G. Hartinger, A. Egger, E. Reisner, M. Galanski, M. a Jakupec, B.K. Keppler, *Dalton Trans.* (**2006**) 1796–802.
- [20] D. Kong, T. Yamori, M. Kobayashi, H. Duan, *Mar. Drugs.* 9 (**2011**) 154–161.
- [21] H. Suna, M. Arai, Y. Tsubotani, A. Hayashi, A. Setiawan, M. Kobayashi, *Bioorg. Med. Chem.* 17 (**2009**) 3968–72.
- [22] K.A. MacGregor, M.K. Abdel-Hamid, L.R. Odell, N. Chau, A. Whiting, P.J. Robinson, A. McCluskey, *Eur. J. Med. Chem.* 85 (**2014**) 191–206.

- [23] A. Nemeikaitė-čėnienė, H. Nivinskas, N. Čėnas, 26 (2015) 46–50.
- [24] M. Itoigawa, Y. Kashiwada, C. Ito, H. Furukawa, Y. Tachibana, K. Bastow, K.-H. Lee, *J. Nat. Prod.* 63 (2000) 893–897.
- [25] J. Benites, J.A. Valderrama, K. Bettega, R.C. Pedrosa, P.B. Calderon, J. Verrax, *Eur. J. Med. Chem.* 45 (2010) 6052–6057.
- [26] J. Šarlauskas, *Chemij.* 26 (2015) 208–217.
- [27] D. Schweinfurth, H.S. Das, F. Weisser, D. Bubrin, B. Sarkar, *Inorg. Chem.* 50 (2011) 1150–1159.
- [28] Z.-L. You, D.-M. Xian, M. Zhang, X.-S. Cheng, X.-F. Li, *Bioorg. Med. Chem.* 20 (2012) 4889–4894.
- [29] S. Bayen, N. Barooah, R.J. Sarma, T.K. Sen, A. Karmakar, J.B. Baruah, *Dye. Pigment.* 75 (2007) 770–775.
- [30] B. Lotina-Hennsen, L. Achnine, N.M. Ruvalcaba, A. Ortiz, J. Hernández, N. Farfán, M. Aguilar-Martínez, *J. Agric. Food Chem.* 46 (1998) 724–730.
- [31] L.C.A. Barbosa, U.A. Pereira, C.R.A. Maltha, R.R. Teixeira, V.M. Moreira Valente, J.R. Oliveira Ferreira, L.V. Costa-Lotufo, M.O. Moraes, C. Pessoa, *Molecules.* 15 (2010) 5629–5643.
- [32] P. Stahl, L. Kissau, R. Mazitschek, A. Huwe, P. Furet, A. Giannis, H. Waldmann, *J. Am. Chem. Soc.* 123 (2001) 11586–11593.
- [33] V. Hahn, a. Mikolasch, K. Manda, D. Gördes, K. Thurow, F. Schauer, *Amino Acids.* 37 (2009) 315–321.
- [34] L.C.A. Barbosa, Espectroscopia no Infravermelho na caracterização de compostos orgânicos, Editora UFV, 2011.
- [35] M.A. Bennett, T.N. Huang, T.W. Matheson, A.K. Smith, *Inorg. Synth.* XXI (1982) 74–78.
- [36] E. Hodson, S.J. Simpson, *Polyhedron.* 23 (2004) 2695–2707.
- [37] R.H. Crabtree, *The Organometallic Chemistry of the Transition Metals*, Fourth Ed, John Wiley & Sons, Inc., 2005.  
<http://pubs.acs.org/doi/abs/10.1021/la015653n>.
- [38] P.S. Pregosin, *NMR in Organometallic Chemistry*, WILEY-VCH Verlag, 2012. [https://books.google.com/books?id=XURJSvAmk\\_0C&pgis=1](https://books.google.com/books?id=XURJSvAmk_0C&pgis=1).
- [39] P. Skehan, R. Storeng, D. Scudiero, A. Monks, D. Vistica, J.T. Warren, H. Bokesch, M.R. Boyd, *J. National Cancer Inst.* 82 (1990) 1107–1112.

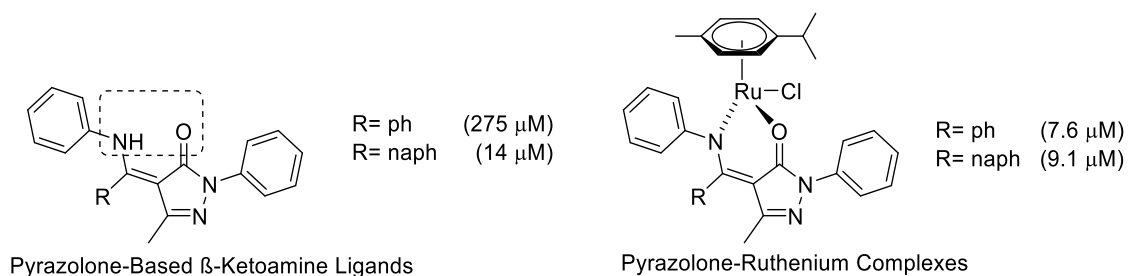
## **CHAPTER 5**

### **SYNTHESIS OF NEW RUTHENIUM COMPLEXES WITH QUINOLINE DERIVATIVES AND THEIR EVALUATION AS ANTIMICROBIAL AGENTS**

## 1. INTRODUCTION

During the last decades, ruthenium(II) complexes have become attractive for the design of new drugs, owing to its promising biological activities, mainly as anticancer agents [1,2]. Among the ruthenium compounds, those bearing the *p*-cymene group, have been used to combine with a large number of organic frameworks. These class of complexes presents anticancer activities of colon [3], breasts [4], ovaries [4], prostate [5], and pancreas [6]. Additionally, antibacterial properties have also been reported [7].

Usually, organic fragments with reported biological activities are used to build ruthenium complexes, such is the case of the pyrazolone derivatives [8,9]. These complexes were shown to be more potent than their respective ligands when their inhibition potential was evaluated against ovarian carcinoma cells, as outline in Figure 5.1. These classes of compounds containing nitrogen and oxygen are able to form stable ruthenium complexes, resulting in complexes with pseudo-octahedral “piano-stool” type molecular geometry. The *p*-cymene group is the “stool top” with three coordination sites occupied by an *N,O*-chelate and a chlorine as a monodentate ligand around the ruthenium center [3].

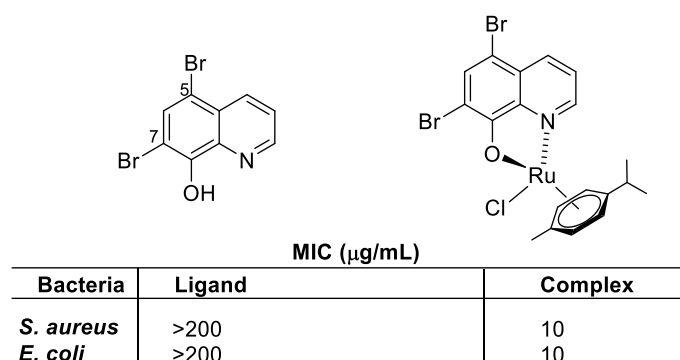


**Figure 5.1.** Structural representation of ruthenium complex of pyrazolone as *N,O*-ligands. The  $IC_{50}$  of these compounds against ovarian carcinoma cells A2780 are also reported in parentheses.

Within a large class of organic frameworks, the 8-hydroxyquinolines have stirred an interest due to its wide potential as an anticancer [10], antibacterial [11], antioxidant [12], antiplasmodial [13], antimalarial [13], anti-HIV [14] and an antifungal [14] agents. 8-hydroxyquinoline is an aromatic heterocyclic compound

able to form complexes with divalent metal ions which make it a potent chelating agent [15].

Since the first synthesis of ruthenium complex using 8-hydroxyquinoline as a ligand [16], several complexes of this class have been reported [7,17–20]. In 2010, Vanparia *et al.* described the synthesis and antibacterial evaluation of derivatives of 8-hydroxyquinoline complexes using Mn(II), Fe(II), Co(II), Ni(II), Cu(II) and Zn(II). Remarkable results were obtained when Ru(II) is coordinated with 5,7-dibromo-8-hydroxyquinoline (See Figure 5.2). The evaluation revealed significantly higher antimicrobial activity for the complex when compared with the single quinoline derivative [7].



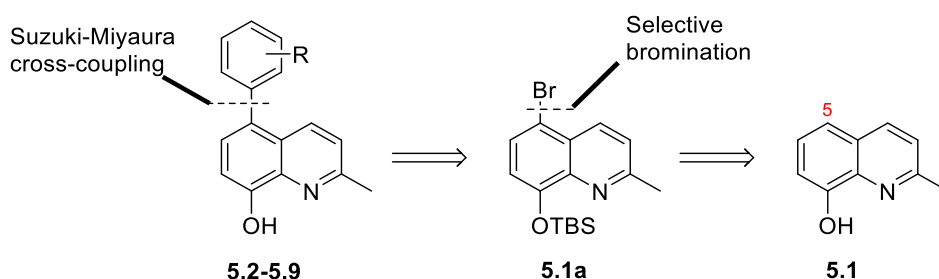
**Figure 5.2.** Structure of 5,7-dibromo-8-hydroxyquinoline and their ruthenium complex which is able to inhibit the bacteria *Staphylococcus aureus* and *Escherichia coli*.

Herein the use of 8-hydroxy-2-methylquinoline as a nucleus to synthesize new derivatives able to form complexes with ruthenium(II) is presented. Aiming to increase of the hydrophobic properties of the new derivatives, different aryl groups at the 5-position will be introduced. In addition to this, electron-withdrawing and donating groups in the aryl fragment will also be introduced, to evaluate the structure-activity relationship. To compare the effect of the methyl at 2-position with the previous report, the preparation of the 5,7-dibromo-8-hydroxy-2-methylquinoline derivative will be discussed as well. Moreover, this chapter will present the structural characterization of all 8-hydroxy-2-methylquinoline derivatives and their corresponding ruthenium complexes along with their potential activity as antimicrobial agents.

## 2. RESULTS AND DISCUSSION

### 2.1. Synthesis

The strategy for the synthesis of the quinoline derivatives **5.2-5.9**, (Figure 5.3) it was envisioned from commercially available 8-hydroxy-2-methylquinoline (**5.1**). In this regard, the protection of the -OH group with a bulky group was required in order to induce a selective bromination in carbon-5, thus affording the intermediated **5.1a**. Accordingly, a Suzuki-Miyaura cross-coupling could be allowed by aryl bromide (**5.1a**) and aryl boronic acids, leading to the new quinoline derivatives.

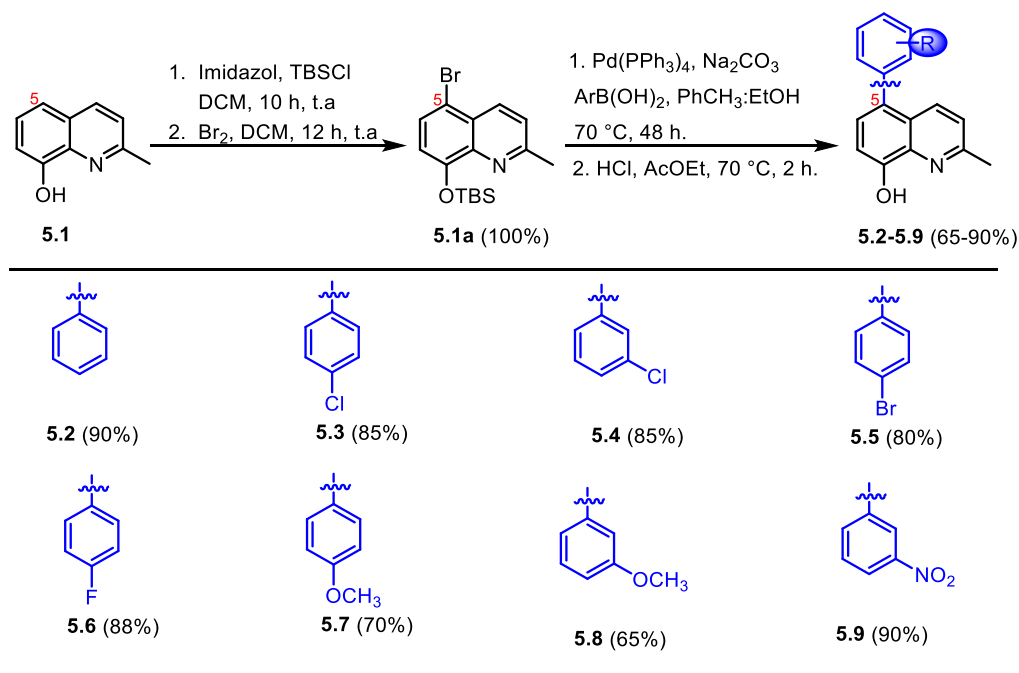


**Figure 5.3.** Retrosynthetic analysis

Several experimental works describe the regioselective bromination at carbon-5 of the hydroxyquinoline core by using different protecting groups to avoid the attack of bromine at the C-7 position. Therefore, different protecting groups have been employed, such as -methyl, -benzyl and -*tert*-butyldimethylsilyl [21–24].

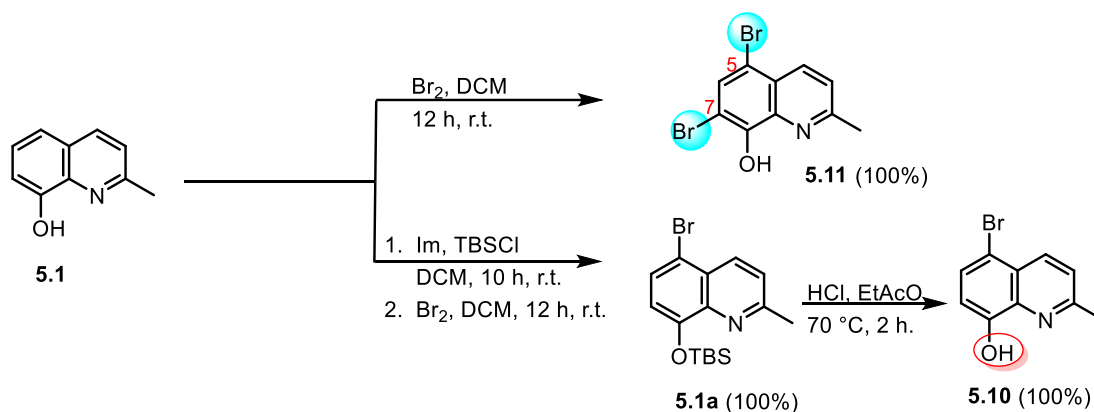
In the present work, intermediate **5.1a** was prepared via treatment of 8-hydroxy-2-methylquinoline (**5.1**) with *tert*-butyldimethylsilyl chloride in the presence of imidazole, as previously reported [24]. In sequence, it was treated with bromine to lead to the substitution at C-5 position, thus affording intermediate **5.1a** in quantitative yield. Subsequently, the resulting bromide **5.1a** was reacted with different aryl boronic acids in the presence of Pd(PPh<sub>3</sub>)<sub>4</sub> through a Suzuki-Miyaura cross-coupling reaction, which resulted in 8 intermediates. To afford the corresponding quinoline derivatives, **5.2-5.9** required a treatment with concentrated HCl in ethyl acetate to generate a total deprotection of the -TBS

group, leading to the formation of the corresponding quinolines in favorable overall yields between 65-90% (Figure 5.4).



**Figure 5.4.** Synthesis of the quinoline derivatives (**5.2-5.9**).

It was possible, however, to obtain the deprotected form of intermediate **5.1a** when it was treated with concentrated HCl in ethyl acetate, affording another quinoline derivative (**5.10**) in a total conversion. Additionally, from commercially available 8-hydroxy-2-methylquinoline (**5.1**), the compound 5,7-dibromo-2-methyl-8-hydroxyquinoline (**5.11**) was obtained through a bromination reaction in 100% yield (Figure 5.5).

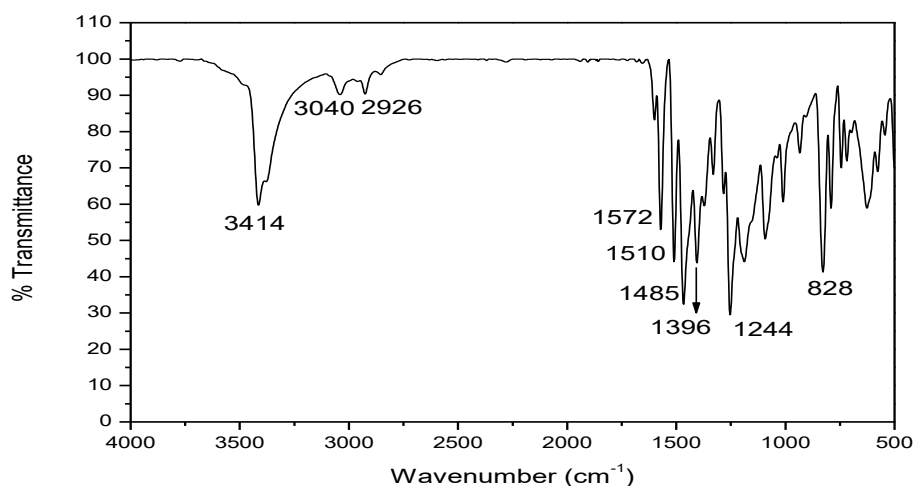


**Figure 5.5.** Synthesis of the quinoline derivatives (**5.10-5.11**).



### 2.1.1. Characterization of quinoline derivatives

All the compounds were characterized by microanalysis and spectroscopic techniques, in which they have shown similar characteristics. The infrared spectra for compounds **5.2-5.11** exhibited a typical absorption in the range from 3330 to 3432  $\text{cm}^{-1}$  which corresponded to an O-H stretching vibration. The IR spectra also show revealed the C-H stretching around 3030-3064  $\text{cm}^{-1}$ . Meanwhile, absorption bands that at range from 1564 to 1606  $\text{cm}^{-1}$  were assigned to the ring stretching modes C=C [25]. Moreover, around 1260  $\text{cm}^{-1}$  the band related to C-O stretching vibrations [26,27] were observed (See Figure 5.6).



**Figure 5.6.** Infrared spectrum in KBr of compound **5.4**.

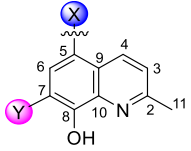
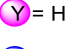
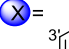
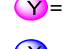
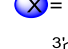
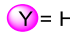
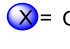
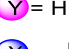
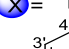

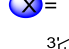
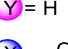
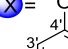
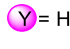
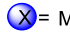
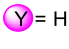
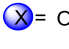
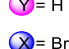

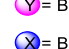

The <sup>1</sup>H-NMR data were grouped in the comparative Table 5.1. In this table, it is possible to observe that the hydrogens in methyl group (H-11) are the most highly shielded type of hydrogen and their signals are found at lower chemical shift values ( $\delta = 2.61-2.72$ ). At the aromatic region  $\delta = 6.83-8.18$  the signals corresponding to the quinoline ring are observed.

The signal related to hydrogen-7 is the most shielded and it is found at the range from 6.89 to 7.13 ppm as a doublet with values of the constant coupling in the range of 7.8-8.2 Hz. Hydrogen-3 is found at  $\delta = 7.17-7.57$  where the signal is usually a doublet with  $J = 7.8-8.3$  Hz. The signal corresponding to hydrogen-6 typically appears as a doublet with a constant coupling about 7.8-8.2 Hz at  $\delta = 7.23-7.50$ .

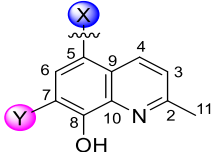
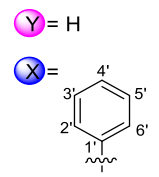
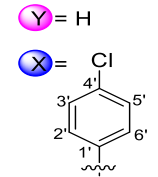
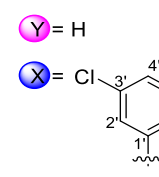
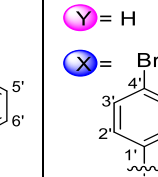
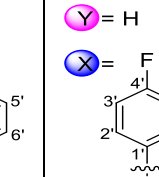
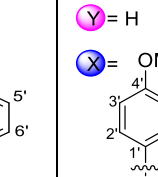
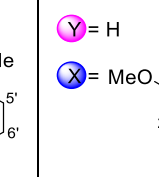
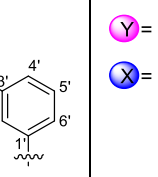
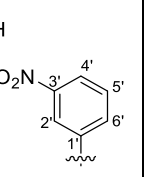
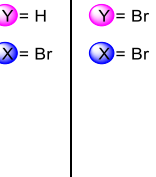
The signal of the most deshielded hydrogen, H-4, usually is a doublet with  $J = 8.3-8.7$  Hz at  $\delta = 7.93-8.18$ . When the quinoline derivatives bears the phenyl ring at the C-5 position with a *para* substitution it is possible to observe the pattern substitution as a doublet with a constant coupling around 8.2-8.7 Hz at  $\delta = 6.93-7.51$ .

Likewise, the  $^{13}\text{C}$ -NMR data are presented in Table 5.2. For all compounds, a characteristic signal of the methyl group is observed, C-11, between  $\delta = 24.7-25.8$ . Another chemical shift characteristic at  $109.6 \pm 2$  ppm is related to the  $\text{sp}^2$  carbon-7. Additionally, the signal related to carbon-3 is observed in the range of  $\delta = 122.7-123.9$ , and the signal corresponding to carbon-4 is observed from 134.4 to 136.2 ppm. Besides this, it is revealed that carbons C-8 and C-2 are at the range of  $\delta = 149.0-152.2$  and 156.8-158.7, respectively. All the spectra data of the compounds are present in Appendix 5.

**Table 5.1.** Comparative  $^1\text{H}$  NMR data of 8-hydroxy-2-methylquinoline derivatives (**5.2-5.11**) in  $\text{CDCl}_3$  (400 MHz)

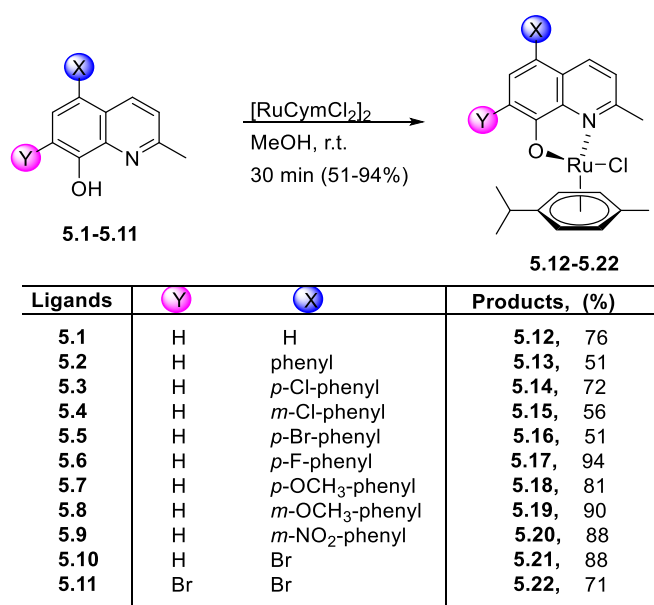
N° H										
	 	 	 	 	 	 	 	 	 	 
	<b>5.2</b>	<b>5.3</b>	<b>5.4</b>	<b>5.5</b>	<b>5.6</b>	<b>5.7</b>	<b>5.8</b>	<b>5.9</b>	<b>5.10</b>	<b>5.11</b>
	$\delta$ (J in Hz)									
<b>H-11</b>	2.65, s	2.65, s	2.72, s	2.65, s	2.64, s	2.64, s	2.64, s	2.67, s	2.63, s	2.61, s
<b>H-3</b>	7.17, d ( $J = 8.6$ )	7.19, d ( $J = 8.8$ )	7.24-7.33, m	7.57, d ( $J = 8.3$ )	7.18, d ( $J = 8.6$ )	7.16, d ( $J = 8.6$ )	7.15, d ( $J = 8.7$ )	7.24, d ( $J = 8.7$ )	7.25, d ( $J = 8.6$ )	7.22, d ( $J = 8.5$ )
<b>H-4</b>	8.06, d ( $J = 8.6$ )	7.93, d ( $J = 8.6$ )	8.08, d ( $J = 8.6$ )	7.99, d ( $J = 8.3$ )	7.99, d ( $J = 8.6$ )	8.06, d ( $J = 8.6$ )	8.11, d ( $J = 8.7$ )	7.96, d ( $J = 8.7$ )	8.18, d ( $J = 8.6$ )	8.06, d ( $J = 8.5$ )
<b>H-6</b>	7.27, d ( $J = 7.8$ )	7.23, d ( $J = 7.8$ )	7.24-7.33, m	7.42, d ( $J = 7.9$ )	7.23, d ( $J = 7.8$ )	7.24, d ( $J = 7.9$ )	7.30, d ( $J = 8.1$ )	7.30, d ( $J = 7.8$ )	7.50, d ( $J = 8.2$ )	7.62, s
<b>H-7</b>	7.11, d ( $J = 7.8$ )	7.10, d ( $J = 7.8$ )	7.17, d ( $J = 7.8$ )	7.10, d ( $J = 7.9$ )	7.05, br. s	7.10, d ( $J = 7.9$ )	6.89, d ( $J = 8.1$ )	7.13, d ( $J = 7.8$ )	6.92, d ( $J = 8.2$ )	-
<b>H-2'</b>	7.41-7.32, m	7.36, d ( $J = 8.2$ )	7.42, s	7.51, d ( $J = 8.4$ )	7.28-7.31, m	7.27, d ( $J = 8.7$ )	7.12, s	8.22, s	-	-
<b>H-3'</b>		7.27, d ( $J = 8.2$ )	-	7.21, d ( $J = 8.4$ )	7.08-7.10, m	6.93, d ( $J = 8.7$ )	-	-	-	-
<b>H-4'</b>		-	7.24-7.33, m	-	-	-	6.95, br. d ( $J = 7.9$ )	8.17, d ( $J = 7.9$ )	-	-
<b>H-5'</b>		7.27, d ( $J = 8.2$ )	7.39, br. s	7.21, d ( $J = 8.4$ )	7.08-7.10, m	6.93, d ( $J = 8.7$ )	7.31, br. t ( $J = 7.9$ )	7.57, t ( $J = 7.9$ )	-	-
<b>H-6'</b>		7.36, d ( $J = 8.2$ )		7.51, d ( $J = 8.4$ )	7.28-7.31, m	7.27, d ( $J = 8.7$ )	6.95, br. d ( $J = 7.9$ )	7.69, d ( $J = 7.9$ )	-	-

**Table 5.2.** Comparative  $^{13}\text{C}$  NMR data of 8-hydroxy-2-methylquinoline derivatives (5.2-5.11) in  $\text{CDCl}_3$  (100 MHz)

N° C										
										
	5.2	5.3	5.4	5.5	5.6	5.7	5.8	5.9	5.10	5.11
	$\delta$ (J in Hz)									
<b>C-11</b>	24.9	24.9	24.9	24.8	24.8	24.9	24.9	25.8	24.8	24.7
<b>C-2</b>	156.9	156.9	157.0	156.9	156.9	156.8	156.9	157.4	157.8	158.7
<b>C-3</b>	122.8	123.0	123.0	122.9	122.8	122.7	122.9	122.2	123.9	123.9
<b>C-4</b>	134.9	134.6	134.4	134.4	134.6	135.1	135.0	136.2	135.9	135.8
<b>C-5</b>	125.0	124.8	124.7	128.7	124.9	125.2	125.0	124.6	110.7	103.6
<b>C-6</b>	127.3	127.5	127.3	127.3	127.4	127.3	127.3	128.1	130.1	132.5
<b>C-7</b>	109.5	109.6	109.4	109.5	109.4	109.6	109.6	109.8	109.8	109.9
<b>C-8</b>	151.3	151.6	151.7	151.8	151.3	151.0	151.5	152.2	151.6	149.0
<b>C-9</b>	127.4	129.4	129.1	127.0	129.6	130.5	130.7	128.0	125.9	124.6
<b>C-10</b>	137.8	137.8	137.7	134.4	137.7	137.8	137.9	137.7	138.9	137.7
<b>C-1'</b>	139.8	138.2	141.6	138.6	135.7, J= 3.3	132.2	141.3	141.5	-	-
<b>C-2'</b>	130.3	131.5	129.7	131.7	131.7, J= 7.9	131.3	116.0	123.5	-	-
<b>C-3'</b>	128.6	128.8	134.4	130.7	115.5, J= 21.2	114.1	159.9	148.6	-	-
<b>C-4'</b>	130.8	133.3	128.3	132.0	162.3, J= 245	159.1	112.8	124.9	-	-
<b>C-5'</b>	128.6	128.8	130.1	130.7	115.5, J= 21.2	114.1	129.9	129.6	-	-
<b>C-6'</b>	130.3	131.5	127.5	131.7	131.7, J= 7.9	131.3	122.8	134.1	-	-

### 2.1.2. Synthesis of complexes 5.12-5.22

The first synthesis of a complex containing ruthenium and 8-hydroxyquinoline as ligand was described in 2000 by Gemel *et al.*, [16]. Through the treatment of dichloro(*p*-cymene)ruthenium(II) dimer (**4.21**) with 2 equivalents of 8-hydroxyquinoline in THF at room temperature for 2 hours, affording the half-sandwich complex was afforded in 94% yield. Then, Schuecker *et al.*, in 2008 [28], reported the synthesis using a reagent ratio of 1:2 (ruthenium/quinoline) with dichloromethane as solvent in 0 °C for 2 hours to yield the product in 92%. Recently, Malipeddi *et al.*, in 2015 [7] demonstrated that by using methanol as a solvent, the time of reaction is reduced to 30 minutes, and the product is obtained in 95% yield. In this context, for the synthesis of complexes **5.12-5.22**, was employed the procedure proposed by Malipeddi *et al.*, was employed [7]. The ruthenium dimer (**4.21**) used was prepared as previously discussed in Chapter 4. When the ruthenium dimer **4.21** is reacted with the corresponding 8-hydroxy-2-methylquinoline derivatives in a ratio of 1:2, a complete color change of solution from yellow to deep orange was observed. The progress of the reaction can follow by TLC and after 30 minutes of stirring at room temperature, the reaction was completed. All the complexes were purified by a chromatographic column using silica gel, leading to the desired complexes (**5.12-5.22**) in promising yields between 51-94% (Figure 5.7).



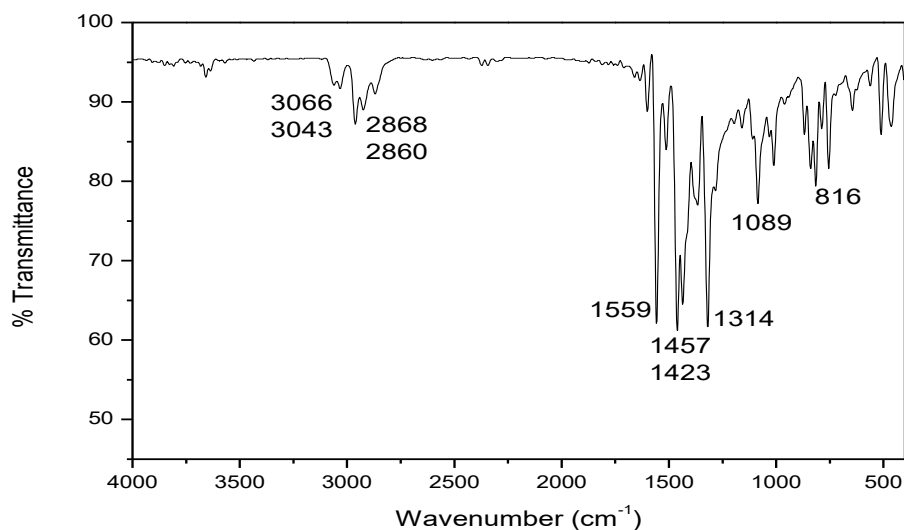
**Figure 5.7.** Synthesis of complexes **5.12-5.22**.

All the complexes were fully characterized through their melting points, microanalysis, infrared,  $^1\text{H-NMR}$ , and  $^{13}\text{C-NMR}$ , which confirmed the proposed structure.

### 2.1.3. Characterization

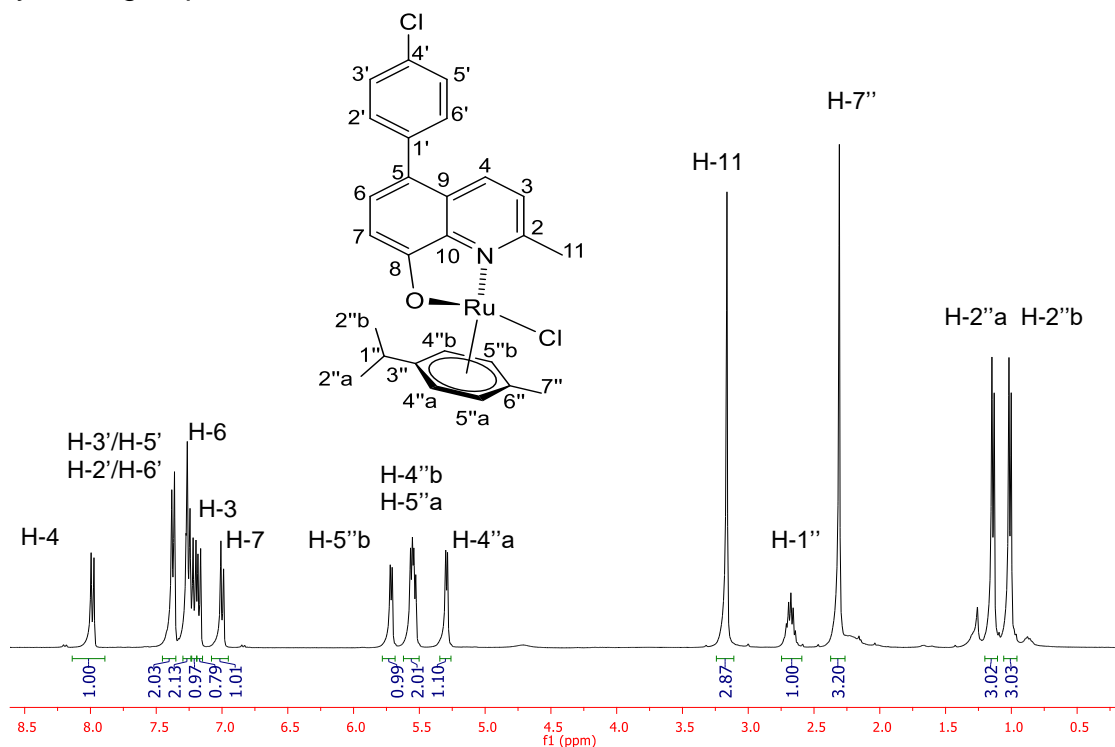
In respect to the complexes (5.12-5.22), compound 5.14 was chosen for description of its structural characterization through IR,  $^1\text{H NMR}$ ,  $^{13}\text{C NMR}$ , and x-ray structure. The spectra of all synthesized complexes exhibited great similarity, with the only variations observed being related to substituents of the aryl group. Therefore, the following discussion is based on data of compound 5.14, although these can be extended to other synthesized products.

In the infrared spectrum (Figure 5.8), a typical absorption in the range from 3070 to 2868  $\text{cm}^{-1}$ , pertaining to the stretching vibration of the aromatic =C-H bonds and to the methyl group was observed. Besides this, the strong absorption in range of 1559-1423  $\text{cm}^{-1}$ , which corresponds to the C=C stretching vibrations, pertain to the aromatic ring. The band at 1314  $\text{cm}^{-1}$  appears as a strong absorption with the stretching bands belonging to C-N [27]. Additionally, the typical  $\nu(\text{O-H})$  stretching disappears and this alteration suggests the deprotonation of the ligand, indicating their coordination to the ruthenium through an oxygen atom.



**Figure 5.8.** Infrared spectrum in KBr of complex 5.14.

In the  $^1\text{H}$  NMR spectrum (Figure 5.9) it is possible to observe at the range from  $\delta = 1.0$  to  $3.5$  five signals related to four methyl and one methine groups. Thus, two doublets at  $\delta = 1.01$  and  $1.13$  ( $J = 6.8$  Hz) integrate for three hydrogens each. These hydrogens are associated with the methyl-2''a and methyl-2''b of *p*-cymene groups.

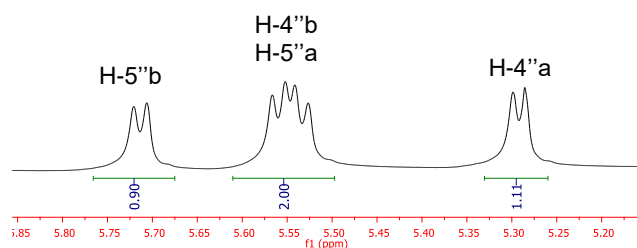


**Figure 5.9.**  $^1\text{H}$  NMR spectrum ( $\text{CDCl}_3$ , 400 MHz) of compound **5.14**.

The methyl groups (H-2''a and H-2''b) in the *p*-cymene fragment are inequivalent (diastereotopic) and therefore resonate at different frequencies. The two distinct doublets that result are not similar at a higher field and being that the case, they are distinguishable from a doublet of doublets. It is because ruthenium does not possess a plane of symmetry [29].

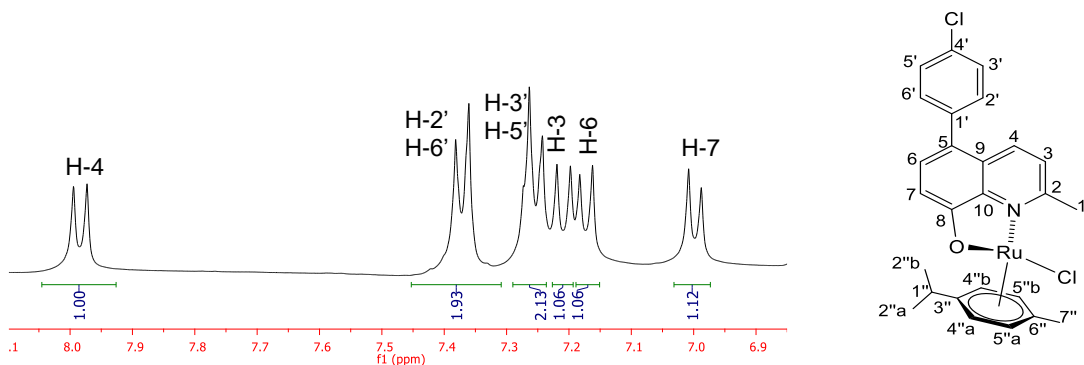
The signal related to methyl-7'' on the *para* position in the cymene ring is represented by a singlet at  $\delta = 2.30$ , and a septet belonging to the methine-1'' is seen at  $\delta = 2.66$  ( $J = 6.8$  Hz). Finally, at  $\delta = 3.16$ , a singlet related to the methyl-11 of the quinoline core is noticeable. In fact, it is important to mention that this signal is more deshielded than into the isolated ligand because of the coordination of the electron pair of the nitrogen with the ruthenium metal center (see Table 5.1 for compare with ligand **5.3**).

In the region between  $\delta = 5.20$ - $5.80$  (Figure 5.10), signals associated with the aromatic hydrogens of the *p*-cymene ring are observed, which appeared in the same chemical shift as the signals of the precursor  $[\text{RuCymCl}_2]_2$  (see Chapter 4). Therefore, a remarkable characteristic of four pairs of doublets with  $J = 5.7$  Hz are assigned to H-4''a, H-4''b, H-5''a, and H-5''b. This behavior in the aromatic hydrogens could be due to the loss of symmetry of the *p*-cymene ring after the coordination of the oxygen and nitrogen of the ligand, where the complex is stereogenic at the metal center [30].



**Figure 5.10.** Expansion of  $^1\text{H}$  NMR spectrum of compound 5.14.

In the last region of the spectrum, from  $\delta = 6.9$  to  $7.9$  (Figure 5.11) the signals correspond to the quinoline core and to the chlorophenyl group, are observed. A doublet at  $\delta = 6.99$  ( $J = 8.4$  Hz) is related to H-7. Subsequently, at  $\delta = 7.17$ , a doublet ( $J = 8.4$  Hz) associated to H-3 and a doublet at  $\delta = 7.20$  ( $J = 8.4$  Hz) belonging to hydrogen-6 are noticed. The *para* substitution of the chlorophenyl group was confirmed by the signal pattern of the two doublets at  $\delta = 7.25$  and  $\delta = 7.37$  ( $J = 8.3$  Hz), for the hydrogens H-2'/H-6' and H-3'/H-5'. Lastly, a signal corresponded to the hydrogen-4 that is represented by a doublet at  $\delta = 7.98$  ( $J = 8.4$  Hz).

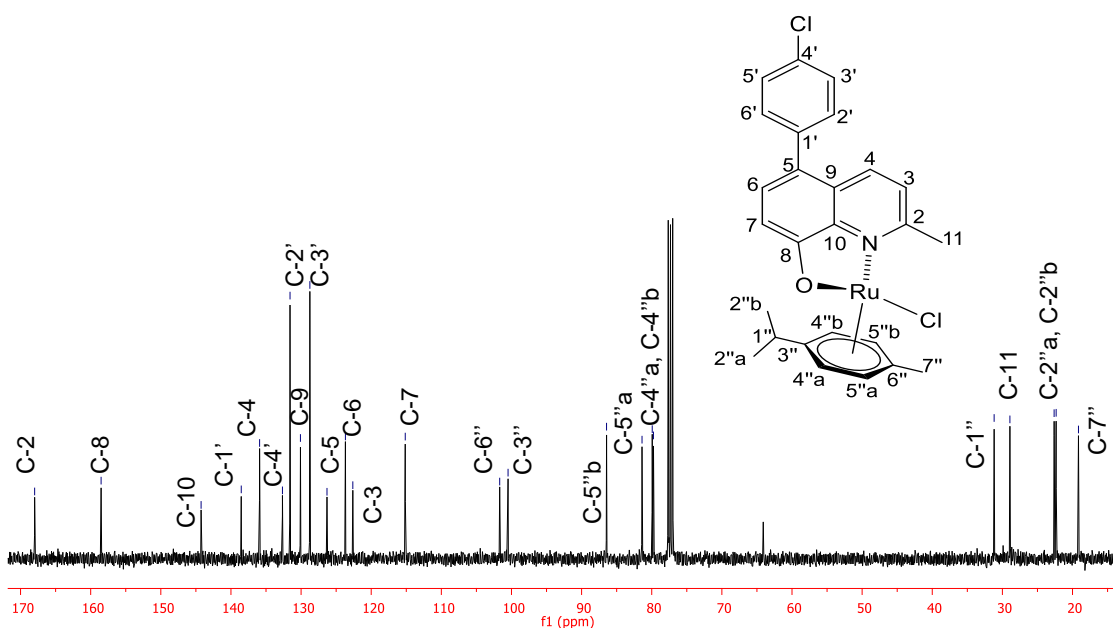


**Figure 5.11.** Expansion of  $^1\text{H}$  NMR spectrum of compound 5.14.



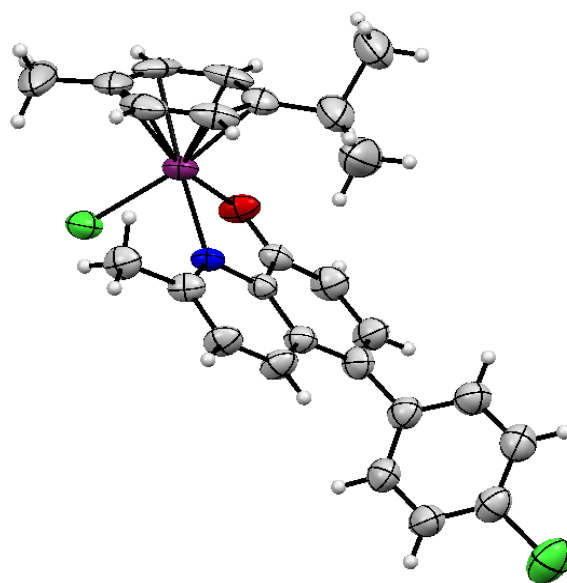
In general, signals associated to the *p*-chloro-phenyl group and pyridinyl moiety appeared in the same chemical shift as the signal of the precursor **5.3**. However, the chemical shift related to H-6 and H-7 decreases in approximately 0.10 ppm when compared with compound **5.3**. This effect could be attributed to the deprotonation of the hydroxyl group and to further electronic donation of the oxygen to the ruthenium.

In the case of  $^{13}\text{C}$  NMR spectrum (Figure 5.12), the signals at  $\delta = 19.0$ - $31.0$  are assigned to the four methyl groups presented in the structure. The signal at  $\delta = 19.1$  is related to carbon-7'', whereas the signals at  $\delta = 22.3$  and  $22.6$  are related to the methyl of the isopropyl group (C-2''a and C-2''b). The signal at  $\delta = 28.9$  is assigned to methyl-11 of the quinoline nucleus and at  $\delta = 31.1$  the signal referred to methine carbon-1''. Subsequently, in the range of  $\delta = 79.7$ - $101.6$ , six signals belonging to carbons of the cymene ring (C-4''a, C-4''b, C-5''a, C-5''b, C-3'', C-6'') are observable. At region of  $\delta = 115.1$ - $167.9$  signals related to the chlorophenyl group are observed and is it also possible to confirm the *para* substitution through the pattern of the carbons C-2' and C-3' carbons at  $\delta = 131.5$  and  $130.0$ , respectively. Additionally, the characteristic signal related to C-8 and C-2 are found at  $\delta = 158.5$  and  $167.9$ , respectively.



**Figure 5.12.**  $^{13}\text{C}$  NMR spectrum ( $\text{CDCl}_3$ , 100 MHz) of compound **5.14**.

Additionally, the structural characterization was confirmed by X-ray diffraction. A single crystal of complex **5.16** was obtained through the slow evaporation of its dichloromethane solutions at room temperature. The figure 5.13 shows the crystalline structure which is formed by the  $\pi$ -bonded on the *p*-cymene fragment, as well as the  $\sigma$ -bond on the chloride ion, and by the *N,O*-atoms on the quinoline bonded to the ruthenium center. The quinoline derivative ligand acted as an *N,O*-chelating bidentate species forming a six-membered chelate ring upon binding to the ruthenium center.



**Figure 5.13.** ORTEP representation of the complex **5.14**.

The distances resulting for Ru-O 2.055(4), Ru-N 2.138(4), and Ru-Cl 2.415(2) Å are typical values reported in the literature for such complexes [31,32]. The ruthenium center exhibits a piano-stool type configuration in this complex with the Ru-Cym distance of 1.667(8) Å, where this bond is significantly shorter than on the other respective ligands. The torsion angles of O-Ru-N, O-Ru-Cl, and Cl-Ru-N were determined as 78.8°, 86.5°, 134.8°, respectively. The angle between Cl-Ru-N increased in comparison with the O-Ru-Cl. This fact, may be related to the methyl substitution in the quinolinic ring causing a repulsion between the methyl group and the chlorine atom.

## 2.2. Biological assay

Antibiotics are drugs employed to treat bacterial infections. A majority of the antibiotics present on the market today, such as penicillin, erythromycin, and all their relatives were known as byproducts of the metabolism of microorganisms in soil, plants, and oceans [33].

Additionally, antibiotic resistance is defined the adaptive change in bacteria in response to the use of these drugs [34]. These bacteria may infect humans and animals, and the infections they cause are therefore more difficult to treat than those caused by non-resistant bacteria [35]. Nowadays, antimicrobial resistance is one of the most problematic public health issues. A worrying example is the prevalence of methicillin-resistant *Staphylococcus aureus* infection, which increased from 5% in 1980 to 50% in 2000 around the world[36]. Additionally, the alarming list of such infections as pneumonia (16% of all pediatric deaths in worldwide in 2015), tuberculosis (250 000 pediatric deaths around the world in 2016), among others, are becoming harder and sometimes impossible to treat as antibiotics become less effective [37,38].

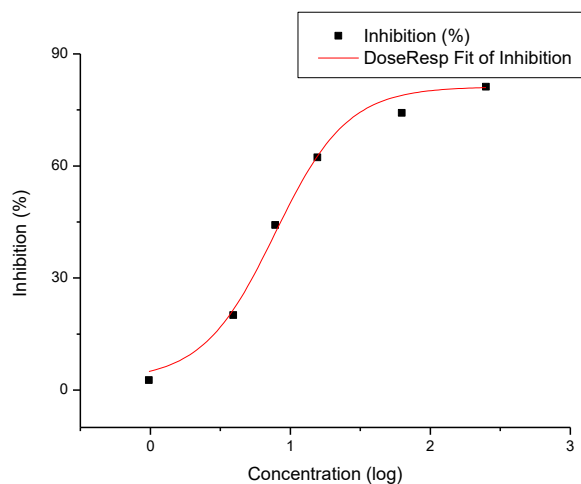
One fact that has contributed to an increased occurrence of hard to treat bacterial infections is the reduced interest in antibiotics by pharmaceutical companies. For example, only 1.6% of drugs in development by the world's pharmaceutical companies were antibiotics [39].

In this context, all 8-hydroxy-2-methylquinoline derivatives and their ruthenium complexes will be employed to assay their antimicrobial activity against different gram-positive and gram-negative bacteria.

### 2.2.1. Antimicrobial activity

For all synthesized 8-hydroxy-2-methylquinoline derivatives (5.2-5.11) and the eleven synthesized complexes (5.12-5.22), the antimicrobial potential against five microorganisms was evaluated; one yeast *Candida albicans*: ATCC 18804, two Gram-positive bacteria *Staphylococcus aureus*: ATCC 29212, *Bacillus cereus*: ATCC 11778 and two Gram-negative bacteria *Salmonella typhimurium*: ATCC 14028, and *Escherichia coli*: ATCC 25922. All the IC<sub>50</sub> values are

presented in Table 5.5. The calculated IC<sub>50</sub> values were obtained from four replicated experiments. A representative sigmoidal dose-response curve (log [compound concentration] versus percentage inhibition of microorganism) is illustrated for compound **5.3** (Figure 5.14). Evaluation of the curves allowed the determination of IC<sub>50</sub> values.

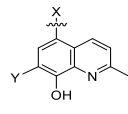
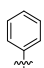
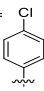
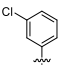
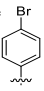
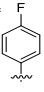
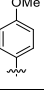
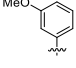
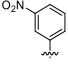


**Figure 5.14.** Inhibition of the yeast *C. albicans* by compound **5.3**. The dose-response curve [log (concentration of **5.3** in  $\mu\text{g}$ ) versus inhibition] was performed in four replicates.

Thus, concerning to the yeast *C. albicans*, it is possible to observe that seven 8-hydroxy-2-methylquinoline derivatives and five complexes can inhibit growth by 50%. Among these compounds, with the exception of **5.2**, **5.7**, and **5.9** a low IC<sub>50</sub> was revealed. Compound **5.6** exhibited an IC<sub>50</sub> = 2.30  $\mu\text{g mL}^{-1}$ , which bears the *p*-fluorophenyl at the C-5 position of the quinoline core. Conversely, *C. albicans* demonstrated be no selectivity to the corresponding complexes (**5.12-5.22**) that requires concentration ranges of 11.59-125.12  $\mu\text{g mL}^{-1}$ . However, the most potent complex, the **5.12**, which carries 8-hydroxy-2-methylquinoline (**5.1**) as a ligand, showed an IC<sub>50</sub> = 11.59  $\mu\text{g mL}^{-1}$ . Complex **5.16**, meanwhile, which possess the *p*-bromophenyl at the C-5 position of quinoline moiety, revealed an IC<sub>50</sub> value of 52.53  $\mu\text{g mL}^{-1}$ .

Regarding the bacterium *S. aureus*, it is possible to observe in Table 5.5 that compounds **5.10** and **5.11** were the only ones able to inhibit this organism's growth. Compound **5.10**, which bears the bromine atom at the C-5 position of the quinoline core, showed and IC<sub>50</sub> = 144.65  $\mu\text{g mL}^{-1}$ .

**Table 5.3.** Concentration of quinolines **5.1-5.11** and the corresponding ruthenium complexes **5.12-5.22** able to inhibit by 50% the growth of five organisms.

	*Compounds	IC <sub>50</sub> (µg/mL)				
		<i>Candida albicans</i>	<i>Staphylococcus aureus</i>	<i>Bacillus cereus</i>	<i>Salmonella typhimurium</i>	<i>Escherichia coli</i>
Y = H X = H	<b>5.1</b> (L <sub>1</sub> ) <b>5.12</b> (Ru+ L <sub>1</sub> )	N.D 11.59	N.D -	N.D -	N.D -	N.D -
Y = H X = 	<b>5.2</b> (L <sub>2</sub> ) <b>5.13</b> (Ru+ L <sub>2</sub> )	- -	- 9.37	- -	- 142.60	- -
Y = H X = 	<b>5.3</b> (L <sub>3</sub> ) <b>5.14</b> (Ru+ L <sub>3</sub> )	7.77 -	- 125.55	- -	- 146.15	- -
Y = H X = 	<b>5.4</b> (L <sub>4</sub> ) <b>5.15</b> (Ru+ L <sub>4</sub> )	4.66 -	- 125.97	- -	- 4.64	- -
Y = H X = 	<b>5.5</b> (L <sub>5</sub> ) <b>5.16</b> (Ru+ L <sub>5</sub> )	6.55 52.53	- 33.38	- -	16.89 24.26	- -
Y = H X = 	<b>5.6</b> (L <sub>6</sub> ) <b>5.17</b> (Ru+ L <sub>6</sub> )	2.30 85.03	- 67.83	- -	- 76.15	- -
Y = H X = 	<b>5.7</b> (L <sub>7</sub> ) <b>5.18</b> (Ru+ L <sub>7</sub> )	- 125.12	- 46.02	16.84 -	- 42.66	- -
Y = H X = 	<b>5.8</b> (L <sub>8</sub> ) <b>5.19</b> (Ru+ L <sub>8</sub> )	6.42 136.54	- 75.21	- -	- 90.56	- -
Y = H X = 	<b>5.9</b> (L <sub>9</sub> ) <b>5.20</b> (Ru+ L <sub>9</sub> )	- -	- -	132.07 90.25	- -	- -
Y = H X = Br	<b>5.10</b> (L <sub>10</sub> ) <b>5.21</b> (Ru+ L <sub>10</sub> )	8.85 -	144.65 -	- -	- -	56.69 -
Y = Br X = Br	<b>5.11</b> (L <sub>11</sub> ) <b>5.22</b> (Ru+ L <sub>11</sub> )	25.02 -	72.14 -	- -	72.14 -	58.17 -
<b>Ampicillin</b>		-	0.25	0.24	0.42	0.27
<b>Miconazole</b>		0.97	-	-	-	-

L= 8-hydroxy-2-methylquinoline derivatives; L+Ru= Ruthenium complexes; N.D= Not determined.

\*The quinolines are represented by L<sub>1-11</sub> and the corresponding ruthenium complexed by Ru+L.

- No inhibition of 50% at 250 µg/mL.

Compound **5.6**, which has the *p*-fluorophenyl at the C-5 position of quinoline core, showed an  $IC_{50} = 67.83 \mu\text{g mL}^{-1}$ . On the other hand, all complexes except **5.12** and **5.20-5.22**, were active against this bacterium, in distinction to the corresponding ligands exhibiting  $IC_{50}$  values between 9.37-125.97  $\mu\text{g mL}^{-1}$ . For this bacterium, the more potent complex is **5.13** which bears the phenyl ring as a substitution of the C-5 position of the quinoline core.

In relation to the Gram-positive bacterium, *B. cereus*, the two 8-hydroxy-2-methylquinoline derivatives bearing the *p*-OCH<sub>3</sub>-phenyl and *m*-NO<sub>2</sub>-phenyl at the C-5 position of quinoline core were able to inhibit by 50% the growth of this organism with  $IC_{50}$  values of 16.84 and 132.07  $\mu\text{g mL}^{-1}$  for **5.7** and **5.9**, respectively. However, complex **5.20**, related to ligand **5.9**, was the only complex capable of inhibiting this bacterium with an  $IC_{50}$  lower than the corresponding ligand (90.25  $\mu\text{g mL}^{-1}$ ).

Regarding the Gram-negative bacterium, *S. typhimurium*, it was shown to be sensitive only to the **5.5** and **5.11** quinoline derivatives with  $IC_{50}$  values at 16.89 and 72.14  $\mu\text{g mL}^{-1}$ , respectively. Nevertheless, the complexes **5.13-5.19** demonstrated selectivity for this bacterium with values as lower as 4.64  $\mu\text{g mL}^{-1}$  for compound **5.15** which possess the *m*-chlorophenyl at the C-5 position of the quinoline core.

Finally, as for *E. coli* bacterium, it was not sensitive when its growth was evaluated against all the compounds, except for quinolines **5.10** (5-bromo) and **5.11** (5,7-dibromo), which presented  $IC_{50}$  values of 56.69 and 58.17  $\mu\text{g mL}^{-1}$ , respectively.

Despite the lack of an observable relationship between the structural activity, within the ligands and complexes, it was nevertheless possible to identify that the complexes were more active than single quinolines against the Gram-positive bacterium, *S. aureus*, and against the Gram-negative bacterium, *S. typhimurium*. Therefore, ruthenium complexes play a significant role controlling the growth of those bacteria. Additionally, when a comparison is draw between the best results from Table 5.5, correspond to compound **5.13** (against *S. aureus*) and **5.15** (against *S. typhimurium*), and some results from the available literature

(ruthenium with 8-hydroxyquinoline against *S. aureus* MIC= 50  $\mu\text{g mL}^{-1}$ ) [7], it is possible to observe that the introduction of the aryl group with or without a substituent, could increase the biological activity of the antimicrobial agents.

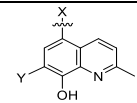
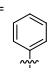
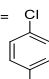
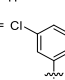
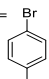
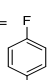
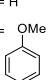
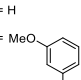
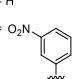
### 2.2.2. Cytotoxic activity

All 8-hydroxy-2-methylquinoline derivatives (**5.2-5.11**) and their ruthenium complexes (**5.12-5.22**) were evaluated for their ability to inhibit the growth of tumor cells *in vitro* by employing five human tumor cell lines (melanoma-518A2, ovarian carcinoma - A2780, colon adenocarcinoma - HT29, breast adenocarcinoma - MCF7, malignant melanoma - A375, and non- malignant mouse fibroblasts - NIH 3T3) by using the well-established photometric sulforhodamine B assay (SRB) [40]. For comparison, betulinic acid was used as a positive standard control. The results of these assays are summarized in Table 5.4. In general, most of the compounds were not soluble in the conditions of the assay. However, it was possible to determine activity for a few of them, which was the case for compounds **5.12**, **5.2/5.13**, **5.7/5.18**, **5.8/5.19**, and **5.21**. With the exception of compounds **5.12** and **5.19**, both 8-hydroxy-2-methylquinoline derivatives and their complexes showed  $\text{EC}_{50}$  values lower as 15  $\mu\text{M}$  and they are comparable to the positive control, betulinic acid.

The 8-hydroxy-2-methylquinoline derivatives (**5.2**, **5.7**, **5.8**) were shown to be more potent than their parent complexes (**5.13**, **5.18**, **5.19**) with  $\text{EC}_{50}$  values as low as 3.1  $\mu\text{M}$  in the case of compounds **5.7** when acting against the malignant melanoma-A375 cell, with a selective index of 3.6. Additionally, compound **5.7** with a *p*-methoxyphenyl at the C-5 position of quinoline moiety, was revealed to be the most active against all the tumor cells with  $\text{EC}_{50}$  values between 3.1 to 5.9  $\mu\text{M}$ .

Although the complexes did not show an increase in cytotoxic activity, compounds **5.13**, **5.18**, and **5.21**, with  $\text{EC}_{50}$  values from 5.2 to 15.0  $\mu\text{M}$ , were more active than other ruthenium complexes reported in the literature [9,17], with  $\text{EC}_{50}$  values >150  $\mu\text{M}$ . However, these complexes exhibit comparable  $\text{EC}_{50}$  values (5.5-9.6  $\mu\text{M}$ ) with cisplatin (12.0  $\mu\text{M}$ ), against the breast adenocarcinoma-MCF7 [41].

**Table 5.4.** Cytotoxicity for quinolines **5.2-5.11** and their corresponding ruthenium complexes **5.12-5.22** (cut-off in all experiments was at 30  $\mu\text{M}$ ); employing human tumor cell lines and non-malignant mouse fibroblasts (NIH 3T3); betulinic acid was used as the standard.

	*Compounds	EC <sub>50</sub> ( $\mu\text{M}$ )*					
		518A2	A2780	HT29	MCF7	A375	NIH 3T3
Y = H	<b>5.1</b> (L <sub>1</sub> )	N.D	N.D	N.D	N.D	N.D	N.D
X = H	<b>5.12</b> (Ru+ L <sub>1</sub> )	>30	>30	>30	>30	>30	>30
Y = H	<b>5.2</b> (L <sub>2</sub> )	5.7±0.6	7.7±0.4	5.9±0.3	5.5±1.2	4.7±0.4	9.3±1.6
X = 	<b>5.13</b> (Ru+ L <sub>2</sub> )	12.1±0.6	8.6±0.1	15.0±0.8	10.6±1.2	7.8±0.6	11.4±1.5
Y = H	<b>5.3</b> (L <sub>3</sub> )	n.s	n.s	n.s	n.s	n.s	n.s
X = 	<b>5.14</b> (Ru+ L <sub>3</sub> )	n.s	n.s	n.s	n.s	n.s	n.s
Y = H	<b>5.4</b> (L <sub>4</sub> )	n.s	n.s	n.s	n.s	n.s	n.s
X = 	<b>5.15</b> (Ru+ L <sub>4</sub> )	n.s	n.s	n.s	n.s	n.s	n.s
Y = H	<b>5.5</b> (L <sub>5</sub> )	n.s	n.s	n.s	n.s	n.s	n.s
X = 	<b>5.16</b> (Ru+ L <sub>5</sub> )	n.s	n.s	n.s	n.s	n.s	n.s
Y = H	<b>5.6</b> (L <sub>6</sub> )	n.s	n.s	n.s	n.s	n.s	n.s
X = 	<b>5.17</b> (Ru+ L <sub>6</sub> )	n.s	n.s	n.s	n.s	n.s	n.s
Y = H	<b>5.7</b> (L <sub>7</sub> )	4.2±0.7	3.7±0.6	5.9±0.4	3.6±0.3	3.1±0.1	11.1±1.1
X = 	<b>5.18</b> (Ru+ L <sub>7</sub> )	10.9±0.9	8.7±0.2	14.7±0.8	9.6±0.7	6.8±0.2	9.8±1.2
Y = H	<b>5.8</b> (L <sub>8</sub> )	5.9±0.4	6.1±0.2	5.7±0.3	5.4±1.0	4.8±0.4	10.4±1.3
X = 	<b>5.19</b> (Ru+ L <sub>8</sub> )	>30	>30	>30	>30	>30	>30
Y = H	<b>5.9</b> (L <sub>9</sub> )	n.s	n.s	n.s	n.s	n.s	n.s
X = 	<b>5.20</b> (Ru+ L <sub>9</sub> )	n.s	n.s	n.s	n.s	n.s	n.s
Y = H	<b>5.10</b> (L <sub>10</sub> )	n.s	n.s	n.s	n.s	n.s	n.s
X = Br	<b>5.21</b> (Ru+ L <sub>10</sub> )	8.5±0.7	5.8±1.1	11.4±0.8	5.8±1.0	5.2±0.3	7.4±1.1
Y = Br	<b>5.11</b> (L <sub>11</sub> )	n.s	n.s	n.s	n.s	n.s	n.s
X = Br	<b>5.22</b> (Ru+ L <sub>11</sub> )	n.s	n.s	n.s	n.s	n.s	n.s
<b>Betulinic acid</b>		13.6±0.8	12.7±0.9	18.4±1.4	11.4±1.4	12.0±1.1	13.1±2.1

L= 8-hydroxy-2-methylquinoline derivatives; L+Ru= Ruthenium complexes; N.D= Not determined; n.s= not soluble; \*EC<sub>50</sub> values in  $\mu\text{M}$  from SRB assay after 96 h of treatment; the values are averaged from at least three independent experiments performed each in triplicate.

\*The quinolines are represented by L<sub>1-11</sub> and the corresponding ruthenium complexed by Ru+L.



### 3. CONCLUSION

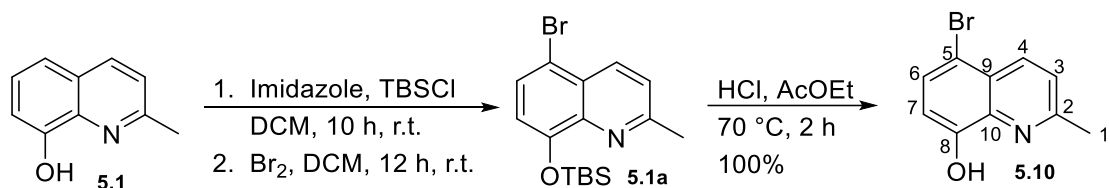
In this present study, the synthesis of new 8-hydroxy-2-methylquinoline derivatives through the introduction of aryl groups at the C-5 position of the quinoline core via a Suzuki cross-coupling reaction was reported. Our findings show that these compounds were obtained in favorable yields of 65-90%. All the new derivatives were employed as ligands to form a new series of ruthenium complexes in favorable yields (51-94%). Furthermore, the ability of the 8-hydroxy-2-methylquinoline derivatives and their respective complexes as inhibitors of the growth of five microorganisms was discussed. The results revealed that ruthenium complexes are promising for the development of specific inhibitors of Gram-negative bacteria, such as *Salmonella typhimurium* and Gram-positive bacterium, such as *Staphylococcus aureus*. The suitable substitution of an aryl group at the C-5 position in the quinoline core could increase the antimicrobial potential as was shown in the case of complexes **5.13** and **5.15**, that presented inhibition by the 50% with IC<sub>50</sub> as low as 9.37 and 4.64  $\mu\text{g mL}^{-1}$ , respectively. Thus, indicating the potential of these fragments as important structural elements in the antimicrobial activity. Due to the low solubility of the most of compounds, the results of cytotoxicity were obtained for a portion of them, avoid the evaluation of structure-activity relationship. Therefore, 8-hydroxy-2-methylquinoline derivatives were more active against tumor cells than the respective ruthenium complexes.

## 4. EXPERIMENTAL PART

### 4.1. General information

For the metal complexes, all manipulations were carried out under an argon atmosphere. The solvents were dried and distilled under argon and degassed by common techniques prior to use. Infrared spectra were recorded on a Perkin-Elmer Paragon 1000 FTIR spectrophotometer, using potassium bromide disks (1% w/w).  $^1\text{H}$  NMR spectra were recorded at 400 MHz and  $^{13}\text{C}$  NMR spectra at 100 MHz with a Bruker Avance. Chemical shifts ( $\delta$ ) are reported from tetramethylsilane with the solvent resonance as the internal standard. Data are reported as follows: chemical shift ( $\delta$ ), multiplicity (s= singlet, d= doublet, t= triplet, q= quartet, br= broad, m= multiplet), integration, coupling constants ( $J$  = Hz) and assignment. Melting points were determined on an MQAPF-301 apparatus. Ruthenium dimer  $[\text{Ru}(p\text{-Cym})\text{Cl}_2]_2$  (**4.21**) was prepared according Chapter 4.

### 4.2. Synthesis of 5-bromo-8-hydroxy-2-methyl-quinoline (**5.10**)

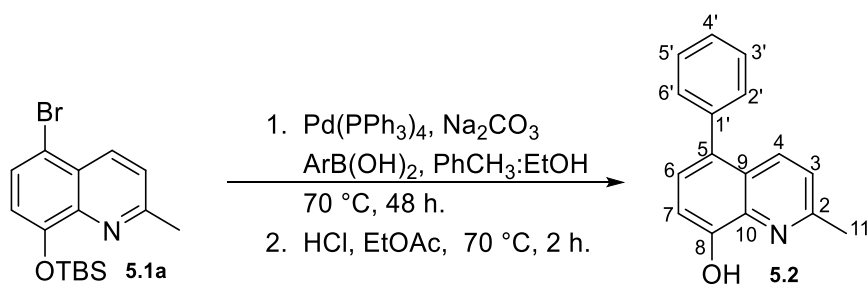


To a round-bottomed flask (100 mL) was added 8-hydroxy-2-methylquinoline **5.1** (2.0 g, 12.6 mmol), dry dichloromethane (20 mL), imidazole (0.90 g, 13.2 mmol) and *tert*-butyldimethylsilyl chloride (2.1 g, 13.2 mmol). The solution was stirred at room temperature overnight, then the mixture was diluted with ethyl ether (100 mL), washed with aqueous HCl (0.1 M, 50 mL), brine (100 mL), water (100 mL). The organic phase was dried over K<sub>2</sub>CO<sub>3</sub> and evaporated under reduced pressure to afford intermediate **5.1a** in a total conversion as a colorless oil. Subsequently, a solution of bromine (1.0 mL, 19.5 mmol) in CH<sub>2</sub>Cl<sub>2</sub> (20 mL) was added dropwise to a vigorously stirred solution of the silyl ether (3.4 g, 12.6 mmol) in CH<sub>2</sub>Cl<sub>2</sub> (20 mL). The mixture of the reaction was stirred overnight at room temperature. Then, the solution was diluted with CH<sub>2</sub>Cl<sub>2</sub> (100 mL), washed with aqueous saturated Na<sub>2</sub>S<sub>2</sub>O<sub>3</sub> (100 mL), aqueous saturated NaHCO<sub>3</sub> (100 mL), brine (100 mL), and water (100 mL), dried over K<sub>2</sub>CO<sub>3</sub>, and evaporated

under reduced pressure to afford 4.4 g (12.6 mmol) of compound **5.1a** as a yellowish oil. Finally, compound **5.1a** was dissolved in 10 mL of ethyl acetate and refluxed in HCl 6 M for 2 hours. The hydrolyzed mixture was cooled and extracted with EtOAc (2 x 50 mL), organic extracts were combined, and the resulting organic phase was dried over Na<sub>2</sub>SO<sub>4</sub>, filtered and the solvent removed under reduced pressure to afford the crude product as a residue. The residue was purified by silica gel column chromatography eluting with Hex/EtOAc 9:1 v/v, to afford compound **5.10** as yellow solid in 100% yield (2.9 g, 12.6 mmol). M.p: 70-72 °C, (lit. [42], 68.5-70 °C). IR ( $\nu_{\max}/\text{cm}^{-1}$ ) 3374, 3048, 2920, 1594, 1564, 1500, 1462, 1388, 1318, 1254, 1198, 924, 824, 784, 556  $\text{cm}^{-1}$ . <sup>1</sup>H NMR (CDCl<sub>3</sub>, 400 MHz)  $\delta$ : 2.63 (s, 3H, H-11), 6.92 (d,  $J$  = 8.2 Hz, 1H, H-7), 7.25, (d,  $J$  = 8.6 Hz, 1H, H-3), 7.50 (d,  $J$  = 8.2 Hz, 1H, H-6), 8.18 (d,  $J$  = 8.6 Hz, 1H, H-4). <sup>13</sup>C NMR (CDCl<sub>3</sub>, 100 MHz)  $\delta$ : 24.8 (C-11), 109.8 (C-5), 110.7 (C-7), 123.9 (C-3), 125.9 (C-9), 130.1 (C-6), 135.9 (C-10), 138.4 (C-4), 151.6 (C-8), 157.8 (C-2). Elemental analysis: calculated C 50.45%; H 3.39%; N 5.88%; found C 50.19%; H 3.51%; N 5.66%. The spectroscopy data matched with those reported by Jampilek *et. al.*, 2005 [42].

#### 4.3. Synthesis of 5-(aryl)-8-hydroxy-2-methyl-quinoline derivatives 5.2-5.9

*Procedure for ligand 2-methyl-5-phenylquinolin-8-ol (5.2):*

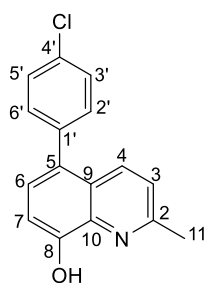


To a Schlenk flask (50 mL) containing intermediate **5.1a** (113 mg, 0.32 mmol) was successively loaded with toluene (11 mL), aqueous Na<sub>2</sub>CO<sub>3</sub> 2 M (13 mL), ethanol (3.0 mL), and benzenboronic acid (43 mg, 0.35 mmol). The mixture was degassed, and Pd(PPh<sub>3</sub>)<sub>4</sub> (12 mg, 0.01 mmol) was rapidly added under a stream of nitrogen. The flask was equipped with a condenser, and the mixture

was refluxed with vigorous stirring for 48 h. The mixture was cooled, diluted with ethyl acetate (100 mL), washed with water (25 mL) and brine (25 mL). Then, organic extracts were combined, and the resulting organic phase was dried over  $K_2CO_3$  and evaporated under reduced pressure. The crude residue was purified by flash column chromatography (Hex/DCM 2:8 v/v) to afford 90% yield (101 mg, 0.29 mmol) of the protected intermediate as a yellowish oil. Subsequently, this intermediate was dissolved in 5 mL of ethyl acetate and refluxed in HCl 6 M for 2 hours. The hydrolyzed mixture was cooled and extracted with EtOAc (2 x 50 mL), organic extracts were combined, and the resulting organic phase was dried over  $Na_2SO_4$ , filtered and the solvent removed under reduced pressure to afford the crude product as a residue. The residue was purified by silica gel column chromatography eluting with Hex/EtOAc 2:1 v/v, to afford compound **5.2** as yellow solid in 100% yield (68 mg, 0.29 mmol). M.p: 103-104 °C. IR ( $\nu_{max}/cm^{-1}$ ) 3432, 2922, 2856, 1630, 1462, 1380  $cm^{-1}$ .  $^1H$  NMR ( $CDCl_3$ , 400 MHz)  $\delta$ : 2.65 (s, 3H, H-11), 7.11 (d,  $J = 7.8$  Hz, 1H, H-7), 7.17 (d,  $J = 8.6$  Hz, 1H, H-3) 7.27 (d,  $J = 7.8$  Hz, 1H, H-6), 7.41-7.32 (m, 5H, H-2'-H-4'), 8.06 (d,  $J = 8.6$  Hz, 1H, H-4).  $^{13}C$  NMR ( $CDCl_3$ , 100 MHz)  $\delta$ : 24.9 (C-11), 109.5 (C-7), 122.8 (C-3), 125.0 (C-5), 127.3 (C-6), 127.4 (C-9), 128.8 (C-4'), 130.3 (C-3'), 130.8 (C-2'), 134.9 (C-4), 137.8 (C-10), 139.8 (C-1'), 151.3 (C-8), 156.9 (C-2). Elemental analysis: calculated C 81.68%; H 5.57%; N 5.95%; found C 81.42%; H 5.80%; N 5.64%.

Compounds **5.3-5.9** were synthesized using a similar method to that of **5.2**.

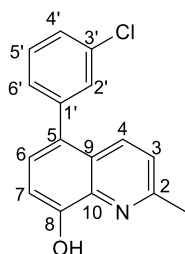
**5-(4-chlorophenyl)-2-methylquinolin-8-ol (5.3):**



Yellow solid; yield: 85% (60 mg; 0.22 mmol). M.p: 92-94 °C. IR ( $\nu_{max}/cm^{-1}$ ) 3414, 3040, 2926, 1600, 1572, 1510, 1468, 1406, 1330, 1254, 1188, 1094, 828, 792, 628, 500  $cm^{-1}$ .  $^1H$  NMR ( $CDCl_3$ , 400 MHz)  $\delta$ : 2.67 (s, 3H, H-11), 7.11 (d,  $J = 7.8$  Hz, 1H, H-7), 7.19, (d,  $J = 8.8$  Hz, 1H, H-3), 7.23, (d,  $J = 7.8$  Hz, 1H, H-6), 7.27 (d,  $J = 8.6$  Hz, 2H, H-3'/H-5'), 7.36 (d,  $J = 8.6$  Hz, 2H, H-2'/H-6'), 7.99 (d,  $J = 8.8$  Hz, 1H, H-4).  $^{13}C$  NMR ( $CDCl_3$ , 100 MHz)  $\delta$ : 24.8 (C-11), 109.4 (C-7), 122.9 (C-3), 124.7 (C-5), 127.4 (C-3), 128.7 (C-3'/C-5'), 129.3 (C-9), 131.4 (C-2'/C-4'), 133.3 (C-4'), 134.4 (C-4), 137.7 (C-10), 138.1 (C-1'),

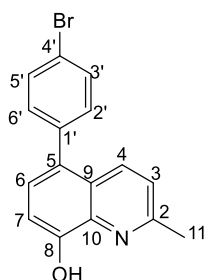
151.5 (C-8), 156.9 (C-2). Elemental analysis: calculated C 71.25%; H 4.48%; N 5.19%; found C 70.97%; H 4.60%; N 5.02%.

**5-(3-chlorophenyl)-2-methylquinolin-8-ol (5.4):**



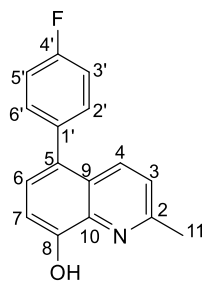
Yellow solid; yield: 85% (60 mg; 0.22 mmol). M.p: 180-181 °C. IR ( $\nu_{\text{max}}/\text{cm}^{-1}$ ) 3392, 3036, 2926, 2856, 1568, 1506, 1466, 1256, 1206, 840, 784, 698, 512  $\text{cm}^{-1}$ .  $^1\text{H}$  NMR ( $\text{CDCl}_3$ , 400 MHz)  $\delta$ : 2.72 (s, 3H, H-11), 7.17 (d,  $J = 7.8$  Hz, 1H, H-7), 7.24-7.33, (m, 3H, H-6, H-3 and H-4'), 7.37 (br. s, 2H, H-5' and H-6'), 7.42 (s, 1H, H-2'), 8.08 (d,  $J = 8.6$  Hz, 1H, H-4).  $^{13}\text{C}$  NMR ( $\text{CDCl}_3$ , 100 MHz)  $\delta$ : 24.9 (C-11), 109.4 (C-7), 123.0 (C-3), 124.7 (C-5), 127.3 (C-6), 127.5 (C-6'), 128.3 (C-4'), 129.1 (C-9), 129.7 (C-2'), 130.1 (C-5'), 134.4 (C-4/C-3'), 137.7 (C-10), 141.6 (C-1'), 151.7 (C-8), 157.0 (C-2). Elemental analysis: calculated C 71.25%; H 4.48%; N 5.19%; found C 71.02%; H 4.63%; N 4.95%.

**5-(4-bromophenyl)-2-methylquinolin-8-ol (5.5):**



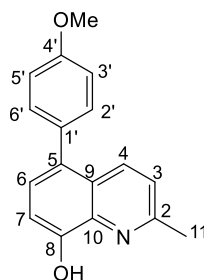
Yellow solid; yield: 80% (66 mg; 0.21 mmol). M.p: 100-101 °C. IR ( $\nu_{\text{max}}/\text{cm}^{-1}$ ) 3412, 1572, 1508, 1470, 1258, 820, 794  $\text{cm}^{-1}$ .  $^1\text{H}$  NMR ( $\text{CDCl}_3$ , 400 MHz)  $\delta$ : 2.65 (s, 3H, H-11), 7.21 (d,  $J = 8.4$  Hz, 2H, H-3'), 7.31, (d,  $J = 7.9$  Hz, 1H, H-7), 7.42 (d,  $J = 7.9$  Hz, 1H, H-6), 7.51 (d,  $J = 8.4$  Hz, 2H, H-2'), 7.57 (d,  $J = 8.3$  Hz, 1H, H-3), 7.99 (d,  $J = 8.3$  Hz, 1H, H-4).  $^{13}\text{C}$  NMR ( $\text{CDCl}_3$ , 100 MHz)  $\delta$ : 24.8 (C-11), 109.5 (C-7), 122.9 (C-6), 127.0 (C-4'), 127.3 (C-3), 128.7 (C-5), 130.77 (C-9), 131.71 (C-2'), 131.77 (3'), 132.0 (C-4), 134.4 (C-10), 138.6 (C-1'), 151.5 (C-8), 156.9 (C-2). Elemental analysis: calculated C 61.17%; H 3.85%; N 4.46%; found C 60.95%; H 3.99%; N 4.29%.

**5-(4-fluorophenyl)-2-methylquinolin-8-ol (5.6):**



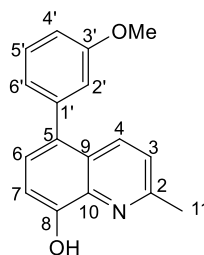
Yellow solid; yield: 88% (58 mg; 0.23 mmol). M.p: 84-85 °C. IR ( $\nu_{\text{max}}/\text{cm}^{-1}$ ) 3350, 3064, 3040, 2922, 2854, 1574, 1512, 1478, 1262, 1218, 1150, 836, 608  $\text{cm}^{-1}$ .  $^1\text{H}$  NMR ( $\text{CDCl}_3$ , 400 MHz)  $\delta$ : 2.64 (s, 3H, H-11), 7.05-7.10 (m, 3H, H-7, H-3'/H-5'), 7.18, (d,  $J = 8.6$  Hz, 1H, H-3), 7.23 (d,  $J = 7.8$  Hz, 1H, H-6), 7.28-7.31 (m, 2H, H-2'/H-6'), 7.99 (d,  $J = 8.6$  Hz, 1H, H-4).  $^{13}\text{C}$  NMR ( $\text{CDCl}_3$ , 100 MHz)  $\delta$ : 24.8 (C-11), 109.4 (C-7), 115.4 (d,  $J = 21.2$  Hz, C-3'/C-5'), 122.8 (C-3), 124.9 (C-6), 127.4 (C-5), 129.6 (C-9), 131.7 (d,  $J = 7.9$  Hz, C-2'/C-6'), 134.6 (C-4), 135.7 (C-1'), 137.7 (C-10), 151.3 (C-8), 156.9 (C-2), 162.0 (d,  $J = 244.9$  Hz, C-4'). Elemental analysis: calculated C 75.88%; H 4.78%; N 5.53%; found C 75.59%; H 4.90%; N 5.36%.

**5-(4-methoxyphenyl)-2-methylquinolin-8-ol (5.7):**



Yellow solid; yield: 70% (60 mg; 0.23 mmol). M.p: 73-75 °C. IR ( $\nu_{\text{max}}/\text{cm}^{-1}$ ) 3330, 3050, 3020, 2960, 2928, 2832, 1578, 1506, 1466, 1428, 1318, 1262, 1224, 1170, 790, 832, 704, 672  $\text{cm}^{-1}$ .  $^1\text{H}$  NMR ( $\text{CDCl}_3$ , 400 MHz)  $\delta$ : 2.64 (s, 3H, H-11), 3.80 (s, 3H, H-12), 6.93 (d,  $J = 8.7$  Hz, 2H, H-3'/H-5'), 7.10 (d,  $J = 7.9$  Hz, 1H, H-7), 7.16 (d,  $J = 8.6$  Hz, 1H, H-3), 7.24 (d,  $J = 7.9$  Hz, 1H, H-6), 7.27, (d,  $J = 8.6$  Hz, 1H, H-2'/H-6'), 8.06 (d,  $J = 8.6$  Hz, 1H, H-4).  $^{13}\text{C}$  NMR ( $\text{CDCl}_3$ , 100 MHz)  $\delta$ : 24.9 (C-11), 55.5 (C-12), 109.6 (C-7), 114.1, (C-3'), 122.7 (C-3), 125.2 (C-6), 127.3 (C-5), 130.5 (C-9), 131.3 (C-2'), 132.2 (C-1'), 135.1 (C-4), 137.8 (C-10), 151.0 (C-8), 156.8 (C-2), 159.1 (C-4'). Elemental analysis: calculated C 76.96%; H 5.70%; N 5.28%; found C 76.77%; H 5.96%; N 5.11%.

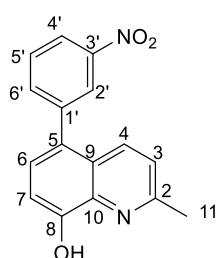
**5-(3-methoxyphenyl)-2-methylquinolin-8-ol (5.8):**



Yellow solid; yield: 65% (56 mg; 0.21 mmol). M.p: 89-90 °C. IR ( $\nu_{\text{max}}/\text{cm}^{-1}$ ) 3402, 3032, 2956, 2926, 2844, 1606, 1574, 1516, 1470, 1406, 1252, 1176, 828, 794, 588  $\text{cm}^{-1}$ .  $^1\text{H}$  NMR ( $\text{CDCl}_3$ , 400 MHz)  $\delta$ : 2.64 (s, 3H, H-11), 3.78 (s, 3H, H-12), 6.89 (d,  $J = 8.1$  Hz, 1H, H-7), 6.95 (d,  $J = 7.9$  Hz, 2H, H-4' and H-6'), 7.12 (s,

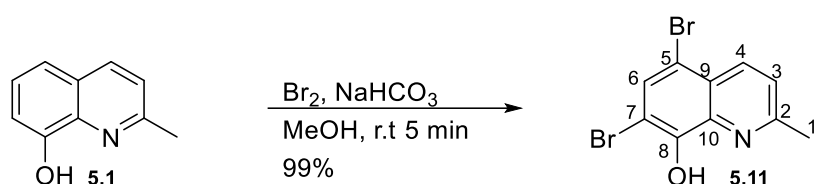
1H, H-2'), 7.15 (d,  $J = 8.7$  Hz, 1H, H-3), 7.31 (br. t,  $J = 7.9$  Hz, 2H, H-5' and H-6), 8.11 (d,  $J = 8.7$  Hz, 1H, H-4).  $^{13}\text{C}$  NMR ( $\text{CDCl}_3$ , 100 MHz)  $\delta$ : 24.9 (C-11), 55.5 (C-12), 109.6 (C-7), 112.8 (C-4'), 116.0 (C-2'), 122.8 (C-6'), 122.9 (C-3), 125.0 (C-6), 127.3 (C-5), 129.6 (C-9), 130.7 (C-5'), 135.0 (C-4), 137.9 (C-10), 141.3 (C-1'), 151.5 (C-8), 156.9 (C-2), 159.9 (C-3'). Elemental analysis: calculated C 76.96%; H 5.70%; N 5.28%; found C 76.80%; H 5.86%; N 5.03%.

**2-methyl-5-(3-nitrophenyl)quinolin-8-ol (5.9):**



Yellow solid; yield: 90% (70 mg; 0.25 mmol). M.p: 211-213 °C. IR ( $\nu_{\text{max}}/\text{cm}^{-1}$ ) 3404, 3064, 2922, 2858, 1574, 1524, 1476, 1342, 1254, 1090, 828, 742, 582  $\text{cm}^{-1}$ .  $^1\text{H}$  NMR ( $\text{CDCl}_3$ , 400 MHz)  $\delta$ : 2.67 (s, 3H, H-11), 7.13 (d,  $J = 7.8$  Hz, 1H, H-7), 7.24 (d,  $J = 8.7$  Hz, 1H, H-3), 7.30 (d,  $J = 7.8$  Hz, 1H, H-6), 7.57 (t,  $J = 7.9$  Hz, 1H, H-5'), 7.68 (d,  $J = 7.9$  Hz, 1H, H-6'), 7.96 (d,  $J = 8.7$  Hz, 1H, H-4), 8.17 (d,  $J = 7.9$  Hz, 1H, H-4'), 8.22 (s, 1H, H-2').  $^{13}\text{C}$  NMR ( $\text{CDCl}_3$ , 100 MHz)  $\delta$ : 25.8 (C-11), 109.8 (C-7), 122.2 (C-3), 123.5 (C-6), 124.6 (C-5), 124.9 (C-4'), 128.0 (C-9), 128.1 (C-2'), 129.6 (C-5'), 134.1 (C-4), 136.2 (C-10), 138.2 (C-6'), 141.5 (C-1'), 148.6 (C-3'), 152.2 (C-8), 157.4 (C-2). Elemental analysis: calculated C 68.56%; H 4.31%; N 9.99%; found C 68.45%; H 4.52%; N 9.74%.

**4.4. Synthesis of 5,7-dibromo-8-hydroxy-2-methyl-quinoline (5.11)**

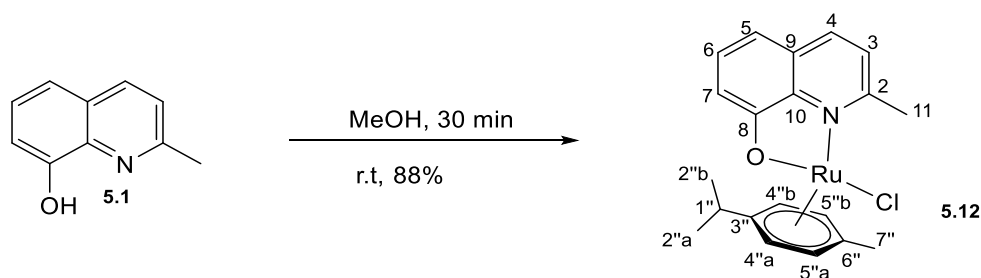


To a round-bottomed flask (25 mL) was added 8-hydroxy-2-methyl-quinoline **5.1** (0.2 g, 0.13 mmol),  $\text{NaHCO}_3$  (0.2 g, 0.24 mmol) and MeOH (2.0 mL), followed by dropwise addition of bromine (0.2 mL, 4.0 mmol) dissolved in MeOH (2.0 mL) at room temperature. The solution was stirred for 5 minutes and then washed with saturated aqueous sodium thiosulfate solution (20 mL), water (20 mL) and brine (20 mL) and the product was extracted with DCM. The organic phase was dried over  $\text{Na}_2\text{SO}_4$ , filtered and concentrated under reduced pressure

to afford the compound **5.11** as a brown solid in 99% yield (0.39 g, 0.13 mmol), which did not require further purification. M.p: 118-120 °C; IR ( $\nu_{\max}/\text{cm}^{-1}$ ) 3430, 3056, 2924, 1584, 1492, 1430, 1368, 1368, 1312, 1246, 1142, 928, 824, 730, 538.  $^1\text{H}$  NMR ( $\text{CDCl}_3$ , 400 MHz)  $\delta$ : 2.61 (s, 3H, H-11), 7.22 (d,  $J = 8.5$  Hz, 1H, H-3), 7.62, (s, 1H, H-6), 8.06 (d,  $J = 8.5$  Hz, 1H, H-4).  $^{13}\text{C}$  NMR ( $\text{CDCl}_3$ , 100 MHz)  $\delta$ : 24.7 (C-11), 103.6 (C-7), 109.9 (C-5), 123.9 (C-3), 124.6 (C-10), 132.5 (C-6), 135.8 (C-9), 137.7 (C-4), 149.0 (C-8), 158.7 (C-2). Elemental analysis: calculated C 37.89%; H 2.23%; N 4.42%; found C 37.57%; H 2.38%; N 4.19%. The spectroscopy data matched with those reported by Lam *et. al.*, 2014 [43].

#### 4.5. Synthesis of complexes 5.12-5.22

Procedure for complex  $[(\eta^6\text{-}p\text{-cymene})\text{RuCl}(\kappa^2\text{-O,N-2-methyl-HyQ})]\cdot\text{Cl}$  (**5.12**):



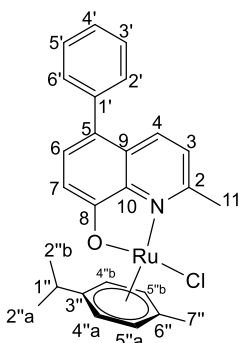
To a Schlenk flask (25mL) containing dichloro *p*-cymene-ruthenium(II) dimer (**4.21**) (50 mg, 0.08 mmol) and 8-hydroxy-2-methyl-quinoline **5.1** (27.1 mg, 0.17 mmol) was added 5 mL of dry methanol and was stirred at room temperature for 2 hours, color change was observed from deep yellow to deep orange. After completion of the reaction, solvent methanol was evaporated under reduced pressure. The crude product was further purified by silica gel column chromatography eluting with Hex/EtOAc 2:1 v/v, to afford compound **5.12** as brown solid in 88% yield (70 mg, 0.15 mmol). M.p: 215-216 °C. IR ( $\nu_{\max}/\text{cm}^{-1}$ ) 3432, 3048, 2960, 2922, 1722, 1564, 1502, 1460, 1430, 1376, 1226, 1108, 830, 738  $\text{cm}^{-1}$ .  $^1\text{H}$  NMR ( $\text{CDCl}_3$ , 400 MHz)  $\delta$ : 0.94 and 1.08 (d,  $J = 6.7$  Hz, 3H, H-2''a and H-2''b), 2.27 (s, 3H, H-7''), 2.54-2.67 (sept,  $J = 6.7$  Hz, 1H, H-1''), 3.12 (s, 3H, H-11), 5.24 (d,  $J = 5.2$  Hz, 1H, H-4''a), 5.49 (d,  $J = 6.7$  Hz, 1H, H-4''b), 5.51 (d,  $J = 6.7$  Hz, 1H, H-5''a), 5.67 (d,  $J = 5.2$  Hz, 1H, H-5''b), 6.70 (d,  $J = 7.7$  Hz,



1H, H-3), 6.94 (d,  $J = 7.7$  Hz, 1H, H-7), 7.17-7.21 (m, 2H, H-5, H-6), 7.86 (d,  $J = 8.2$  Hz, 1H, H-4).  $^{13}\text{C}$  NMR ( $\text{CDCl}_3$ , 100 MHz)  $\delta$ : 18.8 (C-7''), 21.9 and 22.3 (C-2''a and C-2''b), 28.5 (C-11), 30.8 (C-1''), 79.4 (C-4''a), 79.7 (C-4''b), 80.9 (C-5''a), 86.1 (C-5''b), 100.1 (C-3''), 101.1 (C-6''), 110.5 (C-7), 115.1 (C-5), 123.2 (C-3), 128.3 (C-6), 128.7 (C-9), 137.5 (C-10), 144.0 (C-4), 158.1 (C-8), 167.8 (C-2). Elemental analysis: calculated C 56.00%; H 5.17%; N 3.27%; found C 55.83%; H 5.31%; N 3.04%.

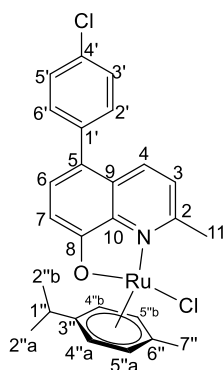
Compounds **5.13-5.22** were synthesized using a similar method to that of **5.12**.

*[( $\eta^6$ -p-cymene)RuCl( $\kappa^2$ -O,N-5-(benzene)-2-methyl-HyQ)]·Cl* (**5.13**):



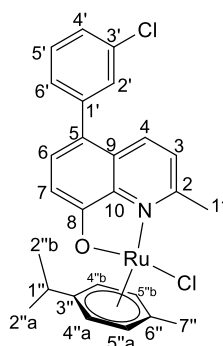
Orange solid; yield: 76% (35.2 mg; 0.065 mmol). M.p: 238-239 °C. IR ( $\nu_{\text{max}}/\text{cm}^{-1}$ ) 3436, 3046, 2960, 2924, 2858, 1600, 1558, 1462, 1436, 1370, 1318, 1112, 818, 762, 706  $\text{cm}^{-1}$ .  $^1\text{H}$  NMR ( $\text{CDCl}_3$ , 400 MHz)  $\delta$ : 0.96 and 1.07 (d,  $J = 6.8$  Hz, 6H, H-2''a and H-2''b), 2.24 (s, 3H, H-7''), 2.61 (sept,  $J = 6.8$  Hz, 1H, H-1''), 3.10 (s, 3H, H-11), 5.22 (d,  $J = 5.4$  Hz, 1H, H-4''a), 5.45 (d,  $J = 5.4$  Hz, 1H, H-4''b), 5.48 (d,  $J = 5.4$  Hz, 1H, H-5''a), 5.63 (d,  $J = 5.4$  Hz, 1H, H-5''b), 6.94 (d,  $J = 7.9$  Hz, 1H, H-7), 7.12 (d,  $J = 8.4$  Hz, 1H, H-3), 7.14 (d,  $J = 7.9$  Hz, 1H, H-6), 7.22-7.35 (m, 5H, H-2', H-3', H-4'), 7.99 (d,  $J = 8.4$  Hz, 1H, H-4).  $^{13}\text{C}$  NMR ( $\text{CDCl}_3$ , 100 MHz)  $\delta$ : 19.0 (C-7''), 22.2 and 22.5 (C-2''a and C-2''b), 28.7 (C-11), 31.0 (C-1''), 79.6(C-4''a), 79.7 (C-4''b), 81.3 (C-5''a), 86.3 (C-5''b), 100.2 (C-3''), 101.5 (C-6''), 115.0 (C-7), 123.3 (C-3), 123.9 (C-6), 126.3 (C-5), 126.5 (C-10), 128.4 (C-3'), 129.9 (C-2'), 130.2 (C-4'), 136.2 (C-4), 139.9 (C-1'), 144.1 (C-9), 158.1 (C-8), 167.6 (C-2). Elemental analysis: calculated C 61.84%; H 5.19%; N 2.77%; found C 61.56%; H 5.32%; N 2.51%.

*[(η<sup>6</sup>-p-cymene)RuCl(κ<sup>2</sup>-O,N-5-(4'-chlorobenzene)-2-methyl-HyQ)]·Cl (5.14):*



Orange solid; yield: 51% (50 mg; 0.087 mmol). M.p: 267-268 °C. IR ( $\nu_{\text{max}}/\text{cm}^{-1}$ ) 3432, 3065, 2960, 2924, 2868, 1600, 1558, 1460, 1436, 1320, 1086, 816, 754, 510  $\text{cm}^{-1}$ .  $^1\text{H}$  NMR ( $\text{CDCl}_3$ , 400 MHz)  $\delta$ : 1.01 and 1.13 (d,  $J = 6.8$  Hz, 6H, H-2''a and H-2''b), 2.30 (s, 3H, H-7''), 2.66 (sept,  $J = 6.8$  Hz, 1H, H-1''), 3.16 (s, 3H, H-11), 5.28 (d,  $J = 5.7$  Hz, 1H, H-4''a), 5.53 (d,  $J = 5.7$  Hz, 1H, H-4''b), 5.56 (d,  $J = 5.7$  Hz, 1H, H-5''a), 5.71 (d,  $J = 5.7$  Hz, 1H, H-5''b), 6.99 (d,  $J = 8.2$  Hz, 1H, H-7), 7.17 (d,  $J = 8.2$  Hz, 1H, H-6), 7.20 (d,  $J = 8.4$  Hz, 1H, H-3), 7.25 (d,  $J = 8.3$  Hz, 2H, H-3'), 7.37 (d,  $J = 8.3$  Hz, 2H, H-2'), 7.98 (d,  $J = 8.4$  Hz, 1H, H-4).  $^{13}\text{C}$  NMR ( $\text{CDCl}_3$ , 100 MHz)  $\delta$ : 19.1 (C-7''), 22.3 and 22.6 (C-2''a and C-2''b), 28.9 (C-11), 31.1 (C-1''), 79.7(C-4''a), 79.9 (C-4''b), 81.3 (C-5''a), 86.4 (C-5''b), 100.4 (C-3''), 101.6 (C-6''), 115.1 (C-7), 122.6 (C-3), 123.6 (C-6), 126.3 (C-5), 128.7 (C-3'), 130.0 (C-9), 131.5 (C-2'), 132.6 (C-4'), 135.9 (C-4), 138.5 (C-1'), 144.2 (C-10), 158.5 (C-8), 167.9 (C-2). Elemental analysis: calculated C 57.89%; H 4.67%; N 2.60%; found C 57.75%; H 4.86%; N 2.41%.

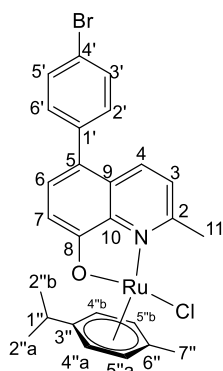
*[(η<sup>6</sup>-p-cymene)RuCl(κ<sup>2</sup>-O,N-5-(3'-chlorobenzene)-2-methyl-HyQ)]·Cl (5.15):*



Orange solid; yield: 72% (77 mg; 0.13 mmol). M.p: 286-287 °C. IR ( $\nu_{\text{max}}/\text{cm}^{-1}$ ) 3430, 3066, 2964, 2924, 2874, 1594, 1558, 1460, 143, 1378, 1316, 1116, 788  $\text{cm}^{-1}$ .  $^1\text{H}$  NMR ( $\text{CDCl}_3$ , 400 MHz)  $\delta$ : 0.92 and 1.06 (d,  $J = 6.9$  Hz, 6H, H-2''a and H-2''b), 2.23 (s, 3H, H-7''), 2.59 (sept,  $J = 6.9$  Hz, 1H, H-1''), 3.09 (s, 3H, H-11), 5.20 (d,  $J = 5.7$  Hz, 1H, H-4''a), 5.44 (d,  $J = 5.7$  Hz, 1H, H-4''b), 5.46 (d,  $J = 5.7$  Hz, 1H, H-5''a), 5.62 (d,  $J = 5.7$  Hz, 1H, H-5''b), 6.91 (d,  $J = 8.4$  Hz, 1H, H-7), 7.11-7.22 (m, 5H, H-3, H-6, H-4', H-5' and H-6'), 7.25 (s, 1H, H-2'), 7.93 (d,  $J = 8.4$  Hz, 1H, H-4).  $^{13}\text{C}$  NMR ( $\text{CDCl}_3$ , 100 MHz)  $\delta$ : 19.1 (C-7''), 22.3 and 22.6 (C-2''a and C-2''b), 28.9 (C-11), 31.1 (C-1''), 79.7(C-4''a), 79.9 (C-4''b), 81.3 (C-5''a), 86.4 (C-5''b), 100.5 (C-3''), 101.6 (C-6''), 115.1 (C-7), 122.3 (C-3), 123.7 (C-5), 126.2 (C-6), 126.7 (C-6'), 128.5 (C-4'), 129.8 (C-9), 130.2 (C-2'), 134.3 (C-5'), 135.8 (C-4/C-3'), 141.9 (C-10), 144.2 (C-

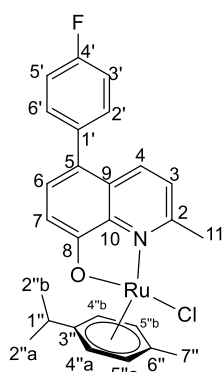
1'), 158.4 (C-8), 168.3 (C-2). Elemental analysis: calculated C 57.89%; H 4.67%; N 2.60%; found C 57.60%; H 4.83%; N 2.36%.

**[[ $\eta^6$ -*p*-cymene)RuCl( $\kappa^2$ -O,N-5-(4'-bromobenzene)-2-methyl-HyQ)]·Cl (5.16):**



Orange solid; yield: 56% (54 mg; 0.09 mmol). M.p: 250-252 °C. IR ( $\nu_{\max}/\text{cm}^{-1}$ ) 3432, 3050, 2962, 2924, 2868, 1602, 1558, 1512, 1462, 1438, 1370, 1322, 1078, 1006, 820, 754, 510  $\text{cm}^{-1}$ .  $^1\text{H}$  NMR ( $\text{CDCl}_3$ , 400 MHz)  $\delta$ : 0.92 and 1.05 (d,  $J = 6.4$  Hz, 6H, H-2''a and H-2''b), 2.22 (s, 3H, H-7''), 2.59 (sept,  $J = 6.4$  Hz, 1H, H-1''), 3.07 (s, 3H, H-11), 5.20 (d,  $J = 5.0$  Hz, 1H, H-4''a), 5.46 (sbr, 2H, H-4''b and H-5''a), 5.63 (sbr, 1H, H-5''b), 6.91 (d,  $J = 8.0$  Hz, 2H, H-7), 7.11 (d,  $J = 8.2$  Hz, 1H, H-3'), 7.16 (d,  $J = 8.0$  Hz, 1H, H-6), 7.32 (d,  $J = 8.0$  Hz, 1H, H-3), 7.43 (d,  $J = 8.2$  Hz, 2H, H-2'), 7.90 (d,  $J = 8.0$  Hz, 1H, H-4).  $^{13}\text{C}$  NMR ( $\text{CDCl}_3$ , 100 MHz)  $\delta$ : 19.1 (C-7''), 22.3 and 22.6 (C-2''a and C-2''b), 28.9 (C-11), 31.1 (C-1''), 79.7(C-4''a), 79.9 (C-4''b), 81.4 (C-5''a), 86.4 (C-5''b), 100.5 (C-3''), 101.7 (C-6''), 115.1 (C-7), 122.6 (C-3), 123.7 (C-6), 126.3 (C-5), 128.7 (C-3'/C-5'), 130.1 (C-9), 131.6 (C-2'/C-6'), 132.6 (C-4'), 135.9 (C-4), 138.5 (C10), 144.2 (C-1'), 158.5 (C-8), 168.0 (C-2). Elemental analysis: calculated C 53.48%; H 4.31%; N 2.40%; found C 53.31%; H 4.56%; N 2.17%.

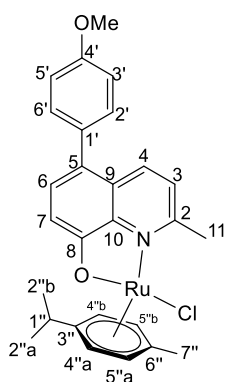
**[[ $\eta^6$ -*p*-cymene)RuCl( $\kappa^2$ -O,N-5-(4'-fluorobenzene)-2-methyl-HyQ)]·Cl (5.17):**



Orange solid; yield: 51% (54 mg; 0.097 mmol). M.p: 275-276 °C. IR ( $\nu_{\max}/\text{cm}^{-1}$ ) 3436, 3062, 3040, 2964, 2926, 2872, 1632, 1602, 1560, 1516, 1464, 1438, 1368, 1322, 1218, 1112, 844, 818, 516  $\text{cm}^{-1}$ .  $^1\text{H}$  NMR ( $\text{CDCl}_3$ , 400 MHz)  $\delta$ : 0.92 and 1.05 (d,  $J = 6.8$  Hz, 6H, H-2''a and H-2''b), 2.22 (s, 3H, H-7''), 2.59 (sept,  $J = 6.8$  Hz, 1H, H-1''), 3.07 (s, 3H, H-11), 5.20 (d,  $J = 5.6$  Hz, 1H, H-4''a), 5.43 (d,  $J = 5.6$  Hz, 1H, H-4''b) 5.46 (d,  $J = 5.6$  Hz, 1H, H-5''a), 5.61 (d,  $J = 5.6$  Hz, 1H, H-5''b), 6.90 (d,  $J = 8.1$  Hz, 2H, H-7), 7.00 (br. t,  $J = 8.6$  Hz, 2H, H-3'/H-5'), 7.07 (d,  $J = 8.1$  Hz, 1H, H-6), 7.11 (d,  $J = 8.7$  Hz, 1H, H-3), 7.18 (m, 2H, H-2'/H-6'), 7.87 (d,  $J = 8.7$  Hz, 1H, H-4).  $^{13}\text{C}$  NMR ( $\text{CDCl}_3$ , 100 MHz)  $\delta$ : 19.1 (C-7''), 22.3 and 22.6 (C-2''a and C-2''b), 28.9 (C-11), 31.1 (C-1''), 79.7(C-4''a), 79.8 (C-4''b), 81.4 (C-5''a), 86.4 (C-5''b), 100.4 (C-3''), 101.6

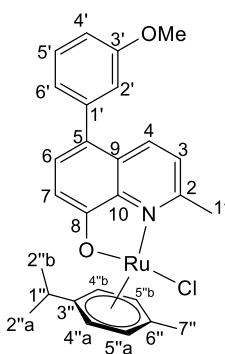
(C-6''), 115.0 (C-7), 115.4 (d,  $J = 21.1$  Hz, C-3'/C-5'), 122.7 (C-3), 123.5 (C-6), 126.4 (C-5), 130.0 (C-10), 131.8 (d,  $J = 7.8$  Hz, C-2'/C-6'), 136.0 (C-4), 144.2 (C-1'), 158.3 (C-8), 162.0 (d,  $J = 244.0$  Hz, C-4'), 167.9 (C-2). Elemental analysis: calculated C 59.71%; H 4.81%; N 2.68%; found C 59.51%; H 5.04%; N 2.51%.

***[(η<sup>6</sup>-p-cymene)RuCl(κ<sup>2</sup>-O,N-5-(4'-methoxybenzene)-2-methyl-HyQ)]·Cl (5.18):***



Orange solid; yield: 94% (84.4 mg; 0.15 mmol). M.p: 253-255 °C. IR ( $\nu_{\max}/\text{cm}^{-1}$ ) 3410, 3044, 2962, 2926, 2870, 1602, 1558, 1514, 1464, 1434, 1366, 1324, 1036, 1286, 826, 784, 728, 710  $\text{cm}^{-1}$ . <sup>1</sup>H NMR (CDCl<sub>3</sub>, 400 MHz)  $\delta$ : 0.91 and 1.04 (d,  $J = 6.8$  Hz, 6H, H-2''a and H-2''b), 2.21 (s, 3H, H-7''), 2.57 (sept,  $J = 6.8$  Hz, 1H, H-1''), 3.07 (s, 3H, H-11), 3.72 (s, 3H, H-12), 5.20 (d,  $J = 5.4$  Hz, 1H, H-4''a), 5.47 (d,  $J = 5.4$  Hz, 2H, H-4''b and H-5''a) 5.64 (d,  $J = 5.4$  Hz, 1H, H-5''b), 6.78 (d,  $J = 7.7$  Hz, 2H, H-3'), 6.83 (d,  $J = 7.8$  Hz, 1H, H-7), 6.91 (d,  $J = 7.8$  Hz, 1H, H-6), 7.12 (d,  $J = 7.7$  Hz, 1H, H-2'), 7.21 (d,  $J = 8.7$  Hz, 1H, H-3), 8.00 (d,  $J = 8.7$  Hz, 1H, H-4). <sup>13</sup>C NMR (CDCl<sub>3</sub>, 100 MHz)  $\delta$ : 19.1 (C-7''), 22.3 and 22.6 (C-2''a and C-2''b), 28.9 (C-11), 31.1 (C-1''), 64.0 (C-12), 79.8 (C-4''a), 79.9 (C-4''b), 81.2 (C-5''a), 86.4 (C-5''b), 100.5 (C-3''), 101.6 (C-6''), 112.3 (C-7), 115.0 (C-3'), 115.9 (C-3), 123.5 (C-6), 124.2 (C-5), 126.4 (C-10), 129.9 (C-2'), 136.4 (C-1'), 141.3 (C-4), 144.0 (C-9), 158.5 (C-8), 159.8 (C-2), 167.2 (C-4'). Elemental analysis: calculated C 60.61%; H 5.27%; N 2.62%; found C 60.32%; H 5.46%; N 2.51%.

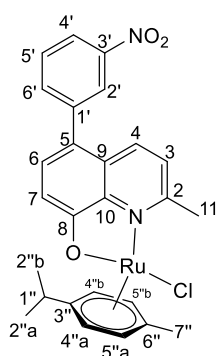
***[(η<sup>6</sup>-p-cymene)RuCl(κ<sup>2</sup>-O,N-5-(3'-methoxybenzene)-2-methyl-HyQ)]·Cl (5.19):***



Orange solid; yield: 81% (73.4 mg; 0.13 mmol). M.p: 235-237 °C. IR ( $\nu_{\max}/\text{cm}^{-1}$ ) 3434, 3038, 2958, 2926, 2868, 1606, 1560, 1518, 1462, 1436, 1322, 1242, 1174, 112, 1032, 822, 520  $\text{cm}^{-1}$ . <sup>1</sup>H NMR (CDCl<sub>3</sub>, 400 MHz)  $\delta$ : 0.91 and 1.04 (d,  $J = 6.8$  Hz, 6H, H-2''a and H-2''b), 2.21 (s, 3H, H-7''), 2.57 (sept,  $J = 6.8$  Hz, 1H, H-1''), 3.07 (s, 3H, H-11), 3.75 (s, 3H, H-12) 5.20 (d,  $J = 5.0$  Hz, 1H, H-4''a), 5.47 (brt,  $J = 5.0$  Hz, 2H, H-4''b and H-5''a), 5.64 (d,  $J = 5.0$  Hz, 1H, H-5''b), 6.86 (d,  $J = 8.3$  Hz, 2H, H-7 and H-6'), 6.90 (d,  $J = 8.3$  Hz, 1H, H-6), 7.08-7.16 (m, 4H, H-3, H-2', H-4', H-5'), 7.95 (d,  $J = 8.3$

Hz, 1H, H-4).  $^{13}\text{C}$  NMR ( $\text{CDCl}_3$ , 100 MHz)  $\delta$ : 19.1 (C-7''), 22.3 and 22.6 (C-2''a and C-2''b), 28.9 (C-11), 31.1 (C-1''), 64.0 (C-12), 79.8 (C-4''a), 79.9 (C-4''b), 81.2 (C-5''a), 86.5 (C-5''b), 100.5 (C-3''), 101.5 (C-6''), 114.0 (C-7), 115.1 (C-3), 123.4 (C-6), 124.1 (C-5), 126.5 (C-4'), 129.8 (C-9), 131.3 (C-2'), 131.9 (C-5'), 132.3 (C-4), 136.4 (C-10), 144.1 (C-6'), 158.4 (C-1'), 158.6 (C-3'), 159.8 (C-8), 166.8 (C-2). Elemental analysis: calculated C 60.61%; H 5.27%; N 2.62%; found C 60.36%; H 5.55%; N 2.41%.

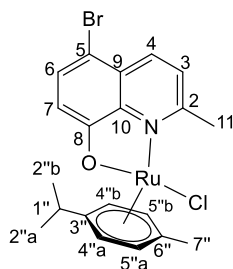
***[(\eta^6-p-cymene)RuCl(\kappa^2-O,N-5-(3'-nitrobenzene)-2-methyl-HyQ)]\cdot Cl (5.20):***



Orange solid; yield: 90% (84 mg; 0.14 mmol). M.p: 230-231 °C. IR ( $\nu_{\text{max}}/\text{cm}^{-1}$ ) 3432, 3054, 2962, 2926, 2868, 1630, 1560, 1530, 1464, 1436, 1346, 1328, 1088, 1034, 744  $\text{cm}^{-1}$ .  $^1\text{H}$  NMR ( $\text{CDCl}_3$ , 400 MHz)  $\delta$ : 0.94 and 1.07 (d,  $J = 6.7$  Hz, 6H, H-2''a and H-2''b), 2.25 (s, 3H, H-7''), 2.60 (sept,  $J = 6.9$  Hz, 1H, H-1''), 3.11 (s, 3H, H-11), 5.23 (d,  $J = 5.0$  Hz, 1H, H-4''a), 5.49 (brt,  $J = 5.0$  Hz, 2H, H-4''b and H-5''a), 5.65 (d,  $J = 5.0$  Hz, 1H, H-5''b), 6.95

(d,  $J = 7.5$  Hz, 1H, H-7), 7.17 (br. t,  $J = 8.0$  Hz, 2H, H-3 and H-6'), 7.50 (t,  $J = 7.8$  Hz, 1H, H-5'), 7.58 (d,  $J = 7.5$  Hz, 1H, H-6), 7.89 (d,  $J = 8.0$  Hz, 1H, H-4), 8.09 (d,  $J = 8.0$  Hz, 1H, H-4'), 8.14 (s, 1H, H-2').  $^{13}\text{C}$  NMR ( $\text{CDCl}_3$ , 100 MHz)  $\delta$ : 19.1 (C-7''), 22.3 and 22.6 (C-2''a and C-2''b), 28.9 (C-11), 31.2 (C-1''), 79.8 (C-4''a), 80.0 (C-4''b), 81.2 (C-5''a), 86.6 (C-5''b), 100.8 (C-3''), 101.8 (C-6''), 115.4 (C-7), 121.2 (C-3), 121.6 (C-6), 124.1 (C-5), 124.8 (C-4'), 126.1 (C-9), 129.6 (C-2'), 130.6 (C-5'), 135.3 (C-4), 136.3 (C-10), 141.7 (C-6'), 144.2 (C-1'), 148.5 (C-3'), 158.8 (C-2), 168.5 (C-8). Elemental analysis: calculated C 56.78%; H 4.58%; N 5.09%; found C 56.63%; H 4.70%; N 4.86%.

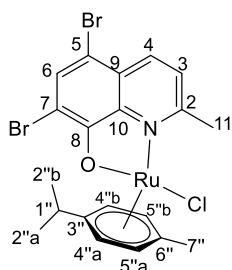
***[(\eta^6-p-cymene)RuCl(\kappa^2-O,N-5-bromo-2-methyl-HyQ)]\cdot Cl (5.21):***



Brown solid; yield: 71% (61.6 mg; 0.11 mmol). M.p: 238-239 °C. IR ( $\nu_{\text{max}}/\text{cm}^{-1}$ ) 3432, 3068, 2962, 2924, 2870, 1556, 1496, 1458, 1430, 1360, 1332, 1084, 826, 646  $\text{cm}^{-1}$ .  $^1\text{H}$  NMR ( $\text{CDCl}_3$ , 400 MHz)  $\delta$ : 0.87 and 1.00 (d,  $J = 6.8$  Hz, 6H, H-2''a and H-2''b), 2.19 (s, 3H, H-7''), 2.51 (sept,  $J = 6.8$  Hz, 1H, H-1''), 3.07 (s, 3H, H-11), 5.15 (d,  $J = 5.6$  Hz, 1H, H-4''a), 5.40

(d,  $J = 5.6$  Hz, 1H, H-4''b), 5.42 (d,  $J = 5.6$  Hz, 1H, H-5''a), 5.58 (d,  $J = 5.6$  Hz, 1H, H-5''b), 6.74 (d,  $J = 8.5$  Hz, 1H, H-7), 7.24 (d,  $J = 8.6$  Hz, 1H, H-3), 7.31 (d,  $J = 8.5$  Hz, 1H, H-6), 8.10 (d,  $J = 8.6$  Hz, 1H, H-4).  $^{13}\text{C}$  NMR ( $\text{CDCl}_3$ , 100 MHz)  $\delta$ : 19.1 (C-7''), 22.2 and 22.5 (C-2''a and C-2''b), 28.8 (C-11), 31.1 (C-1''), 79.5 (C-4''a), 79.9 (C-4''b), 81.2 (C-5''a), 86.5 (C-5''b), 100.6 (C-3''), 101.2 (C-6''), 101.2 (C-5), 115.8 (C-7), 124.4 (C-3), 127.0 (C-10), 132.1 (C-6), 137.3 (C-9), 145.1 (C-4), 158.9 (C-8), 168.3 (C-2). Elemental analysis: calculated C 47.30%; H 4.16%; N 2.76%; found C 47.06%; H 4.30%; N 2.55%.

*[( $\eta^6$ -p-cymene)RuCl( $\kappa^2$ -O,N-5,7-dibromo-2-methyl-HyQ)].Cl (5.22):*



Brown solid; yield: 88% (94 mg; 0.15 mmol). M.p: 250-251 °C. IR ( $\nu_{\text{max}}/\text{cm}^{-1}$ ) 3423, 3042, 2960, 2924, 2868, 1544, 1494, 1430, 1358, 1024, 880, 820, 744, 668  $\text{cm}^{-1}$ .  $^1\text{H}$  NMR ( $\text{CDCl}_3$ , 400 MHz)  $\delta$ : 0.89 and 1.08 (d,  $J = 6.7$  Hz, 3H, H-2''a and H-2''b), 2.26 (s, 3H, H-7''), 2.54-2.69 (sept,  $J = 6.7$  Hz, 1H, H-1''), 3.12 (s, 3H, H-11), 5.21 (d,  $J = 5.1$  Hz, 1H, H-4''a), 5.42 (d,  $J = 5.1$  Hz, 1H, H-4''b), 5.52 (d,  $J = 5.5$  Hz, 1H, H-5''a), 5.70 (d,  $J = 5.5$  Hz, 1H, H-5''b), 7.30 (d,  $J = 8.4$  Hz, 1H, H-3), 7.63 (s, 1H, H-6), 8.12 (d,  $J = 8.4$  Hz, 1H, H-4).  $^{13}\text{C}$  NMR ( $\text{CDCl}_3$ , 100 MHz)  $\delta$ : 19.0 (C-7''), 22.0 and 22.5 (C-2''a and C-2''b), 28.8 (C-11), 31.0 (C-1''), 79.4 (C-4''a), 80.5 (C-4''b), 80.9 (C-5''a), 86.4 (C-5''b), 100.3 (C-3''), 100.8 (C-6''), 102.2 (C-7), 109.0 (C-5), 124.3 (C-3), 126.4 (C-10), 134.5 (C-6), 137.6 (C-9), 144.5 (C-4), 159.7 (C-8), 164.6 (C-2). Elemental analysis: calculated C 40.94%; H 3.44%; N 2.39%; found C 40.61%; H 3.65%; N 2.07%.

#### 4.6. X-ray Crystallography

The single crystal X-ray diffraction measurement of compound **5.14** was performed with an Oxford Gemini A Ultra-radiation instrument with a CCD detector using MoK $\alpha$  radiation ( $\alpha = 0.71073 \text{ \AA}$ ) at room temperature. The data collection, cell refinements and data reduction were performed using the CRYCALISPRO software [44] and the structure was resolved by direct methods and refined by SHELXL-2017 program [45]. All non-hydrogen atoms were refined with anisotropic thermal parameters. H atoms connected to carbon were placed in idealized positions and treated by rigid model, with  $U_{iso}(H) = 1.2U_{eq}(C)$  and H atoms from water molecules were refined with  $O-H = 0.85 \text{ \AA}$  and  $U_{iso}(H) = 1.5U_{eq}(O)$ . and the figures shown were produced using the programs Ortep 3 for Windows [46] and Mercury [47].

#### 4.7. Antimicrobial activity

A pre-inoculum was prepared by transfer of the microorganisms from the culture medium where they were stored to test tubes containing 3.0 ml of culture medium (BHI for bacteria and Sabouraud for yeast). The tubes were then incubated in an oven at 37 °C for 36 h. Then, 500  $\mu\text{L}$  of this pre-inoculum was transferred to test tubes containing sterile distilled water. The tubes were homogenized and the concentration adjusted to 600 nm (bacteria) and 530 nm (yeast), until a transmittance between 74-75% (bacteria) and 75-76% (yeast), corresponding to the 0.5 McFarland standard turbidity, that is, 105 CFU / mL, thus obtaining the suspensions of the inoculums used in the bioassay. To prepare the working solution the samples were previously solubilized in 12.5 mg/mL of dimethylsulfoxide. To an aliquot of 40  $\mu\text{L}$  of those solution was added 960  $\mu\text{L}$  of the culture medium used in the bioassay, obtaining the working solution at the concentration of 500  $\mu\text{g/mL}$ . The bioassays were performed in 96-well plates in duplicate. In the first well 200  $\mu\text{L}$  of the 500  $\mu\text{g/mL}$  working solution was added. In the following wells, 100  $\mu\text{L}$  of culture medium per well was added, then serial (1:1) microdilution of sample solution was performed, in which concentrations ranged from 250 to 0.12  $\mu\text{g/ml}$ . Then, 100  $\mu\text{L}$  of standardized microorganism inoculum was added to each well. Four controls were performed: growth control of the microorganism (to verify cell viability); the blank, which consists of the

sample solution at the same concentrations evaluated, replacing the inoculum with sterile distilled water; positive control (replacement of the working solution by a commercial antibiotic) and sterility control of the culture medium containing 100  $\mu$ L of culture medium and 100  $\mu$ L of sterile distilled water. The microplates were incubated in an oven at 37 °C and after 24 h the plate reader was read from the plate at 490 nm. The IC<sub>50</sub> values were calculated for the samples that showed an inhibition higher than 50% in the highest concentration assayed.

#### **4.8. Cytotoxic activity**

*Was employed the same procedure discussed in Chapter 2.*



## 5. REFERENCES

- [1] G. Gasser, I. Ott, N. Metzler-Nolte, *J. Med. Chem.* 54 (2011) 3–25.
- [2] C. Mari, V. Pierroz, S. Ferrari, G. Gasser, *Chem. Sci.* 6 (2015) 2660–2686.
- [3] F. Aman, M. Hanif, W.A. Siddiqui, A. Ashraf, L.K. Filak, J. Reynisson, T. Söhnel, S.M.F. Jamieson, C.G. Hartinger, *Organometallics*. 33 (2014) 5546–5553.
- [4] L. Biancalana, S. Zacchini, N. Ferri, M.G. Lupo, G. Pampaloni, F. Marchetti, *Dalt. Trans.* 46 (2017) 16589–16604.
- [5] S. Bhattacharyya, K. Purkait, A. Mukherjee, *Dalt. Trans.* 46 (2017) 8539–8554.
- [6] L. Biancalana, A. Pratesi, F. Chiellini, S. Zacchini, T. Funaioli, C. Gabbiani, F. Marchetti, *New J. Chem.* 41 (2017) 14574–14588.
- [7] M. Malipeddi, C. Lakhani, M. Chhabra, P. Paira, R. Vidya, *Bioorg. Med. Chem. Lett.* 25 (2015) 2892–2896.
- [8] R. Pettinari, F. Marchetti, C. Pettinari, A. Petrini, R. Scopelliti, C.M. Clavel, P.J. Dyson, *Inorg. Chem.* 53 (2014) 13105–13111.
- [9] R. Pettinari, C. Pettinari, F. Marchetti, C.M. Clavel, R. Scopelliti, P.J. Dyson, *Organometallics*. 32 (2012) 309–316.
- [10] S.H. Chan, C.H. Chui, S.W. Chan, S. Hon, L. Kok, D. Chan, M. Yuen, T. Tsoi, P. Hang, M. Leung, A. King, Y. Lam, A. Sun, C. Chan, K.H. Lam, J. Cheuk, O. Tang, (2012).
- [11] E.M. Kassem, E.R. El-Sawy, H.I. Abd-Alla, A.H. Mandour, D. Abdel-Mogeed, M.M. El-Safty, *Arch. Pharm. Res.* 35 (2012) 955–64.
- [12] R. Cherdrakulkiat, S. Boonpangrak, N. Sinthupoom, S. Prachayasittikul, S. Ruchirawat, V. Prachayasittikul, *Biochem. Biophys. Reports.* 6 (2016) 135–141.
- [13] Y.Q. Hu, C. Gao, S. Zhang, L. Xu, Z. Xu, L.S. Feng, X. Wu, F. Zhao, *Eur. J. Med. Chem.* 139 (2017) 22–47.
- [14] Y. Song, H. Xu, W. Chen, P. Zhan, X. Liu, *Med. Chem. Commun.* 6 (2015) 61–74.
- [15] V. Prachayasittikul, S. Prachayasittikul, S. Ruchirawat, V. Prachayasittikul, *Drug Des. Devel. Ther.* 7 (2013) 1157–1178.
- [16] C. Gemel, R. John, C. Slugovc, K. Mereiter, K. Kirchner, *J. C. S. Dalt. Trans.* (2000) 2607–2612.
- [17] F. Aman, M. Hanif, M. Kubanik, A. Ashraf, T. Söhnel, S.M.F. Jamieson, W.A. Siddiqui, C.G. Hartinger, *Chem. - A Eur. J.* 23 (2017) 4893–4902.
- [18] M.H. Kaulage, B. Maji, S. Pasadi, S. Bhattacharya, K. Muniyappa, 139 (2017) 1016–1029.
- [19] M. Gobec, J. Kljun, I. Sosič, I. Mlinarič-Raščan, M. Uršič, S. Gobec, I. Turel, *Dalt. Trans.* 43 (2014) 9045–9051.
- [20] A. Mondal, S. De, S. Maiti, B. Sarkar, A.K. Sk, R. Jacob, A. Moorthy, P. Paira, *J. Photochem. Photobiol. B Biol.* 178 (2018) 380–394.
- [21] K. Li, Y. Li, D. Zhou, Y. Fan, H. Guo, T. Ma, J. Wen, D. Liu, L. Zhao, *Bioorganic Med. Chem.* 24 (2016) 1889–1897.
- [22] S. Ökten, O. Çakmak, A. Saddiqa, B. Keskin, S. Özdemir, M. Inal, *Org. Commun.* 9 (2016) 82–93.
- [23] B. Männel, D. Dengler, J. Shonberg, H. Hübner, D. Möller, P. Gmeiner, *J. Med. Chem.* 60 (2017) 4693–4713.
- [24] N. Jotterand, D.A. Pearce, B. Imperiali, (2001) 3224–3228.

- [25] K. Bahgat, A.G. Ragheb, *Cent. Eur. J. Chem.* 5 (2006) 201–220.
- [26] D.L. Pavia, G.M. Lampman, G.S. Kriz, Introduction to Spectroscopy, Third Edit, Thomson Learning, Inc., 2001.
- [27] V. Krishnakumar, R. Ramasamy, *Spectrochim. Acta - Part A Mol. Biomol. Spectrosc.* 61 (2005) 673–683.
- [28] R. Schuecker, R.O. John, M.A. Jakupec, V.B. Arion, B.K. Keppler, *Organometallics.* (2008) 6587–6595.
- [29] R.H. Crabtree, The Organometallic Chemistry of the Transition Metals, Fourth Edi, John Wiley & Sons, Inc., 2005.
- [30] L. Colina-Vegas, L. Luna-Dulcey, A.M. Plutín, E.E. Castellano, M.R. Cominetti, A.A. Batista, *Dalt. Trans.* 46 (2017) 12865–12875.
- [31] E. Hodson, S.J. Simpson, *Polyhedron.* 23 (2004) 2695–2707.
- [32] D. Schweinfurth, H.S. Das, F. Weisser, D. Bubrin, B. Sarkar, *Inorg. Chem.* 50 (2011) 1150–1159.
- [33] D.M. Shlaes, Antibiotics The Perfect Storm, Springer, 2010.
- [34] F. Prestinaci, P. Pezzotti, A. Pantosti, *Pathog. Glob. Health.* 109 (2015) 309–318.
- [35] World Health Organization, (2018). <http://www.who.int/en/news-room/fact-sheets/detail/antibiotic-resistance>.
- [36] N.Y.T. Man, D.R. Knight, S.G. Stewart, A.J. McKinley, T. V. Riley, K.A. Hammer, *Sci. Rep.* 8 (2018) 1–9.
- [37] World Health Organization, (2016). <http://www.who.int/en/news-room/fact-sheets/detail/pneumonia>.
- [38] World Health Organization, (2018). <http://www.who.int/news-room/fact-sheets/detail/tuberculosis>.
- [39] R.J. Fair, Y. Tor, *Perspect. Medicin. Chem.* (2014) 25–64.
- [40] P. Skehan, R. Storeng, D. Scudiero, A. Monks, D. Vistica, J.T. Warren, H. Bokesch, M.R. Boyd, *J. Nationcal Cancer Inst.* 82 (1990) 1107–1112.
- [41] S. Bhattacharyya, K. Purkait, A. Mukherjee, *Dalt. Trans.* 46 (2017) 8539–8554.
- [42] J. Jampilek, M. Dolezal, J. Kunes, V. Buchta, L. Silva, K. Kralova, *Med. Chem. (Los. Angeles).* 1 (2005) 591–599.
- [43] K.H. Lam, R. Gambari, K.K.H. Lee, Y.X. Chen, S.H.L. Kok, R.S.M. Wong, F.Y. Lau, C.H. Cheng, W.Y. Wong, Z.X. Bian, A.S.C. Chan, J.C.O. Tang, C.H. Chui, *Bioorganic Med. Chem. Lett.* 24 (2014) 367–370.
- [44] Rigaku Corporation, (2015).
- [45] G.M. Sheldrick, *Acta Crystallogr. Sect. C Struct. Chem.* 71 (2015) 3–8.
- [46] L.J. Farrugia, *J. Appl. Crystallogr.* 30 (1997) 565.
- [47] C.F. Macrae, I.J. Bruno, J.A. Chisholm, P.R. Edgington, P. McCabe, E. Pidcock, L. Rodriguez-Monge, R. Taylor, J. Van De Streek, P.A. Wood, *J. Appl. Crystallogr.* 41 (2008) 466–470.

## **FINAL CONSIDERATIONS**

This doctoral thesis was inspired in the nucleus of the 2,5-diaminoquinones, which led in to the development of the first total synthesis of abenquine A, B2, C and D. With a well-established route it was also possible to synthesize 4 new analogues for abenquines (Chapter 1) and the further evaluation of their biological potential as phytotoxic was the basis to exploit this promising class of compounds. The results were published as a poster presentation in the Brazilian Meeting on Organic Synthesis (BMOS-2015) and resulted in a poster prize, as well as a publication in a scientific journal, *Tetrahedron Letters* 57 (2016) 1811-1814.

Since the results obtained from these compounds showed a biological potential, the abenquine scaffold was used to design the new series of analogues where the amino acids residues were changing for a different aliphatic amine. As well, were prepared analogues which the amino acids fragment is holding and the acyl moiety was changed for the use of the benzoyl group. This strategy led to 11 new analogues for abenquines and they were used to evaluate their potential as phytotoxic and cytotoxic agents, as described in Chapter 2. As a consequence of this work, the results were presented as a panel in two conferences; Brazil-Spain Workshop on Organic Chemistry (BSWOC-2016) as well as in the International Union of Pure Applied Chemistry (IUPAC-2017). Also, the results caused the publication in two scientific journals, *Journal of Natural Products* 80 (2017) 813-818 and *Bioorganic & Medicinal Chemistry Letters* 27 (2017) 1141-1144.

As the results obtained on Chapters 1 and 2 were so important, they were introduced as a patent in 2017 on the *National Institute of Industrial Property (INPI)*, under the process number: BR1020170227464.

Moreover, a set of new analogues for abenquines was prepared to evaluate their activity as an herbicide (Chapter 3). These analogues were inspired by one analogue that contains the benzylamine group instead of an amino acid. Then, the aiming to introduce different substituents in the benzylamine ring to study their biological activity when changes the structural properties. Additionally, the synthesis of analogues holding the benzylamine

group and varying the size chain of the acyl fragment was planned. The results given for the 14 new compounds were very fascinating since some analogues showed IC<sub>50</sub> values as low as a commercial herbicide diuron. Through further characterization and accompanying with molecular docking studies, it was possible to determine that this class of compounds acts as an inhibitor of the photosystem II. These results were presented in the Brazilian Conference on Natural Products (BCNP-2017) and in the scientific journal, *Journal of Agricultural and Food Chemistry* 65 (2017) 11304-11311.

On the other hand, this thesis involved the synthesis of organometallics frameworks focused on the use of ruthenium *p*-cymene. Firstly, series of 2,5-dialkylamino-benzoquinone were employed as ligands, which resulted in five new ruthenium-quinone complexes as described in Chapter 4. The ruthenium-quinone complexes were screened as cytotoxic, however they were not soluble for the test, although one of them showed an EC<sub>50</sub> > 60 μM. These results are in current process of submission to a scientific journal. Optimization of 2,5-dialkylamino-benzoquinone was presented in the scientific journal, *Chemistry and Biodiversity* 13 (2016) 1008–1017.

From this class of complexes was also possible to recognize that quinone-ruthenium forms an unstable complex, therefore, ligands that content *N,O*-atoms were used to generate new ruthenium complexes. For that, 8-hydroxy-2-methylquinoline was employed as ligand as presented in Chapter 5. Since this class of complex showed high stability as well as a good solubility in the common organic solvents, the 8-hydroxy-2-methylquinoline was used as a nucleus in order to form different ligands. All the 11 new complexes and the 8-hydroxy-2-methylquinoline derivatives were studied as antimicrobial agents showing a promising result. And at the moment, these results are in current process of submission to a scientific journal.

## **APPENDIX**

1. Appendix 1: Infrared,  $^1\text{H}$  and  $^{13}\text{C}$  NMR Spectra of compounds related to Chapter 1

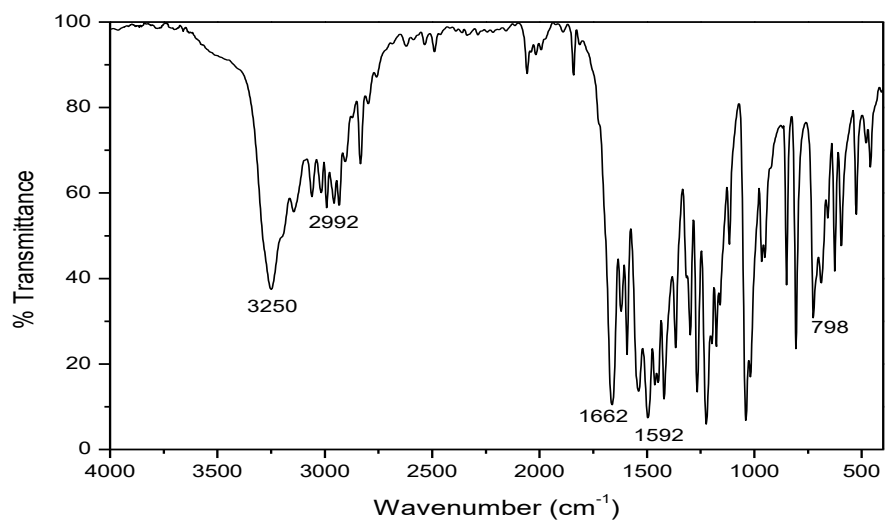


Figure A1.1. Infrared spectrum in KBr of compound 1.12.

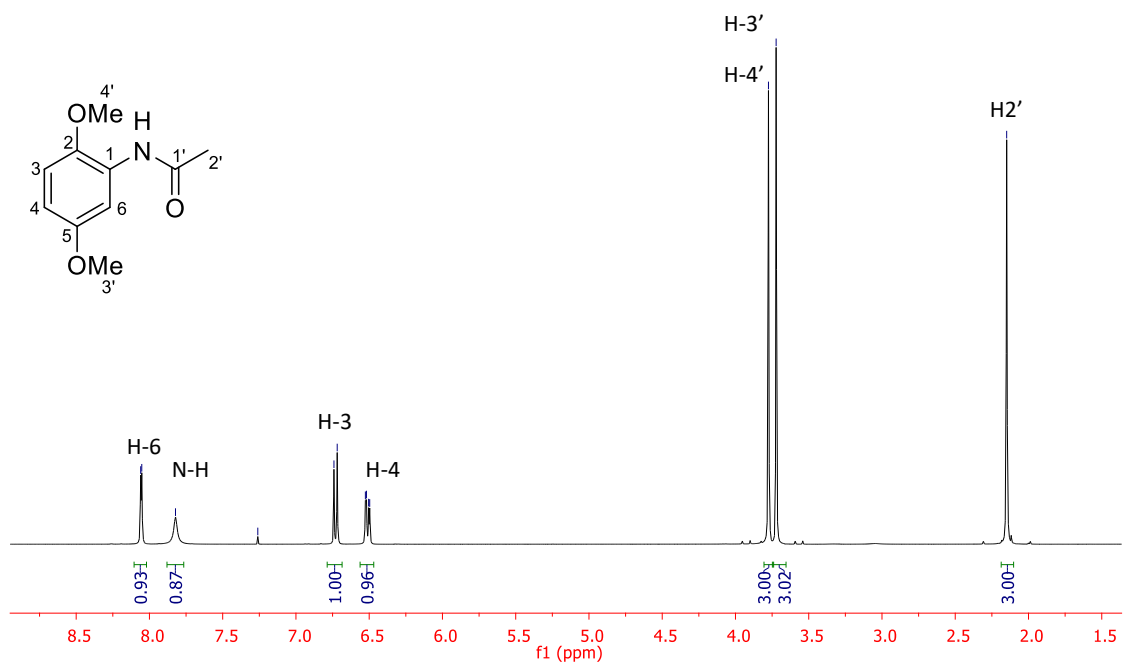
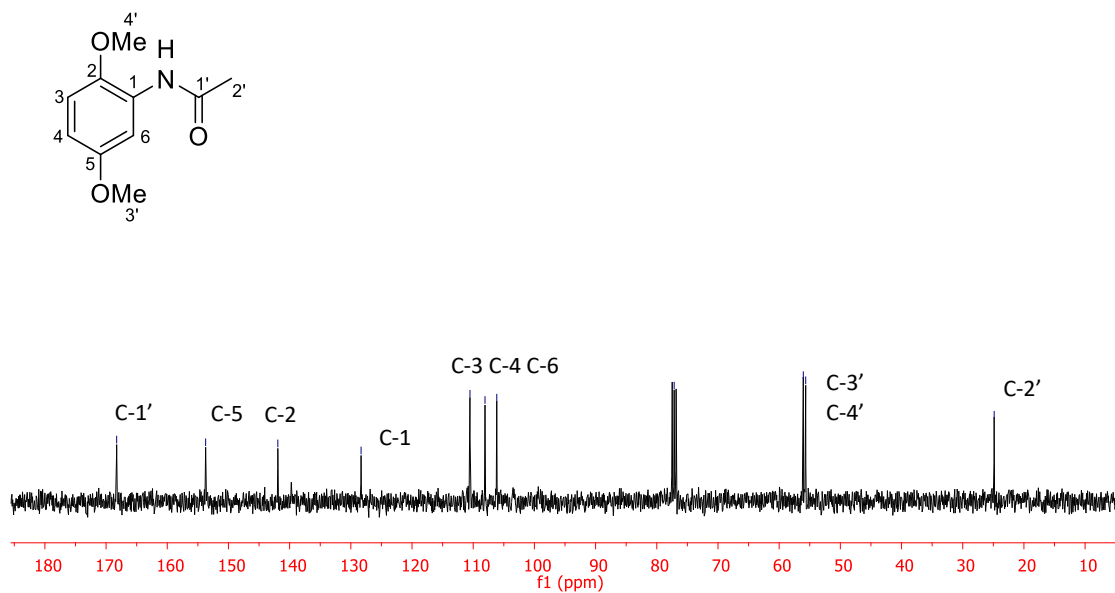
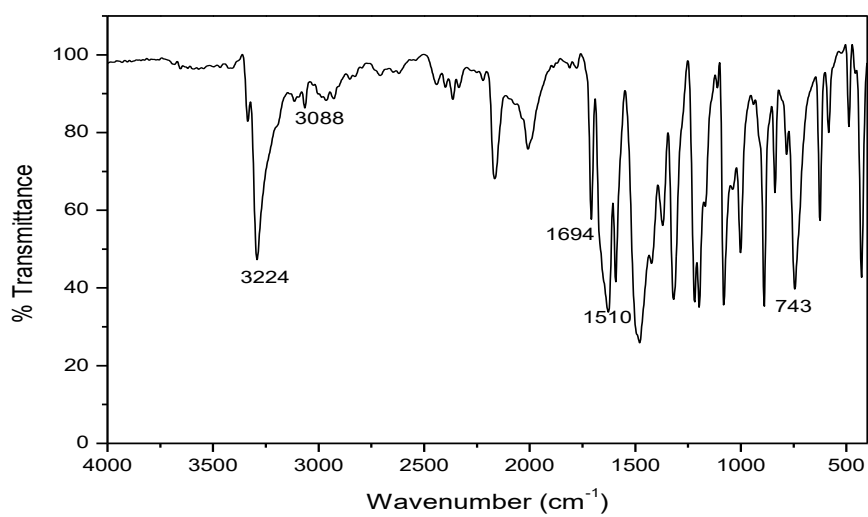


Figure A1.2.  $^1\text{H}$  NMR spectrum (400 MHz,  $\text{CDCl}_3$ ) of compound 1.12.

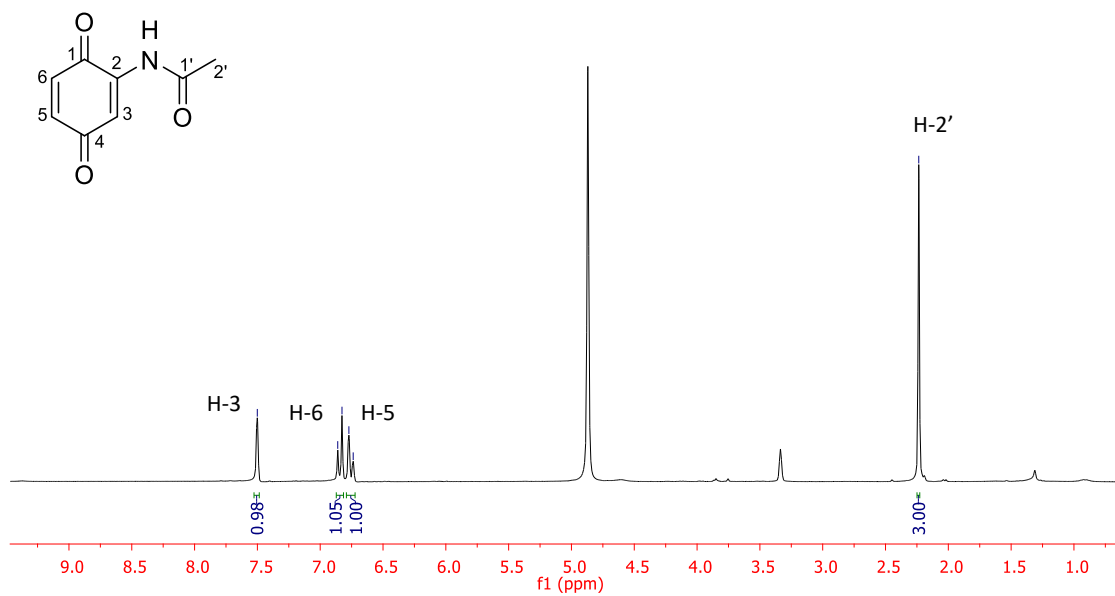


**Figure A1.3.**  $^{13}\text{C}$  NMR spectrum (100 MHz,  $\text{CDCl}_3$ ) of compound 1.12.

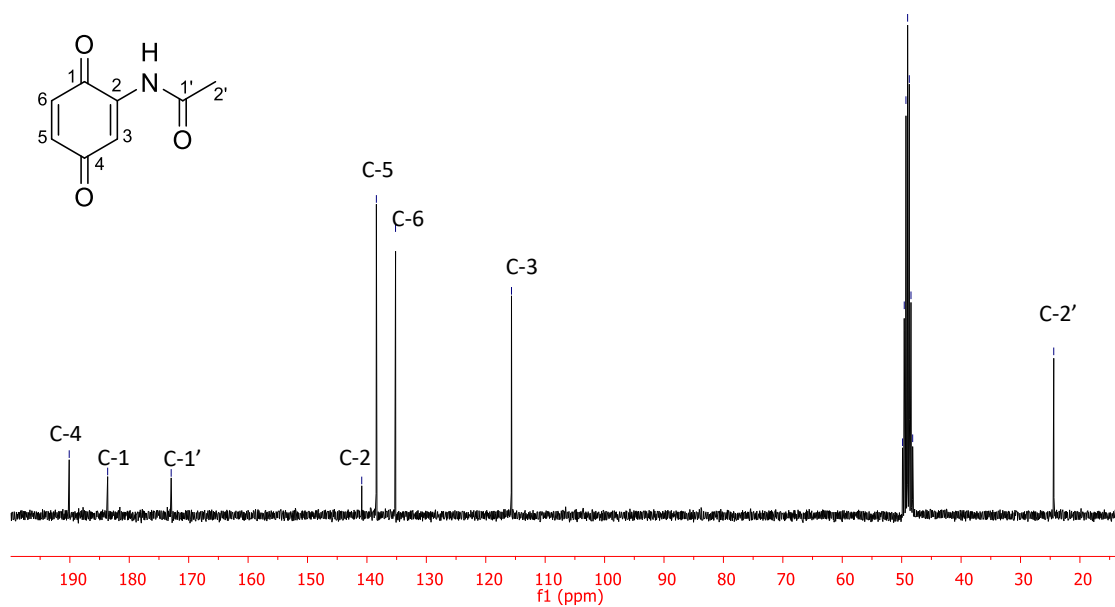


**Figure A1.4.** Infrared spectrum in KBr of compound 1.11.

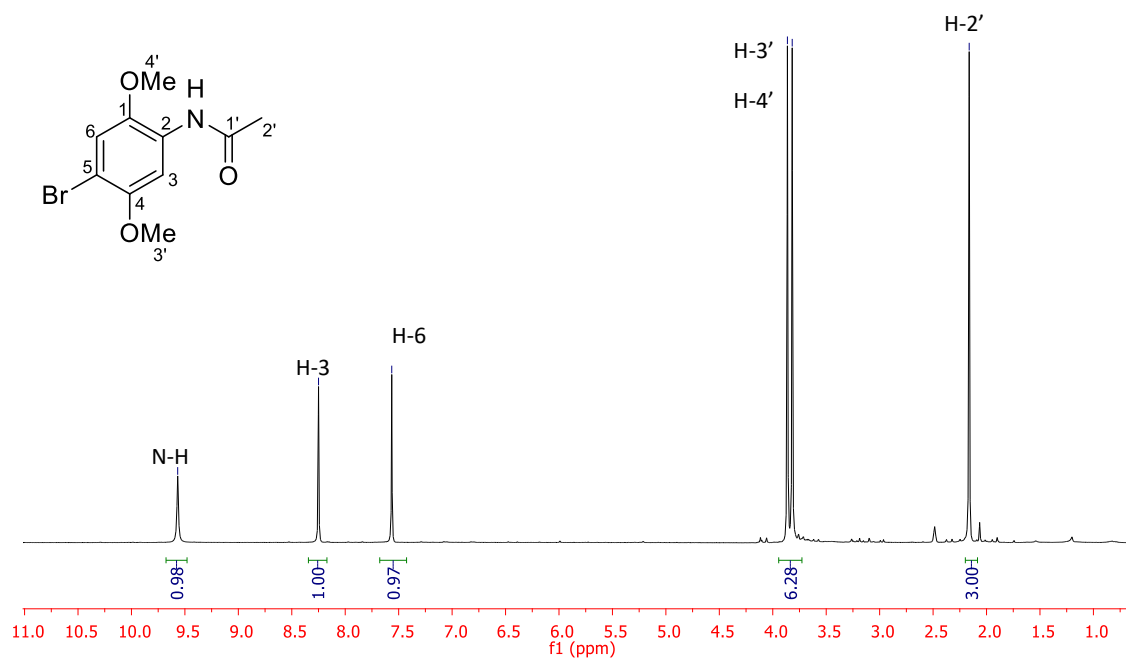




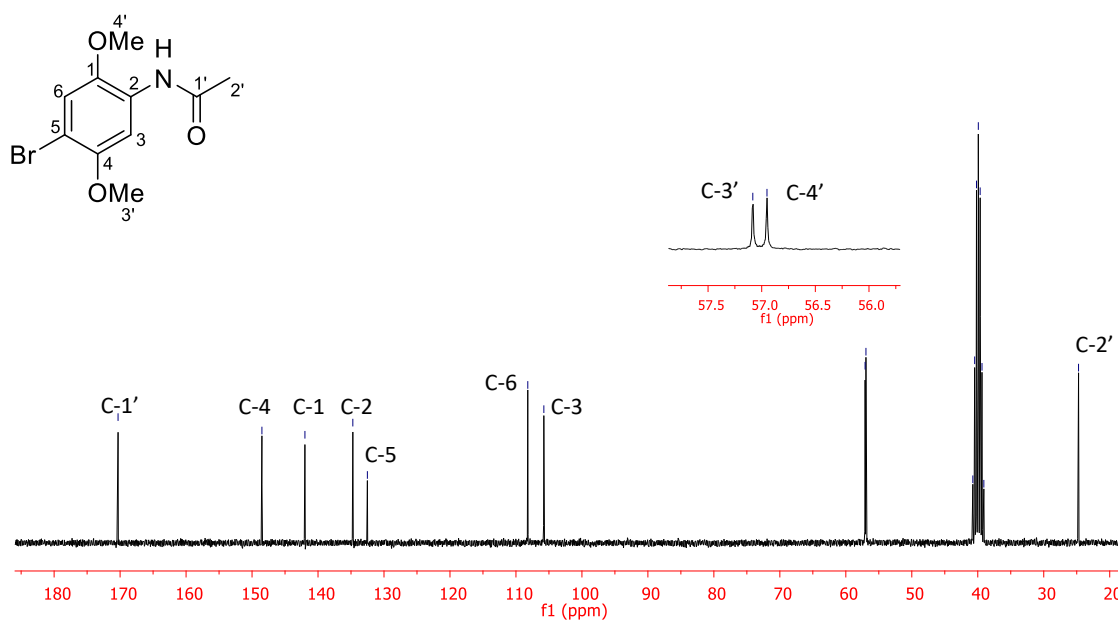
**Figure A1.5.** <sup>1</sup>H NMR spectrum (400 MHz, CD<sub>3</sub>OD) of compound 1.11.



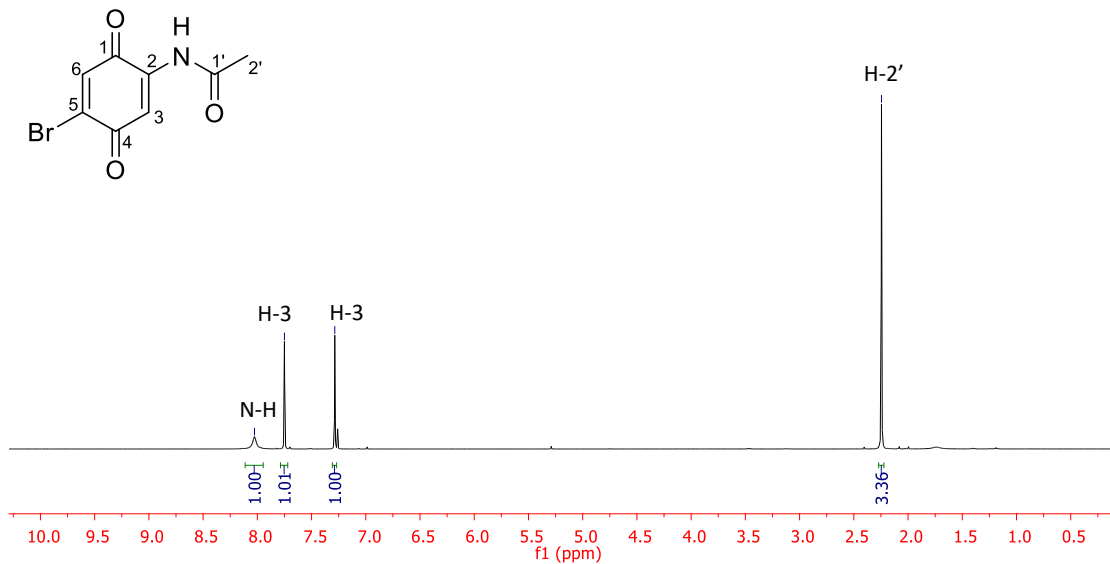
**Figure A1.6.** <sup>13</sup>C NMR spectrum (100 MHz, CD<sub>3</sub>OD) of compound 1.11.



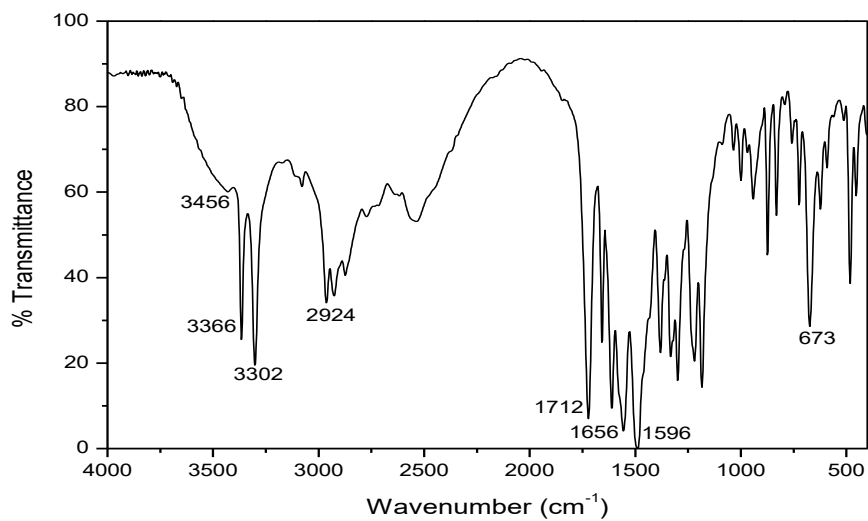
**Figure A1.7.**  $^1\text{H}$  NMR spectrum (400 MHz,  $\text{CDCl}_3$ ) of compound 1.15.



**Figure A1.8.**  $^{13}\text{C}$  NMR spectrum (100 MHz,  $\text{CDCl}_3$ ) of compound 1.15.



**Figure A1.9.** <sup>1</sup>H NMR spectrum (400 MHz, CDCl<sub>3</sub>) of compound 1.16.



**Figure A1.10.** Infrared spectrum in KBr of compound 1.6.

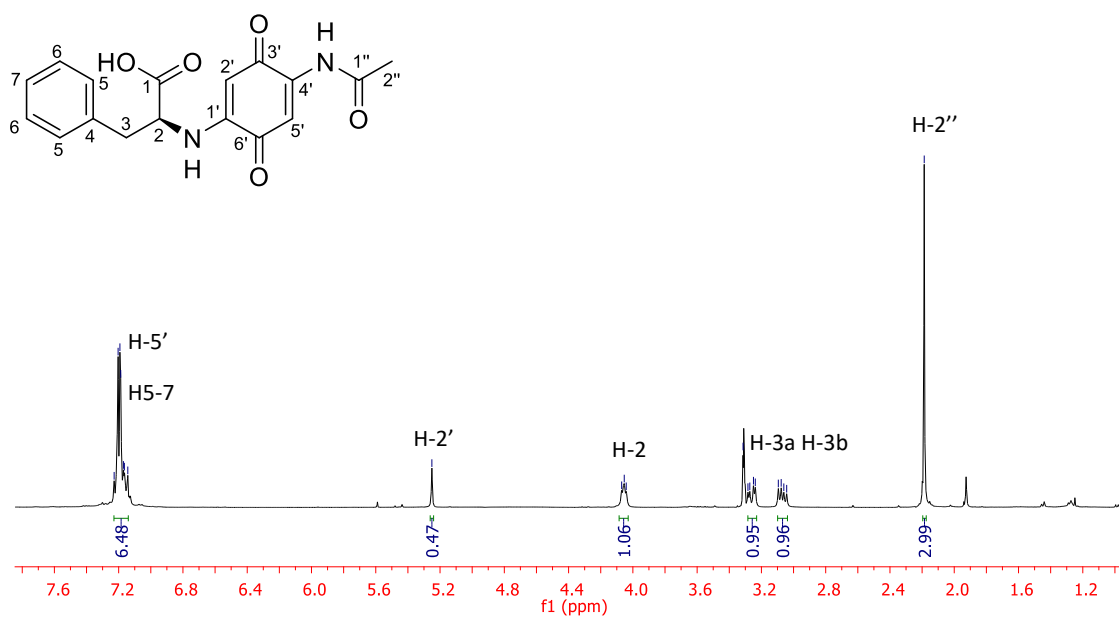


Figure A1.11.  $^1\text{H}$  NMR spectrum (400 MHz,  $\text{CD}_3\text{OD}$ ) of compound 1.6.

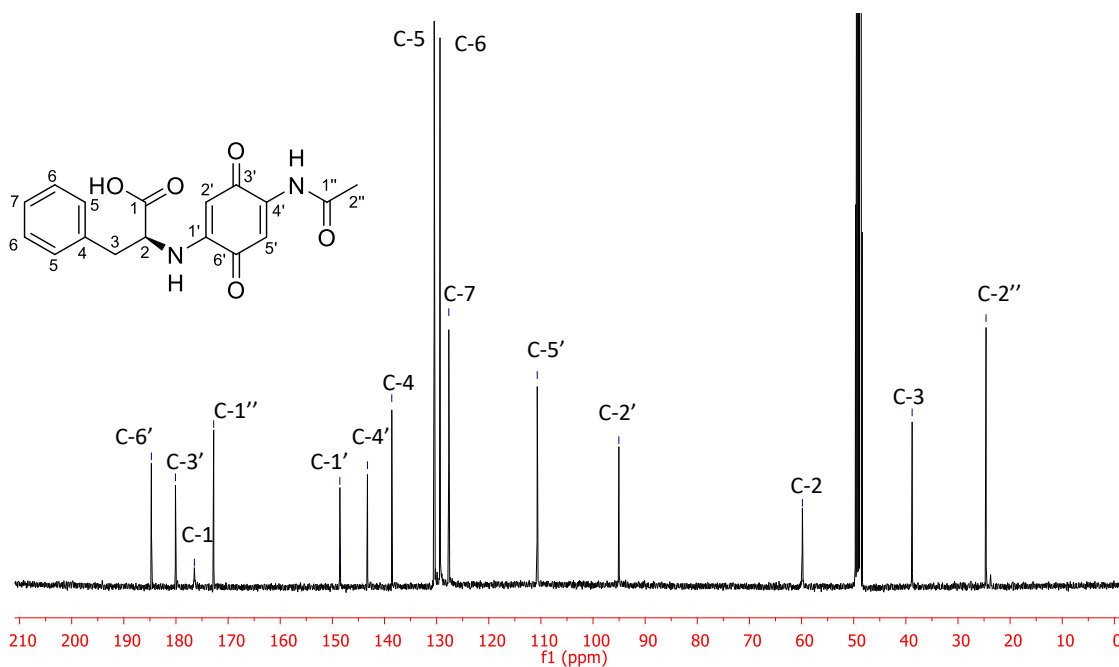
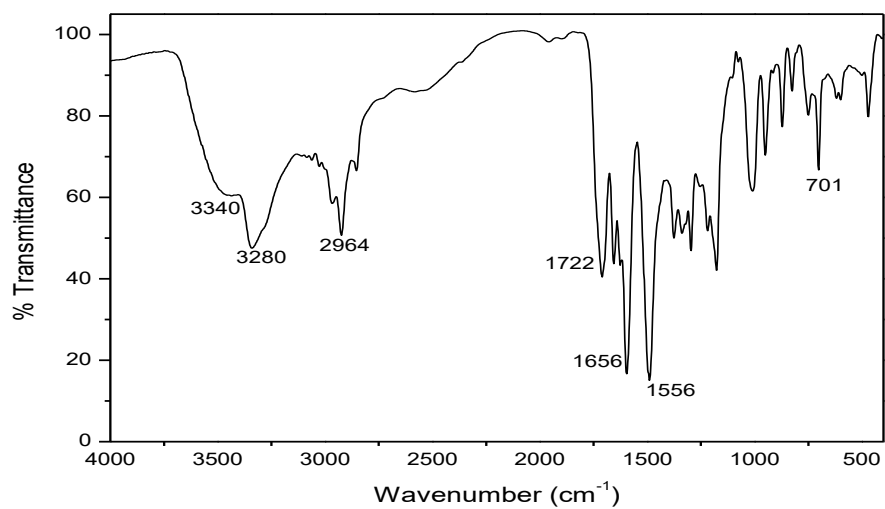
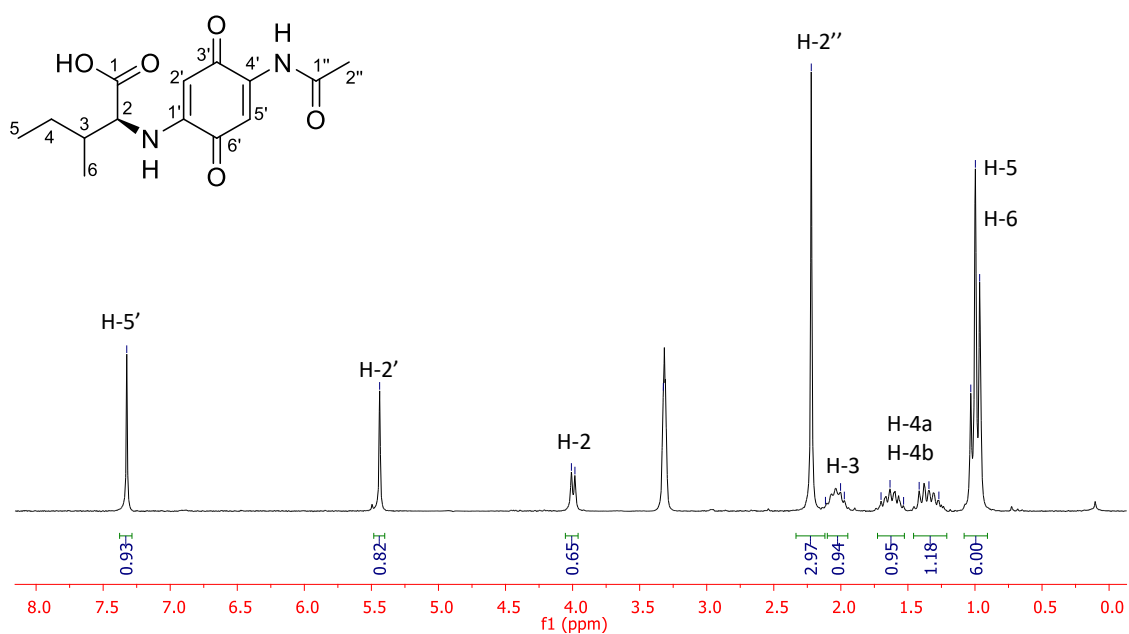


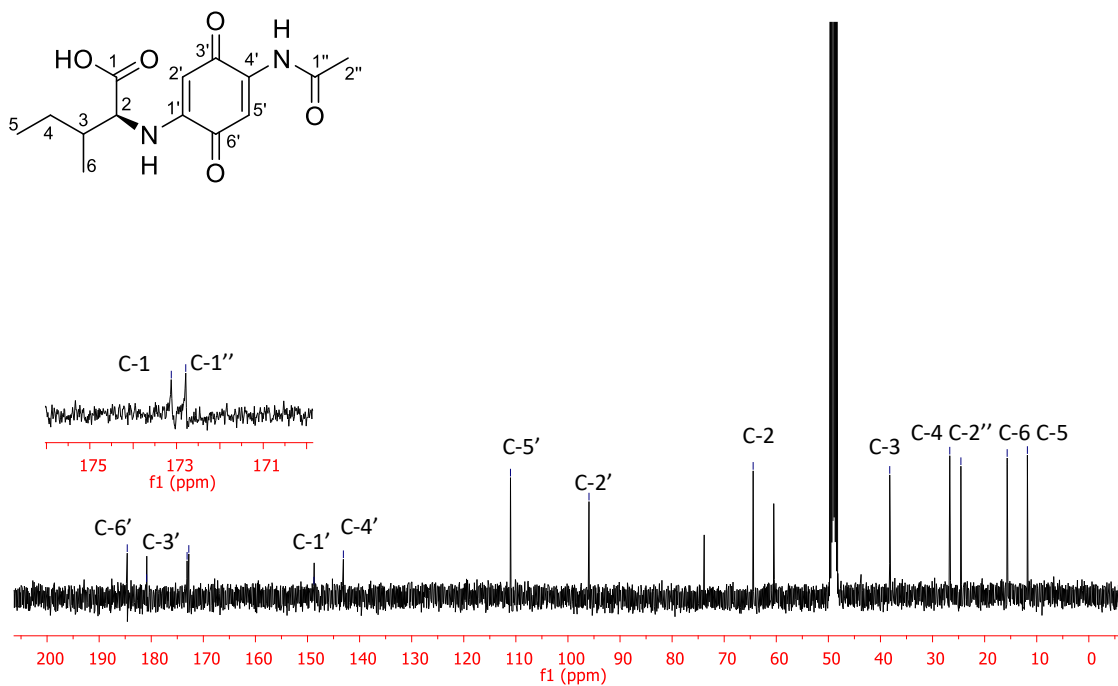
Figure A1.12.  $^{13}\text{C}$  NMR spectrum (100 MHz,  $\text{CD}_3\text{OD}$ ) of compound 1.6.



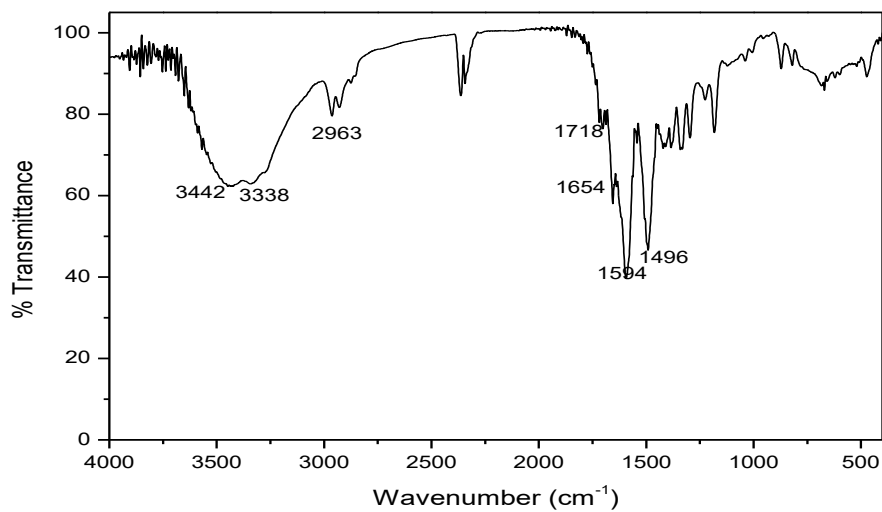
**Figure A1.13.** Infrared spectrum in KBr of compound **1.8**.



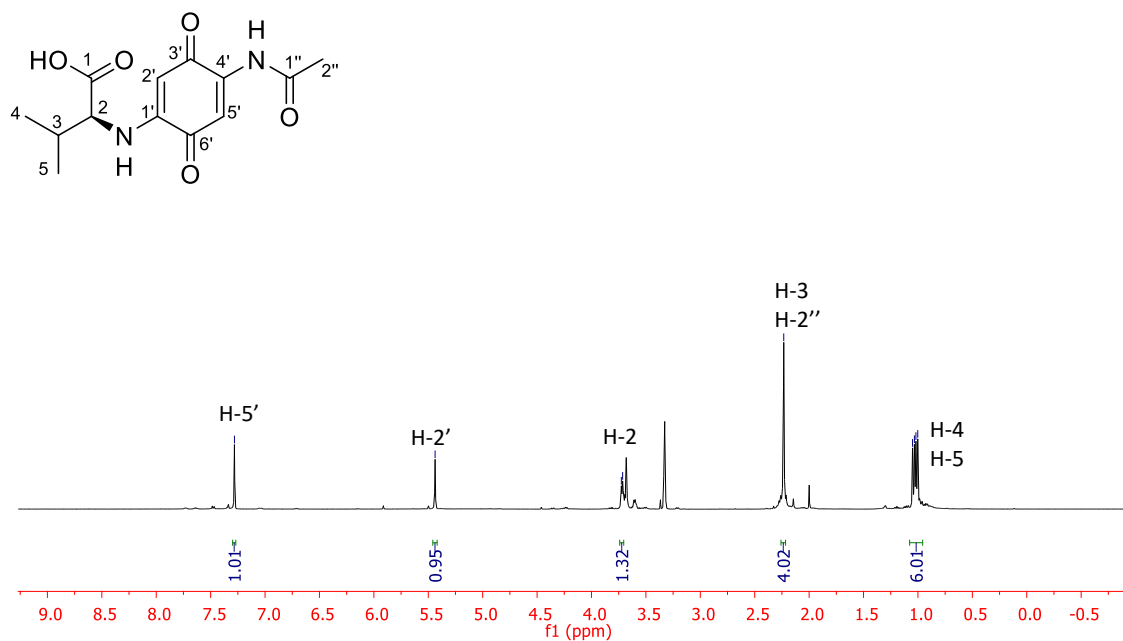
**Figure A1.14.** <sup>1</sup>H NMR spectrum (400 MHz, CD<sub>3</sub>OD) of compound **1.8**.



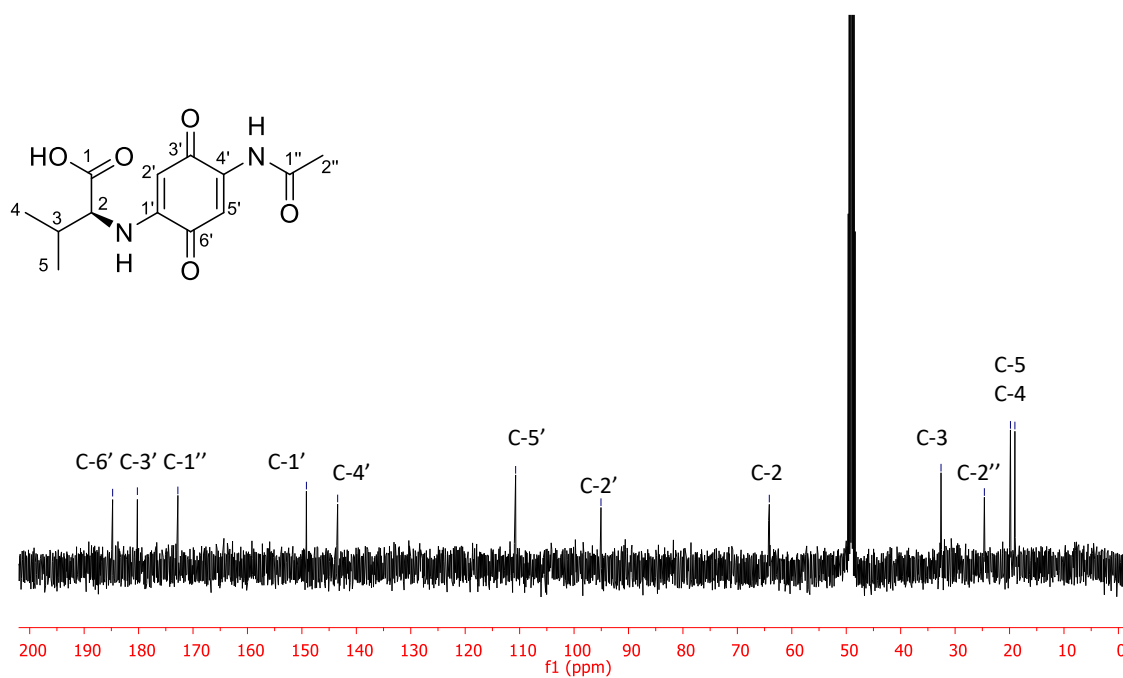
**Figure A1.15.**  $^{13}\text{C}$  NMR spectrum (100 MHz,  $\text{CD}_3\text{OD}$ ) of compound **1.8**.



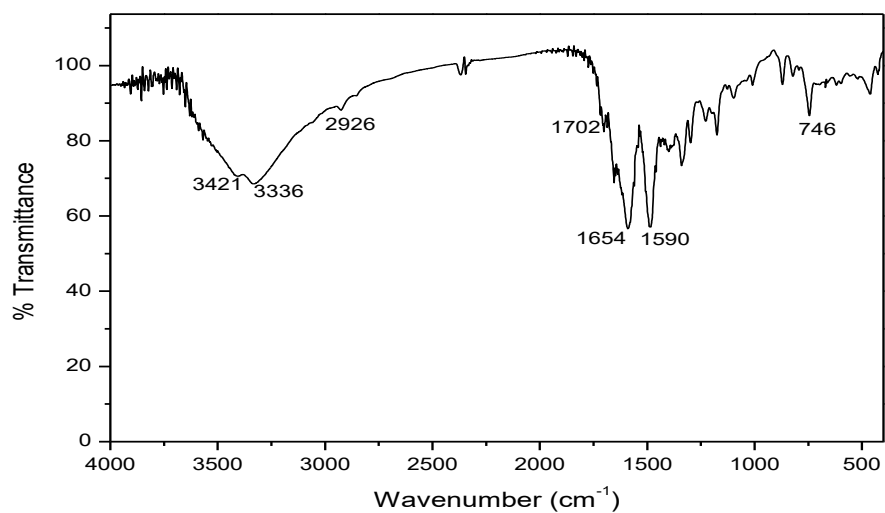
**Figure A1.16.** Infrared spectrum in KBr of compound **1.9**.



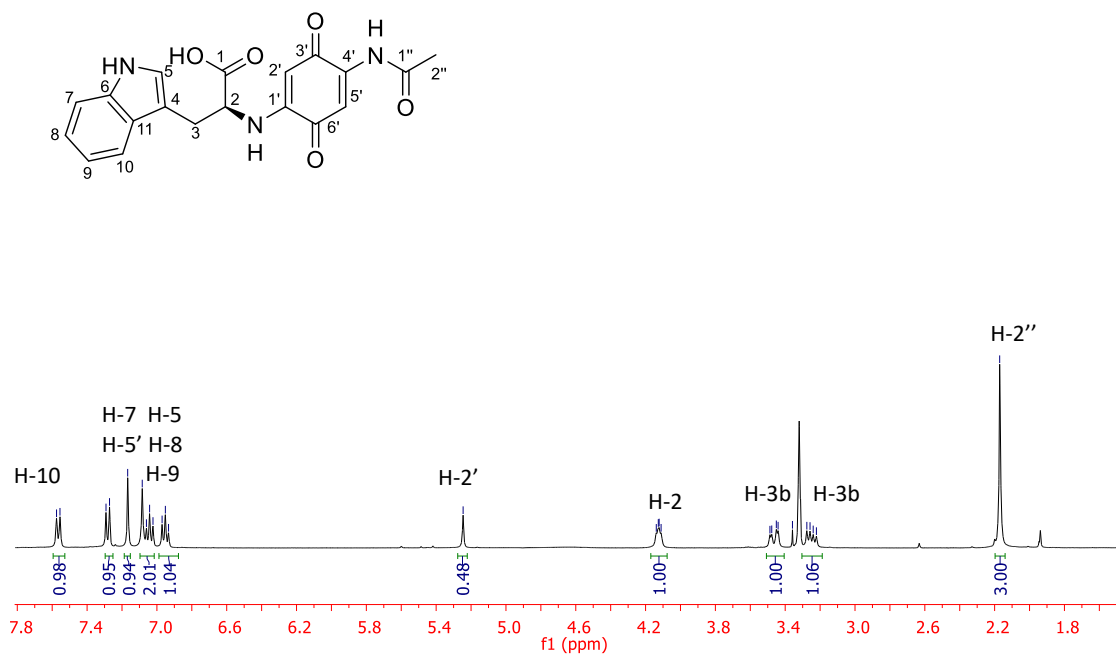
**Figure A1.17.**  $^1\text{H}$  NMR spectrum (400 MHz,  $\text{CD}_3\text{OD}$ ) of compound **1.9**.



**Figure A1.18.**  $^{13}\text{C}$  NMR spectrum (100 MHz,  $\text{CD}_3\text{OD}$ ) of compound **1.9**.

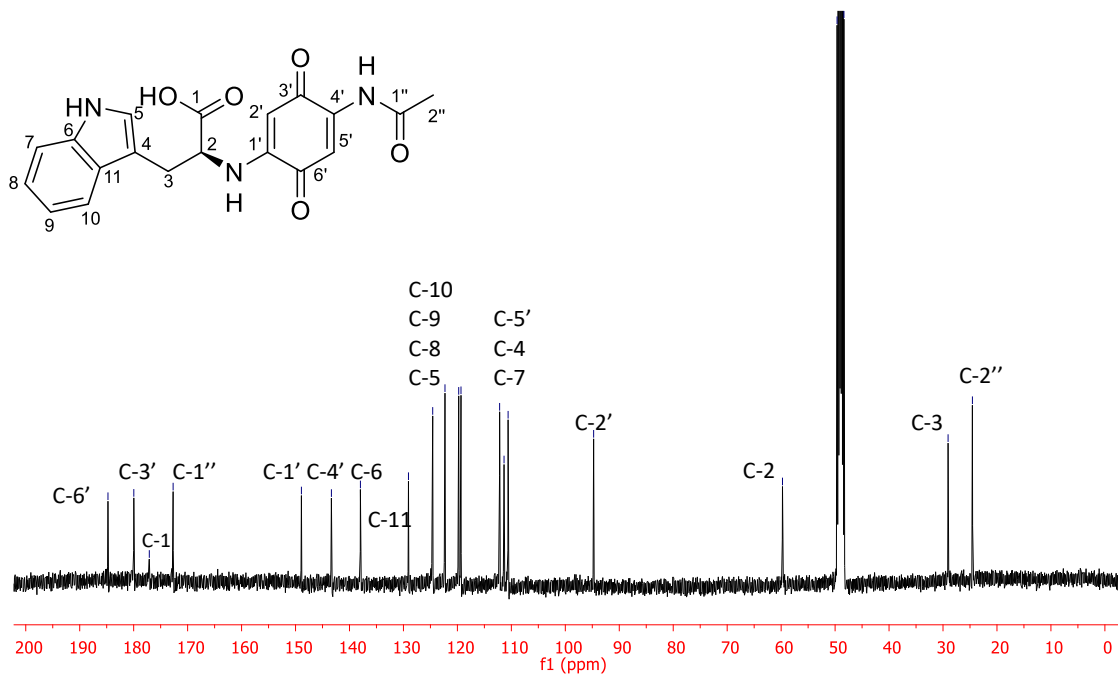


**Figure A1.19.** Infrared spectrum in KBr of compound **1.10**.

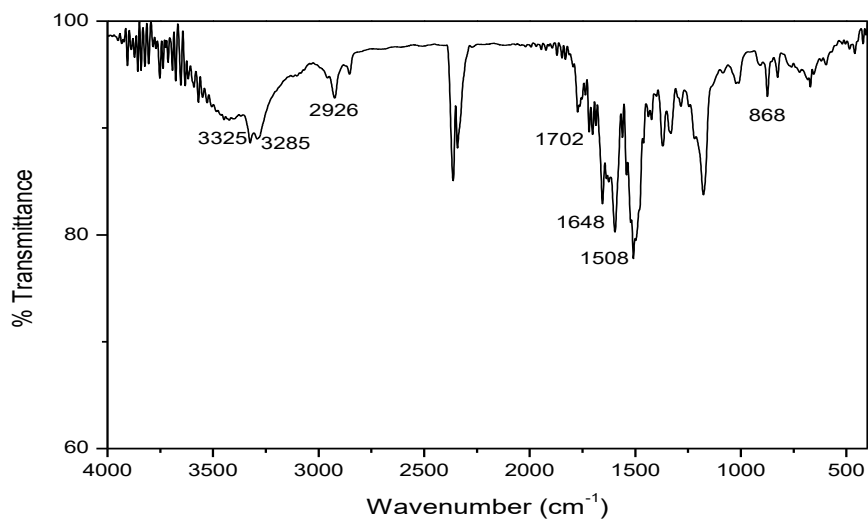


**Figure A1.20.**  $^1\text{H}$  NMR spectrum (400 MHz,  $\text{CD}_3\text{OD}$ ) of compound **1.10**.

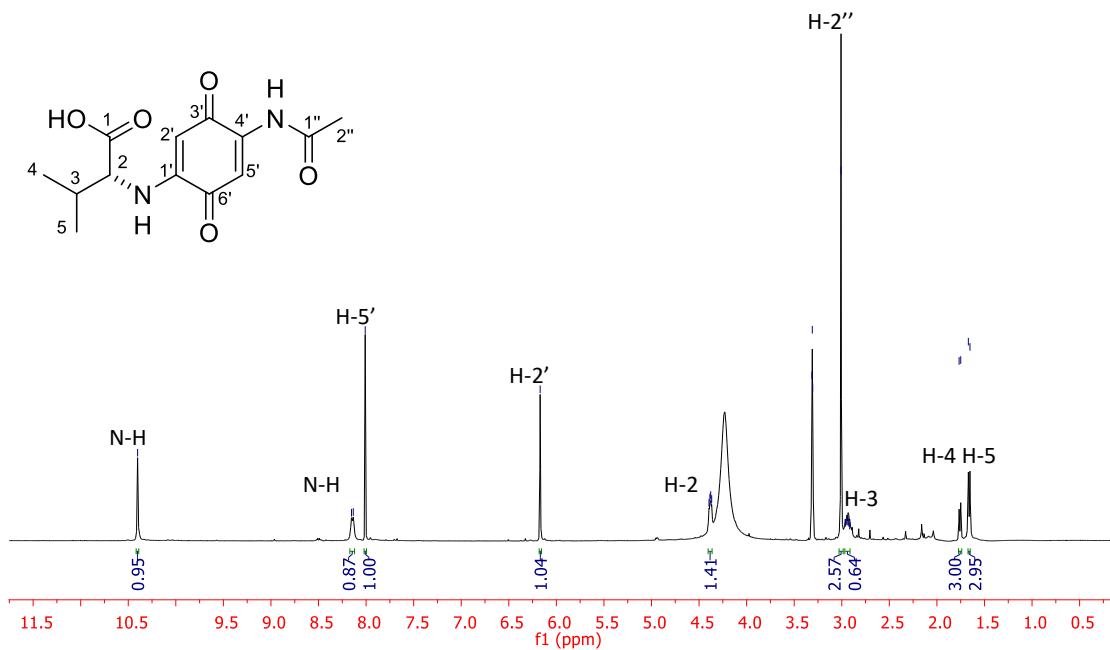




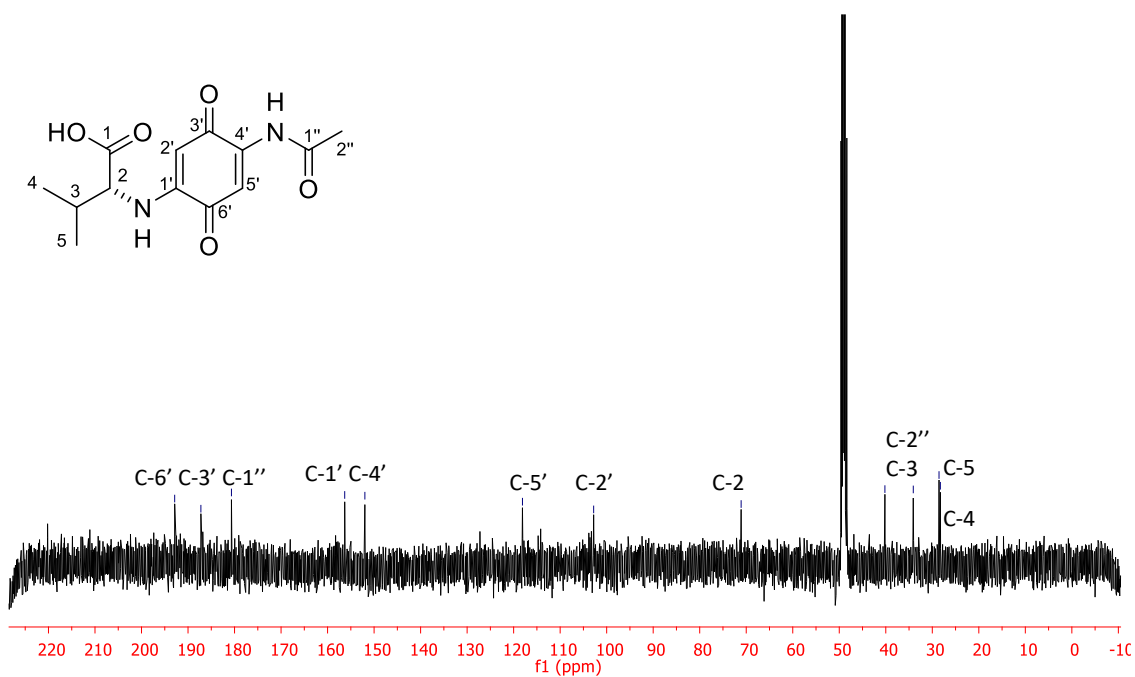
**Figure A1.21.**  $^{13}\text{C}$  NMR spectrum (100 MHz,  $\text{CD}_3\text{OD}$ ) of compound 1.10.



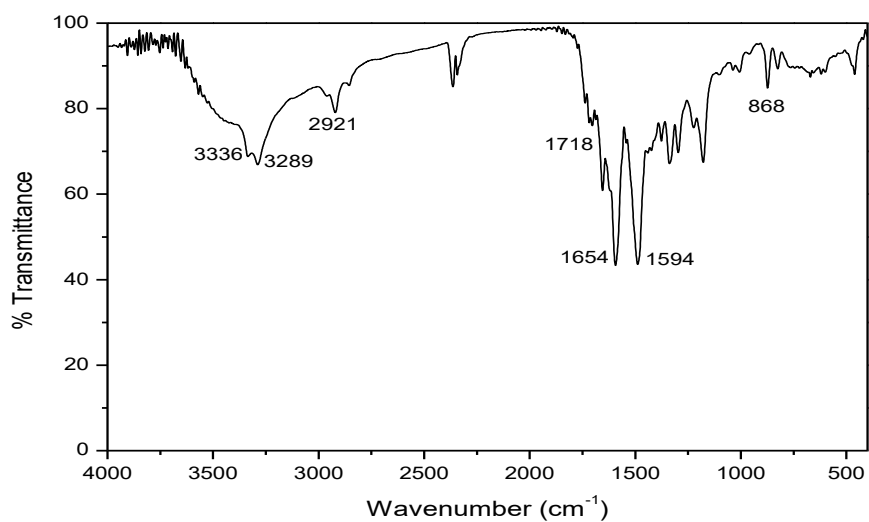
**Figure A1.22.** Infrared spectrum in KBr of compound 1.17.



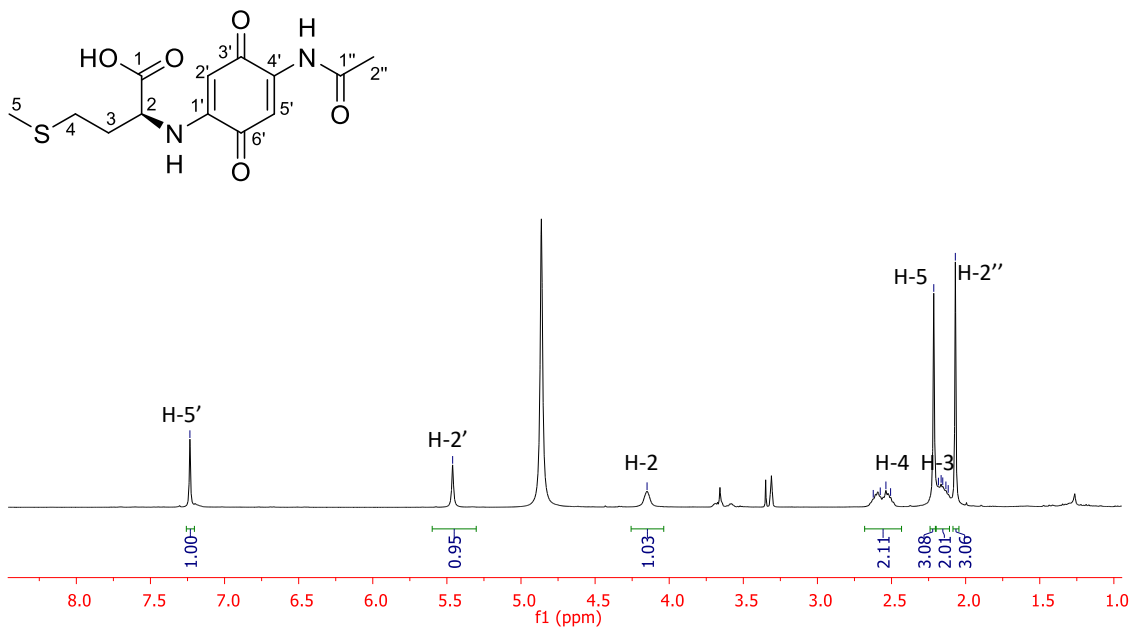
**Figure A1.23.**  $^1\text{H}$  NMR spectrum (400 MHz,  $\text{CD}_3\text{OD}$ ) of compound 1.17.



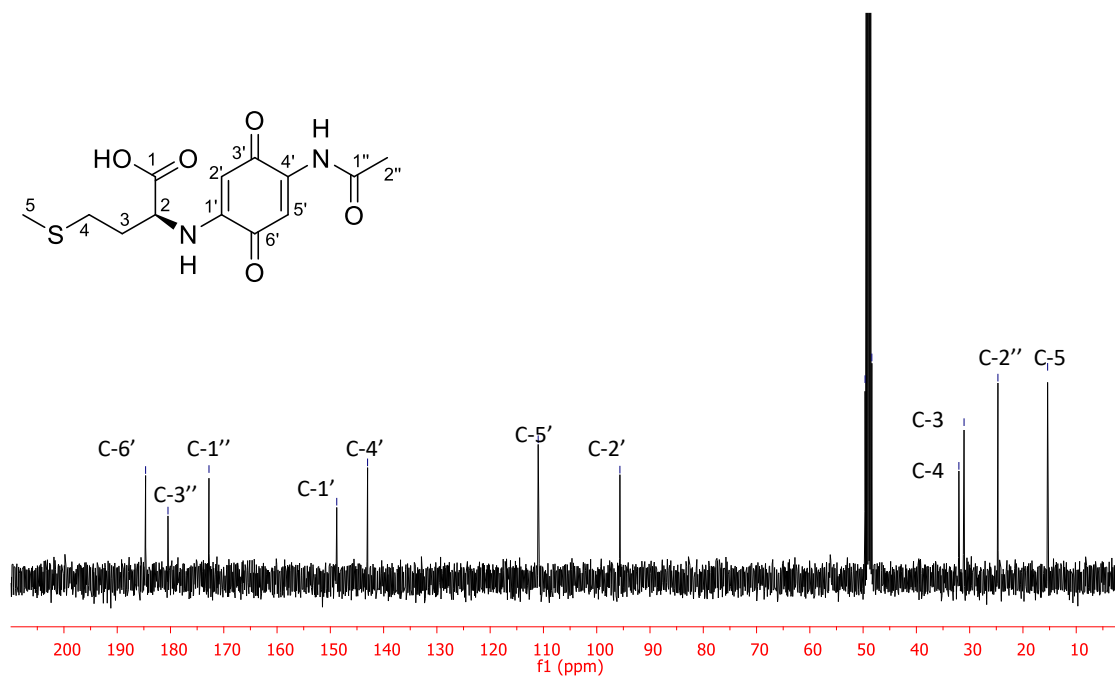
**Figure A1.24.**  $^{13}\text{C}$  NMR spectrum (100 MHz,  $\text{CD}_3\text{OD}$ ) of compound 1.17.



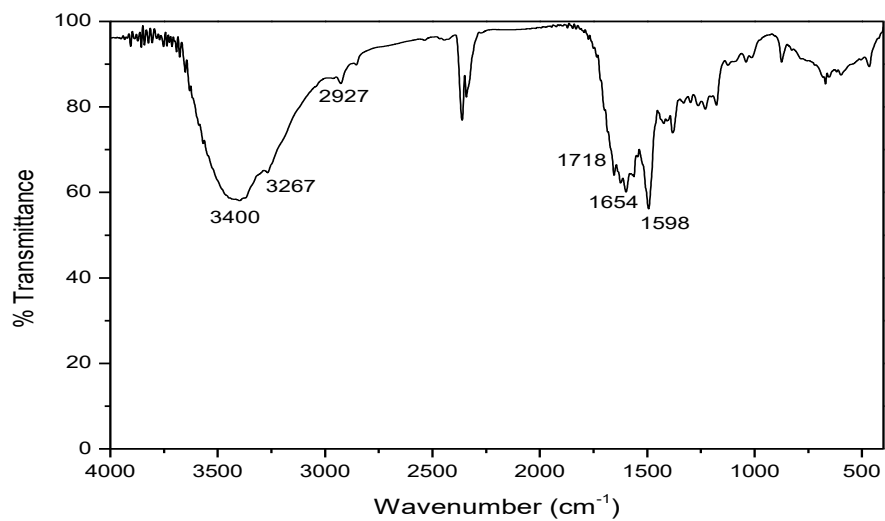
**Figure A1.25.** Infrared spectrum in KBr of compound **1.18**.



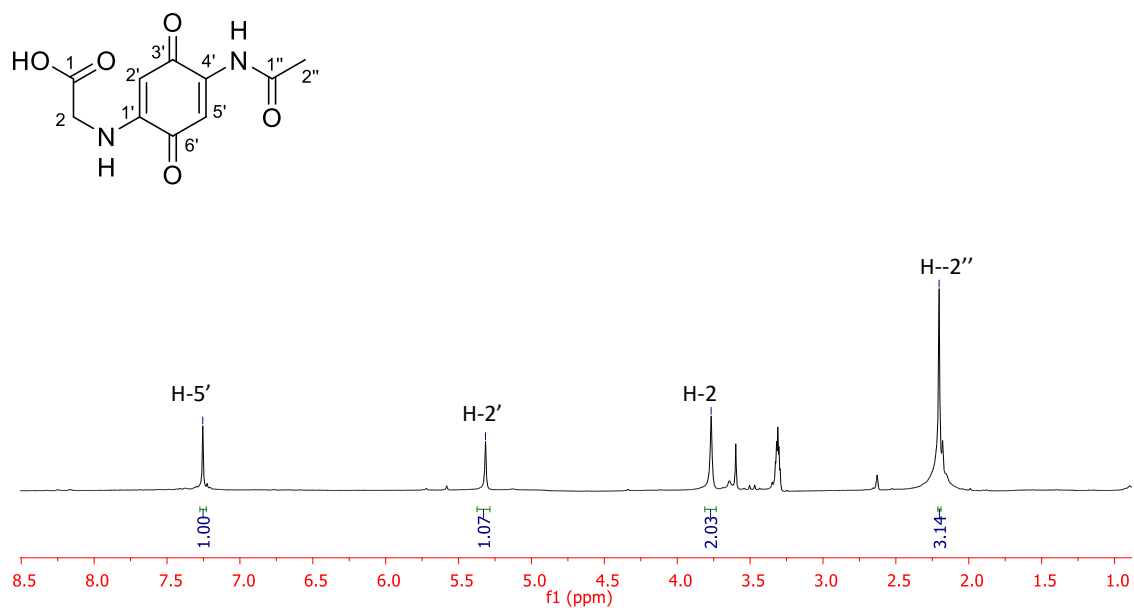
**Figure A1.26.** <sup>1</sup>H NMR spectrum (400 MHz, CD<sub>3</sub>OD) of compound **1.18**.



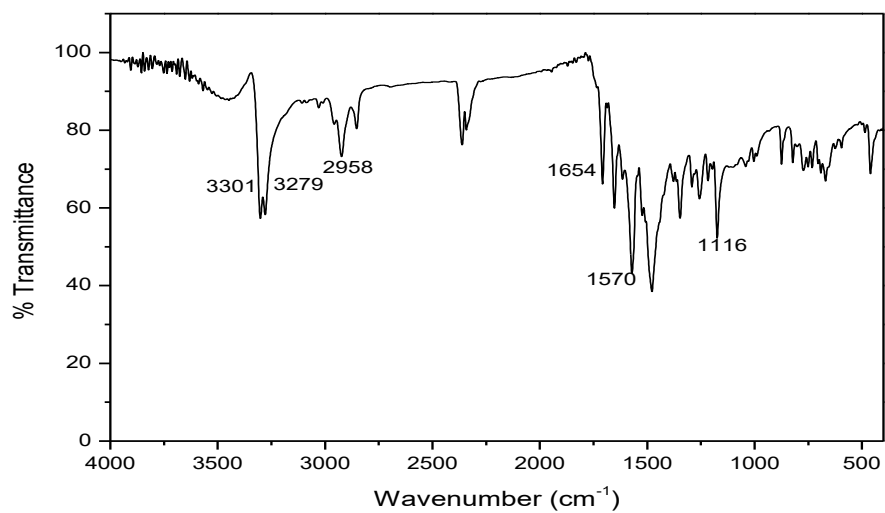
**Figure A1.27.**  $^{13}\text{C}$  NMR spectrum (100 MHz,  $\text{CD}_3\text{OD}$ ) of compound **1.18**.



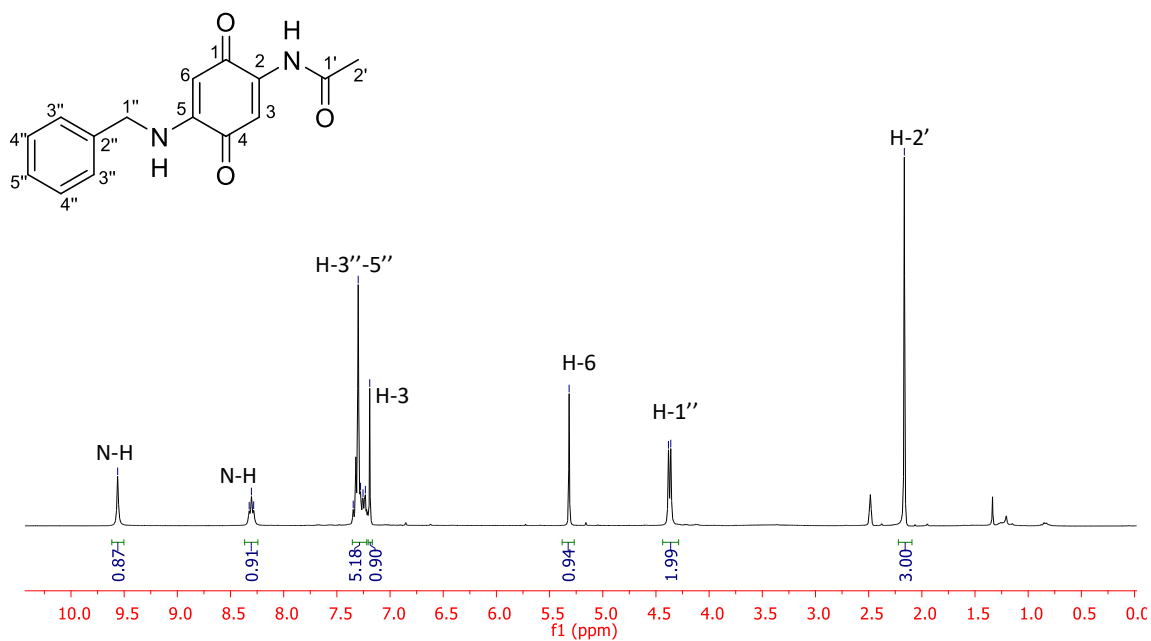
**Figure A1.28.** Infrared spectrum in KBr of compound **1.19**.



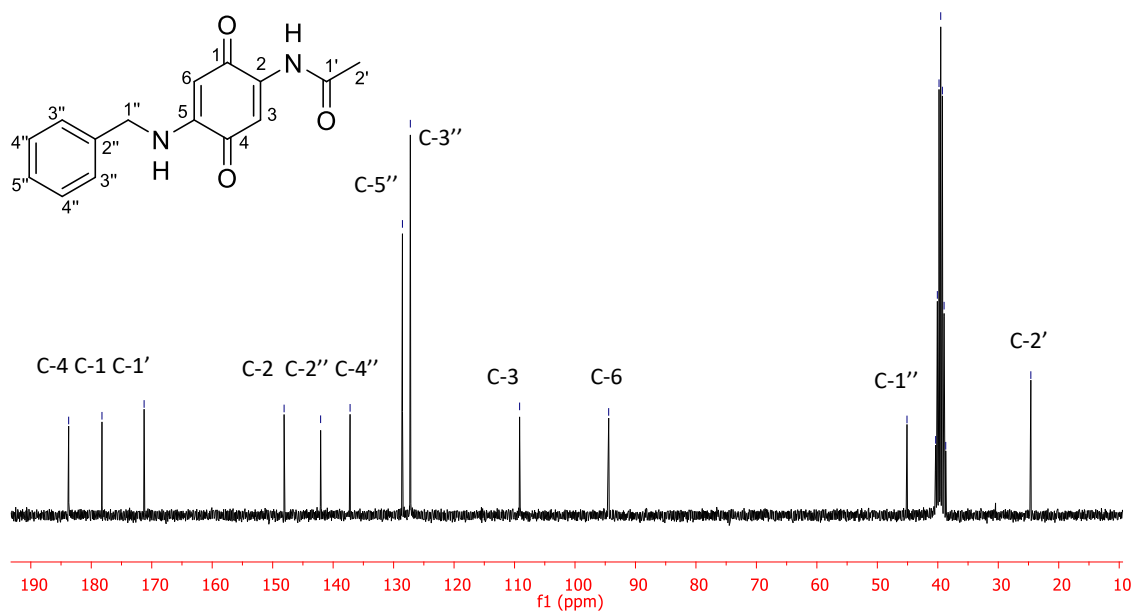
**Figure A1.29.**  $^1\text{H}$  NMR spectrum (400 MHz,  $\text{CD}_3\text{OD}$ ) of compound 1.19.



**Figure A1.30.** Infrared spectrum in KBr of compound 1.20.

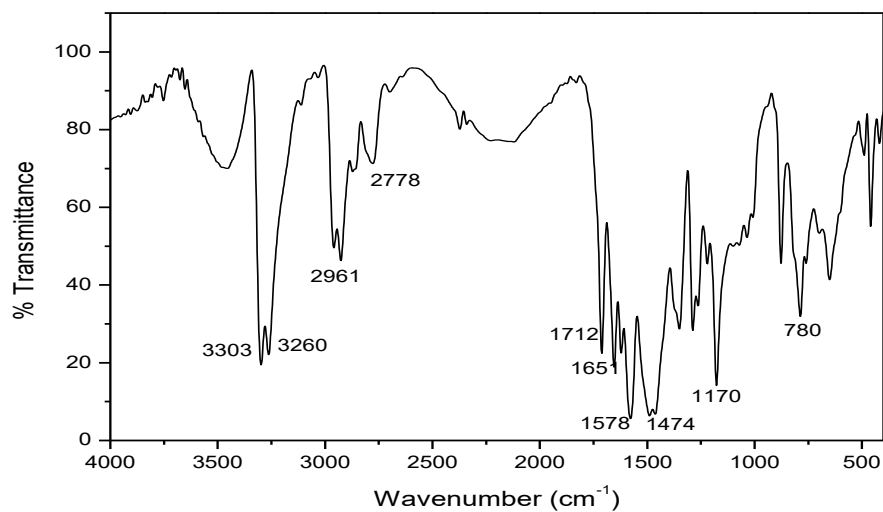


**Figure A1.31.**  $^1\text{H}$  NMR spectrum (400 MHz,  $\text{DMSO-d}_6$ ) of compound 1.20.

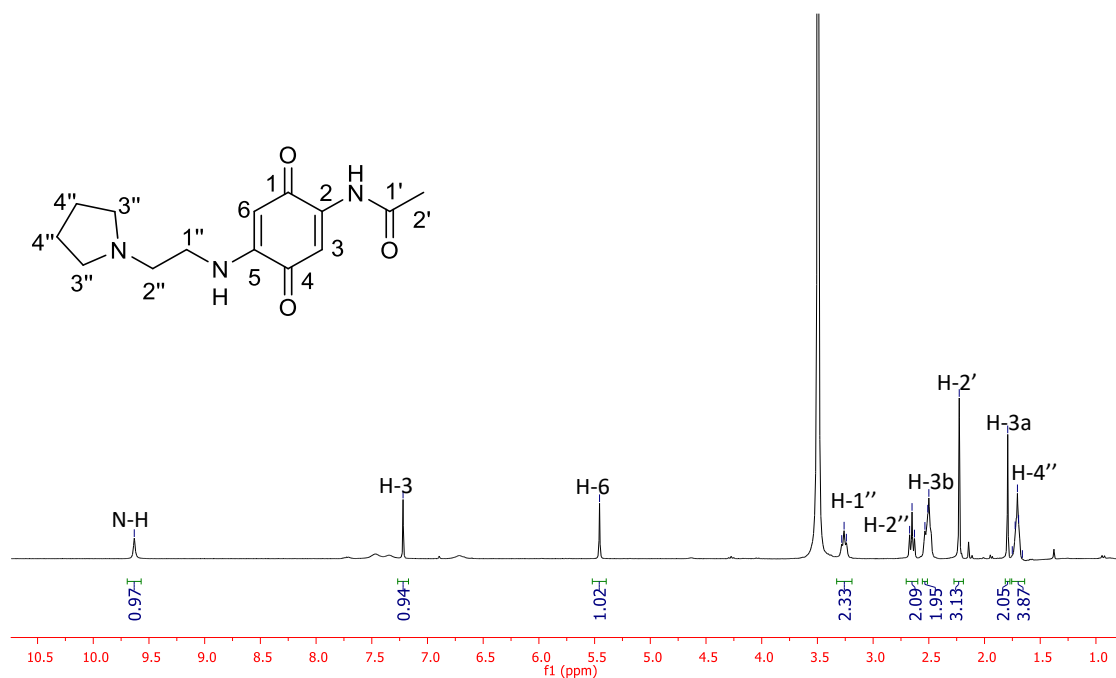


**Figure A1.32.**  $^{13}\text{C}$  NMR spectrum (100 MHz,  $\text{DMSO-d}_6$ ) of compound 1.20.

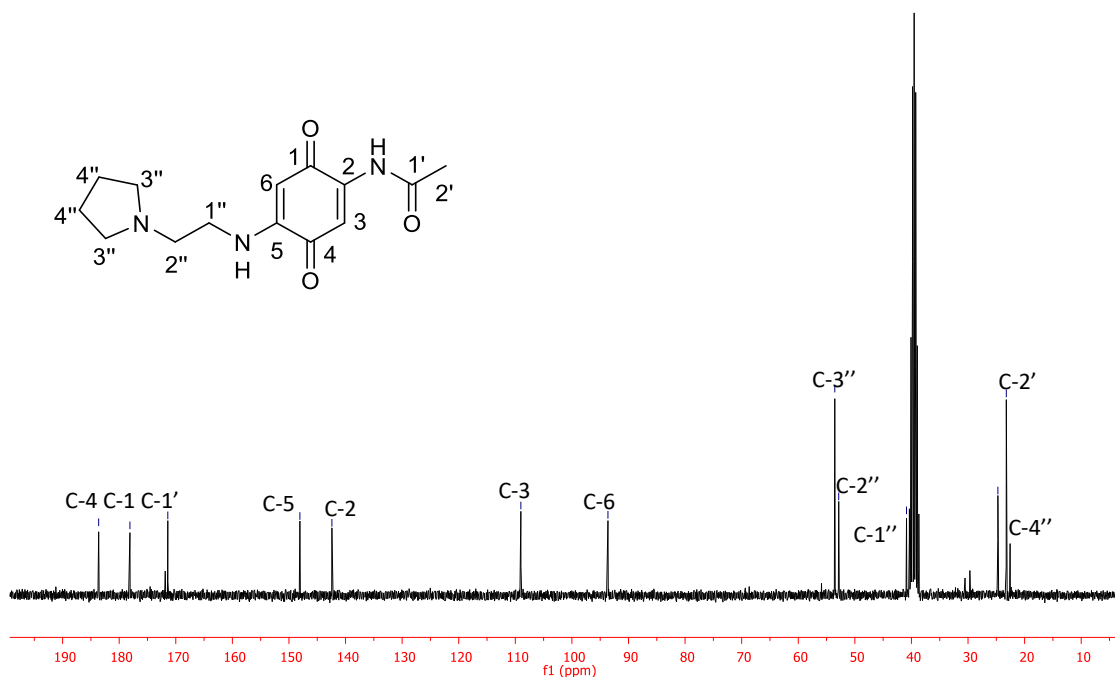
## 2. Appendix 2: Infrared, $^1\text{H}$ and $^{13}\text{C}$ NMR Spectra of compounds related to Chapter 2



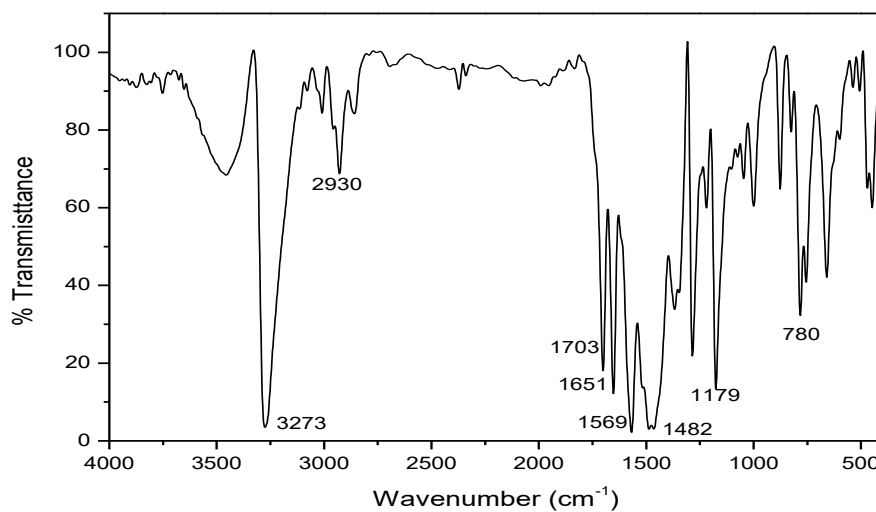
**Figure A2.1.** Infrared spectrum in KBr of compound **2.1**.



**Figure A2.2.**  $^1\text{H}$  NMR spectrum ( $\text{DMSO-}d_6$ , 300 MHz) of compound **2.1**.



**Figure A2.3.**  $^{13}\text{C}$  NMR spectrum ( $\text{DMSO-}d_6$ , 75 MHz) of compound 2.1.



**Figure A2.4.** Infrared spectrum in KBr of compound 2.2.



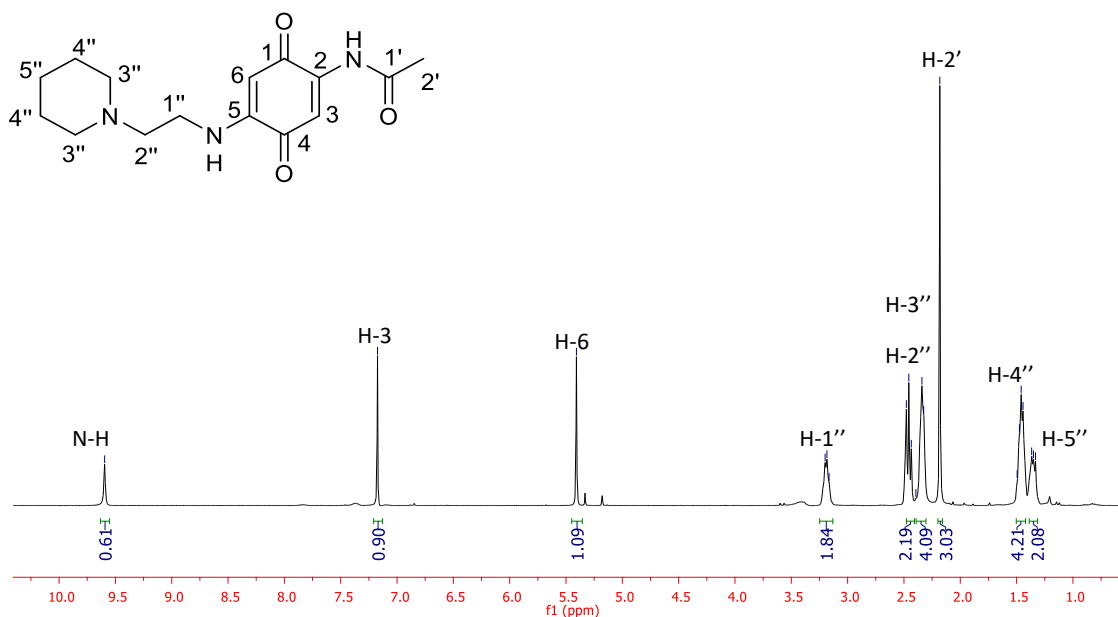


Figure A2.5.  $^1\text{H}$  NMR spectrum (DMSO- $d_6$ , 300 MHz) of compound 2.2.

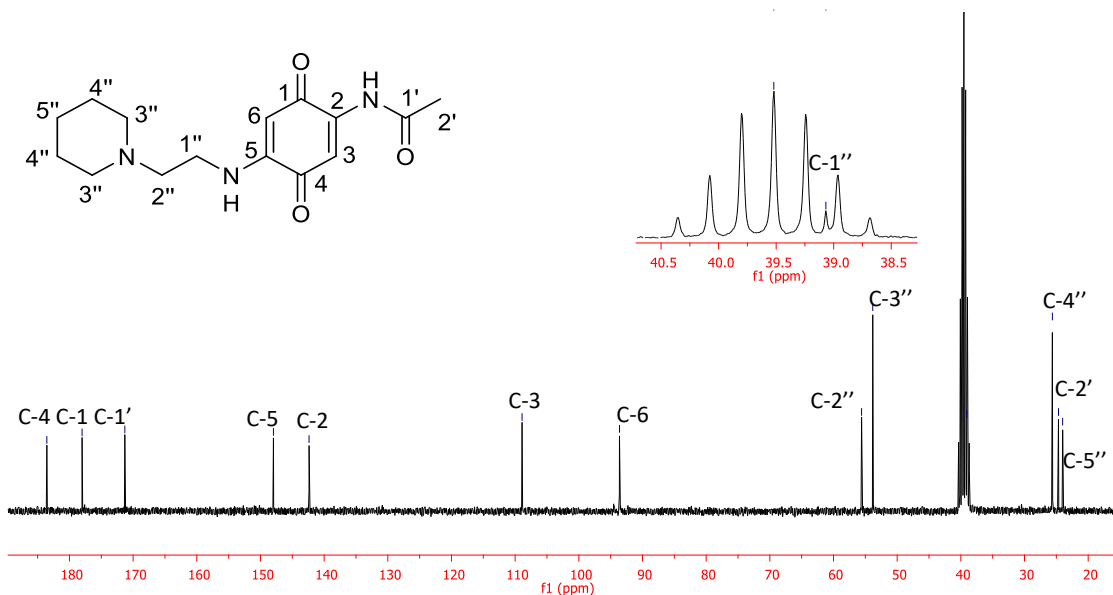
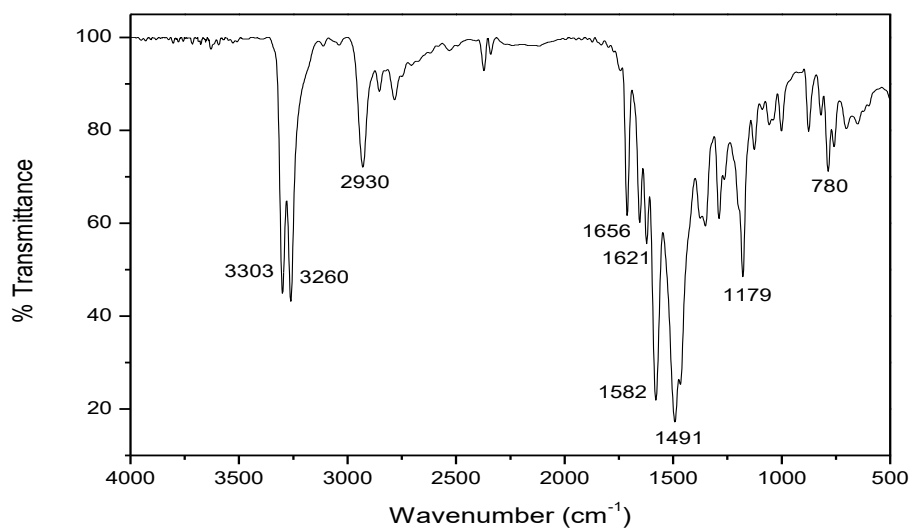
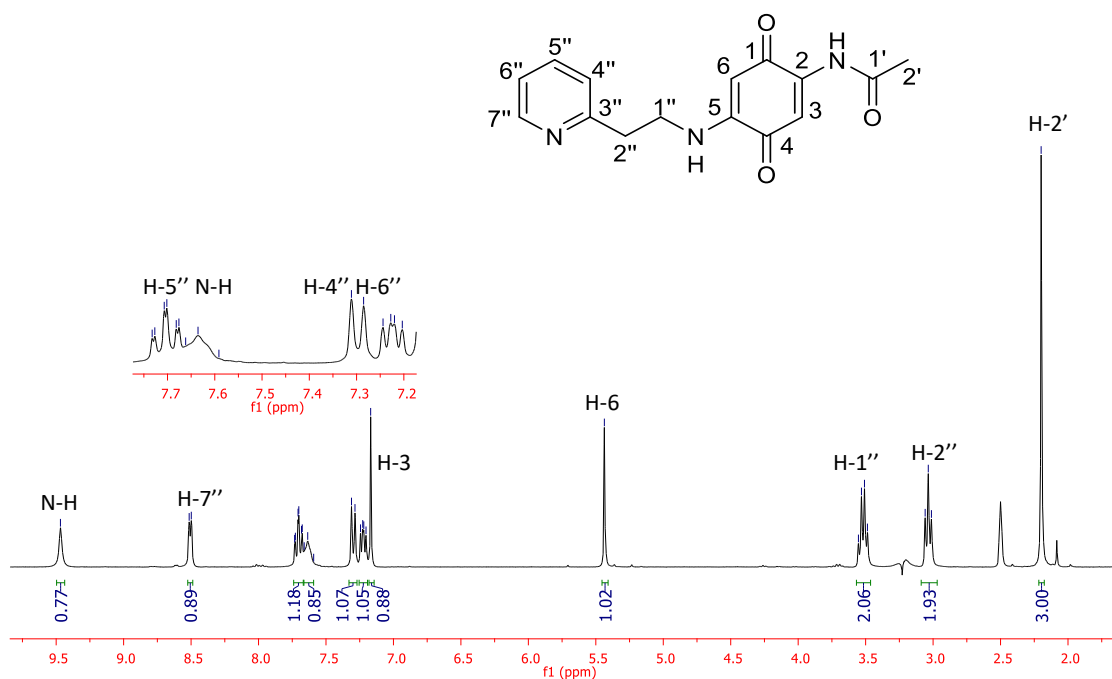


Figure A2.6.  $^{13}\text{C}$  NMR spectrum (DMSO- $d_6$ , 75 MHz) of compound 2.2.



**Figure A2.7.** Infrared spectrum in KBr of compound 2.3.



**Figure A2.8.**  $^1\text{H}$  NMR spectrum ( $\text{DMSO-}d_6$ , 300 MHz) of compound 2.3.

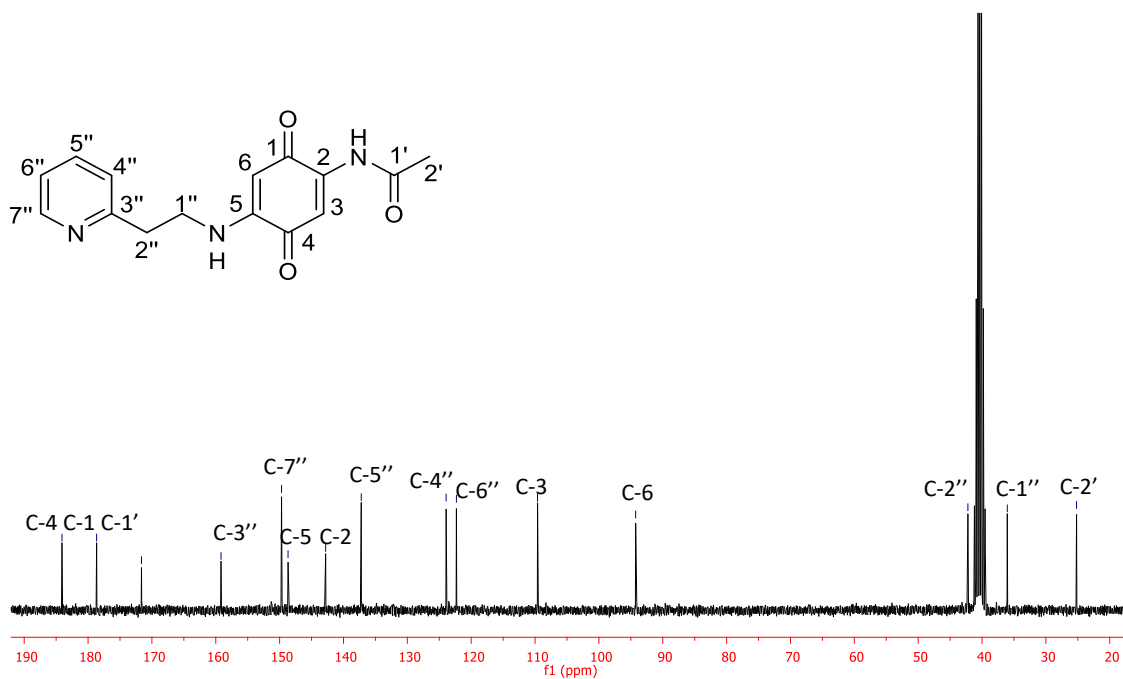


Figure A2.9.  $^{13}\text{C}$  NMR spectrum ( $\text{DMSO-}d_6$ , 75 MHz) of compound 2.3.

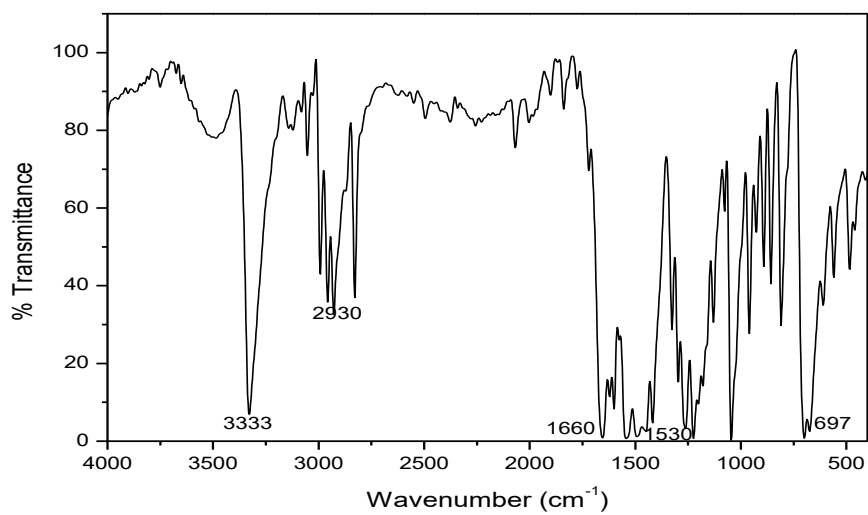
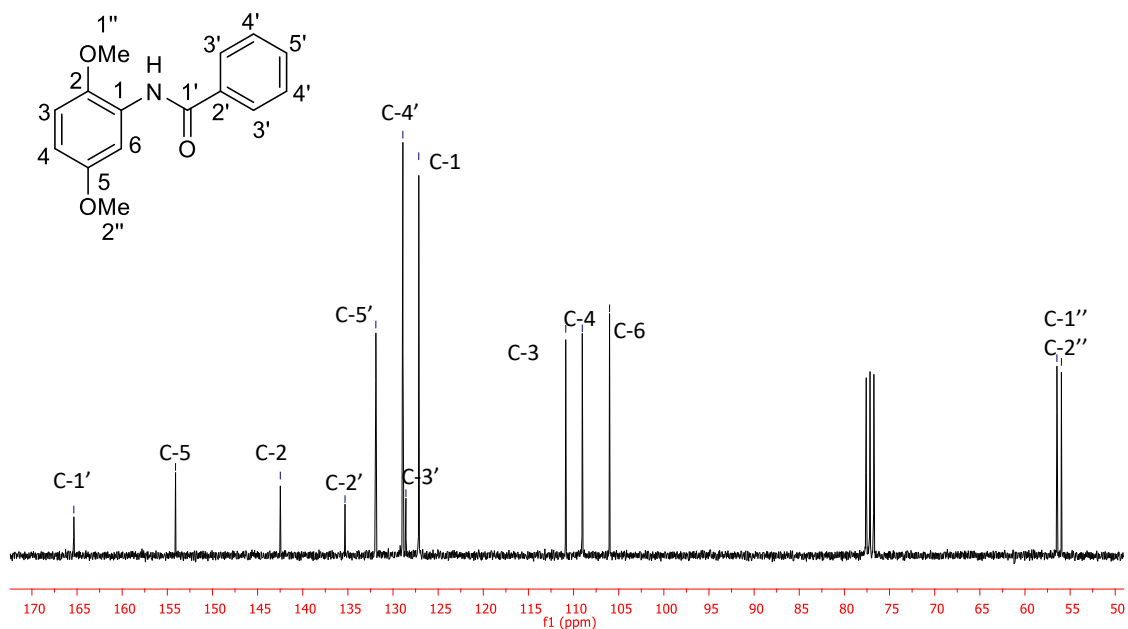
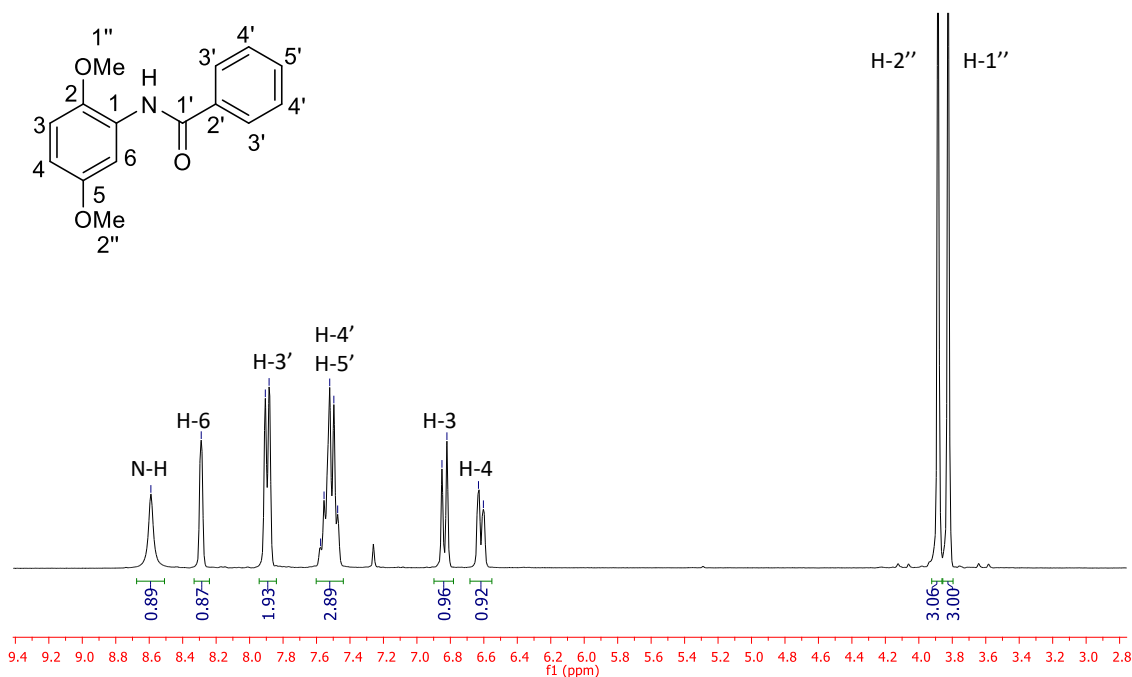
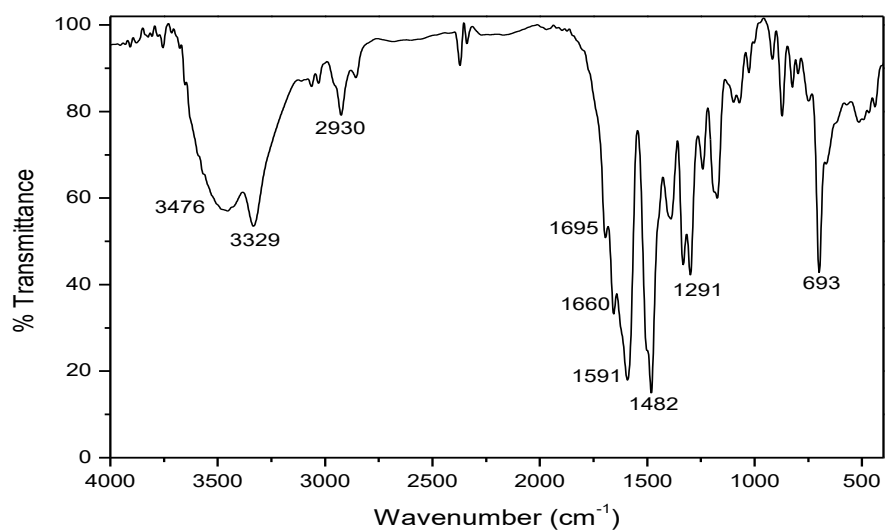
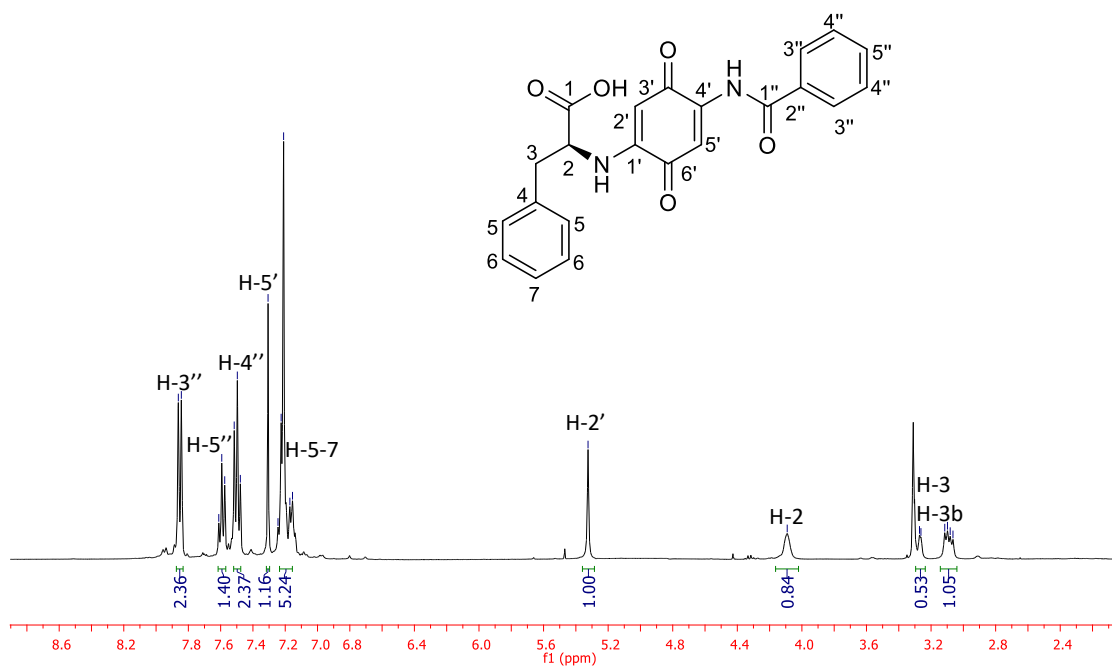


Figure A2.10. Infrared spectrum in KBr of compound 2.4.

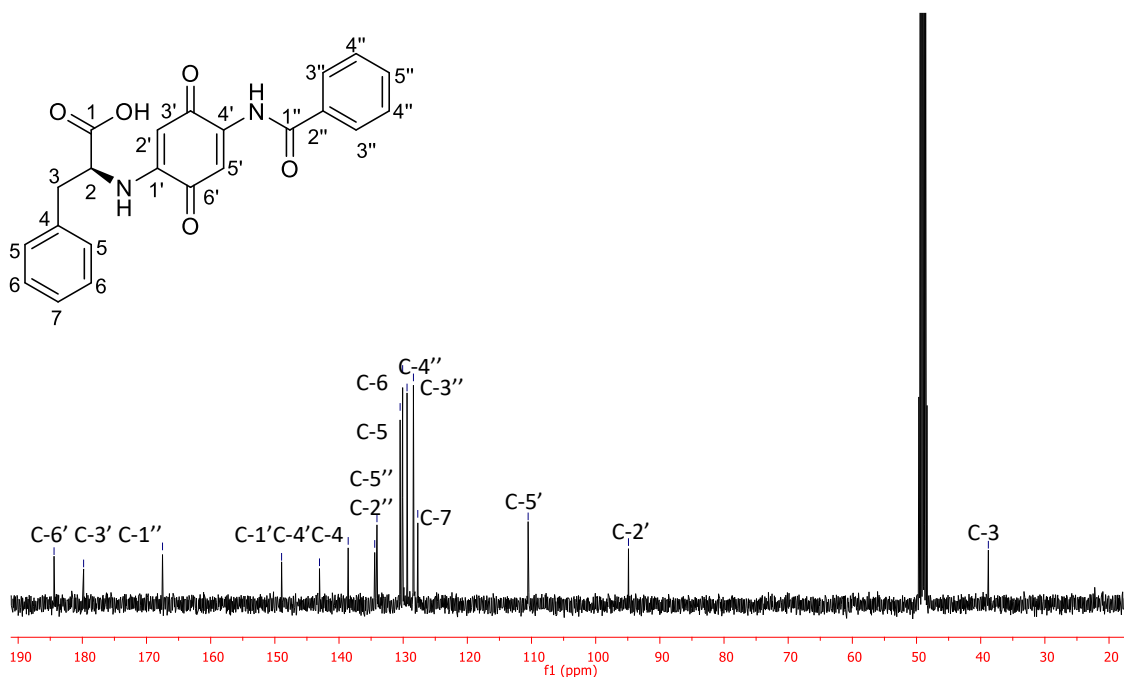




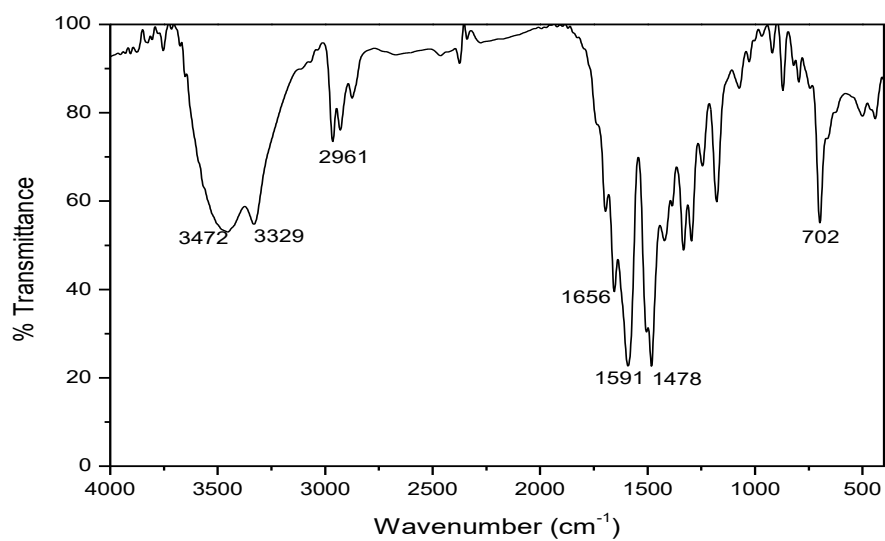
**Figure A2.13.** Infrared spectrum in KBr of compound **2.6**.



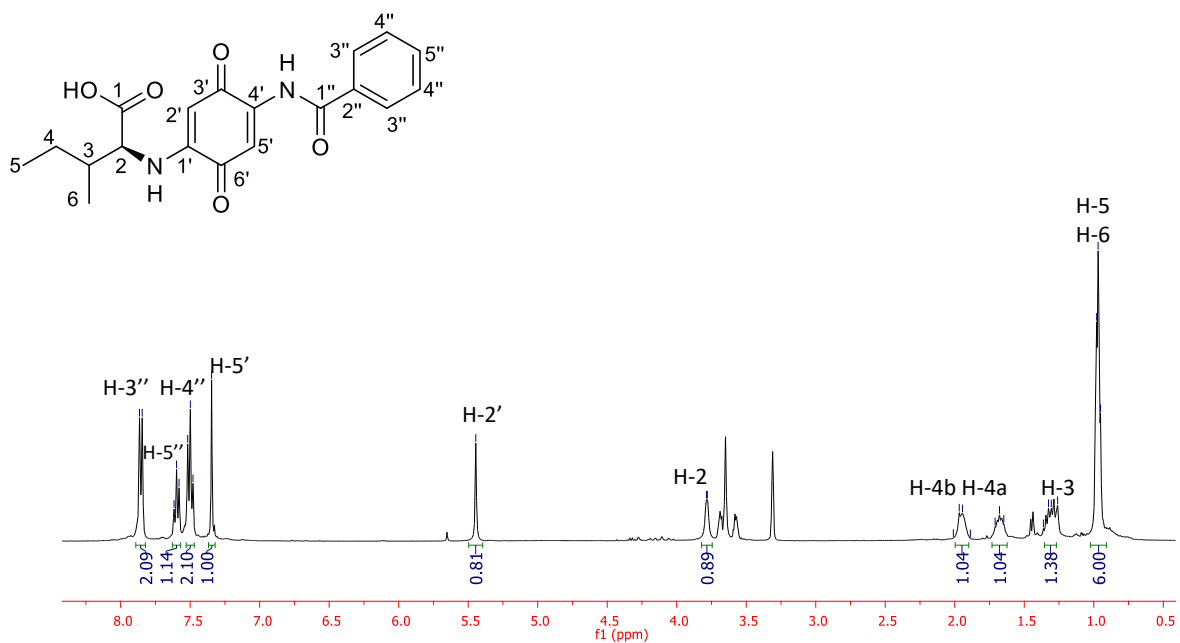
**Figure A2.14.**  $^1\text{H}$  NMR spectrum ( $\text{CD}_3\text{OD}$ , 400 MHz) of compound **2.6**.



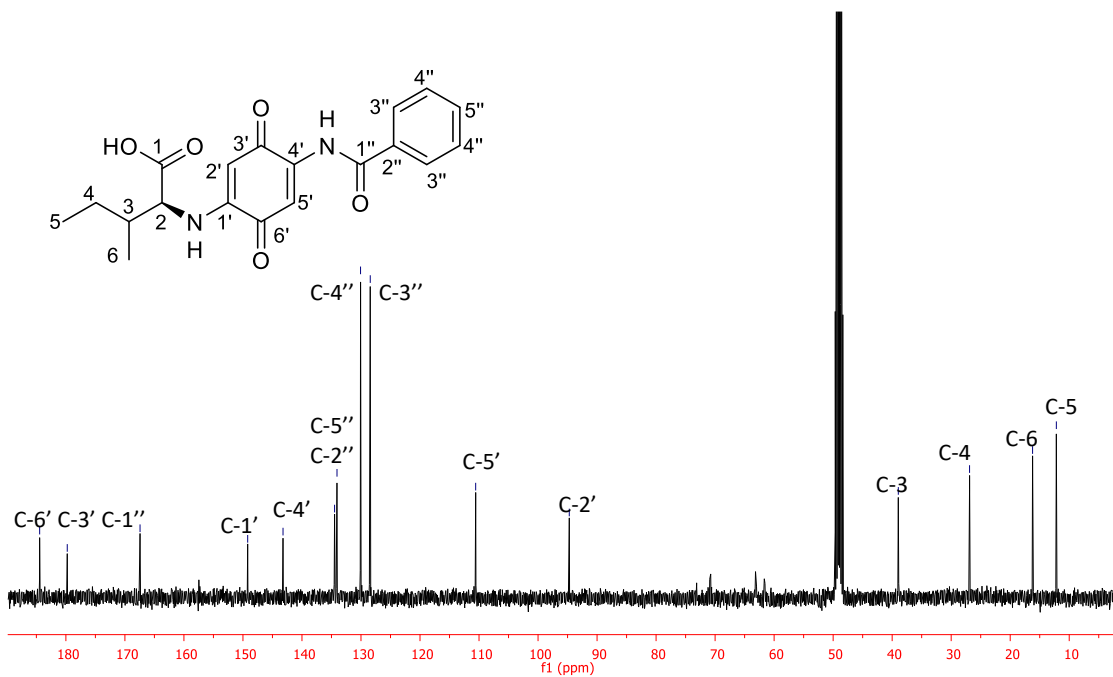
**Figure A2.15.**  $^{13}\text{C}$  NMR spectrum ( $\text{CD}_3\text{OD}$ , 100 MHz) of compound **2.6**.



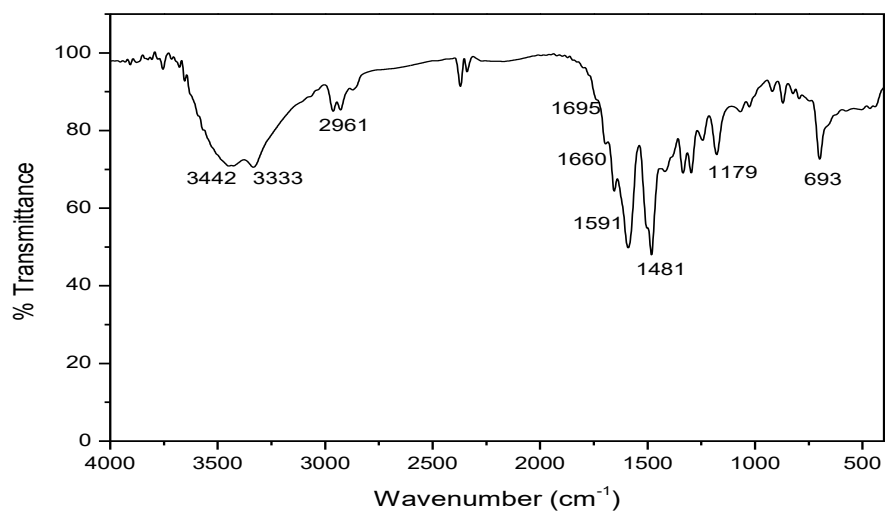
**Figure A2.16.** Infrared spectrum in KBr of compound **2.7**.



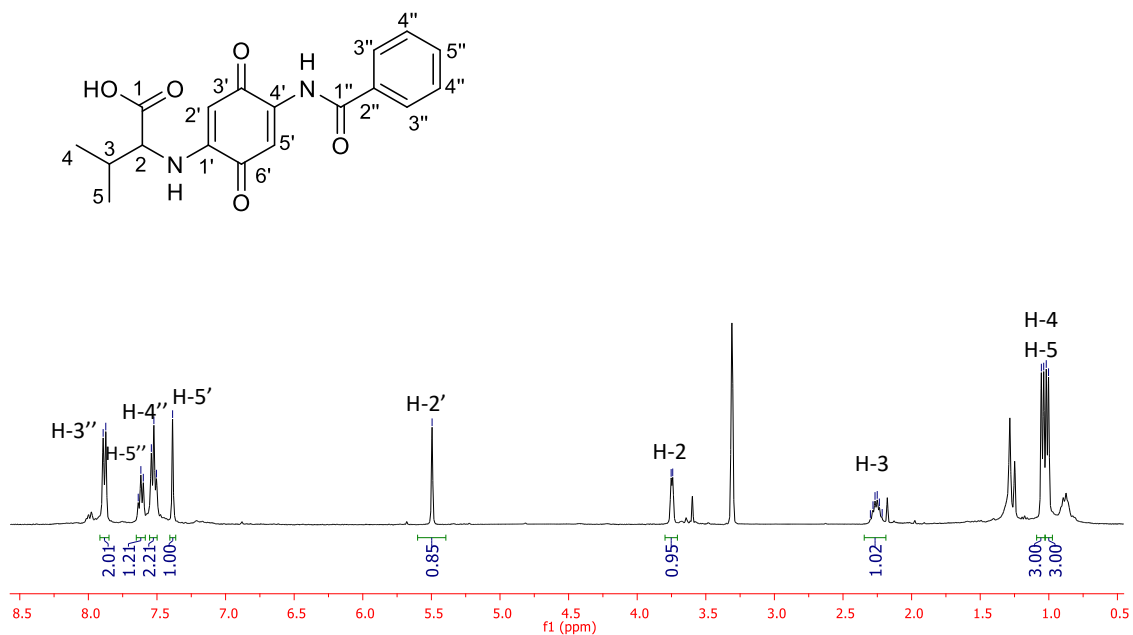
**Figure A2.17.**  $^1\text{H}$  NMR spectrum ( $\text{CD}_3\text{OD}$ , 400 MHz) of compound **2.7**.



**Figure A2.18.**  $^{13}\text{C}$  NMR spectrum ( $\text{CD}_3\text{OD}$ , 100 MHz) of compound **2.7**.

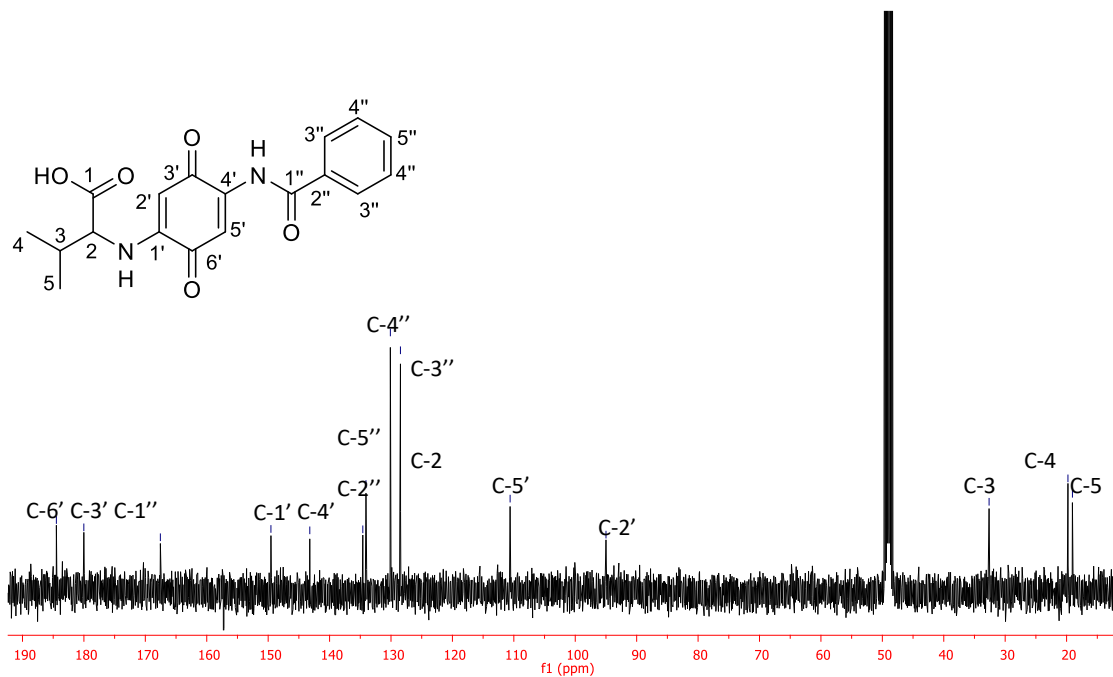


**Figure A2.19.** Infrared spectrum in KBr of compound **2.8**.

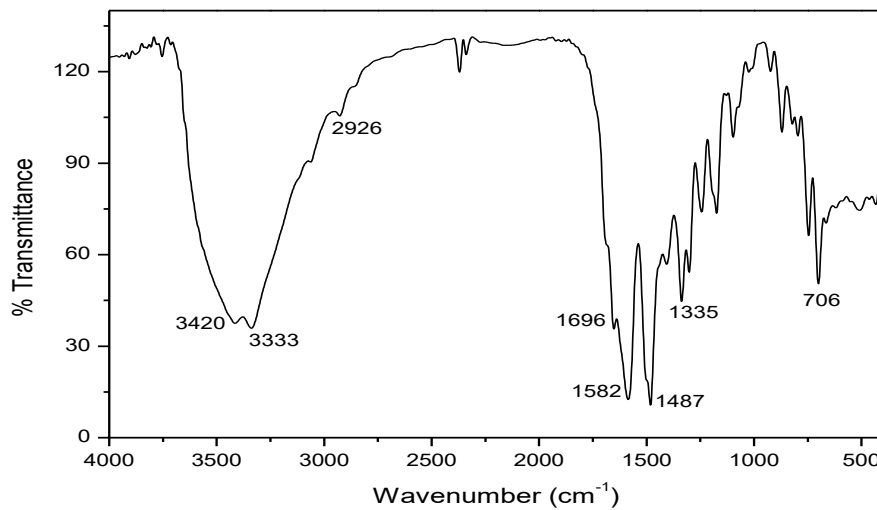


**Figure A2.20.**  $^1\text{H}$  NMR spectrum ( $\text{CD}_3\text{OD}$ , 400 MHz) of compound (**2.8**).

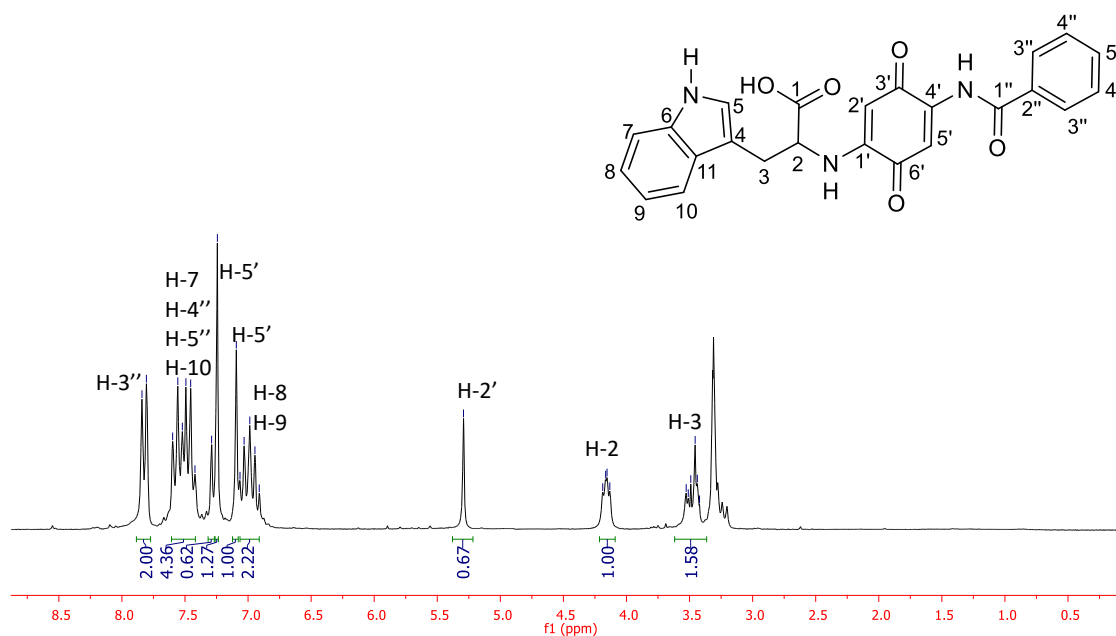




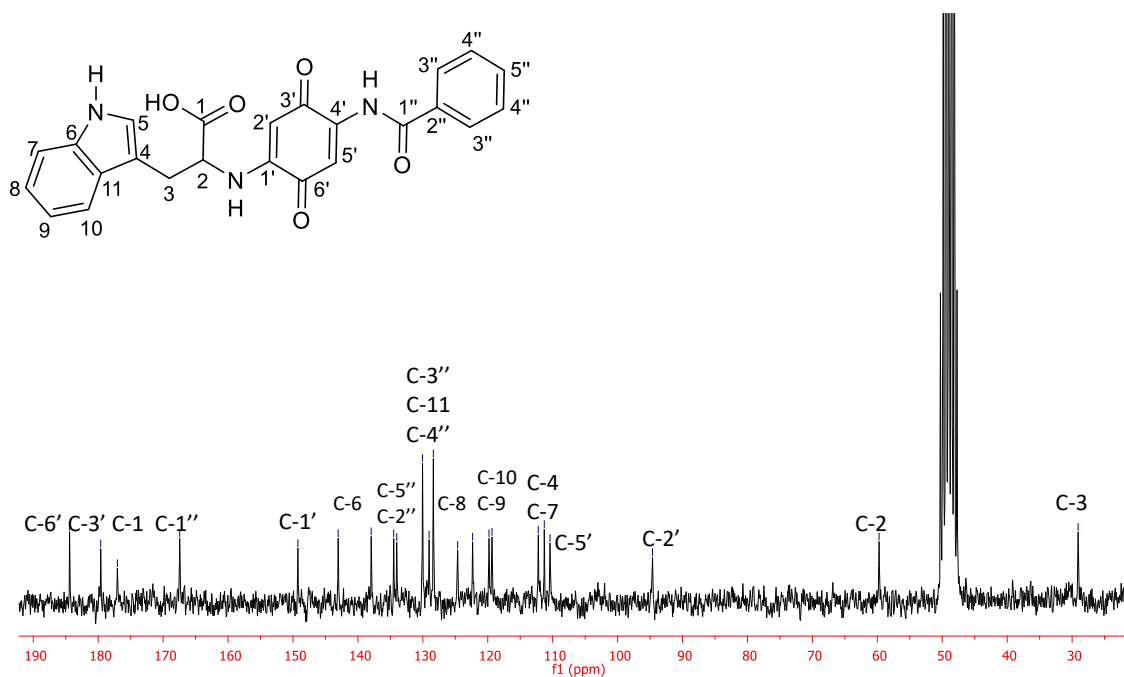
**Figure A2.21.**  $^{13}\text{C}$  NMR spectrum ( $\text{CD}_3\text{OD}$ , 100 MHz) of compound **2.8**.



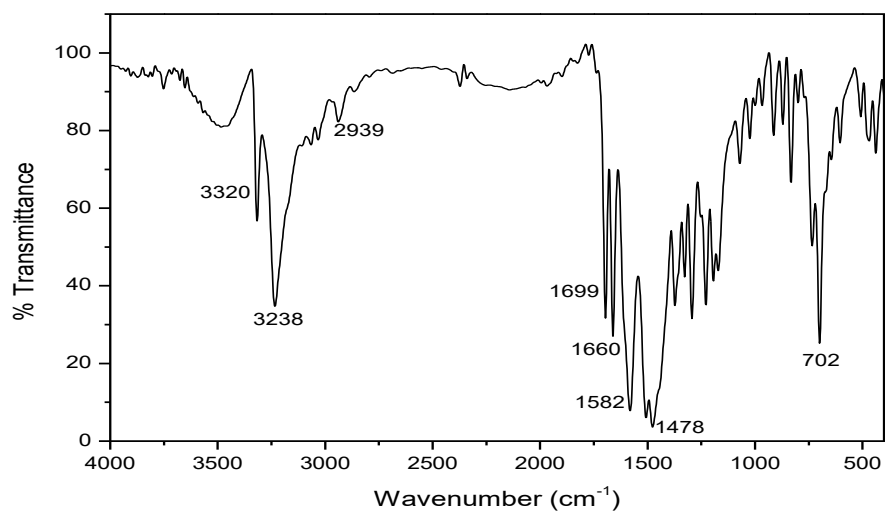
**Figure A2.22.** Infrared spectrum in KBr of compound **2.9**.



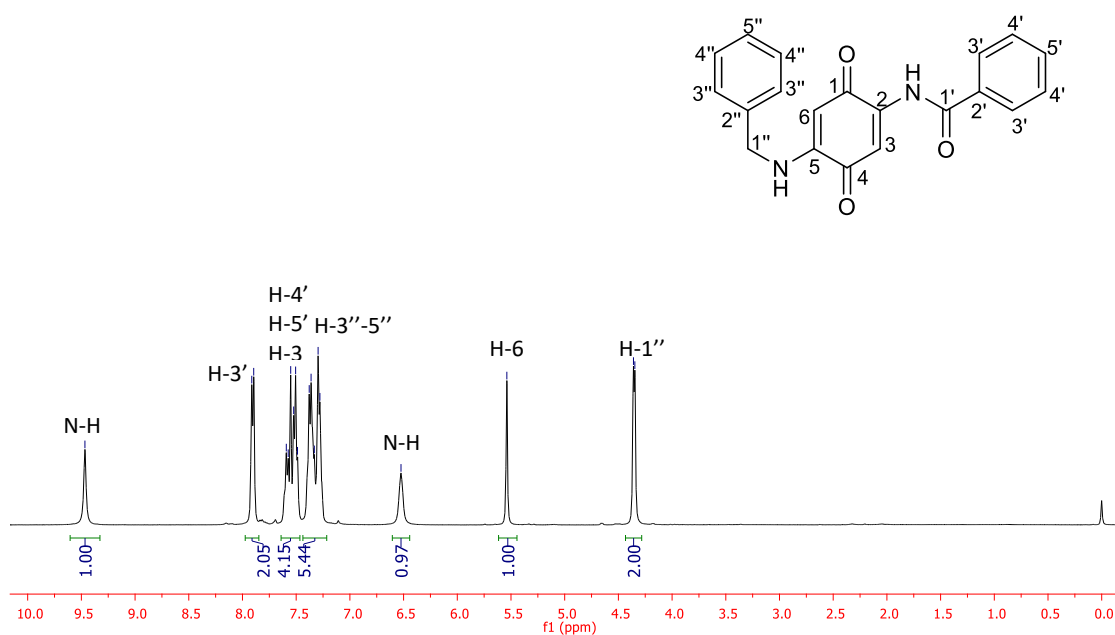
**Figure A2.23.** <sup>1</sup>H NMR spectrum (CD<sub>3</sub>OD, 200 MHz) of compound 2.9.



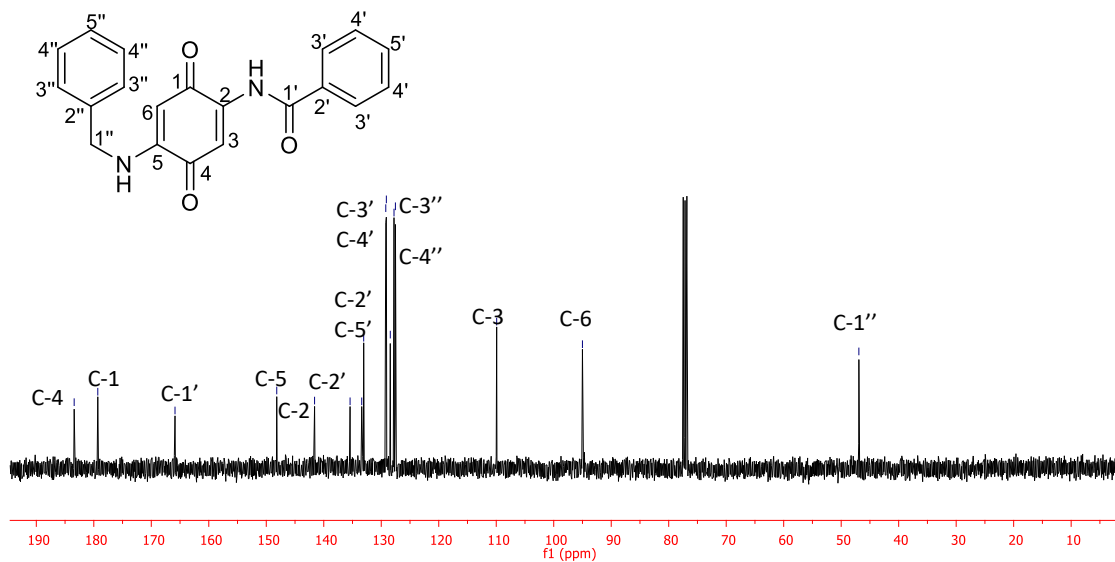
**Figure A2.24.** <sup>13</sup>C NMR spectrum (CD<sub>3</sub>OD, 100 MHz) of compound 2.9.



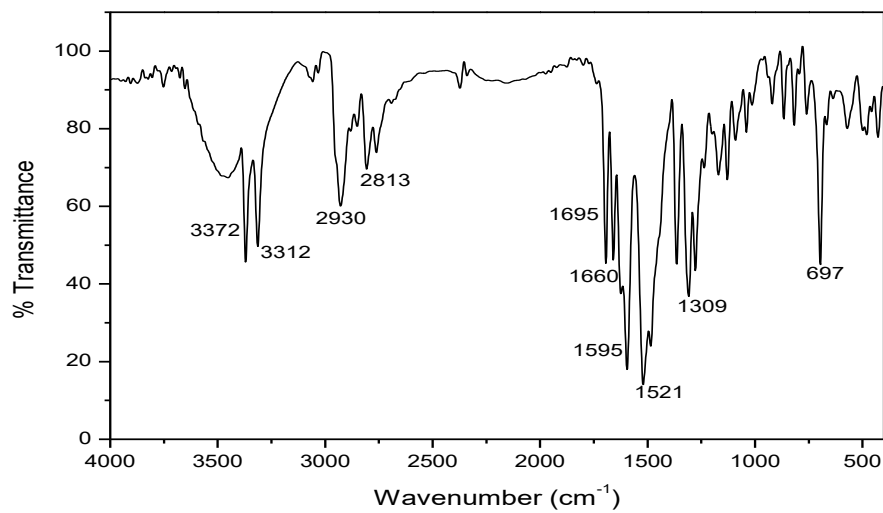
**Figure A2.25.** Infrared spectrum in KBr of compound **2.10**.



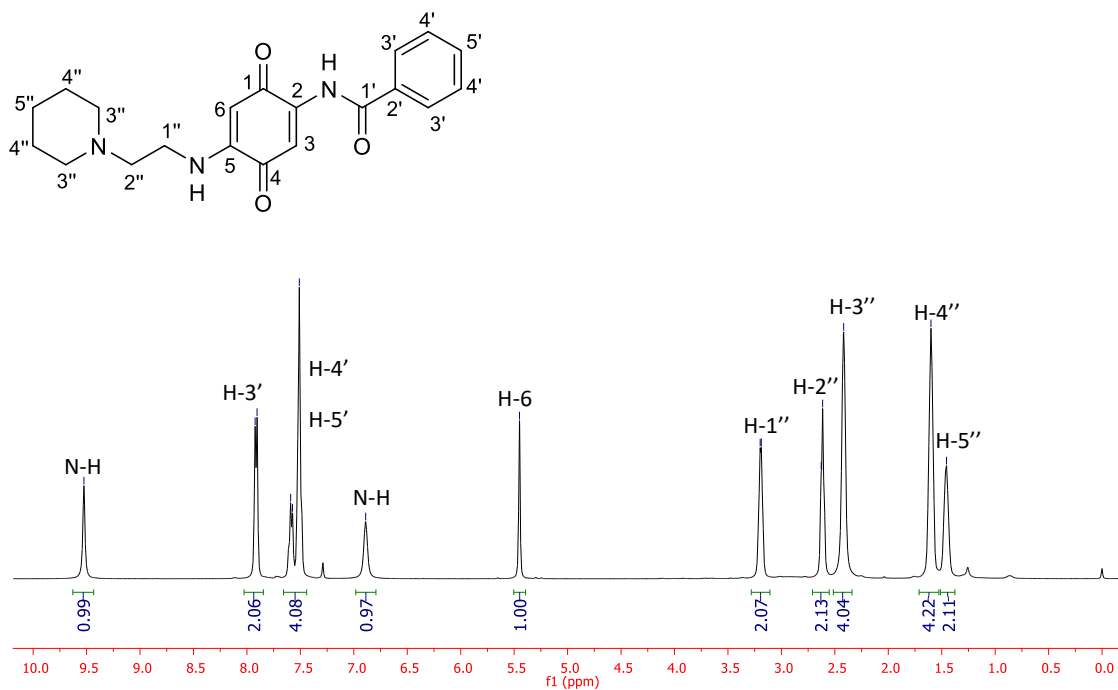
**Figure A2.26.** <sup>1</sup>H NMR spectrum (CDCl<sub>3</sub>, 400 MHz) of compound **2.10**.



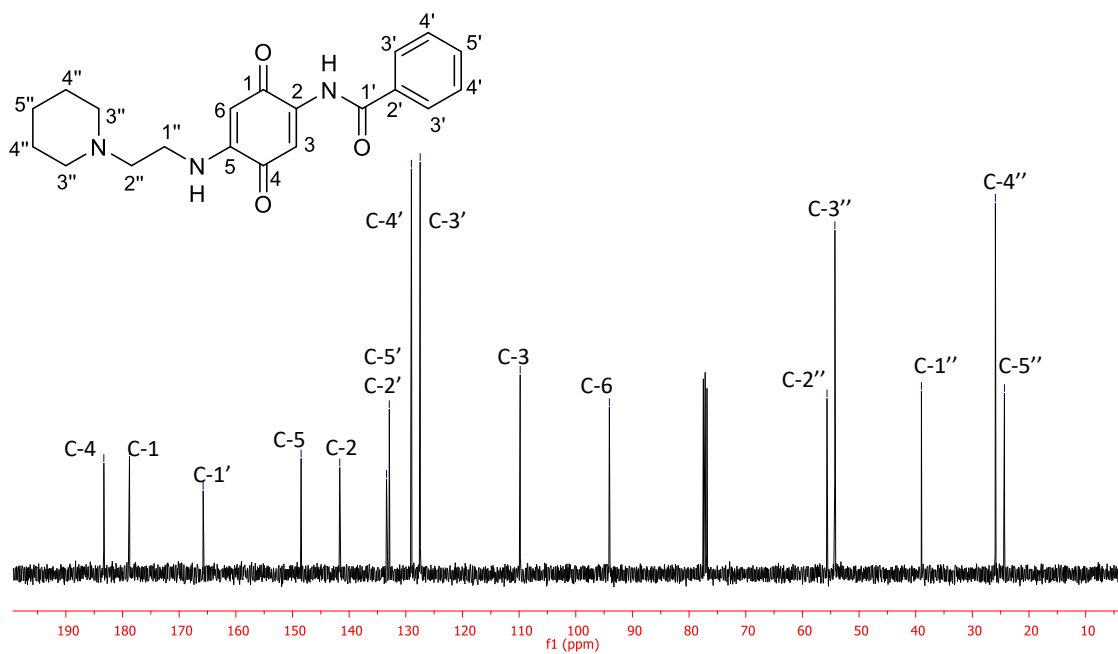
**Figure A2.27.**  $^{13}\text{C}$  NMR spectrum ( $\text{CDCl}_3$ , 100 MHz) of compound **2.10**.



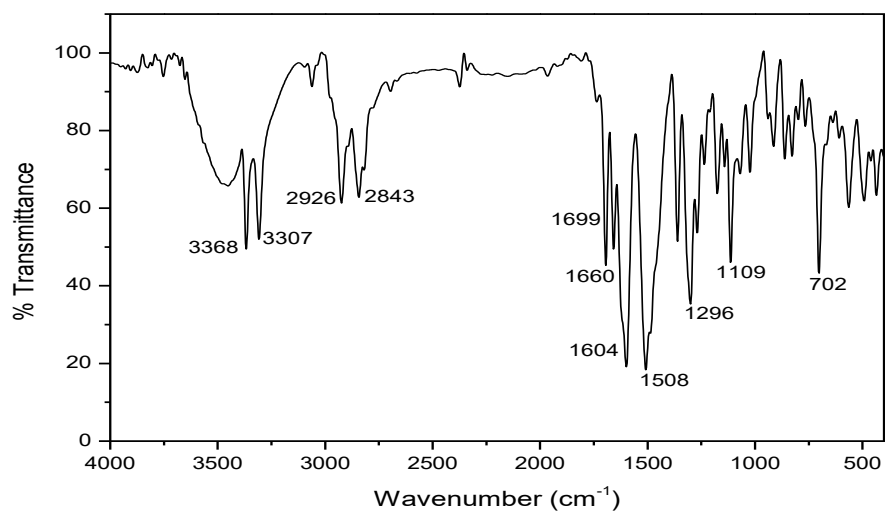
**Figure A2.28.** Infrared spectrum in KBr of compound **2.12**.



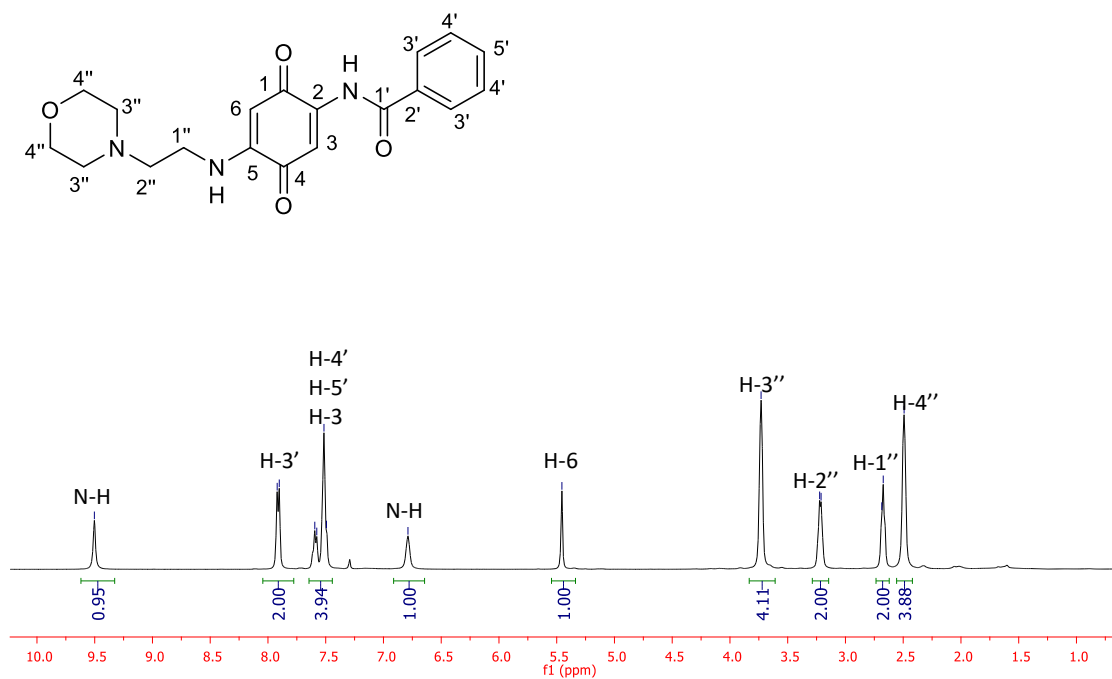
**Figure A2.29.**  $^1\text{H}$  NMR spectrum ( $\text{CDCl}_3$ , 400 MHz) of compound **2.12**.



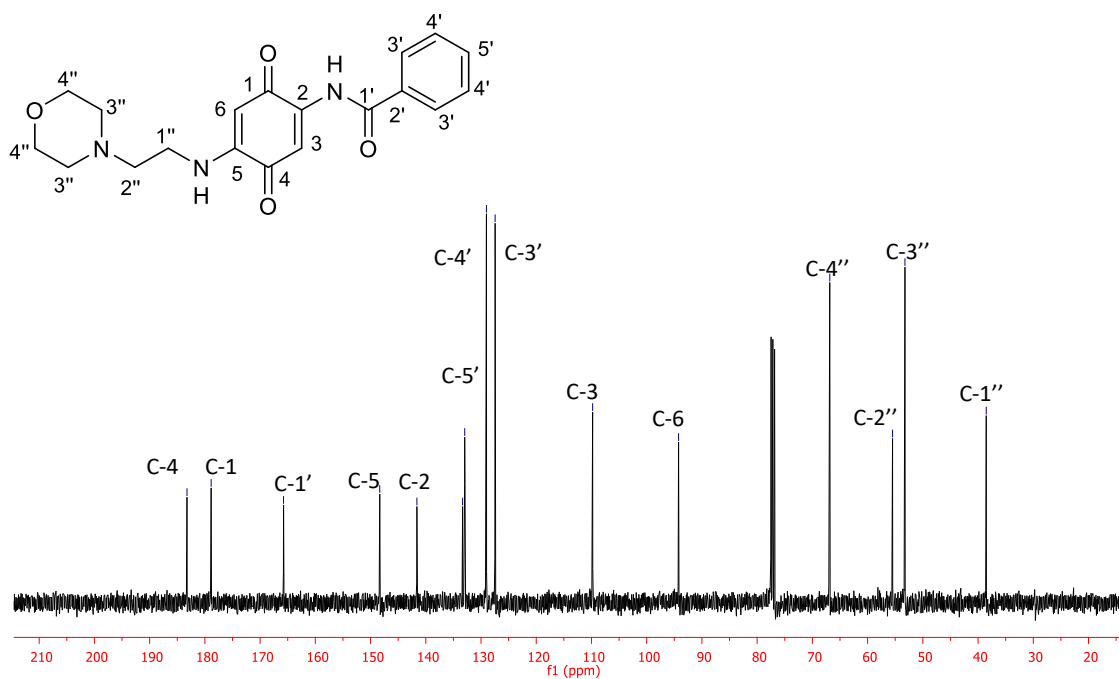
**Figure A2.30.**  $^{13}\text{C}$  NMR spectrum ( $\text{CDCl}_3$ , 100 MHz) of compound **2.12**.



**Figure A2.31.** Infrared spectrum in KBr of compound **2.13**.



**Figure A2.32.**  $^1\text{H}$  NMR spectrum ( $\text{CDCl}_3$ , 400 MHz) of compound **2.13**.



**Figure A2.33.** <sup>13</sup>C NMR spectrum (CDCl<sub>3</sub>, 100 MHz) of compound 2.13.

3. Appendix 3: Infrared,  $^1\text{H}$  and  $^{13}\text{C}$  NMR Spectra of compounds related to Chapter 3

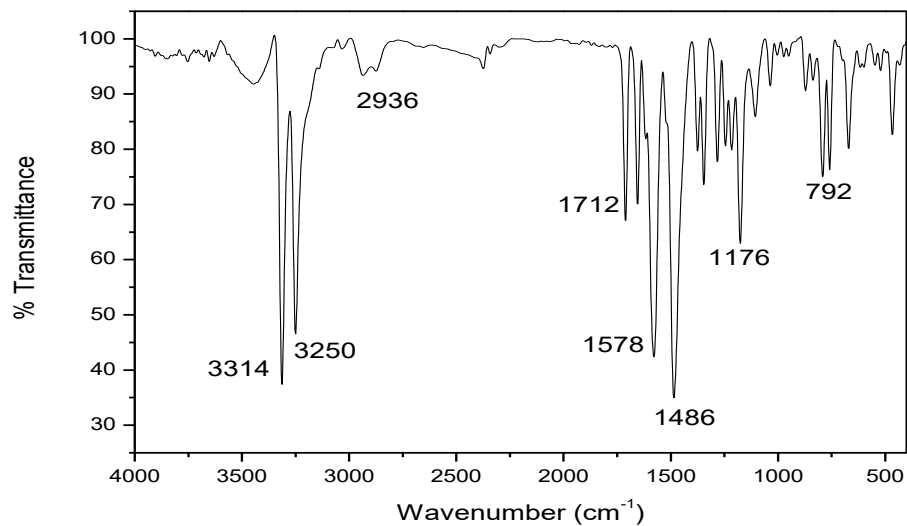


Figure A3.1. Infrared spectrum in KBr of compound 3.1.

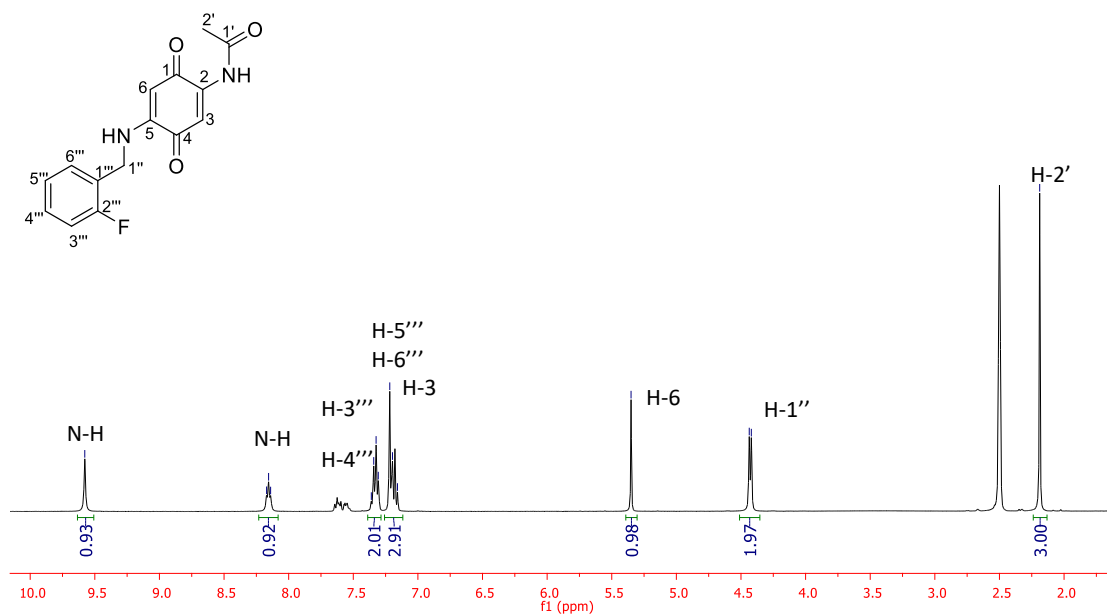
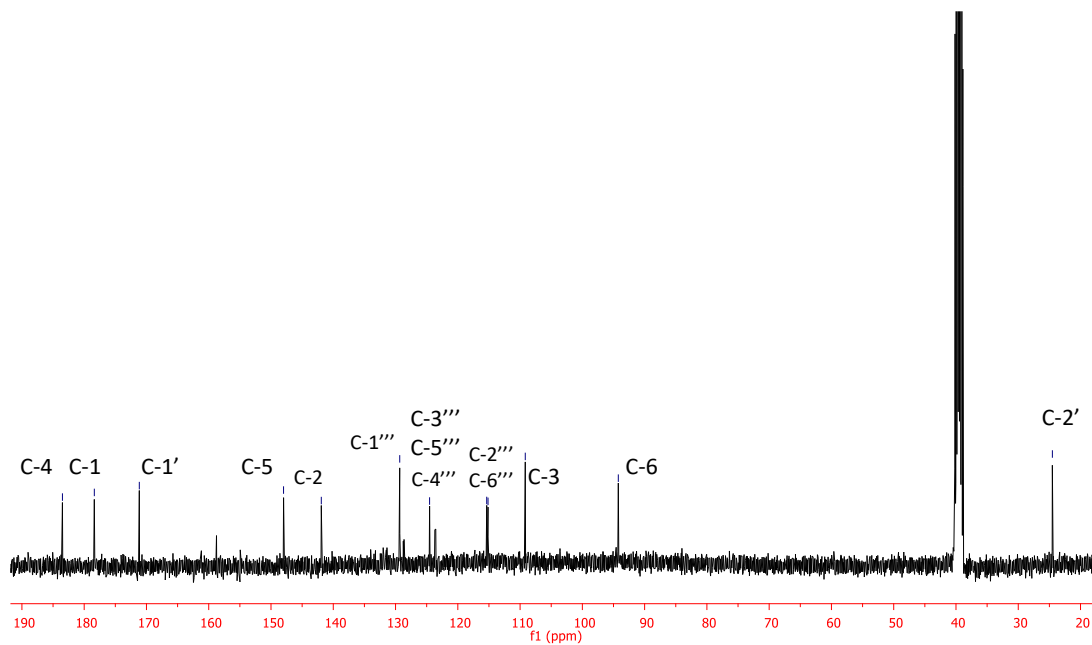
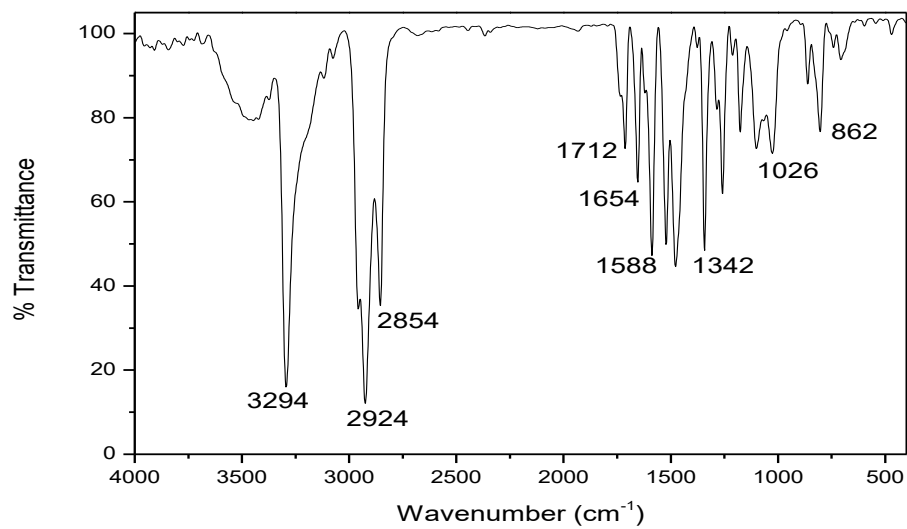


Figure A3.2.  $^1\text{H}$  NMR spectrum (DMSO-*d*<sub>6</sub>, 400 MHz) of compound 3.1.

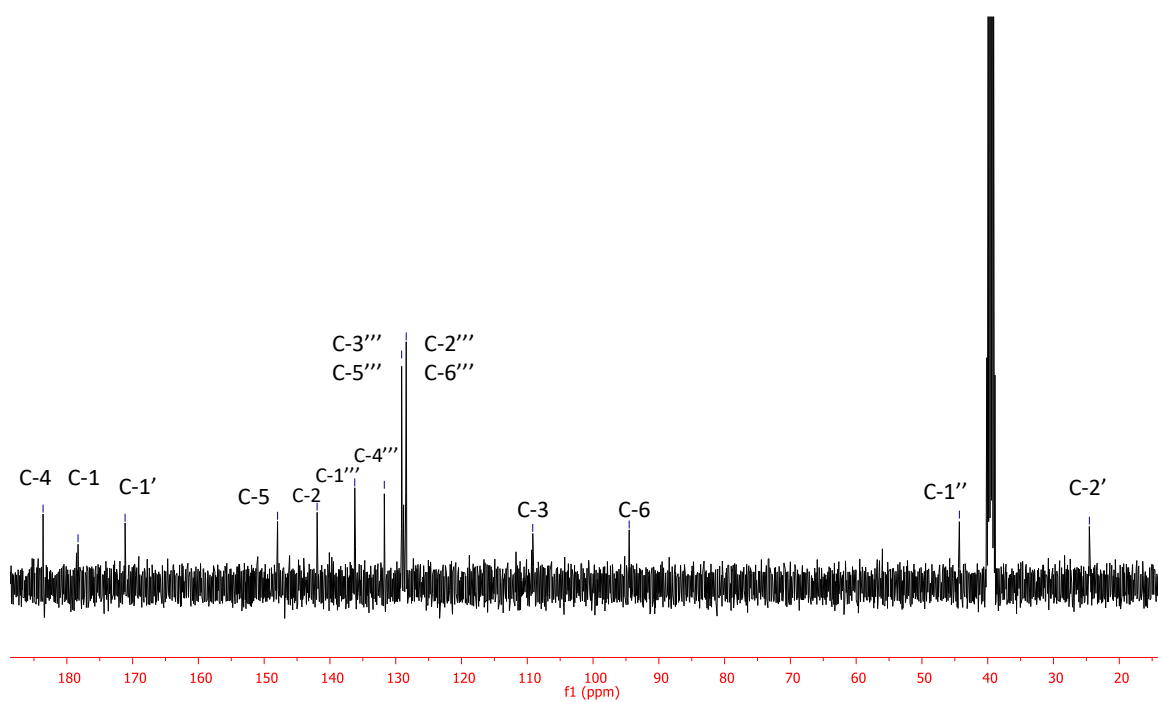
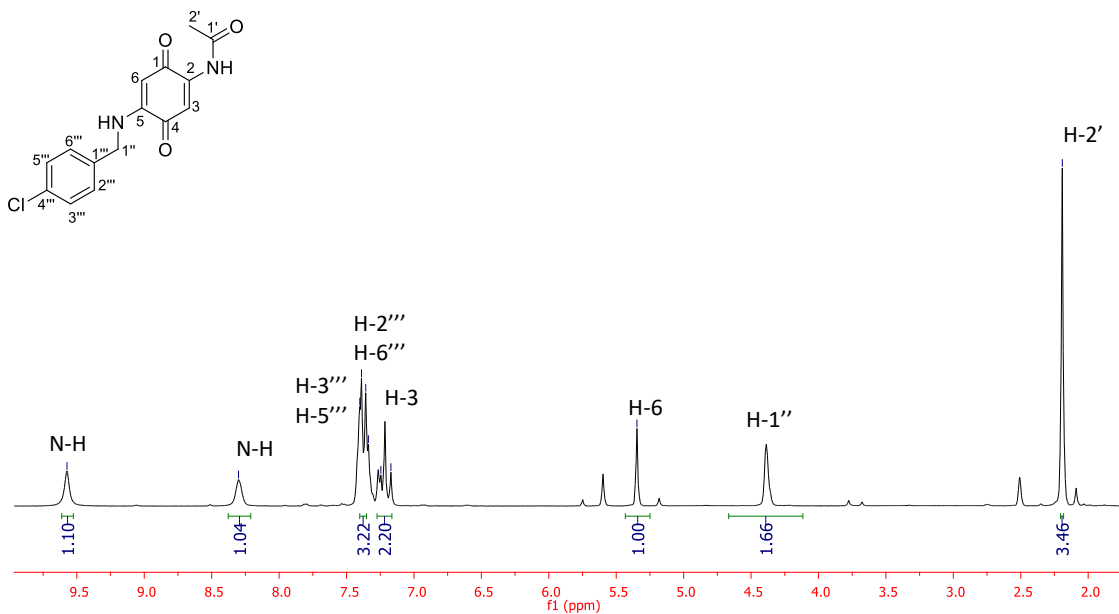


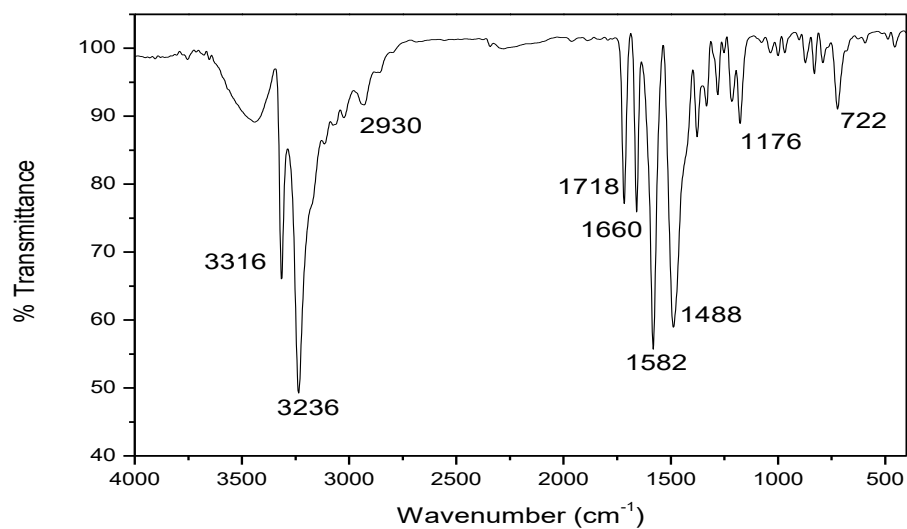


**Figure A3.3.**  $^{13}\text{C}$  NMR spectrum ( $\text{DMSO-}d_6$ , 100 MHz) of compound **3.1**.

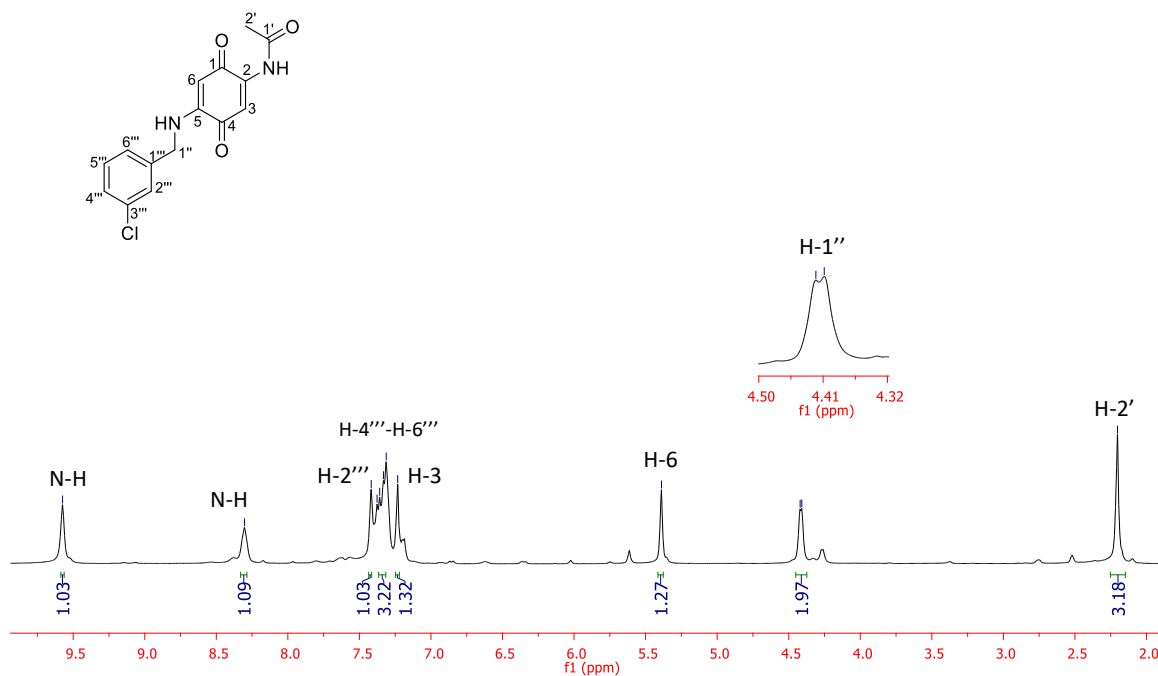


**Figure A3.4.** Infrared spectrum in KBr of compound **3.2**.

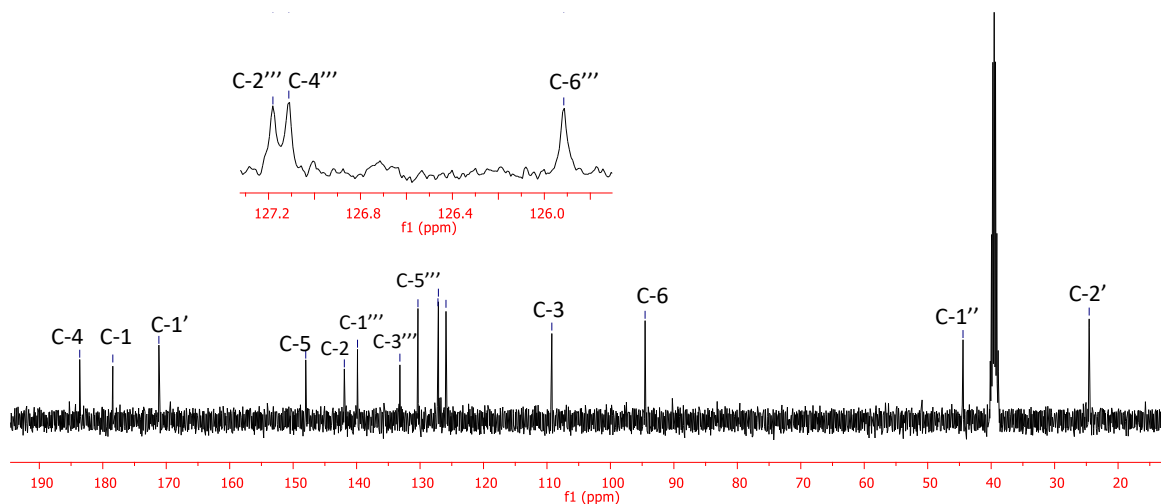




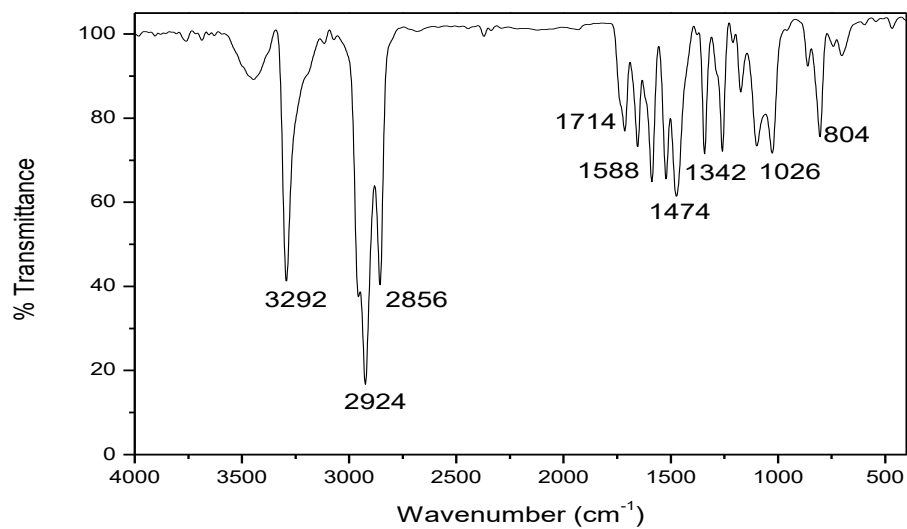
**Figure A3.7.** Infrared spectrum in KBr of compound **3.3**.



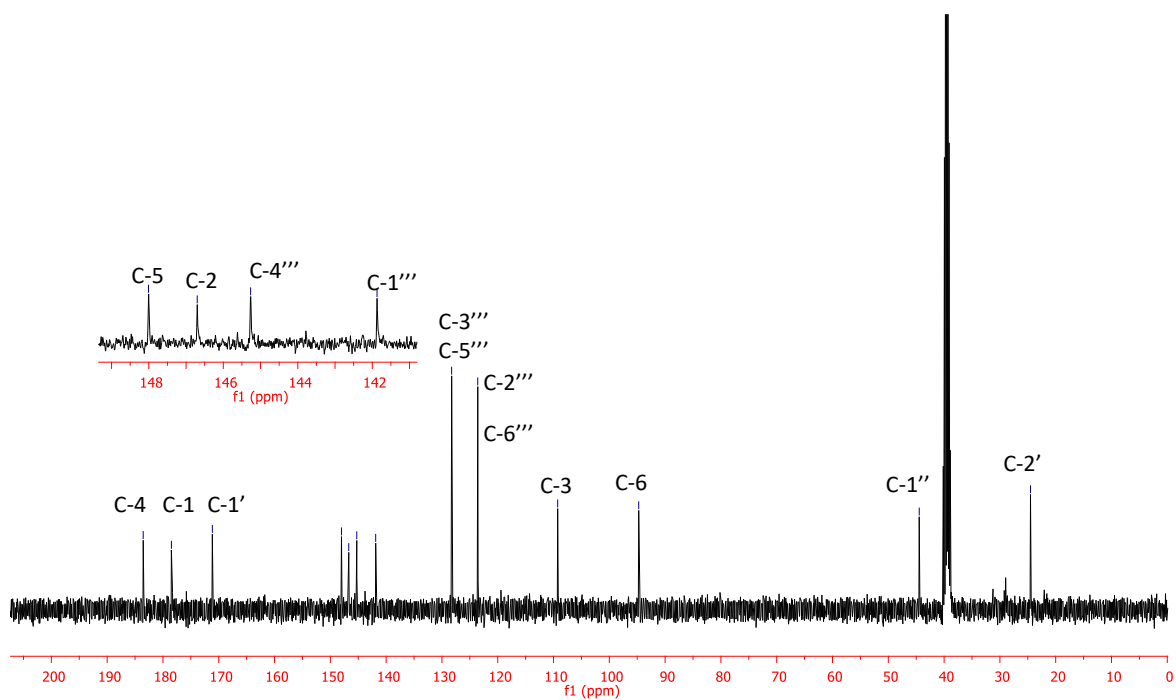
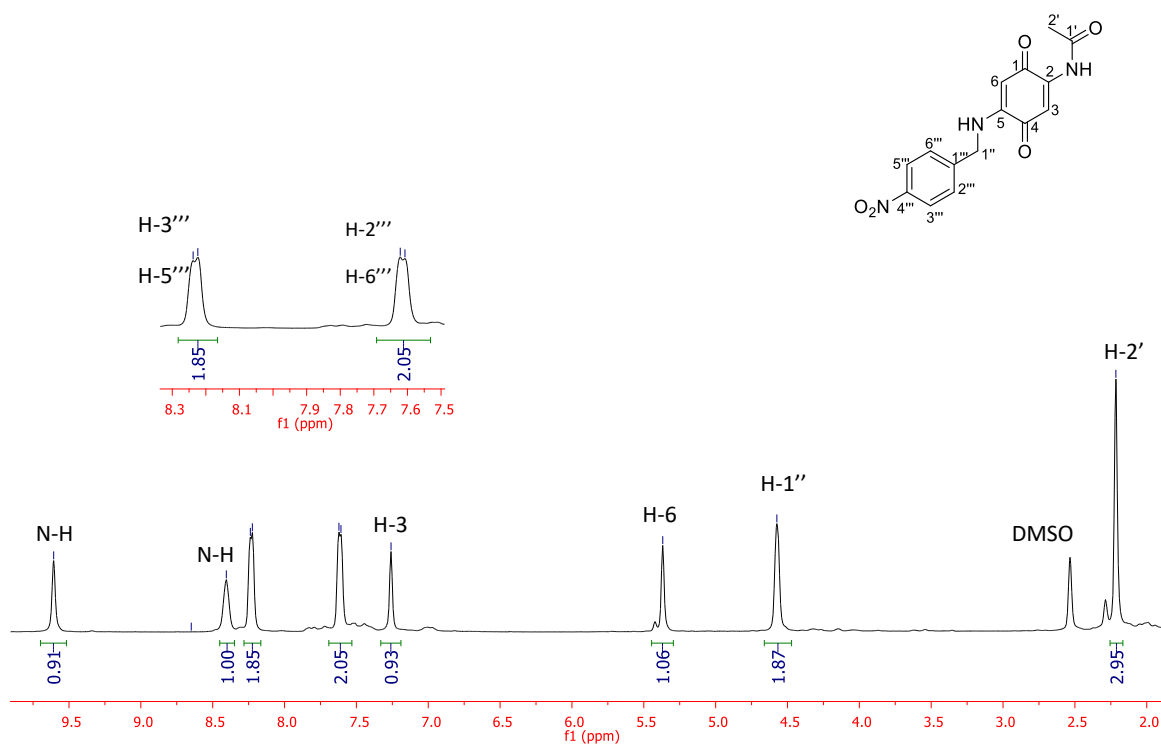
**Figure A3.8.**  $^1\text{H}$  NMR spectrum ( $\text{DMSO-}d_6$ , 400 MHz) of compound **3.3**.

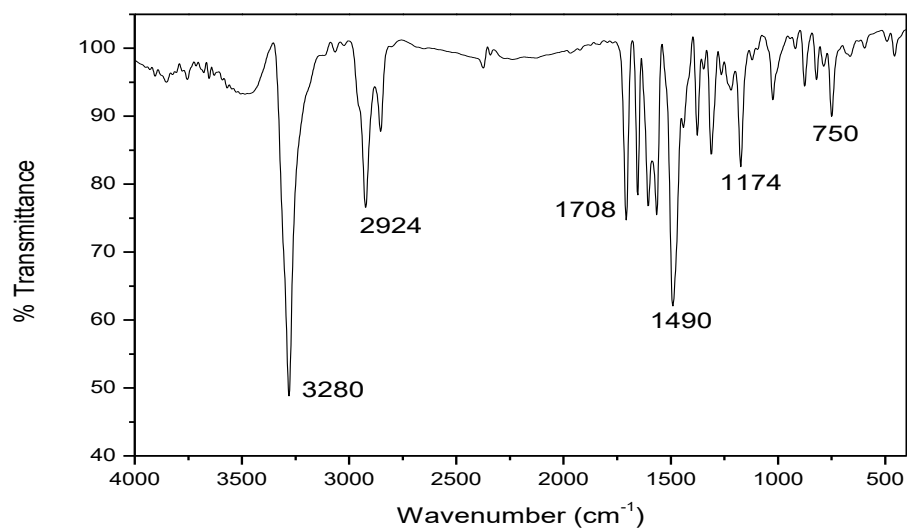


**Figure A3.9.**  $^{13}\text{C}$  NMR spectrum ( $\text{DMSO-}d_6$ , 100 MHz) of compound **3.3**.

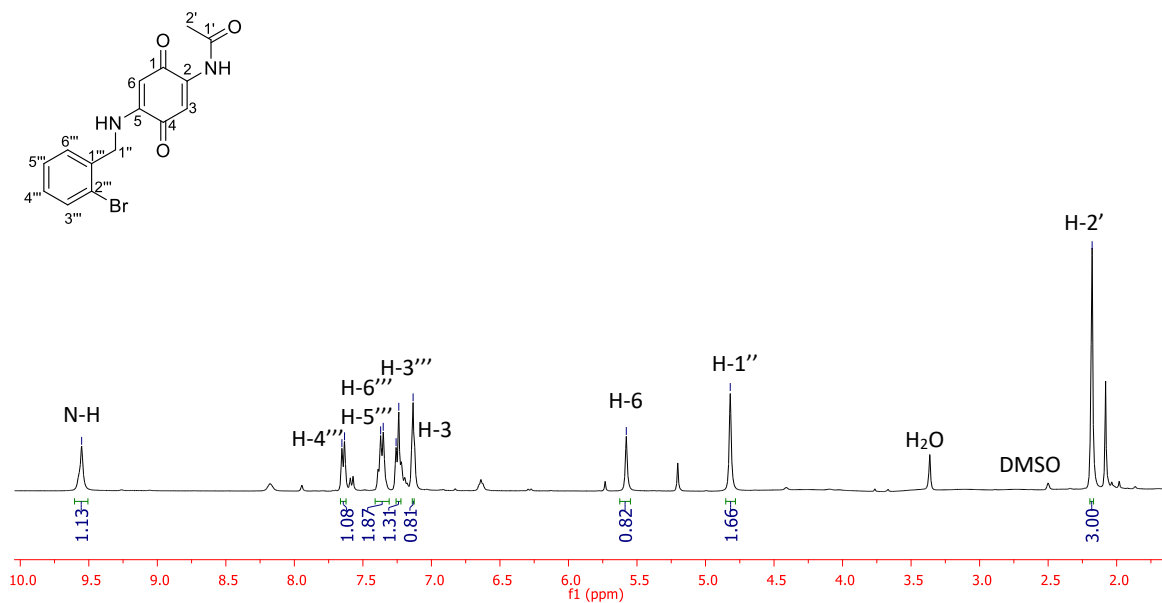


**Figure A3.10.** Infrared spectrum in KBr of compound **3.4**.

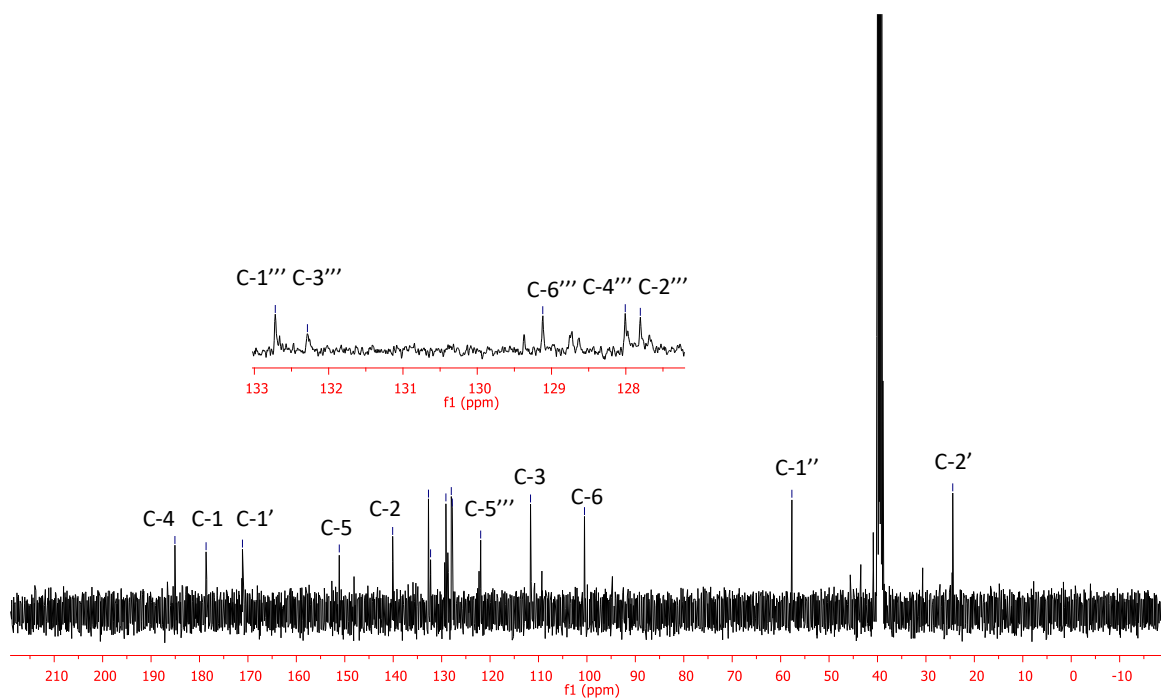




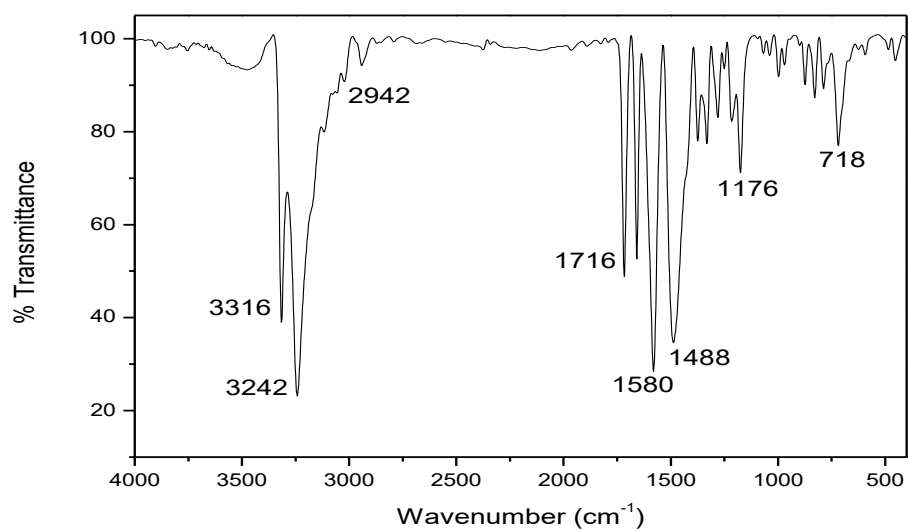
**Figure A3.13.** Infrared spectrum in KBr of compound **3.5**.



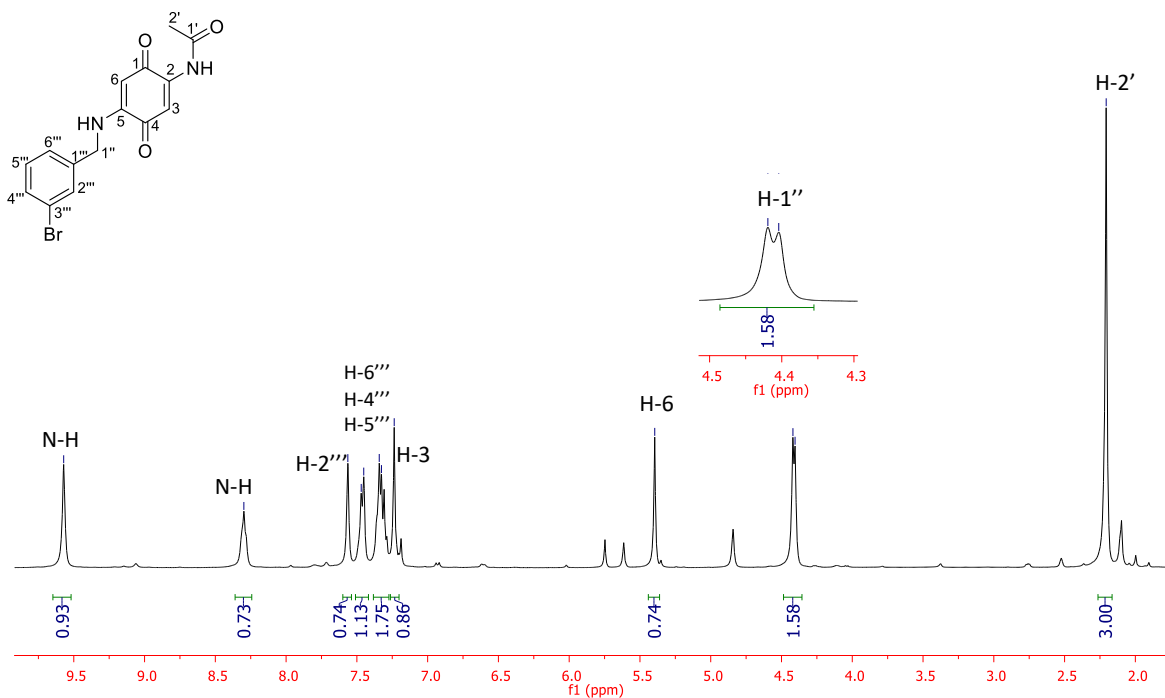
**Figure A3.14.** <sup>1</sup>H NMR spectrum (DMSO-d<sub>6</sub>, 400 MHz) of compound **3.5**.



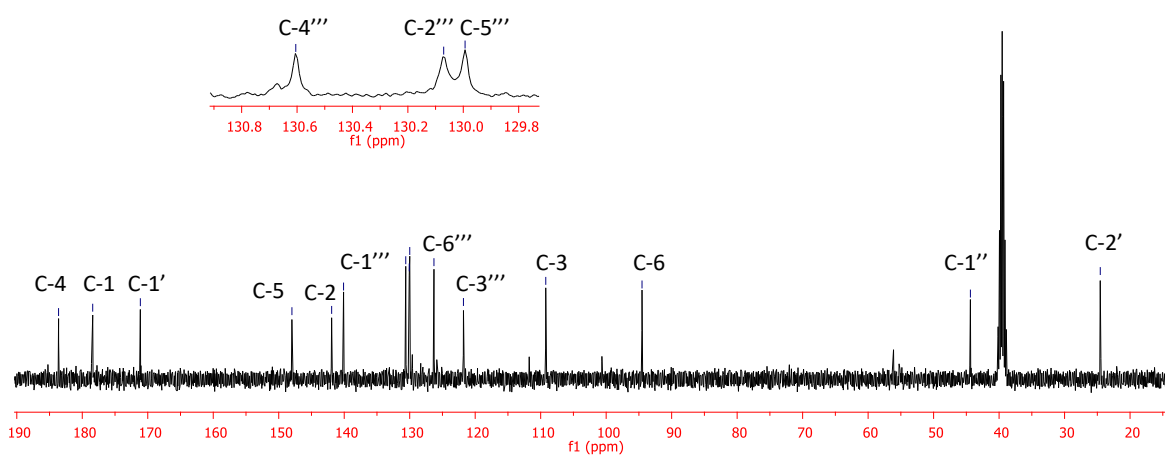
**Figure A3.15.**  $^{13}\text{C}$  NMR spectrum ( $\text{DMSO-}d_6$ , 100 MHz) of compound **3.5**.



**Figure A3.16.** Infrared spectrum in KBr of compound **3.6**.

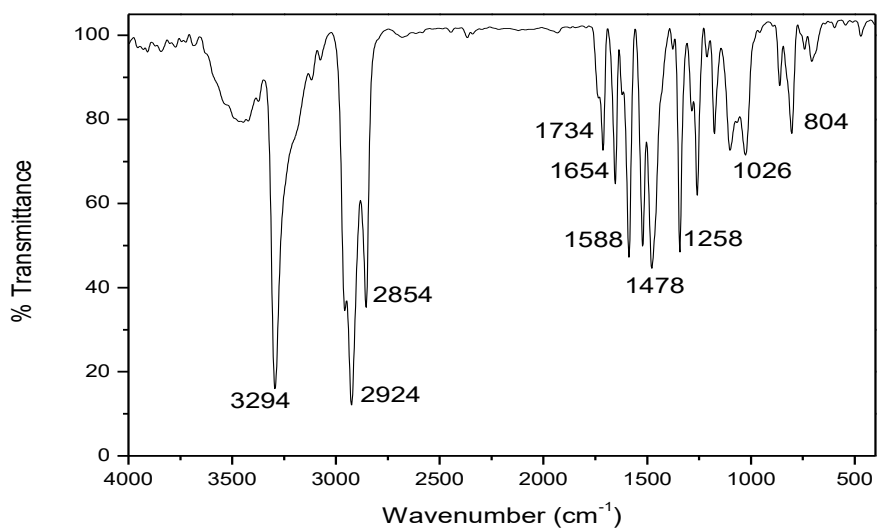


**Figure A3.17.**  $^1\text{H}$  NMR spectrum ( $\text{DMSO-}d_6$ , 400 MHz) of compound **3.6**.

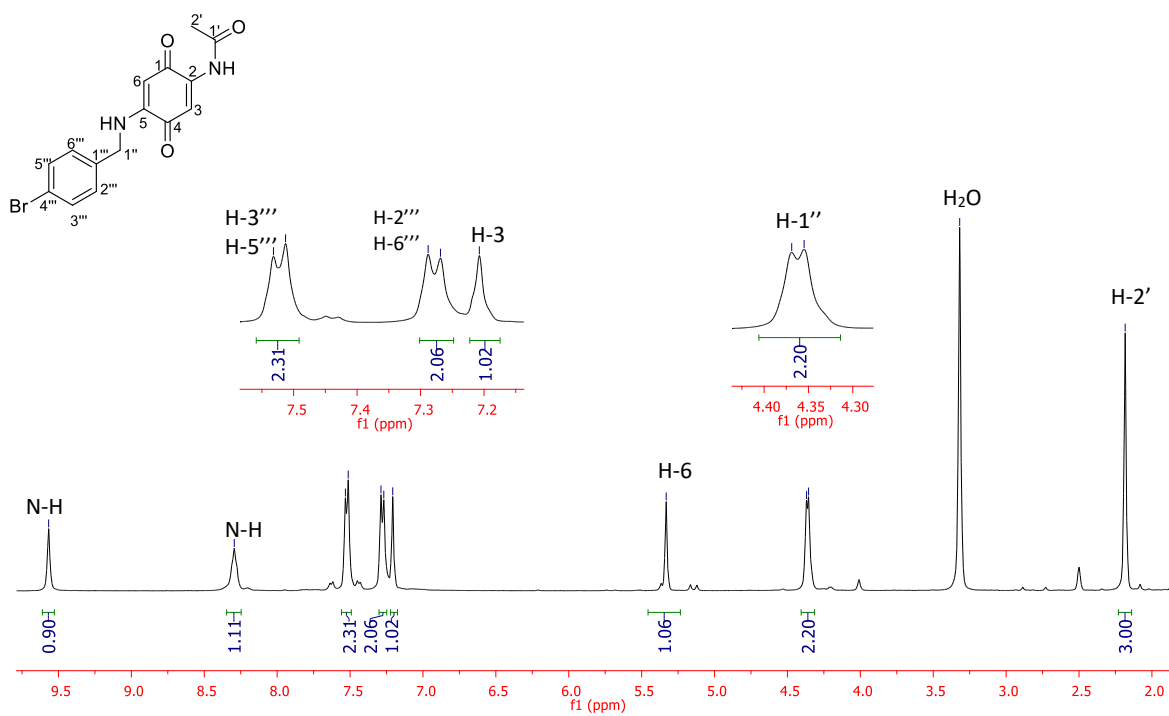


**Figure A3.18.**  $^{13}\text{C}$  NMR spectrum ( $\text{DMSO-}d_6$ , 100 MHz) of compound **3.6**.

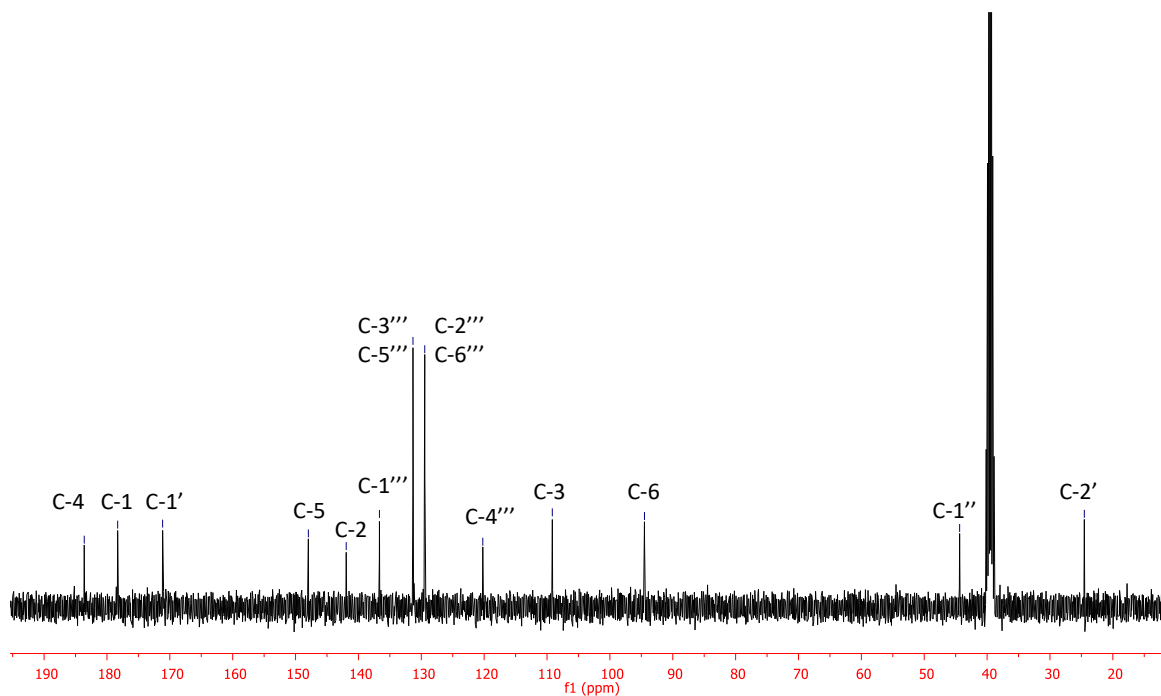




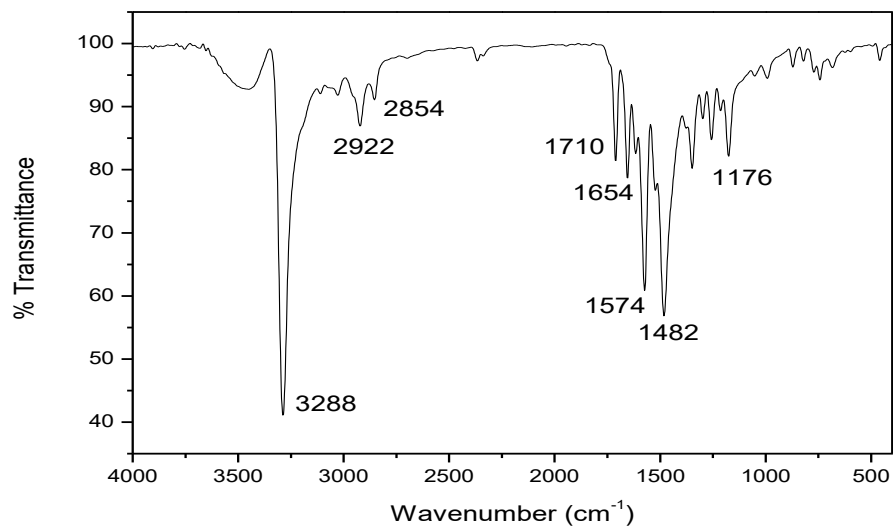
**Figure A3.19.** Infrared spectrum in KBr of compound **3.7**.



**Figure A3.20.**  $^1\text{H}$  NMR spectrum ( $\text{DMSO-}d_6$ , 400 MHz) of compound **3.7**.



**Figure A3.21.** <sup>13</sup>C NMR spectrum (DMSO-*d*<sub>6</sub>, 100 MHz) of compound **3.7**.



**Figure A3.22.** Infrared spectrum in KBr of compound **3.8**.

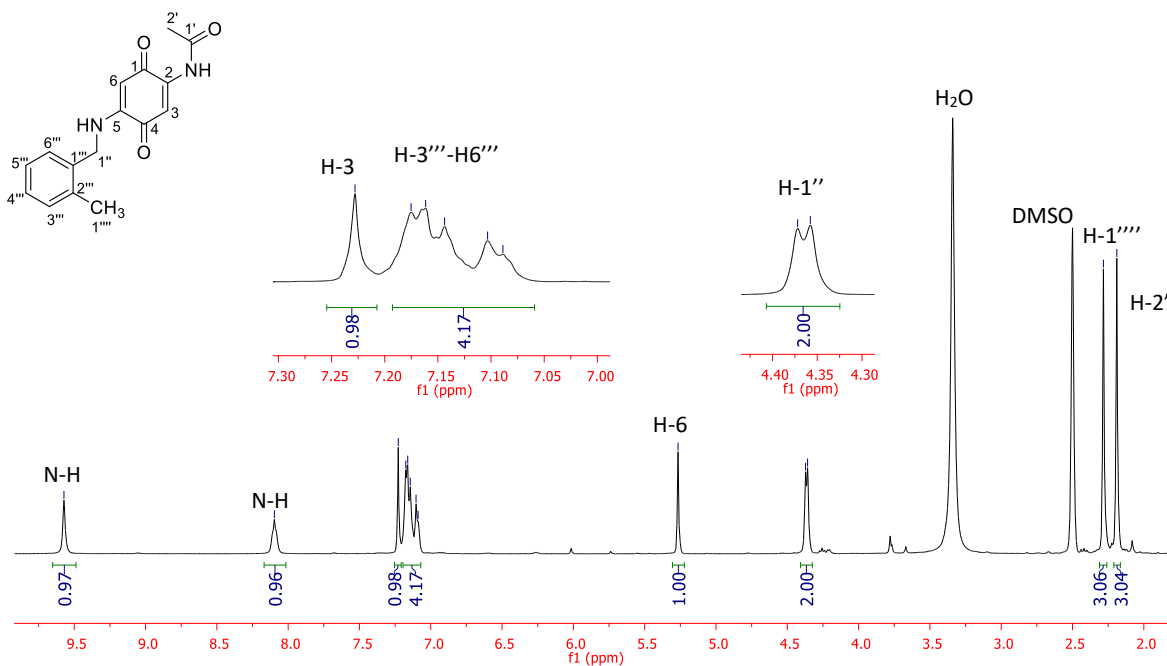


Figure A3.23.  $^1\text{H}$  NMR spectrum ( $\text{DMSO-}d_6$ , 400 MHz) of compound **3.8**.

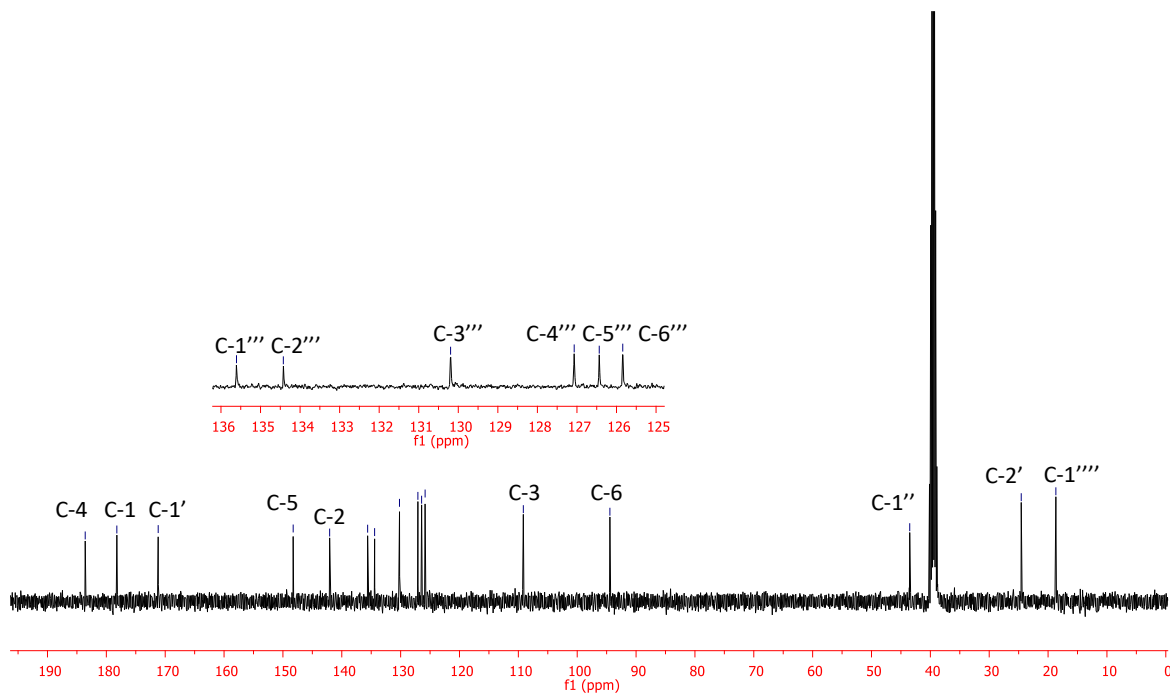
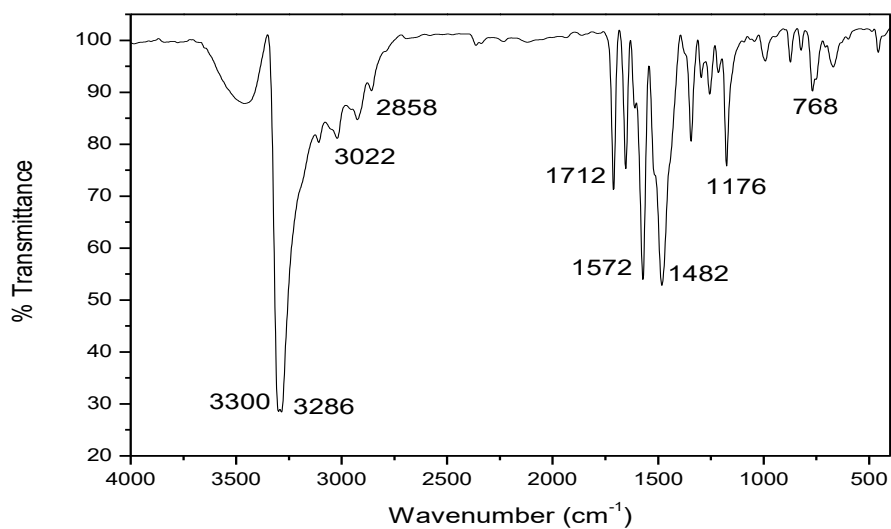
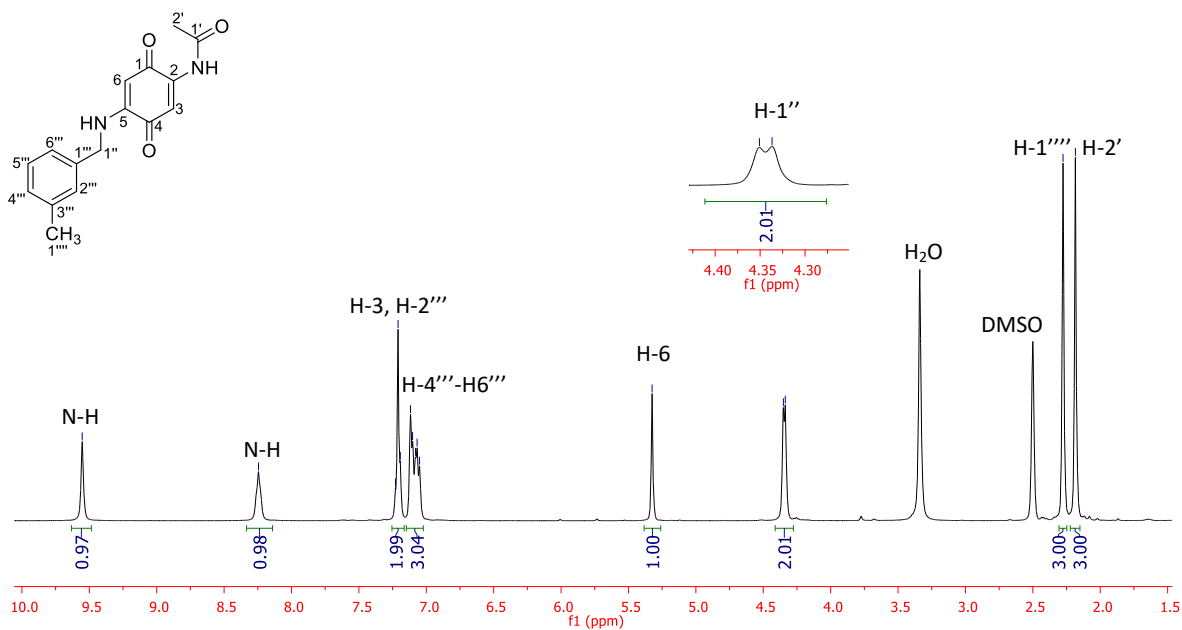


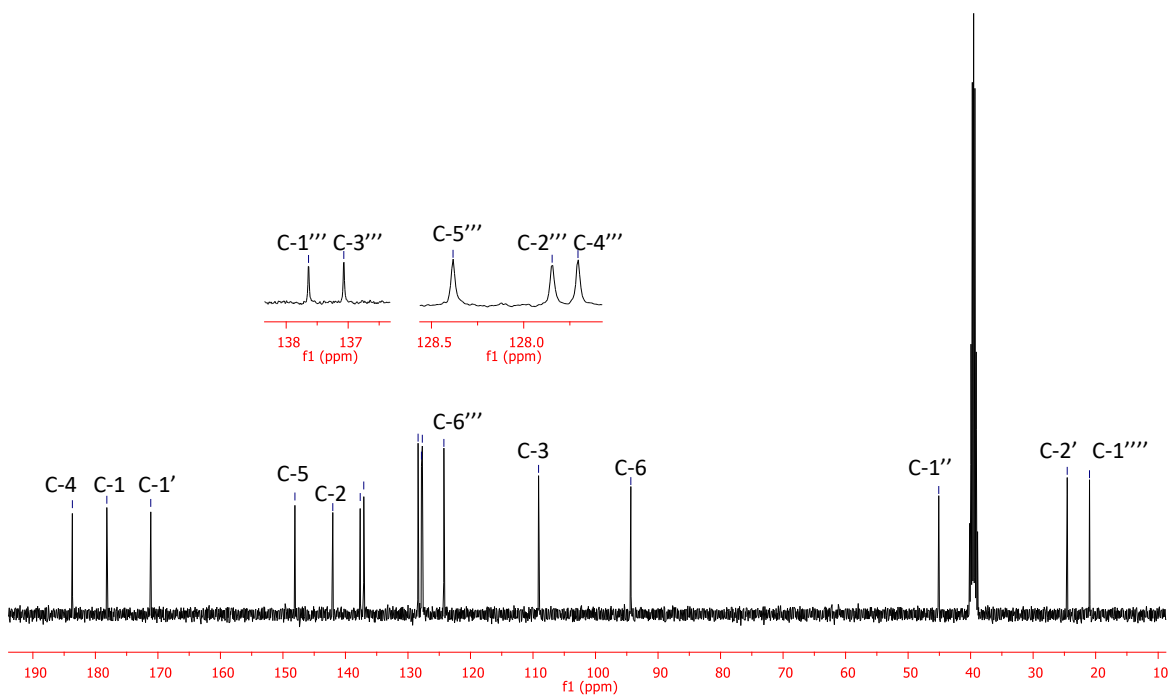
Figure A3.24.  $^{13}\text{C}$  NMR spectrum ( $\text{DMSO-}d_6$ , 100 MHz) of compound **3.8**.



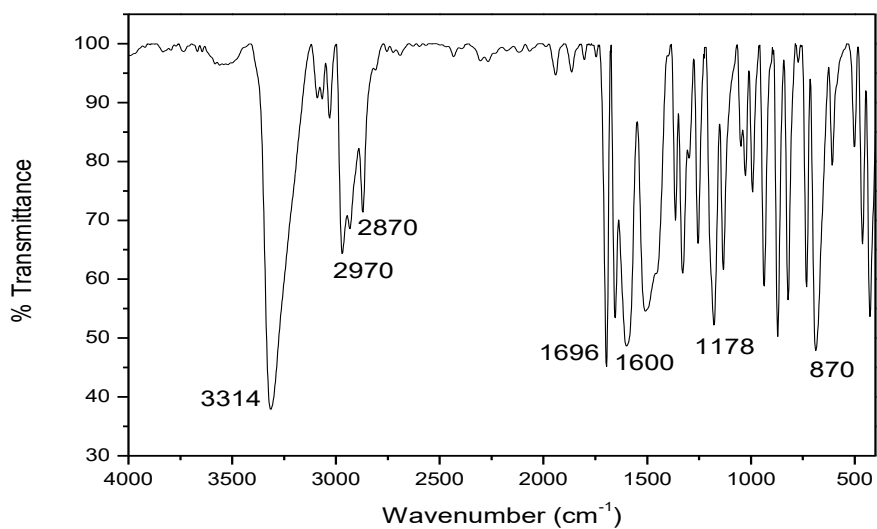
**Figure A3.25.** Infrared spectrum in KBr of compound **3.9**.



**Figure A3.26.** <sup>1</sup>H NMR spectrum (DMSO-*d*<sub>6</sub>, 400 MHz) of compound **3.9**.



**Figure A3.27.**  $^{13}\text{C}$  NMR spectrum ( $\text{DMSO-}d_6$ , 100 MHz) of compound **3.9**.



**Figure A3.28.** Infrared spectrum in KBr of compound **3.12**.

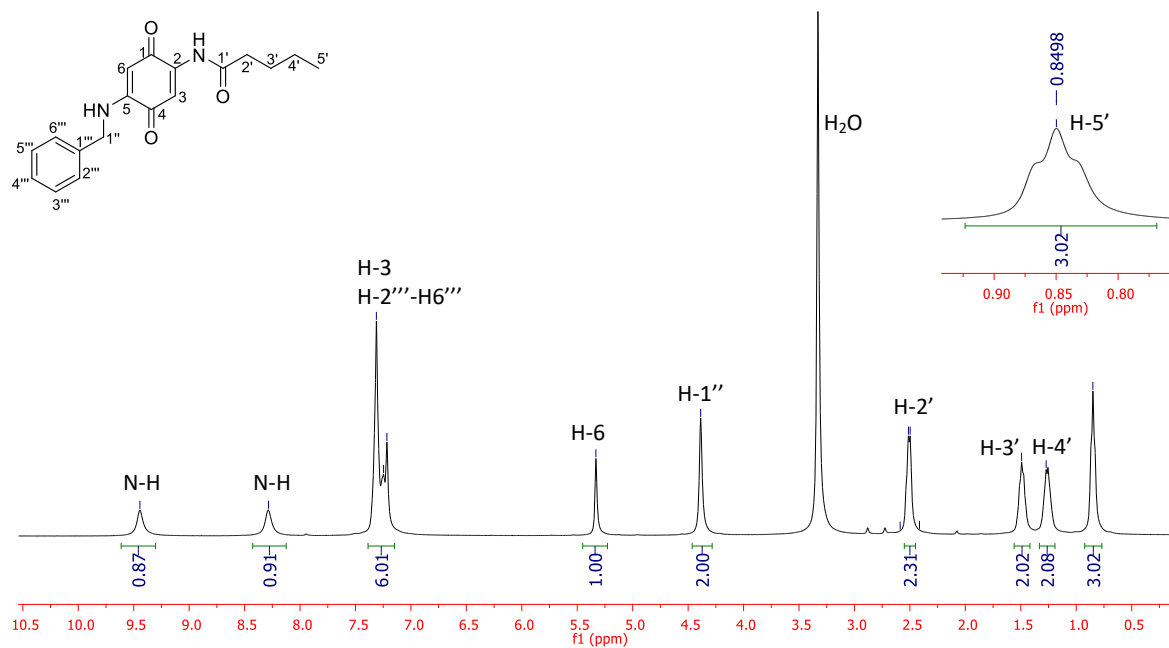


Figure A3.29. <sup>1</sup>H NMR spectrum (DMSO-*d*<sub>6</sub>, 400 MHz) of compound 3.12.

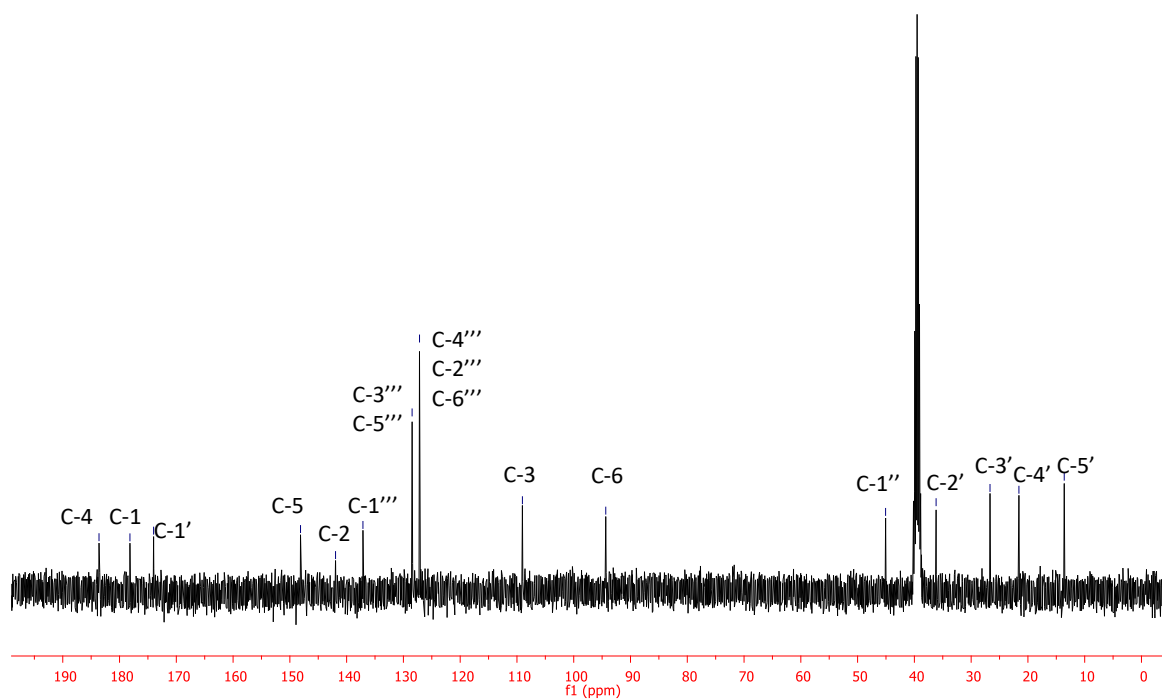
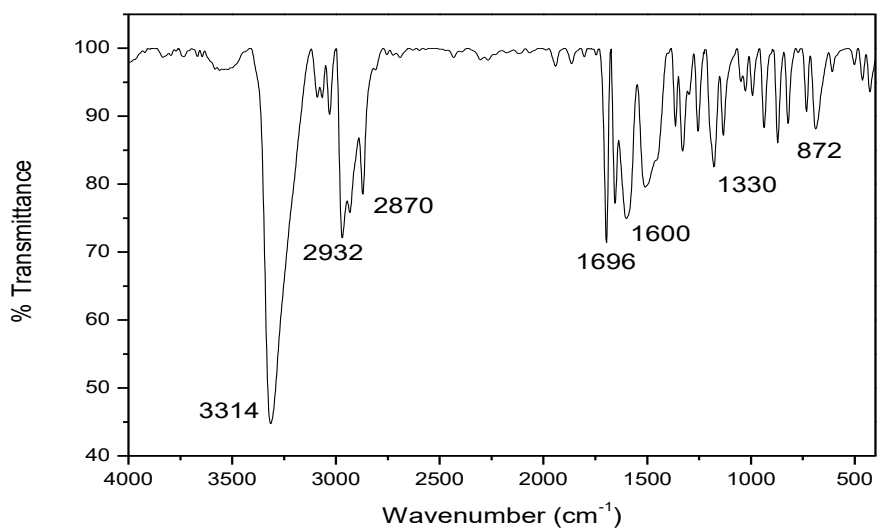
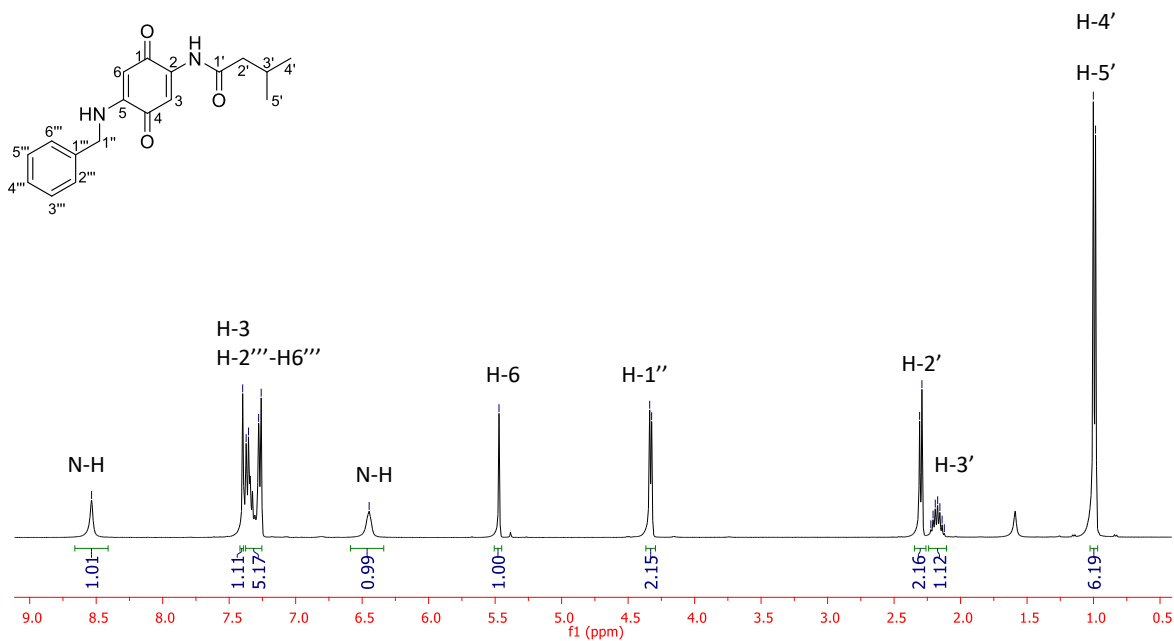


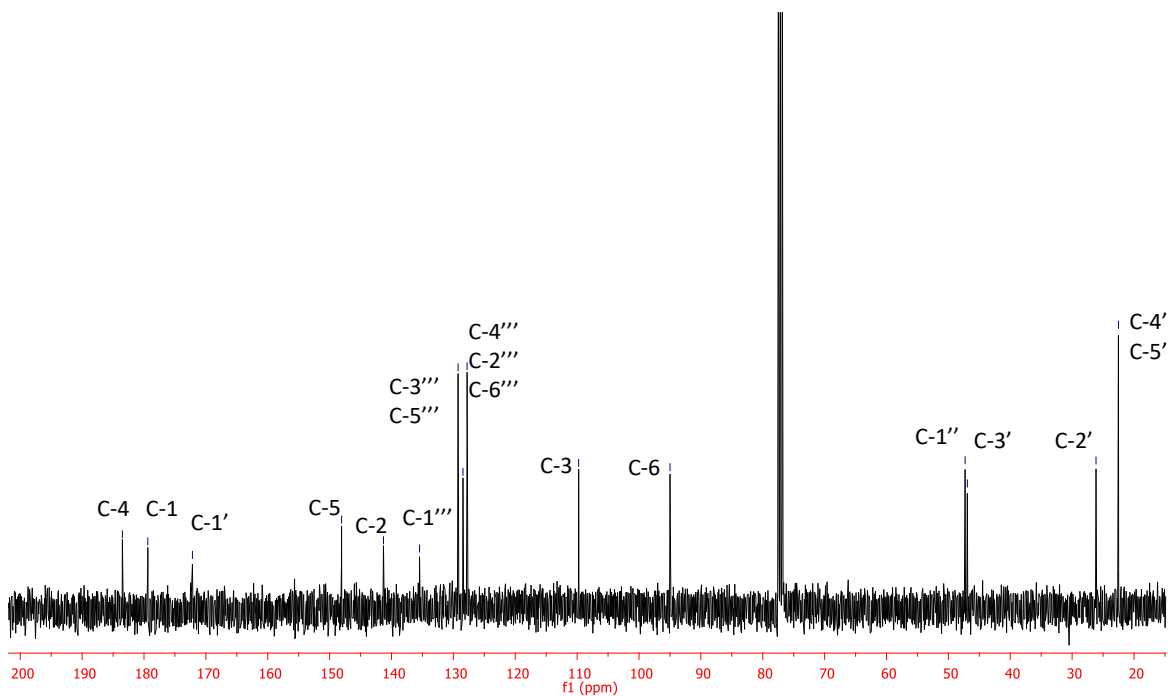
Figure A3.30. <sup>13</sup>C NMR spectrum (DMSO-*d*<sub>6</sub>, 100 MHz) of compound 3.12.



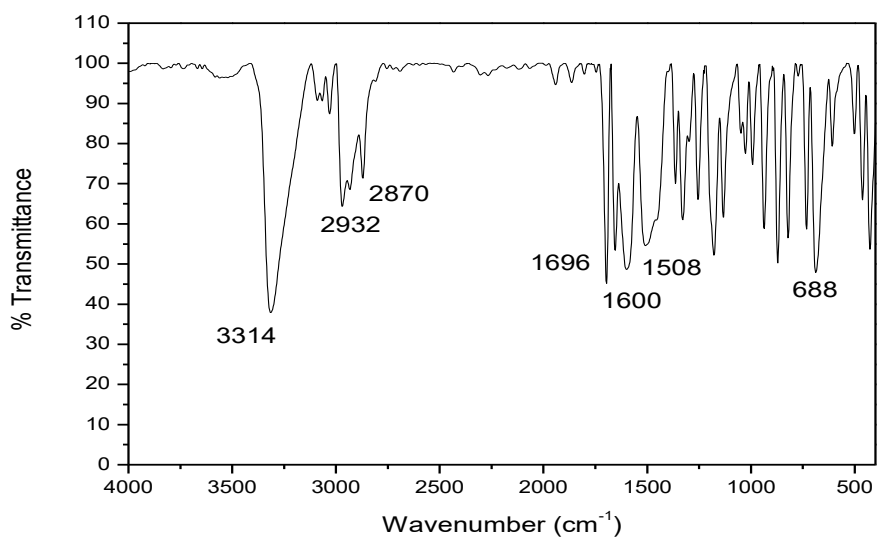
**Figure A3.31.** Infrared spectrum in KBr of compound **3.13**.



**Figure A3.32.**  $^1\text{H}$  NMR spectrum ( $\text{CDCl}_3$ , 400 MHz) of compound **3.13**.

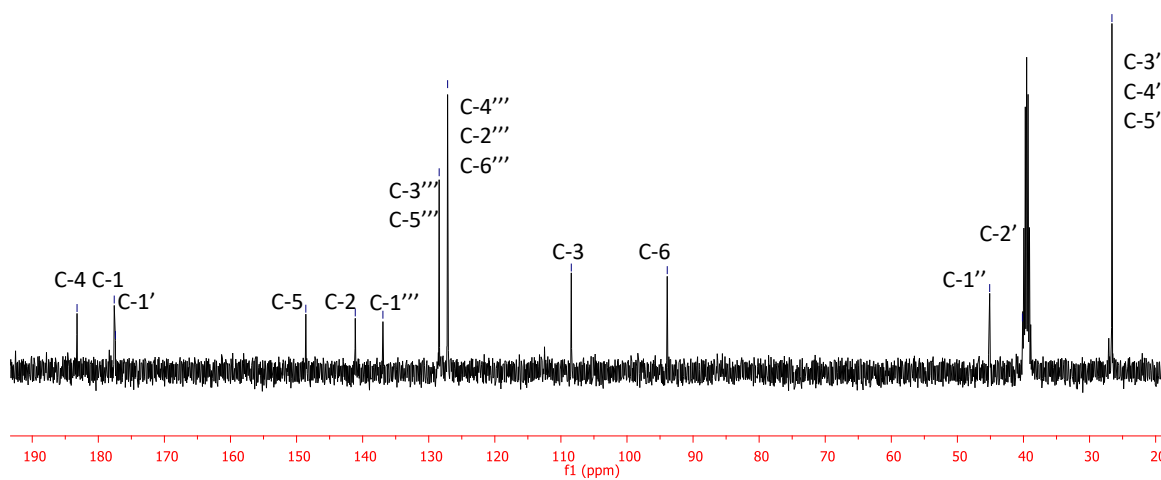
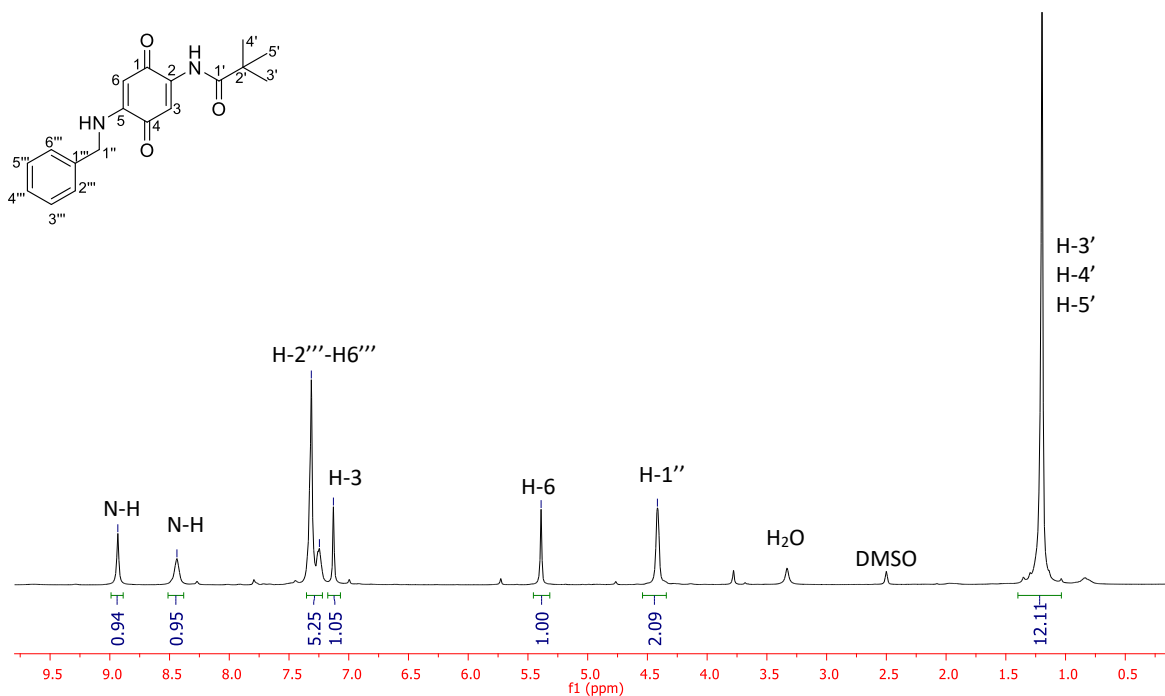


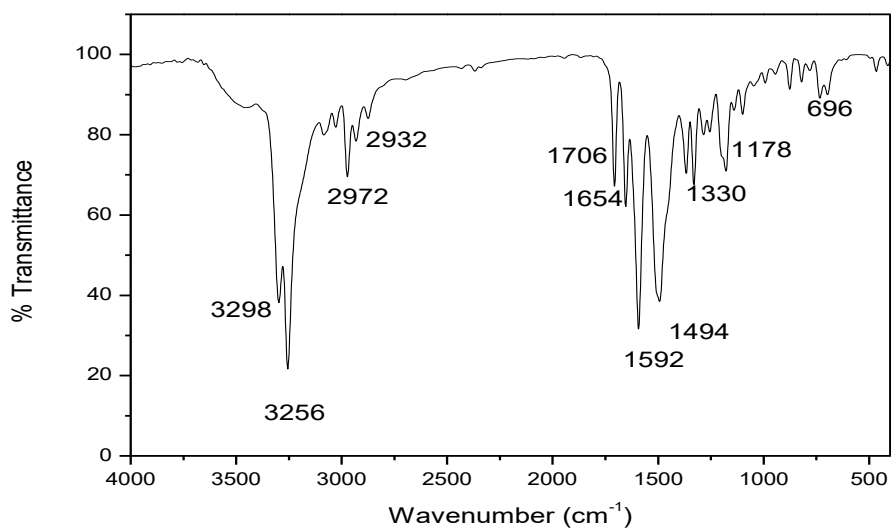
**Figure A3.33.**  $^{13}\text{C}$  NMR spectrum ( $\text{CDCl}_3$ , 100 MHz) of compound **3.13**.



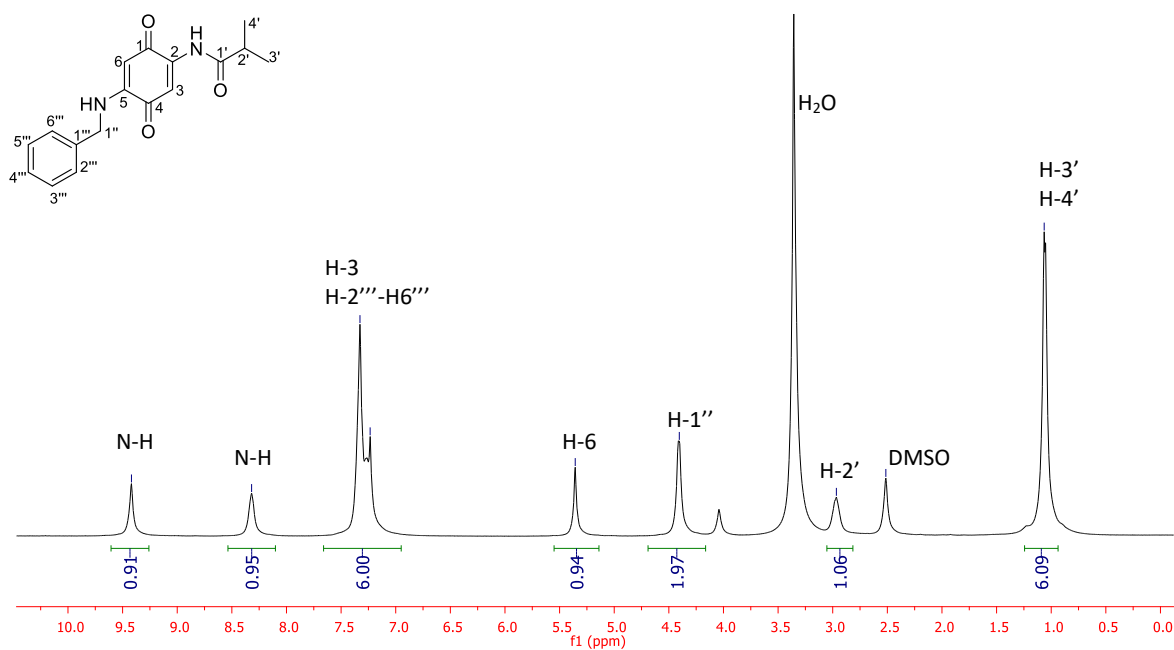
**Figure A3.34.** Infrared spectrum in KBr of compound **3.14**.



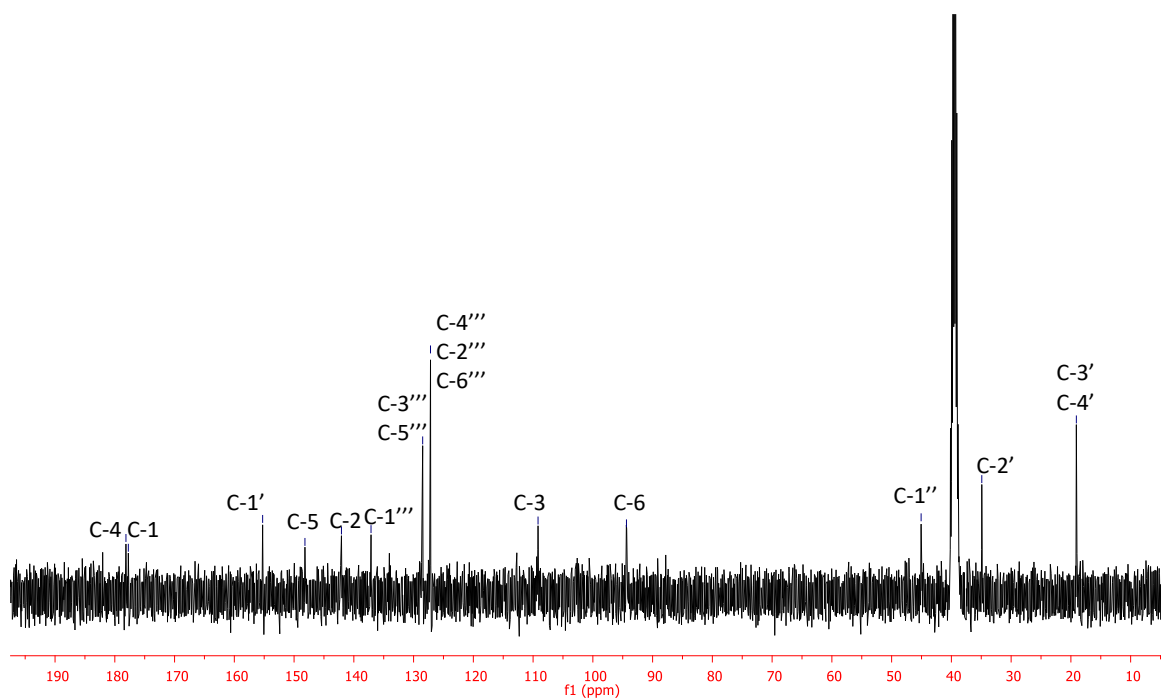




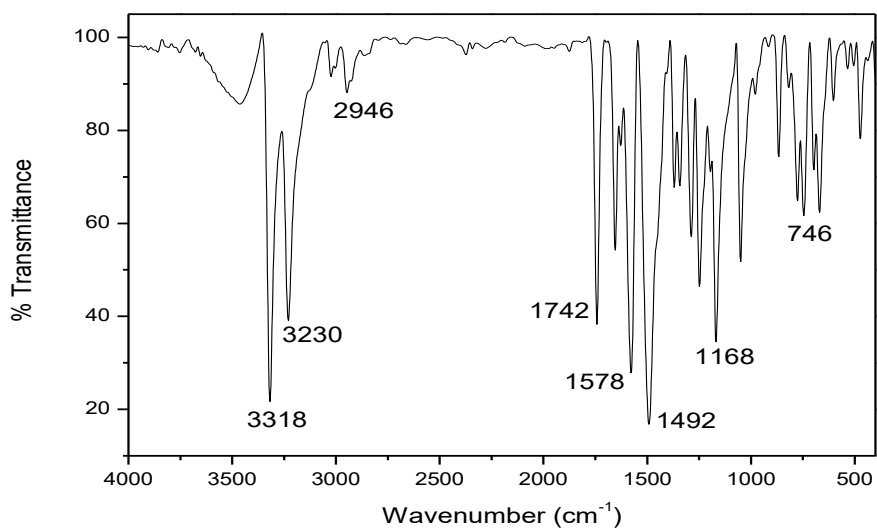
**Figure A3.37.** Infrared spectrum in KBr of compound **3.15**.



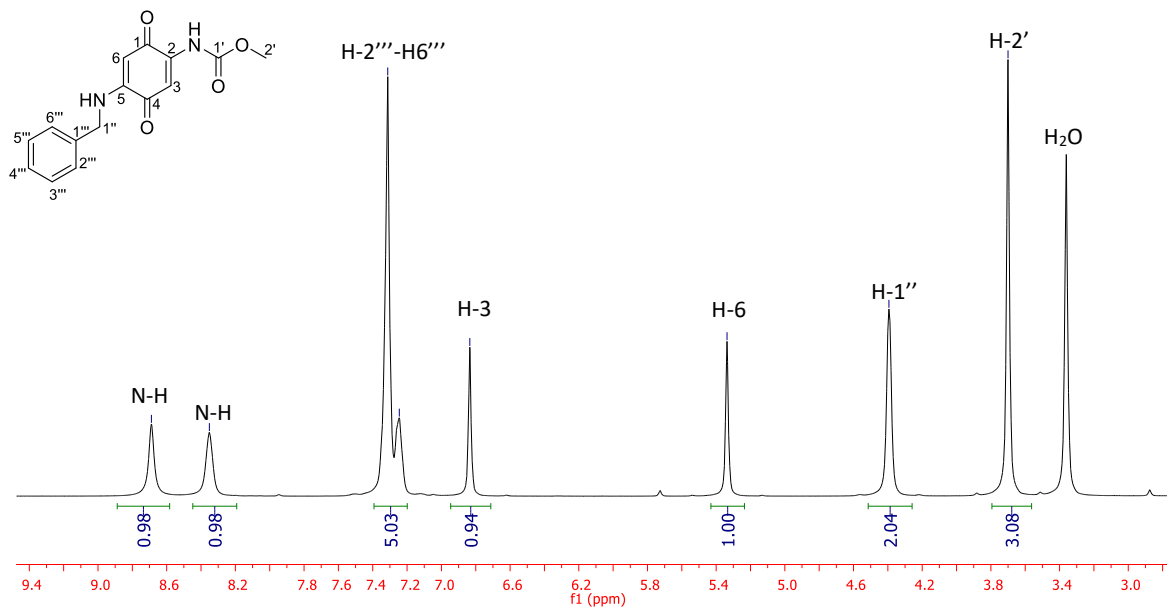
**Figure A3.38.**  $^1\text{H}$  NMR spectrum ( $\text{DMSO-}d_6$ , 400 MHz) of compound **3.15**.



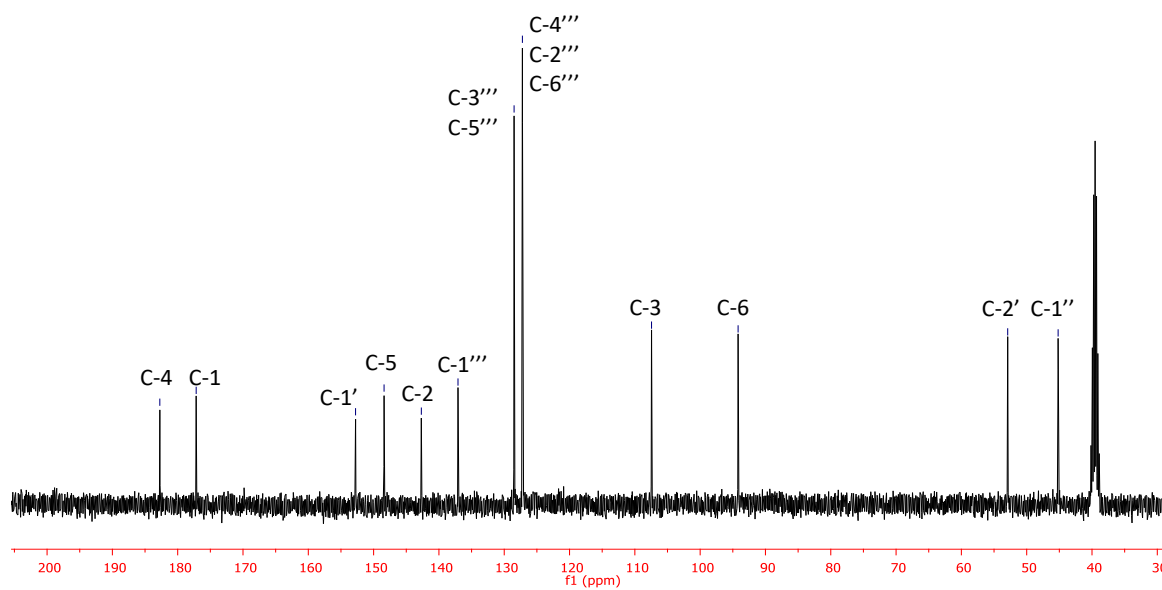
**Figure A3.39.**  $^{13}\text{C}$  NMR spectrum ( $\text{DMSO-}d_6$ , 100 MHz) of compound **3.15**.



**Figure A3.40.** Infrared spectrum in KBr of compound **3.16**.

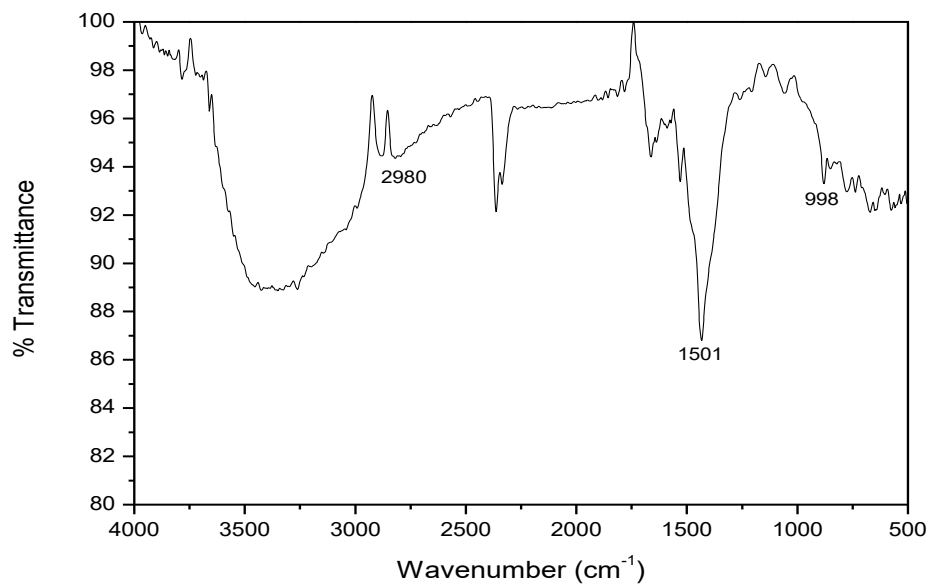


**Figure A3.41.**  $^1\text{H}$  NMR spectrum ( $\text{DMSO-}d_6$ , 400 MHz) of compound 3.16.

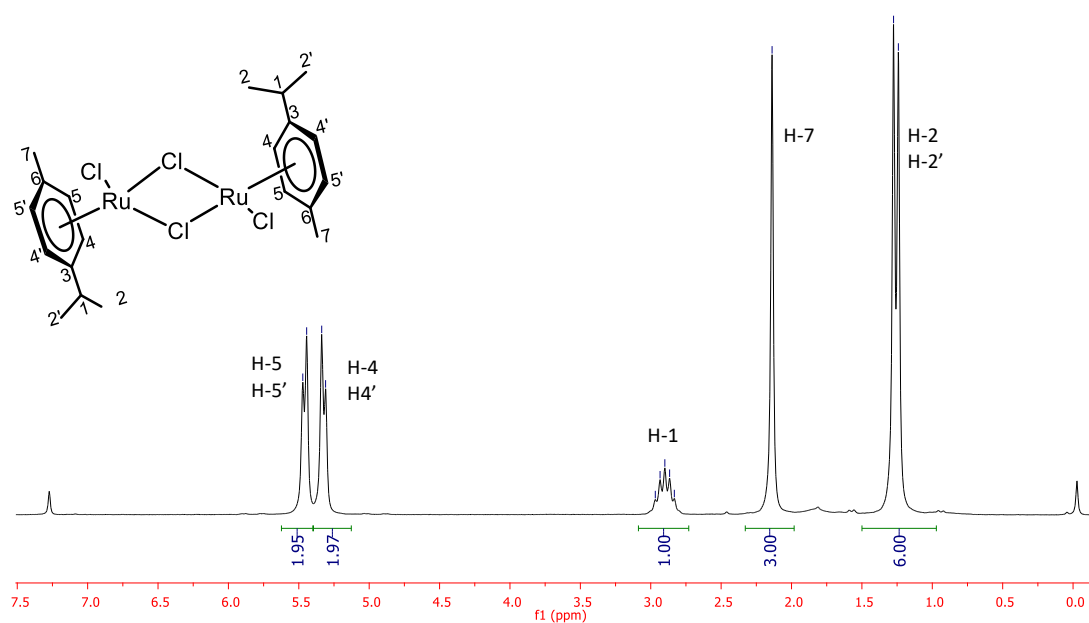


**Figure A3.42.**  $^{13}\text{C}$  NMR spectrum ( $\text{DMSO-}d_6$ , 100 MHz) of compound 3.16.

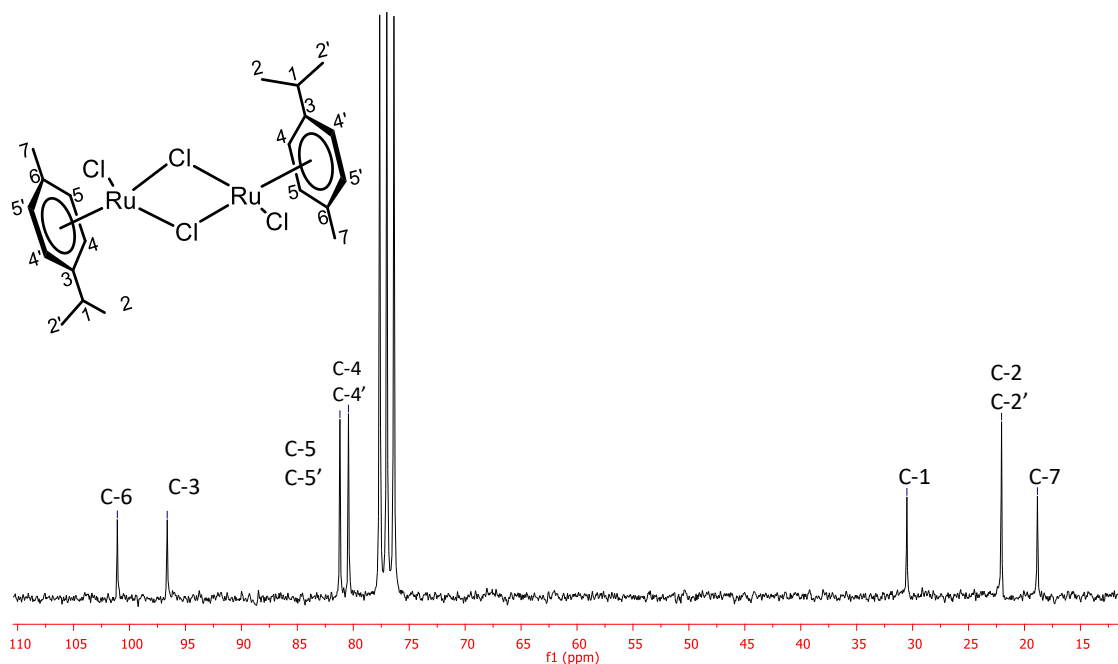
#### 4. Appendix 4: Infrared, $^1\text{H}$ and $^{13}\text{C}$ NMR Spectra of compounds related to Chapter 4



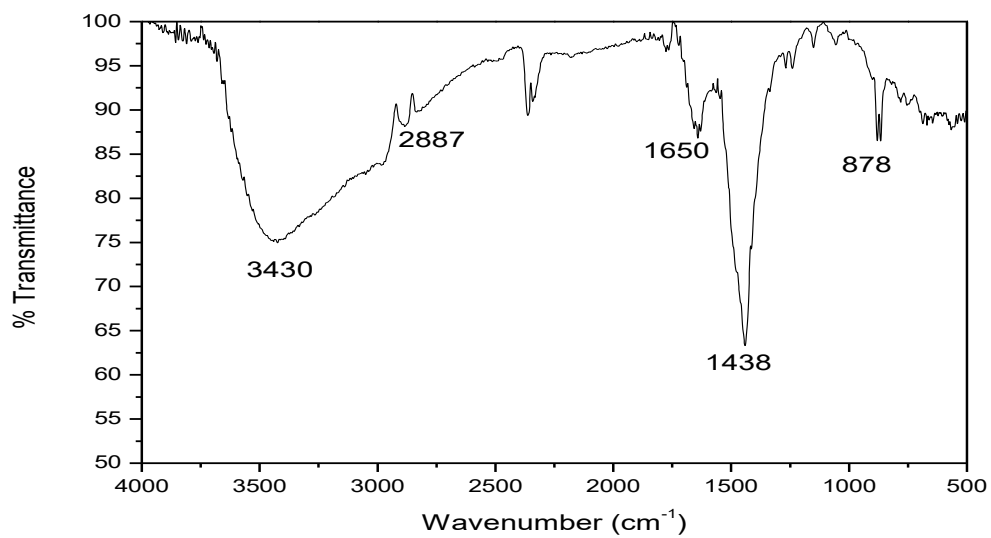
**Figure A4.1.** Infrared spectrum of compound 4.21.



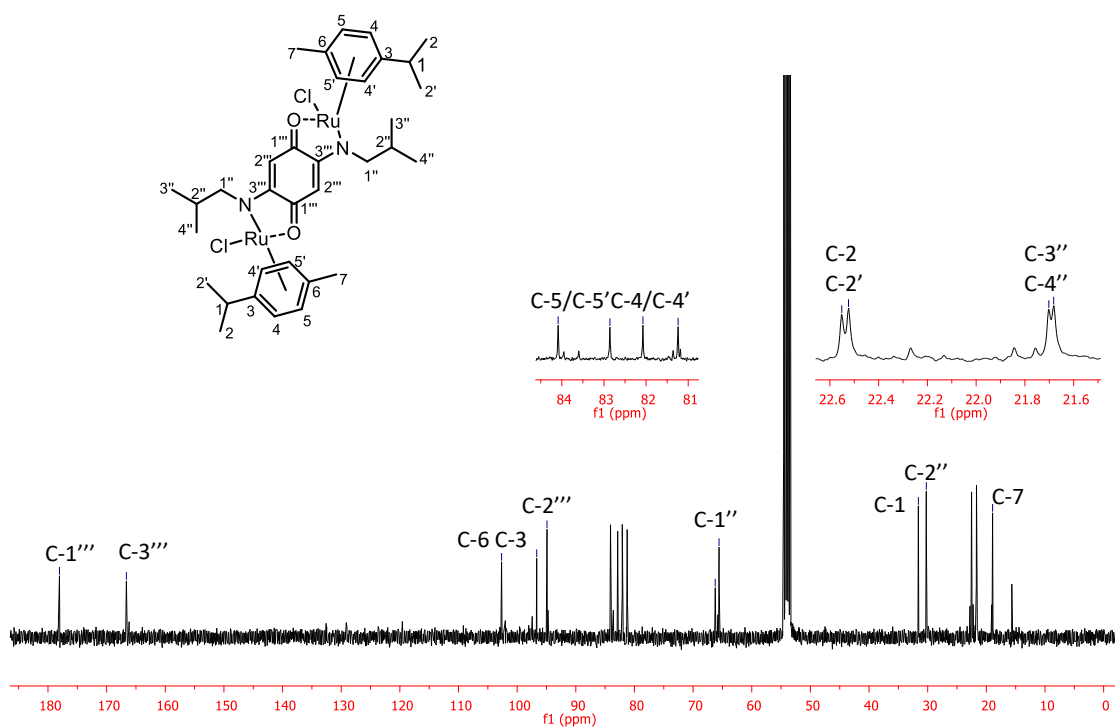
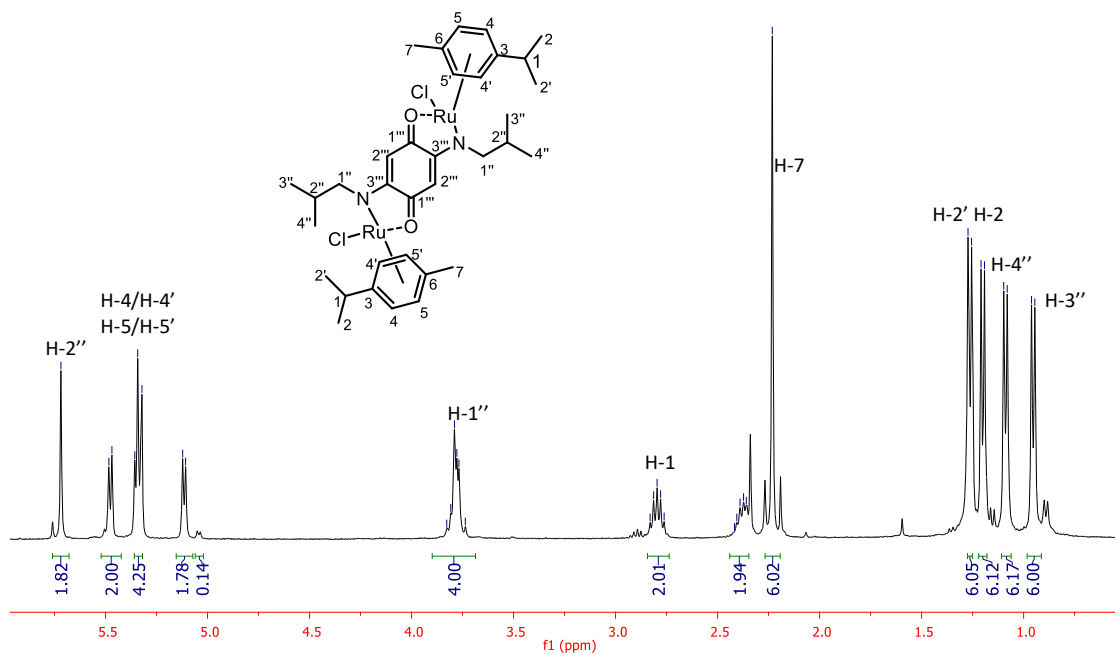
**Figure A4.2.**  $^1\text{H}$  NMR spectrum ( $\text{CDCl}_3$ , 200 MHz) of compound 4.21.



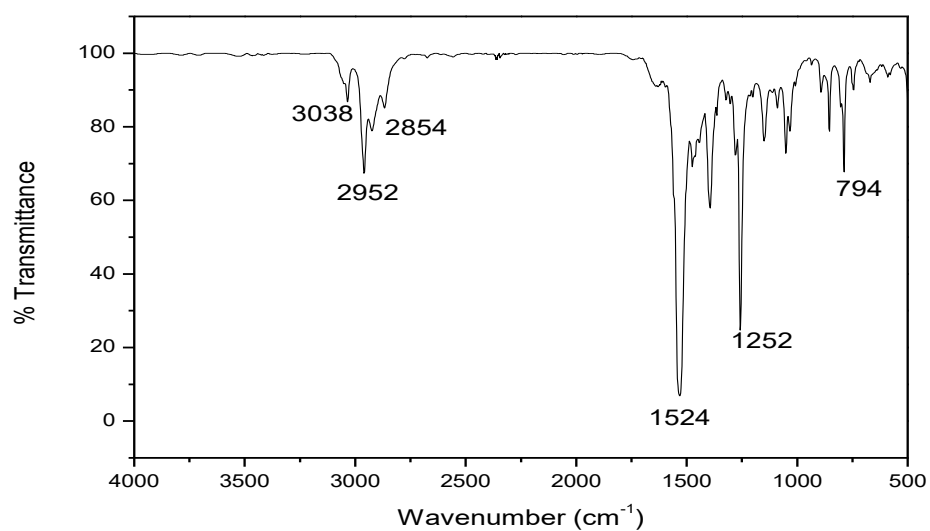
**Figure A4.3.**  $^{13}\text{C}$  NMR spectrum (CDCl<sub>3</sub>, 75 MHz) of compound 4.21.



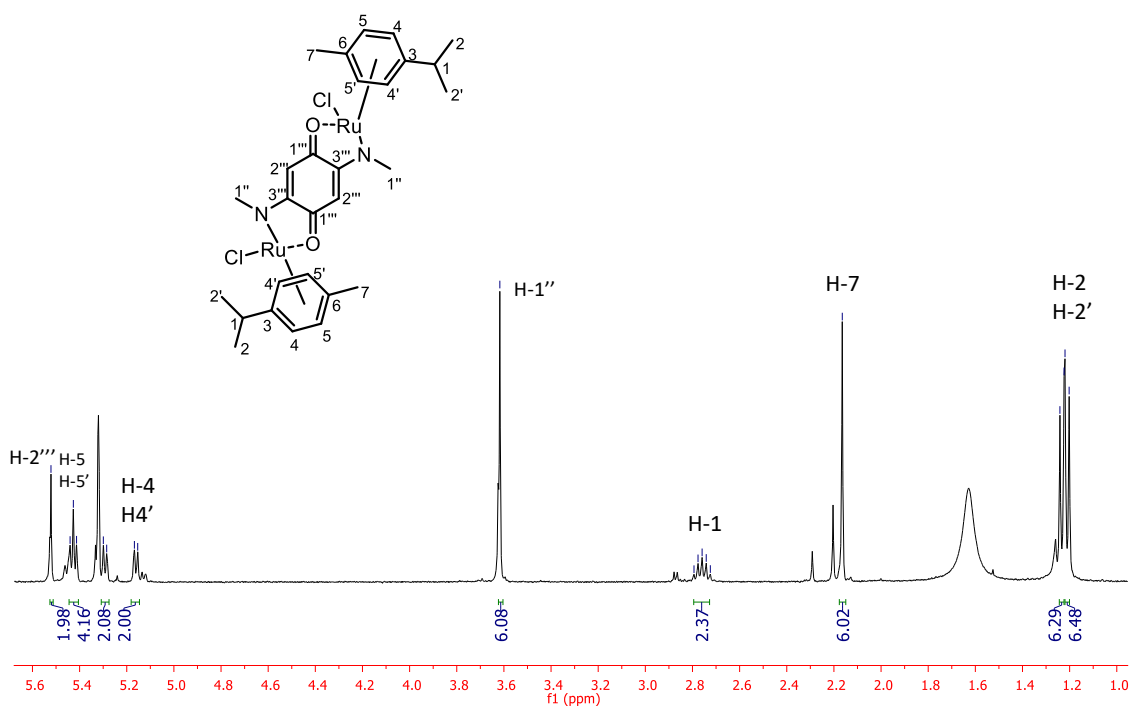
**Figure A4.4.** Infrared spectrum of compound 4.22.



**Figure A4.6.**  $^{13}\text{C}$  NMR spectrum ( $\text{CD}_2\text{Cl}_2$ , 100 MHz) of compound **4.22**.

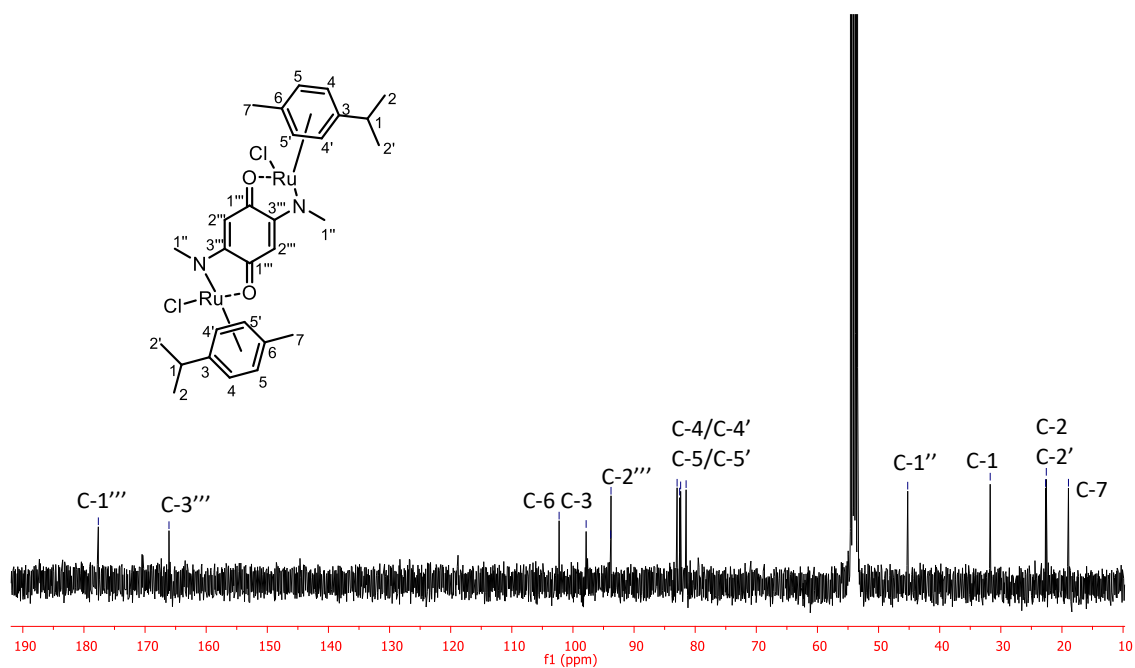


**Figure A4.7.** Infrared spectrum of compound **4.23**.

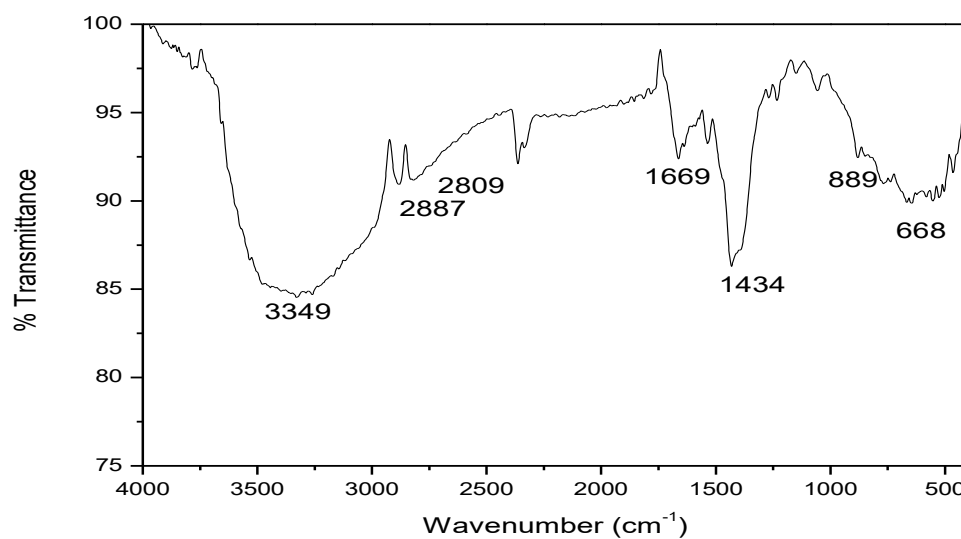


**Figure A4.8.** <sup>1</sup>H NMR spectrum (CD<sub>2</sub>Cl<sub>2</sub>, 400 MHz) of compound **4.23**.





**Figure A4.9.**  $^{13}\text{C}$  NMR spectrum ( $\text{CD}_2\text{Cl}_2$ , 100 MHz) of compound 4.23.



**Figure A4.10.** Infrared spectrum of compound 4.24.

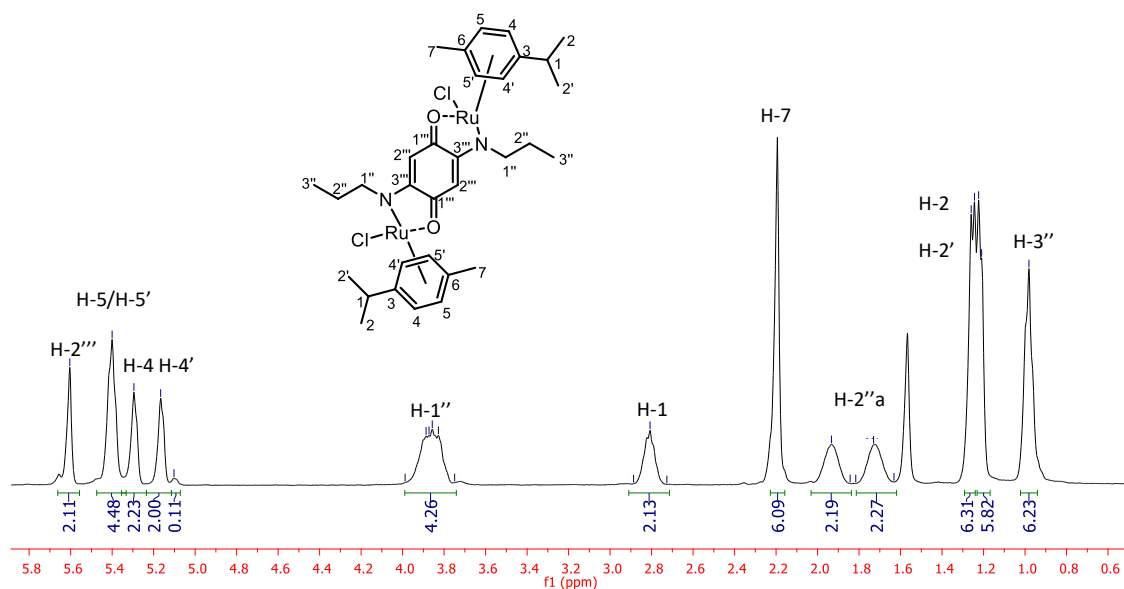


Figure A4.11.  $^1\text{H}$  NMR spectrum ( $\text{CD}_2\text{Cl}_2$ , 400 MHz) of compound 4.24.

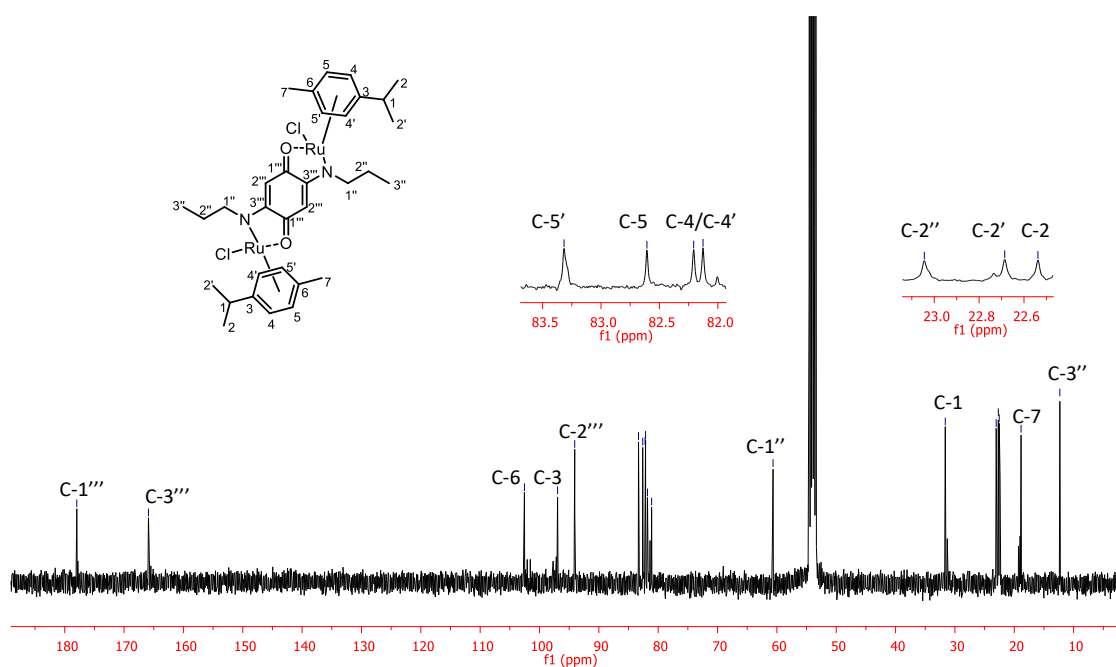
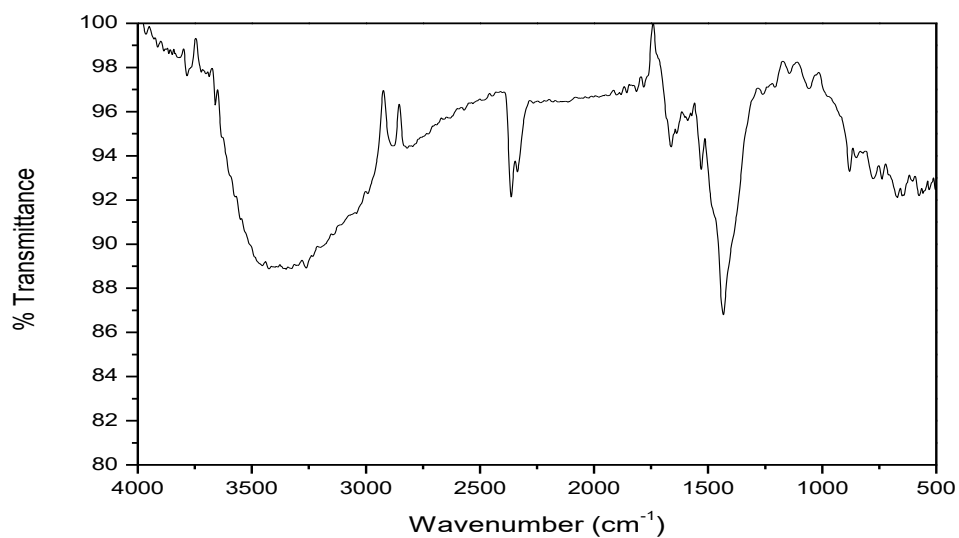
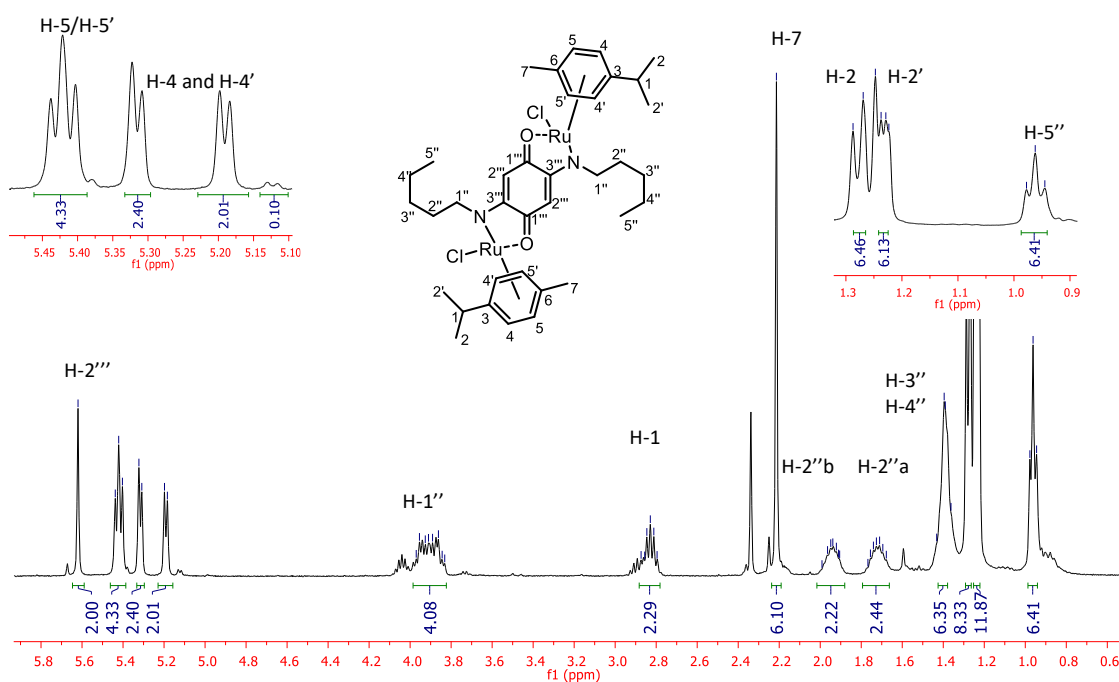


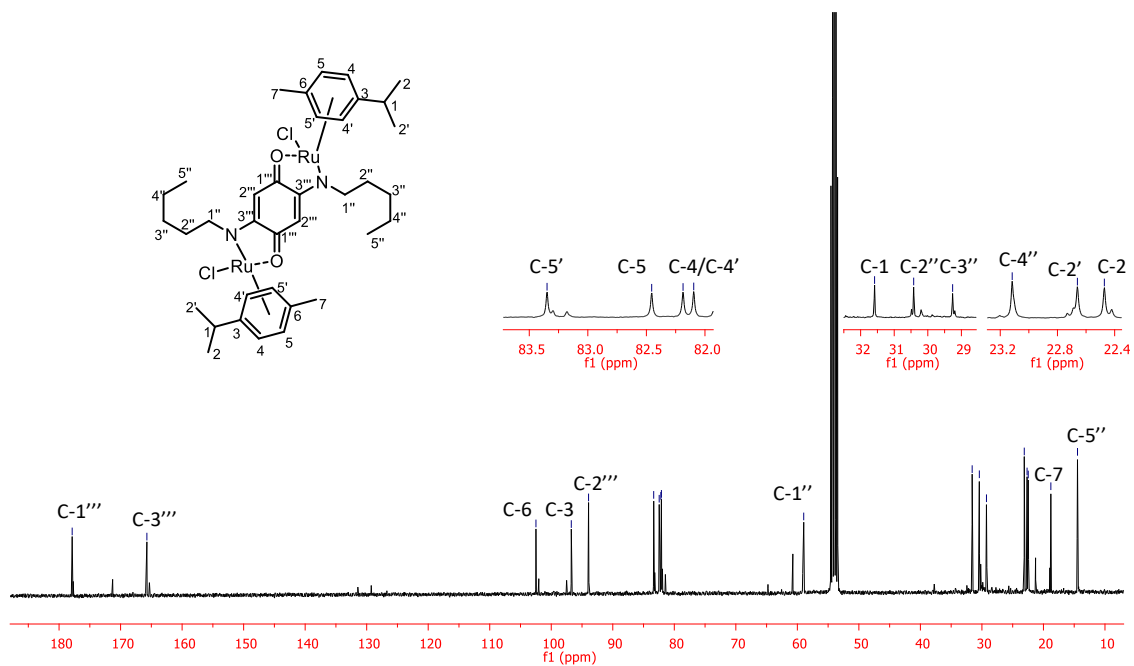
Figure A4.12.  $^{13}\text{C}$  NMR spectrum ( $\text{CD}_2\text{Cl}_2$ , 100 MHz) of compound 4.24.



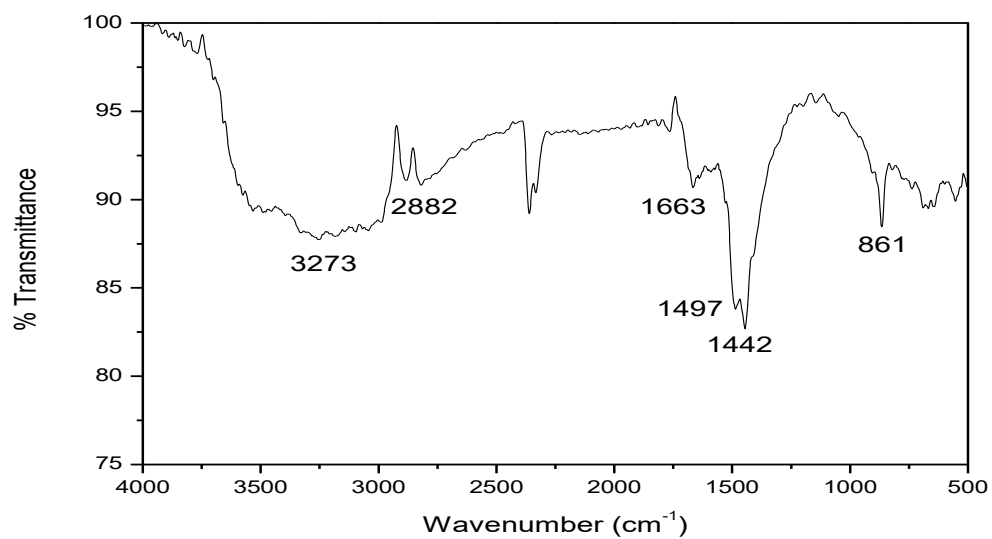
**Figure A4.13.** Infrared spectrum of compound **4.25**.



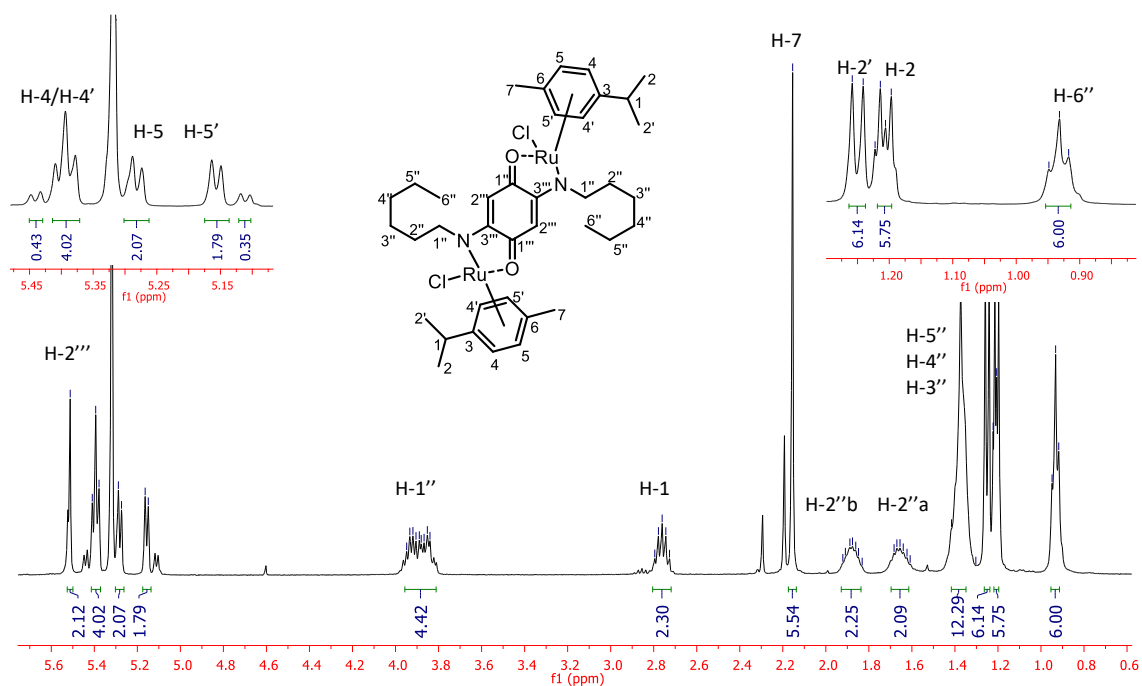
**Figure A4.14.**  $^1\text{H}$  NMR spectrum ( $\text{CD}_2\text{Cl}_2$ , 400 MHz) of compound **4.25**.



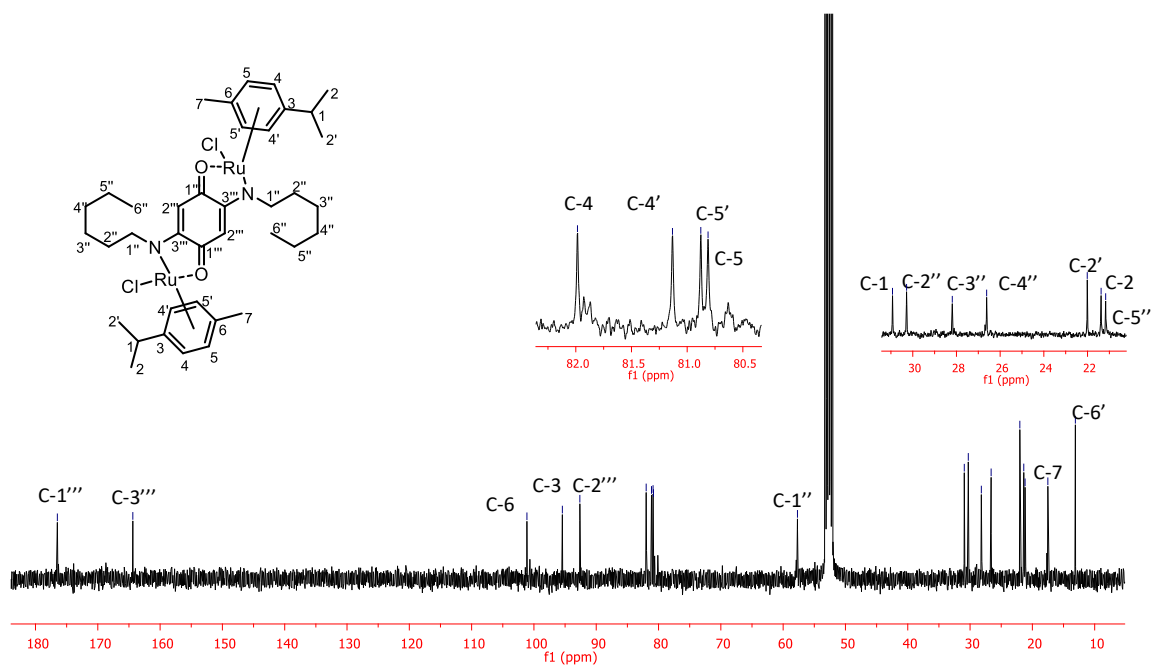
**Figure A4.15.**  $^{13}\text{C}$  NMR spectrum ( $\text{CD}_2\text{Cl}_2$ , 100 MHz) of compound **4.25**.



**Figure A4.16.** Infrared spectrum of compound **4.26**.



**Figure A4.17.**  $^1\text{H}$  NMR spectrum ( $\text{CD}_2\text{Cl}_2$ , 400 MHz) of compound **4.26**.



**Figure A4.18.**  $^{13}\text{C}$  NMR spectrum ( $\text{CD}_2\text{Cl}_2$ , 100 MHz) of compound **4.26**.

5. Appendix 5: Infrared,  $^1\text{H}$  and  $^{13}\text{C}$  NMR Spectra of compounds related to Chapter 5

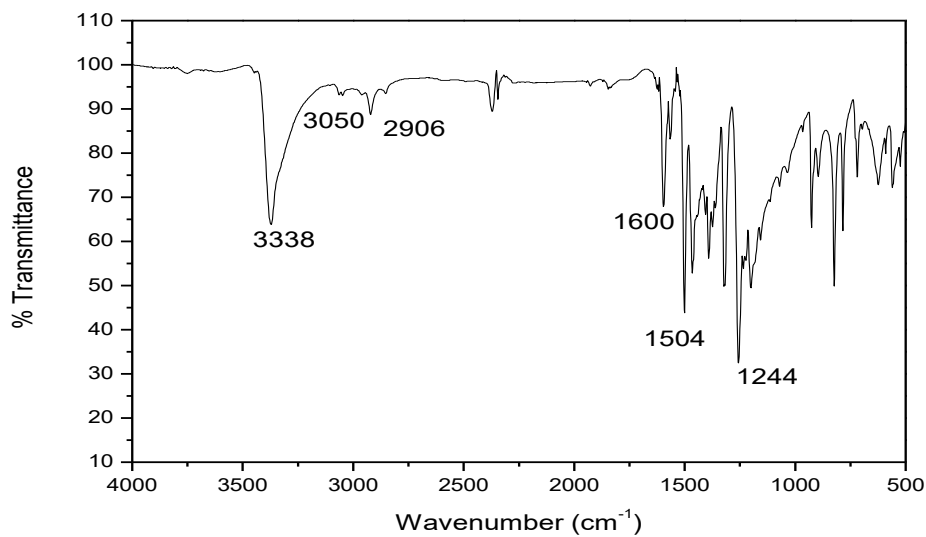


Figure A5.1. Infrared spectrum in KBr of compound 5.2.

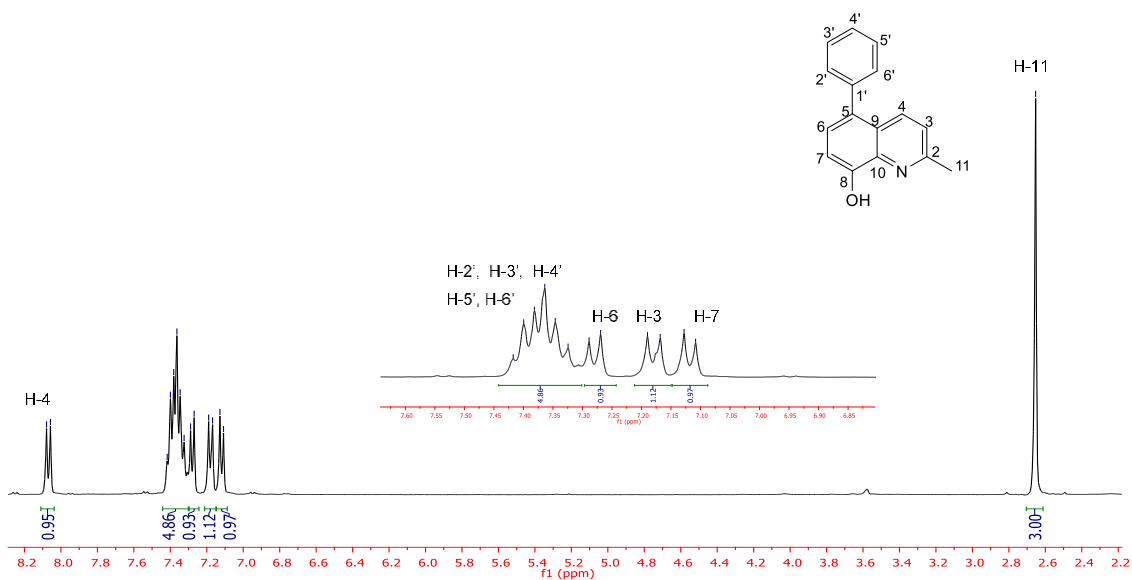
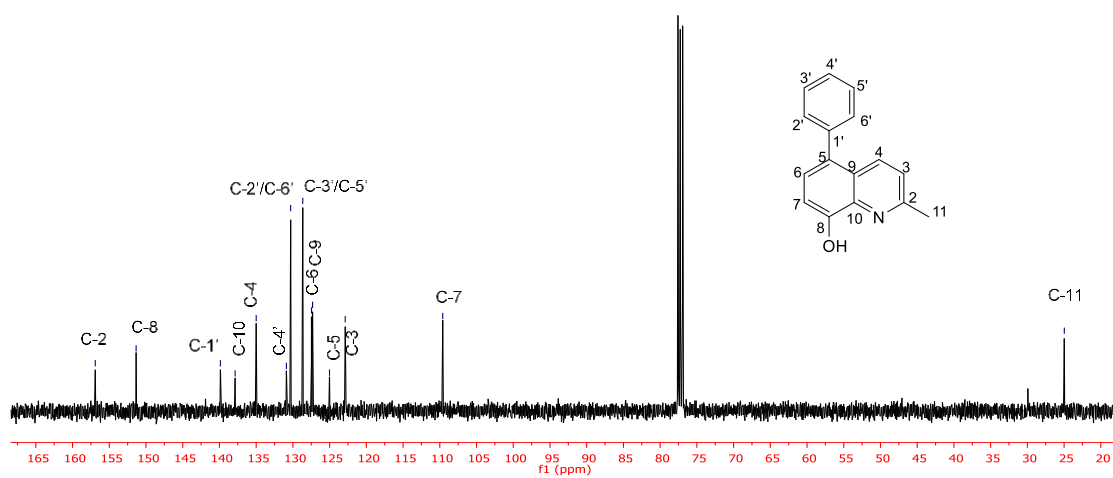
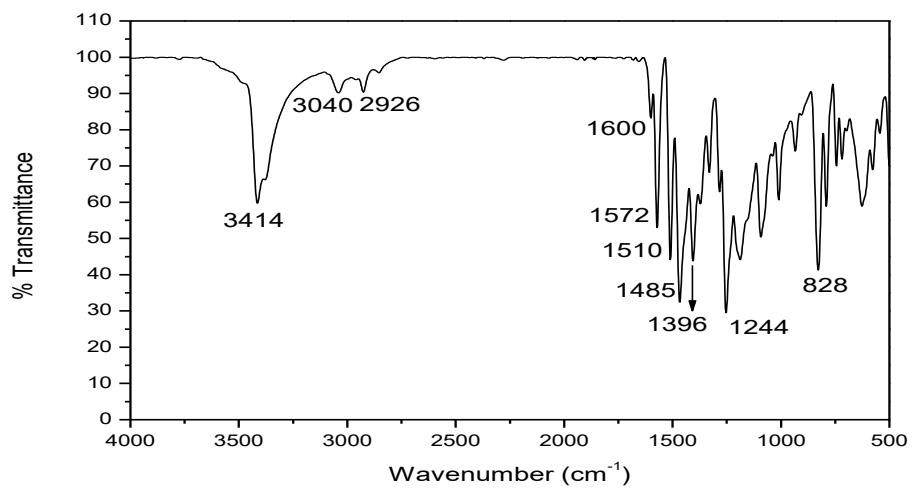


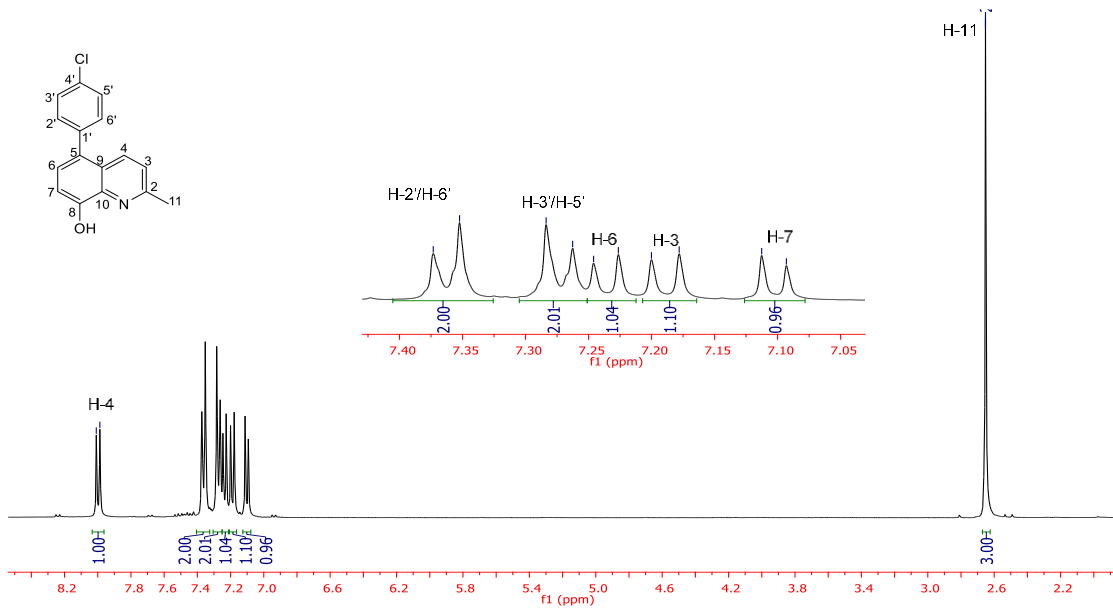
Figure A5.2.  $^1\text{H}$  NMR spectrum (400 MHz,  $\text{CDCl}_3$ ) of compound 5.2.



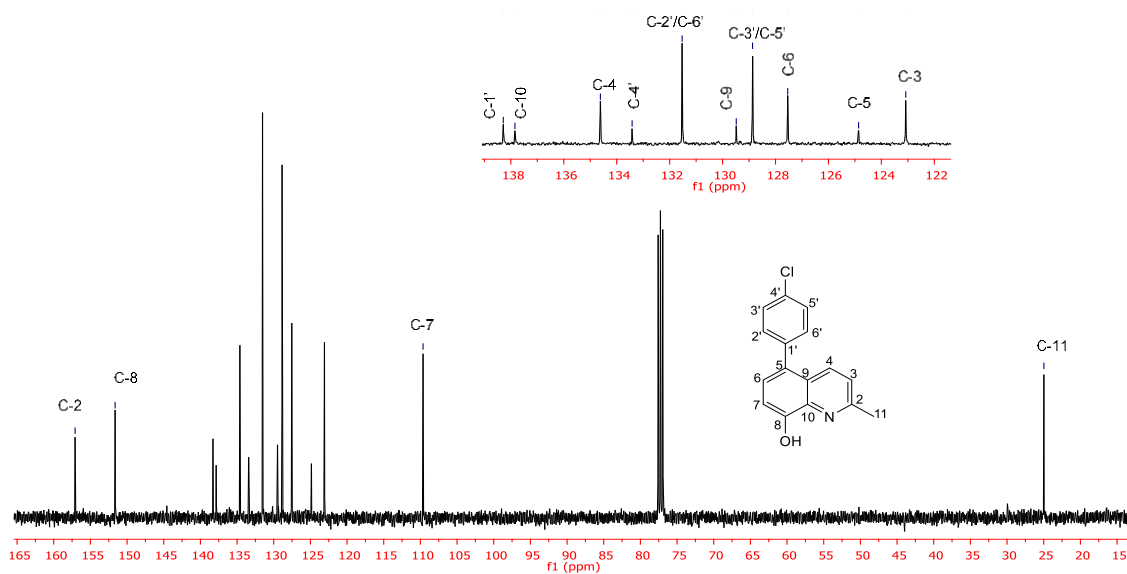
**Figure A5.3.**  $^{13}\text{C}$  NMR spectrum (100 MHz,  $\text{CDCl}_3$ ) of compound **5.2**.



**Figure A5.4.** Infrared spectrum in KBr of compound **5.3**.

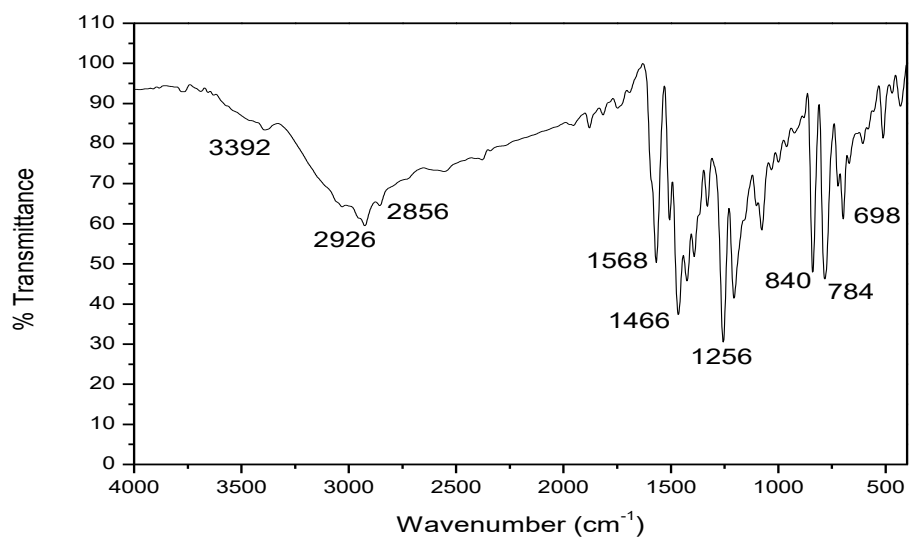


**Figure A5.5.**  $^1\text{H}$  NMR spectrum (400 MHz,  $\text{CDCl}_3$ ) of compound 5.3.

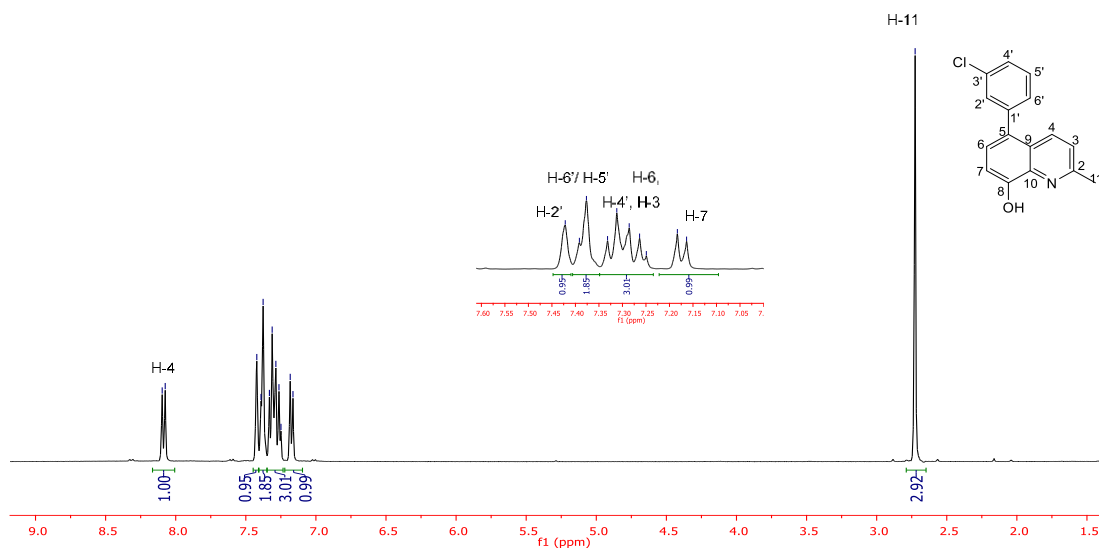


**Figure A5.6.**  $^{13}\text{C}$  NMR spectrum (100 MHz,  $\text{CDCl}_3$ ) of compound 5.3.

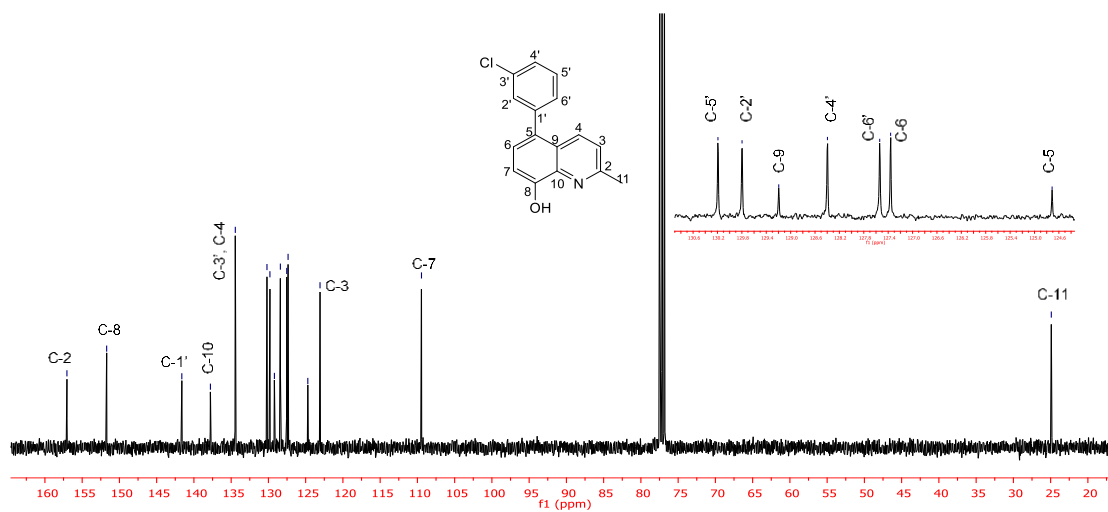




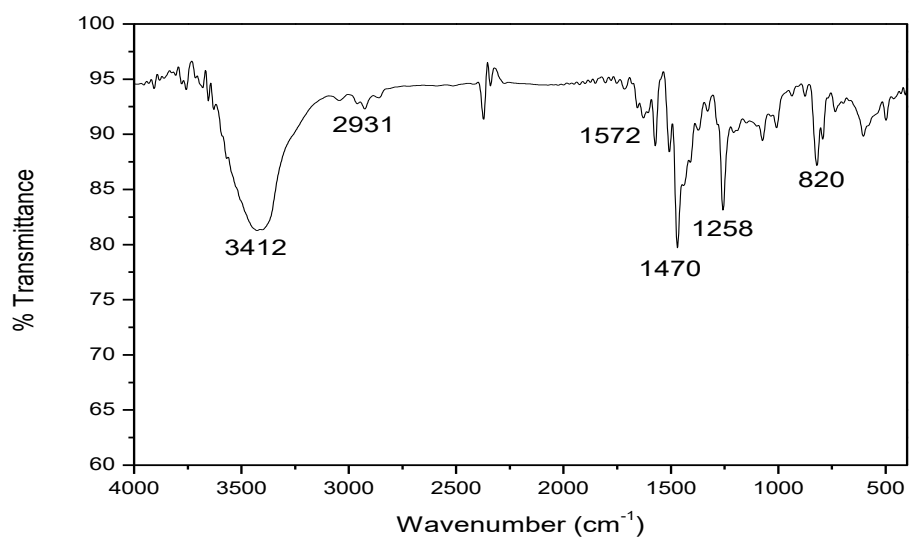
**Figure A5.7.** Infrared spectrum in KBr of compound **5.4**.



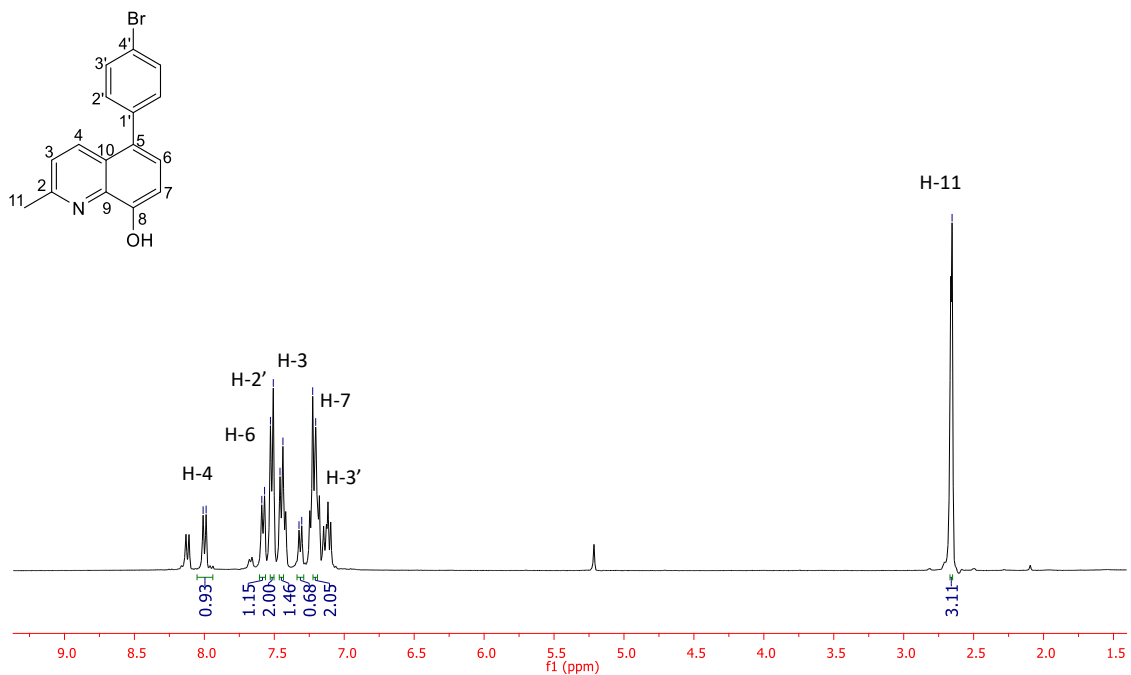
**Figure A5.8.** <sup>1</sup>H NMR spectrum (400 MHz, CDCl<sub>3</sub>) of compound **5.4**.



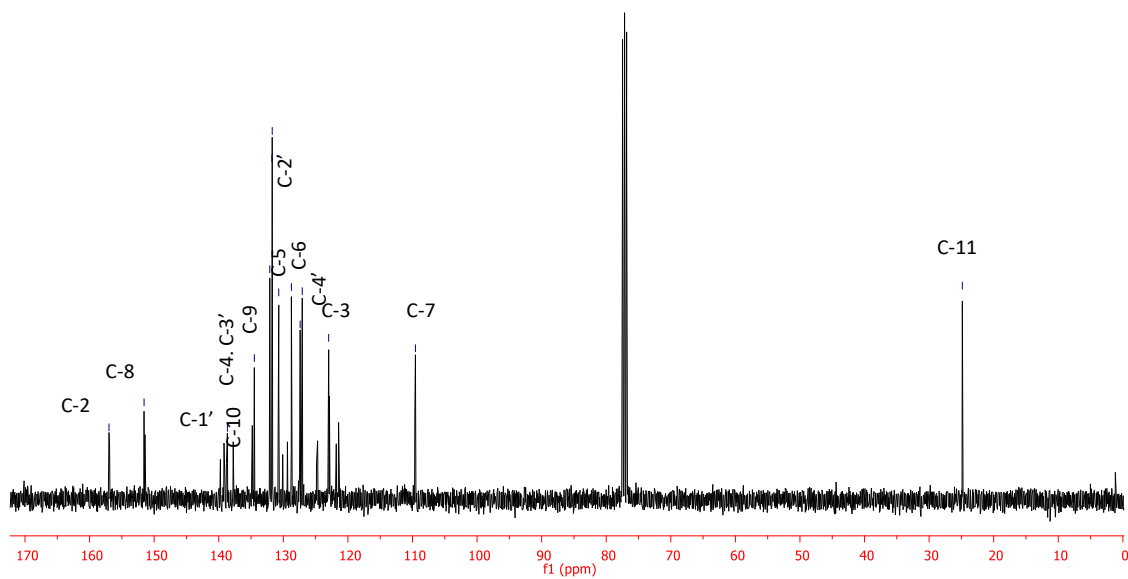
**Figure A5.9.**  $^{13}\text{C}$  NMR spectrum (100 MHz,  $\text{CDCl}_3$ ) of compound 5.4.



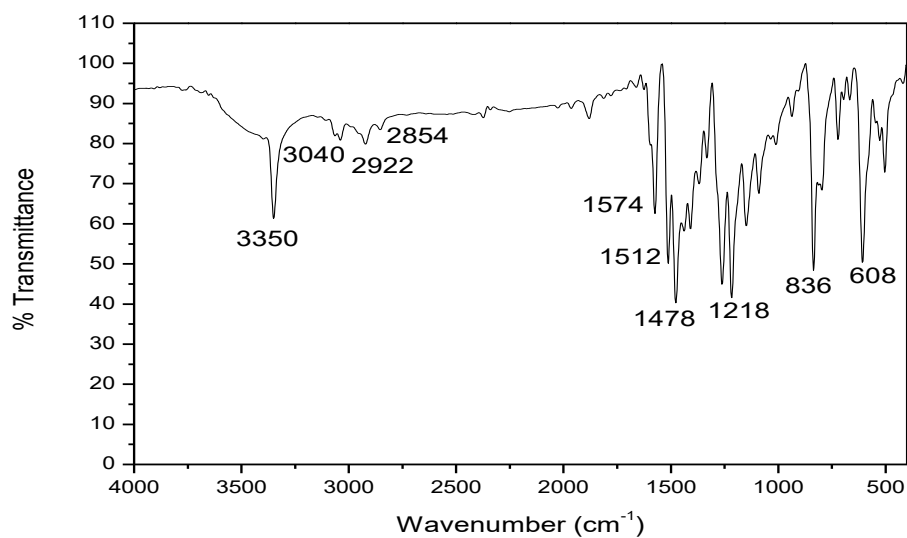
**Figure A5.10.** Infrared spectrum in KBr of compound 5.5.



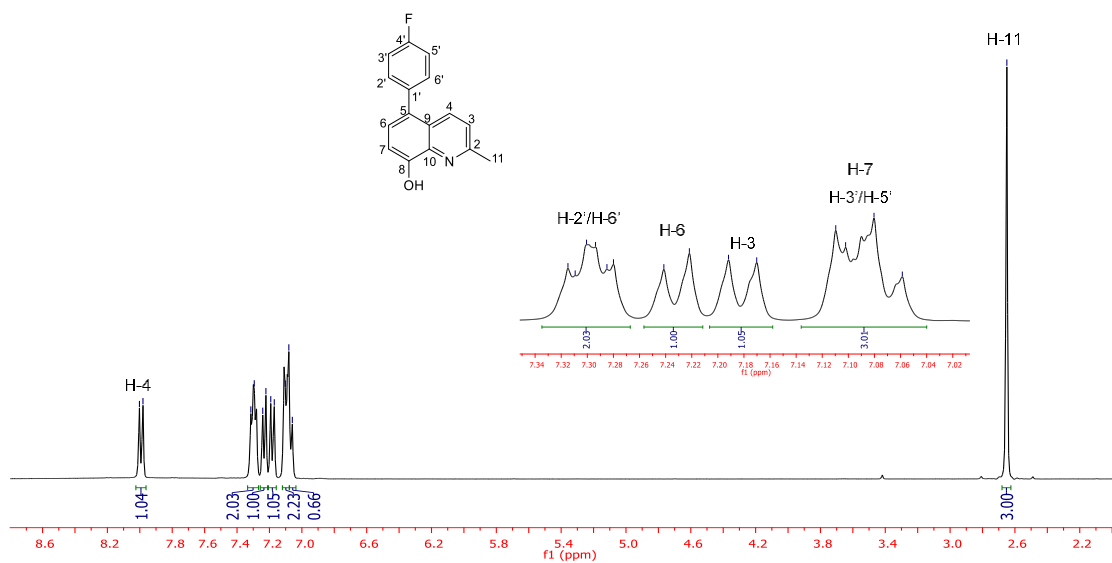
**Figure A5.11.**  $^1\text{H}$  NMR spectrum (400 MHz,  $\text{CDCl}_3$ ) of compound 5.5.



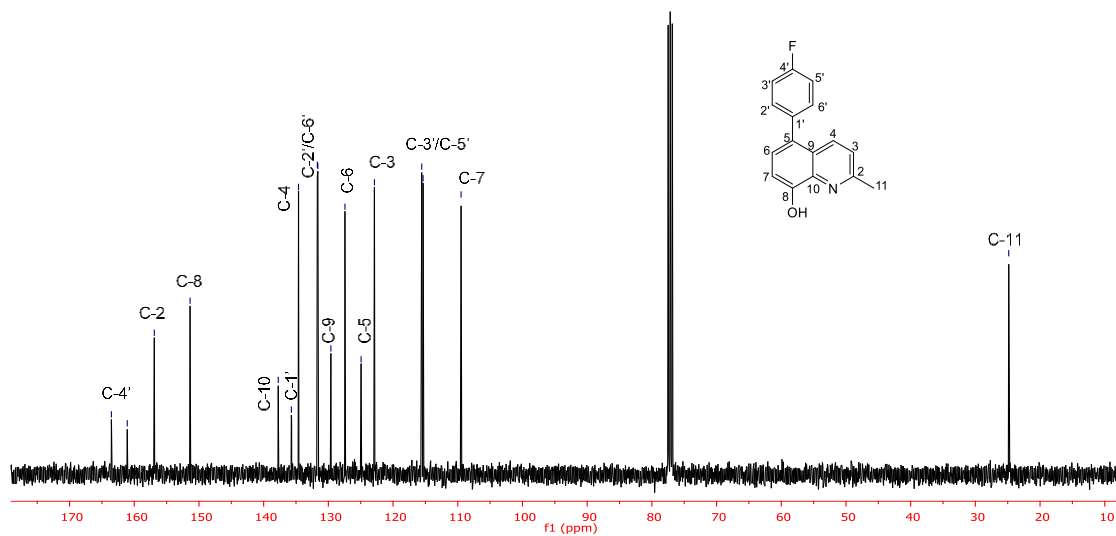
**Figure A5.12.**  $^{13}\text{C}$  NMR spectrum (100 MHz,  $\text{CDCl}_3$ ) of compound 5.5.



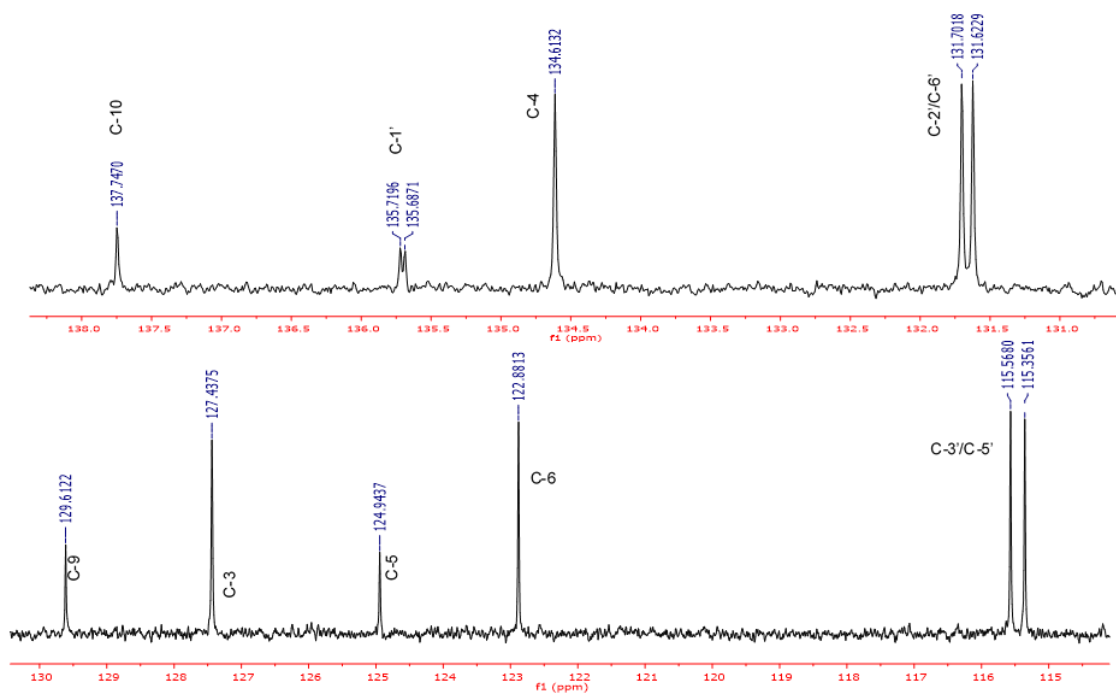
**Figure A5.13.** Infrared spectrum in KBr of compound **5.6**.



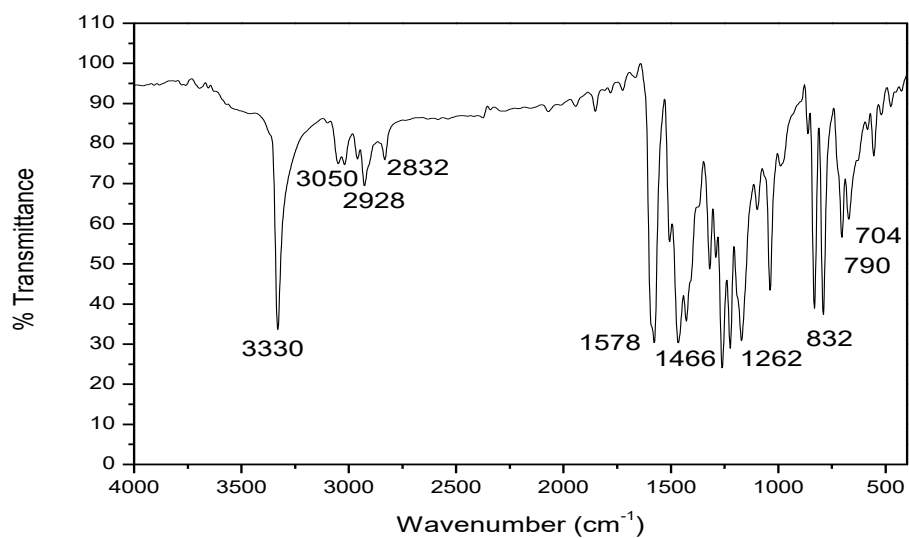
**Figure A5.14.**  $^1\text{H}$  NMR spectrum (400 MHz,  $\text{CDCl}_3$ ) of compound **5.6**.



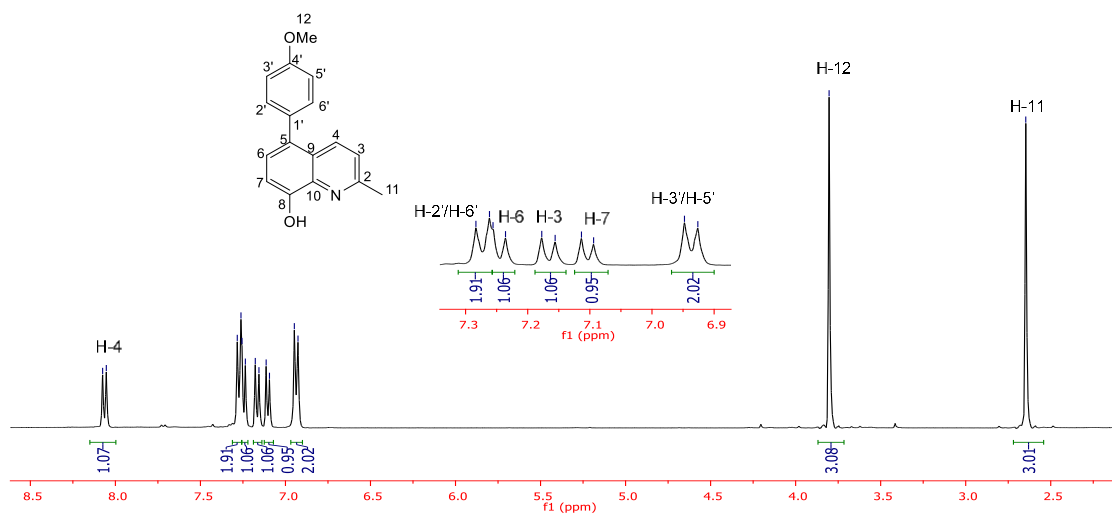
**Figure A5.15.**  $^{13}\text{C}$  NMR spectrum (100 MHz,  $\text{CDCl}_3$ ) of compound **5.6**.



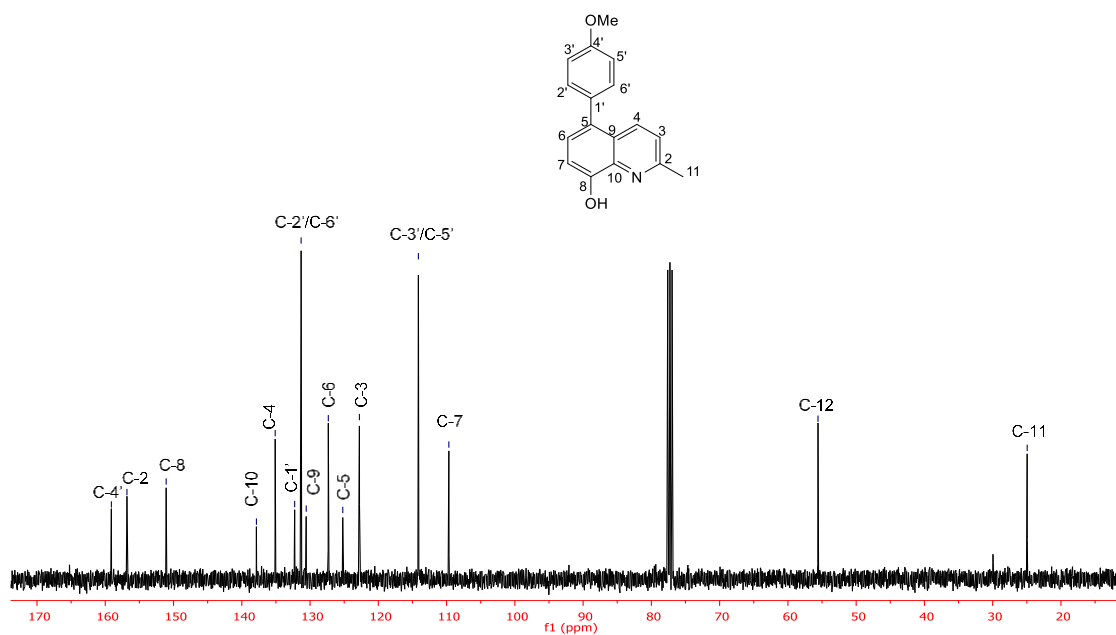
**Figure A5.16.**  $^{13}\text{C}$  NMR expansion of compound **5.6**.



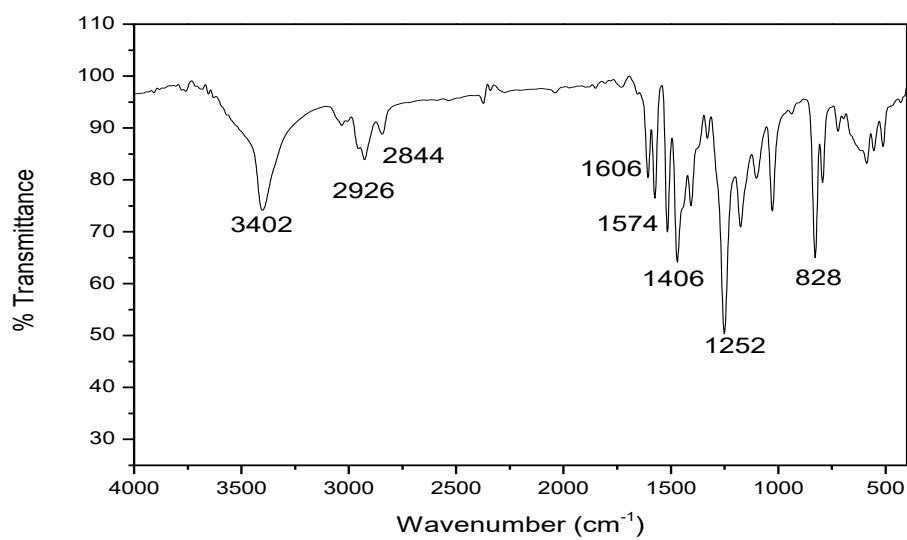
**Figure A5.17.** Infrared spectrum in KBr of compound **5.7**.



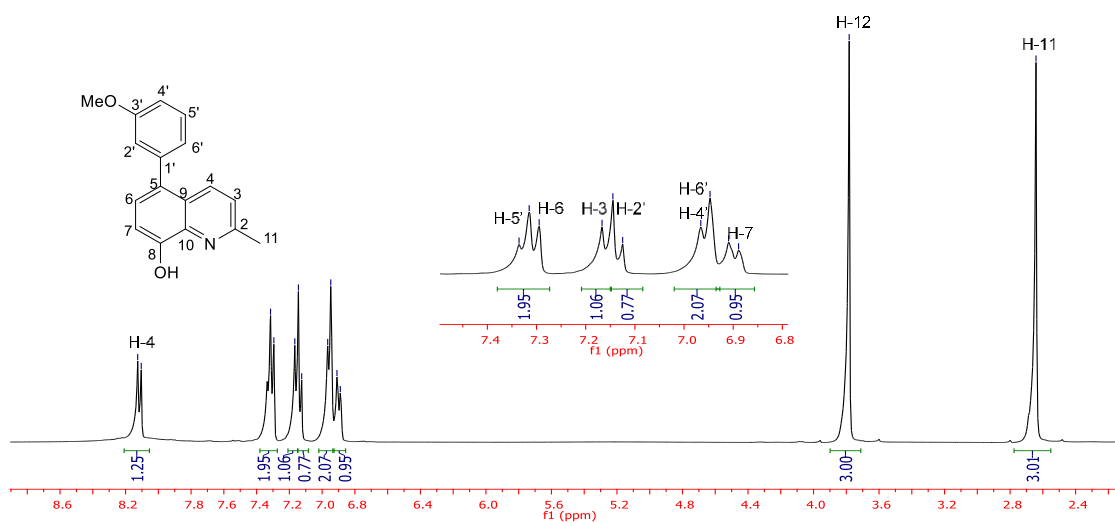
**Figure A5.18.** <sup>1</sup>H NMR spectrum (400 MHz, CDCl<sub>3</sub>) of compound **5.7**.



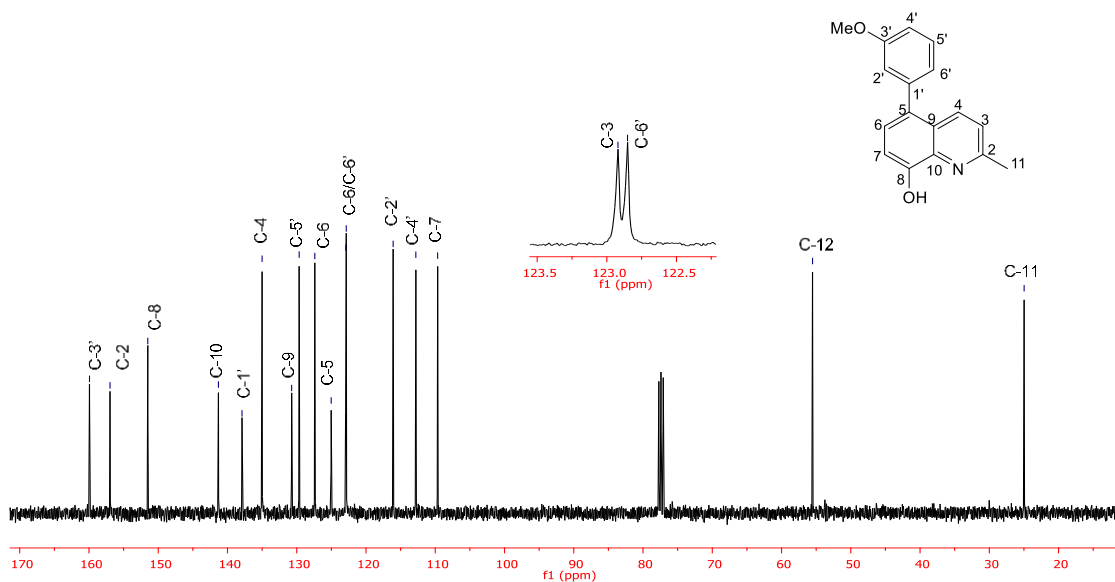
**Figure A5.19.**  $^{13}\text{C}$  NMR spectrum (100 MHz,  $\text{CDCl}_3$ ) of compound 5.7.



**Figure A5.20.** Infrared spectrum in KBr of compound 5.8.

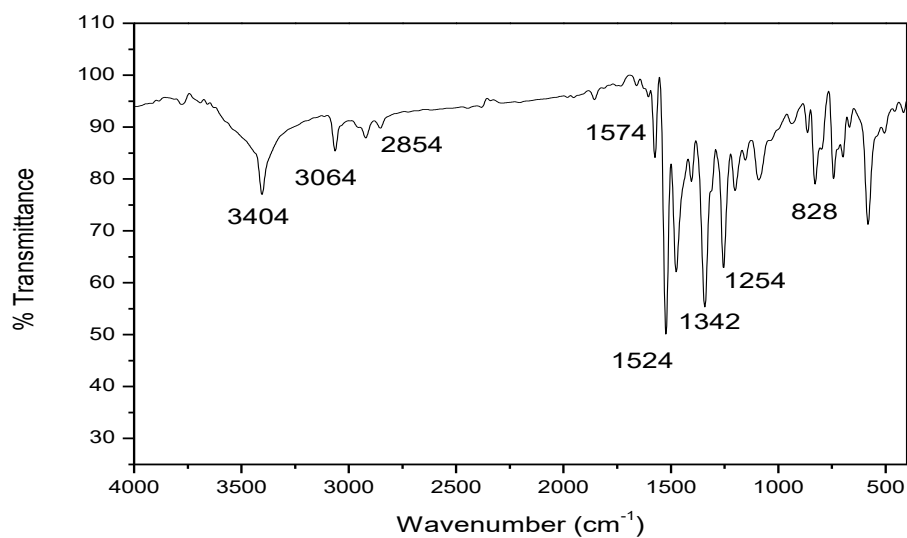


**Figure A5.21.** <sup>1</sup>H NMR spectrum (400 MHz, CDCl<sub>3</sub>) of compound 5.8.

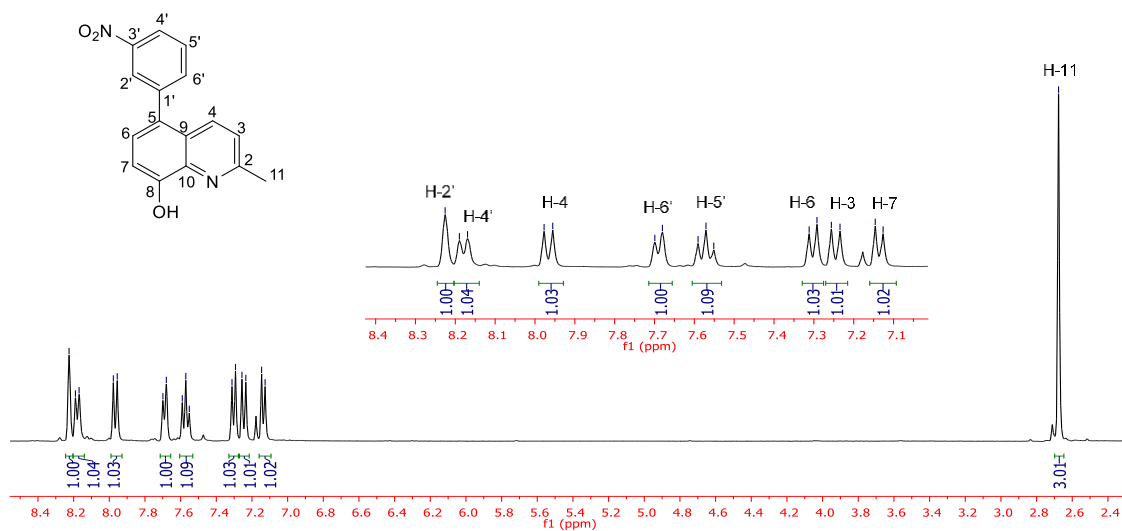


**Figure A5.22.** <sup>13</sup>C NMR spectrum (100 MHz, CDCl<sub>3</sub>) of compound 5.8.

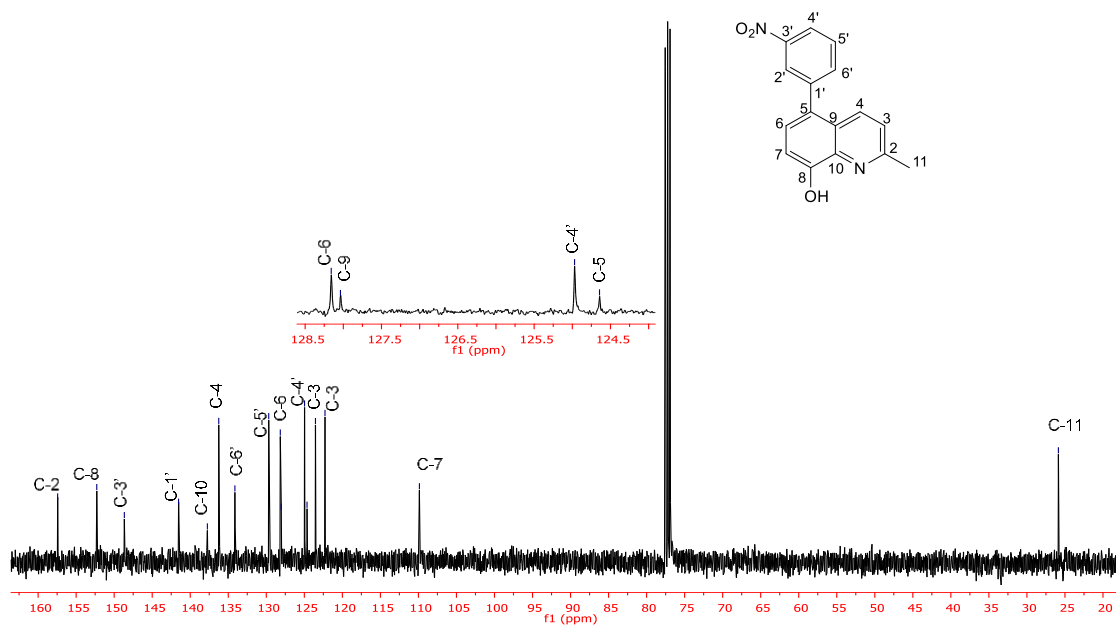




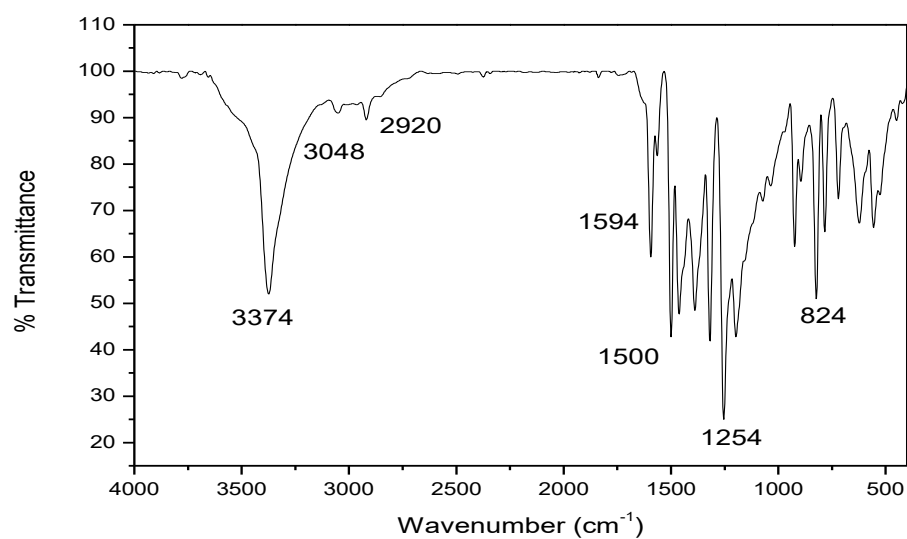
**Figure A5.23.** Infrared spectrum in KBr of compound **5.9**.



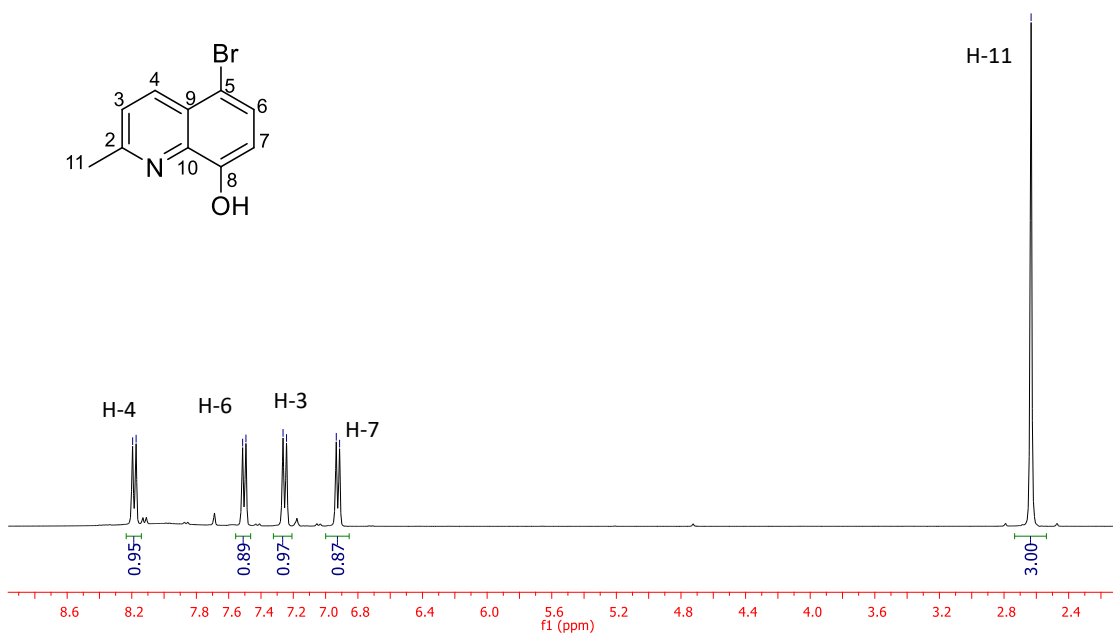
**Figure A5.24.** <sup>1</sup>H NMR spectrum (400 MHz, CDCl<sub>3</sub>) of compound **5.9**.



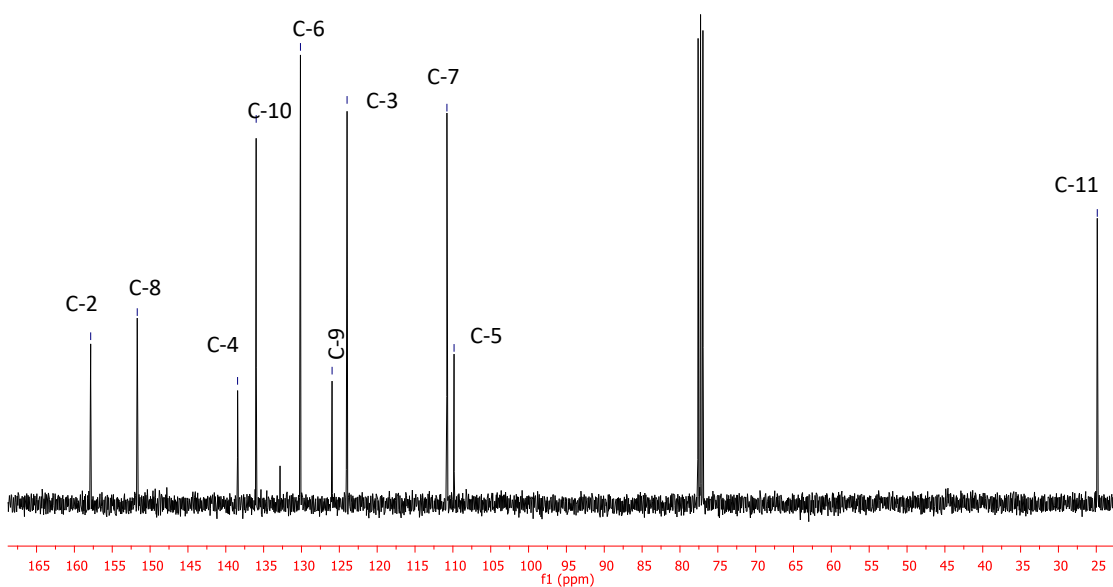
**Figure A5.25.**  $^{13}\text{C}$  NMR spectrum (100 MHz,  $\text{CDCl}_3$ ) of compound **5.9**.



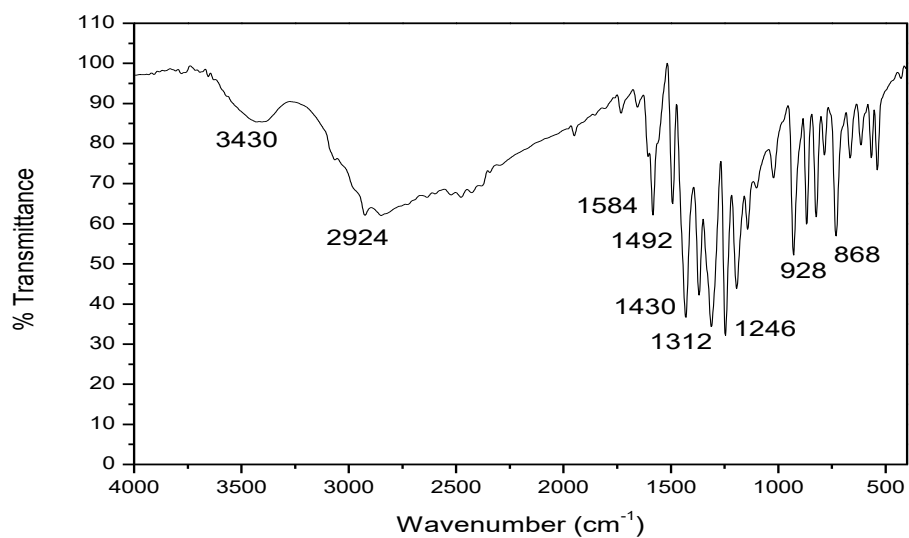
**Figure A5.26.** Infrared spectrum in KBr of compound **5.10**.



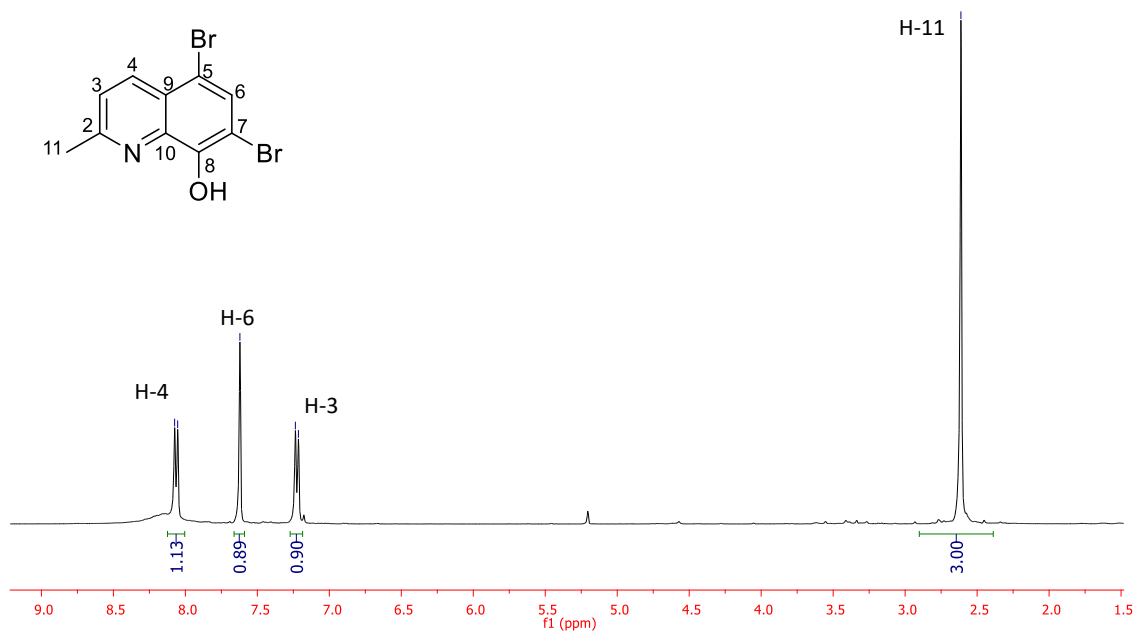
**Figure A5.27.** <sup>1</sup>H NMR spectrum (400 MHz, CDCl<sub>3</sub>) of compound 5.10.



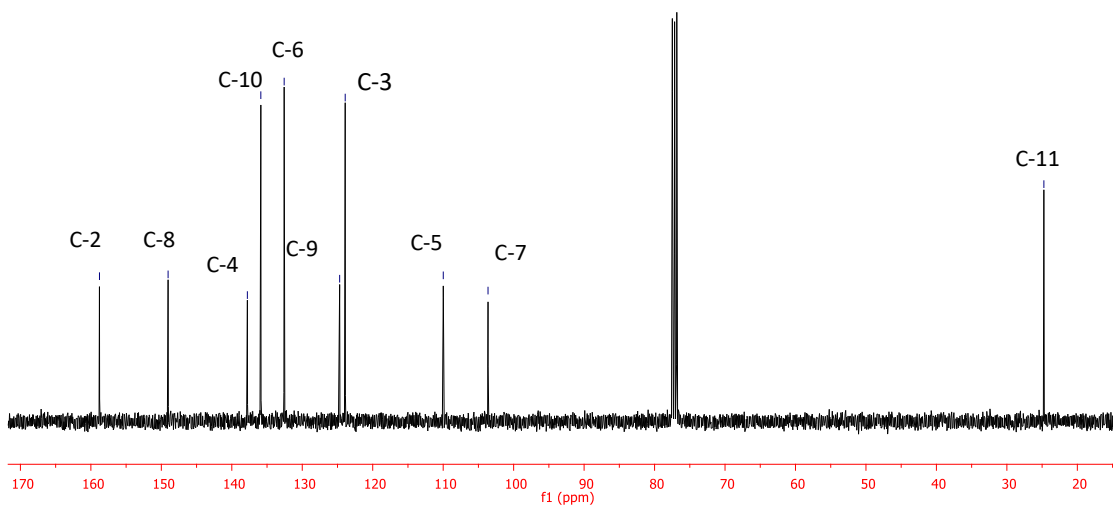
**Figure A5.28.** <sup>13</sup>C NMR spectrum (100 MHz, CDCl<sub>3</sub>) of compound 5.10.



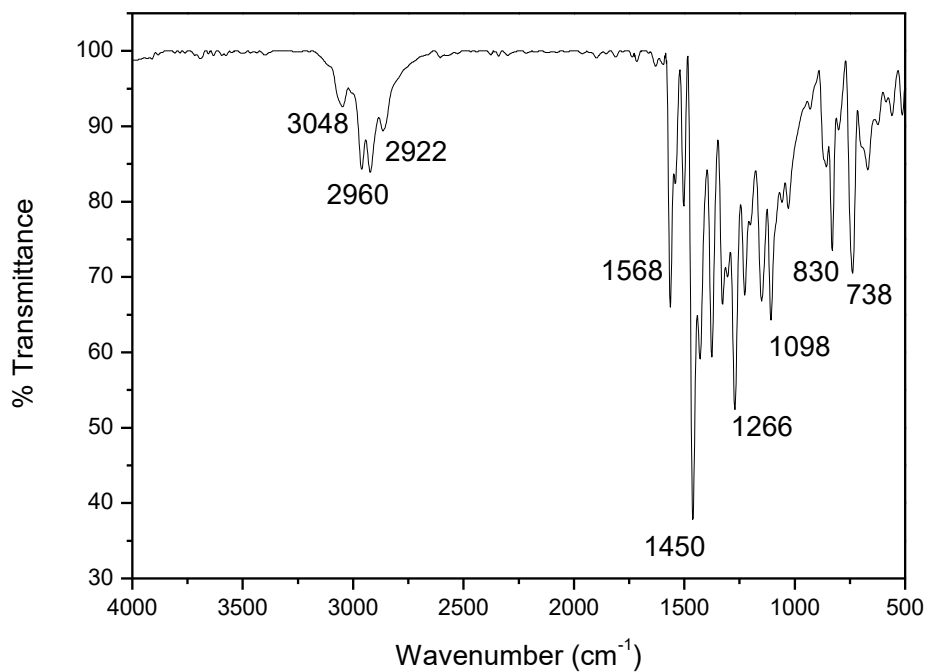
**Figure A5.29.** Infrared spectrum in KBr of compound **5.11**.



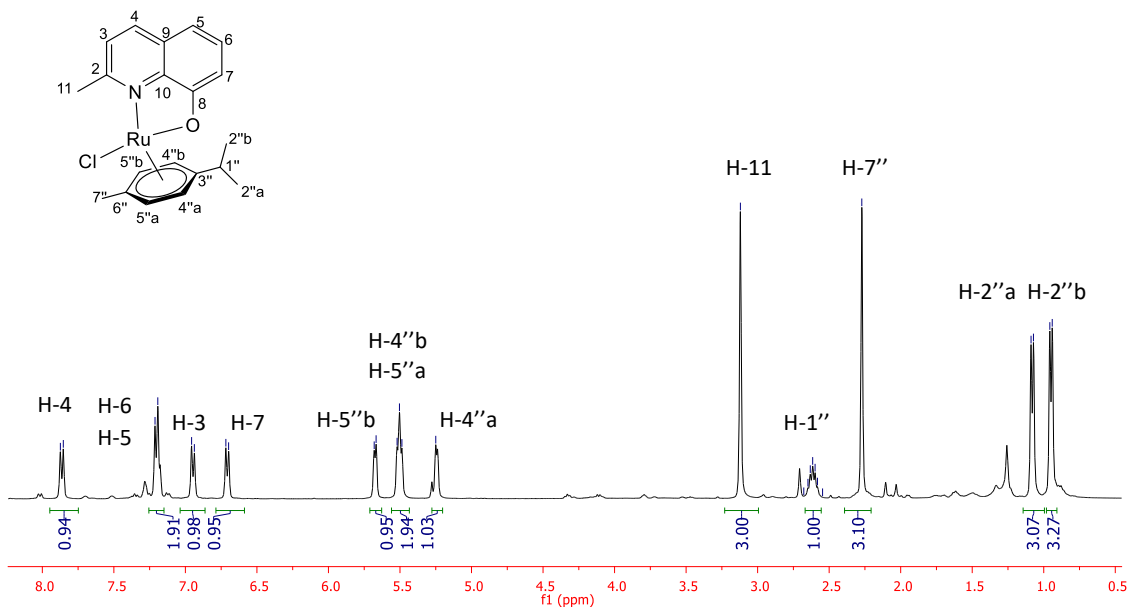
**Figure A5.30.** <sup>1</sup>H NMR spectrum (400 MHz, CDCl<sub>3</sub>) of compound **5.11**.



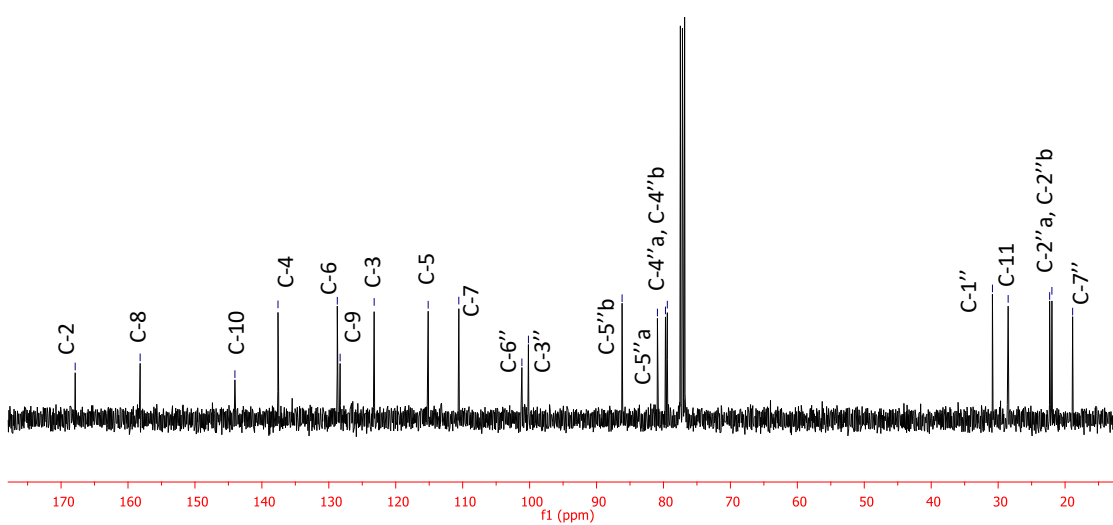
**Figure A5.31.**  $^{13}\text{C}$  NMR spectrum (100 MHz,  $\text{CDCl}_3$ ) of compound 5.11.



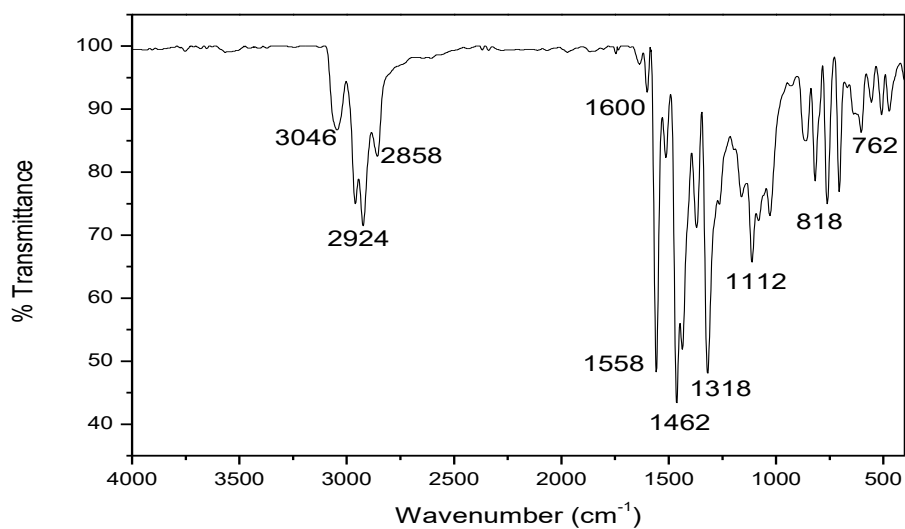
**Figure A5.32.** Infrared spectrum in KBr of compound 5.12.



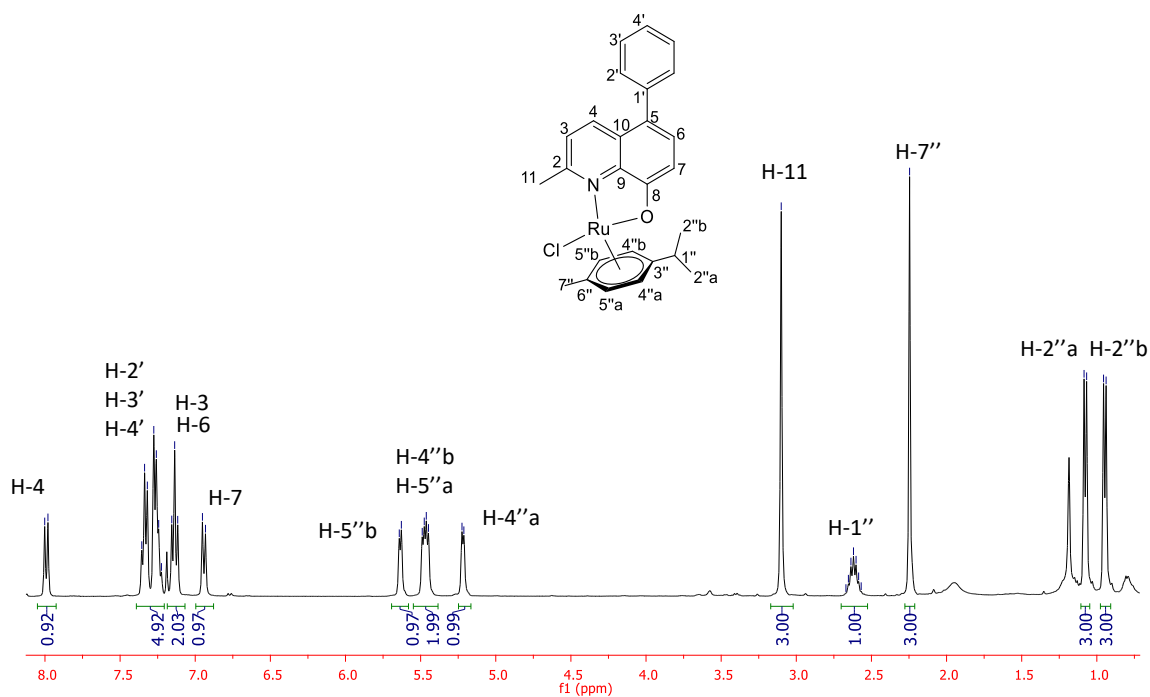
**Figure A5.33.**  $^1\text{H}$  NMR spectrum (400 MHz,  $\text{CDCl}_3$ ) of compound 5.12.



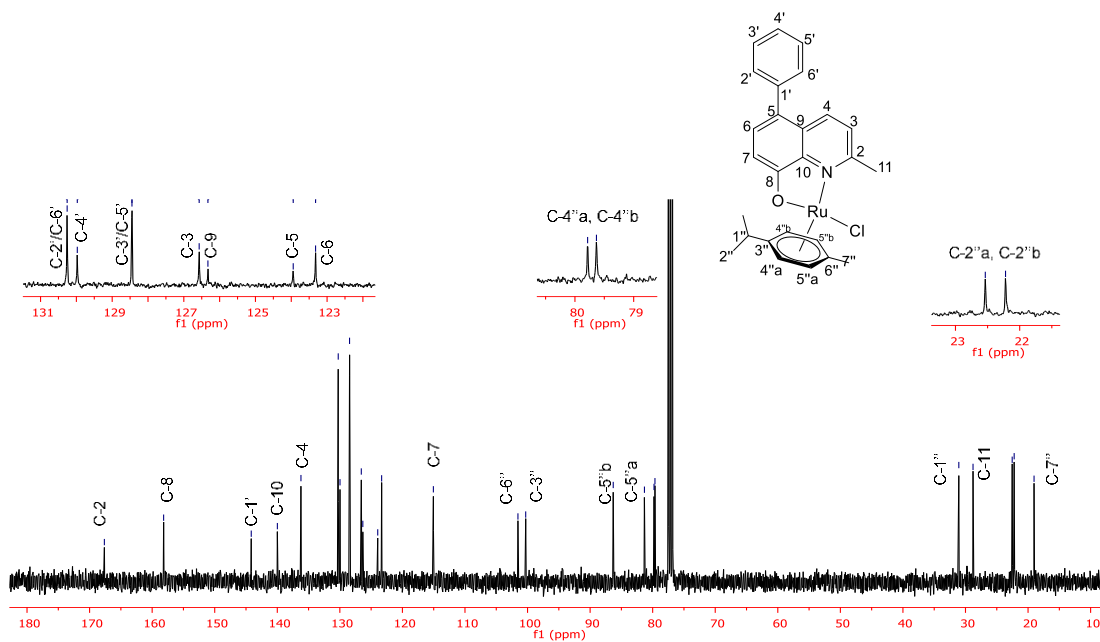
**Figure A5.34.**  $^{13}\text{C}$  NMR spectrum (100 MHz,  $\text{CDCl}_3$ ) of compound 5.12.



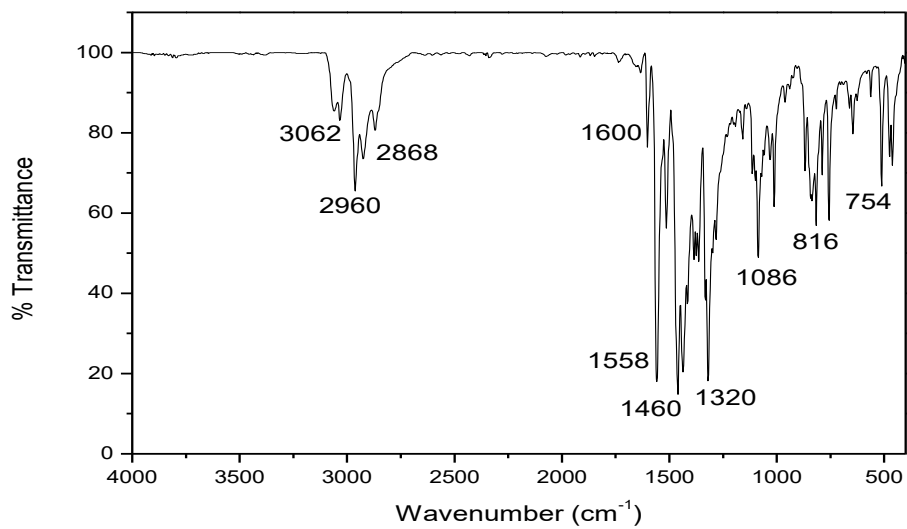
**Figure A5.35.** Infrared spectrum in KBr of compound **5.13**.



**Figure A5.36.**  $^1\text{H}$  NMR spectrum (400 MHz,  $\text{CDCl}_3$ ) of compound **5.13**.

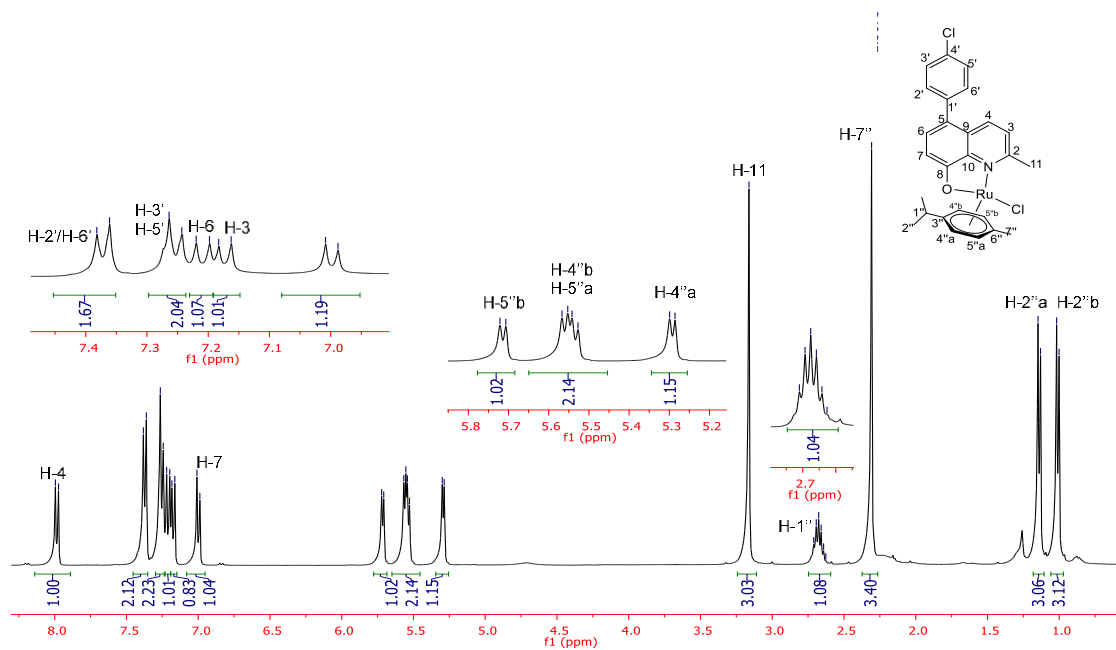


**Figure A5.37.**  $^{13}\text{C}$  NMR spectrum (100 MHz,  $\text{CDCl}_3$ ) of compound **5.13**.

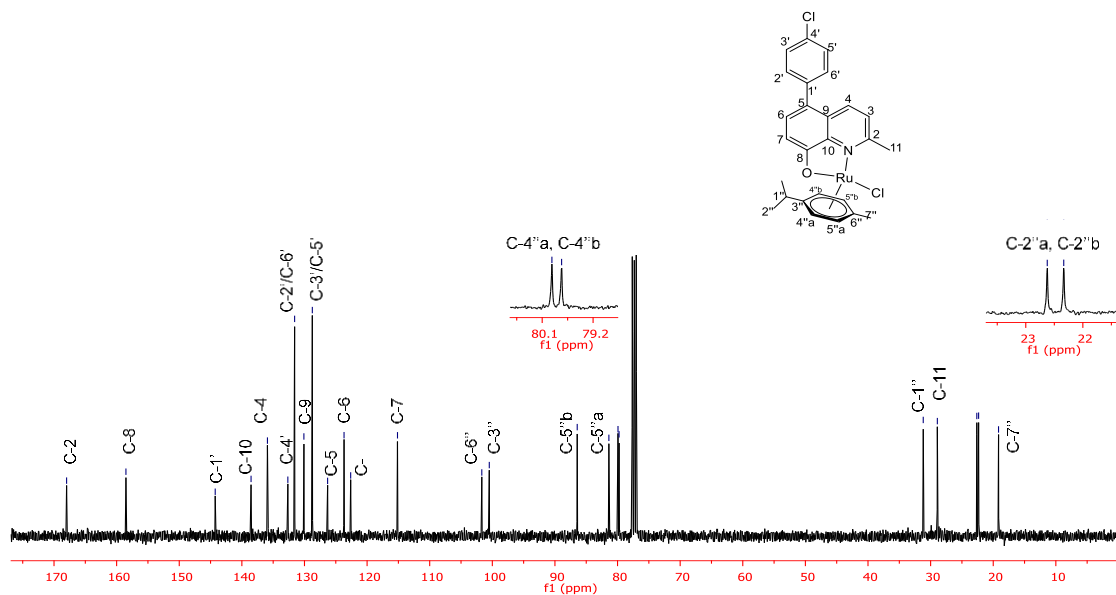


**Figure A5.38.** Infrared spectrum in KBr of compound **5.14**.

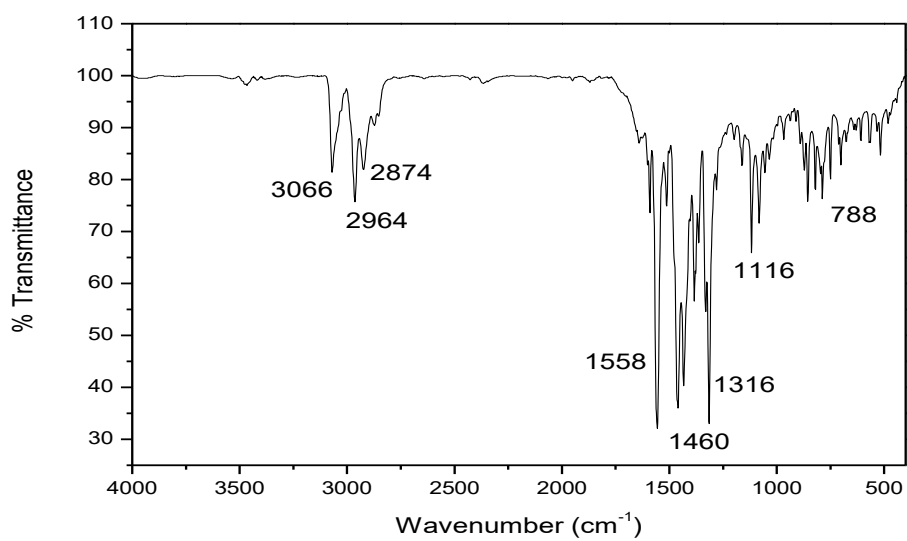




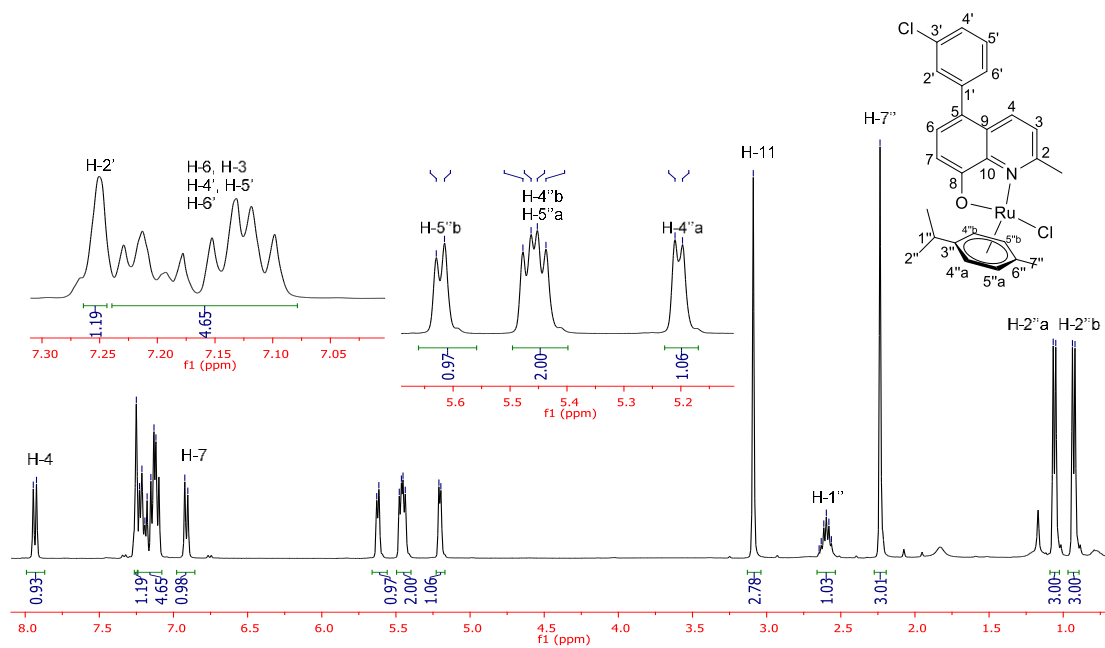
**Figure A5.39.**  $^1\text{H}$  NMR spectrum (400 MHz,  $\text{CDCl}_3$ ) of compound **5.14**.



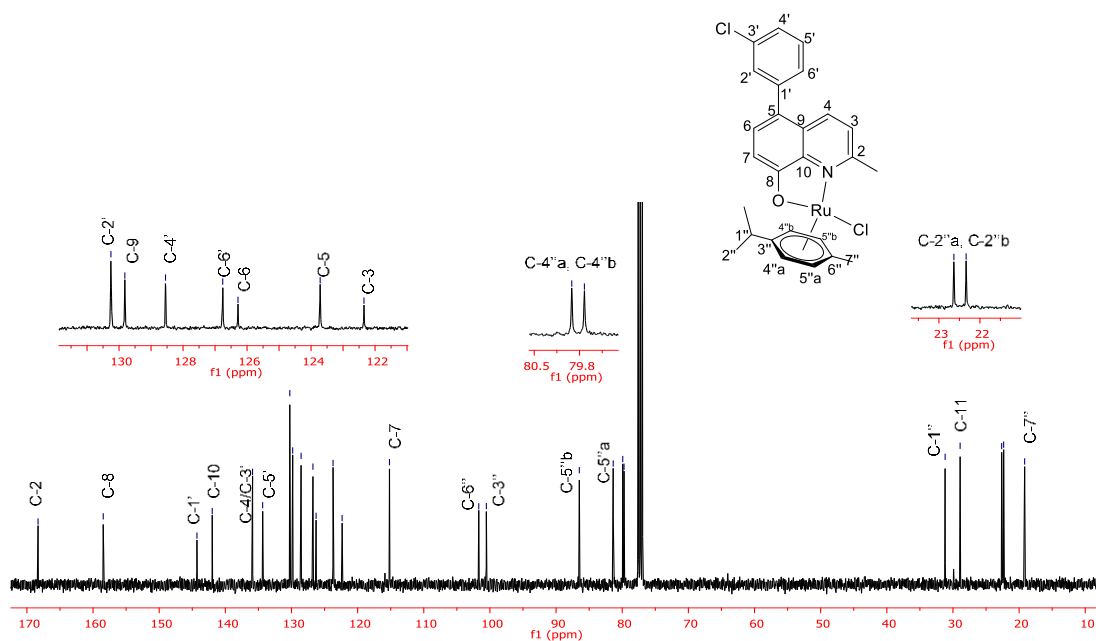
**Figure A5.40.**  $^{13}\text{C}$  NMR spectrum (100 MHz,  $\text{CDCl}_3$ ) of compound **5.14**.



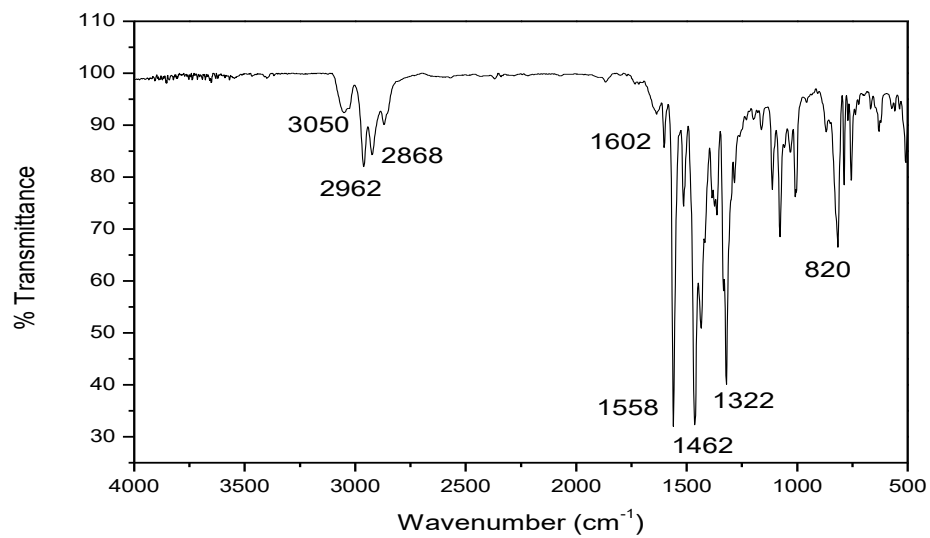
**Figure A5.41.** Infrared spectrum in KBr of compound **5.15**.



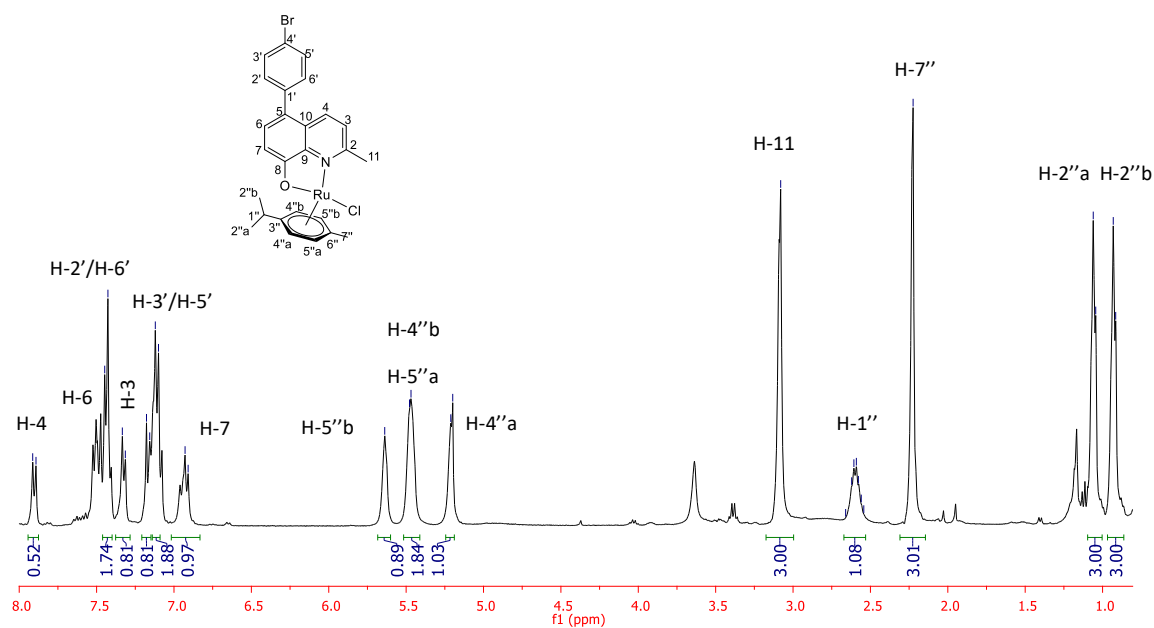
**Figure A5.42.**  $^1\text{H}$  NMR spectrum (400 MHz,  $\text{CDCl}_3$ ) of compound **5.15**.



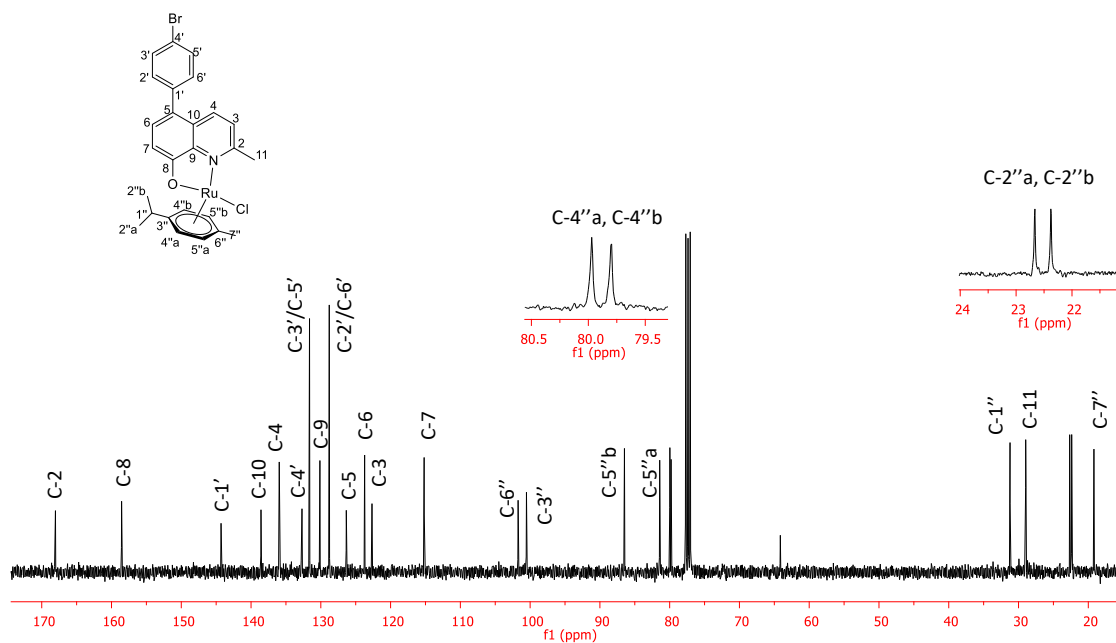
**Figure A5.43.**  $^{13}\text{C}$  NMR spectrum (100 MHz,  $\text{CDCl}_3$ ) of compound **5.15**.



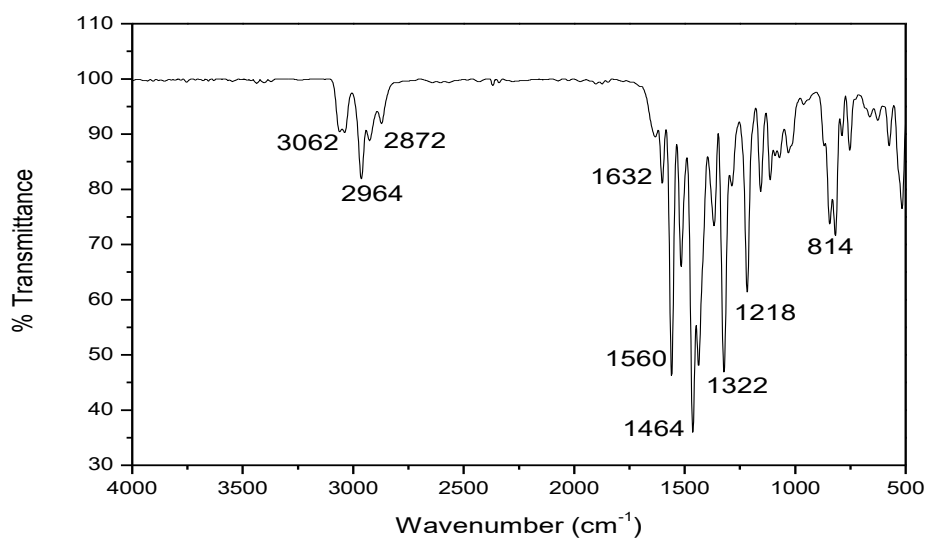
**Figure A5.44.** Infrared spectrum in KBr of compound **5.16**.



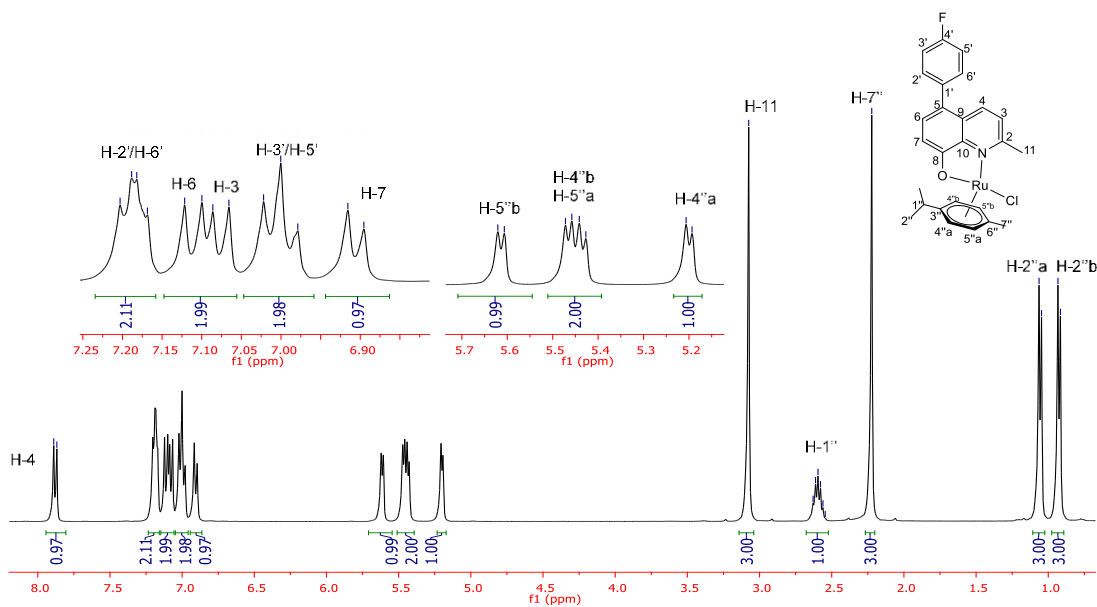
**Figure A5.45.**  $^1\text{H}$  NMR spectrum (400 MHz,  $\text{CDCl}_3$ ) of compound **5.16**.



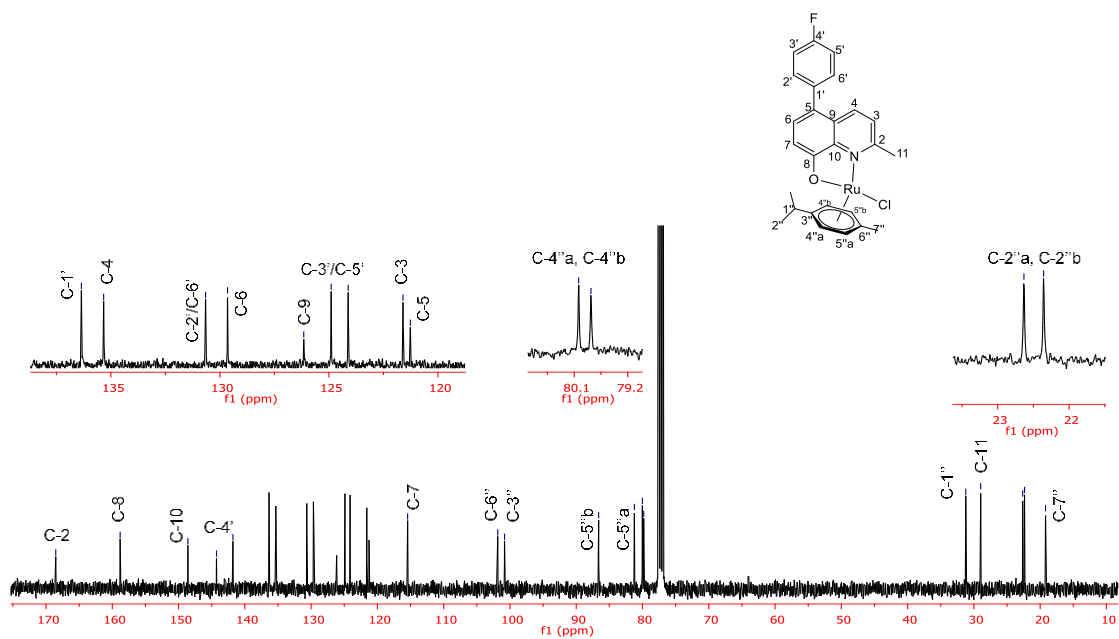
**Figure A5.46.**  $^{13}\text{C}$  NMR spectrum (100 MHz,  $\text{CDCl}_3$ ) of compound **5.16**.



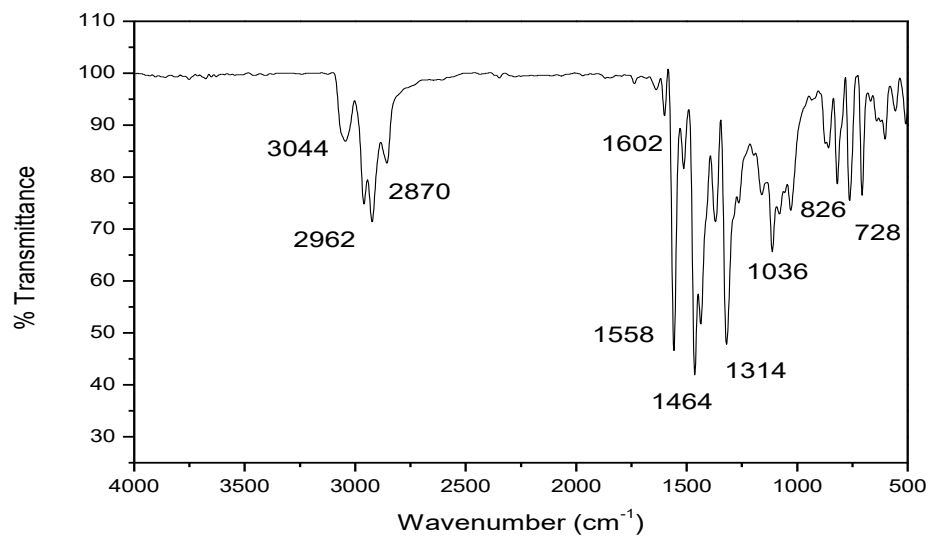
**Figure A5.47.** Infrared spectrum in KBr of compound **5.17**.



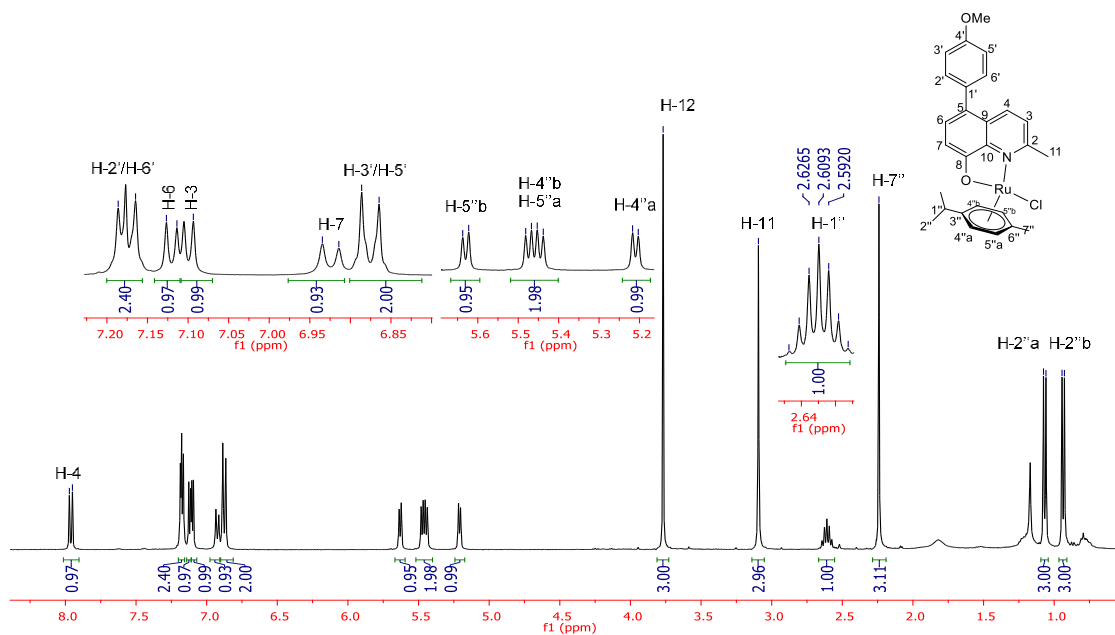
**Figure A5.48.**  $^1\text{H}$  NMR spectrum (400 MHz,  $\text{CDCl}_3$ ) of compound **5.17**.



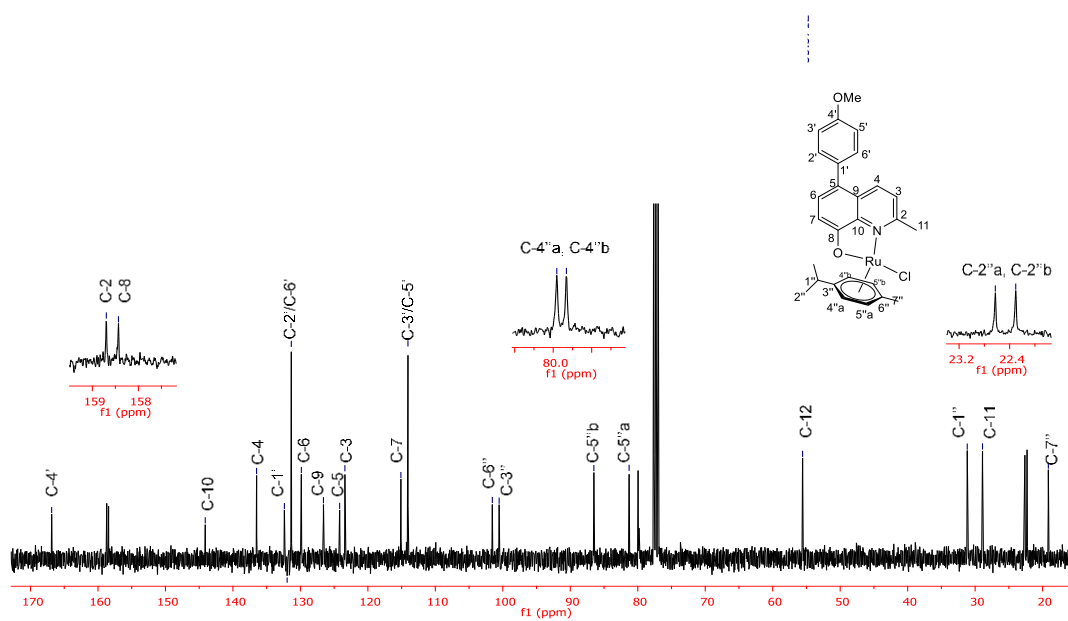
**Figure A5.49.**  $^{13}\text{C}$  NMR spectrum (100 MHz,  $\text{CDCl}_3$ ) of compound **5.17**.



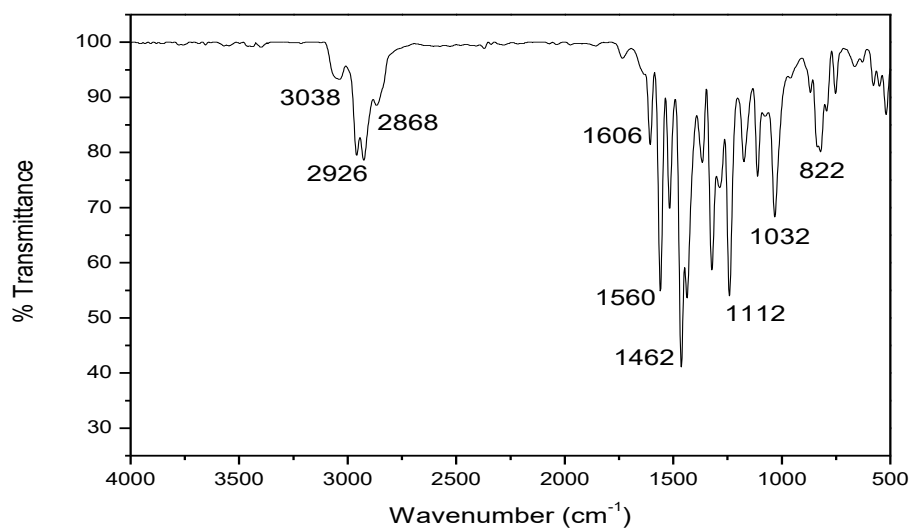
**Figure A5.50.** Infrared spectrum in KBr of compound **5.18**.



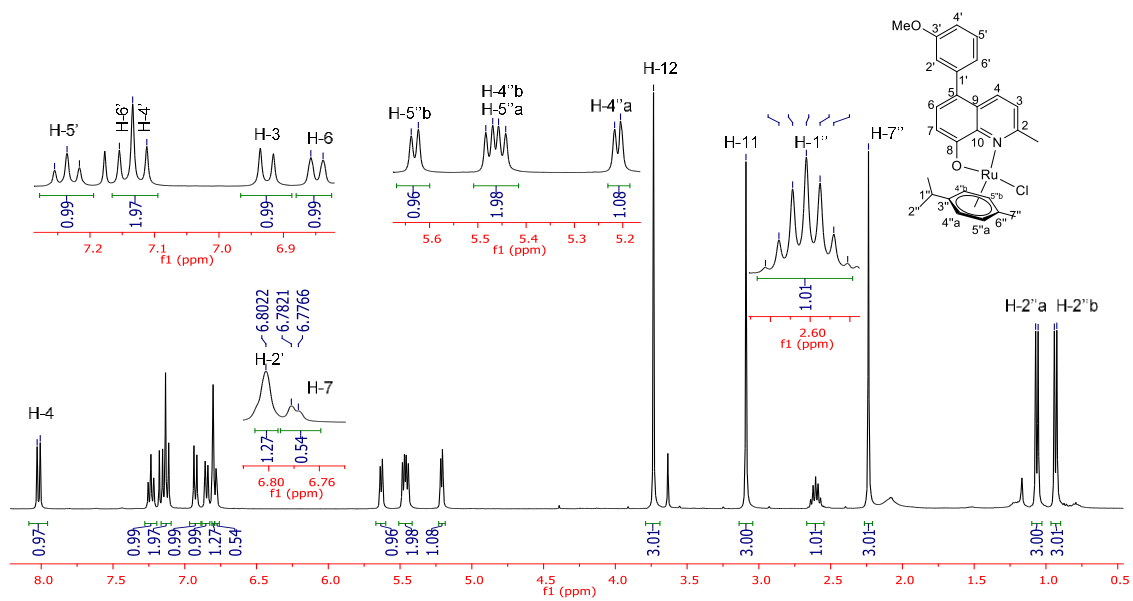
**Figure A5.51.**  $^1\text{H}$  NMR spectrum (400 MHz,  $\text{CDCl}_3$ ) of compound **5.18**.



**Figure A5.52.**  $^{13}\text{C}$  NMR spectrum (100 MHz,  $\text{CDCl}_3$ ) of compound **5.18**.

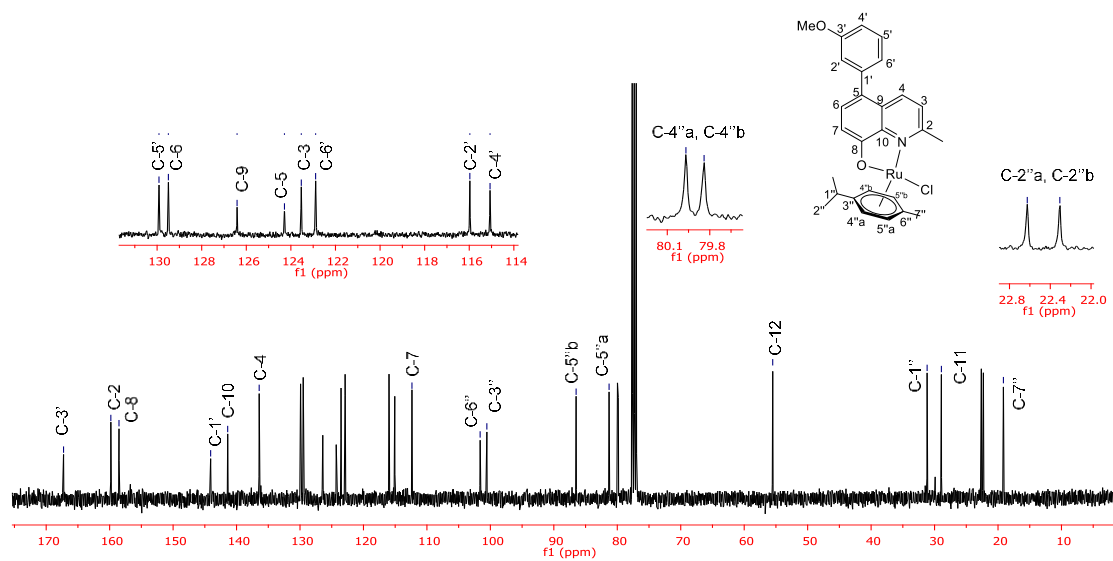


**Figure A5.53.** Infrared spectrum in KBr of compound **5.19**.

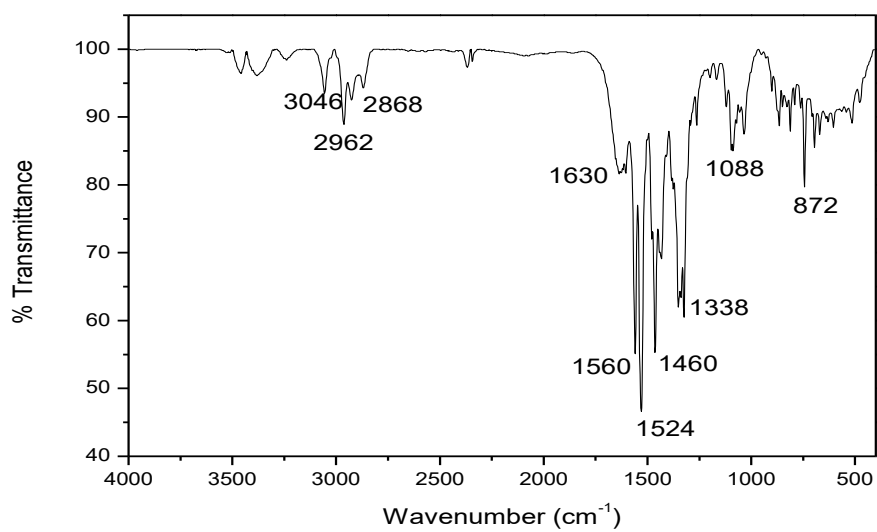


**Figure A5.54.**  $^1\text{H}$  NMR spectrum (400 MHz,  $\text{CDCl}_3$ ) of compound **5.19**.

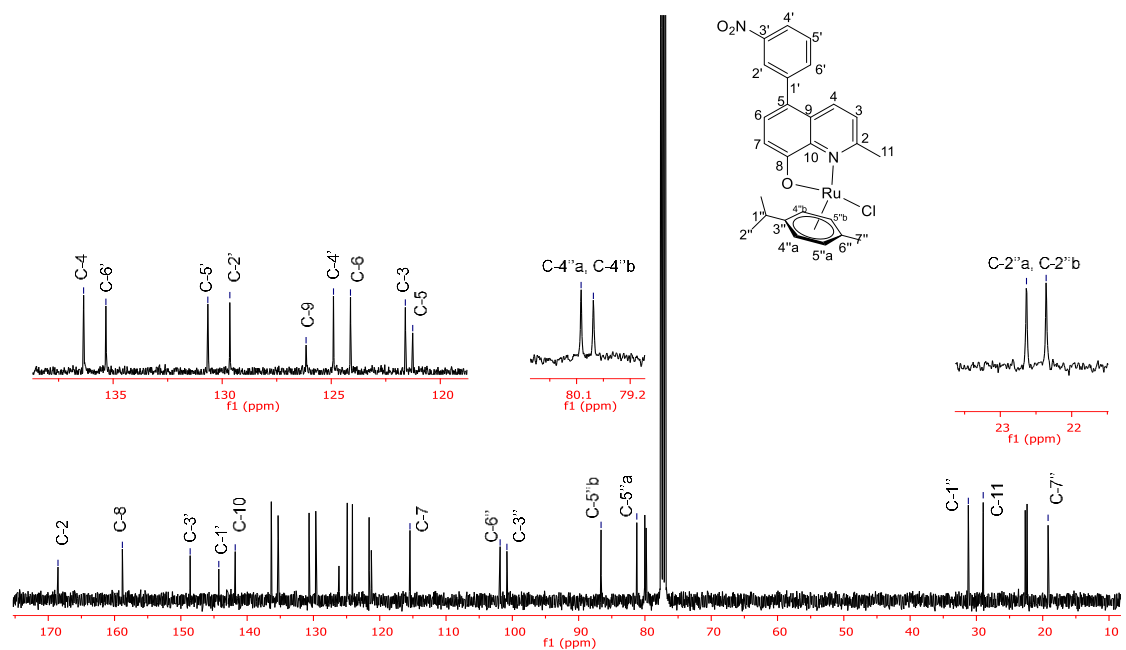
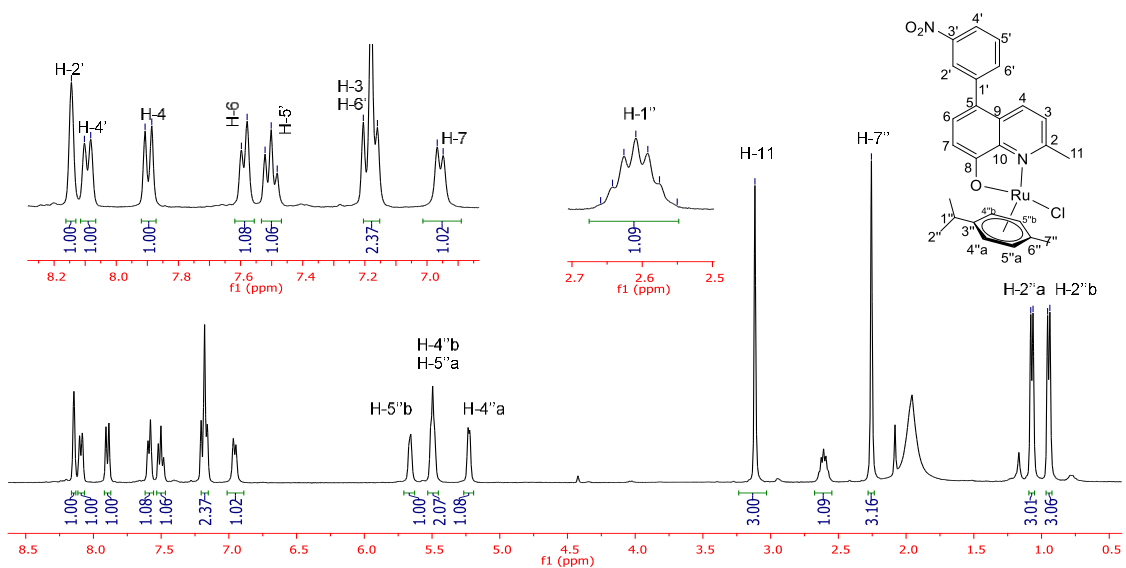


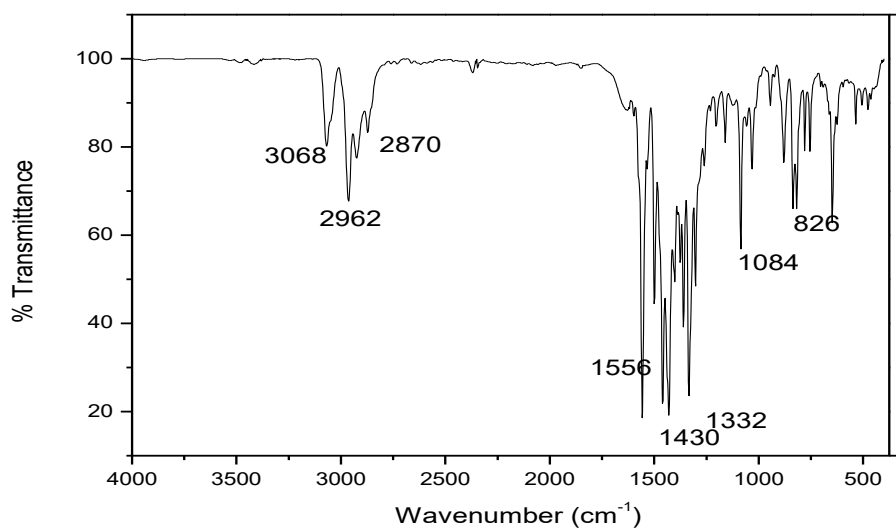


**Figure A5.55.**  $^{13}\text{C}$  NMR spectrum (100 MHz,  $\text{CDCl}_3$ ) of compound **5.19**.

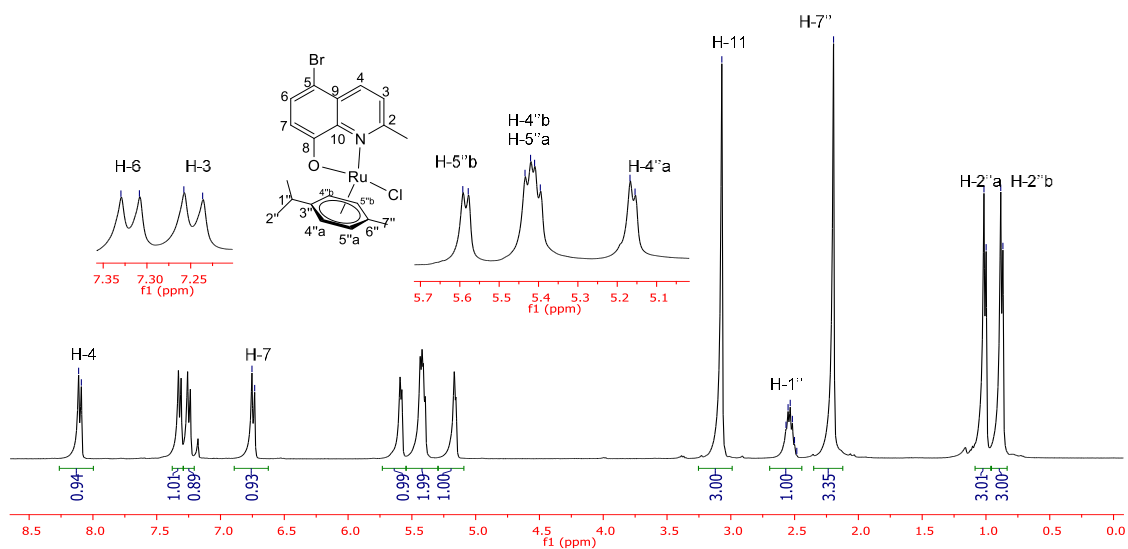


**Figure A5.56.** Infrared spectrum in KBr of compound **5.20**.

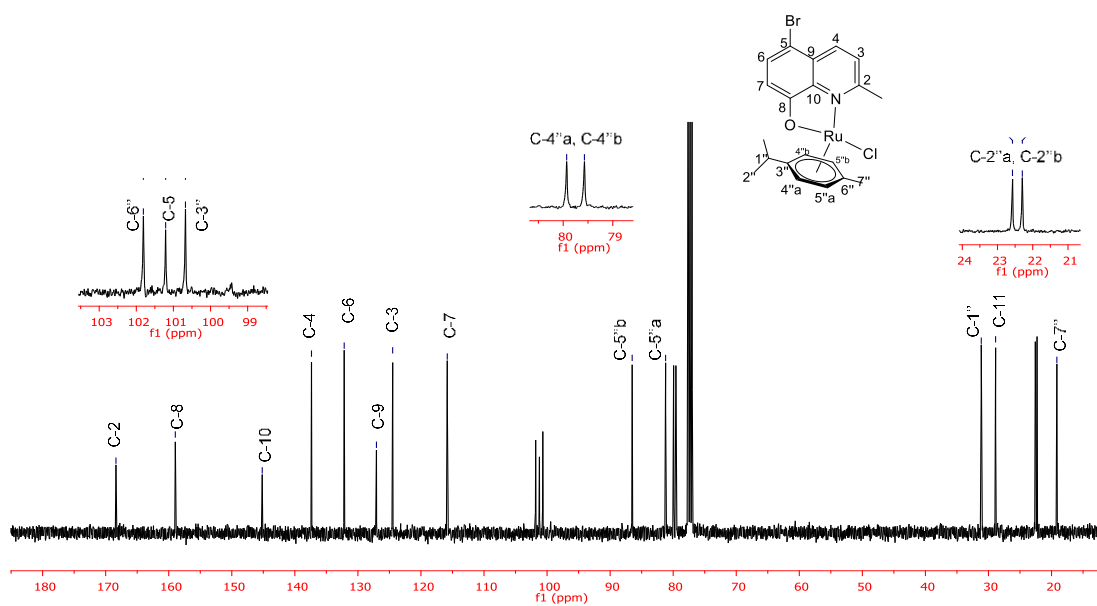




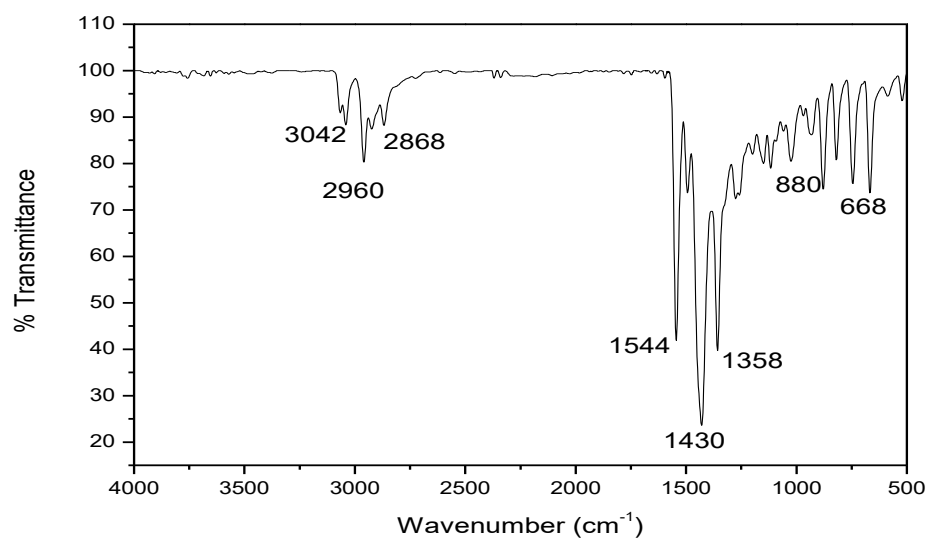
**Figure A5.59.** Infrared spectrum in KBr of compound **5.21**.



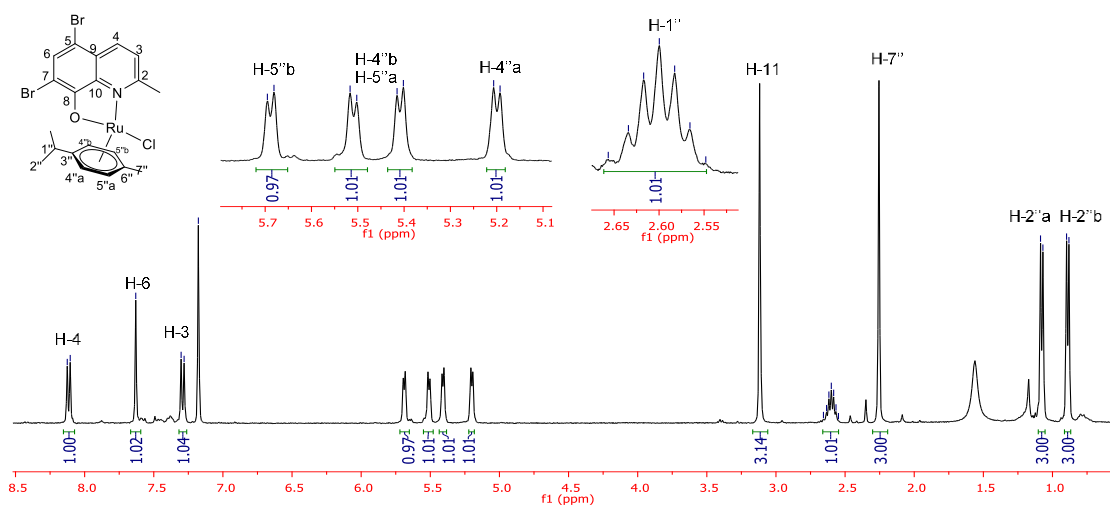
**Figure A5.60.**  $^1\text{H}$  NMR spectrum (400 MHz,  $\text{CDCl}_3$ ) of compound **5.21**.



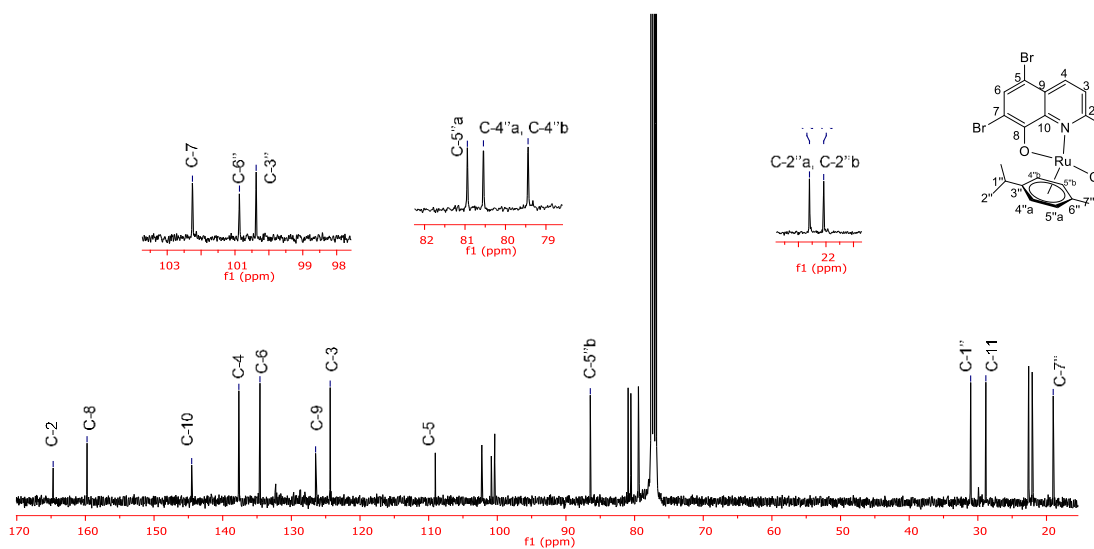
**Figure A5.61.**  $^{13}\text{C}$  NMR spectrum (100 MHz,  $\text{CDCl}_3$ ) of compound 5.21.



**Figure A5.62.** Infrared spectrum in KBr of compound 5.22.



**Figure A5.63.**  $^1\text{H}$  NMR spectrum (400 MHz,  $\text{CDCl}_3$ ) of compound **5.22**.



**Figure A5.64.**  $^{13}\text{C}$  NMR spectrum (100 MHz,  $\text{CDCl}_3$ ) of compound **5.22**.

## **ANNEX**



Contents lists available at ScienceDirect

Tetrahedron Letters

journal homepage: [www.elsevier.com/locate/tetlet](http://www.elsevier.com/locate/tetlet)

## First total synthesis and phytotoxic activity of *Streptomyces* sp. metabolites abenquines

Amalyn Nain-Perez<sup>a</sup>, Luiz C. A. Barbosa<sup>a,b,\*</sup>, Celia R. A. Maltha<sup>b</sup>, Giuseppe Forlani<sup>c</sup><sup>a</sup> Department of Chemistry, Universidade Federal de Minas Gerais, Av. Pres. Antônio Carlos, 6627, Campus Pampulha, CEP 31270-901 Belo Horizonte, MG, Brazil<sup>b</sup> Department of Chemistry, Federal University of Viçosa, Viçosa, MG, Brazil<sup>c</sup> Department of Life Science and Biotechnology, University of Ferrara, via L. Borsari 46, I-44121 Ferrara, Italy

### ARTICLE INFO

#### Article history:

Received 17 February 2016

Revised 8 March 2016

Accepted 11 March 2016

Available online 12 March 2016

#### Keywords:

Abenquines

Aminoquinones

Herbicidal activity

Phytotoxin

### ABSTRACT

The first total synthesis of abenquines A, B2, C and D has been achieved in three steps starting from commercially available 2,5-dimethoxyaniline, with overall yields of 41–61%. Four analogues bearing the amino acids *D*-valine (**17**), *L*-methionine (**18**), and glycine (**19**), and benzylamine (**20**), were also prepared in 45–72% yield. The inhibitory properties of these compounds were evaluated against the photoautotrophic growth of a model *Synechococcus* sp. strain. Abenquine C and its enantiomer were substantially ineffective, whereas all other abenquines significantly inhibited cell proliferation, with concentrations causing 50% inhibition of algal growth ranging from 10<sup>-5</sup> to 10<sup>-6</sup> M.

© 2016 Elsevier Ltd. All rights reserved.

### Introduction

Among the plethora of natural products, such as polyketides, terpenoids, steroids, alkaloids, amino acids, and carbohydrates,<sup>1</sup> the quinones represent an important class of substances endowed with a vast array of biological activities.<sup>2</sup> These compounds are found in plants, microorganisms, and marine organisms.<sup>2</sup> Despite the large structural variation among the natural quinones, those bearing an amino group *ortho* to the carbonyl group are less common. One of the earliest natural aminoquinones identified is streptonigrin (**1**) (Fig. 1), a highly functionalized antibiotic isolated from *Streptomyces flocculus* in 1959.<sup>3</sup> This compound entered phase II clinical trials as an anticancer agent in the 1970s, and has attracted the attention of many research groups.<sup>4</sup> In the early 1980s lavendamycin (**2**), structurally related to streptonigrin, was isolated from *Streptomyces lavendulae*, and was shown to exert cytotoxic and antimicrobial activities.<sup>5</sup> Lavendamycin was also the object of synthetic investigations, including the preparation of analogues for biological studies.<sup>4b,6</sup>

In 1994 two new terpenoid aminoquinones, nakijiquinones A (**3**) and B (**4**), were isolated from a marine sponge (family Spongidae). Besides representing the first sesquiterpenoid quinones with amino acid residues of natural origin, they also exhibited cytotoxic activity against some cancer cell lines.<sup>7</sup> This discovery was

followed by the isolation<sup>8</sup> and synthesis<sup>9</sup> of several new nakijiquinones and analogues bearing amino acid residues. One aminoquinone structurally related to nakijiquinones was then isolated from the marine sponge *Dactylospongia elegans* and named smenospongine.<sup>10</sup> This compound and other natural analogues isolated from marine sources presented antimicrobial and cytotoxic activities.<sup>11</sup> Other natural aminoquinones endowed with biological activities include metachromins,<sup>12</sup> geldanamycin,<sup>13</sup> mytomicin,<sup>14</sup> and dysifragilones.<sup>15</sup>

Recently, a new group of benzoquinones bearing natural amino acid residues (abenquines A–D, **6–10**) (Fig. 1) were isolated from a strain of *Streptomyces* sp. collected from the Atacama desert in Chile. These abenquines showed cytotoxic activity against bacteria and dermatophytic fungi, and were inhibitory of phosphodiesterase type 4b activity.<sup>16</sup> Several groups,<sup>17</sup> including ours,<sup>18</sup> have described aminobenzoquinone phytotoxicity, but little work has been done to address their development as new herbicides. In view of our interest in this area and considering that abenquines are available in short supply, we report here the first total synthesis of such compounds and a preliminary assessment of their phytotoxic effects.

### Results and discussion

Initially we envisaged that all abenquines could be obtained from quinone **11**, which in turn could easily be prepared from the commercially available 2,5-dimethoxyaniline **13** (Scheme 1).

\* Corresponding author. Tel.: +55 31 34093396; fax: +55 31 3899 3065.

E-mail addresses: [lcab@ufmg.br](mailto:lcab@ufmg.br), [lcab@ufv.br](mailto:lcab@ufv.br) (L.C.A. Barbosa).<http://dx.doi.org/10.1016/j.tetlet.2016.03.038>

0040-4039/© 2016 Elsevier Ltd. All rights reserved.

## Natural Abenquines and Their Synthetic Analogues Exert Algicidal Activity against Bloom-Forming Cyanobacteria

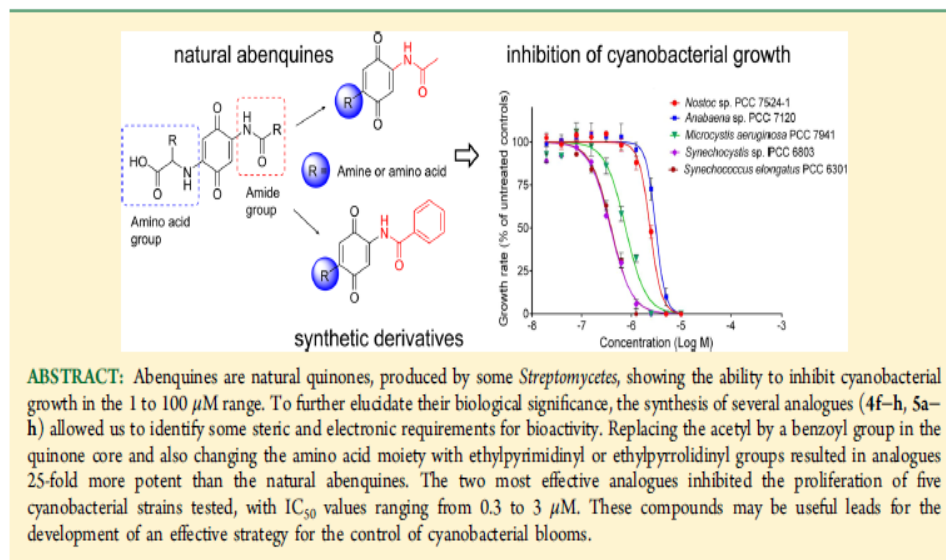
Analyn Nain-Perez,<sup>†</sup> Luiz Cláudio Almeida Barbosa,<sup>\*,†,‡,§</sup> Célia Regina Álvares Maltha,<sup>‡</sup> and Giuseppe Forlani<sup>\*,§</sup>

<sup>†</sup>Department of Chemistry, Universidade Federal de Minas Gerais, Avenida Pres. Antônio Carlos, 6627, Campus Pampulha, CEP 31270-901, Belo Horizonte, MG, Brazil

<sup>‡</sup>Department of Chemistry, Federal University of Viçosa, 36570-000, Viçosa, MG, Brazil

<sup>§</sup>Department of Life Science and Biotechnology, University of Ferrara, Via L. Borsari 46, I-44121 Ferrara, Italy

### Supporting Information



Cyanobacteria, also referred to as blue-green algae, are the only prokaryotes able to perform oxygenic photosynthesis.<sup>1</sup> Widely distributed even in strikingly different and harsh habitats, they play a major role in both carbon and nitrogen global cycling, since several free-living strains can accomplish biological  $\text{N}_2$  fixation.<sup>2</sup> In freshwater bodies and coastal waters under favorable conditions, e.g., warm temperature, sunlight, and increased N and P availability, some cyanobacteria are capable of blooming, rapidly multiplying and forming a dense surface scum.<sup>3</sup> This often leads to the establishment of anoxic conditions, altering the ecological structure and contributing to the ecosystem's decline.<sup>4</sup> Moreover, with the only exception of the genus *Spindelia/Arthrospira*, cyanobacteria produce a variety of potentially harmful toxins, targeting either the liver, the gastrointestinal apparatus, or the nervous system.<sup>5</sup> The release of high concentrations of toxins in cyanobacterial blooms causes concern for public safety and human health, deteriorates freshwater quality affecting drinking water supplies, and threatens aquaculture and fisheries, potentially causing serious economic damage.<sup>6</sup> Since the frequency of cyanobacterial blooms is increasing as a consequence of both pollution and

climate changes,<sup>7</sup> the development of efficient methods for bloom control is urgently required.

With this aim, physical<sup>8</sup> and chemical<sup>9</sup> strategies have been exploited. However, since the former are too costly to be applied on a large scale and the latter can cause further pollution, a biological approach to the problem would be a possibly better choice.<sup>10</sup> Under natural conditions, cyanobacterial proliferation seems to be limited by some algicidal bacteria that are believed to contribute to the control and termination of blooms.<sup>11</sup> Many bacteria showing inhibitory properties *in vitro* against harmful cyanobacteria have been recently isolated whose activity was shown to rely on production and release of active substances.<sup>12–16</sup> Despite the large number of organisms with algicidal activity, the development of effective biological strategies for bloom control requires isolation, characterization, and inexpensive chemical synthesis of these active compounds.<sup>17</sup>

Received: July 7, 2016

Published: March 20, 2017





Contents lists available at ScienceDirect

## Bioorganic &amp; Medicinal Chemistry Letters

journal homepage: [www.elsevier.com/locate/bmcl](http://www.elsevier.com/locate/bmcl)

## Natural abenquines and synthetic analogues: Preliminary exploration of their cytotoxic activity

Amalyn Nain-Perez<sup>a</sup>, Luiz C.A. Barbosa<sup>a,b,\*</sup>, Diego Rodríguez-Hernández<sup>a</sup>, Annemarie E. Kramell<sup>c</sup>, Lucie Heller<sup>c</sup>, René Csuk<sup>c,\*</sup><sup>a</sup> Department of Chemistry, Universidade Federal de Minas Gerais, Av. Pres. Antônio Carlos, 6627, Campus Pampulha, CEP 31270-901, Belo Horizonte, MG, Brazil<sup>b</sup> Department of Chemistry, Universidade Federal de Viçosa, Av. P.H. Rolfs, s/n, CEP 36570-900, Viçosa, MG, Brazil<sup>c</sup> Martin-Luther-University Halle-Wittenberg, Organic Chemistry, Kurt-Mothes-Str.2, D 06120 Halle (Saale), Germany

## ARTICLE INFO

## Article history:

Received 18 November 2016

Revised 24 January 2017

Accepted 25 January 2017

Available online 28 January 2017

## Keywords:

Abenquines

Aminoquinone

Abenquines analogues

Cytotoxicity

SRB assay

## ABSTRACT

In this study, we explore the cytotoxic activity of four natural abenquines (2a–d) and fourteen synthetic analogues (2e–j and 3a–h) against a panel of six human cancer cell lines using a SRB assay. It was found that most of the compounds revealed higher levels of cytotoxic activities than naturally occurring abenquines. The analogues carrying ethylpyrrolidinyl and ethylpyrimidinyl with either an acetyl group (2 h–i) or a benzoyl group (3f–g), were the most potent against all human cancer cell lines and displayed EC<sub>50</sub> between a range of 0.6–3.4 μM. Notably, of the compounds tested, compound 2i proved the most cytotoxic against both ovarian (A2780) and breast (MCF7) cells, showing EC<sub>50</sub> = 0.6 and 0.8 μM respectively. Likewise, the analogues 2i, 3f and 3g showed strong activity against cell HT29 with EC<sub>50</sub> = 0.9 μM for these compounds.

© 2017 Elsevier Ltd. All rights reserved.

The global human population is projected to reach nine billion people by 2050, and this will result in an unprecedented challenge for everyone.<sup>1,2</sup> Together with population growth, the incidence of certain types of cancer is expected to increase due to risk-factors that affect human health as obesity, tobacco and alcohol consumption.<sup>3</sup>

Amongst the major diseases that afflict humanity, cancer has become a major cause of global mortality, with approximately 12.7 million new cases diagnosed every year. According to the World Health Organization, in 2012 approximately 14 million new cases of morbidity and mortality and 8.2 million cancer related cases were reported worldwide. As estimated, the number of new cases could rise to around 70% in the next two decades.<sup>4</sup>

With the growing demand for treatments of cancer, the development of new effective drugs with fewer side effects is a priority for big pharmaceutical industries.<sup>5</sup> Historically, the use of natural products for the treatment and control of various diseases, including cancer is well documented.<sup>6</sup> Currently, 34% of commercial medicines are based on small molecules such as natural products or their derivatives which represent a broad range of chemical

structures.<sup>6,7</sup> Amongst these, naturally occurring quinones are widely distributed across plants, animals and bacteria.<sup>8,9</sup> Among the quinones, several aminoquinones display significant and diverse biological properties. For instance, streptonigrin,<sup>10,11</sup> geldanamycin<sup>12,13</sup> and mitomycin C<sup>14,15</sup> have shown potent anti-tumor and/or antibiotic activities. In 1987, the derivative of mitomycin C known as E09 was developed as a targeted therapeutic agent, and clinical evaluation revealed significant anti-tumor activity.<sup>16</sup>

Recently, a new group of aminoquinones called abenquines A-D (Fig. 1) were isolated from *Streptomyces* sp. strain DB634, collected from the soils of the Chilean highland of the Atacama Desert.<sup>17</sup> These compounds possess an *N*-acetyl-aminobenzoquinone core bearing natural amino acid residues. The abenquines showed low cytotoxic activity against selected bacteria and dermatophytic fungi and were found to be phosphodiesterase type 4 (PDE4b) inhibitors.<sup>17</sup> Recently, these natural compounds were synthesized by our group and showed phytotoxic activity against the cyanobacterium *Synechococcus elongates*.<sup>18</sup>

During the last few years, our group has been using natural products as scaffold for the development of new bioactive substance with potential application as pharmaceuticals or agrochemicals.<sup>19–23</sup> Hence, in order to gain a deeper insight into the biological profile of this poorly investigated group of quinones we now report the cytotoxic profiles of four natural abenquines and fourteen synthetic analogues against several cancer lines.

\* Corresponding authors at: Department of Chemistry, Universidade Federal de Minas Gerais, Av. Pres. Antônio Carlos, 6627, Campus Pampulha, CEP 31270-901, Belo Horizonte, MG, Brazil (L.C.A. Barbosa).

E-mail addresses: [lcab@ufmg.br](mailto:lcab@ufmg.br) (L.C.A. Barbosa), [rene.csuk@chemie.uni-halle.de](mailto:rene.csuk@chemie.uni-halle.de) (R. Csuk).

## Tailoring Natural Abenquines To Inhibit the Photosynthetic Electron Transport through Interaction with the D1 Protein in Photosystem II

Amalyn Nain-Perez,<sup>†</sup> Luiz C. A. Barbosa,<sup>\*,†,‡,§</sup> Celia R. A. Maltha,<sup>‡</sup> Samuele Giberti,<sup>§</sup> and Giuseppe Forlani<sup>\*,§</sup>

<sup>†</sup>Department of Chemistry, Universidade Federal de Minas Gerais, Av. Pres. Antônio Carlos, 6627, Campus Pampulha, CEP 31270-901, Belo Horizonte, MG Brazil

<sup>‡</sup>Department of Chemistry, Universidade Federal de Viçosa, Viçosa, Av. P. H. Rolfs s/n, CEP 36570-000, Viçosa, MG Brazil

<sup>§</sup>Department of Life Science and Biotechnology, University of Ferrara, via L. Borsari 46, I-44121 Ferrara, Italy

### Supporting Information

**ABSTRACT:** Abenquines are natural *N*-acetylaminobenzoquinones bearing amino acid residues, which act as weak inhibitors of the photosynthetic electron transport chain. Aiming to exploit the abenquine scaffold as a model for the synthesis of new herbicides targeting photosynthesis, 14 new analogues were prepared by replacing the amino acid residue with benzylamines and the acetyl with different acyl groups. The synthesis was accomplished in three steps with a 68–95% overall yield from readily available 2,5-dimethoxyaniline, acyl chlorides, and benzyl amines. Key steps include (i) acylation of the aniline, (ii) oxidation, and (iii) oxidative addition of the benzylamino moiety. The compounds were assayed for their activity as Hill inhibitors, under basal, uncoupled, or phosphorylating conditions, or excluding photosystem I. Four analogues showed high effectiveness ( $IC_{50} = 0.1–0.4 \mu\text{M}$ ), comparable with the commercial herbicide diuron ( $IC_{50} = 0.3 \mu\text{M}$ ). The data suggest that this class of compounds interfere at the reducing side of photosystem II, having protein D1 as the most probable target. Molecular docking studies with the plastoquinone binding site of *Spinacia oleracea* further strengthened this proposal.

**KEYWORDS:** abenquine analogues, aminoquinones, photosynthesis inhibitors, photosynthetic electron transport, herbicides

### INTRODUCTION

Presently, agricultural pests<sup>1</sup> and weeds<sup>2</sup> are largely controlled by the use of agrochemicals. Since the introduction of the synthetic auxin 2,4-dichlorophenoxyacetic acid (2,4-D) in 1946, herbicides have become the primary tool for weed management.<sup>3,4</sup> Hence, over the years herbicides contributed considerably to increased crop yields, providing a highly effective, economical, and relatively simple means for weed control.<sup>3,5</sup> They act through different mechanisms, such as inhibition of amino acids or fatty acids biosynthesis, or interference with microtubule formation, or the photosynthetic electron transport light reactions.<sup>2</sup> However, a continuous use of the same herbicide or herbicides sharing the same target leads to the rapid selection of weed biotypes resistant to such chemicals.<sup>3</sup> The identification and characterization of novel herbicides is therefore highly desirable to manage resistant weeds.<sup>5–7</sup> In the past decade, some analogues to natural products have been developed and used as herbicides, but they contribute to only approximately 8% of chemicals used for crop protection.<sup>8</sup> Natural compounds are often environmentally friendly, as their half-life in the soil is usually shorter compared with that of synthetic herbicides.<sup>9,10</sup> Moreover, their wide structural diversity offers opportunities to discover new sites of herbicide action, beyond the targets described to date.<sup>11,12</sup> Several currently used active principles target the photosynthetic process, and these can be classified as (1) electron transport inhibitors, (2) uncouplers, (3) energy transfer inhibitors, (4) inhibitory uncouplers, or (5) electron acceptors.<sup>13</sup>

During recent years, several natural compounds have been investigated for their allelopathic activities.<sup>14–19</sup> Among this large array of natural substances is sorgoleone, a lipophilic quinone produced by *Sorghum bicolor*. The phytotoxic properties of this quinone have been investigated for many years,<sup>20</sup> and its potent herbicidal activity on small-seeded weeds seems due to the interference with the electron transfer process at the photosystem II (PSII) level.<sup>21</sup> On this basis, several sorgoleone analogues were synthesized that showed herbicidal activity against weeds such as *Desmodium tortuosum*, *Hyptis suaveolens*, *Hyptis lophanta*, *Brachiaria decumbens*, and *Euphorbia heterophylla*.<sup>22,23</sup>

Abenquines are natural products isolated from *Streptomyces* sp. strain DB634, a bacterium found in the Atacama Desert in Chile.<sup>24</sup> Abenquines A–D (Figure 1) are *N*-acetylaminobenzoquinones bearing different amino acid residues. We recently described an efficient procedure for their synthesis and that of some analogues.<sup>25</sup> Several of them showed a remarkable algicidal activity, inhibiting cyanobacterial growth by 50% at 1.0  $\mu\text{M}$ .<sup>26</sup> However, their mode of action has not been elucidated.

Here we report that abenquine A and some synthetic analogues inhibit the Hill reaction in vitro and, therefore, are potentially endowed with phytotoxic and herbicidal activity. Some new synthetic analogues showing increased effectiveness

Received: October 10, 2017

Revised: November 30, 2017

Accepted: December 1, 2017

Published: December 1, 2017

## FULL PAPER

Amino-substituted *para*-Benzoquinones as Potential Herbicides

by Amalyn Nain-Perez<sup>a)</sup>), Luiz C. A. Barbosa<sup>a)</sup>), Marcelo C. Picanço<sup>c)</sup>, Samuele Giberti<sup>d)</sup>, and Giuseppe Forlani<sup>a)d)</sup>

<sup>a)</sup> Department of Chemistry, Universidade Federal de Minas Gerais, Av. Pres. Antônio Carlos, 6627, Campus Pampulha, CEP 31270-901, Belo Horizonte, MG, Brazil (phone: +55 31 34095757, e-mail: lcab@ufmg.br)

<sup>b)</sup> Department of Chemistry, Federal University of Viçosa, Av. P. H. Rolfs, s/n, Viçosa, MG, 36570-000, Brazil

<sup>c)</sup> Department of Entomology, Federal University of Viçosa, Av. P. H. Rolfs, s/n, Viçosa, MG, 36570-000, Brazil

<sup>d)</sup> Department of Life Science and Biotechnology, University of Ferrara, via L. Borsari 46, IT-44121 Ferrara (phone: +39 0532 455311, e-mail: flg@unife.it)

Although quinones present a large array of biological activities, a few studies on the herbicidal potential of 2,5-bis(alkyl/arylamino)-1,4-benzoquinones have been reported to date. In this work, starting from benzoquinone, 13 2,5-bis(alkyl/arylamino)-1,4-benzoquinones were prepared in 46 – 93% yield. The products were fully characterized by spectroscopic analyses and their phytotoxicity against *Cucumis sativus* and *Sorghum bicolor* seedlings was investigated. At 100 ppm, compounds caused 10 – 88% growth inhibition of the dicotyledonous species, whereas the monocotyledon was less affected. Most compounds exerted little inhibitory effect on a cyanobacterial model strain. However, at 100  $\mu$ M, compounds **8** – **10** caused about 50% inhibition of algal growth, and compounds **1** and **2** reduced cell viability in the 1 – 10  $\mu$ M range. The ability of benzoquinone derivatives to interfere with the light-driven ferricyanide reduction by isolated spinach chloroplasts was evaluated. Some substances showed a moderate effect as uncouplers, but no relationship was found between this property and their biological activity, indicating that the herbicidal effect is not associated with the inhibition of the photosynthetic electron transport chain. Phytotoxic compounds were not toxic to insects, strengthening the possibility that they may serve as lead for the development of eco-friendly herbicides.

**Keywords:** Herbicidal activity, Algicidal activity, Insecticidal activity, Photosynthetic inhibitors, 2,5-Bis(alkyl/arylamino)-1,4-benzoquinones.

## Introduction

Modern agriculture is highly dependent on the use of synthetic chemicals, such as fertilizers and pesticides, including insecticides, herbicides, and fungicides, which are used worldwide to increase crop yield [1][2]. However, the repeated use of substances that act by the same mechanism of action continuously leads to the development of resistance in several organisms, such as insects, fungi, and weeds, representing a major issue in crop protection [3 – 5]. Thus, there is a continuous need for the development of new agrochemicals to provide farmers with effective tools to control pests [6].

New pesticides should be endowed with ‘ecological selectivity’, *i.e.*, be effective in pest control without affecting nontarget organisms, such as pest natural enemies and pollinators [7][8]. Among the formers are the predatory ants, as *Solenopsis saevissima* (SMITH) (Hymenoptera: Formicidae) [9]; among the latter bees (Hymenoptera: Apidae) constitute an essential group of beneficial insects, accounting for 90% of the reproductive success of flowering plants [10]. In this perspective, the stingless bee

*Tetragonisca angustula* LATREILLE (Meliponinae) is important in the Neotropics [11].

Biologically active quinones have recently attracted great interest due to their broad-spectrum effects, such as antibacterial, antifungal [12], herbicidal [13 – 17], antifeedant [18], urease inhibitory [16], and insecticidal [19][20] activities. Some naturally occurring quinones are redox active molecules that play a main role as electron carriers in photosynthesis, respiration, and information-transfer processes [21]. With this background, we set our study directed to the synthesis and characterization of a series of 2,5-bis(alkyl/arylamino)-1,4-benzoquinones. Even though there are several reports on the preparation of this type of compounds [14][16][22][23] and their substituted derivatives [18], to date their potential use as herbicides has been poorly investigated [24][25].

Here, we report the synthesis of a set of aminobenzoquinone derivatives **1** – **13** and the assessment of their inhibitory effects on plant and algal growth, as well as their ability to interfere with the photosynthetic electron transport chain in isolated spinach chloroplasts. In view of the great concern about the impact of new herbicides on



**Pedido nacional de Invenção, Modelo de Utilidade, Certificado de  
Adição de Invenção e entrada na fase nacional do PCT**

**Número do Processo:** BR 10 2017 022746 4

**Dados do Pedido**

---

**Natureza Patente:** 10 - Patente de Invenção (PI)

**Título da Invenção ou Modelo de Utilidade (54):** "ANÁLOGOS DE ABENQUINAS, PROCESSO DE OBTENÇÃO, COMPOSIÇÃO FARMACÊUTICA E USOS"

**Resumo:** A presente invenção trata de análogos de abenquinas e do seu processo de obtenção através da modificação dos substituintes no núcleo da benzoquinona. O processo de obtenção dos compostos constitui-se de uma rota sintética de três etapas com altos rendimentos, de 45 a 85%. A invenção trata ainda das composições farmacêuticas contendo análogos de abenquinas e seus usos. Os análogos às abenquinas podem ser utilizados como potentes inibidores da proliferação de cianobactérias em águas frescas. E finalmente, os análogos às abenquinas assim como as composições contendo esses compostos podem ser utilizados como potentes inibidores da proliferação de diferentes linhagens de células tumorais.

**Dados do Inventor (72)**

---

Inventor 1 de 6

**Nome:** LUIZ CLÁUDIO ALMEIDA BARBOSA

**CPF:** 26179687668

**Nacionalidade:** Brasileira

**Qualificação Física:** Professor do ensino superior

**Endereço:** Rua Alagoas, 997, apto. 1503, Bairro Funcionários

**Cidade:** Belo Horizonte

**Estado:** MG

**CEP:** 30130-167

**País:** BRASIL

**Telefone:** (31) 340 93932

**Fax:**

**Email:** patentes@ctit.ufmg.br

Inventor 2 de 6

**Nome:** AMALYN NAIN PEREZ

**CPF:** 02031852698

**Nacionalidade:** Venezuelana

**Qualificação Física:** Estudante de Pós Graduação

**Endereço:** Avenida Fleming, 1113, apto. 104, Bairro Ouro Preto

**Cidade:** Belo Horizonte

**Estado:** MG

**CEP:** 31310-490

**País:** BRASIL

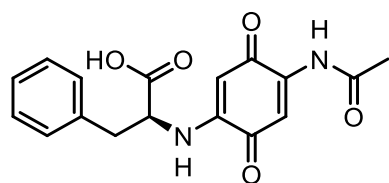
**Telefone:** (31) 340 93932

**Fax:**

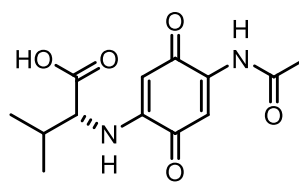
**Email:** patentes@ctit.ufmg.br

## **CHART OF PRODUCTS**

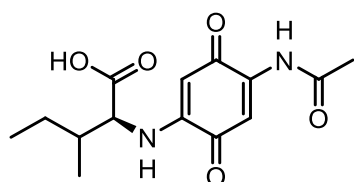
## Chapter 1:



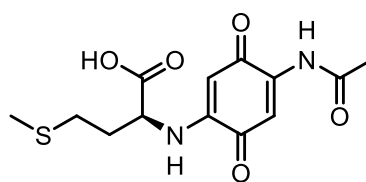
**Abenquine A (1.6)**



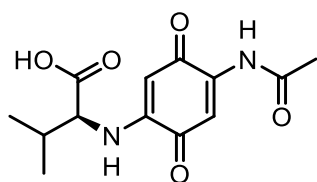
**1.17**



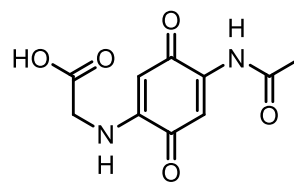
**Abenquine B (1.8)**



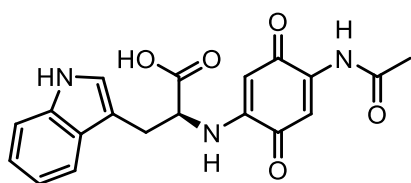
**1.18**



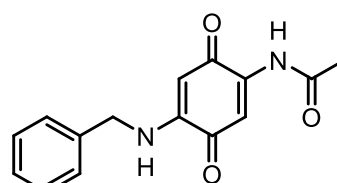
**Abenquine C (1.9)**



**1.19**

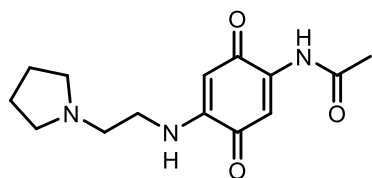


**Abenquine D (1.10)**

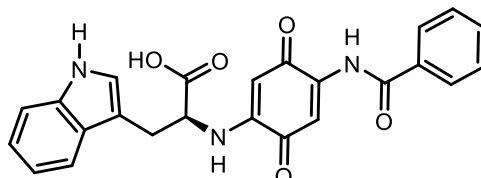


**1.20**

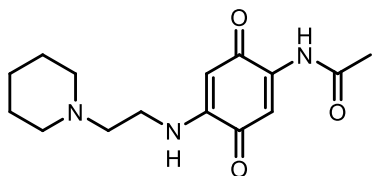
## Chapter 2:



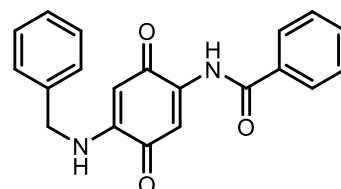
2.1



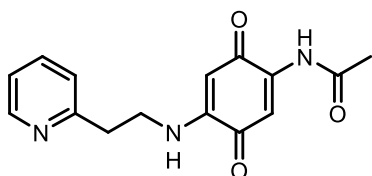
2.9



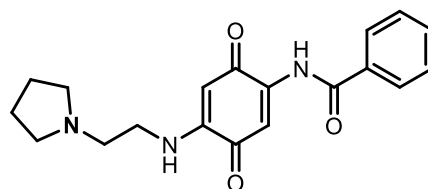
2.2



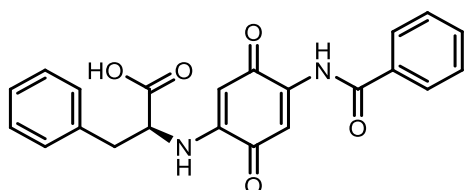
2.10



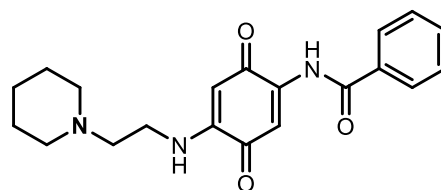
2.3



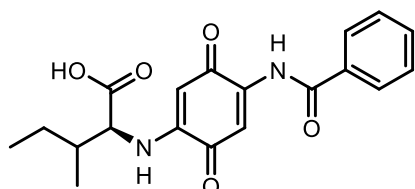
2.11



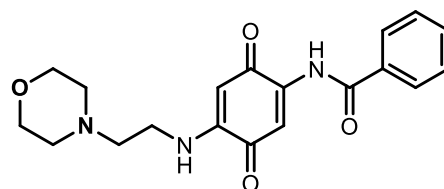
2.6



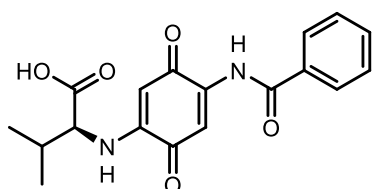
2.12



2.7

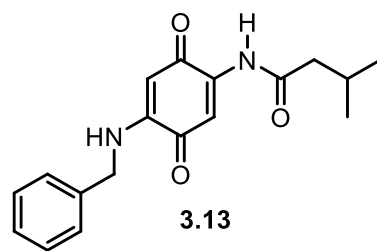
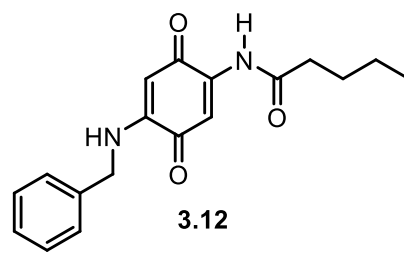
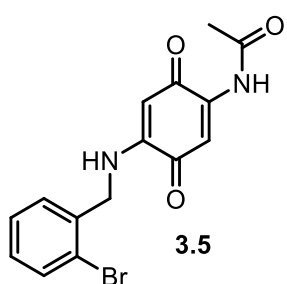
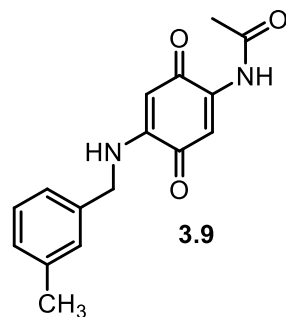
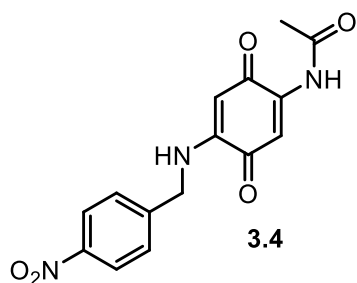
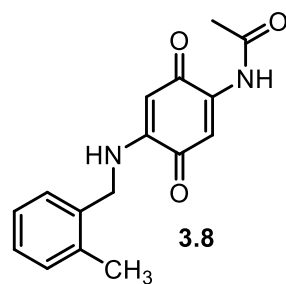
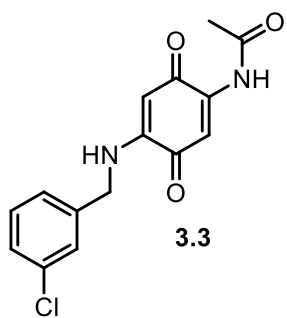
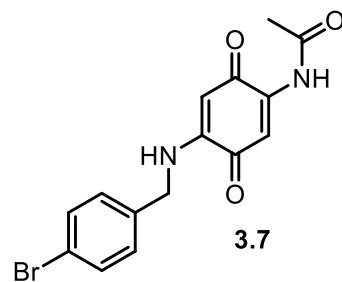
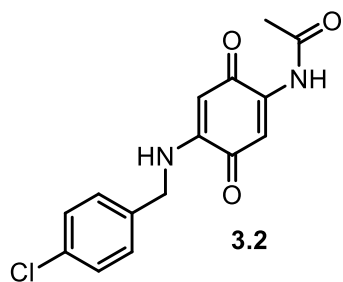
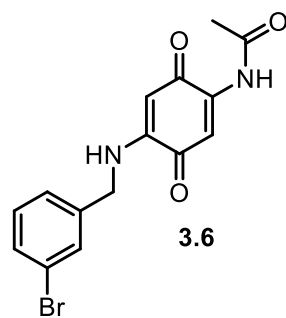
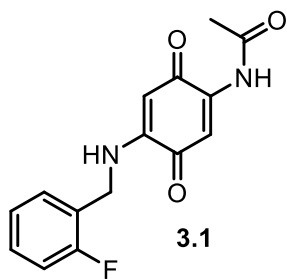


2.13

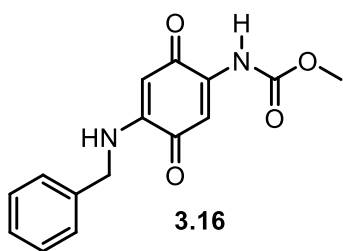
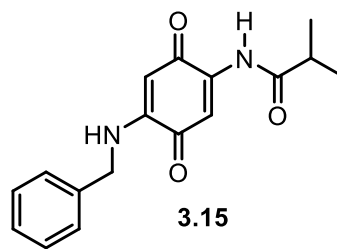
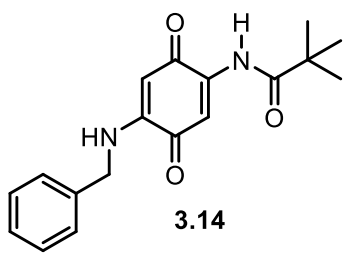


2.8

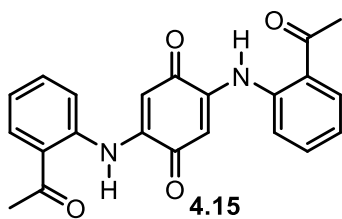
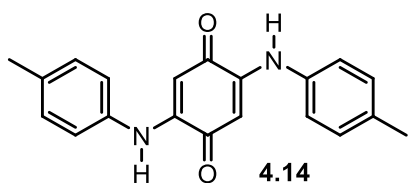
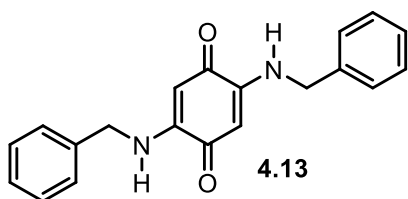
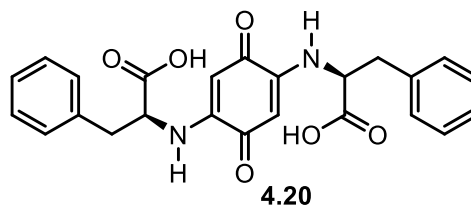
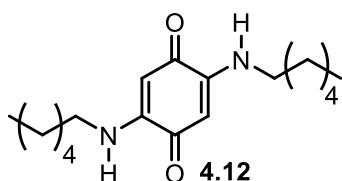
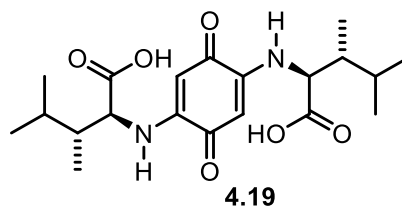
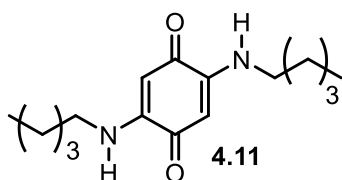
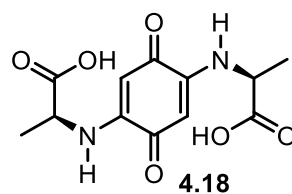
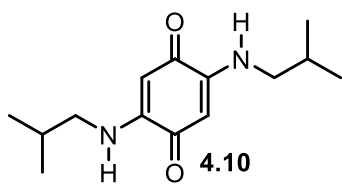
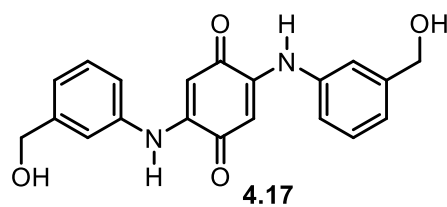
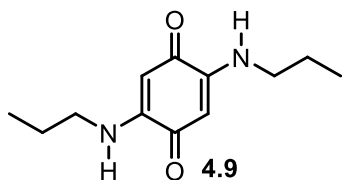
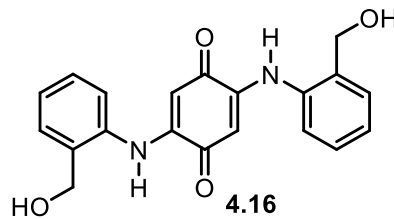
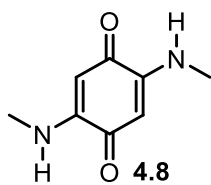
### Chapter 3:

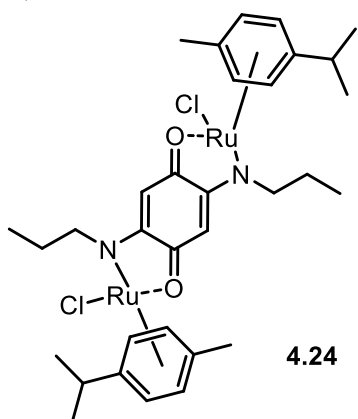
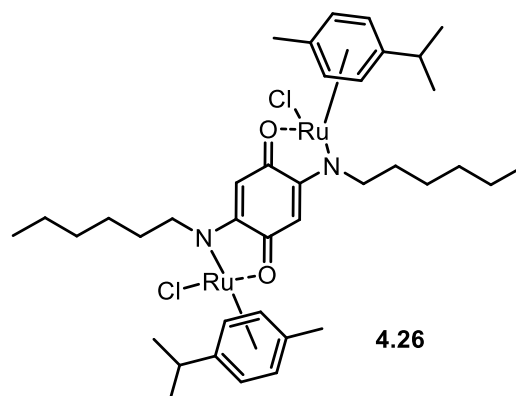
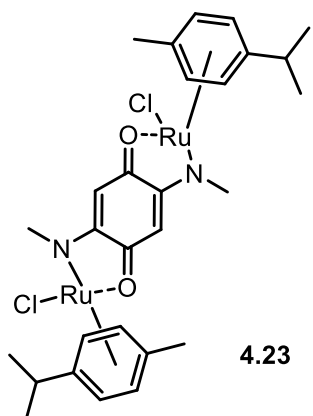
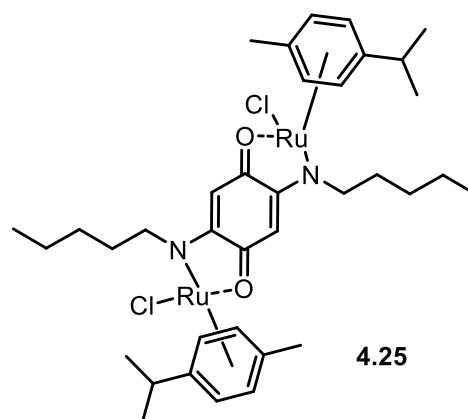
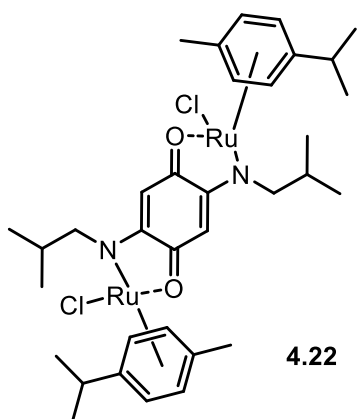






## Chapter 4:





## Chapter 5:

